

Università degli Studi di Milano-Bicocca

*Facoltà di Scienze Matematiche, Fisiche, Naturali
Dipartimento di Scienze Geologiche e Geotecnologie*

**Doctor of Philosophy
in
Earth Sciences**



MULTI SCALE HEURISTIC AND QUANTITATIVE MULTI-RISK ASSESSMENT IN THE LOMBARDY REGION, WITH UNCERTAINTY PROPAGATION

Serena Lari

Supervisor

Prof. Giovanni Battista Crosta

Academic year 2008/2009

SUMMARY

Introduction.....	5
Chapter 1. Risk assessment and acceptability.....	7
1 Background and definitions.....	7
1.1 Risk assessment	8
1.2 Quantitative risk measures.....	9
1.3 Acceptability of risk.....	13
1.4 Overview of risk measures.....	24
1.5 Multi-risk assessment.....	25
Chapter 2. Uncertainties in risk assessment.....	27
2 Uncertainty evaluation methodology.....	27
2.1 Aleatory and epistemic uncertainties.....	28
2.2 Uncertainty propagation.....	29
Chapter 3. Countermeasures for risk mitigation.....	38
3 Cost-benefit analysis.....	38
PART I: Multi risk assessment, regional scale	
1 Introduction.....	43
2 Study area.....	44
2.1 State of risks in lombardy.....	49
3 General methodology.....	51
3.1 Databases.....	52
3.2 Exposed elements.....	54
3.3 Weighting strategies.....	56
4 Physical risk indicators.....	57
4.1 Hydrogeological risk.....	58
4.2 Other risks.....	60
5 Aggravating factor.....	61
6 Total risk assessment.....	63
7 Risk integration	66
8 Hot spot identification.....	68

9	Sensitivity analysis.....	70
10	Discussion.....	73
10.1	Spatial pattern of risk.....	73
10.2	Influence of risk perception on weighting process.....	77
10.3	High risk/hot-spot areas.....	78
11	Conclusions.....	79

PART II: Integrated area planning

1	Introduction.....	81
2	Integrated area plans.....	86
3	Study areas.....	87
3.1	Lower Valtellina.....	87
3.2	Brescia.....	93
4	Data implementation.....	98
4.1	Exposed elements.....	99
4.2	Hazard.....	99
5	Methodology.....	104
5.1	Societal and individual risk.....	105
5.2	Economic risk.....	113
6	Natural risk assessment.....	116
6.1	Rockfalls.....	116
6.2	Shallow landslides.....	136
6.3	Debris flow risk.....	151
6.4	Floods on alluvial fans.....	163
6.5	River floods.....	172
6.6	Seismic risk.....	184
6.7	Wildfire risk.....	204
6.8	Total natural risk.....	213
7	Technological risk assessment.....	225
7.1	Work injuries.....	225
7.2	Road accident risk.....	229
7.3	Transport of hazardous materials.....	232
7.4	Industrial risk.....	238
7.5	Total technological risk.....	246
8	Conclusions.....	249

PART III: Uncertainty in multi risk assessment at local scale

1	Introduction.....	251
2	Study area.....	251
2.2	Context for risk analysis and data availability.....	252
3	Risk assessment and uncertainty evaluation.....	255

3.1	Methodology.....	255
3.2	Risk analysis.....	259
4	Discussion and conclusions.....	278
4.2	Risk evaluation	278
4.3	Uncertainty.....	279

PART IV: Indicators for priority and efficacy evaluation of mitigation works

1	Introduction.....	282
2	Purposes of the study.....	283
3	Existing practices in Lombardy region.....	284
3.1	Hydrogeological risk.....	284
3.2	Wildfire risk.....	284
4	Methodology.....	286
4.1	Level 1: recognition of risk level.....	286
4.2	Level 2: multi criteria analysis.....	287
4.3	Level 3: cost-benefit analysis.....	298
5	Application.....	302
5.1	Level 2: multi criteria analysis.....	303
5.2	Level 3: cost-benefit analysis.....	307
6	Conclusions.....	312
	References.....	313
	Data sources.....	331
	Appendix I.....	334

INTRODUCTION

In spite of a growing understanding and a great effort of society in disaster mitigation, the management and reduction of existing risks continue to challenge disaster prone communities (Tyagunov et al., 2005). Frequency and severity of natural and technological disasters are increasing worldwide; combined with the development of urbanised areas and with the growth of population, they result in a dramatic growth of losses. Their reduction becomes a strategic goal, and is being recognized as an integral component of both emergency management and sustainable development, also involving social, economic, political, and legal issues (Durham 2003).

Risk management is more effective when: (1) it is an integral part of a total community risk management approach, (2) it involves all levels of government and community, (3) it is proposed as a prevention and preparedness approach, rather than purely response (Durham 2003). A condition to prevention, management and reduction of risk is its quantification, analysis and assessment.

In this thesis, some methodologies for multi-risk assessment are presented, that can be applied to regional or local scale. At the local scale, the problem of uncertainty propagation in risk assessment is treated, testing different methodology for calculation.

The work is organised in four parts:

1. Multi risk analysis at the regional scale in Lombardy (PRIM project, 2007). The methodology integrates information with different degree of accuracy into an indicator based approach, in order to develop a regional scale multi-risk assessment and to identify “hot spot” risk areas for more detailed analysis. Eventually, the sensitivity of weights is investigated, and the effect on risk assessment of different individual attitudes and perception (i.e., expert, social, political, risk aversion).
2. Quantitative multi risk assessment (QRA) at the local scale on the hot spots, for lower Valtellina and the area of Brescia and lower Val Trompia, Val Sabbia, and Valcamonica. The methodology is based on the use of historical data and modelling to assess for each threat the expected number of casualties and the expected economic damage.
3. Quantitative risk assessment (QRA) for floods, earthquakes and industrial accidents in the area of Brescia (420 km²), with uncertainty propagation analysis. Frequency-damage curves were calculated. Three methods were

used and compared to calculate the uncertainty of the expected economic losses: Monte Carlo Simulation, First Order Second Moment approach, and Point Estimate.

4. Realization of a tool based on a system of indicators aimed at assigning a priority for the realization of new mitigation works, at the evaluation of efficacy of existent works, and at the comparison of different alternatives for the same risk scenario. Indicators are referred to the risk scenario, to the most recent and most significant event occurred in the analysed area, to the planning stage of the work, and to the technical characteristics of realization and maintenance of the work itself.

CHAPTER 1. RISK ASSESSMENT AND ACCEPTABILITY

1 BACKGROUND AND DEFINITIONS

Risk is generally agreed to be dependent on probability of occurrence of hazardous events and on expected consequences (Baecher and Christian, 2003). According to Kaplan and Garrick (1981) risk is defined by a combination of the expected consequences of a set of scenarios, each with a probability and a consequence.

Specific risk is the expected degree of loss for one or more elements at risk, characterised by specific vulnerability, exposition, due to a phenomenon of a given hazard.

$$R_s(P, I, E, V) = H * E_s * V$$

where:

P = probability of occurrence;

I = intensity, geometric or mechanic severity of a potentially hazardous phenomenon. It is expressed as a function of a characteristic descriptor (mass, energy, etc.) or according to a relative scale;

E = elements at risk: population, goods (properties, facilities, cultural and environmental goods) and activities which can undergo damages due to an hazardous phenomenon.

V = vulnerability, degree of loss for an element or type of elements due to the occurrence of an hazardous event of a given intensity. It is expressed in a 0-1 ranging scale (0=no loss, 1= complete loss);

H = Hazard is the probability that a particular threat occurs within a given period of time at a specific site (e.g. annual exceeding probability of an event of specified magnitude). In technological risk, hazard is also referred to as the probability of an Accidental Event (NORSOK, 2001) or Initiating Event (NASA, 2002);

E_s = exposition, probability that an element at risk is exposed to the effects of an hazardous phenomenon of a given intensity in a definite time interval at a certain place.

Vulnerability is the predisposition of some portions of the physical, social and economical space to suffer damages in consequence of impact with potentially harmful phenomena (United Nations Development Programme, 2004). Physical vulnerability is the degree of loss to a given element or set of elements within the area affected by a hazard, and it can be expressed through a mathematical function on a scale of 0 (no loss) to 1 (total loss). Vulnerability functions are commonly available only for flood and earthquakes (Porter et al., 2001; FEMA, 1999; USACE, 2000), and in some examples for landslides (Glade et al., 2003; Roberds, 2005; Birkmann, 2006; Fuchs et al., 2007; Galli and Guzzetti, 2007).

As for the other dimensions of vulnerability, a set of heuristic or empirical indicators are reported in the literature (Coburn et al., 1994; CEPAL/BID, 2000; Barbat, 2003; Glade, 2003; UNDP, 2004).

1.1 RISK ASSESSMENT

The risk assessment includes the identification, quantification and evaluation of risks associated with a given system. It is performed because involved parties (designers, managers, decision makers, stakeholders) want to identify and evaluate the risks and decide on their acceptability and on mitigations to be implemented. Outcomes of risk assessment can be used in the design process to decide on the required safety levels of new systems or to support decisions on the acceptability of safety levels and the need for mitigation measures in existing systems. A quantitative measure is needed to transfer decisions on acceptable safety into a technical domain (Voortman, 2004). Overall, the risk assessment aims to support rational decision-making regarding risky activities (Apostolakis, 2004), territorial planning and management.

Decision-making related to risks is very complex and involves not only technical aspects but also political, psychological and social processes. In this complex decision-making process a clear identification of the risks and of the effects of risk reduction measures is very useful (Jonkman et al., 2002). From a technical point of view, the extent of the risks and the effects of risk reduction measures can be quantified in a Quantitative Risk Assessment (QRA). Generally four phases are distinguished in literature on quantitative risk assessment, see for example Vrouwenvelder et al. (2001):

- *Qualitative analysis*: Definition of the system and the scope, identification and description of the hazards and scenarios;
- *Quantitative analysis*: Determination of the probabilities and expected consequences of the defined events. Quantification of the risk as a function of probabilities and consequences;
- *Risk evaluation*: Evaluation of the risk based on the results of the former analyses. In this phase the decision is made whether or not the risk is tolerable;
- *Risk control and risk reduction measures*: Depending on the outcome of the risk evaluation, measures may have to be taken to reduce the risk. It should also be determined how the risks can be controlled (for example by inspection, maintenance or warning systems) (Jonkman et al., 2002).

1.2 QUANTITATIVE RISK MEASURES

A quantitative risk measure is a mathematical function of the probability of an event and the consequences of that event. Risk measures can consider loss of life and economic damage as a consequence. For a more complete overview of the study of risk measures reference is made to Jonkman et al. (2003).

1.2.1 PROBABILISTIC AND DETERMINISTIC APPROACH

The probabilistic approach is based on an inventory of probabilities and consequences for all possible accident scenarios. Next to the probabilistic approach a deterministic or scenario analysis is sometimes used in the design phase (Jonkman et al., 2003). The deterministic approach analyses one (or a limited number of) design scenario(s) for which all conditions are uniquely given. This scenario is generally analysed in a qualitative and descriptive way and gives useful insight in possible event development. It mainly focuses on specific phases of the event development. As the event's causes are generally not involved in the analysis, it becomes difficult to give a complete analysis of measures. The two approaches are complementary as the deterministic analysis focuses on one of the scenarios investigated in the probabilistic analysis. The application of one single accident scenario (i.e. a purely deterministic analysis) as a basis for a design without inclusion of probabilities and consequences in general does not contribute to an effective design. This implies that the uncertainty that is always present is neglected. In practice, the probability of a scenario is often implicitly considered in the deterministic analysis with the selection of the "representative" or design scenario. Therefore it is assumed here that the probabilistic risk analysis (based on all scenarios) provides the best basis for rational decision-making regarding risks.

1.2.2 INDIVIDUAL RISK MEASURES

Individual risk to life is the increment of risk imposed on particular individual by the existence of the hazard. It is usually expressed as the annual probability of the individual being killed as a result of the hazard (Leroi et al., 2005).

According to Diamantidis et al. (2006), the annual probability of being harmed describes the risk to an individual due to a hazardous situation. This probability is called the individual risk. With respect to fatality risks, the individual risk is the annual probability of being killed.

The individual risk can also be defined as the frequency at which an individual may be expected to face a given level of harm from the realisation of specified hazards such as geohazards. The individual risk criterion is occasionally used for the definition of acceptable risk values in landslide hazards (Diamantidis et al., 2006).

The measure of individual risk (IR) used by the Dutch Ministry of Housing, Spatial Planning and Environment (VROM) is defined as the probability that an average unprotected person permanently present at that point location, would get killed due to an accident at the hazardous activity (Bottelberghs, 2000).

$$IR = P_f \cdot P_{d|f} \quad (1)$$

where:

P_f probability of failure (yr^{-1})

$P_{d|f}$ probability of dying of the individual in the case of failure, assuming the permanent unprotected presence of the individual.

A slightly different definition, in which the actual presence of the individual is considered, is used by the Dutch Technical Advisory Committee on Water Defences (TAW, 1985) and by Bohlenblust (1998) to describe the actual personal risk. An overview of other measurements to express the individual risk is given by Bedford and Cooke (2001), examples are the “activity specific hourly mortality rate” and the “death per unit activity”.

Besides the individual risk, other expressions are described. The ‘loss of life expectancy’ expresses the decrease of life expectancy due to various causes. The ‘delta yearly probability of death’ computes the intensity at which a given activity is to be performed (in suitable units) to increase the yearly probability of death by 10^{-6} . The activity ‘specific hourly mortality rate’ is the probability per time unit while engaged in a specified activity. An example is the fatal accident failure rate (FAFR) which gives the number of fatalities per 1000 h of exposure to a certain risk. A variant is the ‘death per unit activity’, which replaces the time unit by a unit measuring the amount of activity. The risks of travel by car, train or aeroplane are often expressed as the number of deaths per kilometre travelled.

The UK’s Health and Safety Executive (HSE) defines the individual risk as the risk that a typical user of a development is exposed to a dangerous dose or worse of toxic substance, heat or blast overpressure (HSE, 1989). A dangerous dose is likely to cause the person severe distress or injury, but it does not necessarily lead to death.

The IR is a property of the place and as such useful in spatial planning. Locations with equal individual risk levels can be shown on a map with so-called risk contours.

1.2.3 SOCIETAL RISK MEASURES

To society as a whole or to a company or institution responsible for a specific activity, the total damage due to a hazard is of major interest. The notion of societal risk R (casualties/year) is introduced.

$$R = \sum_{i=1}^n p_i \cdot C_i \quad (2)$$

where p_i is the probability of occurrence (per year) of event i , and C_i are the related consequences. Societal risk is also referred as total risk in landslide risk assessment (e.g. Fell, 1994). With respect to fatality risks, the societal risk R corresponds to the annual expected number of fatalities. It depends on the probability as well as on the size of the consequences of events. In most practical studies the societal risk of an installation is given in the form of a numerical F-N-curve (Fig.2). An F-N-curve (N representing the number of fatalities, F the frequency of accidents with more than N fatalities) shows the relationship between the annual frequency F of accidents with N or more fatalities.

Societal risk is defined by Institute of Chemical Engineering (1985) as the relationship between frequency and the number of people suffering from a specified level of harm in a given population from the realisation of specified hazards. Where individual risk gives the probability of dying on a certain location, the societal risk gives a number for a whole area no matter where precisely within that area the event will occur. The difference is shown in Fig.1.

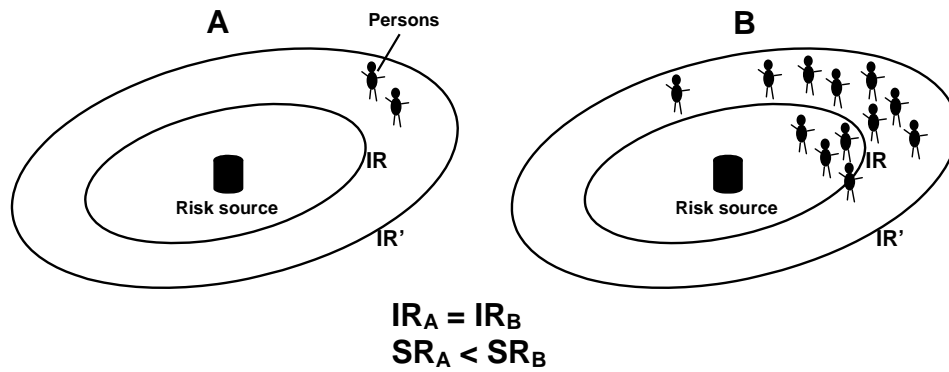


Fig. 1. The difference between individual and societal risk. Both situations have equal individual risk levels (shown by IR' and IR). Because of the larger population density of situation B, B has a larger societal risk (based on Stallen, 1996)

The basis of the calculation of societal risk is formed by the probability density function (pdf) of the yearly number of fatalities. From the pdf an FN curve can be derived which shows the probability of exceedance as a function of the number of fatalities, on a double logarithmic scale.

$$1 - F_N(x) = P(N > x) = \int_x^{\infty} f_N(x) dx \quad (3)$$

where:

$f_n(x)$ the probability density function (pdf) of the number of fatalities per year

$F_N(x)$ probability distribution function of the number of fatalities per year, signifying the probability of fewer than x fatalities per year.

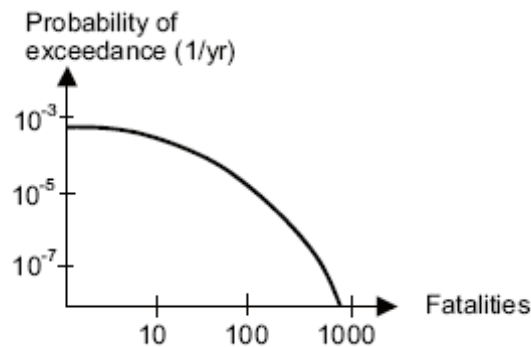


Fig.2. Example of an FN curve

A simple measure for societal risk is the expected value of the number of fatalities per year, $E(N)$, in literature often referred to as the Potential Loss of Life (PLL):

$$E(N) = \int_0^{\infty} x \cdot f_N(x) \cdot dx \quad (4)$$

Ale et al. (1996) propose the area under the FN-curve as a measure for societal risk. Vrijling and van Gelder (1997) show that this measure equals the expected number of fatalities per year:

$$\int_0^{\infty} (1 - F_N(x)) dx = \int_0^{\infty} \int_x^{\infty} f_N(u) du dx = \int_0^{\infty} \int_0^u f_N(u) dx du = \int_0^{\infty} u f_N(u) du = E(N) \quad (5)$$

The British Health and Safety Executive (HSE) has defined a risk integral as a measure for societal risk (Carter, 1995):

$$RI = \int_0^{\infty} x \cdot (1 - F_N(x)) \cdot dx \quad (6)$$

Vrijling and van Gelder (1997) proved mathematically that the RI can be expressed in two characteristics of the pdf of the number of fatalities, the expected value $E(N)$ and the standard deviation $\sigma(N)$:

$$RI = \frac{1}{2}(E^2(N) + \sigma^2(N)) \quad (7)$$

From the pdf also the expected value of the number of deaths, $E(N)$ (or potential loss of life (PLL), and the standard deviation, $\sigma(N)$, can be derived. Combining these two elements the total risk (TR) has been proposed by Vrijling et al. (1998) as a measure for societal risk:

$$TR = E(N) + k \cdot \sigma(N) \quad (8)$$

This measure takes into account the risk aversion towards rare accidents with large numbers of fatalities by multiplying a risk aversion index k with the standard deviation. Although the equations may look different, the societal risk measures described here are all based on the pdf of the number of fatalities.

1.2.4 ECONOMIC RISK MEASURES

Besides the danger of loss of life due to certain activities, the economic risks plays an important role in decision-making. Different approaches have been proposed to quantify economic risks and their applications.

A FD curve displays the probability of exceedance as a function of the economic damage (D representing the economic damages, F the frequency of accidents with a damage higher than D). The FD curve and the expected value of the economic damage can be derived from the pdf of the economic damage ($f_D(x)$)

$$1 - F_D(x) = P(D > x) = \int_x^{\infty} f_D(x) \cdot dx \quad (9)$$

$$E(D) = \int_0^{\infty} x \cdot f_D(x) dx \quad (10)$$

where:

$F_D(x)$ the probability distribution function of the economic damage

$E(D)$ expected value of the economic damage

Analogous to the FN-curve and the expected number of fatalities, it can be shown that the area below the FD-curve equals the expected value $E(D)$ (Jonkman et al., 2002).

The expected value of the economic damage is used as a part of cost benefit analysis of flood prevention measures in the UK (Parker, 1987). The benefits of a measure are determined by calculating the expected value of the economic damage before and after the measure has been taken. The difference between these two values results in the benefits, which can be weighed against the costs of the measures.

1.3 ACCEPTABILITY OF RISK

The definition of acceptable risk levels is a very complex issue. Tolerable risks are risks that society can live with. It is a range of risk regarded as non-negligible and needing to be kept under review and reduced further if possible (Leroi et al., 2005). According to Bell et al., (2004), tolerable risks define the level of risk society is prepared to live with under the condition that risk is monitored and risk management options are taken to reduce it.

Acceptable risks are risks which everyone affected is prepared to accept. Action to further reduce such risk is usually not required unless reasonably practicable measures are available at low cost in terms of money, time and effort (Leroi et al., 2005). It represents the level of risk society is prepared to accept without any specific risk management options (Glade et al., 2004, Lee and Jones, 2004, Australian Geomechanics Society, 2000, IUGS 1997).

IUGS (1997) listed some common general principles that can be applied when considering tolerable risk criteria.

- a) The incremental risk from a hazard to an individual should not be significant compared to other risks to which a person is exposed in everyday life.
- b) The incremental risk from a hazard should, wherever reasonably practicable, be reduced, i.e. the As Low As Reasonably Practicable (ALARP) principle should apply, as defined by Health and Safety at Work etc. Act 1974, UK.

- c) If the possible loss of life or economic damages due to an event is high, the risk that the event might actually occur should be low. This accounts for society's particular intolerance to events that cause many simultaneous casualties, and is embodied in societal tolerable risk criteria.
- d) Persons in society will tolerate higher risks than they consider acceptable, when they are unable to control or reduce the risk because of financial or other limitations.
- e) Higher risks are likely to be tolerated for existing contexts than for planned projects, and for workers, than for society as a whole.
- f) Tolerable risks may vary from country to country, and within countries, depending on historic exposure to hazard, and the system of control of natural hazards.

Smith (1992) stated that risk means different things to different people because each person holds a unique view of the environment and of environmental risk. To tackle this problem both social and natural scientists have spent enormous efforts on developing suitable approaches, including for instance the technical approach (e.g. Starr 1969; Geotechnical Engineering Office 1997), the mathematical approach (Plattner 2005), the psychometric approach (e.g. Slovic 1987), the Dual-process approach (summarized by Epstein 1994) and the System theoretical approach (e.g. Luhmann 1995) (Bell, 2004). They all contributed to the question of risk perception and risk acceptance.

The definition of acceptable risk is a necessary stage in risk management (Leroi et al., 2005). It enables the elaboration of risk analysis and reduction methodologies on the basis of clear and shared objectives. The criteria can be multiple, and so can their value; acceptable risk can be defined in a qualitative, quantitative or even implicit way (Leroi et al., 2005).

The concept of risk acceptance criteria is also widely used in many industrial sectors. Comparative risk thresholds have been established which allow a responsible organisation to identify activities having an unacceptable level of risk on the participating individuals or society as a whole. Risk acceptance can be defined by two different methods: implicitly or explicitly. Implicit criteria often involve safety equivalence with other industrial sectors (e.g. stating that a certain activity must impose risk levels at most equivalent to those imposed by another similar activity). In the past, this approach was very common because some industrial sectors (for example nuclear and offshore) developed quantitative risk criteria well before others, and thus also constituted a basis for comparison. While this methodology has been surpassed by more refined techniques, it is still used occasionally today. Explicit criteria are applied in many industrial sectors, as they tend to provide either a quantitative decision tool or a comparable requirement for the industry when dealing with the certification / approval of a particular structure or system.

The nature of risk determines its acceptability which is associated with several properties and related factors such as (Osei et al., 1997): voluntary vs. involuntary, controllability vs. uncontrollability, familiarity vs. unfamiliarity, short/long-term consequences, presence of existing alternatives, type and nature of consequences, derived benefits, media communication, information availability, personal involvement,

memory of consequences. In the landslide case for example, natural and engineered slopes can be considered as voluntary and involuntary, respectively. Informed societies can have better preparedness for natural hazards, while societies having frequent natural disasters have fresh memories about the consequences

When people are familiar with risk involved in an activity they are more willing to accept it. Societies experiencing frequent landslides and/or earthquakes may have different level of landslide risk acceptance than those experiencing rare landslide and/or earthquake situations. Risk acceptability is also influenced by the failure/accident consequences. For example, people leaving on a slope which has very small movement rate may accept the landslide risk unless the movement is accelerated by a triggering event. Existence of alternatives has also impact on the level risk acceptability. If there are no alternatives, many risks can be tolerated by the people.

Type and nature of consequences are another important property of risk, since risks due to events causing more damage and fatality are more difficult to accept (e.g., landslides threatening a rural area vs. earthquake in an urban area). Derived benefits of society and the individual play significant role in risk acceptance. In addition, presentation of consequences of a geohazard in media has some influence on risk acceptability.

Acceptable risk levels, hence, cannot be defined in an absolute sense. Each individual has their own perception of acceptable risk which, when expressed in decision theory terms, represents their own “preferences”.

1.3.1 INDIVIDUAL RISK

According to IUGS (1997) the incremental risk from a hazard should not be significant compared to other risks to which a person is exposed in the every-day life. The probability of the individual risk is therefore compared with the probability of natural death. A normally accepted order of magnitude of a hazard of death related to a particular activity is around 10^{-4} per year (Archetti and Lamberti, 2003).

For individual risk acceptability, instead, some criteria included in Italian law can be considered. DM 28/10/2005 includes some threshold for acceptability:

- 10^{-1} to 10^{-5} for risk freely faced
- 10^{-6} to 10^{-8} for non voluntary faced risk

HSE uses a framework for judging the tolerability of risks, considering an unacceptable, a tolerable and a broadly acceptable region (HSE, 2001) Fig.3. Using HSE's definition of individual risk, a value of 10^{-6} should be used as a guideline for the boundary between the broadly acceptable and the tolerable regions for both workers and the public. For the boundary between the tolerable and the unacceptable regions no widely applicable criterion is given. However, an HSE document on the tolerability of risks in nuclear stations (HSE, 1992) suggests values of 10^{-3} for workers and 10^{-5} for the members of the public, as a boundary between the tolerable and the acceptable regions.

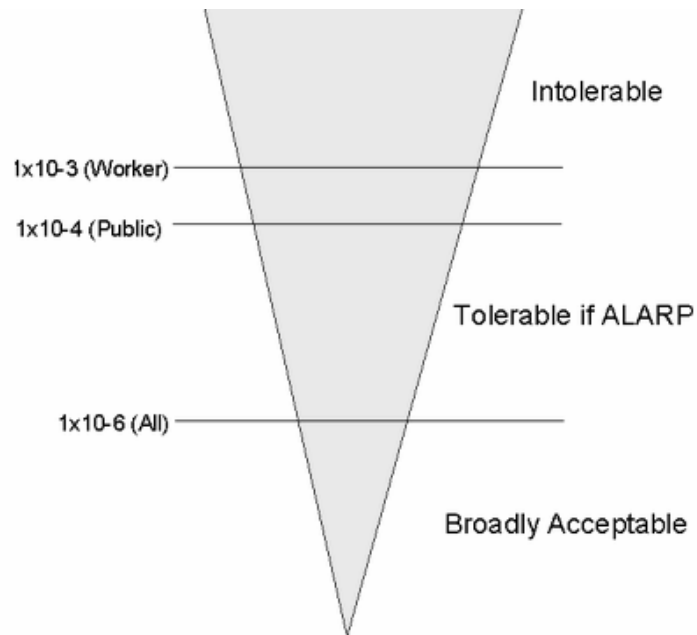


Fig.3. R2P2 Individual risk criteria, HSE (2001)

The Dutch Ministry of Housing, Spatial planning and Environment (VROM) has set the following standard for populated areas (Bottelberghs, 2000):

$$IR < 10^{-6} (\text{yr}^{-1}) \quad (11)$$

Risks lower than 10^{-6} per year should always be reduced to a level as low as is reasonably achievable (ALARA).

The method of TAW (TAW, 1985) gives the opportunity to limit a broader set of risks ranging from voluntary activities, such as mountaineering, to more involuntary risks, such as those of hazardous installations:

$$IR < \beta \cdot 10^{-4} (\text{yr}^{-1}) \quad (12)$$

In this expression the value of the policy factor β varies according to the degree of voluntariness of the activity and with the benefit perceived. In Tab.1. some β values are proposed for different activities. This method has been used in case studies concerning various risks in Vrijling et al., (1995).

Tab.1. Policy factor β as function of voluntariness and benefit of the activity (Vrijling, 1995).

β	Voluntariness	Benefit	Example
100	Completely voluntary	Direct	Mountaineering
10	Voluntary	Direct	Motorbiking
1	Neutral	Direct	Car driving
0.1	Involuntary	Some	Factory
0.01	Involuntary	None	Living nearby an LPG station

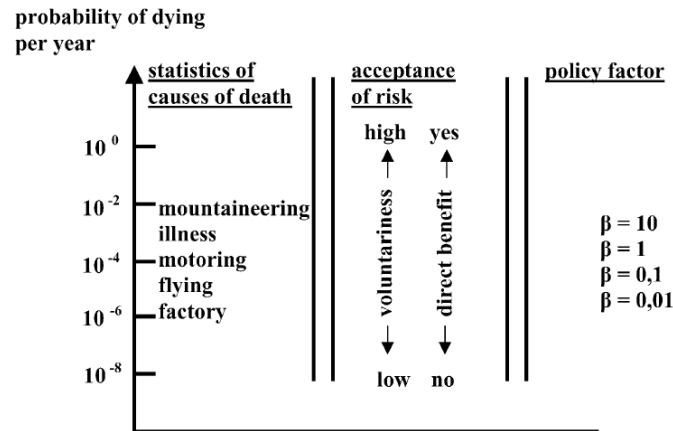


Fig.4. Policy factor β for different activities and various degrees of voluntary participation and benefit (Jonkman et al., 2002)

The background of the standard proposed by Bohnenblust (1998), is comparable with the TAW standard. Bohnenblust limits the acceptable IR, taking into account the extent to which participation in an activity is voluntary and the degree of self-control in the activity. Four risk categories have been determined, ranging from voluntary to involuntary. The proposed limits of Bohnenblust and TAW are shown in Fig.5. Bohnenblust studies the safety of the railway system in Germany (Bohnenblust, 1998).

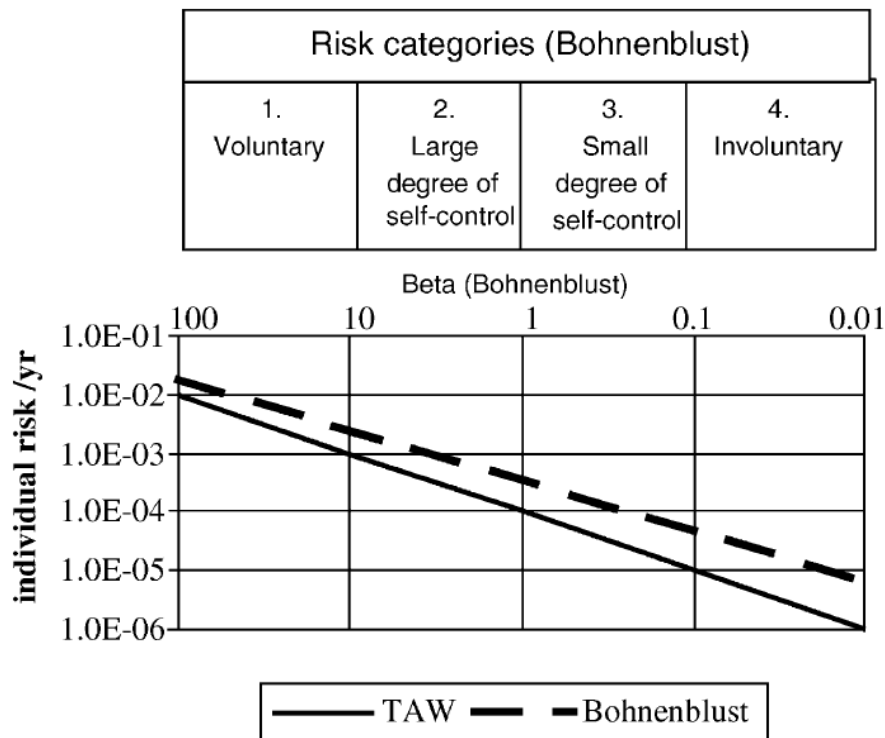


Fig.5. Individual risk standard according to Bohnenblust and TAW (Jonkman et al., 2002).

1.3.2 SOCIETAL RISK

A FN-criterion is defined by three variables: (1) its base point (the exceedance frequency of 1 fatality), (2) its slope, and (3) its frequency and/or consequence cut-off. Fig. 6 shows the different constraints that together make up an FN-criterion.

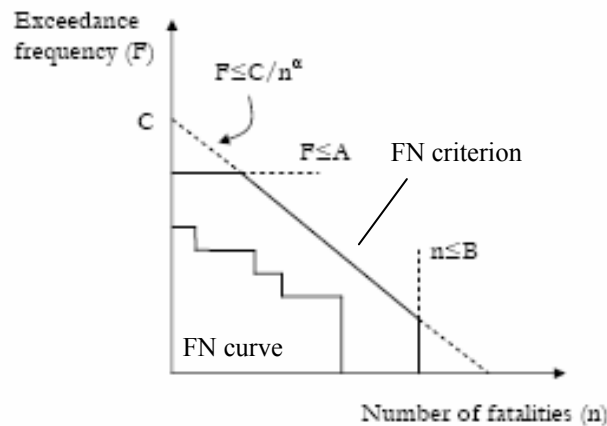


Fig.6. A fictitious FN-curve and an FN-criterion (Jongejan, 2008).

FN-criteria generally have slopes between between -1 and -2 (Ball and Floyd, 1998). A horizontal FN-criterion would limit the cumulative frequency of accidents ($F \leq A$), regardless of accident size. A vertical FN-criterion ($n \leq B$) would limit accident size, regardless of accident frequency. Slopes smaller than -1 reflect aversion to larger accidents. To support such aversion, one could argue that larger accidents increasingly affect the ability of a community to function, both socially and economically (e.g. Stallen et al., 1996). Empirical work also shows that typically decision makers place greater weight on larger accidents (e.g. Hubert et al., 1991).

The acceptable region, the unacceptable region, and the ALARP (as low as reasonably possible) region are thereby identified as shown as an example in Fig.7. A number of open issues have been pointed out regarding the validity of the ALARP criteria, including public participation, political reality, morality and economics.

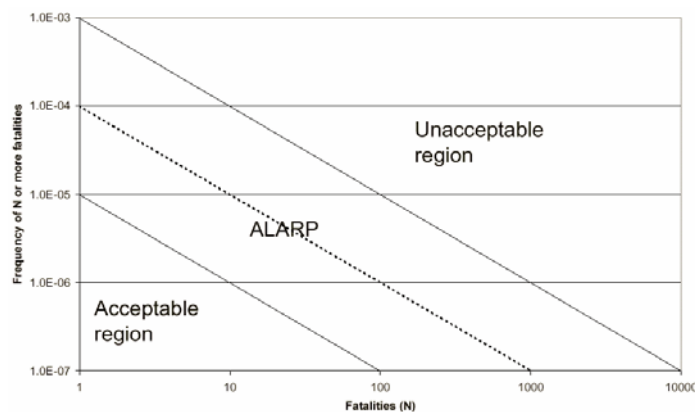


Fig.7. Example of F N-curve and illustration of ALARP range

F-N curves form the basis of developing societal acceptability and tolerability levels. However, it is to be noted that as F-N curves are frequently derived based on historical data (number of events and related fatalities) and consequently they represent the current situation.

The authority is usually responsible for defining the tolerability of the risk combinations contained within the risk classification matrix. In several countries a FN criterion line limits the risks of various hazardous activities. These standards can be described with the following general formula:

$$1 - F_N(x) < \frac{C}{x^n} \quad (13)$$

where n is the steepness of the limit line and C the constant that determines the position of the limit line. A standard with a steepness of $n = 1$ is called risk neutral. If the steepness $n = 2$, the standard is called risk averse (Vrijling and Van Gelder, 1997). In this case larger accidents are weighted more heavily and are thus only accepted with a relatively lower probability. Tab.2 gives the values of the coefficients for some international standards and the FN limit lines are shown in Fig. 8.

Commonly, as a part of the standard, an ALARA (or ALARP) region has been determined below the limit line, in which the risk should be reduced to a level that is as low as reasonably achievable (or possible).

Tab.2. Some international standards limiting the FN-curve (Jonkman et al., 2002)

Country	n	C	Application
UK (HSE)	1	10^{-2}	Hazardous installations
Hong Kong (truncated)	1	10^{-3}	Hazardous installations
The Netherlands (VROM)	2	10^{-3}	Hazardous installations
Denmark	2	10^{-2}	Hazardous installations

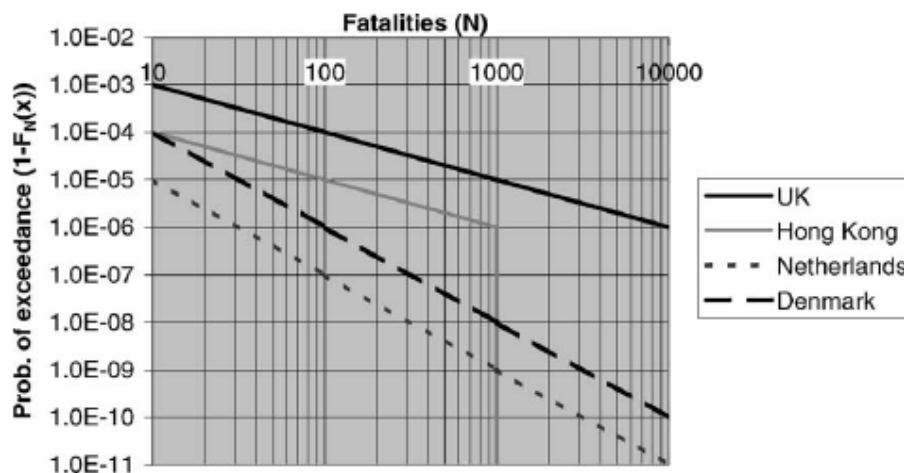


Fig.8. Some international standards in FN format (Jonkman et al., 2002)

Vrijling et al. (1995) proposed a standard for the acceptable risk. It limits the Total Risk on a national level, considering the policy factor β , which is has already been presented before (Tab.1).

$$TR < \beta * 100, \quad TR = E(N) + k \sigma (N) \quad (14)$$

This national criterion for acceptable risk can be translated into a standard for a single installation or location. This criterion has the typical form of a FN limit, with a quadratic steepness ($\alpha = 2$):

$$1 - F_N(x) < \frac{C}{x^2} \quad (15)$$

Behavioural decision theorists have however criticized the oversimplified nature of risk criteria that model the social costs of accidents by a function of the number of fatalities (Slovic et al., 1984). A criticism of the use of FN-criteria in regulatory contexts is that uniform criteria are typically applied to systems of different character and size.

Setting limits with FN-curves on a local level can be not adequate on a national level. If a risk criterion is defined on an local level, the national criterion is determined by the number of locations. An increase in the number of scenarios, each of them acceptable according to the local limit, can therefore lead to an unacceptable high-risk level on a national scale. To prevent these problems it is proposed to set a limit on a national level and to distribute the acceptable risk over the locations (Jonkman et al., 2002).

A similar problem with the use of FN limit lines is illustrated by Evans and Verlander (1997). While the risks of single scenarios are each acceptable by the FN limit line, the risks of the “probabilistic mixture” can exceed the limit, although the number of installations has not changed. Evans and Verlander (1997) conclude that the use of FN criterion can lead to unreasonable and inconsistent decisions and that the use of expected (dis)utility functions is therefore preferable. FN criteria are however difficult to connect to expected utility theory. Considering for instance a hazardous event that could cause n_1 fatalities with probability p_1 , and n_2 fatalities with probability p_2 ($n_1 < n_2$; $p_1 > p_2$), a decision maker is asked to evaluate risk acceptability. Assuming that the decision maker's disutility function U is a function of the number of fatalities and that the decision maker is risk averse (Fig.9), expected disutility equals $p_1 U(n_1) + p_2 U(n_2)$.

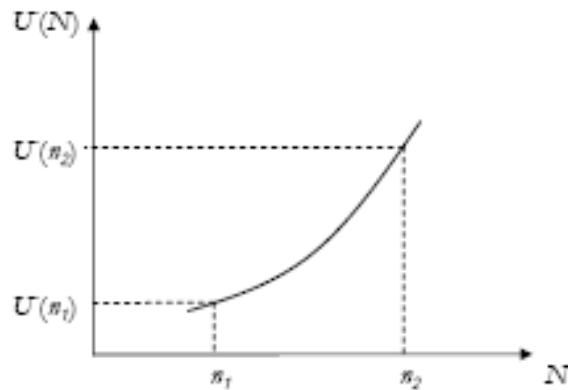


Fig.9. The decision maker's disutility function

When the decision maker considers the risk just acceptable, he could define the FN-criterion shown in Fig.10. Any increase in p_1 or p_2 (or n_1, n_2) would cause expected disutility to increase.

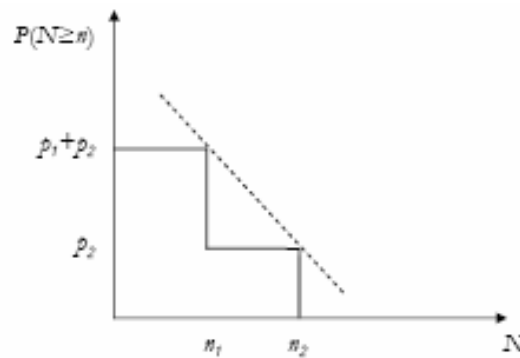


Fig.10. An FN-curve and an FN-criterion corresponding to the decision maker's judgment. (Jongejan, 2008).

If the second scenario with the n_2 fatalities could be avoided ($p_2=0$), this would probably affect the probability of an accident with n_1 fatalities that the decision maker would consider acceptable. The previously defined FN-criterion would only still be appropriate when its value of $P(N \geq n_1)$ would still be the same, which presupposes:

$$U(n_2) = U(n_1)$$

Hence, the same FN-criterion would only still be appropriate if the decision maker were to value n_1 fatalities similarly as n_2 fatalities. Every fatal accident would then be considered equally regrettable, irrespective of accident size, which hardly seems realistic. When the decision maker is risk neutral or risk-averse, an accident with n_2 fatalities would be considered worse than an accident with n_1 fatalities: $U(n_2) > U(n_1)$. Without the probability of an accident with n_2 fatalities ($p_2=0$), the decision maker would allow higher values of p_1 and/or n_1 . Numerical examples are shown in Fig.11. The figure shows a two-scenario FN-curve (with $n_1=10$; $p_1=10^{-2}$; $n_2=100$; $p_2=10^{-4}$), and four single-scenario FN-curves that would be considered just as unpleasant by decision makers with disutility functions $U(n)=\gamma n$ ($\gamma > 0$), $U(n)=n^2$, $U(n)=e^{0.01n}$, and $U(n)=e^{0.1n}$.

respectively. With the appropriateness of an FN-criterion depending on the FN-curve that is to be evaluated (unless $dU(n)/dn=0$), it becomes problematic to set FN-criteria in a manner consistent with expected utility theory (Jongejan, 2008).

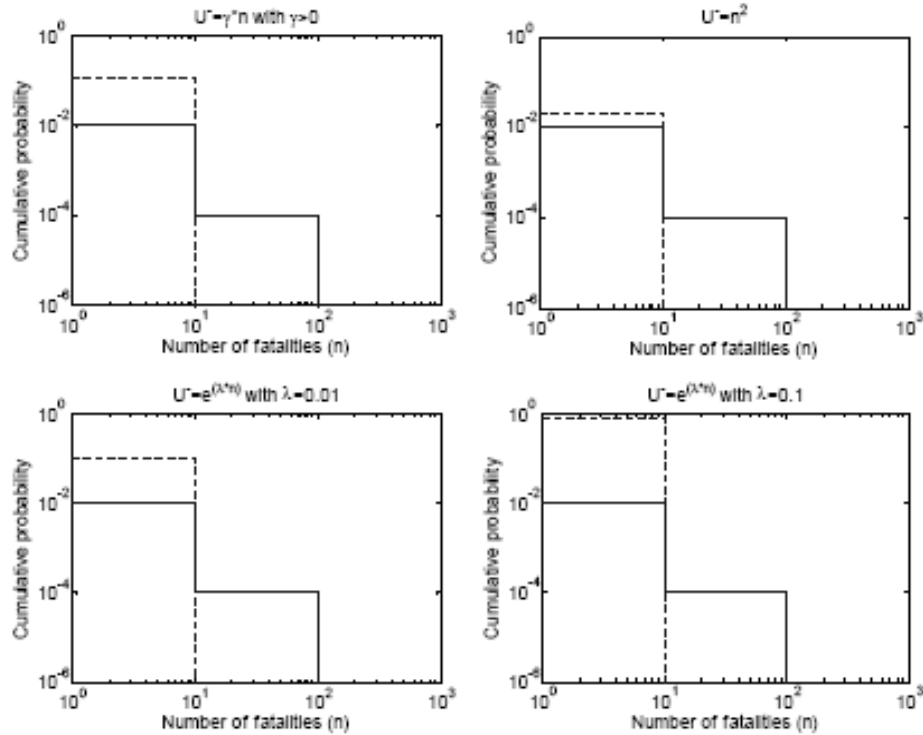


Fig.11. FN-curves that would be considered just as bad for different utility functions (Jongejan, 2008).

English Health and Safety Executive, HSE (2001) defines for some couples values of gravity of the effects - frequency of the event , three classes of societal risk acceptability (Tab.3).

Tab..3. Classes of societal risk acceptability, (HSE, 2001)

	1 death	2-10 deaths	11-50 deaths	51-100 deaths	+ 100 deaths
$>10^{-2}$	intolerable	intolerable	intolerable	intolerable	intolerable
$10^{-2} / 10^{-3}$	intolerable	intolerable	intolerable	intolerable	intolerable
$10^{-3}/10^{-4}$	tolerable	tolerable	intolerable	intolerable	intolerable
$10^{-4}/10^{-6}$	tolerable	tolerable	tolerable	tolerable	intolerable
$10^{-6}/10^{-8}$	acceptable	acceptable	tolerable	tolerable	tolerable

1.3.3 ECONOMIC RISK

The problem of identifying an acceptable level of risk can also be formulated as an economic decision problem (van Danzig, 1956). According to the method of economic optimisation, the total costs in a system (C_{tot}) are determined by the sum of expenditure for a safer system (I) and the expected value of the economic damage $E(D)$. In the optimal economic situation, the total costs in the system are minimised:

$$\min(C_{tot}) = \min(I + E(D)) \quad (16)$$

In this way the optimal probability of failure of the system can be determined, being investments (I) and $E(D)$ functions of the probability of failure. Slijkhuis et al. (1997) showed how uncertainty and risk aversion can be modelled in the method of economic optimisation. Investments and economic damage are modelled as random parameters. The determination of the optimal level of protection takes into account the standard deviation of total cost and a risk aversion factor (k). The attitude towards uncertainty and the risk aversion can be varied by adjusting the value of k . The economic optimum is given by:

$$\min(\mu(C_{tot}) + k\sigma(C_{tot})) \quad (17)$$

The study of Yelokhin, (1997) on the economic risks in the Russian region is an example of the use of a FD-curve. Also Jansen (1988) has tried to obtain a financial economic risk limit in the form of a FD-curve. However, research of the economic risks in various fields, did not lead to a consistent economic risk limit. Baecher (1982b) proposes some acceptability criteria for FD and FN curves, for a variety of traditional civil facilities and other large structures or projects (Fig.12)

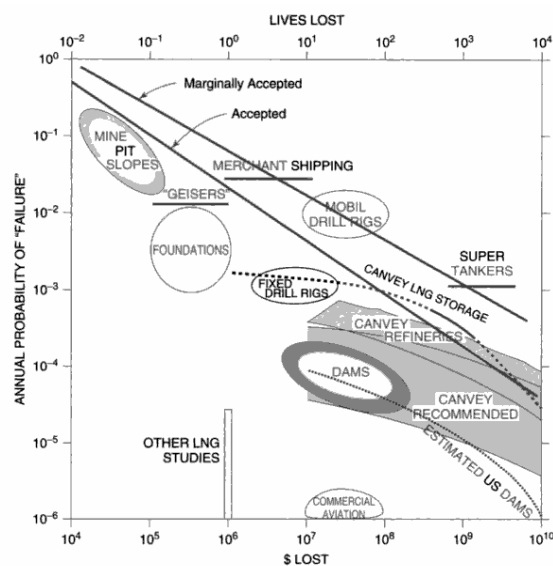


Fig. 12. F-N chart showing average annual risks posed by a variety of traditional civil facilities and other large structures or projects (Baecher, 1982b)

The expected value of the economic damage is used as part of cost benefit analyses of flood prevention measures in the UK (Parker, 1987) and in The Netherlands (Zhou,1995). In both approaches the benefits introduced by a mitigation measure are determined by calculating the expected value of the economic damage before and after implementing the measure. The difference between these two values is the benefit, which can be weighed against the costs of the measures.

A limit for the expected economic damage per year for dams has been proposed by BC Hydro (Hydropower & Dams, 1998), in which the financial risks for one dam should not exceed:

$$E(D) < \$10.000 \cdot (yr^{-1}) \quad (18)$$

The method of economic optimisation has originally been applied by van Danzig (1956) to determine the optimal level of flood protection (i.e. dike height) for Central Holland. The total investments in dike heightening (I_{tot}) are determined by the initial costs (I_0) and the variable costs (I'). If the dike is heightened X metres, the difference between the new dike height (h) and the current dike height (h_0).

$$I_{tot} = I_0 + I' \cdot X \quad \text{and} \quad X = h - h_0 \quad (19)$$

The expected value of the economic damage can be calculated from the occurrence probability of the event (P_b), the damage caused by the event (D), and the discount rate (r'). The flood level h is modelled as exponentially distributed with parameters A and B .

$$P_b = e^{-\frac{h-A}{B}} \quad \text{and} \quad E(D) = \frac{P_b \cdot D}{r'} \quad (20)$$

The total costs are formulated as the sum of investments and the expected value of the economic damage. The economic optimum is found by minimising the total costs. By taking the derivative of the total costs and the dike height, the optimal flooding probability ($P_{b,opt}$) and the optimal dike height (h_{opt}) are found.

$$P_{b,opt} = \frac{I' \cdot B \cdot r'}{D} \quad \text{AND} \quad h_{opt} = A - B \cdot \ln(P_{b,opt}) \quad (21)$$

The method of economic optimisation has also been applied for the design of various hydraulic structures, for example for breakwaters in (Vrijling et Van Gelder, 1995).

1.4 OVERVIEW OF RISK MEASURES

In Tab.4 the most important characteristics of the described risk measures are shown: the mathematical expression, the field of application, the standards and a reference to literature.

Tab.4. Overview of risk measures

Risk measure	Mathematical expression	Field of application	Criteria	Reference
Individual risk VROM	$IR = P_f \cdot P_{d f}$	VROM: hazardous installations/ transport routes	$<10^{-6}$	Bottelberghs, 2000
Individual risk TAW	$IR = P_f \cdot P_{d f}$	Case studies, floods	$<\beta \cdot 10^{-4}$	TAW, 1985
FN curve	$1 - F_N(x) = \int_x^{\infty} f_N(x) \cdot dx$	Hazardous installations	VROM: $1 - F_N(x) < 10^{-3} / x^2$	Stallen et al., 1996
Expected value of the number of fatalities/year	$E(N) = \int_0^{\infty} x \cdot f_N(x) \cdot dx$	Dams (USA, Canada)	$<10^{-2}$ USBR $<10^{-3}$ BC Hydro	USBR, 1997 Bowles, 1999
Risk Integral	$RI = \int_0^{\infty} (1 - F_N(x)) \cdot x \cdot dx$	HSE (UK): land use planning	-	Carter, 1995
Total risk	$TR = E(N) + k \cdot \sigma(N)$	Different case studies	$<\beta 100$	Vrijling et al., 1998
FD Curve	$1 - F_D(x) = \int_x^{\infty} f_D(x) \cdot dx$	-	-	-
Expected economic damage	$E(D) = \int_0^{\infty} x \cdot f_D(x) \cdot dx$	Dam safety	$E(D) < \$ 10.000$	Parker, 1987
Economic Optimisation	$\min(C_{tot}) = \min(I + E(D))$	Flood protection	Economic optimum	van Danzig, 1956

1.5 MULTI-RISK ASSESSMENT

Despite many approaches have been proposed to assess specific natural and technological hazards and risks, only few studies combine multiple typologies into a multi-risk holistic assessment. The methodological approaches in risk assessment studies range from very coarse index to elaborate assessments.

Trans-national studies have been performed to compare risk levels in different countries (Cardona et al, 2004; UNDP, 2004; ESPON, 2005) or to identify key “hot-spots” where the risks of natural disasters are particularly high (Dilley et al., 2005). These studies are based on approaches that make use of national-level indicators (e.g., number of hazardous events, Gross Domestic Product, total population), without a spatial analysis of hazard and element-at-risk patterns. The United Nations Development Programme (UNDP, 2004) developed a multiple-hazard risk model at a global scale, integrating expected damages in terms of deaths from different hazard types (earthquakes, floods, tropical cyclones). UNDP has begun the development of a Disaster Risk Index (DRI) in order to improve understanding of the relationship between development and disaster risk. The European project ESPON 1.3.1 (2005), developed an indicator based approach for the analysis of the spatial patterns of natural and technological hazards in Europe (avalanches, droughts, earthquakes, extreme temperatures, floods, forest fires, landslides, storm surges, tsunamis, volcanic eruptions, winter and tropical storms, technological hazards, air traffic accidents, major accident hazards at chemical plants, nuclear power plants, oil processing, transport and storage), accounting for the domino effects and identifying the possible impacts of climate

change. The method also provide an integration of different risks using a multi criteria approach based on a Delphi panel of experts.

Local scale multi-risk analysis have been proposed including multiple sources of natural (Granger et al, 1999; Granger and Hayne, 2001; Middleman and Granger, 2001; Van Westen et al., 2002) and natural/technological hazards (na-tech; Barbat and Cardona, 2003; Ferrier and Haque, 2003). These studies require an accurate description of each hazard and risk, at the temporal and spatial scale, and are suitable only for small areas already recognized as “hot spots”.

The AGSO Cities project (Granger et al, 1999) for geohazards in Australian urban communities analysed earthquakes, landslides, floods, storm surge, severe winds, bushfires, and tsunamis risks in urbanized areas, at a local scale. The vulnerability and resilience of the population have been taken into account, but risk assessment was performed separately for each of the hazard sources, in order to compare them, without an attempt to integrate them. Van Westen et al. (2002) propose a local-scale methodology for the assessment of flooding, landslides and earthquake risk in Turrialba, Costa Rica. For each hazard source, the methodology combines cost maps with vulnerability and hazard maps for the different return periods, in order to obtain graphs of probability versus potential damage. The estimation of annual losses for each hazard type and each return period represents a “standardization process”, which allows to put hazards into perspective and prioritise accordingly, and to display a total risk map. Ferrier and Haque, (2003) developed for Toronto a local scale study indicator based methodology, accounting for both natural and technological hazards. On the basis of social hazard identification, estimation of vulnerability, consequences evaluation, they produced for each hazard source a score of risk to be compared, or added. This is an example of coarse index approach based on readily available data and expert knowledge about the hazards and their possible effects on the municipality. For urban centres, Cardona and Hurtado (2000), Masure (2003) Cardona (2001), and Barbat and Cardona (2003), developed an holistic multidisciplinary indicator based approach, and a model for seismic risk analysis (Carreno et al., 2007). These models have the purpose of supporting the decision making in risk management, helping the identification of critical zones and their vulnerability. The evaluations consider exposure, socio-economic characteristics of the city, and its coping capacity or degree of resilience. Another example of detailed multi-risk assessment is given by Blong (2003) who developed a damage scale for Australia which quantifies the damages to buildings resulting from a range of natural hazards.

CHAPTER 2. UNCERTAINTIES IN RISK ASSESSMENT

2 UNCERTAINTY EVALUATION METHODOLOGY

The problems of analysis and management of many technological and natural risks are dominated by the uncertainties about fundamental phenomena, reflecting incomplete knowledge (Patè-Cornell, 1995) or intrinsic randomness of the processes. For this reason, it is becoming increasingly important to decision makers that, when presented with the results of a Probabilistic Risk Assessment (PRA), the uncertainty in the results of the PRA is correctly characterized (Parry, 1996). Furthermore, since a PRA is used to model very rare events, there can be no experimental verification of its validity. In addition, because of the rare nature of the events being modelled, statistical uncertainties in the estimates of the parameters of the model can be significant.

Uncertainties about the impact of physical phenomena create different opinions about how to model and treat them (Parry, 1996). The question of how to define, measure and describe the nature of different types of uncertainties is particularly critical in the analysis of high consequence phenomena (e.g., global climate change or failures of nuclear reactors) because of public sensitivities to the magnitude of the potential consequences. In these cases, policy making is generally guided by a mix of public interests and scientific research results, with a link between the two. In other instances, however, full uncertainty analysis is not needed, for example, because the best risk management strategy is fairly obvious. Uncertainties in decision and risk analyses can be divided into two categories: those that account for variability in processes and phenomena and, therefore, represent randomness in samples (aleatory uncertainties), and those deriving from lack of knowledge about fundamental phenomena (epistemic uncertainties) (Hoffman and Hammonds, 1994).

2.1 ALEATORY AND EPISTEMIC UNCERTAINTIES

Aleatory uncertainty is associated with the inherent randomness of natural processes, intended as variability over time for phenomena that take place at a single location (temporal variability) or as variability over space for phenomena that take place at different locations but at the same time (spatial variability), or as variability over both time and space. Such natural variability is approximated using mathematical simplifications, or models. These models may or may not provide a good fit to naturally phenomena. In the best case, they are close but only approximate fits (Baecher and Christian, 2003). The aleatory aspect of uncertainty is related to the characterization of the events or phenomena being modelled as occurring in a 'random', or 'stochastic' manner, and described by probabilistic models. It is this aspect of uncertainty that gives the Probabilistic Risk Assessment the probabilistic part of its name (Parry, 1996). By contrast to epistemic uncertainty, aleatory (also known as randomness or stochastic uncertainty) representing variations in samples, is generally more easily acknowledged and integrated in mathematical models (Patè-Cornell, 1996).

The epistemic uncertainty is attributed to lack of data, lack of information about the events and processes, or lack of understanding of the physical laws that limits the modelization of the real world (Baecher and Christian, 2003). The epistemic uncertainty is that associated with the analyst's confidence in the predictions of the PRA model itself, and is a reflection of his assessment of how well his model represents the system he is modelling (Parry, 1996). These epistemic uncertainties play an important role when the evidence base is small, for example, in seismic hazard analyses in regions where earthquakes are rare, or in the assessment of the failure risks of technical systems operating in poorly known environments. These uncertainties are sometimes ignored and tend to be underestimated.

Both types of uncertainty can affect qualitative and numerical variables (e.g., the frequency of a phenomenon). Most risk analysis problems involve both known statistical samples, and unknown or partially known mechanisms. Bayesian probability theory allows the measurement and combination of randomness (aleatory uncertainties) and fundamental (epistemic) uncertainties (Patè-Cornell, 1996). It is essential to maintain the distinction between these two types of uncertainty as they perform different functions in the model of the system created by the analyst. The aleatory uncertainty is a fundamental and integral part of the structure and form of the PRA model, whereas the epistemic uncertainty is related to a characterization of how well we can represent the system by the model. In practice, however, many analysts have found that, for certain issues, especially those related to the modelling of the occurrence or the impact of particular physical phenomena, particularly in regimes that are outside our direct experience, it is difficult for them to distinguish between the two types.

2.2 UNCERTAINTY PROPAGATION

Interpreting the results of a PRA in the light of the uncertainties is important if the results are to be applied to making meaningful decisions. For example, probability distributions on the numerical results, such as the damage frequency, can be used to calibrate the confidence level at which a safety goal is achieved. It may be important to characterize the overall uncertainty, but also to understand which factors drive the uncertainty.

Methods for the propagation of the uncertainty on the basic events through the quantification process, to generate a characterization of uncertainty on the outcomes of the PRA, are relatively well established. The most common technique is Monte Carlo analysis or variants, such as the Latin Hypercube Sampling, because epistemic uncertainties on parameters are generally characterized as probability distributions, whether the distributions are continuous or discrete. Probability distributions give both the range of values that the variable could take, and the likelihood of occurrence of each value within the range (Hall, 2006).

In this thesis, different strategies for uncertainty modelling (Monte Carlo simulation, First Order Second Moment, FOSM, and Point Estimate, PE analysis) were applied and compared. The methods were applied to assess and aggregate the uncertainty to the evaluation of hazards, values of the exposed elements and process-specific vulnerabilities.

2.2.1 MONTE CARLO SIMULATION

A wide range of engineering and scientific disciplines use simulation methods based on randomized input, often called Monte Carlo methods. They have been employed to study both stochastic and deterministic systems (Baecher and Christian, 2003). Monte Carlo methods are a class of computational algorithms that rely on repeated random sampling to compute their results. Because of its reliance on repeated computation and random or pseudo-random numbers, the Monte Carlo method provides approximate solutions to a variety of mathematical problems related to physical and mathematical systems (Fishman, 1996). Monte Carlo methods tend to be used when it is infeasible or impossible to compute an exact result with a deterministic algorithm. There is no single Monte Carlo method; instead, the term describes a large and widely-used class of approaches. However, these approaches tend to follow a particular pattern:

1. Define a domain of possible inputs.
2. Generate inputs randomly from the domain, and perform a deterministic computation on them. An essential component of every Monte Carlo experiment is the generation of random samples from a possible range of the input parameter values, followed by model evaluations for the sampled values. These generating methods produce samples drawn from a specified distribution. The random numbers from this distribution are then used to transform model parameters according to some predetermined transformation equation (Hall, 2006)
3. Aggregate the results of the individual computations into the final result.

Note, also, two other common properties of Monte Carlo methods:

- the computation's reliance on good random numbers
- its slow convergence to a better approximation as more data points are sampled.

Monte Carlo simulation provides a number of advantages over deterministic analysis:

- Probabilistic Results. Results show not only what could happen, but how likely each outcome is.
- Graphical Results. Because of the data a Monte Carlo simulation generates, it is easy to create graphs of different outcomes and their chances of occurrence. This is important for communication.
- Sensitivity Analysis. With just a few cases, deterministic analysis makes it difficult to see which variables impact the outcome the most. In Monte Carlo simulation, it's easy to see which inputs had the biggest effect on the results.
- Scenario Analysis. In deterministic models, it is very difficult to model different combinations of values for different inputs to see the effects of truly different scenarios. Using Monte Carlo simulation, analysts can see exactly which inputs had which values together when certain outcomes occurred.
- Correlation of Inputs. In Monte Carlo simulation, it is possible to model interdependent relationships between input variables. It's important for accuracy to represent how, in reality, when some factors increase, others increase or decrease accordingly.

Monte Carlo simulation can perform risk analysis by building models of possible results by substituting a range of values—a probability distribution—for any factor that has inherent uncertainty. It then calculates results over and over, each time using a different set of random values from the probability functions. Depending upon the number of uncertainties and the ranges specified for them, a Monte Carlo simulation could involve thousands or tens of thousands of recalculations before it is complete. Monte Carlo simulation produces distributions of possible outcome values. In general, a variable to measure is related to other quantities by a function of the type

$$\theta = f(\mu_1, \mu_2, \dots, \mu_n)$$

The unknown values of $\mu_1, \mu_2, \dots, \mu_n$ are subjected to uncertainty when measured, so random variables X_1, X_2, \dots, X_n are associated with discrete observations. The uncertainty in the value $\hat{\theta}$, as an estimate of θ , is calculated by propagating distributions associated with the uncertainty of the estimated values of $\mu_1, \mu_2, \dots, \mu_n$ through the measurement equation. Distributions that can be numerically simulated, denoted as M_1, M_2, \dots, M_n , are assigned to each of $\mu_1, \mu_2, \dots, \mu_n$. A simulation calculates multiple scenarios of a model by repeatedly sampling values from the probability distributions for the uncertain variables and using those values for the output calculation. An uncertainty statement about $\hat{\theta}$ can be formulated by observing the frequency distribution of

$$Y = f(M_1, M_2, \dots, M_n)$$

The accuracy of the MC method depends on the distributions chosen for the variables that can be numerically simulated (M_1, M_2, \dots, M_n) (Hall, 2006).

Monte Carlo sampling techniques are entirely random, any given sample may fall anywhere within the range of the input distribution. Samples, of course, are more likely to be drawn in areas of the distribution which have higher probabilities of occurrence. A problem of clustering, however, arises when a small number of iterations are performed (Fig.13). The values in the outer ranges of the distribution are not represented in the samples and thus their impact on the results is not included in the simulation output. Latin Hypercube sampling, samples more accurately from the entire range of distribution functions. The input probability distributions are stratificated, that is, cumulative curve is divided the into equal intervals on the cumulative probability scale (0 to 1). A sample is then randomly taken from each interval or stratification (Fig.14).

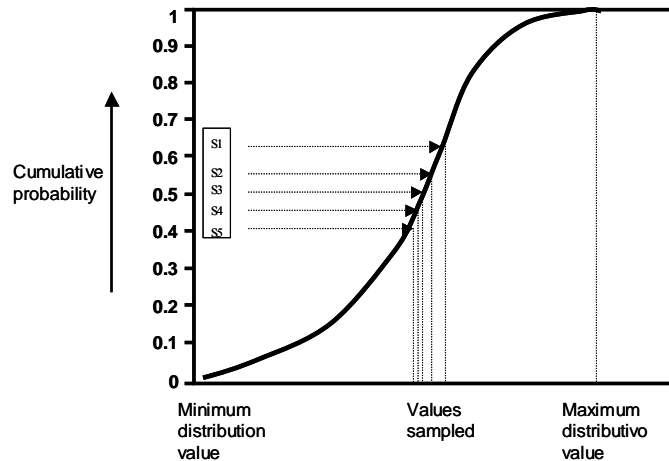


Fig.13. Five iterations of Random Sampling

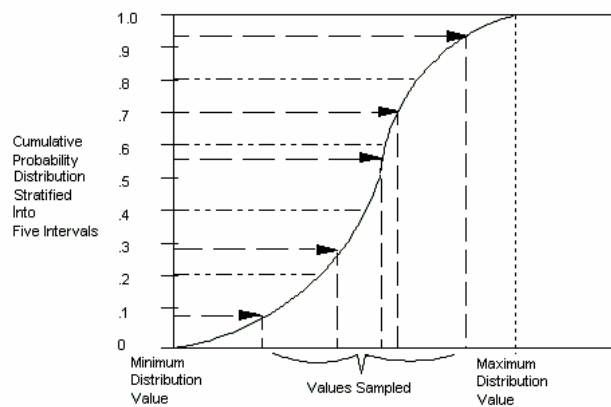


Fig.14 Five iterations of Latin Hypercube Sampling

2.2.2 FOSM

The First Order Second Moment (FOSM) method result from the truncation of the multivariate expansion of Taylor's series expansion of the performance function, considering only the first order terms. It estimates the mean (first moment) and the variance (second moment) of model output through computation of the derivative of model output to model input at a single point (Yen et al., 1986). The discarded terms are functions of the second and higher order derivatives of the performance function, the variances and shapes of the probability density functions of the input variables, and the correlations among input variables. For a linear function, the second order derivatives are equal to zero and the FOSM method is exact. For nonlinear functions, the accuracy of the FOSM method diminishes as the nonlinearity of the performance function increases (El-Ramly et al., 2003). This method is initially designed for uncertainty propagation but it provides measures of sensitivity as well. The treatment of error propagation starts by recognizing that the result of the calculations can be considered a function f of the several input parameters and variables, X_1, X_2, \dots, X_n evaluated at some points (x_1, x_2, \dots, x_n)

$$\theta = f(x_1, x_2, \dots, x_n) \quad (23)$$

If there is only one independent variable X and the value of f is known for some value of X , say X^* , then the value of f can be found for any other value by using the well known Taylor series. The equation is exact, provided all terms out to infinity are used. In practical applications x is chosen to be near X , so higher order terms become small and the series can be truncated after only a few terms. In the simplest form, a first-order Taylor series approximation requires computing the model output at a single point and determining the derivative (i.e. change of model output due a change in model input):

$$\theta(x) = f(\mu_x) + \sum_{i=1}^n \frac{\partial f}{\partial x_i} (x_i - \mu_{x_i}) \quad (24)$$

where $x_i = (x_1, \dots, x_n)$ are the input random variables with means $\mu_i = (\mu_1, \dots, \mu_n)$, and $\frac{\partial f}{\partial x_i}$ are derivatives evaluated at the mean values μ_i .

The mean of the output function μ_θ and the standard deviation σ_θ^2 are then calculated as:

$$\mu_\theta \approx g(\mu_{x_1}, \mu_{x_2}, \dots, \mu_{x_n}) + \sum_{i=1}^n \int_{-\infty}^{+\infty} (x_i - \mu_{x_i}) f_{x_i}(x_i) dx_i \quad (25)$$

$$\begin{aligned} \sigma_\theta^2 &\approx \sum_{i=1}^n \sum_{j=1}^n \rho_{x_i x_j} \sigma_{x_i} \sigma_{x_j} \frac{\partial g}{\partial x_i} \frac{\partial g}{\partial x_j} \\ &= \sum_{i=1}^n \sigma_{x_i}^2 \left(\frac{\partial g}{\partial x_i} \right)^2 + \sum_{i=1}^n \sum_{j \neq i}^n Cov(X_i, X_j) \frac{\partial g}{\partial x_i} \frac{\partial g}{\partial x_j} \end{aligned} \quad (26)$$

The calculation of the first two moments of the dependent variable allows to express its uncertainty as a Coefficient of Variation (COV or Ω), deriving from the propagation of the Coefficients of Variation of the dependent variables:

$$\Omega = \frac{\sigma}{\mu} \quad (27)$$

In particular, in case of a function of a single variable:

$$\mu_{\theta} \approx \theta(\mu_x) \quad \text{and} \quad \sigma_{\theta}^2 \approx \sigma_x^2 \left(\frac{d\theta}{dx} \right)^2 \quad (28)$$

in case of a sum of uncorrelated independent variables:

$$\mu_{\theta} \approx \sum_{i=1}^n \mu_{X_i} \quad \text{and} \quad \sigma_{\theta}^2 = \sum_{i=1}^n \sigma_{X_i}^2 \quad (29)$$

in case of a product of uncorrelated independent variables:

$$\mu_{\theta} \approx \prod_{i=1}^n \mu_{X_i} \quad \text{and} \quad 1 + \Omega_{\theta}^2 = \prod_{i=1}^n (1 + \Omega_i^2) \quad (30)$$

While the FOSM method is a useful tool for probabilistic analyses, the simplifying assumptions made in formulating this technique are seldom mentioned in the literature. To avoid the incorrect use of the FOSM method, its limitations must be clear. Furthermore, the method requires the evaluation of partial derivatives. For many complex problems, this may not be possible, or too complicated and time costly.

2.2.3 TWO POINT ESTIMATE

In many problems, like risk assessment for instance, uncertainty in data and in theories is significant in a measure that a probabilistic treatment is required. Frequently, a deterministic treatment is preferred in order to remove the complications of a rigorous probabilistic analysis. In Point Estimate method (Rosenblueth, 1981) random variables are replaced with point estimates, that is, each variable is replaced with a central value (expectation, median, or mode), or with one consciously biased: the estimates are treated as deterministic. Results are also expressed as point estimates without giving an idea of their differences with the corresponding central values or of the magnitude of the resulting bias or dispersion. In decision making, a calculation of the first moment - expectation - of functions of the random variables would often suffice (Rosenblueth, 1981).

The aim of the two point estimate is to calculate the first two or three moments of a random variable, function of one or more random variables. The method overcomes

the deficiencies of a deterministic treatment, sacrificing the accuracy of a rigorous probabilistic analysis (Rosenblueth, 1981). The method aims to reduce the computational demands of propagating uncertainty through a function by eliminating the calculation of derivatives or use of Monte Carlo sampling. The PDF of each random variable is represented by discrete points, located according to the first, second and third moments. The method replaces the probabilistic distribution with a limited number of discrete points that match the distribution up to the third statistical moment.

Rosenblueth's method is a computationally efficient method of estimating the first 3 moments of functions of a small number of uncertain input variables, which may be correlated and skewed. The method provides better estimates than the first order second moment (FOSM) approximation, often without significantly more computation. It may be easily applied to simulation modelling, given limitations and assumptions below. The disadvantages of the method are related to the evidence that it does not evaluate moments higher than the third. Furthermore, Christian and Baecher (1999) note that it is never reliable for moments higher than second, and not generally reliable for non-linear functions with high input variance. The method neglects non-linear inter-dependencies of input variables (i.e. represents them using correlation coefficients). Information about input-output sensitivities is not implicit to the method (as it is in FOSM and in Monte Carlo). The most appropriate application cases are where an approximation of output variance is required, rather than probabilistic risk analysis or sensitivity analysis, and where variance of inputs is not high, or where function is linear or nearly linear.

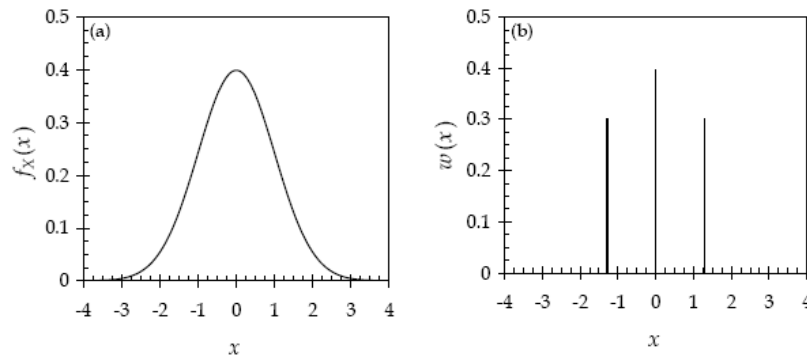


Fig. 15. Discretization (b) of a continuous distribution (a) maintaining the same moments

Cases and notation

Considering a real function $Y=Y(X)$ of the real random variable X , the i moment of X is

$$M_i(X) = \int_{-\infty}^{+\infty} x^i p_x(x) dx \quad (31)$$

$p_x(x)$ is the probability density function of X at $X=x$.

The central moments are:

$$M_i(X) = \int_{-\infty}^{+\infty} (x - E(X))^i p_x(x) dx \quad (32)$$

$E(X)$ denotes the expectation of X , $M_1(X)$.

For symmetric distributions skewness is nil and the same holds for all other central moments of odd order. In uncertainty evaluation, we are interested in obtaining the expressions for the expectation, standard deviation, and coefficient of skewness of Y , respectively, and to do it independently from X 's distribution. To do this, an arbitrary distribution is assigned to X , having four parameters so as to comply with expressions for the moment of order and for the first three moments of X . A particularly simple function satisfying this requirement consists in two concentrations, P_1 and P_2 , of the probability density function $pX(x)$, respectively at x_1 and x_2 (see Rosenblueth, 1981). With four equations it is possible to calculate the first three moments of Y . In most cases the calculations are made at two points, and Rosenblueth uses the following notation:

$$E(Y^m) \approx P_+ y_+^m + P_- y_-^m \quad (33)$$

where $E(Y^m)$ = expected value of Y raised to the power m ; y_1 = value of Y evaluated at a point x_1 , which is greater than the mean; y_2 = value of Y evaluated at a point x_2 , which is less than the mean; and P_1, P_2 = weights. The problem is then to find appropriate values of x_1, x_2, P_1 , and P_2 . If two concentrations are used, equal to 0.5 each, placed symmetrically with respect to X 's expectation, X 's first two moments can be taken into account, estimating those of Y with a second-order approximation to its expected value:

$$P_+ + P_- = 1 \quad (34)$$

$$P_+ + P_- = \mu_x \quad (35)$$

$$P_+ + P_- = 1 \quad (36)$$

$$P_+(x_+ - \mu_x)^2 + P_-(x_- - \mu_x)^2 = \sigma_x^2 \quad (37)$$

$$P_+(x_+ - \mu_x)^3 + P_-(x_- - \mu_x)^3 = \nu_x \sigma_x^3 \quad (38)$$

A great simplification occurs when the skewness is zero or negligible. The distribution of X is then symmetric, and

$$P_+ = P_- = \frac{1}{2} \quad (39)$$

$$x_+ = \mu_x + \sigma_x \quad (40)$$

$$x_- = \mu_x - \sigma_x \quad (41)$$

The estimation increases to 2^n points for functions of n variables. Generalization of the method to functions of several variables, that is often the case in risk analysis, requires solution of large numbers of simultaneous equations, many of which are generally nonlinear. It is preferable to concentrate the density function at a superabundant number of points and impose conditions on their coordinates. If 2^n points are considered, when the number of random variables is n , and the concentrations at all points are left unknown, such as the coordinates of two of them not having coordinates in common, distributing the rest so as to form a rectangle, prism, or hyperprism, an adequate number of unknowns is obtained to satisfy the moments of orders zero, first, and second of the form

$$\int_{-\infty}^{\infty} (x_i - \bar{X}_i)^2 p_{x_i}(x_i) dx_i \quad (42)$$

$i = 1 \dots n$, and $p_{x_i}(x_i)$ = marginal probability density function of x_i . The other third order moments are forced without necessarily satisfying the corresponding conditions, but the sacrifice implies a significant simplification. The resulting equations are simple and can indeed be solved almost by inspection.

Thus for the case $Y = Y(X_1, X_2)$ and $\rho = 0$, the rectangle in Fig. 16 is obtained, where p = coefficient of variation of X_1 and X_2 ; P_{ij} indicates the variable and ξ_{ij} identifies each of the values that the variable can assume; P_{ij} and σ_i are computed as for functions of a single variable. In this special case $v_1 = v_2 =$

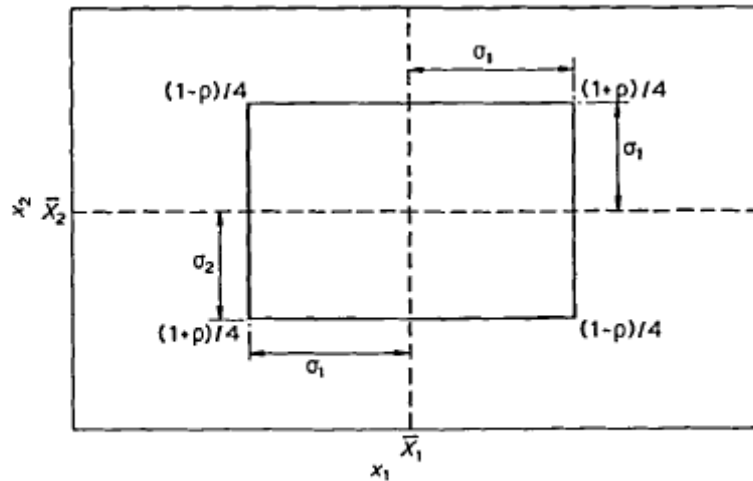


Fig. 16 Special case, $v_1=v_2=0$ (Rosenblueth, 1981)

The procedure chooses 2^n points selected so that the value of each variable is one standard deviation above or below its mean. If the variables are not correlated, the function Y is evaluated at each of the four points, and the weight for each point is 0.25.

When Y is a function of three variables, X_1 , X_2 , and X_3 , there are eight points, which are located at each combination one standard deviation above or below the mean of all the variables. In defining the weights, Rosenblueth uses a set of + and - signs as subscripts on the weight P . The convention is that the first sign refers to X_1 , the second to X_2 , and the third to X_3 . If the point is $\mu_{X_i} + \sigma_{X_i}$, the sign is positive; otherwise it is negative. Then,

$$P_{+++} = P_{---} = \frac{1}{8}(1 + \rho_{12} + \rho_{23} + \rho_{31}) \quad (43)$$

$$P_{++-} = P_{+-} = \frac{1}{8}(1 + \rho_{12} - \rho_{23} - \rho_{31}) \quad (44)$$

$$P_{+--} = P_{-+-} = \frac{1}{8}(1 - \rho_{12} - \rho_{23} + \rho_{31}) \quad (45)$$

$$P_{+--} = P_{-++} = \frac{1}{8}(1 - \rho_{12} + \rho_{23} - \rho_{31}) \quad (46)$$

The generalization to more than three variables follows the same logic.

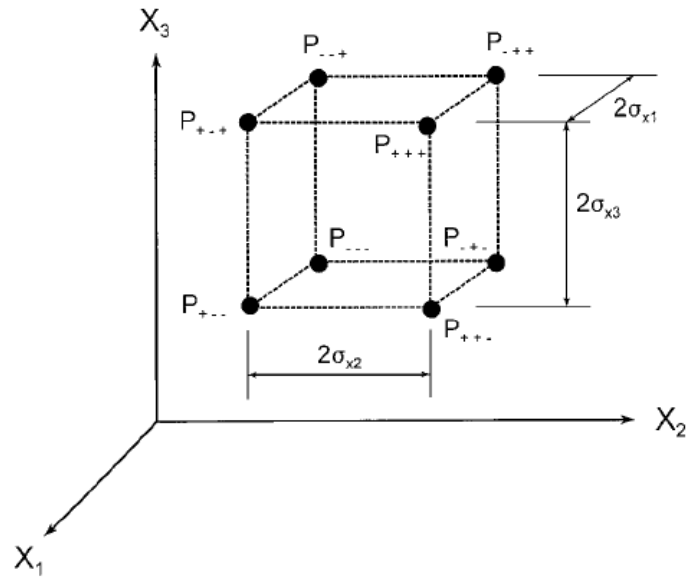


Fig. 14 Rosenblueth's points and weights for three variables, correlated or uncorrelated (Rosenblueth, 1981)

CHAPTER 3. COUNTERMEASURES FOR RISK MITIGATION

3 COST-BENEFIT ANALYSIS

The problem of optimising economical resources and of evaluating of works in terms of economic efficacy of the investment have been widely treated in the literature with different approaches. The most rigorous one is cost-benefit analysis (CBA).

Cost-benefit analysis is one of the instruments most common in support decision making, in order to evaluate the relationships between the costs and the benefits induced by the projects proposed to the public authorities. It can turn up to be very useful for the evaluation and the comparison of the advantages of different strategic approaches, also in different contexts.

An important distinction should be made between *ex-ante* and *ex-post* CBA.

- *Ex-ante* CBA is the CBA procedure that helps in the decision of whether to allocate scarce resources to a prospective policy.
- *Ex-post* CBA is conducted at the end, or in the middle of a policy and looks back in time. This analysis has the purpose of showing whether particular policies are successful, and eventually drive a policy change (Boardman et al., 1996). *Ex-post* analyses are clearly useful as guides to decisions in later, similar situations.

A wide literature and specific manuals are available regarding the use of cost-benefit analysis and other comparable methods in the context of natural risks (Benson and Twigg, 2004; Benson et al., 2007). In USA, on the projects of flood mitigation, BCA has been made compulsory from the Congress in the Flood Control Act dating 1936, and has become a standard practice for FEMA e U.S. Army Corps of Engineers. In England, DEFRA and Agriculture Ministry promote this kind of analysis, such as the World Bank, also if the method is scarcely applied in risk management activities (Ministry of Agriculture, 2001; Penning-Rowsell et al., 1992).

In Tab.5, different applications of BCA in risk mitigation are resumed:

Tab.5. Existing Appraisals of the Costs and Benefits in risk management (Guidance note on the Costs and Benefits of Disaster Risk Reduction, ISDR, 2007)

Source and type of analysis	Actual or potential benefits	Result/return
Appraisals (assessment before implementation)		
Kramer (1995): Appraisal of strengthening of roots of banana trees against windstorms	Increase in banana yields in years with windstorms	Expected return negative as expected Yields decreased, but increase in stability as variability of outcomes decreased
World Bank (1996): Appraisal of Argentinean Flood Protection Project. Construction of flood defence facilities and strengthening of national and provincial institutions for disaster management	Reduction in direct flood damages to homes, avoided expenses of evacuation and relocation	IRR: 20.4% (range of 7.5%-30.6%)
Vermeiren and Stichter (1998): Hypothetical evaluation of benefits of retrofitting of port in Dominica and school in Jamaica	Potentially avoided reconstruction cost in one hurricane event each	B/C ratio: 2.2 – 3.5
Dedeurwaerdere (1998): Appraisal of different prevention measures against floods and lahars in the Philippines	Avoided direct economic damages	B/C ratio: 3.5 – 30
Mechler (2004a): Appraisal of risk transfer for public infrastructure in Honduras and Argentina	Reduction in macroeconomic impacts	Positive and negative effect on risk adjusted expected GDP dependent on exposure to hazards, economic context and expectation of external aid
Mechler (2004b): Prefeasibility appraisal of Polder system against flooding in Piura, Peru	Reduction in direct social and economic and indirect impacts	Best estimates: B/C ratio: 3.8 IRR: 31% NPV: 268 million Soles
Mechler (2004c): Research-oriented appraisal of integrated water management and flood protection scheme for Semarang, Indonesia	Reduction in direct and indirect economic impacts	Best estimates: B/C ratio: 2.5 IRR: 23% NPV: 414 billion Rupiah
Ex-post evaluations (assessment after implementation of measures)		
FEMA (1998): Ex-post evaluation of implemented mitigation measures in the paper and feed industries in USA	Reduction in direct losses between 1972 and 1975 hurricanes	C/B ratio: ca. 100
Benson (1998): Ex-post evaluation of implemented flood control measures in China over the last four decades of the 20 th century	Unclear, probably reduction in direct damages.	\$3.15 billion spent on flood control have averted damages of about \$12 billion
IFRC (2002): Ex-post evaluation of implemented Red Cross mangrove planting project in Vietnam for protection of coastal population against typhoons and storms	Savings in terms of reduced costs of dike maintenance	Annual net benefits: 7.2 mill. USD B/C ratio: 52 (over period 1994-2001)
Venton & Venton (2004) Ex-post evaluations of implemented combined disaster mitigation and preparedness program in Bihar India and Andhra Pradesh, India	Reduction in direct social and economic, and indirect economic impacts	Bihar: B/C ratio: 3.76 (range: 3.17-4.58) NPV: 3.7 million Rupees (2.5-5.9 million Rs) Andhra Pradesh: B/C ratio: 13.38 (range: 3.70-20.05) NPV: 2.1 million Rupees (0.4-3.4 million Rs)
ProVention (2005): Ex-post evaluation of Rio Flood Reconstruction and Prevention Project, Brazil. Construction of drainage infra-structure to break the cycle of periodic flooding	Annual benefits in terms of avoidance of residential property damages.	IRR: > 50%

3. Countermeasures for risk mitigation

FEMA (1997): evaluation of National Flood Insurance Program: 18,700 communities adopting floodplain regulations, zoning, building requirement, flood insurance	Reduction or elimination of flood damage and associated costs of recovery.	Annual benefits of \$770 million Costs: Program largely funded by insurance premiums
MMC (2005): review of FEMA mitigation programs	Programs to help mitigate effects of multiple natural hazards from 1988-2000.	Average B/C ratio: 4 based on a review of 4,000 mitigation programs.
FEMA (1997): Acquisition/relocation of Castaic School District buildings, California	Relocation of schools away from dam inundation & gas pipeline burst due to earthquakes. Buildings built to earthquake code.	Cost: \$27million Estimated benefits: cost of reconstruction, building rental, daily education, 1300 lives saved
MMC (2005): Cost effective analysis of Freeport, New York flood mitigation project	Elevation of homes, businesses, main roads above 100-yr flood level. Electrical lines moved underground. Early warning systems and education programs initiated	
MMC (2005): Cost effective analysis of Jefferson County, Alabama mitigation projects	Early warning systems, vulnerability and hazard maps, education programs	B/C ratio averaged over all projects 2.6
MMC (2005): Cost effective analysis of Tuscola County, Michigan mitigation projects	Mapping of flood vulnerable areas, improved drainage, acquisition and retrofitting of homes and businesses	B/C ratio averaged over all projects 12.5
MMC (2005): assessment of the National Earthquake Hazards Reduction Program	Seismic retrofitting of multiple buildings reduction in fatalities and injuries in US development of shake maps	B/C ratios: 1.4 – 2.5
Mizina (1999): evaluation of mitigation programs for agriculture in Kazakhstan under climate change scenarios	Projects range from education, capacity building, and reducing soil erosion	Cost effectiveness using ADM range from: 0.65 – 5.5
Fuchs et al. (2006): cost effectiveness of avalanche risk reduction strategies in Davos, Switzerland	Reduction in deaths and damage to infrastructure, better land use planning and zoning, snow fences	B/C ratios range from: 0 – 3.72

There are two areas where the use of CBA in natural disaster risk mitigation can be very useful (ISDR, 2007):

1. Judging risk management measures: in the context of scarce resources, performing CBA for potential risk management projects can help in selecting the most profitable projects in terms of damages avoided (ISDR, 2007).

2. Mainstreaming risk: there is a need for including disaster risk and risk management measures in project and development planning, called mainstreaming. Including disaster risk and risk management may help in developing more robust projects (ISDR, 2007).

Furthermore, CBA can be an important instrument for awareness and education.

The costs of a project include direct (expenditures on materials, labor, and long-term maintenance of the project) and indirect (activities or services not charged to the project costs, consequences such as reduction in land or property value, and lost opportunities) costs.

Calculating the benefits of mitigation activities is even more difficult than calculating costs, as benefits are measured as the avoided losses that would have occurred without the mitigation project.

There are essentially four steps to analysing the costs and benefits of works to reduce risk:

- risk analysis;
- identification of risk management options and the costs associated with them;
- risk analysis with and without project implementation;
- estimation of cost and benefit probabilities.

Despite attempts such as those by FEMA (1999) and other organizations to incorporate more factors into cost-benefit estimates, existing methods for CBA are limited with respect to the factors considered (ISDR, 2007). Particular limitations include:

1. The dynamic nature of hazards and vulnerability, and therefore risk
2. Difficulties in assessing avoided losses and the often non-market nature of benefits from many disaster risk reduction investments
3. Variety coupled with lack of unanimity regarding the types of activities that actually contribute to disaster risk reduction
4. The distribution of costs and benefits
5. Indirect costs and benefits
6. The lifetime of a mitigation effort
7. Limited data availability
8. Choice of discount rates
9. Limited familiarity with economic efficiency concepts by sponsors and field staff

Estimating the full costs of events and the true benefits of mitigation measures can be difficult. Although a number of manuals exist, such as FEMA's Hazard Mitigation Grant Program Desk Reference (FEMA,1999), and the literature on CBA and the valuation of human lives and other non-market values is extensive, neither the manuals nor results in the literature are fully consistent (FEMA 1999; Navarro 2005). As a result, there are no fully accepted and institutionalized methods for determining what is a cost, a benefit, how to discount the future or how to value a human life. In general, however, costs and benefits of mitigation measures suggest that investment returns are likely to be robust when investments address simultaneously multiple hazards and serve multiple purposes in addition to their risk reduction function. In these cases, they are often both more sustainable and capable of generating revenue streams, compensating project costs. These results are completely in accordance with the general approach of this thesis, introducing multi-risk theme as a base of the research. The costs are likely to be higher and the benefits lower when they are developed and implemented as "stand-alone" activities that are implemented separately or in isolation from existing programs and systems (ISDR, 2007).

Furthermore, the benefits are maximum when the investments are not sensitive to strong assumptions and uncertainties. The results of the development of mitigation strategies are strongly connected with background assumptions, such as a flood volume, the frequency of extreme meteorological events, etc. In general, in the case of hazard sources or vulnerability in a continuous evolution, the role of the uncertainties and of the assumptions is critical.

PART I

MULTI-RISK ASSESSMENT REGIONAL SCALE

1 INTRODUCTION

Multi-risk assessment is becoming a valuable tool for land planning, emergency management and the deployment of mitigation strategies. Multi-risk maps combine all available information about hazard, vulnerability, and exposed values related to different dangerous phenomena, and provide a quantitative support to complex decision making.

Through an indicator-based approach nine major threats affecting the Lombardy Region (Northern Italy, 25,000 km²), namely landslide, avalanche, flood, wildfire, seismic, meteorological, industrial (technological) risks; road accidents, and work injuries, were analysed and integrated. For each threat, a set of indicators was developed, expressing the physical risk and the coping capacity or system resilience. By combining these indicators through different weighting strategies (i.e. budgetary allocation, and fuzzy logic), a total risk for each threat was calculated. Then, these risks were integrated by applying AHP (Analytic Hierarchy Process) weighting, and a set of multi-risk maps was derived. Eventually, the dominant risks for each zone, and a number of risk hot-spot areas were identified.

Relative risk scores are provided from this methodology, not directly accounting for the temporal occurrence probability of the phenomena.

The methodology for multi-risk assessment can be applied to regional scale analyses. In the following, risk is defined as the measure of the probability and severity of a damage to life, health, property, and environment. The methodology integrates information with different degree of accuracy into an indicator based approach, in order to develop a regional scale multi-risk assessment and to identify “hot spot” risk areas for more detailed analysis. Finally, the sensitivity of weights, and the effect on risk assessment of different individual attitudes and perception (i.e., expert, social, political, risk aversion) were investigated.

The proposed approach can be applied with different degree of detail depending on the quality of the available data. This allows the application of the method even in case of non homogeneous data, which is often the case for regional scale analyses. Moreover, it allows the integration of different risk types or metrics.

2 STUDY AREA

Lombardy (Northern Italy) covers an area of 23,855 km². 17% of the Italian population (almost 9,000,000 people, ISTAT Istituto nazionale di statistica, 2006) lives in Lombardy and about 25% of the Gross Domestic Product (GDP) is produced here (ISTAT, 2005).

The region presents a wide variety of landscapes and environments, but it can roughly be subdivided into 3 different sectors: the Alps, the Po alluvial plain, and the Apennines (Fig. 1).

Climate of Lombardy is continental, with local variations related to the orographic setting. Mean annual precipitation ranges from 650 to 800 mm/year in the lower plain, gradually increasing towards the Alps. Here we observe a strong orographic effect, with maximum precipitation in the southern Alps (2000-2200 mm/year) and minimum values in the northern sector (700-900 mm/year).

The most populated cities (Milano, Bergamo, Brescia, Varese) are located in the upper plain area, where 80% of population and most industrial facilities, services and lifelines are located (Fig.1).

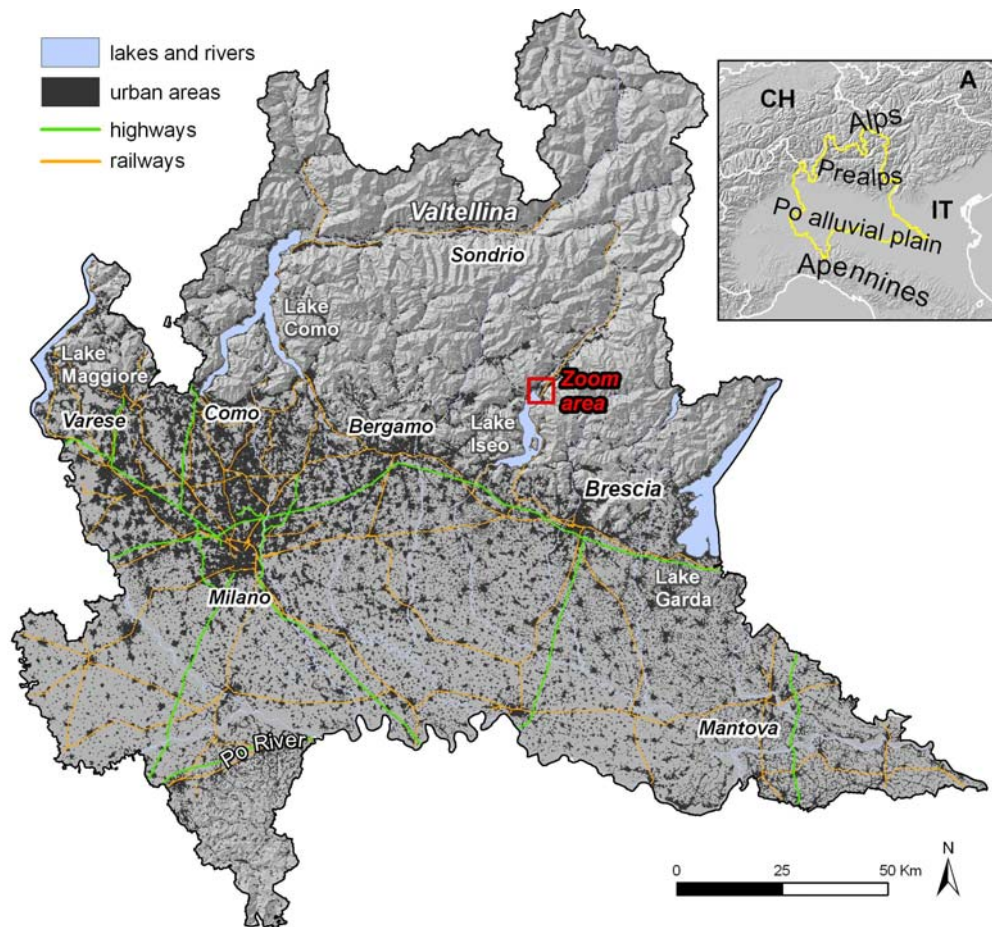


Fig. 1. Map of Lombardy. Urban areas and main transportation network used for the analysis are shown.

The Alps, (11,940 km²), with elevations up to 4025 m a.s.l., are composed of three major structural domains, namely: southern Alps, Penninic and Austroalpine domain (Fig.2). Lombardy is located in a central position of the Alpine chain. The territory presents a large variety of landscapes, with valleys trending North-South, with the exception of Valtellina. The East trending Insubric line bounds the southern Alps to the north. The Lombardy alpine lakes cover over 800 km².

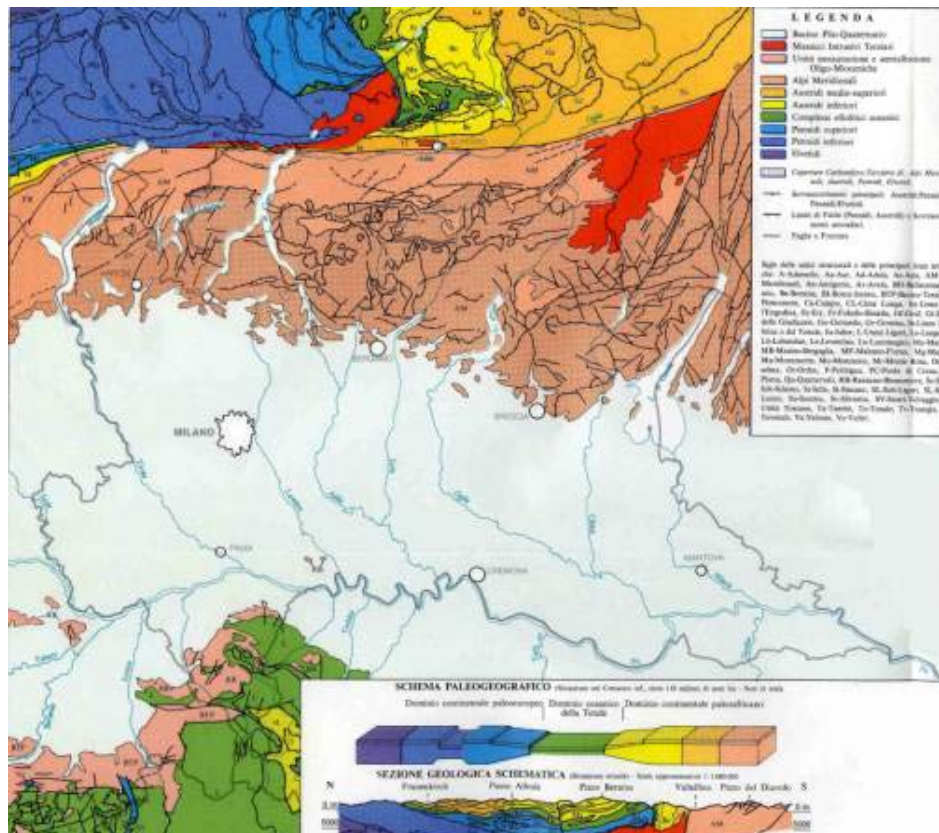


Fig. 2. Simplified geologic scheme of Lombardy (Carta Geologica 1:250,000, Regione Lombardia)

Penninic and Austroalpine units are mainly composed of metamorphic rocks and sedimentary layers, while Southern Alps units present a metamorphic basement and a thick sediment cover. Two significant late-alpine intrusive bodies are present, namely Adamello and Val Masino-Bregaglia plutons. Penninic units form the deepest part of the alpine chain, while the Austroalpine ones include the more elevated structural units. The high energy of the range is the product of endogenous and exogenous processes. Deformation and uplift processes are still active, and during the Quaternary, glaciers deeply modelled the landscape. The actual morphology is further controlled by climatic changes and water regime.

The pre-alps, constitute the zone of connection between Alps and Po alluvial plain. This zone is characterised by the presence of extended glacial, fluvio-glacial deposits and alluvium. Carbonatic massifs developed particular slope morphologies connected to karstic processes.

The Po river plain, (11,221 km²), covers most of the southern part of the region, and half of its total area. It is a fertile plain, thanks to the abundance of water courses and springs. The plain is highly populated, and hosts intensive industrial and commercial activities. It is limited by river Ticino to the West, and by river Mincio to the East. The mean elevation is above 100 m. s.l.m., with negligible gradient. Deposits are mainly connected with material eroded in the mountains and deposited during the floods of river Po and its tributaries.

The Apennines extend for about 700 km² in the South-West of the region, with elevations up to 1724 m a.s.l.. The Apenninic domain is characterised by allochthonous Ligurian units, sedimented in the ancient deep sea of the Ligurian basin, and by marly-arenaceous deposits on the Ligurian units, taking the name of Epiligurian units or Ranzano – Bismantova successions. The main structure of northern Apennine is a fold and thrust belt, built by the superimposition of different tectonic units. Slopes are gentle, and valleys are mainly modelled by water flow and lope movements. In some cases, the morphology is influenced by gully erosion due to the presence of scaly clays and limestones.

In Lombardy, anthropic areas (urbanised, industrial, commercial areas, communication networks, mining zones, dumps, building yards) represent the 9% of the regional territory, mainly located in the plain and, in minor quantity, in the valley floors. Wooden cultivations are scarcely diffused, while sowable land is widely diffused. Agricultural territories cover 48,6% of the regional surface. Coppices, forests, grass lands and bare zones are concentrated on the slopes in the Alps and in the Apennines (Fig.3).

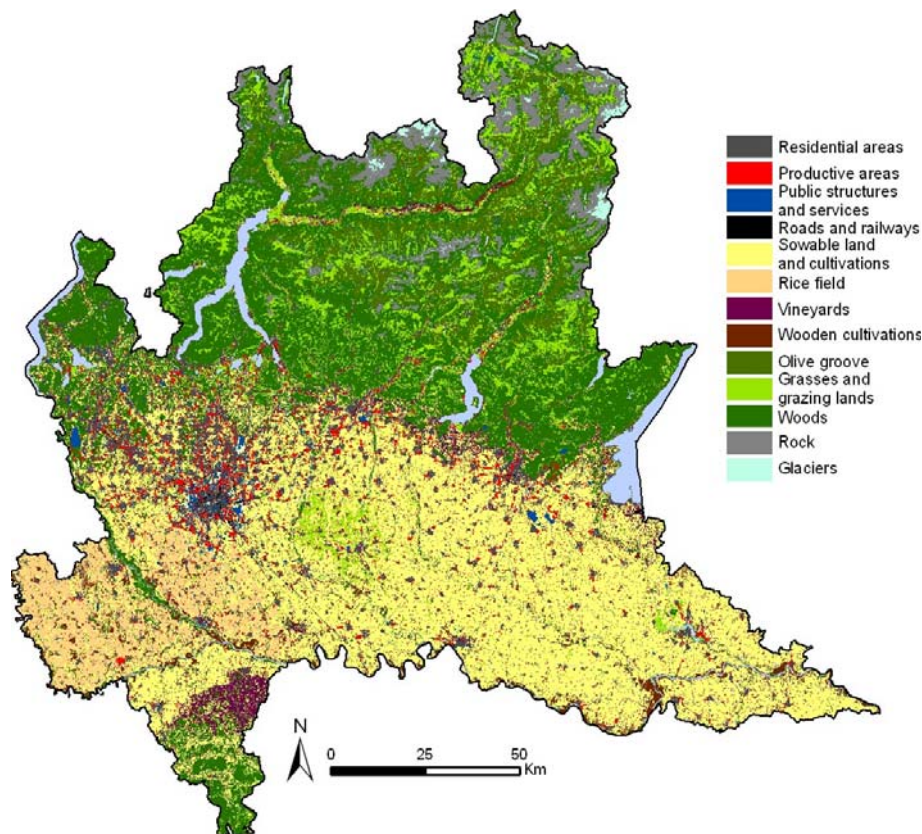


Fig. 3. Soil use map of Lombardy (DUSAF,2007)

The distribution of the geologic units in Lombardy is the result of deep transformations induced by the orogenesis. The area presents a noticeable geological and geomorphic complexity (Fig.4).

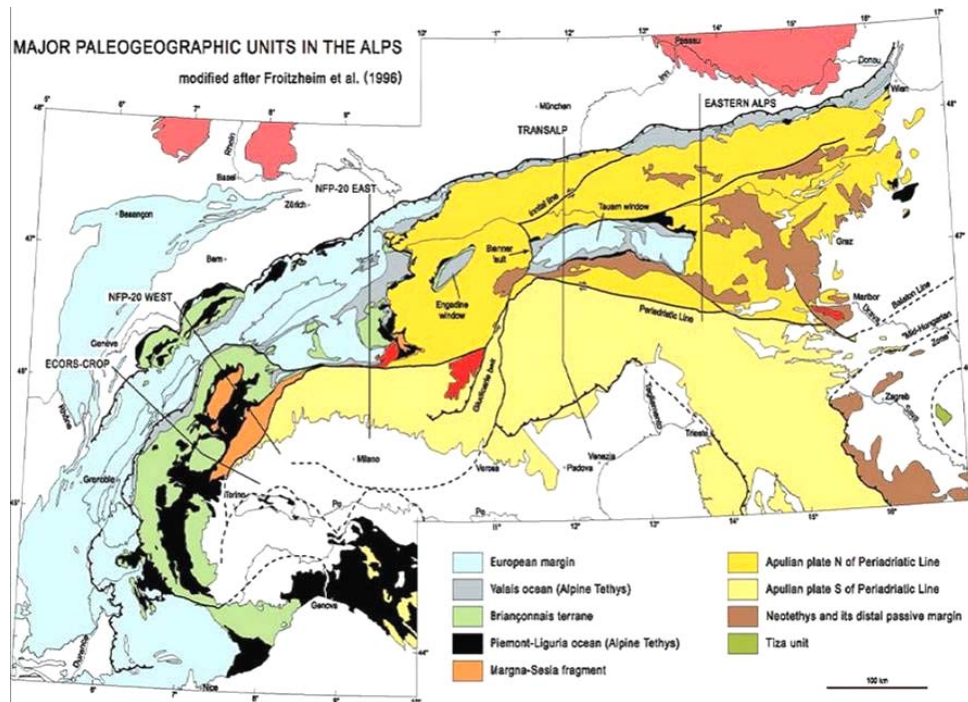


Fig. 4. Map of the major paleogeographic and tectonic units in the Alps (Shmid et al, 2004).

In Lombardy three alpine domains are present: in the northern part of Insubric line, Australpine units, belonging to the African domain, covers the Penninic Units, belonging to European domain (Fig.5 and 6). The Southern Alps domain characterises the southern side of the Line, and it is built by south oriented thrusts.

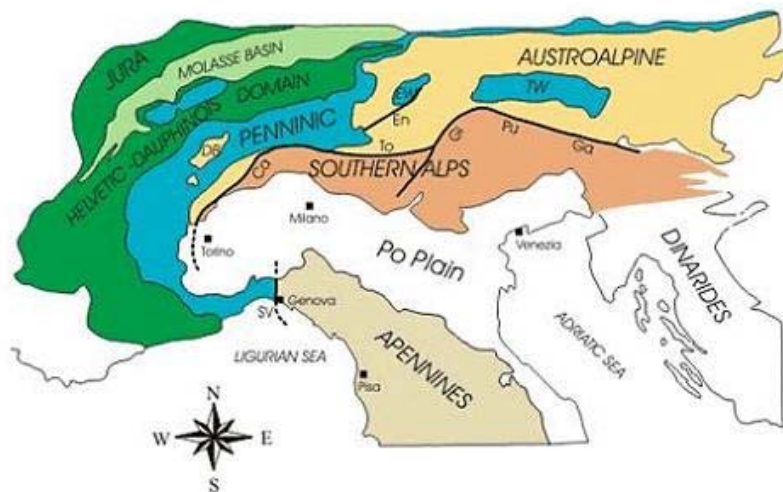


Fig.5. Major domains of the Alps DB = Dent Blanche; EW = Engadina window; TW = Tauern window. Periadriatic lines are:: Ca = Canadese line; To = Tonale line; Gi = Giuicarie line; Pu = Punteria line; Ga = Gail line; En = Engadina line; SV = Sestri-Voltaggio line.

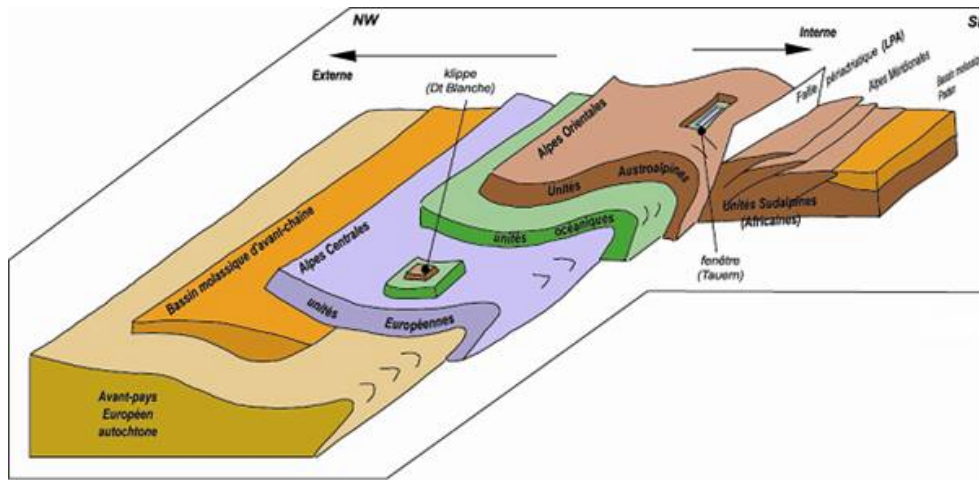


Fig.6. Structural scheme of the Alps (Marthaler, 2001)

The Insubric Line is marked by levels of mylonite E-W oriented, involving all the rocks in correspondence of the line for almost 1 Km width. Cataclastic boundaries are present, connected to more recent and superficial movements.

2.1 STATE OF RISKS IN LOMBARDY

Lombardy is characterized by many risks that threaten the population and the economic activities. The Regional Civil Protection Agency (PRIM, 2007), identified nine major threats, whose analysis has been considered a priority: landslide, avalanche, flood, wildfire, seismic, meteorological, and industrial (technological) risks; road accidents, and work injuries. Some potentially relevant threats were not considered, as pollution, sanitary risks, terrorist attacks.

Landslides, floods and snow avalanches have been grouped in the “hydrogeological risk” in accordance to the standards of the Regional Civil Protection Office (PRIM, 2007).

In order to highlight the impact on the territory of the analysed threats on Lombardy, data about fatalities occurred in the last century were collected (Fig.7). Unfortunately, data were available only for some threats and limited time intervals, and were not usable in the successive risk analysis.

Since 1906, floods and landslides caused 421 and 239 fatalities, respectively (AVI, Aree Vulnerate Italiane da frane ed inondazioni, 2007), while snow avalanches caused 53 fatalities and a global amount of 104 injured people since 1985 (SIRVAL, Sistema Informativo Regionale Valanghe, 2007). Road accidents and work injuries show a much larger impact on human life than other risks, the annual number of fatalities being orders of magnitude higher with respect to the other risks. In the period 1999-2004 almost 45,000 road accidents per year occurred causing about 800-900 fatalities per year (Fig. 2; source: ISTAT). 160,000 work injuries per year were recorded on average between 2001 and 2006, with almost 200 fatalities per year (source: INAIL, national insurance for work injuries, 2007) (Fig.7).

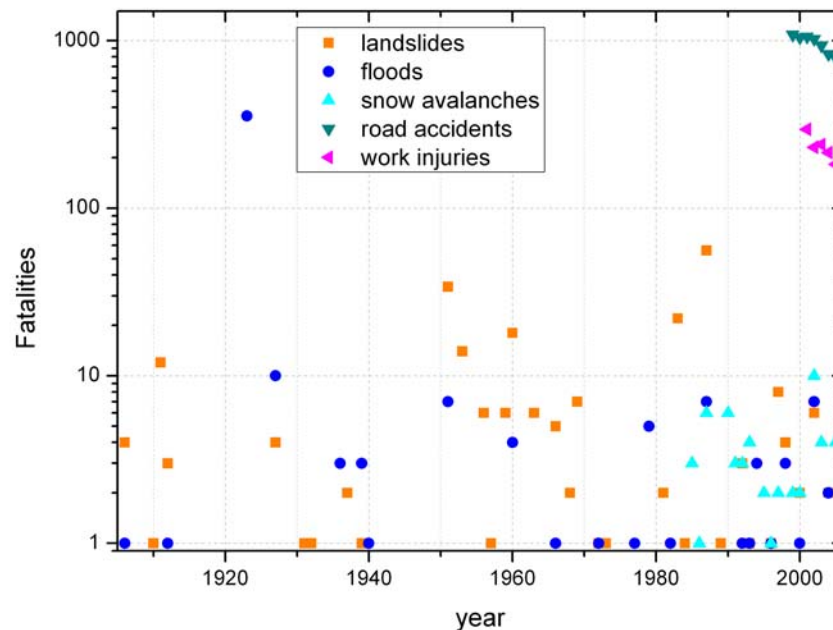


Fig.7 Number of fatalities per year in Lombardy caused by floods and landslides between 1906 and 2005 (AVI), by avalanches between 1985 and 2005 (SIRVAL), by road accidents between 1999 and 2005 (source: ISTAT), and by work injuries in the period 2001-2005 (source: INAIL).

Wildfires and earthquakes did not have relevant consequences on human lives in the last century. Lombardy has in general a low seismic risk, with respect to other Italian regions, with some exceptions in the eastern sector, close to the Lake Garda (max historical magnitude 6 Richter, 1222 A.D., Gruppo di lavoro CPTI, 2004). A moderate seismicity characterizes also the Apenninic zone (max magnitude 5.5 Richter, 1541 A.D., Gruppo di lavoro CPTI, 2004), the upper Valtellina and the south eastern part of the region.

Other data collected to give a general overview of the state of risk in Lombardy regard the regional expenditure for risk mitigation. This is not necessarily a good proxy for risk severity, though it provides a rough idea of the economical and effective impact of different risks on the community, from the perspective of the Regional Administration, as a result of a politic perception.

The mitigation costs sustained in 2006 by public administrations for the period 2007-2010 amount to 2,1 billion euros. 72.95 % of the costs have been planned for the mitigation of road accidents, 24.89 % for landslides, floods and avalanches, 0.95 % for seismic risk mitigation, 0.89 % for wildfires, 0.24% for industrial accidents and 0.06 % for work injuries. It is worth to note that no significant event in 2006 required planning exceptional mitigation expenditure. Thus, the 2006 planning can be considered representative of ordinary mitigation costs. It is also worth to note that public administration expenditures for seismic risk, industrial risk, and work injuries are not representative of the actual economic impact, because most of the mitigation costs for these risks are covered by privates or/and insurances.

Though the expenditure for road accidents and hydrogeological risk is orders of magnitude higher than the others, also the other threats have been included in the analysis. The planning of a civil protection strategy of risk management and prevention, which is the purpose of this study, needs to account for all the possible threats active and interacting in a specified territory, even if their public costs are not so relevant.

3 GENERAL METHODOLOGY

The methodology was developed starting from available data at different scales, in order to be suitable for use at different scales and with data at different levels of detail. Risk analyses were performed at the regional scale using as terrain units 1km x 1km square polygons. The subdivision of the study area in vector square polygons reduces the loss of spatial information with respect to the raster format. Besides, the geometry of the elements at risk and of the areas involved by dangerous processes is maintained with a high detail within each polygon. The impacted areas are calculated through geometric analysis maintaining the highest precision available, and referred only in the end to each polygon.

The constant area of terrain units ensures the homogeneity of the analysis in spatial resolution, starting from heterogeneous input data with different scale and resolution.

The adopted methodology for risk assessment is based on indicators (Fig.8). These indicators are developed at different levels of complexity according to the availability of data for each threat, thus allowing both to manage heterogeneous data (in quality and quantity) and to integrate them iteratively using all the available information.

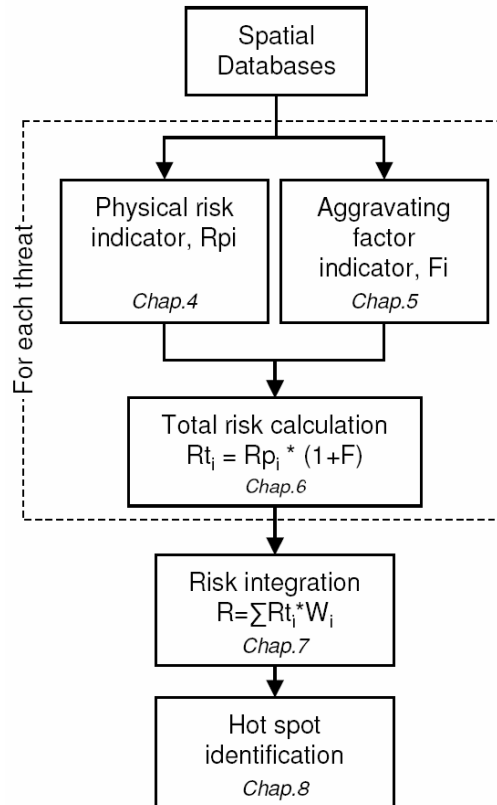


Fig.8 Methodological scheme of the analysis. Subscript i refers to each threat.

3.1 DATABASES

Sources of hazard for landslide, snow avalanche and flood were mapped using inventory maps, susceptibility models, or national regulatory maps (see Tab.1,2, and 3 for data sources and scales). Through inventory maps areas that are potentially hazardous were identified, under the assumption that past events can be reactivated or occur in the future under the same conditions (Varnes, 1984). These data were integrated with susceptibility zoning for some phenomena considered not exhaustively represented in the inventory maps, such as rockfalls and shallow landslides. For rockfalls, a shadow angle approach was applied (Hungr and Evans, 1988; Jaboyedoff and Labiouse, 2003), using 20 m x 20 m DTM and two different angles for the identification of higher (39°) and lower (33°) hazard zones. For shallow landslides, a coupled slope-stability and steady-state hydrological model was applied (Dietrich and Montgomery, 1998; Crosta and Frattini, 2003). A 20 m x 20 m DTM was used, and the model was parameterized considering different combinations of superficial lithology and land use, and assigning parameter values according to the literature and past experiences (Crosta and Frattini, 2003). Both models provide an approximate assessment of susceptibility, but appear to be consistent with the scale and the aim of the analysis, and they have been constrained and calibrated through available event data.

For floods, hazard zones delimited according to national regulatory maps were adopted, for both major rivers and 73 dam break scenarios (Tab 2).

Tab 1 Hazard sources and relative scores adopted for landslide risk assessment. See chap.6 for scores explanation.

Symbol	Hazard source	Data source	Scale	Ref	Score
HRF	Areas susceptible to high-hazard rockfall	Shadow cone model	1:10,000	1	0.40
LRF	Areas susceptible to low-hazard rockfall	Shadow cone model	1:10,000	1	0.30
AL	Active landslide	Inventory map	1:10,000	2	1.00
DL	Dormant landslide	Inventory map	1:10,000	2	0.90
IL	Inactive landslide	Inventory map	1:10,000	2	0.40
ADF	Active debris flow	Inventory map - buffer 10 m	1:10,000	2	0.80
DDF	Dormant debris flow	Inventory map - buffer 10 m	1:10,000	2	0.40
SL	Areas susceptible to rainfall-induced shallow landslide	Slope stability Model	1:10,000	3,4	0.20
DSSD	Deep seated gravitational slope deformation	Inventory map	1:10,000	2	0.20
ADL	Active diffused landsliding	Inventory map	1:10,000	2	0.70
DDL	Dormant diffused landsliding	Inventory map	1:10,000	2	0.40
UDL	Unclassified diffused landslides	Inventory map	1:10,000	2	0.55

¹ Jaboyedoff and Labiouse, 2003, ² PROGETTO IFFI, ³ Dietrich and Montgomery, 1998, ⁴ Crosta and Frattini, 2003

Tab.2 Hazard sources and scores adopted for flood risk assessment. See chap.6 for scores explanation.

Symbol	Hazard source	Data source	Scale	Ref	Score
FA	80% of 200 yr flood	Regulatory map	1:25,000	5	1.00
FB	200 yr flood	Regulatory map	1:25,000	5	0.70
FC	500 yr flood	Regulatory map	1:25,000	5	0.20
LF	Lacustrine flooding	Historical data and LIDAR analysis	1:10,000	7	0.50
AAF	Active alluvial fan	Inventory map	1:10,000	2	0.80
DAF	Dormant alluvial fan	Inventory map	1:10,000	2	0.20
MiR	River network	Topographic map - buffer 10 m	1:10,000	8	0.60
DBF	Dam-break flooding area	Regulatory map	1:10,000	9	0.10

² PROGETTO IFFI, ⁵ PAI, ⁷ Il bacino lariano, 2007 ⁸ CTR, ⁹ CIRC.MIN.LL.PP 352/1987,

Tab.3 Hazard sources and scores adopted for snow avalanche risk assessment. See chap.6 for scores explanation.

Symbol	Hazard source	Data source	Scale	Ref	Score
SA	Snow avalanche	Inventory map	1:10,000	6	0.5

⁶ SIRVAL

Data for wildfire risk derive from a Regional database which includes wildfire events occurred in the period 1975-2005 (SIAB). For each event, the location of initiation point, the affected areal extent, and the damages are available.

For seismic risk, the Italian seismic hazard map was used (MPS working Group, 2004), that expresses the hazard in terms of peak ground acceleration (PGA) with a return period of 475 years (exceedance probability of 0.1 in 50 years).

Regarding the industrial risk, due to incomplete documentation about the productive processes and the accident scenarios, only explosion-related accidents were considered, neglecting those related to the release of toxic gas and pollutants. Sources of industrial hazard are represented by 246 major risk plants, identified by a national law (D.Lgs. 238/05, according to Seveso Directive 96/82/CE), and mainly located in the plain, in highly urbanised areas. To define a hazard zone, a 1 km radius buffer around the external bordure was considered. This is not fully realistic because it does not account for wind direction and velocity, and other meteorological conditions for which not enough data are available. Nevertheless, in defining a buffer of 1 km a conservative approach was adopted. In fact, most industrial accidents are entirely limited in the plant itself.

Work injury statistics regard accidents occurred to workers regularly registered to INAIL (national insurance for work injuries). Irregular non-insured workers are excluded from the statistics. The database used for work injuries was provided by INAIL and refers to the period 1999-2001. Accidents are classified according to the causes of injuries, and their severity.

Road accidents include the ones occurring on different road typologies (i.e. highway, state, municipal, urban and extra urban roads) and involving all types of vehicles. Accidents also include injuries to pedestrians. Road accidents statistics were extracted from the ISTAT database for the 1999-2004 period. A regional traffic model for the main road network was used to normalise road accidents with respect to the expected traffic flux.

As for meteorological risk, due to the lack of complete and homogeneous data, only lightnings were considered, although they represent only a small part of the whole meteorological risk. For the 1996-2005 period, data relative to the number of annual lightnings per 4 km² cells were provided by the network of the Italian Survey Lightnings System (SIRF-CESI). The network is composed of 16 sensors on the whole Italian territory.

3.2 EXPOSED ELEMENTS

The identification and mapping of the elements at risk, were conducted with a high spatial accuracy, by using different databases. Human life was not included in the analysis as an independent element at risk. The number of people potentially involved in dangerous phenomena was indirectly considered, by attributing a value of human presence to each class of exposed elements (Tab.4), based on the average assumed annual occupancy.

23 classes of exposed and vulnerable elements, T_j , were identified, and each element was mapped by using different 1:10,000 maps available at a regional scale.

Main categories of exposed elements include: residential areas, lifelines, major industrial plants, strategic buildings (schools, hospitals, etc.) and natural resources (Tab 4, Fig. 9).

Tab. 4: List of the exposed elements and scores for the different dimensions of value: HL=human life, ENV=environmental, DIR=direct economic, INDIR=indirect economic, MIT=Relevance for mitigation. Map scale 1:10,000. See chap.6 for scores explanation.

Exposed elements	ref	HL	ENV	DIR	INDIR	MIT	Aggregated fuzzy score
Continuous residential area	1	Very high	null	Very high	High	Moderate 2	0.080
Discontinuous residential area	1	High	null	High	Moderate	Moderate	0.066
Main road	2	High	null	Moderate	High	High	0.069
Secondary road	2	Moderate	null	low	Moderate	Moderate	0.031
Railway line	2	High	null	Moderate	High	Very high	0.071
Powerline	2	null	null	low	High	High	0.082
Power plant	3	null	null	High	High	Moderate	0.067
School	3	Very high	null	High	low	High	0.086
Hospital	3	Very high	null	Very high	Very high	Very high	0.103
Tourist facility	3	Low	null	Moderate	low	low	0.029
Sport structure	1	Low	null	low	low	low	0.010
Industrial plant	4	Moderate	null	High	High	null	0.066
Railway station	3	High	null	High	High	High	0.086
Airport	3	High	null	Moderate	High	low	0.067
Industrial area	1	High	null	High	High	Low	0.077
Forest	1	null	low	low	low	null	0.002
Coppice	1	null	low	low	low	null	0.001
Bank vegetation	1	null	low	null	low	null	0.000
Pasture	1	null	low	null	low	null	0.000
Natural park	1	null	Moderate	low	low	null	0.001
Wooden cultivation	1	null	low	low	low	low	0.002
Sowable land	1	null	low	low	low	low	0.002
Urban park	1	low	low	low	low	low	0.002

¹DUSAF, ²CTR, ³MISURC, ⁴D.Lgs. 238/05

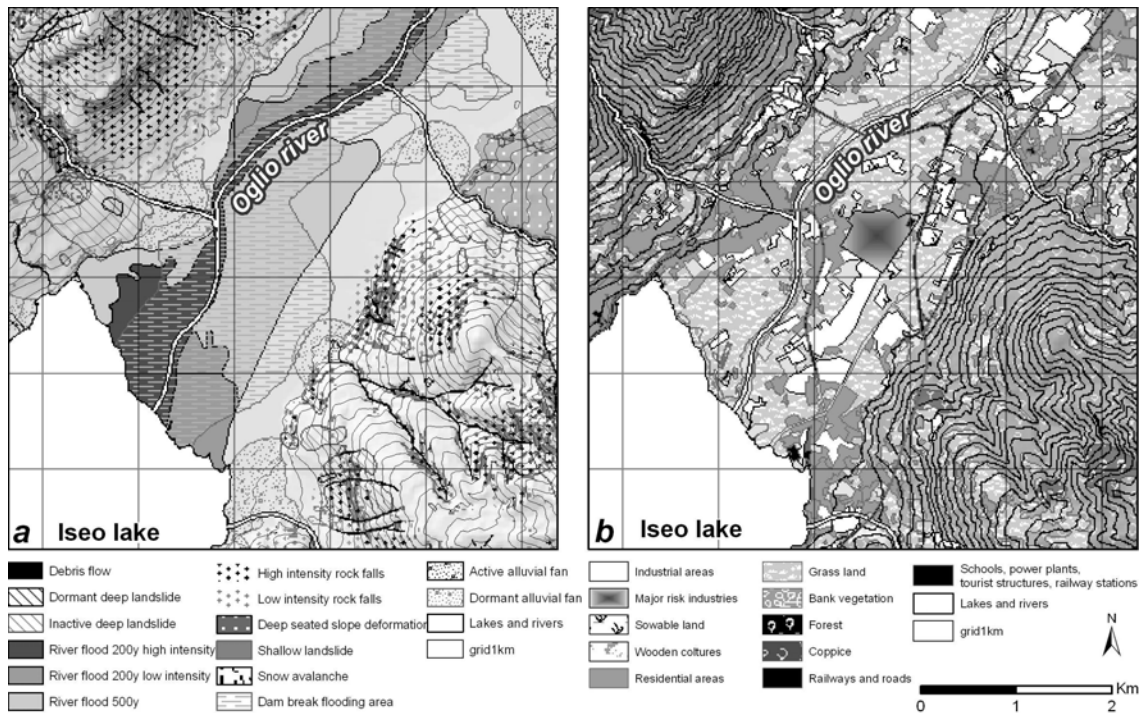


Fig.9. Sources of hydrogeological hazard (a) and exposed elements (b): example for a selected area (see Fig.1 for location). The 1 km x 1 km square polygons used for the analysis are shown.

3.3 WEIGHTING STRATEGIES

The different indicators were aggregated by applying appropriate weights based on expert knowledge. Case by case, the most convenient weighting strategy was selected (Budgetary Allocation, Fuzzy Sets, and Analytic Hierarchy Process).

Budgetary Allocation is the simplest and more direct way to find weights based on the personal believe. The technique is based on the distribution and allocation of a budget (i.e., 100 scores in our analysis) over the different indicators (Cardona et al., 2004). It was adopted to assign weights to the indicators of physical risks and aggravating factors due to its capability to manage a large number of variables.

Fuzzy sets (Zadeh, 1965) are useful while attempting to aggregate different dimensions of a complex problem, expressed also in a linguistic way. For each dimension, the linguistic attributes correspond to fuzzy sets with Gaussian membership functions. These are aggregated using the union defuzzification method (Cardona et al. 2004) in order to provide a final score This approach was used to aggregate the different dimensions of the target value scores (Tab.4) due to its capability to account for multidimensional linguistic attributes.

Analytic Hierarchy Process (AHP, Saaty, 1990) is a widely used technique for multi-attribute decision making. AHP enables the decomposition of a problem into hierarchy and assures that both qualitative and quantitative aspects of a problem are included in the evaluation process. The opinion about the dominance of risks is systematically extracted by means of pair-wise comparisons. A preference of 1 indicates equality between two indicators while a preference of 9 indicates that one indicator is 9

times larger or more important than the other. The weights are obtained by rescaling between 0 and 1 the eigenvectors relative to the maximum eigenvalue for the matrix of the coefficients, resulting from the pair-wise comparisons. We used this technique for the integration of the different risks, due to its capability to check the internal coherence of the expert's attributions through the calculation of the Consistency Ratio (CR, ranging from 0 to 100). CR values lower than 10 assures an excellent coherence of the attributions (Saaty, 1990).

For Budgetary allocation, Fuzzy logic and AHP, 15 experts from different disciplines were involved. They are:

- 5 research geologists with expertise on landslide, flood and avalanche risk
- 3 Civil Protection officers responsible for the allocation of economic resources for mitigation projects
- 2 environmental researchers working on natural and technological risks
- 5 public administrators with expertise in natural and technological risk

4 PHYSICAL RISK INDICATORS

The physical risk indicator, R_p , is a dimensionless score expressing the expected direct loss consequent to a hazardous event. According to the intrinsic nature of each threat and data quality and availability, the physical risk has been evaluated at three different levels of complexity.

The simplest level of analysis was applied to road accidents, work injuries and lightnings. For these threats, we built sets of indicators based on statistics of available data (PRIM, 2007). The physical risk was calculated as a weighted sum of these indicators.

For landslide, avalanche, flood, industrial and seismic risks, impact indicators, I were built. Each indicator is defined as the portion of 1km x 1km cell where a specific target is impacted by a specific hazard (Fig.10). The physical risk, R_p , is then calculated as:

$$R_p = \frac{\sum_{i,j=1}^N (h_i \cdot v_{i,j} \cdot w_j) I_{i,j}}{\sum_{i,j=1}^N (h_i \cdot v_{i,j} \cdot w_j)} \quad (1)$$

where h is the score for the hazard source i (see Tab. 1, 2, 3), w is the score of the exposed element value j (see Tab. 4), and v is the score for the vulnerability of the impacted target. The vulnerability score expresses the level of potential damage of each target in response to each hazard.

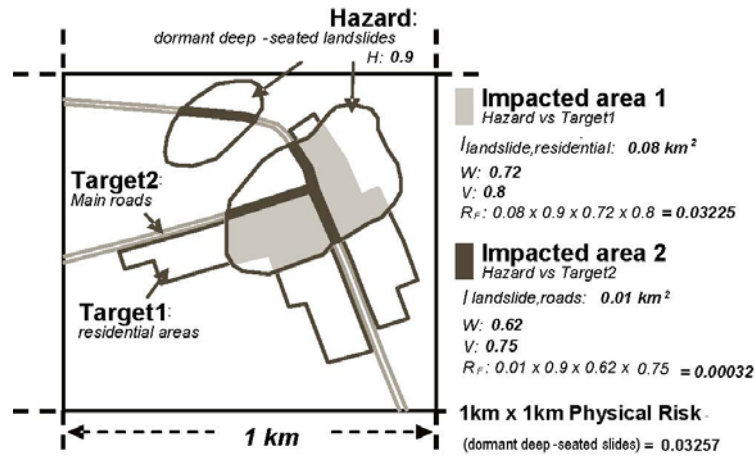


Fig.10. Example of calculation of physical risk with two impact indicators (i.e. dormant deep-seated landslides impacting on residential areas and roads). The same methodology has been applied for landslide, avalanche, flood, industrial and seismic risk.

Due to the large number of scores to be assessed, AHP was not applicable in this case. Scores h and v have been assessed by means of a budgetary allocation method, while the scores w have been obtained through a fuzzy logic approach. The score w expresses a multi-dimensional value accounting for: the economic (direct and indirect) and environmental value, the potential for human losses, and the relevance for mitigation. The economic value was assigned on the basis of regional-averaged economic estimations, without considering site-specific value distribution (e.g., value of buildings according to proximity of city centre). The other value components (e.g., human lives, environmental value, relevance for mitigation) were assigned on the basis of expert knowledge.

For wildfires, a large amount of data was available, and it was possible to develop a scenario-based risk assessment (PRIM, 2007). For each terrain unit, the wild-fire risk was calculated by summing up the product of hazard H , vulnerability V and value W :

$$R_p = \sum_{m=1}^M \sum_{n=1}^N H_m V_{m,n} W_n \quad (2)$$

where M is the number of wild-fire scenarios and N the number of exposed elements.

In order to allow a comparison of physical risks, each value was normalized by the corresponding regional mean.

4.1 HYDROGEOLOGICAL RISK

The hydrogeological risk appears to be strongly controlled by the physiographic setting (Fig.11), and mainly affects mountainous areas, alluvial plains and valley floors, with maximum values along alpine valleys, where flood and landslide risks co-exist with a high urban density. Although this result was expected, it is important to stress that the analysis allowed to quantitatively estimate the risk levels among different

terrain units, which is important for the development of mitigation strategies, for the allocation of economic resources, for the planning of new urban areas, and for prioritising the mitigation actions.

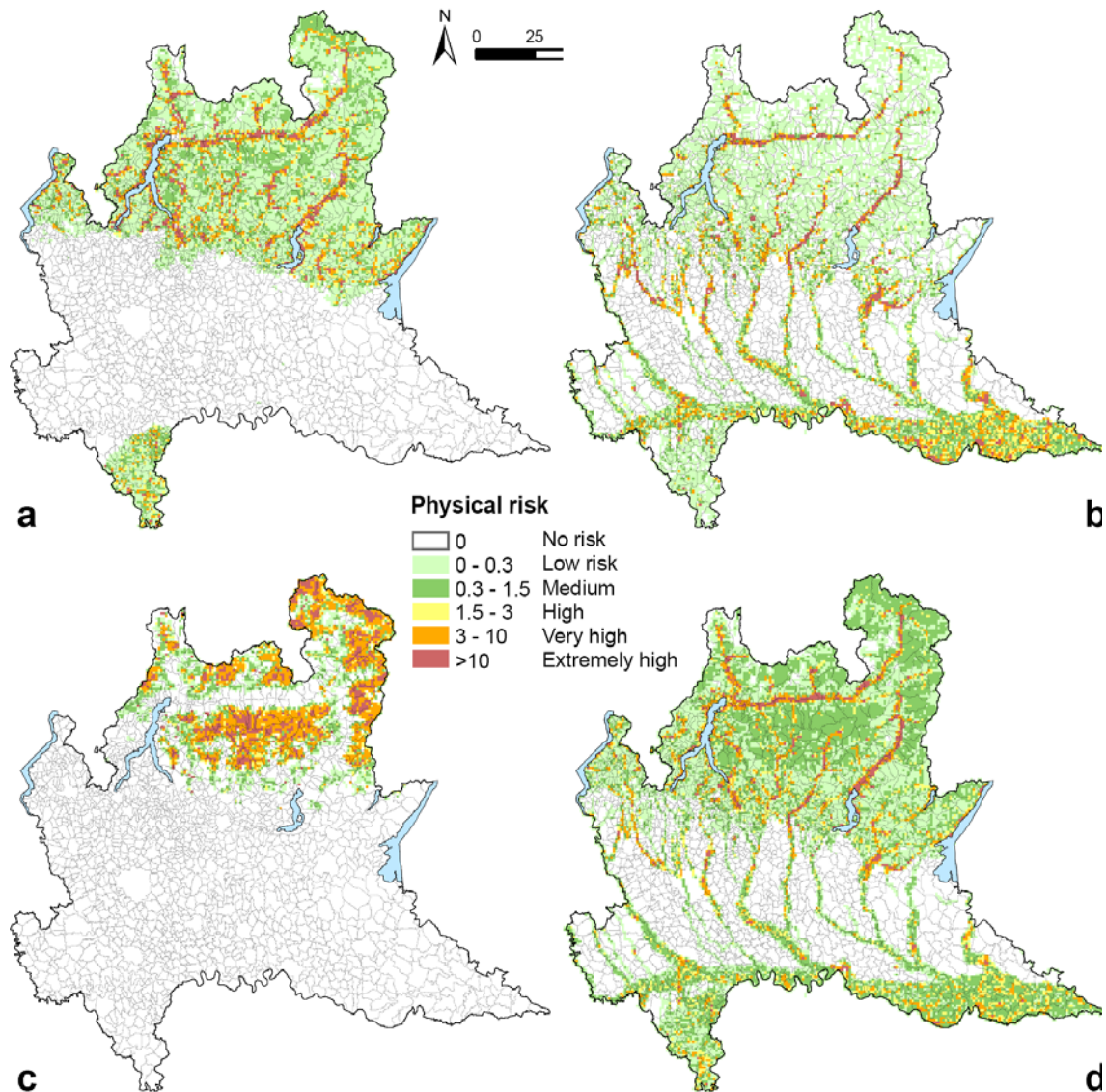


Fig. 11. Landslide (a), flood (b), avalanche (c) and aggregated hydrogeological (d) physical risks, RP. Values of risk are normalized by the regional mean.

To investigate the control of physiographic setting on hydrogeological risk the terrain units were grouped according to the mean elevation in classes of 100 units. For each class, the mean physical risk for landslide, flood, and snow avalanche was calculated (Fig.12). The maximum landslide risk is reached at 500 m a.s.l., where the density of exposed urban settlements and infrastructures is higher. The snow avalanche risk is negligible below 1500 m a.s.l. (Fig.12a), and is generally low because these processes are common in non urbanised areas (Fig.12b). The flood risk is very relevant in two different elevation intervals corresponding to either the lower Po plain or the

main alpine valleys (e.g. Valtellina), where rivers are not entrenched below the plain level and population density is relatively high.

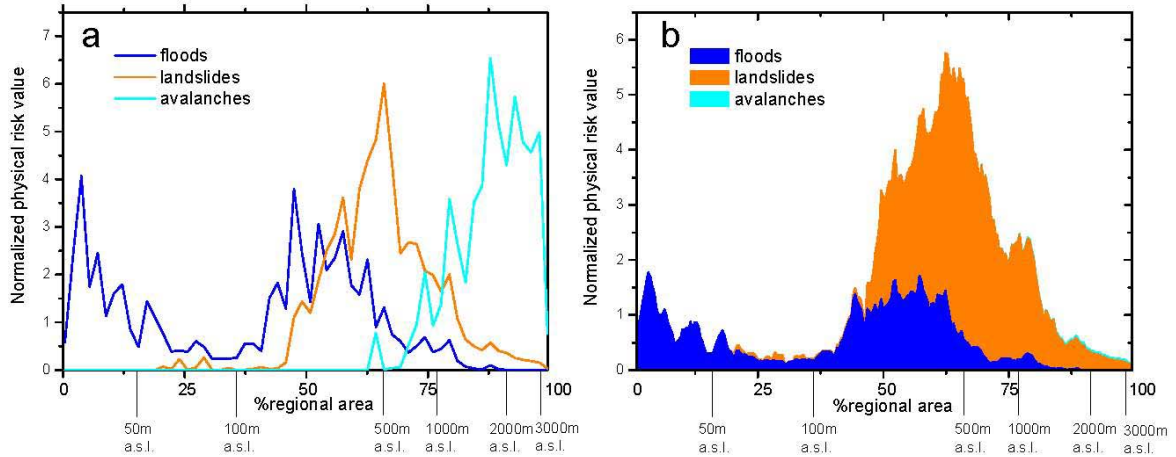


Fig. 12. Flood, landslide, and avalanche physical risk for different elevation quantiles. Risk values are normalised with respect to the regional mean of: a) each single threat; b) the hydrogeological physical risk.

4.2 OTHER RISKS

Wildfire hazard was assessed for three reference scenarios of wildfire size (Fig.13). The choice of the scenarios derives from the regional fire-prevention plan (Piano Antincendi Boschivi, 2006). For each scenario, an exceedance probability was extracted from frequency-size analysis of 2880 events occurred in the 1975-2005 period (Fig.13).

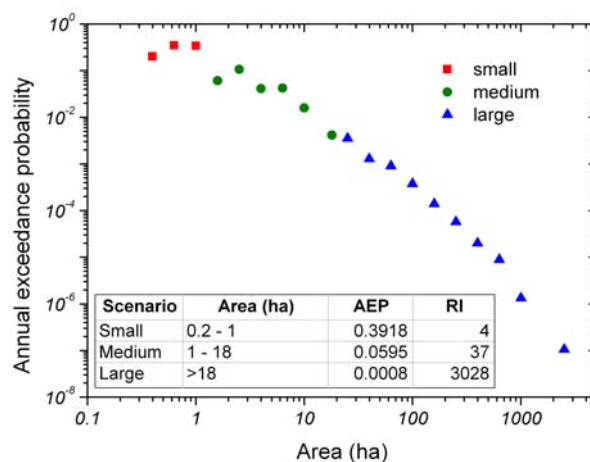


Fig. 13. Wildfire area vs annual exceedance probability, for the three scenarios. Annual exceedance probability (AEP) and recurrence interval (RI) of each scenario are reported in the table. The exceedance probability was calculated from annual frequency (wildfire n° /total wildfire n° /30 years) of logarithmically binned wildfire areas.

By means of a discriminant analysis (Klecka, 1980), the wildfire spatial susceptibility was assessed for each land unit as a function of both the previous fire distribution and the predisposing factors (e.g. slope, elevation, aspect, land use, type of vegetation, pirologic potential, river network density, road density). This susceptibility expresses the wildfire potential for each unit. Hazard was then calculated by multiplying this susceptibility by the regional probability of occurrence of each scenario (Fig.13). In the assessment of the value of the exposed territory, a great importance has been assigned to the presence of protected natural areas, according to their environmental value (i.e. EU Relevant Places, Special Protection areas, Natural reserves, Natural Parks, National and Regional parks).

Seismic risk was assessed using the same approach adopted for hydrogeological risk, with the same targets except for buildings, that have been subdivided according to their period of construction (before 1919, between 1920 and 1945, 1946-1961, 1962-1971, 1972-1981, 1982-1991, after 1992), in order to account for different vulnerability.

Industrial risk was assessed by means of impact indicators using the same targets of hydrogeological risk and the 1 km wide buffer around the plant as source of hazard.

Meteorological risk was assessed using the mean number of annual lightnings for 30 km x 30 km grid cells (SIRF-CESI). Differently from the other threats, this is more a hazard rather than a risk indicator, because it does not include any assessment of the impact on the exposed elements. However, since lightnings are ubiquitous and impacting all exposed elements in an homogeneous way, this limitation should not introduce significant errors in the analysis.

For road accidents, a composite indicator was used, aggregating the number of accidents, the number of injured people and the number of fatalities. These data were analysed for each municipality and for different road typologies (i.e. highway, state, municipal, urban or extra urban road).

For work injuries, the accident rate for different typologies of activity was used as a risk indicator. This rate expresses the possibility of an accident for a given activity at a certain place and in a given time period for a certain number of operators.

For both work injuries and road accidents, the physical risk was assessed by a weighted sum of these indicators. Weights were assigned through budgetary allocation

5 AGGRAVATING FACTOR

The aggravating factor, F , is an indicator that expresses the lack of coping capacity and resilience of the society, potentially inducing to an aggravation of risk, in terms of indirect costs. It varies from 0 to 1, under the assumption that it can induce costs amounting to a maximum of 100% of the physical risk (Cardona, 2004).

F was assessed through a multi-criteria approach based on indicators. For each risk we used the same set of indicators, with different weights (Tab.5). The aggravating factor was calculated through the weighted average of the indicators (weights in Tab.5), normalized by the maximum value. The effective distances from each cell to emergency management facilities was calculated through a cost distance function, which minimizes

the travel time. A budgetary allocation was performed to assign the weights to the 10 indicators with respect to their importance in coping with risks. The aggravating factor was then mapped at a regional scale in 1 km x 1 km square polygons.

Tab. 5: Weights for aggravating factor indicators

Indicator	Hydro	Wildfire	Seismic	Meteo	Industr	Road	Work
Presence of volunteer civil protection group	0.01	0.02	0	0	0	0	0
Presence of municipal civil protection group	0.02	0.05	0.02	0.02	0.01	0	0
Presence of inter-municipal civil protection group	0.02	0.05	0.02	0.02	0.01	0	0
Distance from closest first aid station (basic equipment)	0.04	0.04	0.04	0.04	0.03	0.07	0.08
Distance from the closest first aid station (advanced equipment)	0.06	0.05	0.06	0.06	0.05	0.11	0.12
Distance from the closest fire brigade department	0.09	0.08	0.09	0.09	0.11	0.08	0.07
Distance from the closest police department	0.03	0.03	0.03	0.03	0.03	0.12	0.05
Distance from the closest hospital	0.42	0.27	0.42	0.42	0.23	0.47	0.63
Presence of a municipal civil protection plan	0.24	0.27	0.24	0.24	0.4	0	0
Interconnection level (number of road network nodes)	0.03	0.12	0.03	0.03	0.1	0.12	0.03

The aggravating factor for the hydrogeological risk is presented (Fig. 14). The factor is null in densely populated regions, where the connectivity is high, the emergency structures are closer, and the civil protection groups can be quickly activated. Due to the presence of civil protection plans and groups, the aggravating factor is low even in some mountain areas with poor connectivity. This behaviour is similar for the aggravating of the other threats.

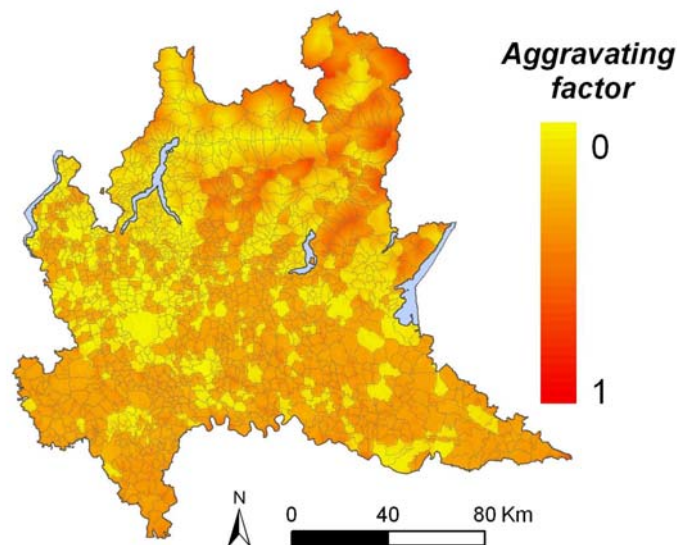


Fig. 14. Map of the aggravating factor, F , normalised with respect to the maximum value. Example for the hydrogeological risk

6 TOTAL RISK ASSESSMENT

For each risk, the Total Risk (R_T) indicator was calculated following Cardona et al., (2004):

$$R_T = R_P * (1 + F) \quad (3)$$

where R_P is the Physical Risk, and F is the aggravating factor.

The spatial pattern of risk seems controlled by different factors depending on the threats.

Wildfire risk is evenly distributed on forested areas, and appears to be independent from the distribution of man-made elements, being the forest itself the principal element at risk (Fig.15 and 16). It is quite rare, in fact, that other targets (e.g. buildings) are completely surrounded by forests and impacted by wildfires. It was also considered that roads are not destroyed or damaged by fire. On the contrary, they are able to break the forest continuity, thus stopping or slowing down the fire propagation, or to favour the intervention.

Seismic risk is mostly present in the eastern part of the Region, where seismic hazard is higher (Fig.15 and 16), whereas the meteorological risk spreads over the whole study area, with a slight increase in the southern Alps, due to more frequent stormy conditions (Fig.15 and 16). Industrial risk shows a spot distribution controlled by the location of major risk plants, close to the main cities (Milano, Varese, Bergamo and Brescia) (Fig.15 and 16). Road accidents and work injuries show a spatial pattern which is largely controlled by the distribution of urbanized areas (Fig.15 and 16).

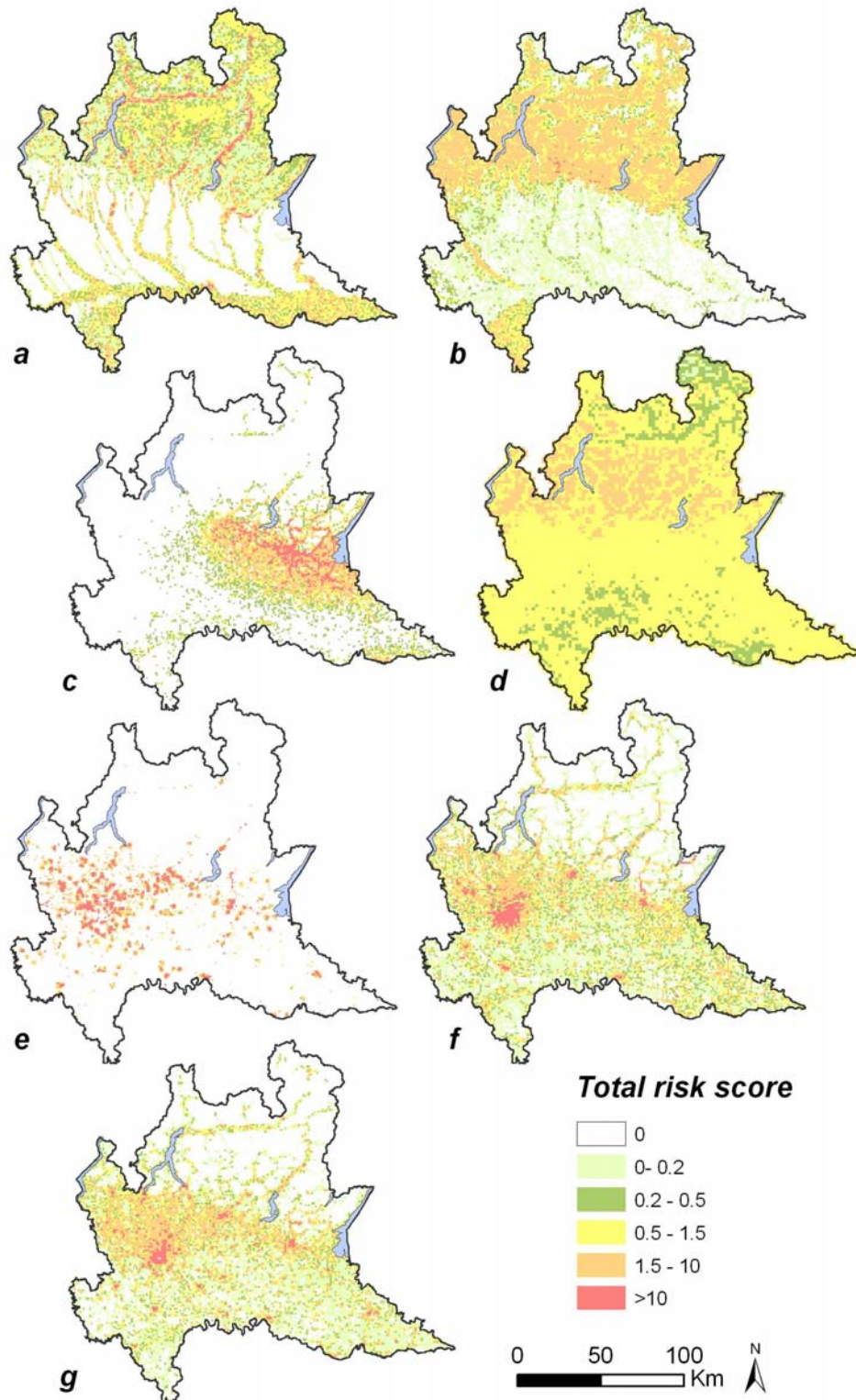


Fig. 15. Maps of normalized total risk, RT, for: hydrogeological risk (a), wildfire (b), seismic (c), meteorological (d), industrial (e), road accidents (f), work injuries (g). Risk values are expressed with respect to the regional mean.

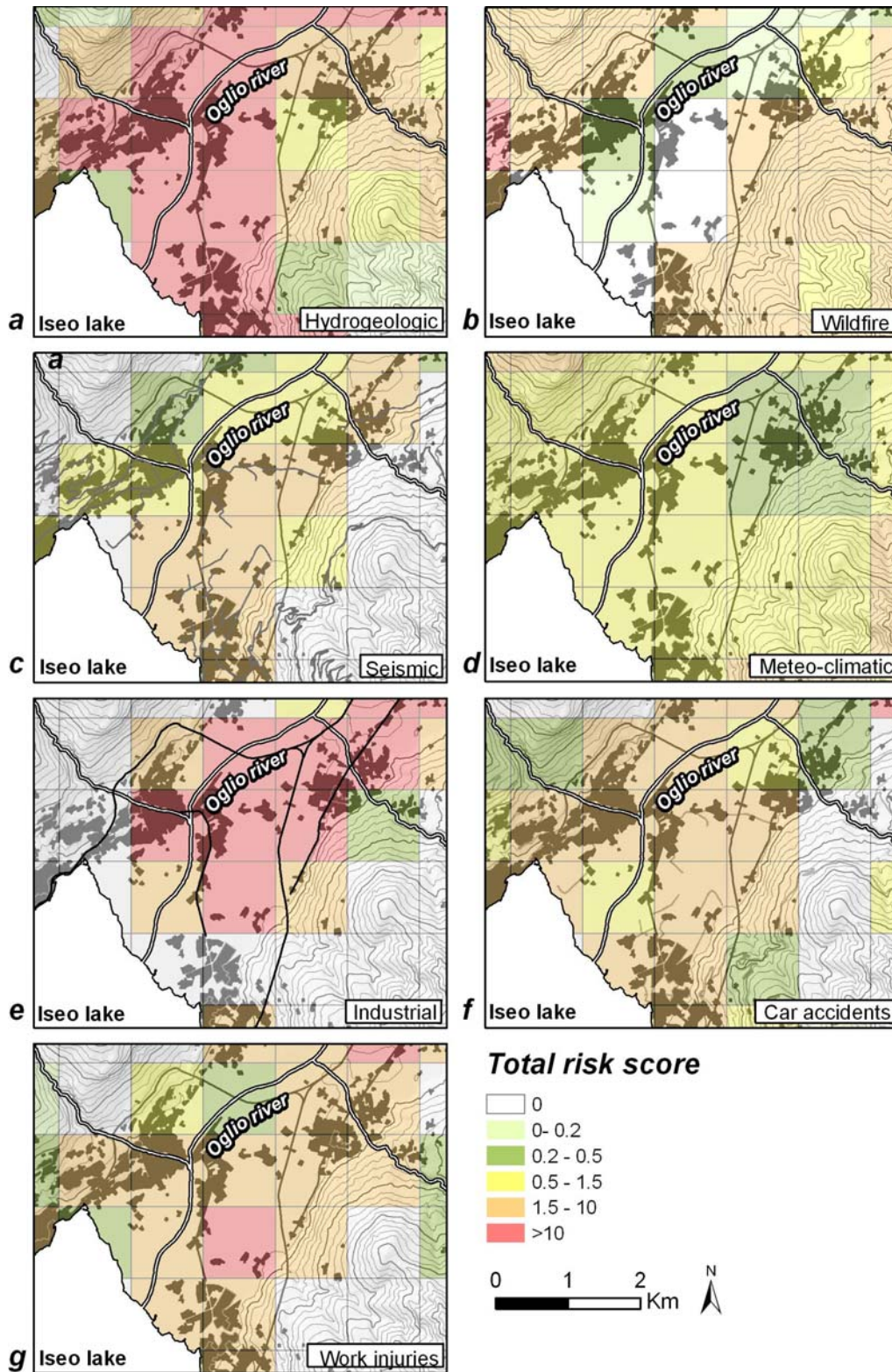


Fig.16. Normalized total risks, RT, for a specific area (see Fig.1) : hydrogeological risk (a), wildfire (b), seismic (c), meteorological (d), industrial (e), road accidents (f), work injuries (g). Risk values are expressed with respect to the regional mean.

7 RISK INTEGRATION

Total risks, R_T , normalized by their regional mean value, were aggregated into a multi-risk index with AHP which provided a robust set of weights and allowed to evaluate the internal coherence of each expert by means of the Consistency Ratio, (CR) (Saaty, 1990) (Fig.17, Tab.6).

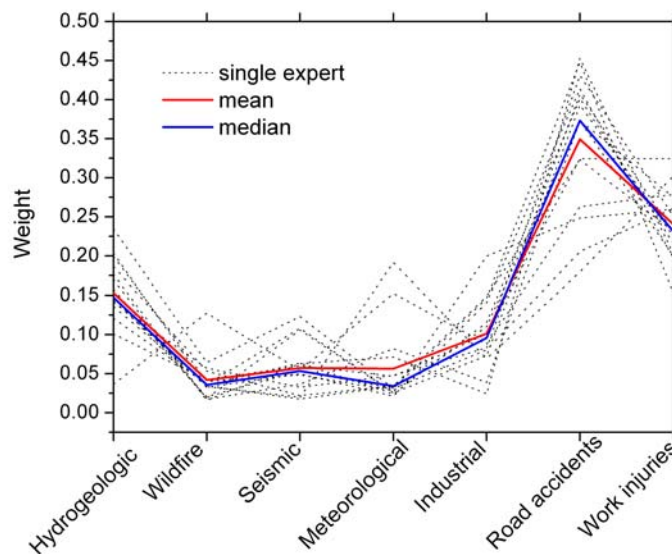


Fig. 17. Risk weights attributed by each of the 15 members of the technical panel, by means of the AHP method

Tab. 6: Weights associated to each risk typology for the production of the integrated multi-risk map as resulting from AHP analysis.

Risk	mean	median	Std.dev	Range
Hydrogeological	0.16	0.15	0.05	0.12
Wildfire	0.04	0.04	0.03	0.11
Seismic	0.06	0.05	0.03	0.11
Meteorological	0.06	0.03	0.05	0.17
Industrial	0.10	0.10	0.05	0.18
Road accidents	0.35	0.37	0.09	0.27
Work injuries	0.24	0.23	0.04	0.17
Consistency Ratio	14.85	11.75	6.77	20.29

By selecting different subsets of threats, we produced maps of 1) natural risks, including hydrogeological, seismic, wildfire and meteorological risk (Fig.18a); 2) social accidents, including work injuries and road accidents(Fig.18b); 3) na-tech risk including

both natural risks and industrial risk; (Fig.18c), and 4) integrated risk, including all risks (Fig.19a). In order to analyse the dominance of the threats over the region, we identified for each cell the risk with the highest weighted value (Fig.19b).

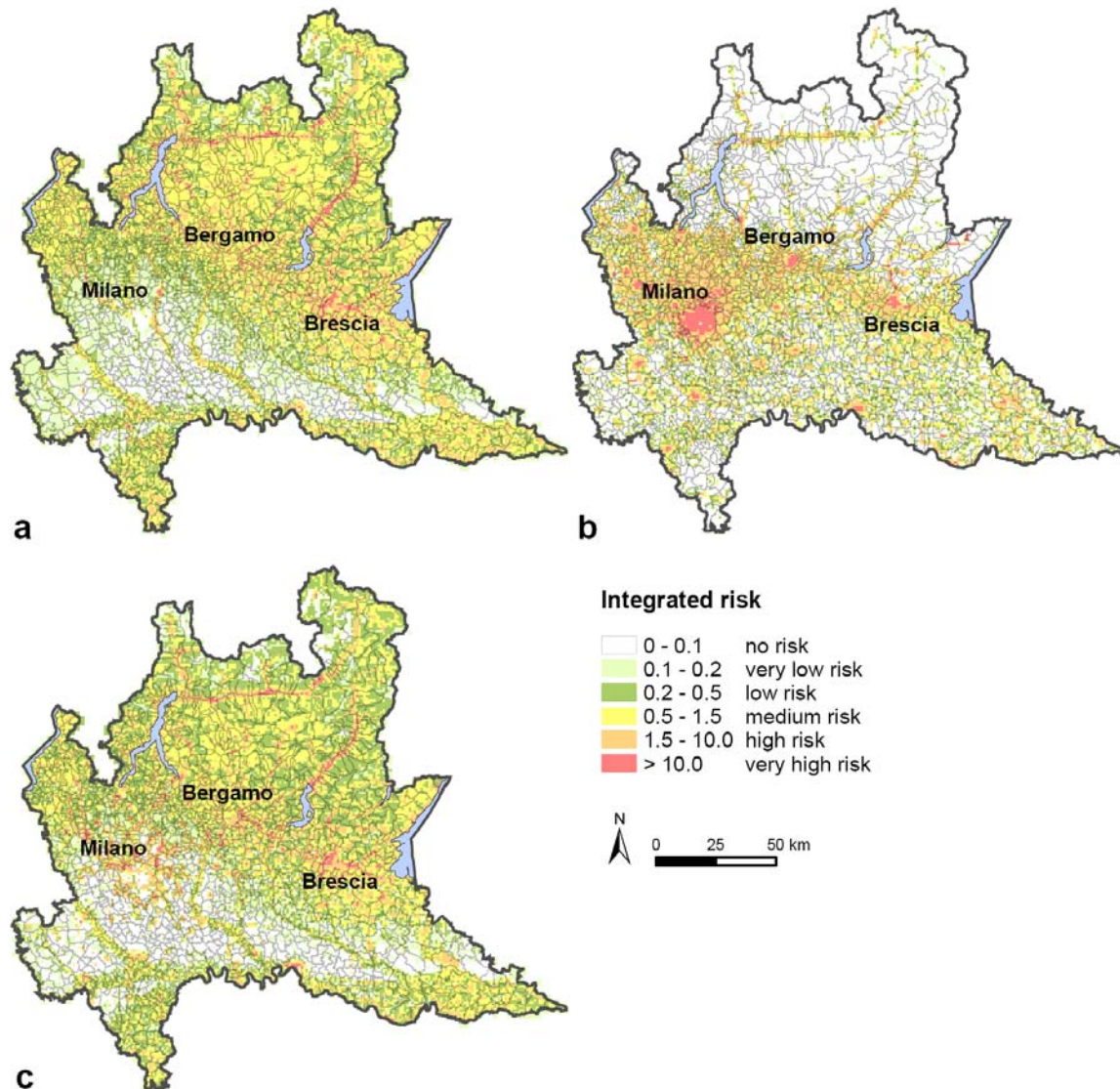


Fig. 18. Integrated risk maps normalized with respect to mean regional value, by expert weighting, for a) natural risks, b) road and work accidents. c) Na-tech risks (hydrogeological, seismic, wildfire, meteorological and industrial risks).

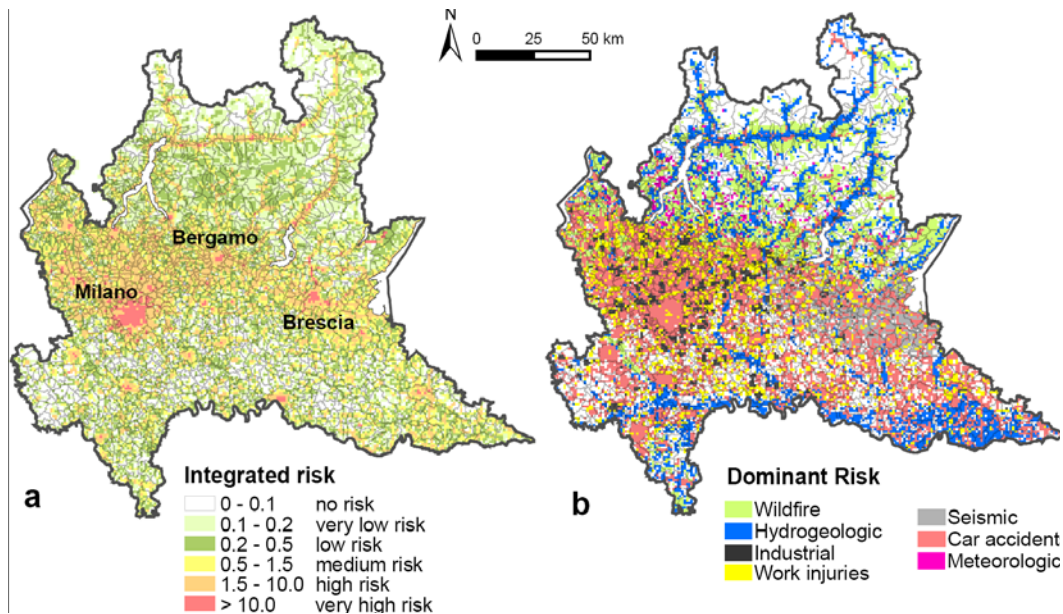


Fig.19. a) Integrated risk map of all the considered threats by expert weighting, normalized with respect to mean regional value. b) Dominant risk map, for risk values > 0.05

8 HOT SPOT IDENTIFICATION

On the basis of the integrated risk map, we finally detected risk hot-spots, defined as contiguous areas that respect the conditions of a minimum number of co-existing threats having a relevant risk level. By changing these conditions we developed three maps characterized by: at least 1 threat with a very high risk value, 10 times the regional mean, or more (Fig.20a); at least 3 threats with medium risk value, 1.5 times the regional mean, or more (Fig.20b); at least 2 threats with high risk value, 3 times the regional mean, or more (Fig.20c).

To delineate the hot-spots, first the number of risks and their level with respect to the regional mean was calculated for each 1 km x 1 km square polygon. Then, all the terrain units satisfying the given set of conditions were selected, and contiguous terrain units were merged into large polygons. Finally, the area of each polygon was calculated, and the hot spots were reclassified according to their size.

In general, high risk hot spots include large urban areas, their main industrialized districts and the main traffic corridors (Milano and its northern neighbourhoods, Bergamo and neighbourhoods, Brescia, Sondrio, Varese), due to the high value of the exposed elements, together with a high number of road accidents and work injuries. When considering the co-existence of different threats with lower risk values (Fig.20b, Fig.20c), hot-spots appear also in rural areas in Valtellina, in the northern area of the Milano province, in the prealpine valleys into the north of Brescia and Bergamo, and in the low Po plain.

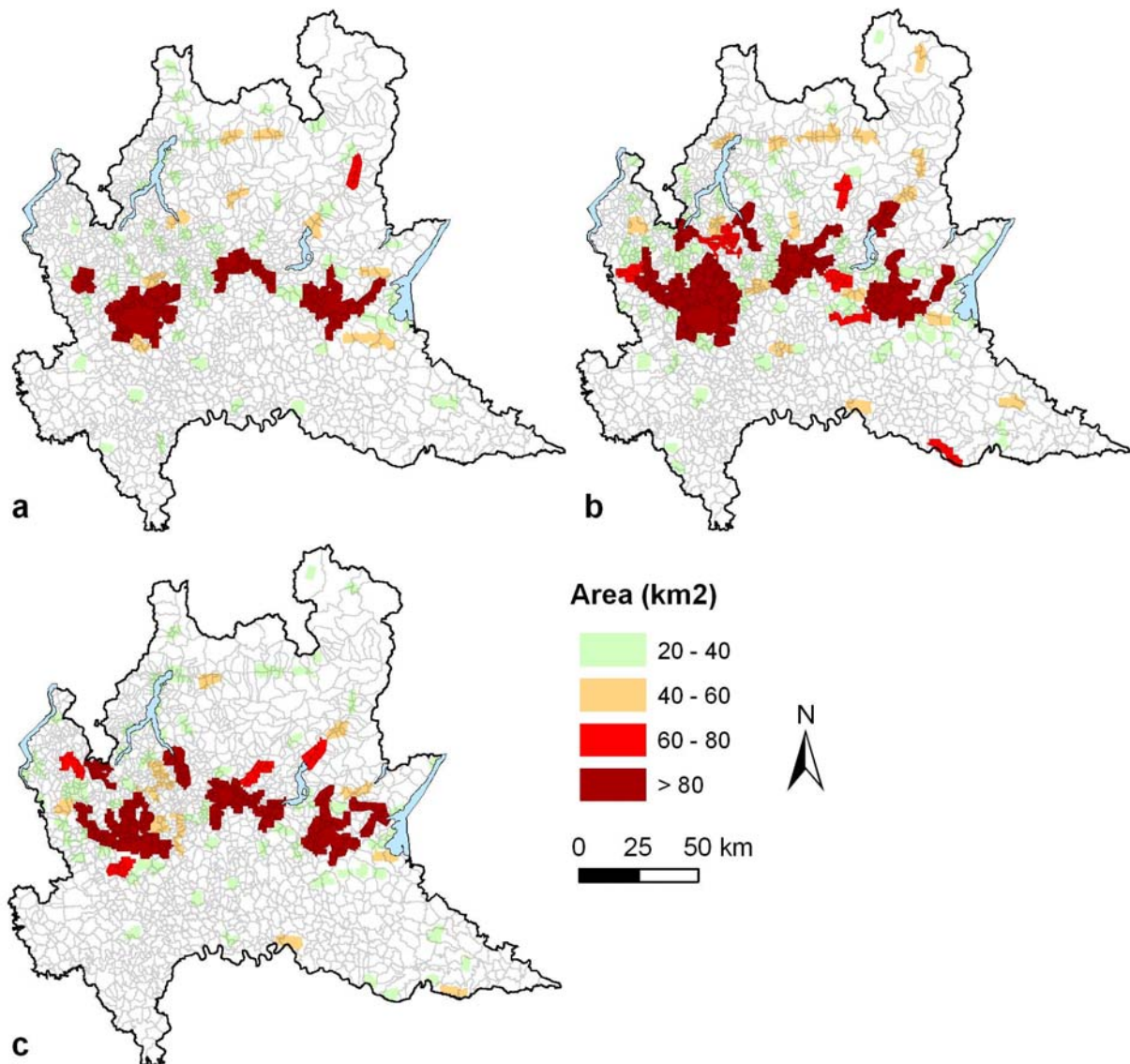


Fig. 20. Hot spot risk areas, delimited by the number and relevance of coexisting risks, reclassified according to the size of the contiguous area: a) at least one threat with very high risk (10 times the regional mean); b) two threats with high risk (3 times the regional mean); c) three threats with medium risk (1.5 times the regional mean).

The analysis of the percentage of square polygons with more than a certain number of threats (Fig.21) shows that many cells are affected by more than one threat, especially for moderate risk level (e.g., 40% of cells have more than 2 risks exceeding level 1). This suggests that the coexistence of threats in Lombardy is significant, thus justifying the analysis of the risks in an holistic way. Large areas and many people are threatened by various risks that do not reach high levels, but can interact to originate complex or domino effects. In order to develop an efficient mitigation strategy, the coexistence of them must be taken into account.

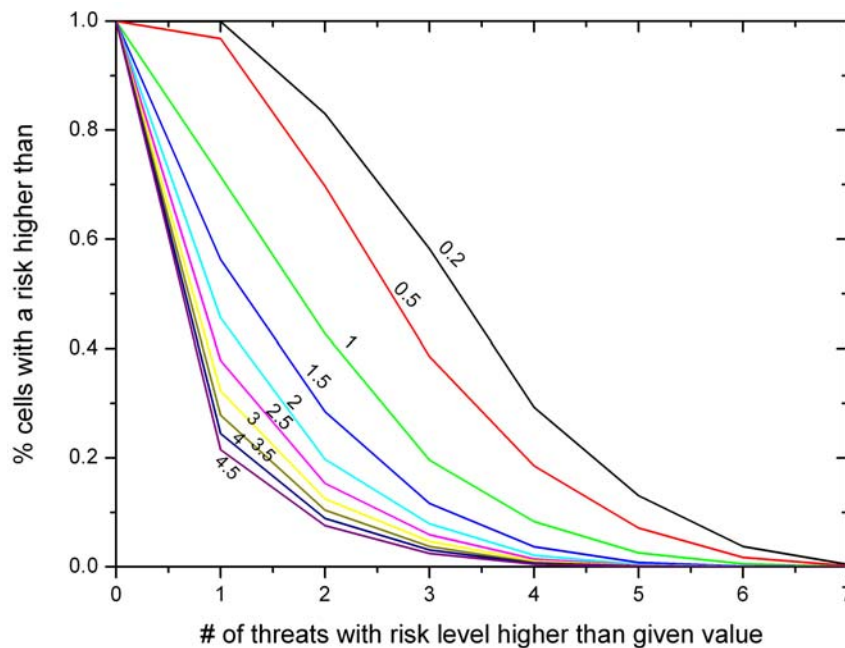


Fig. 21. Percentage of cells affected by a number of risks exceeding a certain risk level (normalized by the regional mean).

9 SENSITIVITY ANALYSIS

Due to the uncertainties associated to the weighting of the indicators, a sensitivity analysis was performed to evaluate the variation of outputs to small changes in the weight. As example, the sensitivity analysis are presented, related to: 1) the scores of hazards and exposed elements for hydrogeological physical risk, 2) the weights of aggravating indicators of hydrogeological risk, and 3) the weights of all different threats for their aggregation.

The hydrogeological physical risk is linearly correlated to the variation of both hazard sources and target scores. The sensitivity is higher for variables characterised by high scores, and large spatial diffusion (e.g., 500 years flood, Fig.22; discontinuous residential areas, Fig. 23). For the aggravating factor, F , the most sensitive indicators are the presence of a civil protection plan and the distance from hospitals (Fig. 24). For the integration of risks (Fig.25), the slope of the trend line simply corresponds to the weight of each threat, since the integrated risk is a weighted mean of the total risks. Hence, a percent variation in the larger weight causes larger variations in the integrated risk.

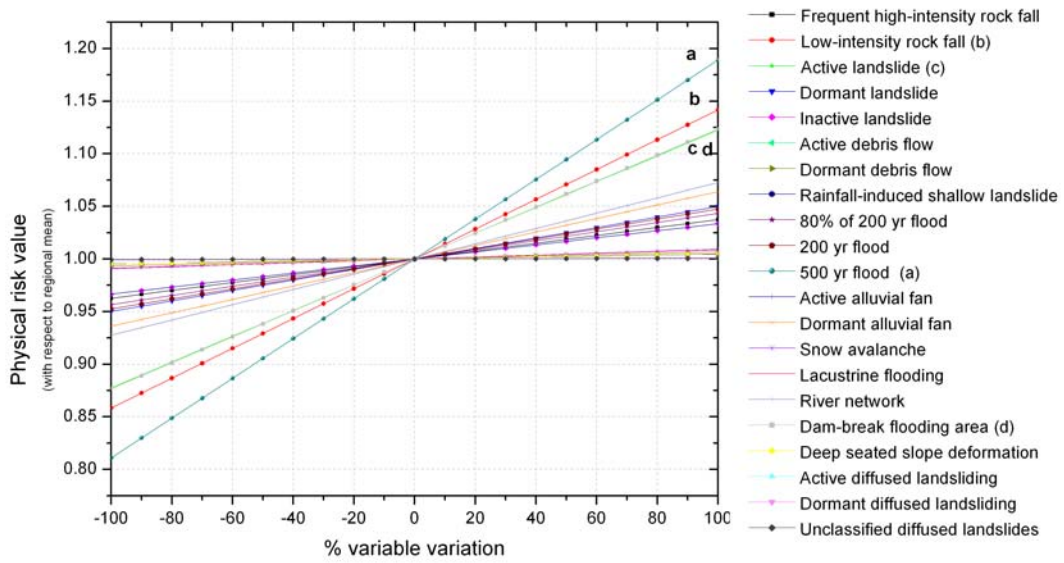


Fig.22. Sensitivity analysis for hazard sources scores. See legends for reference of letters a, b, c, d.

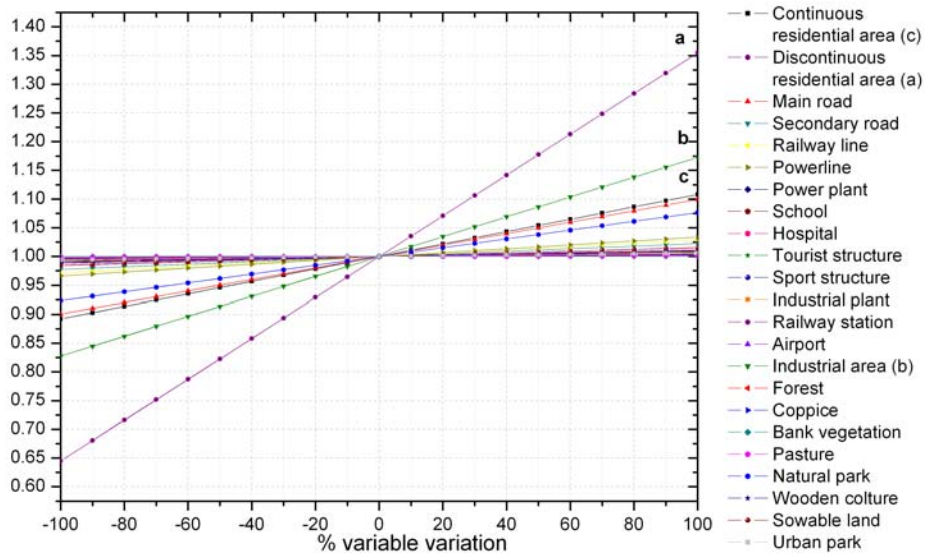


Fig.23. Sensitivity analysis for target value scores. See legends for reference of letters a, b, c, d.

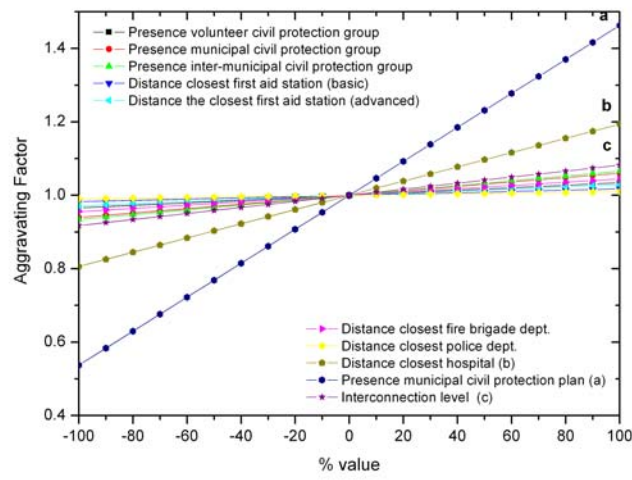


Fig.24 Sensitivity analysis for aggravating factor for hydrogeological risk. See legends for reference of letters a, b, c.

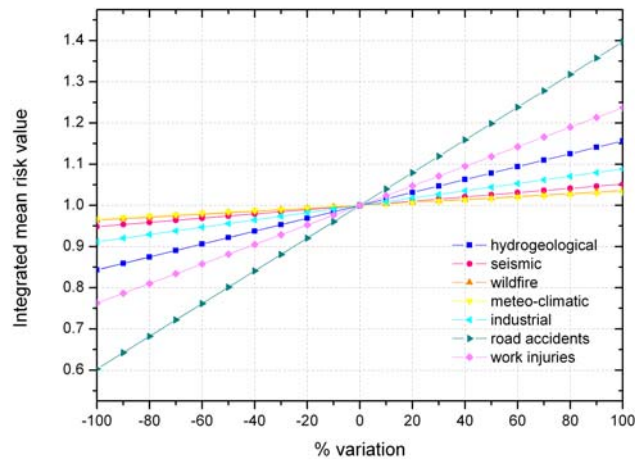


Fig.25. Sensitivity analysis for threat weights

10 DISCUSSION

The generation of multi-risk maps is a complex task that has been tackled in this part of the thesis. The first step of the analysis consists in the identification and mapping of the hazard sources. This step can present some difficulties related to: the data spatial resolution (especially for landslides, work injuries, lightnings, road accidents), the temporal window covered by the databases (e.g. work injuries, road accidents), the difficulty in defining the area of influence of some hazards (e.g., industrial accidents, wildfires), the availability of data for some risks (e.g. meteorological, industrial), for which we needed to limit our analysis to a sub-set of specific phenomena. As a consequence, the hazard sources are characterized with different accuracy and homogeneity, thus hampering the use of more rigorous methods (e.g., Probabilistic Risk assessment, PRA).

Weighting of indicators is a step that may introduce uncertainty. On a case by case approach, different techniques were selected to reduce this uncertainty, all based on expert knowledge: fuzzy logic was used to aggregate different dimensions of value, while AHP was used when the number of considered variables was limited. Otherwise, the use of AHP would have been too complex and time costly. This forced to perform a simpler budgetary allocation. Evaluating the uncertainty and its propagation in risk assessment is not simple at this scale of analysis, and feasible only for more detailed studies (Lari, 2009).

However, due to these uncertainties, a conservative approach was adopted, by always considering the worst possible case. This was done both in the identification and mapping of hazard scenarios, and in the evaluation of the aggravating factors.

With respect to previous multi-risk assessment studies, the methodology allows a higher spatial resolution. The spatial detail of local scale studies is preserved (Cardona and Hurtado, 2000; Masure, 2003; Cardona, 2001, and Barbat and Cardona, 2003) within a regional scale analysis, also considering different risks as in ESPON (2005) and UNDR/HOT SPOT projects (Dilley et al., 2005).

10.1 SPATIAL PATTERN OF RISK

The spatial pattern of different risks in Lombardy is governed by the distribution of either the hazards or the exposed elements: the first case is common for risks related to larger and infrequent events (hydrogeological, seismic, wildfire, and industrial risks), whereas the second is common for frequent, and evenly distributed events (road accidents and work injuries).

The spatial distribution of different threats in Lombardy is strongly controlled by the physiographic setting (e.g. landslides, avalanches), as results from the analysis of normalised total risk for all the municipalities located in plain, hilly, or mountainous areas, according to ISTAT (National Institute of statistics) classification (Fig. 26). To refine this analysis, we also grouped the terrain units according to the mean elevation in classes of 100 units, and we analysed the risk of each threat within all the elevation classes (Fig.27).

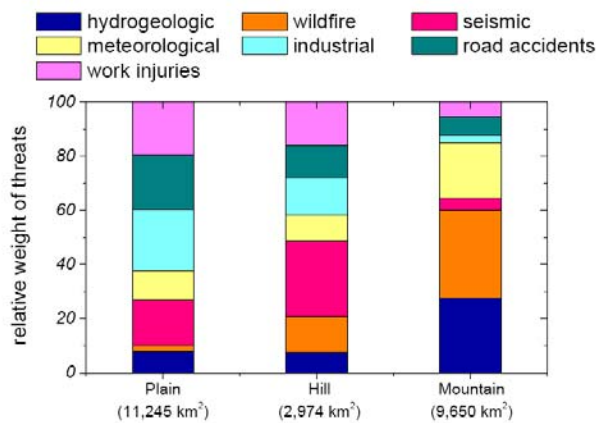


Fig.26. Total risks relevance for municipalities classified according to the physiographic setting.

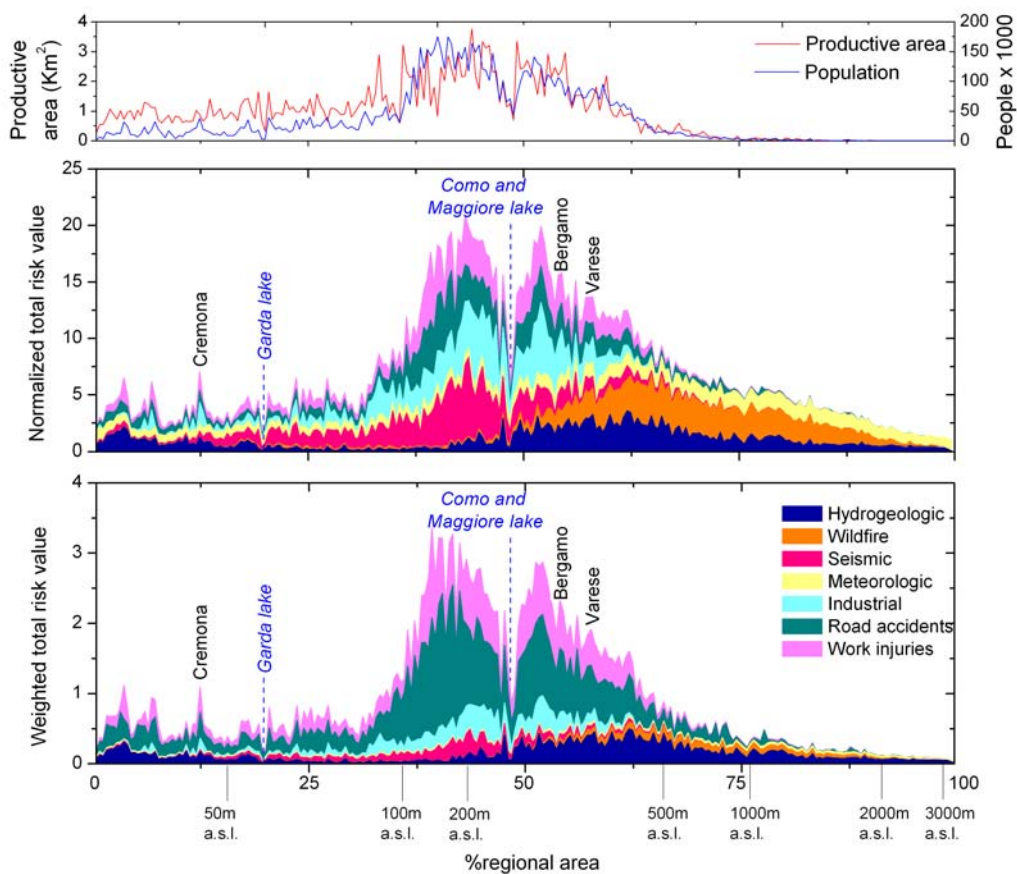


Fig. 27. Relevance of each total risk for different elevation quantile classes: a) distribution of population and productive activities, b) normalised superimposed risk values with respect to the regional mean, c) superimposed risk values weighted according to expert AHP weighting (Fig. 29).

The area below 100 m a.s.l., which occupy almost 35% of Lombardy, is characterised by a overall low risk level. This is a rural area, with a relatively low population density, scarce industrial activities, and with dominant threats related to road accidents, hydrogeological risk in the flooding area of the Po river, and a few localised industrial risks and work injuries (e.g. Cremona area).

The area between 100 and 200 m a.s.l. (almost 15% of the territory) shows the highest risk value. This includes the most populated zones (e.g., Milano and Brescia), and is affected by severe threats related to human activities (industrial risk, road accidents and work injuries) and to seismic risk (Brescia). Considering weighted risks, a strong dominance of road accidents is observed (Fig.27).

In the area between 200 and 500 m a.s.l. (almost 15% of the territory), we observe a decrease of the overall risk level, linked to a decrease of population density and economic activities. The dominant threats change progressively from technological to natural (landslide, wildfire) with the exception of seismic risk, which is independent from altitude. Above 500 m a.s.l (almost 35% of the area), the risk level decreases because of the scarcity of human-related exposed elements. In this area the meteorological threat appears to be dominant, merely because other risks are absent. Road accidents in mountain areas are locally relevant (e.g. higher Valtellina, Fig.20c) along strategic transnational roads (Fig.27).

In order to observe the relations with the population density, the mean physical risk value for each municipality was calculated (Fig 28). Work and road accidents are linearly correlated with population density: these threats are diffused on the whole study area, and then controlled by the spatial distribution of the elements at risk, i.e. people.

Industrial and seismic risks appear to be mostly influenced by the distribution of the hazard sources: spot-like in the first case, diffused but increasing towards north-east in the second.

Wildfire and hydrogeological risks do not show a clear correlation with the population density: being relatively localised, they affect only some towns of the area, generally in the mountainous part and characterised by low population density (e.g. Sondrio).

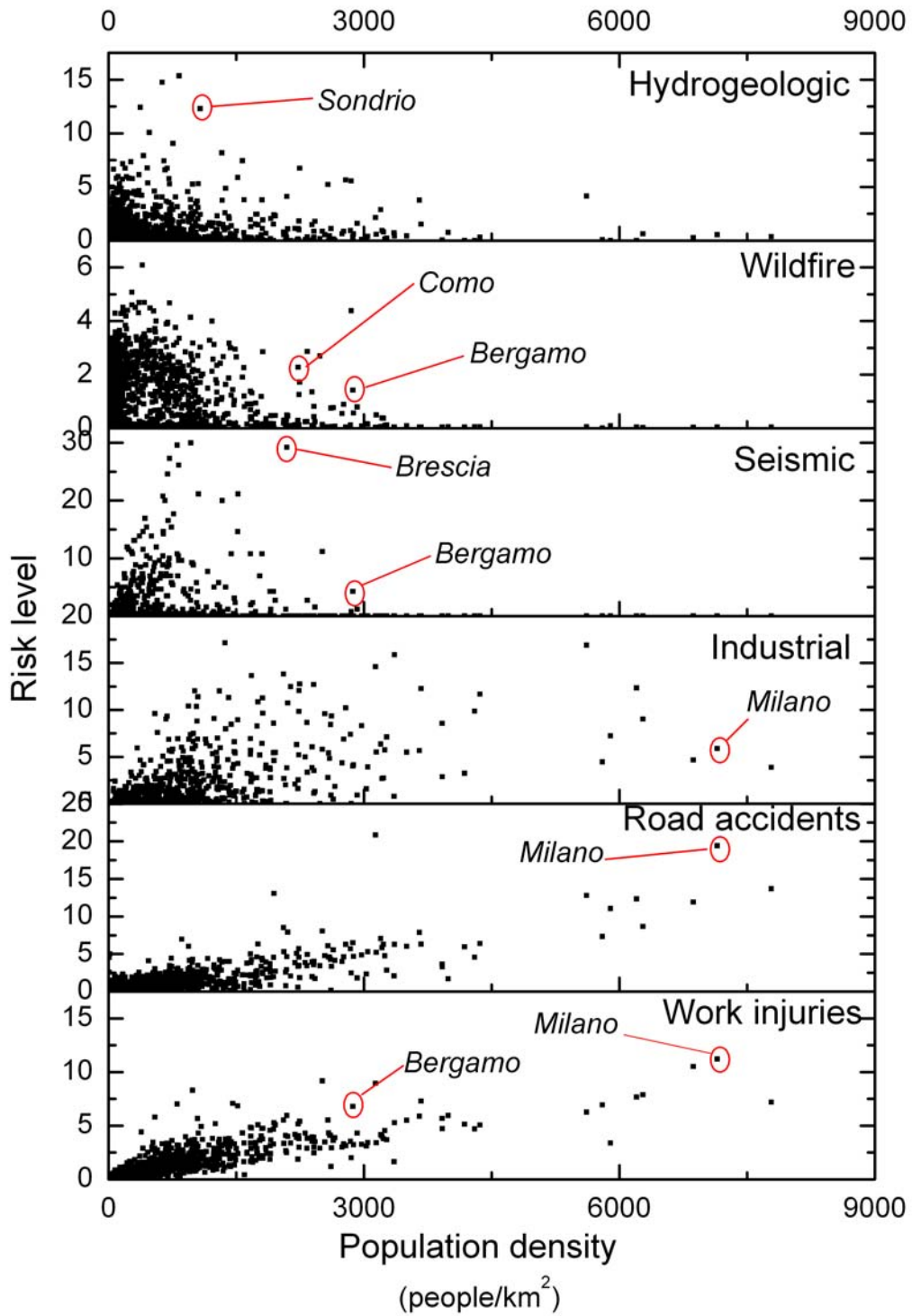


Fig. 28. Averaged level of risk (normalised by the regional mean) with respect to the population density of each municipality.

10.2 INFLUENCE OF RISK PERCEPTION ON WEIGHTING PROCESS

As mentioned above, the weighting process is intrinsically subjective. For this reason, the results can be conditioned by the individual attitude or point of view of stakeholders, inhabitants and experts involved in weighting. In order to further investigate this issue, a simple Budgetary Allocation was performed, considering four possible alternatives: expert opinion, risk averse attitude, social perception, and political perception. In Figure 25, the relative averaged weights assigned to each threat from the different perspectives are shown.

Weights obtained through Budgetary Allocation differ from those derived by the AHP method. The AHP weights show a stronger importance of road accidents and work injuries, that together amount to 60 % of the total. In the Budgetary Allocation method, the attribution of the weights is direct; this can lead single experts to be reluctant and more cautious in attributing strongly unbalanced weights.

Risk aversion is an attitude to risk where relatively frequent small accidents are more easily accepted than one single rare accident with large consequences, although the total expected losses are equal in both cases. In this case, industrial and seismic risks, which can potentially have catastrophic consequences, are perceived to be more severe than road accidents and work injuries (Fig.29).

The social perception is considered as the perception of common non-expert people who accept more easily voluntary rather than non-voluntary risks, and who consider more critical those risks that could be potentially controlled by the public administrator through defensive works, regulations and other mitigation strategies. In this analysis, this implies that a typical risk related to single behaviour, such as road accident, is perceived as less important, and seismic risk is also under-estimated because fatalistically perceived as uncontrollable (Fig.29).

Finally, the political perception is strongly conditioned by the public administration objectives and by the management duties: a strong importance is given to the threats related to human activities or to planning strategies (Fig.29).

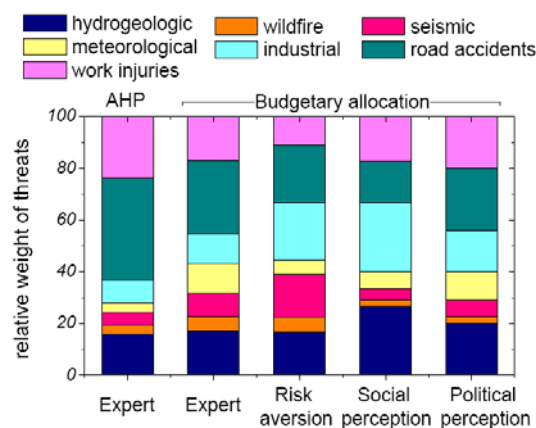


Fig. 29. Different risk weights as obtained through various expert panels (technical, political, social, risk averse)

10.3 HIGH RISK/HOT-SPOT AREAS

Within a multi-risk framework, the criticality of an area depends on: 1) the number of interacting risks that co-exist at the same place, 2) the level of each risk (a lonely risk, if acute, can be problematic and conditioning for land planning and development). On the basis of these criteria, contiguous areas were detected representing risk “hot spots”. Three possible scenarios for the identification of hot spot areas are proposed here. The first scenario highlights areas with maximum risk level, but does not account for the co-existence of risks. The other scenarios consider the simultaneous presence of more than one risk. Since this is a predisposing factor for domino effects and interactions that can increase the criticality of an area, for example by increasing the aggravating factor (destruction of facilities, roads, infrastructures), the second and third scenarios look preferable (Fig.20). The choice among these two scenarios depends on the characteristics of the territory, and the complexity of the interactions among different processes.

The extent of the “hot-spots” can be important for land planning, for development and prioritisation of mitigation strategies. Large “hot spots” are more critical for risk management because they include large and complex socio-economic systems with potentially strategic infrastructures and services. The larger the “hot-spot”, the larger the external area of influence that can be potentially affected in case of a system breakdown.

Only few large “hot spots” (Fig. 30) affect high percentages of the total exposed value: the three largest areas include 30% (scenario b), 22% (scenario c), 19% of the regional value (scenario a) and most of the population (see Tab.7). For this reason, some actions focused on these areas could be significant to control a large part of the regional criticalities. This underlines the relevance of these results in developing a risk mitigation and management policy.

Tab. 7: Hot-spot risk areas, extension and exposed value

scenario	# threats	Risk level	Hot spot area (km ²)	population (# people)	residential area (km ²)	productive area (km ²)	% regional area	% value exposed elements
a	<i>At least 1</i>	<i>Very high</i>	3264	5,300,516	620.4	284.8	14	40
b	<i>At least 2</i>	<i>high</i>	5228	6,637,056	911.3	384.2	21.9	56
c	<i>At least 3</i>	<i>medium</i>	4164	5,866,495	778.4	327.9	17.4	48

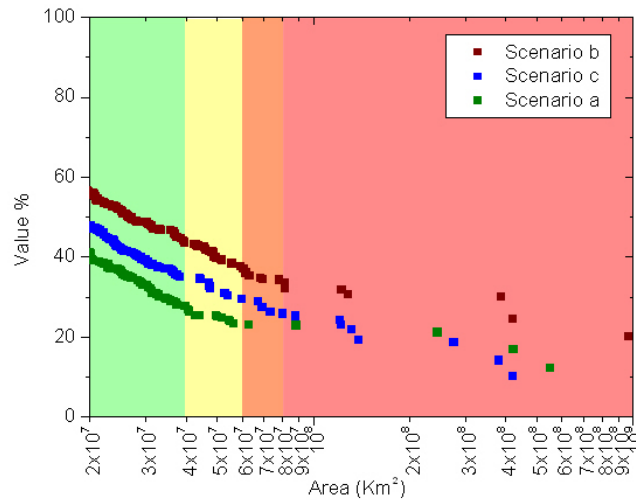


Fig. 30. Plot of the percentage of total exposed value for each hot spot and for the three scenarios (cfr. Fig.16) with respect to the extent of the area. Colours indicate classification of area extents as in Fig.20.

11 CONCLUSIONS

Combining risks with different characteristics, metrics and distributions is extremely difficult, but, as demonstrated by the recent trend in public administration requests, it is useful for some public administrations, which have to manage and plan mitigation strategies not only for critical situations deriving from a single specific risk, but for the territory in its complexity and interaction between threats, processes, and dynamics.

Presently, the Lombardy region lacks the conditions for a fully quantitative, probabilistic multi-risk analysis, because of heterogeneity in data quality and availability. For this reason, only an indicator based approach was possible at the scale of the analysis. For the same reason 1 km x 1 km terrain units were adopted, which can be considered reasonable with the current data availability and scale of the analysis.

Although the analysis is perfectible, it allows the detection of integrated risk areas and “hot-spot” areas useful for decision making and prevention policies, and for the realisation of integrated area management plans.

c

PART II

INTEGRATED AREA PLANNING

1 INTRODUCTION

Among the hot spot areas identified with the regional scale analysis (Part I), some areas present high risk levels combined with the coexistence of natural and anthropogenic threats. Lower Valtellina (Fig.1) resulted to be the most critical mountainous territory, together with Lower Val Camonica, Val Trompia and Val Sabbia (Fig.1). The nature of these mountainous and hilly territories is coupled with a strong urbanisation and development of productive activities, increasing the possible damaging effects of natural hazardous phenomena.

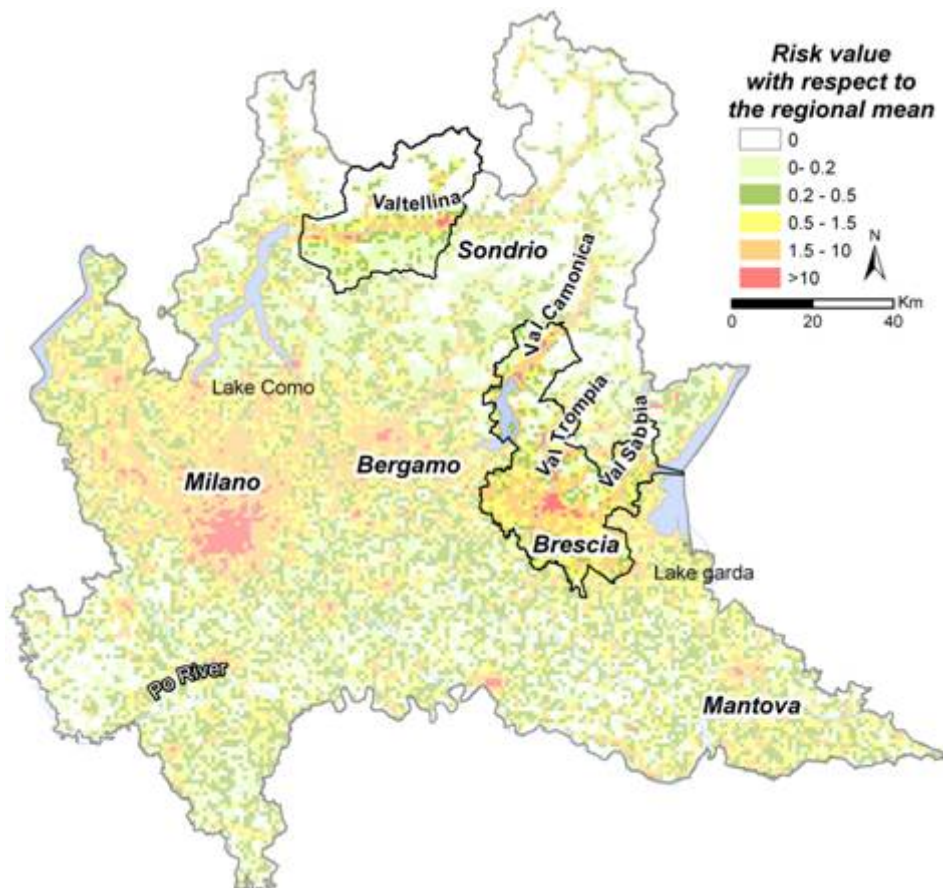


Fig.1. Study areas for integrated area plans. Integrated risk is shown (see Part I).

Lower Valtellina presents different sources of risk, both natural and anthropogenic. Road accidents are very frequent in this area (Fig.2). The main road is State Road (S.S.) n.38 dello Stelvio, where ordinary, goods and tourist traffic is very intense. The traffic runs through a double way road passing through major settlements

in the valley (mostly Delebio and Morbegno) with some critical passages. In Delebio, for instance, two deaths per year are registered.

In the study area of Brescia (Fig.3), the Ex SS510 Sebina Orientale is one of the provincial roads with the highest level of risk in Lombardy. It registered 39 casualties and 479 injuries in the period 1996-2000 along its 47,5 km.

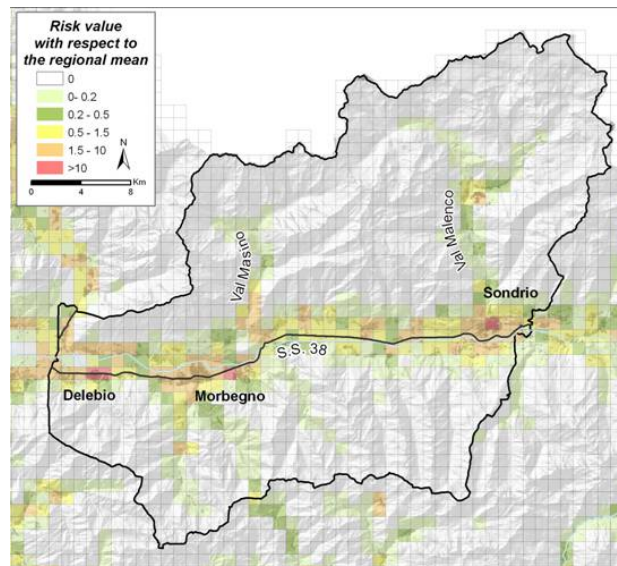


Fig 2. Road and work accidents risk distribution for lower Valtellina, represented by 1 km x 1 km cell (see Part I). Locally (Delebio, Morbegno, Sondrio), the risk level is more than 10 times the regional mean.

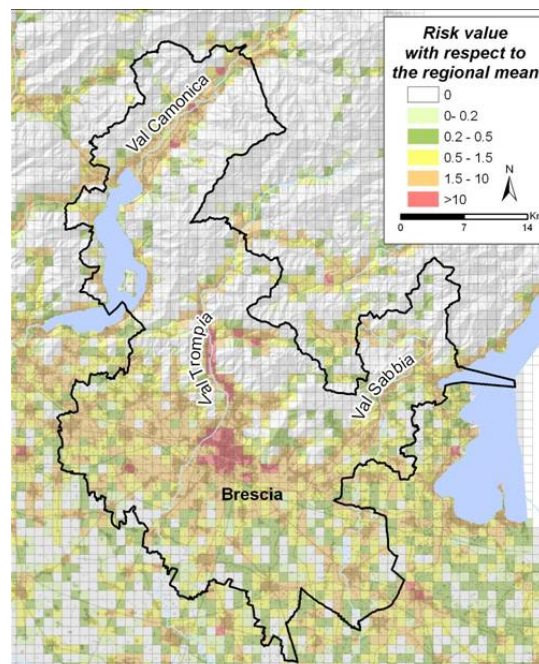


Fig 3. Road and work accidents in Brescia and valleys. An some places (Brescia, low Val Trompia), the risk level is more than 10 times the regional mean.

The two study areas are both characterized by a large number of different productive activities. In lower Valtellina Major accident plants (as defined by D.lgs. 238/2005), are absent. In the Brescia area, 11 Major accident plants are present. In both cases, the risk deriving from diffused productive activities is in general more significant.

Natural risk is very significant in correspondence of urbanised zones, for both study areas (Fig.4 and 5). Along the valley bottom, dominant risks are river floods, fan floods, shallow landslides and debris flows. In the secondary valleys, landslides and locally wildfires are significant. The last event occurred in Valtellina dates July 2008, involving many torrents that damaged the village of Rodolo and Selvetta producing heavy damages to the buildings. In 2000, a debris flow in Dubino caused two deaths.

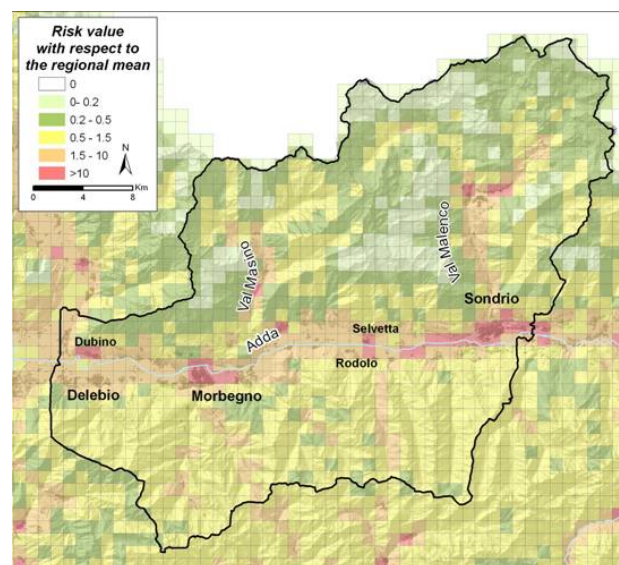


Fig 4. Natural risk in lower Valtellina. In some areas of the valley bottom and of secondary valleys the risk level is more than 10 times the regional mean.

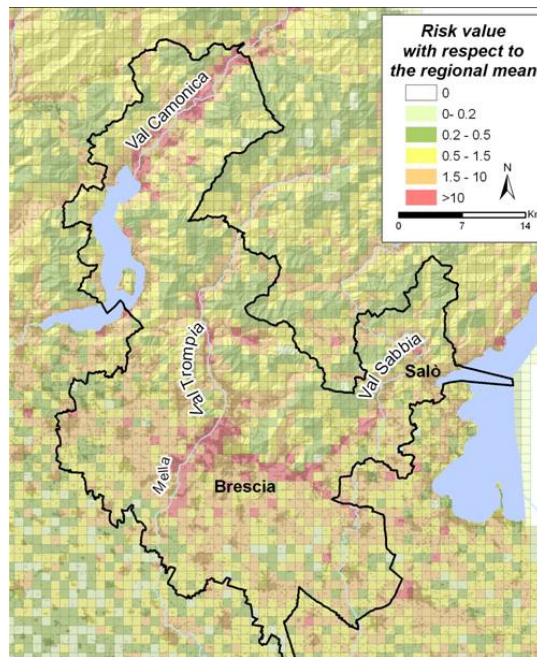


Fig 5. Natural risk for the Brescia area. In some areas of the city of Brescia and of valleys, the risk level is more than 10 times the regional mean.

The integrated risk map shows that the risk reaches larger values at the valley bottom and in the secondary valleys (Fig.6 and 7). On the valley bottom, the most critical sectors are the alluvial fans, where the urbanization has been intense. In Valtellina, the high level of risk is not related to the floods of the river Adda, which is strongly embanked and whose floods involve cultivated areas immediately near to the river, but it is mostly due to slope processes, alluvial fan floods or road accidents along State Road 38. In the area of Brescia, the river Mella threatens the city of Brescia. All the territory is affected by a high level of seismic risk, the highest in the framework of region Lombardy. The last event of magnitude 5.2 took place in 2004 in Salò and Val Sabbia area.

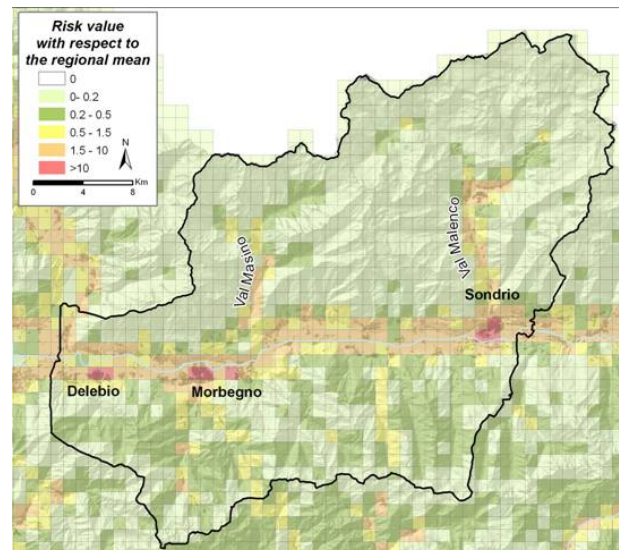


Fig 6. Integrated risk in lower Valtellina. Risk is concentrated in the valley bottom, where the population density is higher. Risk values are also significant in Val Masino and Valmalenco.

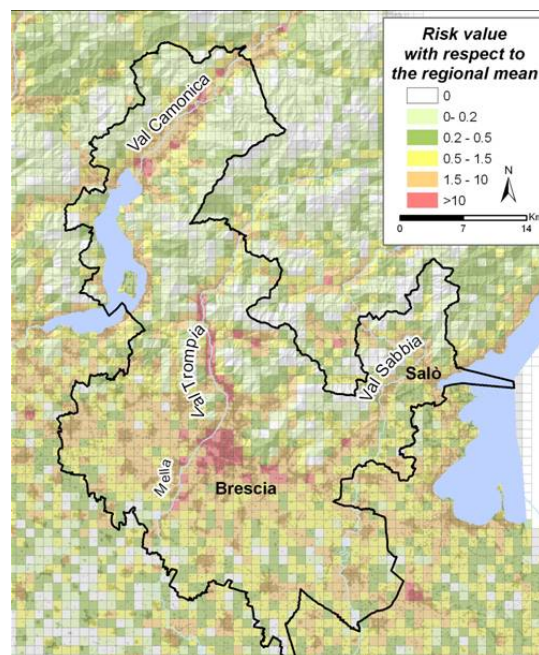


Fig 7. Integrated risk for the Brescia area. Risk is concentrated in the piedmont zone, including the city of Brescia, and valley bottoms, where the population density is higher.

2 INTEGRATED AREA PLANS

Integrated area plans are local development programs, aimed at the creation of a synergy among economic development, environmental resources, and social context, with the purpose of favouring a better quality of life for people living or working in the area, and of designing a development strategy accounting for the complexity of the context.

Integrated area plans are developed by the Administrations in collaboration with public and private stakeholders, and with the participation of local population. Lombardy region in 2008 activated 4 integrated area plans on the risk hot spots detected by PRIM (2007), for the areas of Milano, Lecco, lower Valtellina, and the valleys of Brescia.

In planning the future of a territory, natural and technological risks and their interactions must be considered. Integrated area plans provide a quantitative tool to design structural and non structural actions, with the aim of preventing risk, reducing or mitigating its components: hazard, vulnerability, or exposed value.

To design an effective prevention strategy it is important to detect the most vulnerable areas with respect to the different threats, or the ones potentially involving the largest number of people or economic value.

In order to achieve this objective, the steps for the realization of an integrated area plan are:

- mapping of the sources of hazard
- simulation of the propagation of the phenomena
- assessment of a risk value

For the lower Valtellina and the Brescia valleys rockfalls, shallow landslides, debris flows, river floods, alluvial fan floods, and earthquakes were simulated and analysed. For Valtellina, work injuries, road accidents, transport of dangerous materials, and industrial accidents were also considered.

In this thesis, no domino effects were considered, even if they are extremely important in areas with strong natural and human components. Domino effects analysis will be developed based on the results obtained in this work.

To develop integrated area plans, datasets of events and exposed elements related to Lombardy region were strongly implemented by means of bibliographic researches, digital database construction, and field work (Bordonaro, 2009; Bariselli, 2009; CRASL, 2009). In the analysis at the regional level (see Part 1) the entire area was divided in 1 km x 1 km square polygonal territorial units. At the scale of analysis of the integrated area plans, the level of detail was improved, considering 20 m x 20 m territorial units, which allowed a higher spatial resolution, and a better calculation process and revision. Data were analysed in a raster format.

3 STUDY AREAS

3.1 LOWER VALTELLINA

3.1.1 GEOGRAPHIC AND ECONOMIC SETTING

The area spreads over 1150 km² and includes 40 municipalities, among them Sondrio and Morbegno, which are the two most populated municipalities (almost 22,000 and 12,000 inhabitants, respectively) (Fig.8). In total, 90,278 people live in the study area (ISTAT, 2007), with a mean density of population of 76 people/km². It is a low value if compared with the Italian national mean (197,6 p/km²) and regional mean (404,1 p/km²), since it includes a wide mountainous territory with a very low density. Considering only the valley bottom, the density grows up to 790 p/km².

The road network, due to the mountainous territory, is not very developed. The whole area is crossed by the Stelvio state street SS 38, which is also the main road along the valley.

The orientation of the valley influences sun exposure, so that the mountain side exposed to South and the one exposed to North have different vegetation and agricultural use. The first one has been used since centuries to develop an intensive agricultural production up to 600-700 m a.s.l., the second has a prevalent silvo-forestal vocation.

The agricultural activities in the area are widely diffused: 2,512 ha are sowable land, 3,078 ha wooden cultures (apple trees and vines), 2,185 ha permanent grasses and 75,088 ha grazing land. In the valley bottom permanent grasses and corn cultures are prevalent. On the alluvial fans, especially between Sondrio and Tirano, the fruit-farming is very diffused (50% of regional production of apples comes from this area). In most cases, vineyards occupy the south-facing slopes.

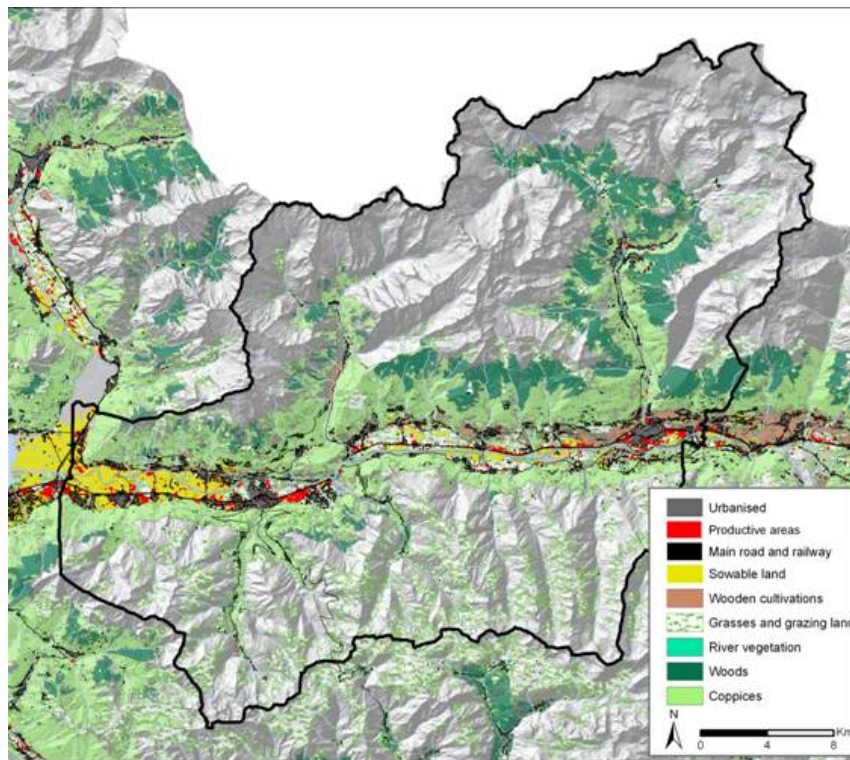


Fig.8. Land use of the lower Valtellina area considered in risk assessment (DUSAF, 2007)

3.1.2 GEOLOGIC SETTING

Valtellina is the major valley of Lombardy, trending East-West, being superimposed on the Insubric Line. Insubric Line is visible on the low northern side of the valley, especially in the North of Dubino, in low Val Masino, in the area of Postalesio and in lower Val Malenco till the area of Treviso. It runs from Ponte in Valtellina to Boalzo; after the alluvium of the valley bottom, it is again observable in Stazzona on the eastern side of the valley, along Val Camonica. In Valtellina, Insubric Line runs parallelly to the rock formations, in other places it can become transverse. As said in Part I, the Insubric Line divides the Southern Alps from Austroalpine and Penninic domain. In particular, see Fig.9.

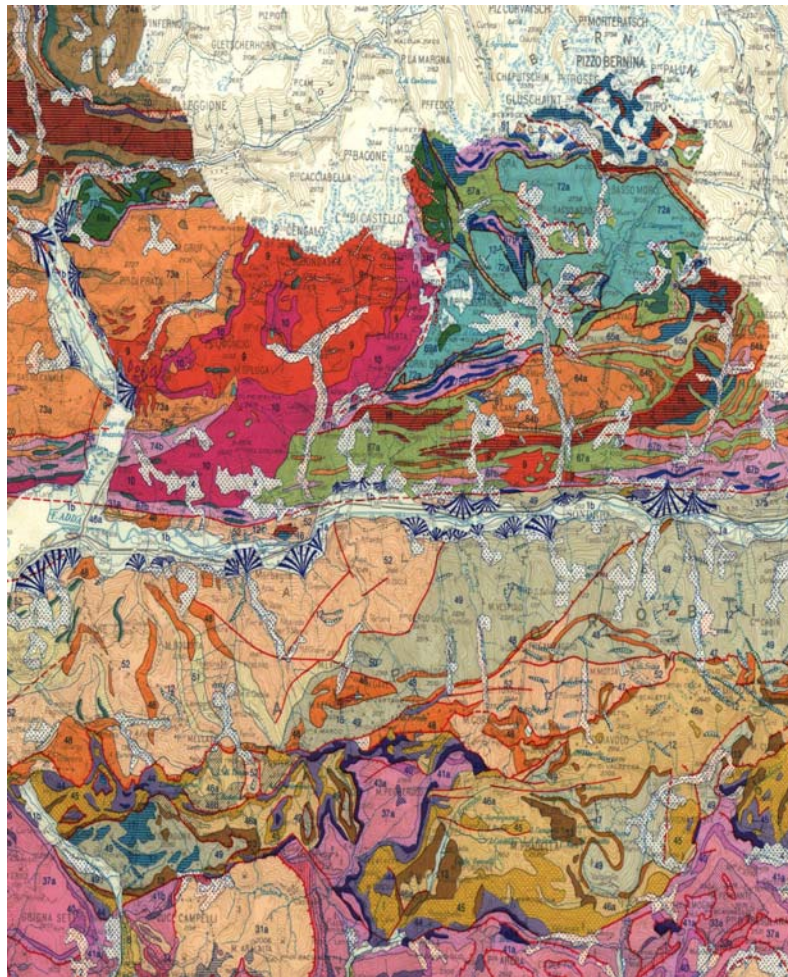


Fig. 9. Geologic map of the study area. Carta Geologica 1:250,000, Regione Lombardia

3.1.3 GEOMORPHOLOGICAL SETTING

Valtellina is surrounded by high mountain groups (Bernina, Ortles, Orobic), closing the valley to the North, East and South, with the outlet in correspondence of Como lake. In general, the two flanks are morphologically different (Fig.10). The north exposed side is characterised by many secondary deep and narrow valleys, North-South oriented. In general, they appear to be mature valleys, lacking intra basin sediment stores.

The South oriented side is characterised by fewer wide catchments. These are morphologically evolved basins, with secondary valleys and significant sediment storages in alluvial and debris fans inside the basins. On the southern exposed side many villages are located, aligned along a climatically favourable area suspended over the main valley. This is an important element in risk analysis, offering an alternative communication line with respect to the main roads in the valley bottom.



Fig 10. Elevation difference between northern (on the left) and southern sides (on the right) (from Google Earth).

Quaternary deposits are largely represented, and can reach significant depths in the valley bottom. At the outlets of the tributary valleys, rivers built large alluvial fans, (e.g. at Sondrio and Morbegno) (Fig.11).

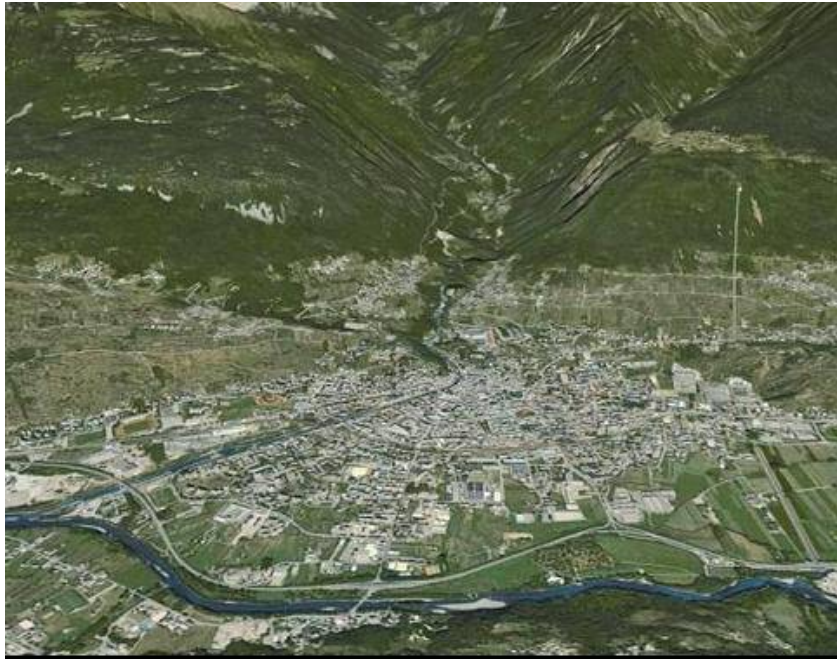


Fig 11. Alluvial fan of Sondrio (from Google Earth).

The deposits of river Adda, along the valley bottom, are often delimited and constricted by the wide alluvial fans. These sediments are recent, and built of coarse materials, in prevalence gravel, in tracts of river bed with a higher energy, and of finer sediments, sand and silt, in marshy areas with low or null energy.

3.1.4 HYDROGEOLOGIC AND HYDROGRAPHIC SETTINGS

The geographic position and the geological-geomorphological conditions of Valtellina control its hydrologic structure.

The area is in the context of a typically alpine climatic and morphologic landscape, with abundant precipitation, large water reservoirs (lakes and glaciers) and steep slopes. Furthermore, the presence of highly-permeable formations structure, contributes to accentuate the irregular distribution of water resources. The hydrologic system of Valtellina is composed by a main collector (river Adda) and by a large number of tributaries discharging from the lateral valleys (Fig.12).

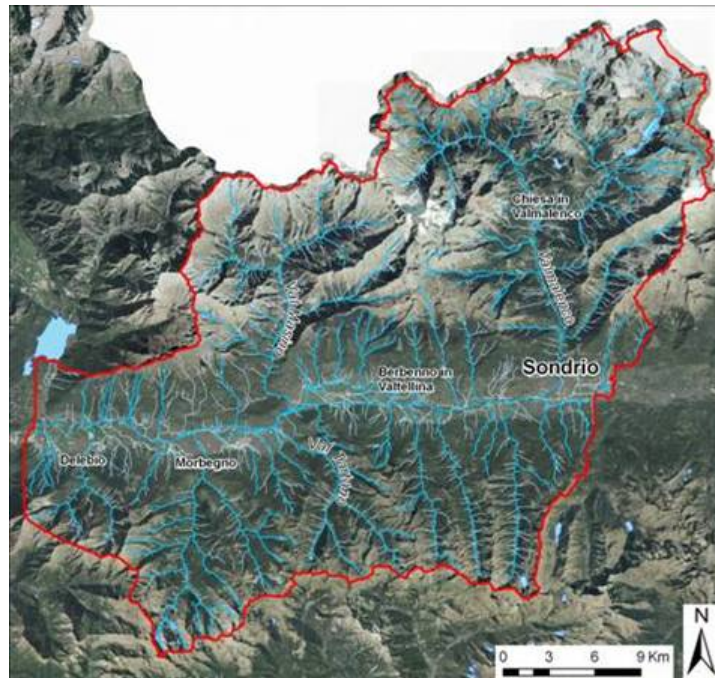


Fig 12. Hydrographic network of the study area

Hydrography has a regular structure, being strongly conditioned by the Insubric line, and by the secondary ones. River Adda is imposed sub-parallelly to the Line, while the secondary torrents are generally disposed orthogonally. River Adda flows from East to West into Como Lake.

A large number of springs is present in the valley, often with significant discharge, sometimes used for urban supply.

Main rivers are Adda, Bitto, Masino, and Mallero (Fig.13).

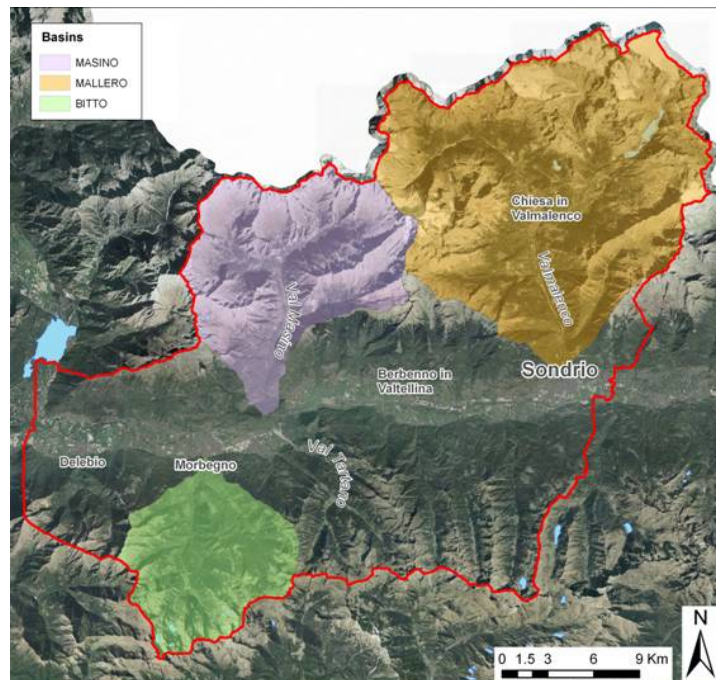


Fig 13. Masino, Mallerio and Bitto basins

3.2 BRESCIA

3.2.1 GEOGRAPHICAL AND ECONOMIC SETTING

The study area of Brescia is located between Lake Iseo and Lake Garda, and includes lower Valcamonica, lower Valtrompia, lower Valsabbia and part of the plain.

The area has an extension of 1,508 km² and includes 82 municipalities, among them Brescia, Darfo Boario Terme, Gardone Valtrompia, Salò and Montichiari. 727,000 people live in this area (ISTAT, 2007), with a mean population density of almost 250 p/km². Valley bottoms are strongly urbanised, and densely populated, especially in Val Trompia.

Productive activities are quite developed in the valley bottom and in the plain. (Fig.14).

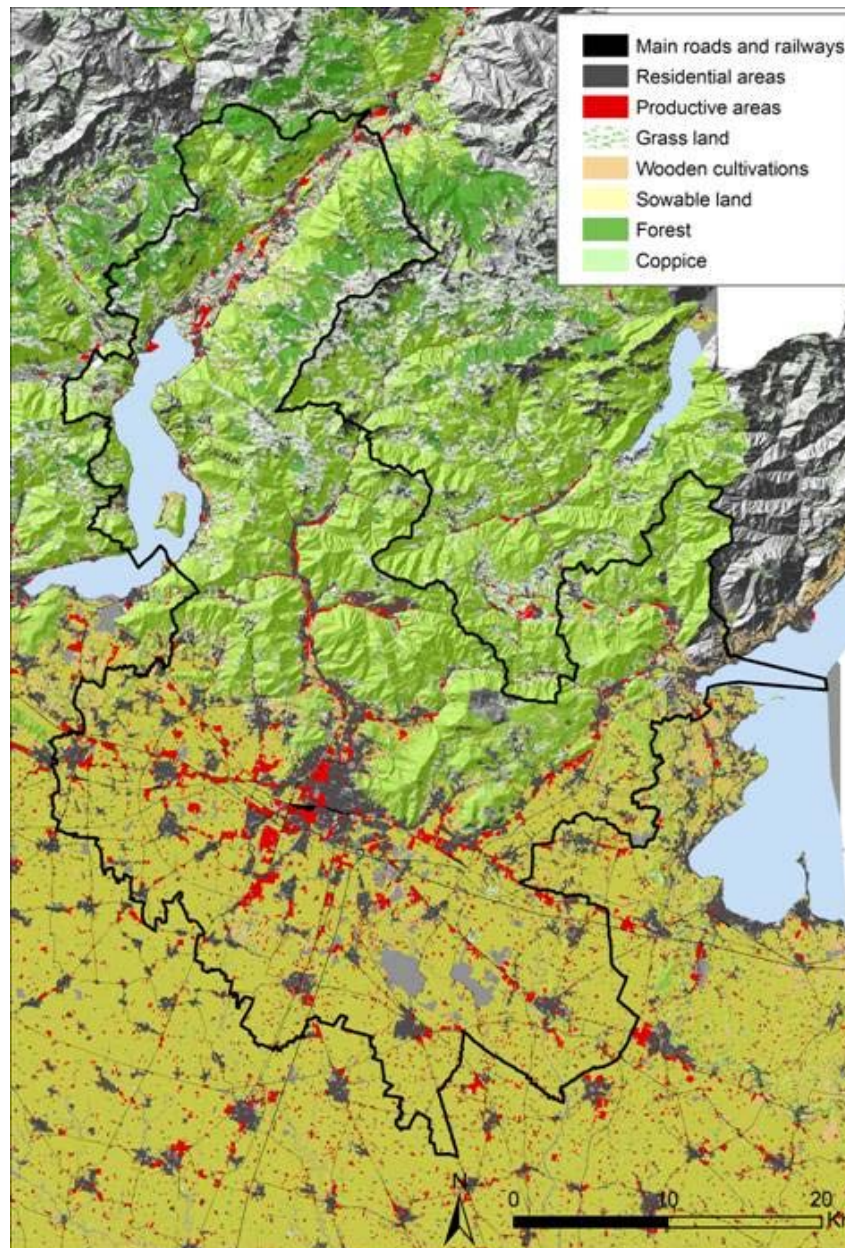


Fig.14. Study area of Brescia

3.2.2 GEOLOGIC AND GEOMORPHOLOGICAL SETTING

Lower ValCamonica, crossed by river Oglio, is characterised by a large and plain valley bottom, built of sands and silts of fluvial (or in minor part lacustrine) origin, deposited after the retreat of the Wurm glacier. Slopes are asymmetrical, less steep the oriental one, where Permian and basement rocks crop out, steep and rocky the western one, built of a Triassic sedimentary succession. The dominant tectonic structures are faults, some of them already active during Permian and Trias, and thrusts of the western slope of the valley.

River Mella crosses orthogonal the main structures of Val Trompia. Towards the North, more and more ancient terrains crop out. The cause of this structural asset is to be found in the presence of some tectonic surfaces immersing to the north, with variable inclinations, causing the superimposition of the more ancient units on the more recent ones. The sense of the tectonic transport is from north to south. Mella tributaries incise laterally and in orthogonal direction its course some minor valleys west-east oriented. Slope morphology is generally irregular.

Val Sabbia is incised by the river Chiese and its tributaries. The morphology is quite complex. In the south, morainic hills face the plain. A karstic plateau is located in the municipality of Serle, where sinkholes, caves and underground tunnels allow the flow of the water. Following the Chiese river towards the north, it suddenly changes direction to north-west. On the left, two lateral valleys: Val Collio and Val Degagna. Rocky slopes characterise the landscape, passing from limestone to dolomite. Large fluvial terraces are here located.

The plain included in the study area is characterised by the presence of rivers Mella and Chiese and by some weak relieves. In correspondence of the prealpine margin, the rocky outcrops immerse suddenly under pliocenic-quaternary deposits of the plain. These are continental sediments of fluvioglacial, eolic, deltaic and fluvial origin, followed in depth by sea deposits, dating lower Pleistocene and Pliocene. Quaternary deposits are more than 1.000 m. deep. Geotechnical and geophysical data and surveys show the presence of a buried ridge crossing the plain with south west - north east direction, justifying the emergency of some smooth relieves (Fig.15 and 16).

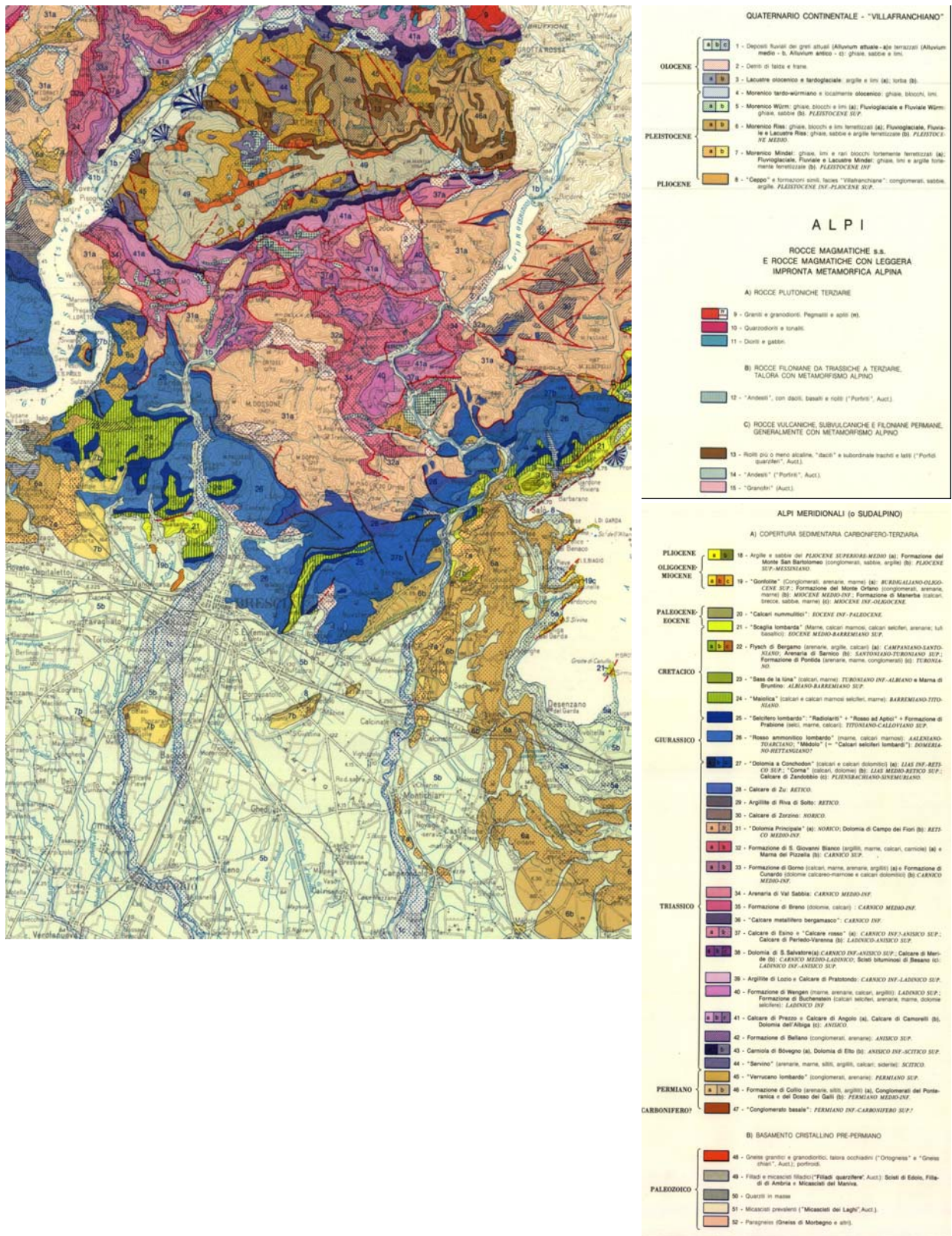


Fig.15. Geologic map of the study area. Carta Geologica 1:250,000, Regione Lombardia

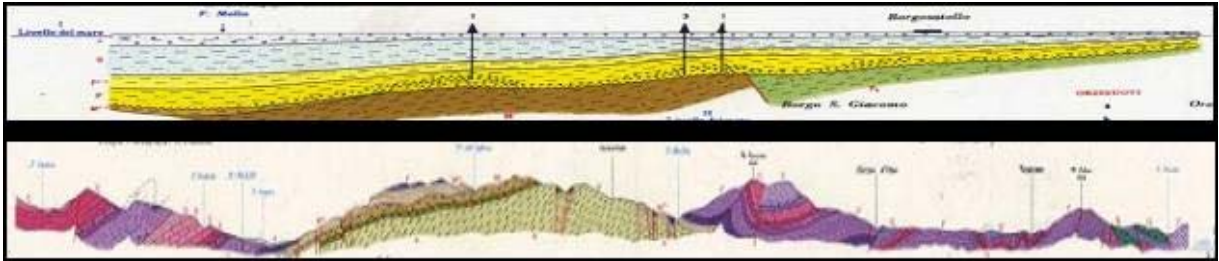


Fig.16. Sections- type of the study area: Leno-Brescia (a), Esine –Vestone (b)

3.2.3 HYDROGEOLOGIC AND HYDROGRAPHIC SETTINGS

River Oglio is an important affluent of River Po. It runs through Val Camonica receiving a large number of tributaries, among them Mella and Chiese, on the left side, in the plain. In Val Camonica it feeds Lake Iseo. River Mella runs through Val Trompia and crosses the city of Brescia, flowing toward Oglio. Chiese runs through Val Sabbia, and flows toward Oglio in the lower plain (Fig.17).

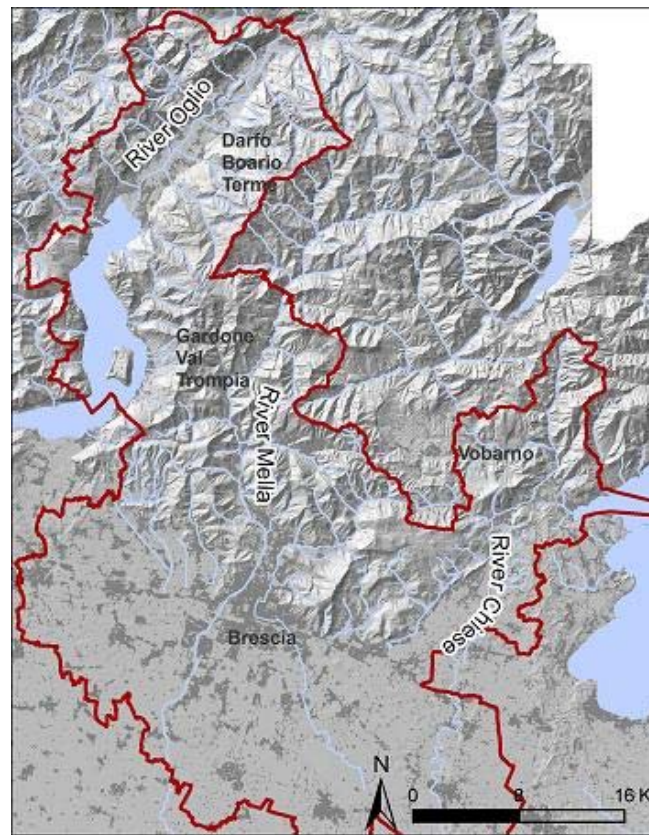


Fig.17. Hydrographic network of the study area

4 DATA IMPLEMENTATION

4.1 EXPOSED ELEMENTS

With respect to the analysis at the regional scale, for the two hot spot areas a higher level of detail was required for developing Integrated Area Plans.

First, a manual detailed validation of the data provided for the whole Region was performed, in relation to the localization of sensitive elements as schools, hospitals, and power plants. This allowed to improve the precision of the localization and the number of mapped elements (Bordonaro, 2009; CRASL, 2009). Then, new elements were introduced in this step of the analysis, such as commercial centres, markets, cinemas, fairs, airports, filling stations, hospices, barracks, first aid stations, heliports, churches, cemeteries (Bordonaro, 2009; CRASL, 2009).

4.2 HAZARD

All existing studies and databases related to the study areas were collected and elaborated to be available for the present study. The historical data analysis was based on all the available data sources (books, catalogues, web sources). The purpose was to collect the data required for the calculation of occurrence frequency w for each threat, and to have historical data to evaluate risk values resulting from the analysis

4.2.1 FLOODS

Hazard maps are available (PAI, 2007) for rivers Adda and Mallerio, in Valtellina. In addition, the 1987 flood was mapped, based on aerial photos realised with a zonation of flood plain in 3 zones according to flood intensity and return period immediately after the event. This flood had an exceptional impact on the whole Valtellina, and presents an extension comparable with zone C of PAI zonation (Fig.18) which corresponds to the extent of 500 years return time flood.

For the area of Brescia, the PAI zonation is available for rivers Oglio, Mella, and Chiese. In addition, all data related to past events and damages were mapped starting from available data sources (Berutti, 1998; Pedersoli, 1992; CNR, 1998; CNR, 1999; Guzzetti, 2000; Regione Lombardia, 2009; AVI, 2007) (Fig.19).

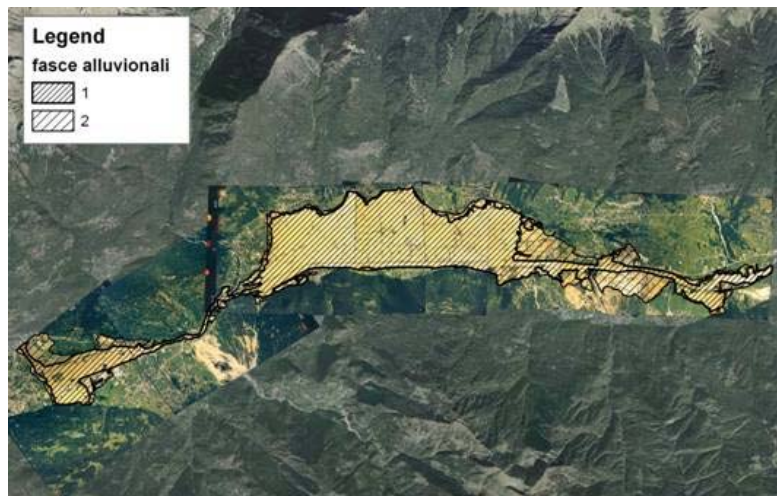


Fig.18. Mapping of 1987 event and distinction of two zones: 1: large water depth. 2: shallow water depth.

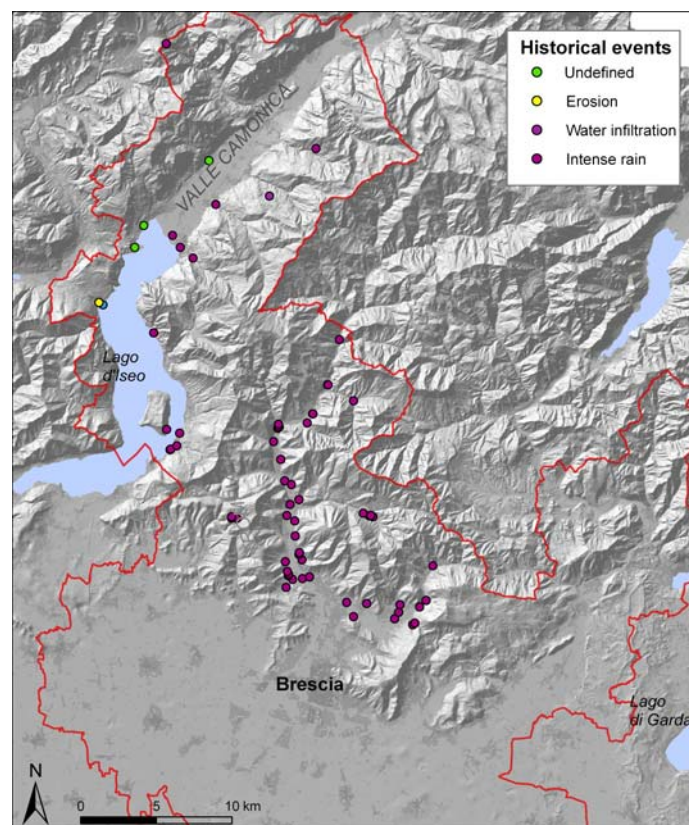


Fig.19. Localization of floods and related causes. Events are concentrated in lower Val Trompia, and were generally triggered by intense and prolonged rainfalls.

4.2.2 DEBRIS FLOWS

The existing inventory of debris flows in Lombardy (1:10,000 scale) was used, providing a detailed description of distribution landslide phenomena (progetto IFFI, 2007). The inventory was produced at 1:10,000 scale, based on aerial photo interpretation, field checks (Frattini et al., 2000) and historical data. The database was further implemented with detailed information referred to 1987, 2000, 2002 and 2008 events in Valtellina (Fig.20), and those deriving from aerial photo interpretation for Val Trompia and the area of Brescia (Fig.21).

Debris flows in Valtellina are mainly concentrated in the northern flank of the valley, and within secondary valleys (e.g. Valtartano (1987) and Val Gerola). Debris flows along the main valley often originated on terraced slopes, and were favoured by bad maintenance of both the terraces and the drainage systems (Crosta et al., 2003).

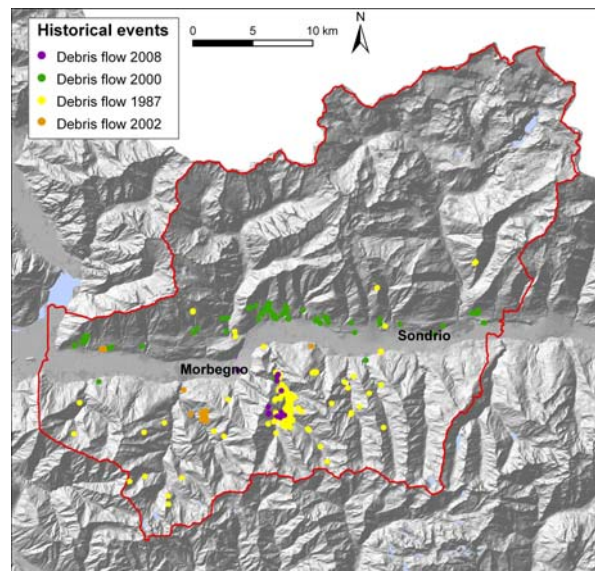


Fig 20. Recent historical events in Valtellina (years 1987, 2000, 2002 and 2008).

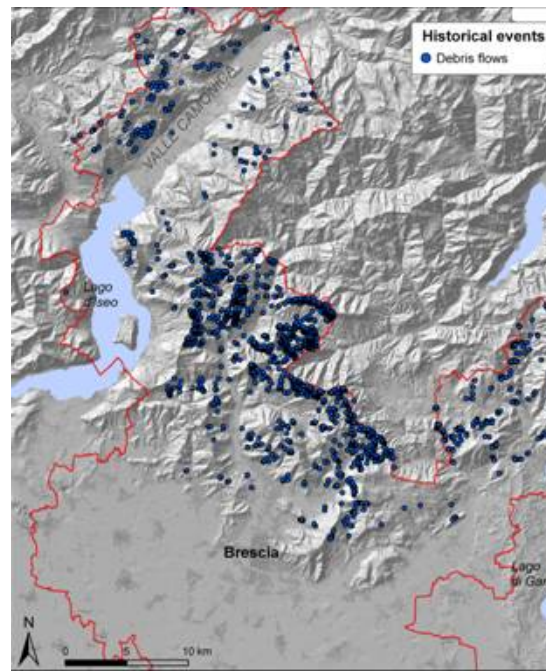


Fig.21. Localization of debris flow events, for the Brescia study area (1954-2004).

4.2.3 ROCKFALLS

Rockfall events and related damages were mapped for the two study areas starting from many data sources (Guzzetti, 2000; Regione Lombardia, 2009) (Fig.22 and 23).

For Valtellina, 330 events were mapped for a 20 years period, with events evenly distributed in the study area. The maximum density of rockfall events can be observed along the steep slopes of Val Masino.

For Brescia area, 374 events were mapped for the same period. The density of events is higher in upper Val Trompia and along the eastern flank of lake Iseo. The northern part of Valcamonica, which is known to be prone to rockfall activity, presents a very few events, this suggesting a strong undersampling of real events.

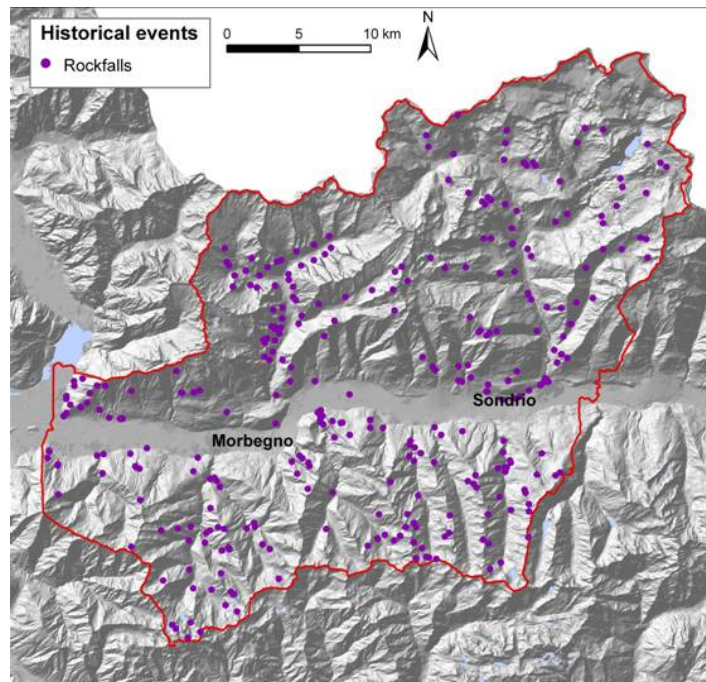


Fig.22. Distribution of rockfalls in Valtellina: localization of the historical events (1907-2000)

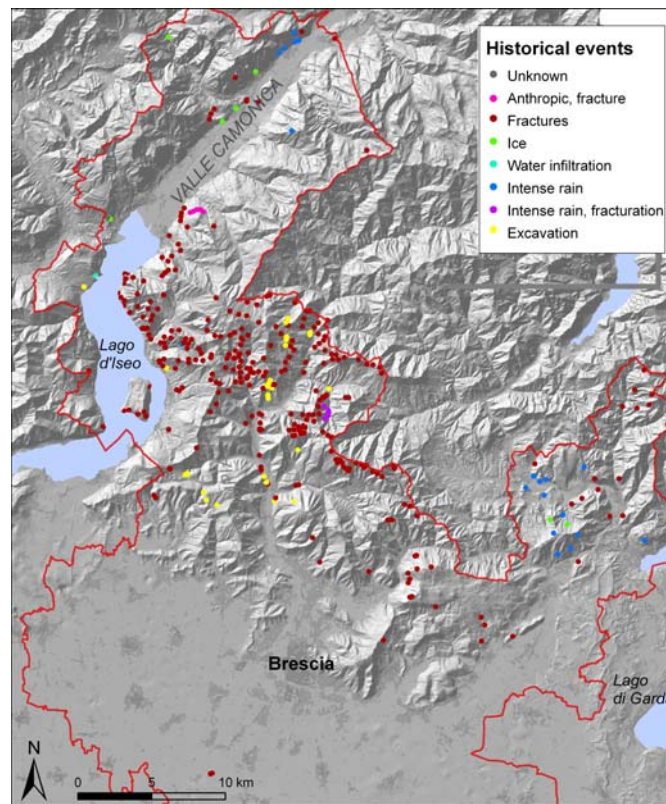


Fig. 23 Rockfall events for Brescia area: localization and cause of the historical events (1954-2004). The areas mostly affected by rockfalls are Val Trompia and the eastern shore of lake Iseo

4.2.4 FLOODS IN ALLUVIAL FAN

Similarly to the other hazards, events and related damages were mapped for the two study areas starting from different data sources (Berutti, 1998; Pedersoli, 1992; CNR, 1998; CNR, 1999; Guzzetti, 2000; Progetto IFFI, 2007; AVI, 2007, Crosta and Frattini, 2003).

Floods and debris flows on alluvial fans are among the most critical hazards, especially for Valtellina area (Fig.24), where the settlements are mostly located on the fans.

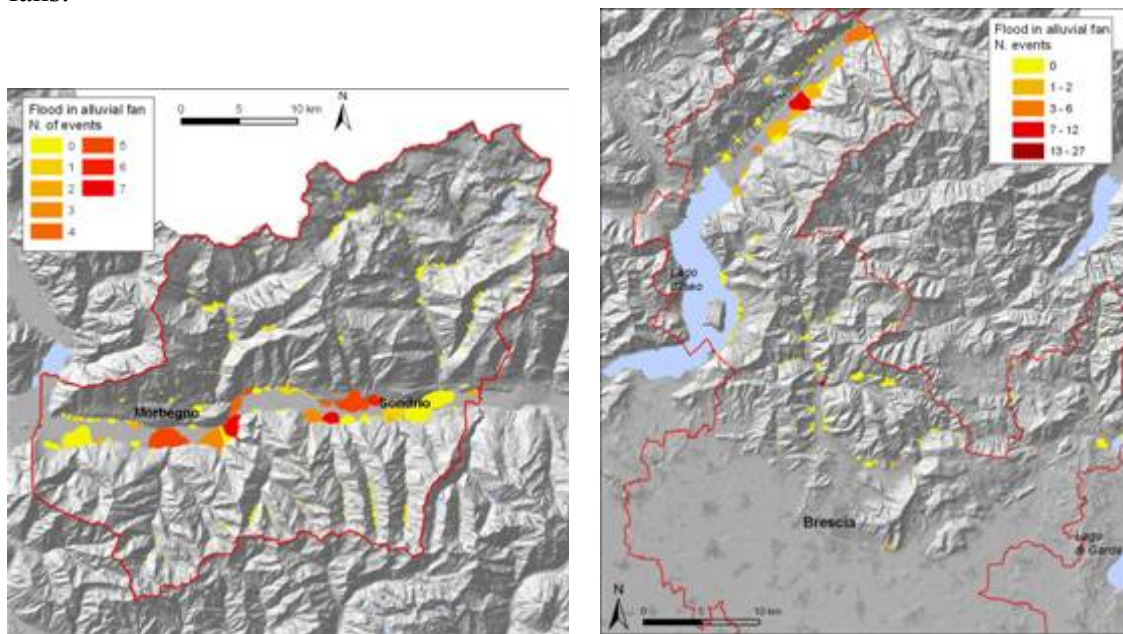


Fig. 24. Number of historical floods in the alluvial fans, for the two study areas. Alluvial fans in the main valleys are the most affected

5 METHODOLOGY

The adopted methodology leads to the quantification of risk induced by natural and technological events, with respect to

- risk for man safety (societal and individual risk)
- risk for goods (economic risk)

The two aspects are in general scarcely comparable: assigning an economic value to human life or safety is a difficult task that is not tackled here. Risk assessment leads in the first case to the quantification of annual casualties, in the second to the economic annual damage, in euro.

In order to take into account the main scenarios related to the study areas, different natural and technological threats were analysed:

1. Hydrogeological risk (including river floods, dam failure, snow avalanches, rockfalls, shallow landslides, debris flows, alluvial fan floods)
2. Wildfire
3. Seismic risk
4. Industrial accidents, related to Major risk plants (RIR, according to D.Lgs. 238/05, and Seveso Directive 96/82/CE) and to other minor productive/commercial activities
5. Work injuries
6. Transport of dangerous materials, on road and railway
7. Road accidents

For each threat, a preliminary bibliographic search was performed, followed by a mapping of historical events and impacted areas. The work was organised as follows:

- calculation of the expected occurrence frequency (n. events per year) based on historical data, known recurrence periods and probabilities obtained by numerical models.
- evaluation of an exposure value (probability that a certain exposed element is effectively impacted by an event)
- evaluation of the vulnerability: probability of exposed element, if impacted, of undergoing a damage
- risk assessment.

Although the analysis involves threats which have significant differences of distribution, impact, frequency, the same general model was used to assess the different typologies of risk, in order to ensure the homogeneity of the evaluations and the possibility of making comparisons and additions.

The methodology allows a comparison of the results with acceptability curves and criteria presented in the Literature (see Chap. 1).

For man safety, risk is measured as

- societal risk, as n. of impacted persons per year, at a given place

- individual risk, as annual probability that a person, standing at a given place, dies for one of the considered events
For goods, risk is expressed as
- economic risk, as expected euros of damage, per year, in a given place for one of the considered events

5.1 SOCIETAL AND INDIVIDUAL RISK

One of the main purposes of the analysis is to obtain a numerical index allowing the rough detection of hot spots, where to develop local scale analysis. In the adopted methodology, societal risk, RF is assessed, for each threat i , based on the general model (Tab.1):

$$RF_i = g_i * c_i * w_i \quad (1)$$

$$\text{and } c_i = e_i * p_i * N \quad (2)$$

Individual risk IR_i is obtained as

$$IR_i = RF_i / (p_i * N) \quad (3)$$

Where parameters are presented in Tab.1.

Tab 1. Parameters used for societal risk assessment.

Name	Symbol	Definition
Impacted area	A_{dp}	<i>Impact areas related to a certain scenario</i>
Gravity factor	g	<i>Probability that a person, if impacted, undergoes a certain type of damage (death)</i>
Exposure factor	e	<i>Probability of a person present in the area A_{dp} to be effectively impacted. The factor does not account for implemented mitigation interventions.</i>
Presence factor	p	<i>Probability of a person, potentially present in the impacted area A_{dp}, to be effectively present</i>
N. potentially exposed elements	N	<i>Number of people present in the impacted area A_{dp}</i>
Expected occurrence frequency	w	<i>Expected annual frequency of the scenario</i>
Conversion factor	c	<i>Number of people effectively impacted</i>
Physical risk	R_F	<i>Societal risk for a certain place deriving from a threat</i>
Individual risk	IR	<i>Probability of a person to be killed by an event</i>

Only for seismic societal risk, a slightly different methodology was adopted. It will be described in the related chapter.

5.1.1 MAP OF EQUIVALENT POPULATION: P_i AND N

In order to assess a societal and individual risk for the study areas, it was necessary to take into account the localization and the time of permanence of people, living, working, using structures or crossing the areas. The equivalent people present in each place in each moment is expressed by a map of equivalent population. With reference to the general methodology described above, equivalent population is defined as:

$$\text{Equivalent population} = p_i * N$$

For the Brescia study area, the equivalent population map was already available (CRASL, personal communication) and was developed corresponding to the maximum number of persons being simultaneously present at a given place (Fig.25).

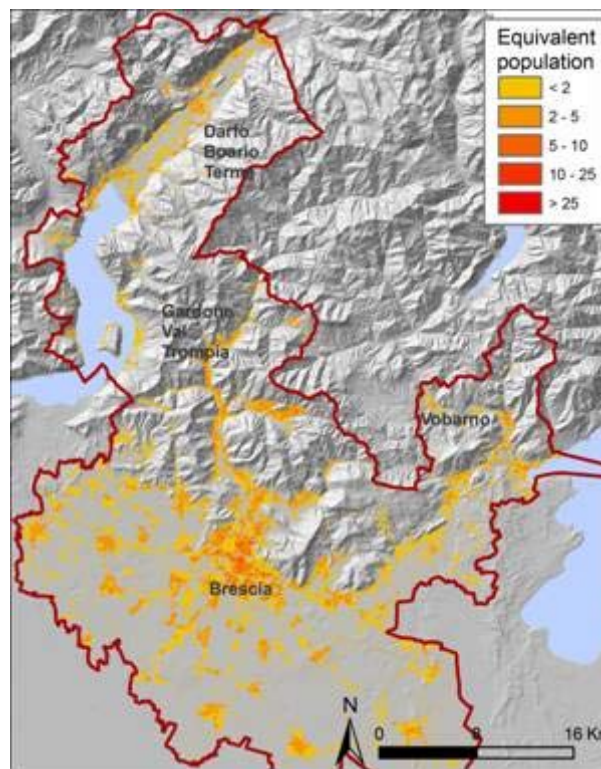


Fig.25. Equivalent population, Brescia study area, (CRASL, personal communication)

For Valtellina, two scenarios were considered (day and night) taking into account the different distribution of population in the two periods of the day. The two scenarios are defined as:

- day (10 hours) from 8 a.m. to 6 p.m. (Fig.26)
- night (14 hours) from 6 p.m. to 8 a.m. (Fig.27)

In the following, data used to develop the equivalent maps of Valtellina are illustrated into detail.

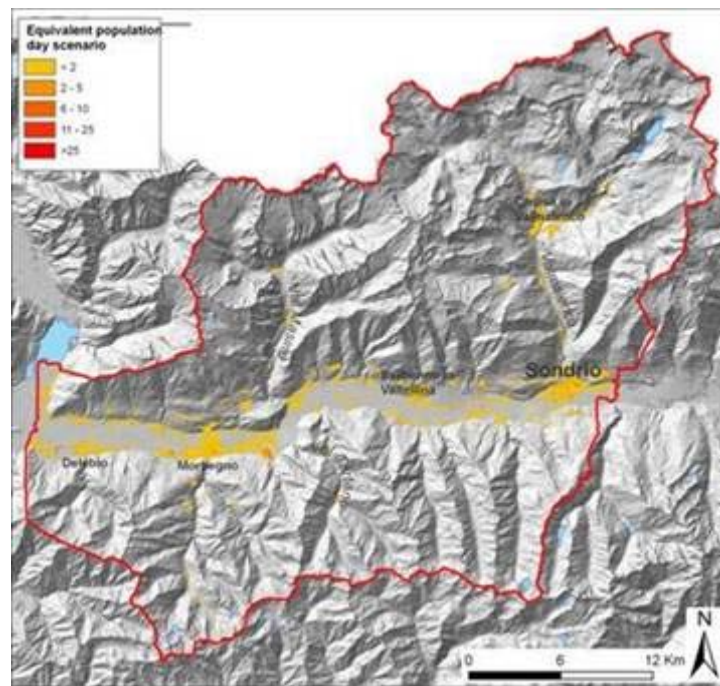


Fig.26. Equivalent population for day scenario, Valtellina

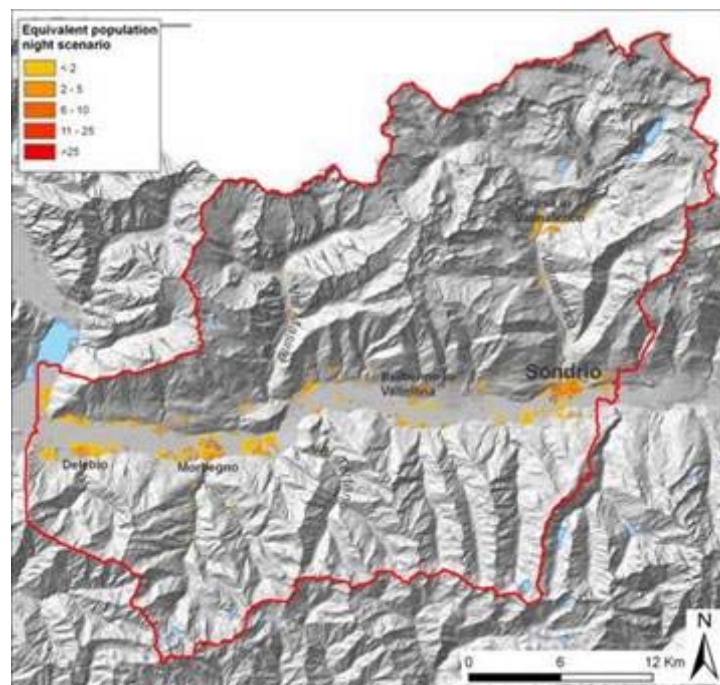


Fig.27. Equivalent population for night scenario, Valtellina

Residents

Data were provided from ARPA Lombardia (ARPA, 2007) for 100 x 100 m cells. The data were resampled at 20 m x 20 m cells to be used consistently with the detail of the analysis. Occupation time for residential buildings included 3.5 hours during the day, and the entire night.

People in public buildings

For each kind of element, the expected number of people simultaneously present was evaluated. In order to do this, it was necessary to evaluate data relative to each specific element (source: specific web sites, health boards, local administrations) and to estimate the time of permanence of people in specific category of structure or buildings.

- *Commercial centres*

For commercial centres, the number of parking places was considered as the maximum number of people simultaneously present. During the day, one person per car staying inside the centre for 2 hours was assumed. It is worth to consider that during the working days the parking is never full, but during the weekend it often is, and that a car is frequently occupied by more than one person. From 8 p.m. to 8 a.m., only the presence of two guards is considered for each centre.

- *Hospitals*

The number of available beds (ISTAT, 2001) was obtained for both public and private hospitals. During the day, both day-hospitals and in-patients were considered, supposing the hospital is always full. During the night, only in-patients were considered.

- *Schools*

The number of students for each building was derived from databases of the Ministry of Education. For the day scenario, their presence was quantified as 1200 hours per year, corresponding to 0.33 hrs/day for the whole year (1200hrs/(365days*10hrs)). For the night scenario, no people was supposed to stay in the buildings.

- *Railway stations*

Data related to annual flux of people in the stations is available only for the major stations (Centostazioni s.p.a., www.centostazioni.it). In Valtellina this information is available for Sondrio, with 2.000.000 people/year pass by, corresponding to about 5500 people per day. For the other stations, a proportion was assumed, attributing a weight according to their importance (Tab.2).

Tab 2. People in transit per day in railway stations

Station	weight	pp/day
Sondrio	1	5500
Morbegno	0,5	2750
others	0,1	550

Half of the total flux was supposed to belong to the day scenario, and half to the night scenario. For the day, each person was supposed to stay within the station for an average time of 12 minutes (0.2 hrs), waiting for, or getting off the train. For the night, 6 minutes of permanence were supposed (0.1 hrs).

- *Airports*

The only airport present in the study area is touristic. No data were available related to the flux of people. According to the dimension of the airport, 2 people were supposed to be present during the day, and 1 during the night, for all the days of the year.

- *Hospices and nursing homes*

For hospices, the number of patients was provided by ASL (health boards). For nursing homes, it was supposed equal to 15. Patients were supposed to be present the entire day and night for every day of the year, as confirmed by the presence of many people in the waiting lists.

- *Cinemas*

The number of seats in the halls was obtained contacting each cinema directly or on the web. For the day scenario, 8 hours of opening a week were calculated (4 on Saturdays and 4 on Sundays, during the afternoon), that is $8 \text{ hrs} / 7 \text{ days} = 1,14 \text{ hrs/day}$. For the night scenario, two shows of in mean two hours a day were considered, giving 4 hrs per day each day of the year.

- *Fairs*

Only one single fair is present in the study area, the Fiera di Morbegno. In lack of data, we assumed to be 5000 the maximum number of people simultaneously visiting the fair, for 13 hours of daily opening of the structure (10 a.m. to 11 p.m.), 9 h in the day scenario and 4 h in the night one. $5000 \text{ visitors} / 13 \text{ hours} = 384,62 \text{ pp/hours}$. The hypothesis was that a visitor stays inside the fair in mean for 2 hours. Based on the annual programme of the fair, calculation of equivalent people was performed for 30 days/year of activity.

- *Sport facilities*

In the study areas athletic tracks, football, rugby and golf fields are located, together with swimming pools and ski-lifts. In general, for both day and night scenarios, a density of 20 people/hour was supposed to be present at each facility during opening times, during all the year, with some exceptions. For ski-lifts, 500 people were supposed to be present per year: $500 / 365 = 1,37 \text{ pp/day}$, only in the day scenario. For golf fields, 10 people were considered, staying in mean for 2 hours each, only during the day: $10 \text{ pp} * (2 \text{ hours} / 10 \text{ hours}) = 2 \text{ pp/hrs}$. For swimming pools, a density of 40 people/hour was considered during the day, while in the evening a higher density of 60 people was supposed.

- *Churches*

A number of churches is present in the study areas, and they can host a variable number of believers. For simplicity, a constant number of 50 people was considered to be inside the building during celebrations. For the day scenario, one hour of celebration was considered for the 313 ferial days and 2 hours for the 52 Sundays. For the night scenario, only two celebrations on Saturdays and Sundays were considered.

- *Cemeteries*

Lots of cemeteries of different size are present in the study areas. The presence of 20 visitors on Sundays was assumed. 30 minutes (0.5 hours) of permanence were considered all the Sundays of the year, only during the day.

- *Heliports*

No certain data were available for heliport frequentation. 20 people were supposed to be present, for 6 hours, only during the day.

- *Markets*

52 days of market per year were considered, with a presence of 45 visitors simultaneously present for 5 hours during the day

- *Fire brigades and barracks*

No certain data were available in relation to people living in these structures, as officials and their families. 5 peoples for barracks and 6 for fire brigades were supposed to occupy the buildings during both the day and the night.

- *Filling stations*

Filling stations were mapped by means of aerial photos and direct field survey. For each of them, one person was supposed to be present in each moment, for 8 hours during the day from Monday to Saturday.

Tab 3. Number of people N_p and presence p in structures and buildings for day and night scenarios. n is the number of people assumed for the calculation.

	Day		Night		n
	p	N_p	p	N_p	
Commercial centres	2/10 hrs	n	1	2	n. of parking places
Hospitals	1	day hospital + n	1	n	n. patients
Schools	0,33 hrs	n	1	0	n. children
Stations	0,2/10hrs	$n*0,5$	0.1/14 hrs	$n*0,5$	n. passengers
Airport	1	n	1	1	2
Hospices	1	n	1	n	n. patients
Cinemas	1,14/10 hrs	$n+5$	4/14hrs	$n+5$	n. places cinema halls
Fairs	2/10 hrs* 30/365 days	3462	2/14 hrs* 30/365 days	1538	5000
Sport facilities	2/10 hrs	n	4/14 hrs	n	density of people
Swimming pools	8/10 hrs	n	3/14 hrs	60	40
Churches	1/10 hrs* 313/365 days 2/10 hrs*52/365 days	n	2/10 hrs* 52/365 days	n	Mean density
Cemeteries	0,5/10 hrs* 52/365 days	n	1	0	Mean density visitors
Heliports	6/10 hrs	n	1	0	Mean density visitors
Markets	5/10 hrs* 52/365 days	n	1	0	45
Barracks	1	n	1	n	5

Fire brigades	1	n	1	n	6
Filling stations	8/10 hrs* 313/365 days	n	1	0	1

Workers

For each category of economic activity, the number of workers was provided for each census parcel by ISTAT (Censimento Industria, 2001). Workers were further localised by attributing them to areas classified according to sector of activity (industrial production, agricultural production, urban area, hospital, school, sport facilities) by using DUSAF (2007) (Tab.5).

Where available, data were integrated with detail data referring to single structures. (Tab.4).

Tab 4. Number of workers and presence in structures and buildings

	Day		Night		n
	p	N _p	p	N _p	
Hospitals	9/10 hrs	0.75* n	8/14 hrs	0.25*n	n. workers
Schools	0,33 hrs	n	1	0	n. teachers
Cinemas	1,14/10 hrs	n	4/14hrs	n	5 workers
Fairs	9/10 hrs* 30/365 days	n	4/14 hrs* 30/365 days	n	200 workers
Heliports	6/10 hrs	n	1	0	Mean density visitors
First aid	6/10 hrs	n*0.5	6/14 hrs	n*0.5	20 workers

Tab.5. Correspondence between ISTAT classification of economic activities and DUSAF classification of land use.

ISTAT Category	DUSAF
Industrial productions	Productive areas
Agricultural productions	Productive areas
Quarries	Quarries
Schools	Schools
Hospitals	Hospitals
Commercial activities	Urban areas
Services	Urban areas
Technologic plants	Productive areas
Sport facilities	Sport facilities

5.1.2 FACTOR G: GRAVITY

For societal risk, gravity is intended as the probability of loss of life, if a person is impacted by a certain phenomenon. It is a process-specific index, expressing the vulnerability of man to each threat.

The definition of severity scales of damage effects is largely treated in the literature, for which no universal solution is accepted in the scientific community. A common need is to find a measure unity to define the levels of damage (e.g. death, serious injuries, minor injuries, etc.). A suitable approach was recently proposed by Tweeddale (Tweeddale, 1992), providing scores related to different effects on humans (Tab.6).

Tab 6. Scores related to levels of damage on human life (Tweeddale, 1992)

Effects on humans	Score
One death	1
High probability of dying	0.8
Low probability of dying or strong damages for many people (permanent disability)	0.3
Strong damages for few people or modest damages to many people	0.1
Damages for few people	0.01
Light damages for few people	0.001

An alternative approach is adopted by INAIL (2007). Gravity is defined as the ratio between the indemnified consequences of events and the number of exposed people. All the typologies of consequences are expressed as loss of working days, quantified as in the international conventions adopted by U.N.I. (Italian Standard Agency, 2009)

- Temporary inability: number of lost working days
- Permanent disability: each degree of disability is equal to 75 working days lost;
- Death: each case is equal to 7500 working days;

On the basis of the described approaches, a scale of gravity for damages on man health was defined by Buldrini (2009), selecting a score for three degrees of consequences, as in Tab.7.

Tab.7. Scores related to levels of damage on human life

Gravity level on man	score	Examples
Death	1	-
Heavy injuries	0,25	<i>Permanent damages, permanent disability of 25%</i>
Light injuries	0,01	<i>Reversible damages, 75 days of temporary inability, 1% of permanent disability</i>

Once defined the gravity scale, the gravity factor g is calculated as:

$$g_i = 1 \times P_{\text{death},i} + 0,25 \times P_{\text{heavy injuries},i} + 0,01 \times P_{\text{light injuries},i} \quad (4)$$

where P_{death} is the probability of being damaged to death, $P_{\text{heavy injuries}}$ is the probability of getting permanent damages or 25% disability, and $P_{\text{light injuries}}$ is the probability of getting reversible damages.

5.2 ECONOMIC RISK

In the adopted methodology, economic risk is assessed, for each threat i , based on the general model (Tab.8).

$$RF_i = g_{ij} * c_{ij} * w_i \quad (5)$$

$$\text{and } c_{ij} = e_{ij} * p_{ij} * V_j * N_j \quad (6)$$

where symbols are defined as in Tab.

Tab.8. Parameters used for economic risk assessment.

Name	Symbol	Definition
Impacted area	A_{dp}	Impact areas related to a certain scenario
Gravity factor	g_{ij}	Probability that an exposed element, if impacted, undergoes a certain degree of damage (damage > 10 mln euros)
Exposure factor	e_{ij}	Probability of an exposed element present in the area A_{dp} to be effectively impacted. The factor does not account for implemented mitigation works.
Presence factor	p_{ij}	Probability of an exposed element, potentially present in the impacted area A_{dp} , to be effectively present
Value	V_j	Value, in euros, of the impacted element of the type j
N. potentially exposed elements	N_j	Number of exposed elements of the j^{th} typology, present in the impacted area A_{dp}
Expected occurrence frequency	w_i	Expected annual frequency of the scenario
Conversion factor	c_{ij}	Number of exposed elements of the j^{th} type, effectively impacted
Physical risk	RF_i	Economic risk at a certain place deriving from a threat i

Only for seismic economic risk, a slightly different methodology was adopted. It will be described in the related chapter.

5.2.1 ECONOMIC VALUE

Economic value was evaluated for each element at risk, accounting for all the available studies (Tab.9). In general, where specific studies were not available, a market research was performed, by means of Internet, public administrations and private companies.

Tab.9. Economic value of exposed elements

Exposed element	Value	Source
Technologic plants	3,000,000 €/m ² 50,000 €/m ²	<i>Buldrini, 2009</i>
Commercial centres	1400 €/m ²	<i>Market researches</i>
Hospitals	1500 €/m ² 1800 €/m ²	<i>Regional administration</i>
Schools	1300 €/m ²	<i>Market researches</i>
Sowable land	0.24 €/m ²	<i>CRASL, personal Communication</i>
Railway station	1400 €/m ²	<i>Market researches</i>
Airport	1500 €/m ²	<i>Market researches</i>
Cinema	1400 €/m ²	<i>Market researches</i>
Fair	1400 €/m ²	<i>Market researches</i>
Agricultural productive	800 €/m ²	<i>Market researches</i>
Commercial and productive activity	1000 €/m ²	<i>Market researches</i>
Electric power line	80 €/m	<i>Provincial administration</i>
Railway	2500 €/m	<i>Italian Railways</i>
Wood	11 €/m ²	<i>ERSAF (2009)</i>
Rural houses	1500 €/m ²	<i>Market researches</i>
Campings	50 €/m ²	<i>Market researches</i>
Orchard	5,2 €/m ²	<i>CRASL, personal Communication</i>
Vineyard	7 €/m ²	<i>CRASL, personal Communication</i>
Olive grove	6,3 €/m ²	<i>CRASL, personal Communication</i>
Residential	1500 €/m ²	<i>Market researches</i>
Sport facilities	1300 €/m ²	<i>Market researches</i>
Double lane road	2500 €/m	<i>Provincial administration</i>
Single lane road	1900 €/m	<i>Provincial administration</i>

5.2.2 FACTOR G: GRAVITY

The approach proposed by Tweeddale (Tweeddale, 1992) for gravity of industrial accidents was first considered to evaluate the factor of gravity for goods, since it is free from monetary equivalences and provides the scores presented in Tab.10.

Tab 10. Scores related to levels of damage to buildings (Tweeddale, 1992)

Effects on goods- Gravity of damage	Score
Many houses destroyed (n)	<i>n</i>
All the neighbouring plants destroyed	<i>3-10</i>
One house destroyed	<i>1</i>
Plant of origin of the event destroyed or part of the neighbouring plants destroyed	<i>0.3</i>
Part of the plant of origin of the event destroyed or minor damages to neighbouring plants	<i>0.03-0.1</i>
Light damages for the plant of origin of the event	<i>0.001-0.01</i>

On the basis of this approach, a scale of gravity for damages on goods is here defined (Buldrini, 2009), selecting a score for three degrees of consequences, as in Tab.11.

Tab 11. Scores related to levels of damage on buildings

Gravity of damage to goods	Score	Examples
Strong damages	<i>1</i>	<i>Houses destroyed</i>
Partial damages	<i>0,25</i>	<i>Neighbouring structures partially destroyed</i>
Light damages	<i>0,01</i>	-

Once defined the gravity scale, the gravity factor g is calculated as:

$$g_i = 1 \times P_{\text{strong } d,i} + 0,25 \times P_{\text{partial } d,i} + 0,01 \times P_{\text{light } d,i} \quad (7)$$

where P_{strong} is the probability of a building or structure to be destroyed, P_{partial} is the probability of undergoing partial destruction, and P_{light} the probability of light damaging.

6 NATURAL RISK ASSESSMENT

6.1 ROCKFALLS

For rockfall risk analysis a 3D modelling was performed using the mathematical model HY-STONE (Crosta et al., 2004). It simulates the possible three-dimensional trajectories of rock blocks starting from previously identified areas.

6.1.1 ROCKFALL SIMULATION

The code used for the simulation allows to simulate the motion of rocky blocks non interacting in a three-dimensional reference system, using a DTM to describe slope topography. The program simulates free fall motion (parabolic motion), impact/rebound and rolling. Energy loss of following impacts is described by means of restitution coefficients (normal and tangential). Energy loss due to rolling is described by means of a dynamic friction at rolling. The code incorporates both kinematic (lumped mass) and hybrid (mixed kinematic-dynamic) algorithms, allowing to model free fall, impact and rolling, with different damping relationships available to simulate energy loss at impact or by rolling.

The rocky block is described as a solid geometric shape with a certain volume and a certain mass. The model can simulate rotational motion (Crosta et al., 2004).

To account for the uncertainty of the parameters and of their space-time variability, it is possible to perform stochastic simulations, launching more than one block from each source area and varying parameters according to a certain probability distribution within a certain stochastic range. These simulations allow to:

- introduce the natural variability of the parameters;
- obtain a higher and more reliable coverage of the territory;
- verify the dispersion of the trajectories and arrival points starting from a single source area;
- obtain representative distributions for the variables of higher interest for the model (height, velocity, energy, etc.).

The code allows, where necessary, to simulate the presence of vegetation, of defence interventions, and of fragmentation processes of the blocks.

Simulation results are produced partially in a raster format and partially in vectorial format, and provide:

1. number of blocks in transit for each cell;
2. number of blocks in transit for each cell weighted for triggering probability
3. number of blocks stopped within each cell;
4. translational and rotational velocity (minimum, medium e maximum) of the blocks in transit for each cell;
5. heights (minimum, medium e maximum) of the trajectories for each cell;

6. translational and rotational energy (minimum, medium e maximum) of the blocks in transit for each cell;
7. instant data of the motion;
8. three-dimensional trajectories;
9. starting and stopping points of the trajectories.

The input data were elaborated by means of GIS, and consisted in thematic maps already available or purposely prepared during the study.

The DTM provided by Region Lombardy was used. It is prepared by interpolating the contour lines of the Regional Technical Map, with a 20 m x 20 m resolution.

Each source area includes a number of pixels from which blocks are launched. For the purposes of the study, simulations were performed starting from diffused source areas selected using an empirical criterion, that is considering all the cells with slope more than 40° as potential sources. Ten blocks were launched from each source cell for the study area of Brescia, and 30 for Valtellina. The final source map involves 1.246.882 cells for a total extent of 499 km² for Valtellina and 807.434 cells for a total extent of 322,9 km² for Brescia area (Fig.28).

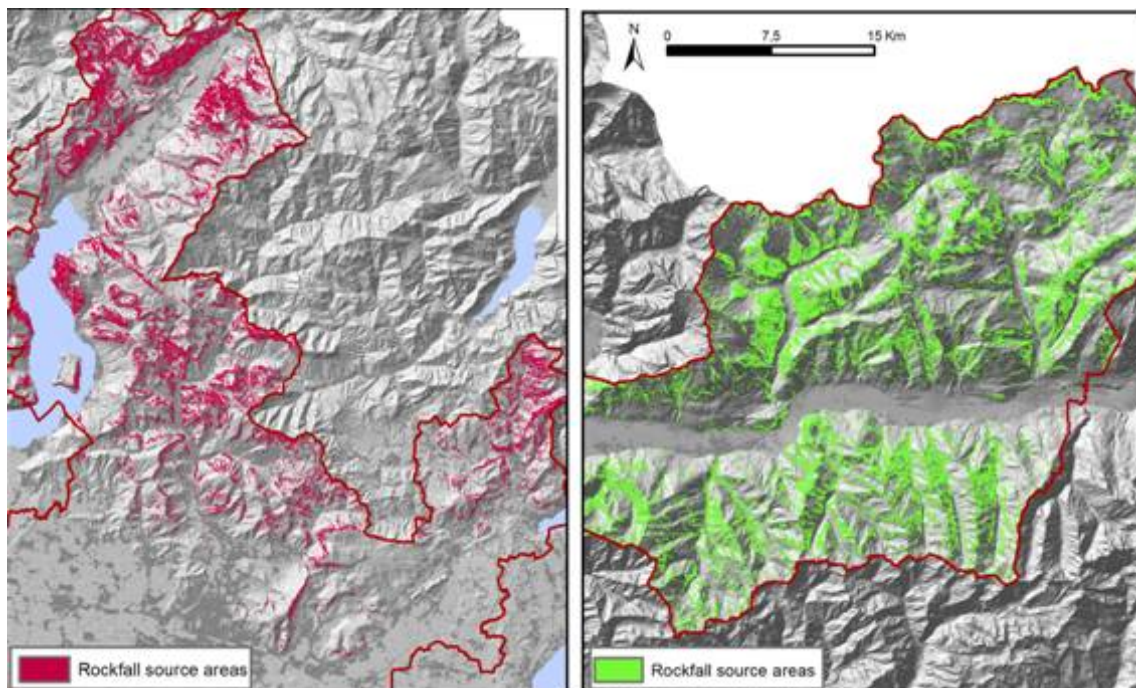


Fig.28. Source areas for rockfall simulations

In order to characterize the variability of land surface with respect to energy restitution and rolling resistance, we identified unique condition sub-areas (Fig.29), i.e., homogeneous zones characterized by a certain combination of environmental factors. We built the unique-condition sub-areas by overlying surface lithology and land-use maps. Geo-environmental maps of the Regional Administration, and maps derived from photo interpretation were integrated. Coefficient values were assigned comparing these

surfaces with reference-cases for which values have been presented in the literature (Azzoni et al, 1995; Agliardi e Crosta, 2003) (Tab.12). These values were further adjusted during the model calibration phase. To introduce the stochastic component, the radius of the blocks was varied (exponential distribution, mean value: 0.75 m) and, with normal distribution, the initial degree of the trajectory with respect to the direction of maximum slope, the coefficient of normal, tangential restitution and the friction coefficient at rolling. The normal and tangential coefficients of restitution express energy restitution, which is the amount of energy that each block conserves after the impact with the topographic surface. The rolling friction angle expresses the resistance of surface to rolling. Similarly to the coefficients of restitution, this parameter has been assigned to each unique-condition sub-area using literature data and successively calibrated. These values have been iteratively calibrated with a trial and error approach in order to fit the simulation results with observed data.

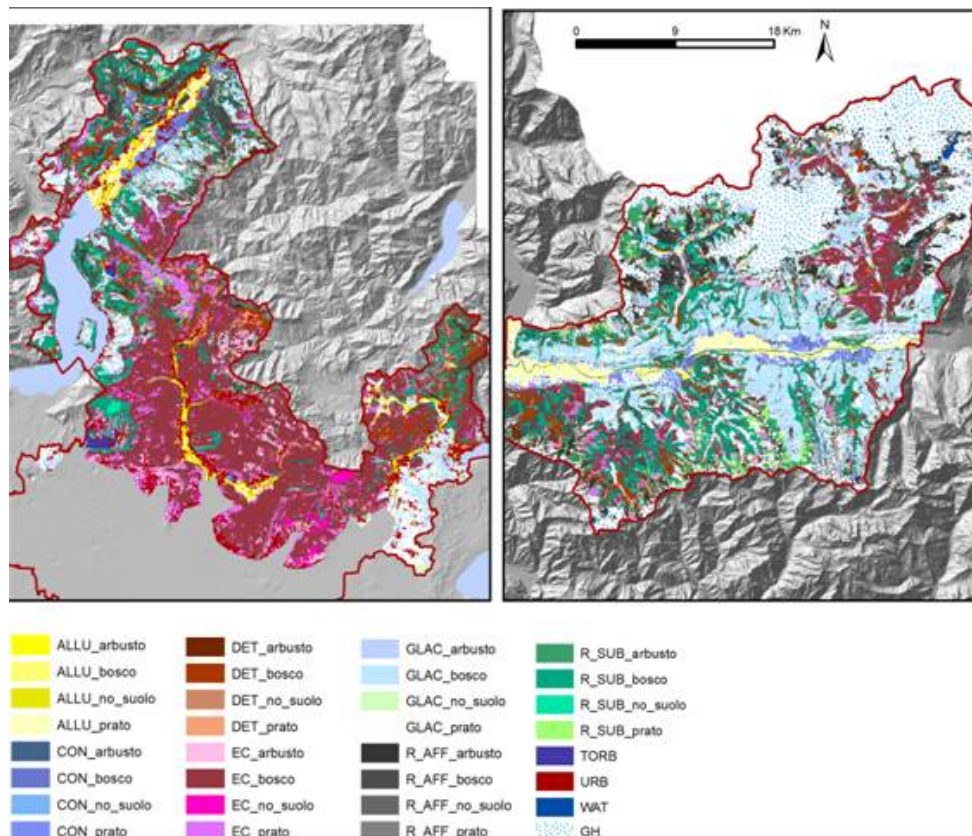


Fig.29. Unique condition map for the two study areas, see Tab.12 for legend

Tab.12. Values of restitution coefficients and rolling friction angle for unique-condition sub-areas

Surface lithology	Land use	Unic class	Crf(°)	CRn(%)	CRt(%)
Debris	Bare land	DET_nosuolo	0.60	35	55
Debris	Forest land	DET_bosco	0.50	30	50
Debris	Sparse forest land	DET_arbusto	0.55	33	53
Debris	Grass land	DET_prato	0.57	34	55
Eluvio-Colluvial deposit	Bare land	EC_nosuolo	0.60	25	60
Eluvio-Colluvial deposit	Forest land	EC_bosco	0.65	25	55
Eluvio-Colluvial deposit	Sparse forest land	EC_arbusto	0.63	25	57
Eluvio-Colluvial deposit	Grass land	EC_prato	0.62	25	60
Fluvial deposit	Bare land	ALLU_nosuolo	0.60	25	58
Fluvial deposit	Forest land	ALLU_bosco	0.65	25	54
Fluvial deposit	Sparse forest land	ALLU_arbusto	0.63	25	56
Fluvial deposit	Grass land	ALLU_prato	0.62	25	58
Alluvial fan	Bare land	CON_nosuolo	0.60	30	60
Alluvial fan	Forest land	CON_bosco	0.58	28	56
Alluvial fan	Sparse forest land	CON_arbusto	0.58	29	58
Alluvial fan	Grass land	CON_prato	0.59	30	60
Glacial deposit	Bare land	GLAC_nosuolo	0.60	25	50
Glacial deposit	Forest land	GLAC_bosco	0.60	20	45
Glacial deposit	Sparse forest land	GLAC_arbusto	0.60	22	47
Glacial deposit	Grass land	GLAC_prato	0.60	23	50
-	Peat	TORB	0.70	25	55
Outcropping bedrock	Bare land	R_AFF_nosuolo	0.45	50	68
Outcropping bedrock	Forest land	R_AFF_bosco	0.55	50	63
Outcropping bedrock	Sparse forest land	R_AFF_arbusto	0.52	50	65
Outcropping bedrock	Grass land	R_AFF_prato	0.49	50	68
Shallow eluvio- colluvial deposits	Bare land	R_SUB_nosuolo	0.52	44	65
Shallow eluvio- colluvial deposits	Forest land	R_SUB_bosco	0.55	40	60
Shallow eluvio- colluvial deposits	Sparse forest land	R_SUB_arbusto	0.53	42	63
Shallow eluvio- colluvial deposits	Grass land	R_SUB_prato	0.52	44	65
-	Urban and suburban	URB	0.70	40	30
-	Water body	WAT	1.00	20	20
	Glaciers	GH	0.3	50	70

Rockfall frequency

Rockfall frequency represents the number of blocks that passes through a single cell. This value depends on the number of block launched from each source cell, the number of source cells above, the topographic effect of convergence/divergence.

The first is a model parameter, and it is equal to 10 or 30. The number of uphill source cells also depends on the extension of rocky areas and on the dimension of the DTM cells. The number of source cells increases where the cell dimension is smaller. Topographic effects induce a deviation of the trajectories towards convergence zones, causing a higher number of passages. In general, the number of transits can be considered as a *proxy* of the probability that a block reaches a certain portion of the territory (Fig.30). Since 30 blocks were launched for each source area in Valtellina, and 10 in the area of Brescia, a significant difference in the number of passages is evident in Fig.30.

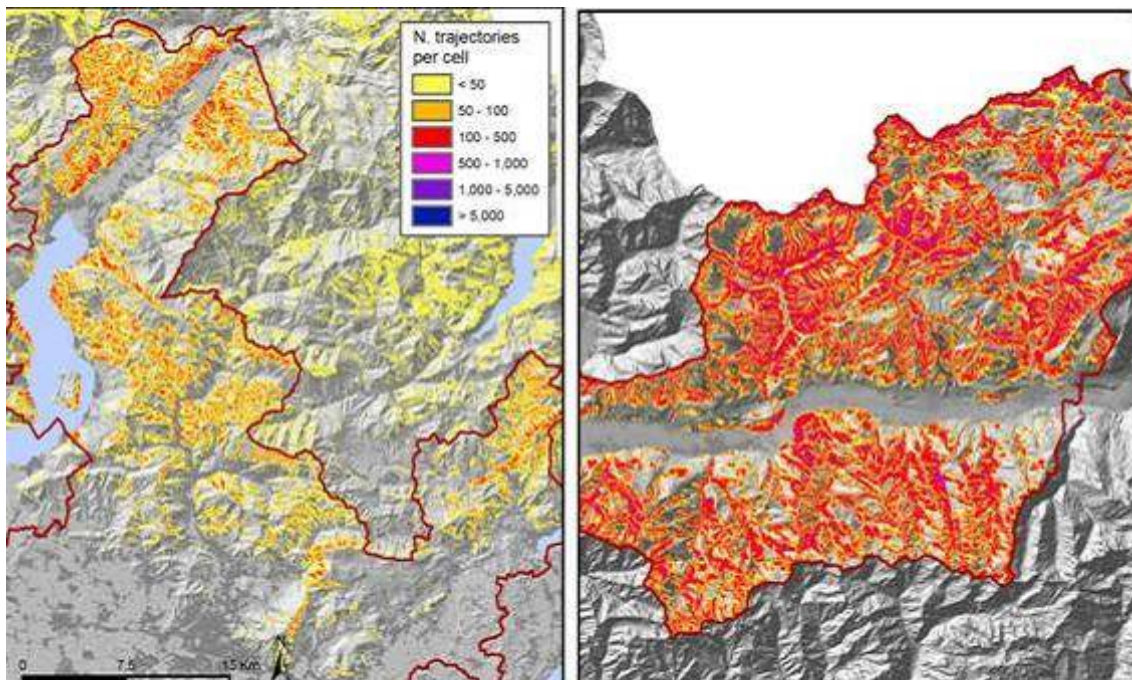


Fig.30. Number of blocks in transit for each cell.

Trajectory height

The minimum, maximum, and mean height of the trajectories are statistics of the heights of all the trajectories that pass through each cell. An important value is the maximum height, expressing the maximum potential elevation above ground of the blocks that can pass through a cell. This value is a proxy for the potential energy of the block, and is very important in countermeasure design because it allows for a good dimensioning (in height) of rockfall nets or barriers.

Block velocity

Maximum, mean and minimum velocity of each block crossing each cell are calculated by the model. An important value is the maximum velocity, which is related to the maximum energy of the blocks which pass through a cell. This value is important in countermeasure design because it allows for a good dimensioning of rockfall nets or barriers. In the case of a kinematic simulation, the velocity is the only variable that can be used for the calculation of the kinematic energy involved into the rockfall process. In the case of hybrid simulation, this variable can be directly substituted by kinetic energy.

Block kinetic energy

Maximum, mean and minimum energy of each block crossing each cell are calculated. The kinetic energy depends linearly on the block mass, that is sampled randomly by the model using an exponential distribution. The values of energy that are represented by the raster outputs are functions of the block masses, that are always different, and not explicitly expressed in the output. For instance, a very high energy can be due to a large mass simulated by chance. This makes the comparison of energies rather difficult, especially if a few blocks are launched. For this reason, velocity is preferred than energy for the development of risk scenarios.

6.1.2 EXPECTED FREQUENCY OF OCCURRENCE, W_{RF}

For the evaluation of the expected frequency of occurrence, W_{RF} , two different frequencies were taken into account: the frequency of block detachment and the frequency of transit in each pixel.

The detachment frequency was estimated from intensity-frequency curves, obtained adapting and calibrating curves found in the literature (Hungar et al., 1999; Dussauge et al., 2003) using historical events of Lombardy Region. For Valtellina, the inventory map of Lombardy Region records 330 events in a period of almost 20 years. This corresponds to an annual frequency of 16.5 events. In the Brescia study area, 374 events were recorded for the same period, giving an annual frequency of 18.7 events.

Transit frequency derives from HY-STONE and is expressed as the number of blocks passing through each cell, independently from their volume.

Considering that detachment frequency depends from the size of the block, 7 different scenarios were analysed, each of them characterised by the detachment of blocks with different volume and diameter (Tab.13).

Tab.13. Volume and mass characteristics of blocks for each rockfall scenario.

Scenario	V (m ³)	Diameter (m)	Av. Block V (m ³)	Block unit weight (Kg)	Av. Block mass (Kg)
F0-1	0,01	0,26	0,0045	2750	12,375
F0-2	0,1	0,58	0,045	2750	123,75
F0-3	1	1,24	0,45	2750	1237,5
F0-4	10	2,67	4,5	2750	12375

F0-5	100	5,76	45	2750	123750
F0-6	1000	12,40	450	2750	1237500
F0-7	10000	26,73	4500	2750	12375000

The frequency associated to each scenario was calculated using an intensity-frequency relationship presented in the literature for similar rockfall scenarios, but in different geographic and geological contexts (Fig.31) (Hungur et al., 1999; Dussauge et al., 2003). It is a power law describing the distribution of rockfall events for some volumetric classes

$$\log N(V) = N_0 + b \cdot \log V \quad (8)$$

where:

$N(V)$ = annual frequency increment for larger volume events

N_0 = total number of fall events

b = exponent of the power law

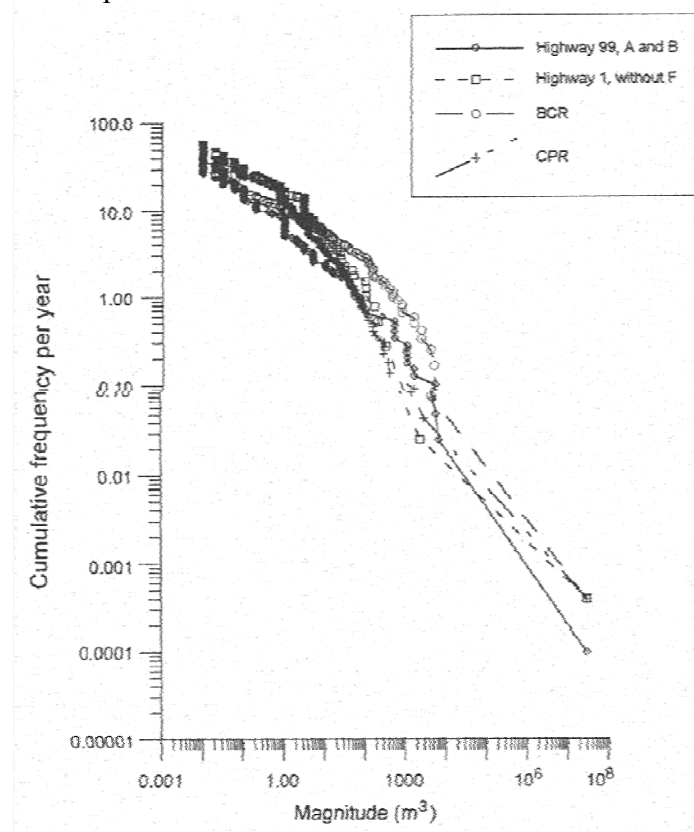


Fig.31. Frequency-intensity curve, (Hungur et al., 1999; Dussauge et al., 2003)

The frequency-intensity curve allows to determine the rockfall frequency for unit length of rock slope. For the calculation of the overall frequency it was necessary to determine the length of slopes affected by rockfalls in the study areas. This operation

was performed in a GIS environment. In Valtellina, the length of the rock slopes was about 577 km. In the Brescia study area, was 461 km (Tab.14).

Tab 14. Data related to rockfall sources

	Valtellina	Brescia
Length (Km)	577	461
Number of cells	1,246,882	807,434
Source cells area (Km²)	498.7	322.9
n. historical events	330	374
Observation period (years)	20	20

Since the events registered in the catalogues are the ones that cause the most visible damages, it was assumed that they belong to scenarios F0-6 and F0-7. The value of N_0 was then calibrated in order to obtain a number of expected events in scenarios F0-6 and F0-7 comparable to the actual ones. The other parameters of the curve were derived from the literature (b value is the exponent presented for carbonatic rocks) (Tab.15., Fig. 32 and 33).

Tab.15. Parameters of the intensity-frequency curve

N0	V0	T	b
1	0,001	1	-0,41

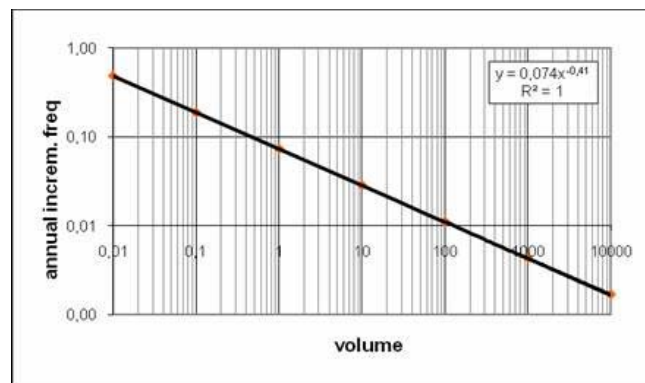


Fig.32. Intensity-frequency curve for Valtellina

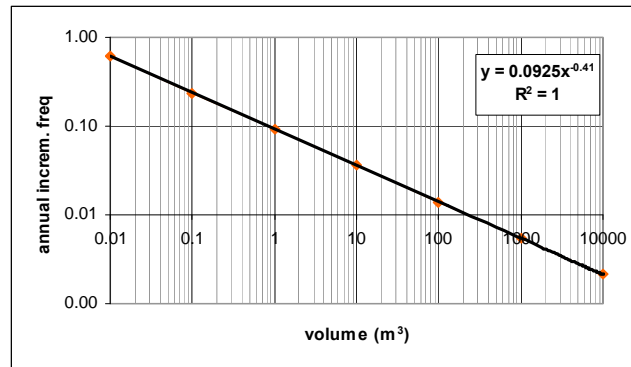


Fig 33. Intensity-frequency curve for the Brescia study area

Once the event frequency for the two study areas was estimated, it was possible to estimate the frequency of detachment for each block of a given size launched by the model, dividing the total frequency of the size class for the number of launched blocks. This was performed for each volume/intensity classes (Tab.16).

Tab.16. Rockfall frequency related to each scenario (block size)

Scenario	Valtellina			Brescia		
	Freq/km ²	freq /area	freq/block	Freq/km ²	freq /area	freq/block
F0-1	0.49	282.2	7.5 10 ⁻⁶	0,61	281,7	8.8 10 ⁻⁵
F0-2	0.19	109.8	2.9 10 ⁻⁶	0,24	109,6	3.4 10 ⁻⁵
F0-3	0.07	42.7	1.1 10 ⁻⁶	0,09	42,6	1.3 10 ⁻⁵
F0-4	0.03	16.6	4.4 10 ⁻⁷	0,04	16,6	5.2 10 ⁻⁶
F0-5	0.01	6.5	1.7 10 ⁻⁷	0,01	6,5	2 10 ⁻⁶
F0-6	0.00	2.5	7 10 ⁻⁸	0,01	2,5	8 10 ⁻⁷
F0-7	0.00	1.0	3 10 ⁻⁸	0,00	1,0	3 10 ⁻⁸

Finally, for the calculation of the occurrence frequency w_{RF} at each cell, the detachment frequency was multiplied for the transit frequency (counter), provided by HY-STONE

$$w_{RF} = \text{freq/block} * \text{counter}$$

For the Valtellina study area, the expected occurrence frequency was assigned to day and night scenarios, considering the different length of the scenario (10 and 14 hours, respectively).

6.1.3 SOCIETAL RISK ASSESSMENT

Gravity factor, g_{RF}

To assess the gravity factor for the study area, the empiric vulnerability curve proposed by Agliardi et al. (2009) was used (Fig.34). This curve was built for buildings and successively adapted to people. As typical for vulnerability functions, the curve is a sigmoid:

$$g = \frac{A_1 - A_2}{1 + e^{(x-x_0)/dx}} + A_2 \quad (9)$$

where:

A_1, A_2, x_0, dx = empirical constants

$x (= Ec)$ = kinetic energy

The constants in the function were derived interpolating some percentage damage and energy data referred to the 2004 Fiumelatte (LC) event (Tab.17.).

Tab 17. Value of constants and kinetic energy, introduced in eq. 9.

A_1	A_2	x_0	dx
-0,35824	1,00	128887,94	120332,95

For all the scenarios, the kinetic energy was obtained as:

$$Ec = \frac{1}{2}mv^2 \quad (10)$$

where:

m = block mass.

v = mean velocity of the blocks as by HY-STONE modelling

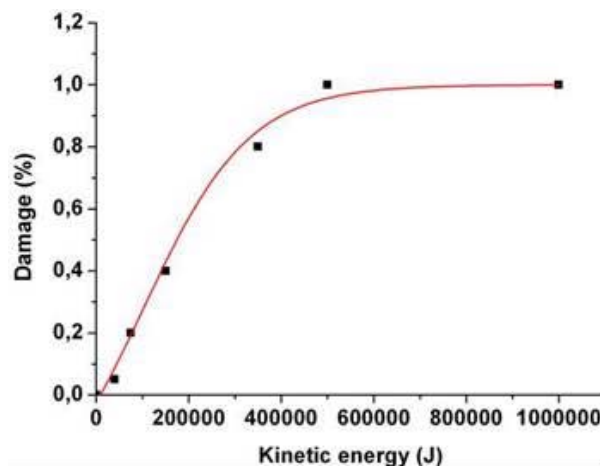


Fig.34. Vulnerability curve (Agliardi et al., 2009)

Exposure factor, e_{RF}

The exposure factor expresses the probability of a person to be effectively impacted within a terrain unit. In the case of rockfalls, it is linked to the dimension of a block crossing the terrain unit. The larger the block, the higher is the probability. In this case, we actually refer to a spatial exposure, related to the size of the block and to the land unit area. Considering the blocks as spheres, the radius of each block is:

$$r = \sqrt[3]{\frac{3V}{4\pi}} \quad (11)$$

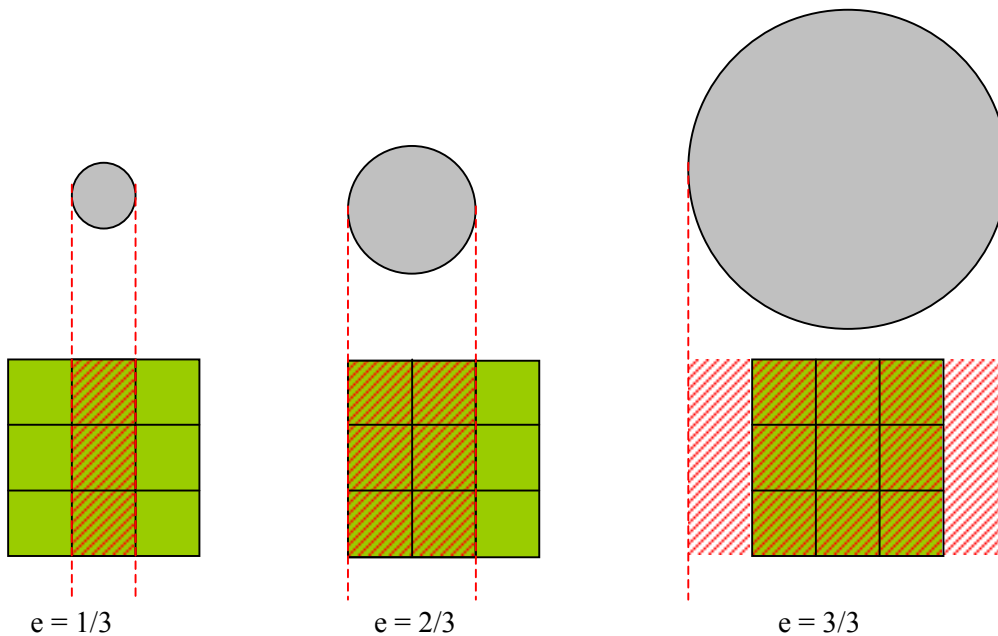


Fig.35. Blocks with different volume affect different portions of a cell

Given the fact that the terrain unit is a 20 x 20 m cell, the exposure factor e was calculated as (Fig.35):

$$e_{RF} = \text{diameter} / 20 \text{ m}$$

Considering that the block could be intercepted by a structure or could not impact all the exposed people, a corrective factor of 0.5 was further introduced (Tab.18).

$$e_{RF\text{correct}} = e_{RF} * 0,5$$

Tab 18. Exposure factors, e for each rockfall scenario

Scenario	V (m ³)	Radius (m)	Diameter (m)	e _{RF}	e _{RF-correct}
F0-1	0,01	0,133	0,267	0,0133	0,006
F0-2	0,1	0,287	0,575	0,028	0,014
F0-3	1	0,62	1,240	0,062	0,031
F0-4	10	1,336	2,673	0,133	0,066
F0-5	100	2,879	5,758	0,287	0,143
F0-6	1000	6,203	12,407	0,620	0,310
F0-7	10000	13,365	26,730	1	0,5

Societal physical risk

For each of the 7 scenarios, the societal physical risk was calculated by eq.1. The rockfall scenarios are considered among them independent.

Range of volumes do not overlap, implying that event frequencies for each of them are independent. To obtain the total societal risk (R_{tot}), simply summing the physical risk of each scenario(R_i):

$$R_{tot} = \sum R_i \quad (12)$$

For Valtellina, the map of societal risk shows risk values ranging from 0 to $4.8 \cdot 10^{-4}$ casualties/year/cell for the day scenario and from 0 to $1.3 \cdot 10^{-3}$ casualties/year/cell for the night scenario. $2.6 \cdot 10^{-2}$ casualties/year is the expected value of societal risk for the whole area for the day scenario, $5.5 \cdot 10^{-2}$ casualties/year for the night scenario (Tab.19). In general, societal risk is localised in few small areas, in the settlements located under steep rocky slopes (Fig.36 and37)

Map of total societal risk in the Brescia area (Fig. 38) shows that the western slope of Valle Camonica, Val Trompia and partially Val Sabbia are risky areas. Risk values range from 10^{-6} to $5.8 \cdot 10^{-3}$ casualties/year/cell. 0.678 casualties/year is the expected value of societal risk for the whole area.

Considering the overall number of expected casualties, we should remember that the two study areas have different extensions ($1,508 \text{ km}^2$ for Brescia, and $1,150 \text{ km}^2$ for Valtellina) and a different population (727,000 vs 90,278 residents). These values both influence the overall societal risk.

Tab.19. Rockfall societal risk values

	Valtellina day scen	Valtellina night scen	Brescia
Range (cas/year/cell)	$4.8 \cdot 10^{-4}$	$1.3 \cdot 10^{-3}$	$5.8 \cdot 10^{-3}$
Total (cas/year)	$2.6 \cdot 10^2$	$5.5 \cdot 10^2$	0,678

In the area of Brescia, both the overall risk and the maximum value per cell are higher. This is due to the different morphology of the areas. Brescia valleys are

narrower with steeper slopes. The higher values of the equivalent population of the valley bottoms also contribute to increase risk level.

499 km² for Valtellina and 323 km² for the Brescia area are identified as potential source areas of rockfalls. This means that, according to the assumptions here adopted, Valtellina is, in general, potentially more subjected to the phenomenon. However, societal risk is lower because the impacted areas are often limited or uninhabited. It is also important to notice that the triggering frequency for the single scenarios was considered homogeneous for the whole study area. This is clearly a simplifying assumption, since rockfall triggering depends on geological, geomorphologic, climatic and hydrologic conditions. As a consequence, risk is overestimated at some places (e.g.: Val Trompia) and underestimated at others (e.g.: slopes above Darfo, Valcamonica).

The analysis of historical data reveals that in both areas rockfalls did not cause many casualties in the past: and so, the results produced by the modelling in terms of victims is overestimated. On the other side, the morphologic characteristics of the study areas make the hazard potentially relevant. For this reason, the models are considered consistent with the study areas.

In the analysis, moreover, no mitigation works were taken into account, so that total and not residual risk was assessed.

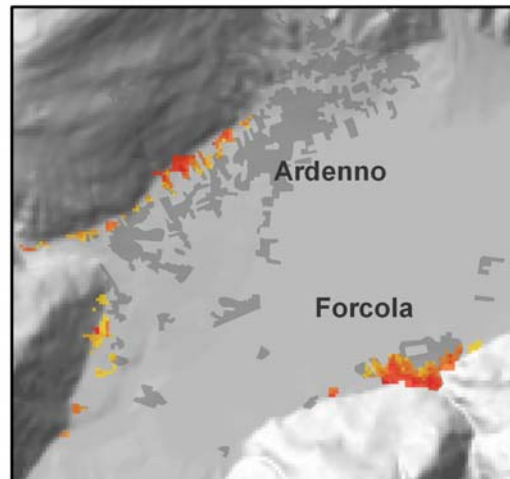
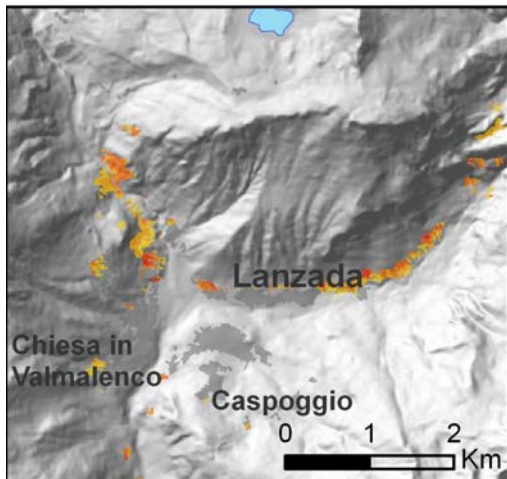
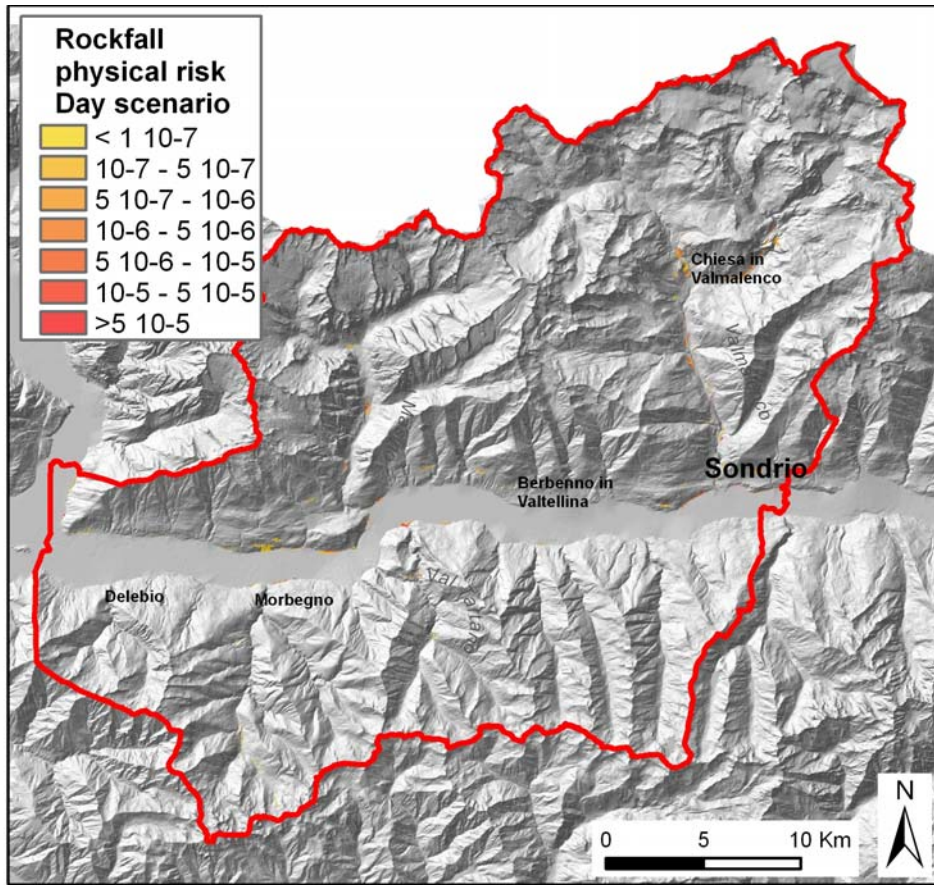


Fig.36. Map of societal physical risk for rockfalls, day scenario, Valtellina. Risk values are expressed in terms of casualties per year.

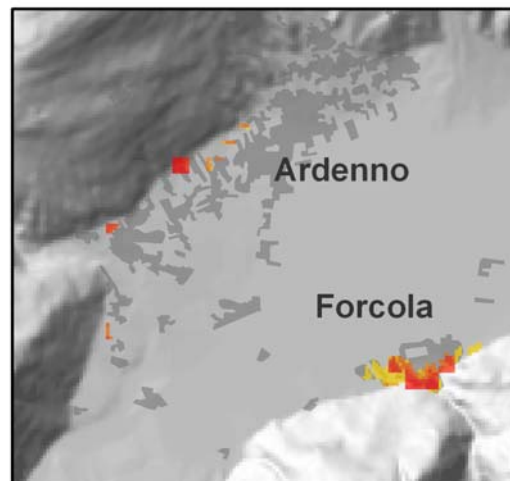
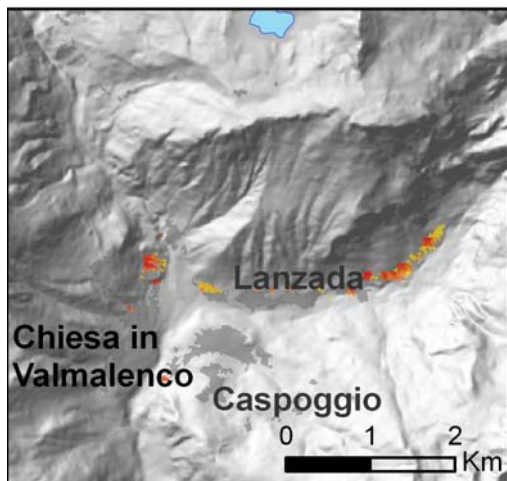
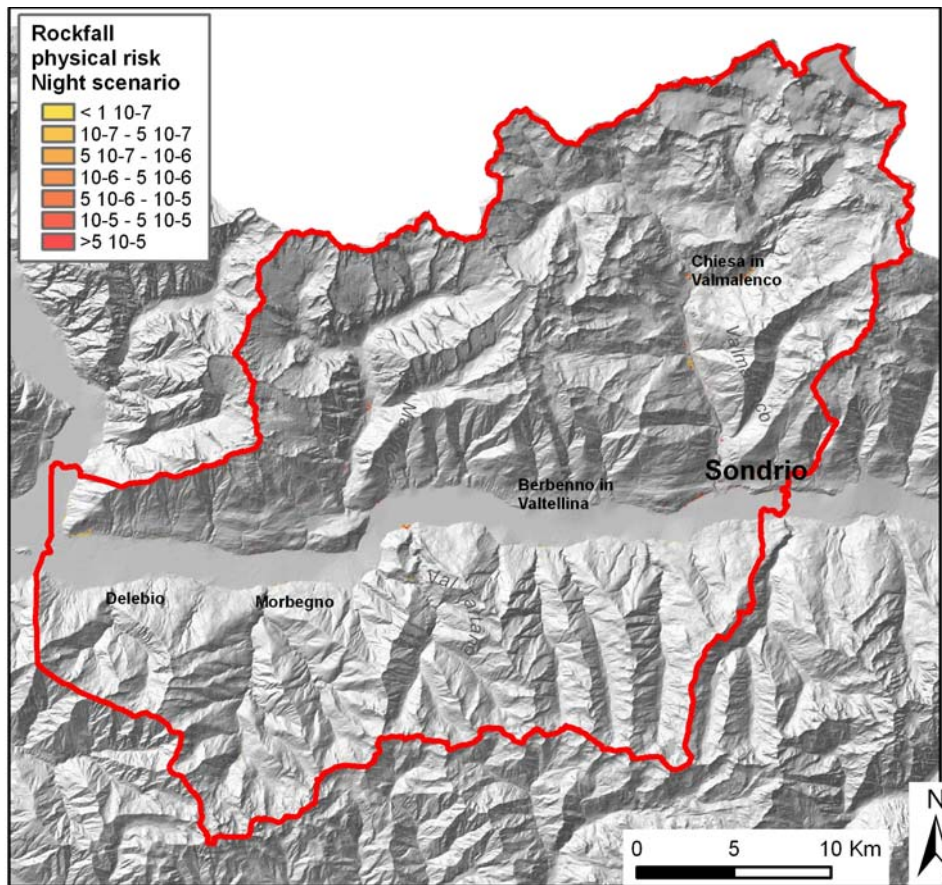


Fig.37. Map of societal physical risk for rockfalls, night scenario, Valtellina. Risk values are expressed in terms of casualties per year.

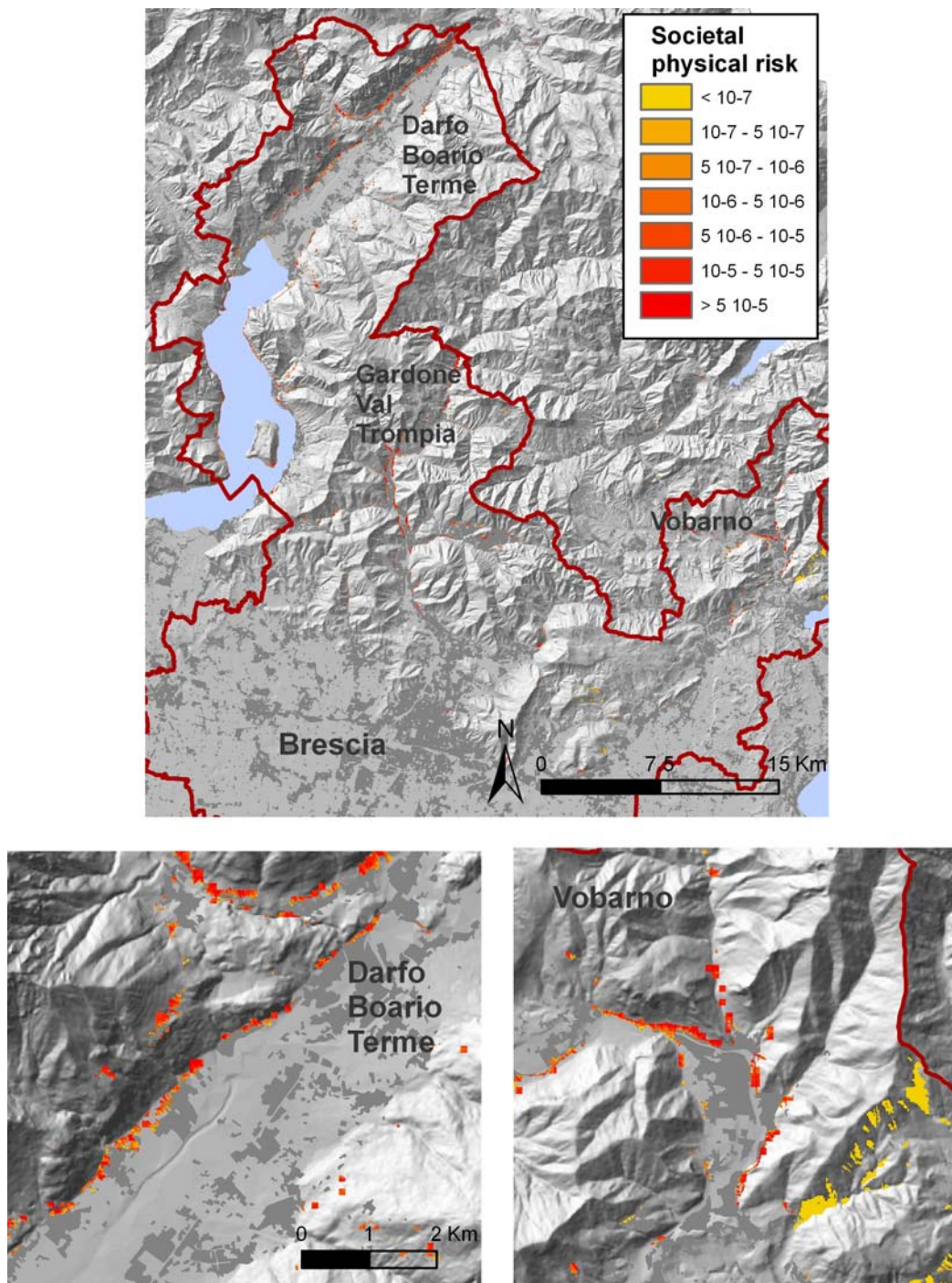


Fig.38. Map of societal physical risk for rockfalls, Brescia study area. Risk values are expressed in terms of casualties per year.

6.1.4 ECONOMIC RISK ASSESSMENT

The approach used for the assessment of economic risk is similar to the one used for societal risk.

Values of rockfall frequency w were the same as for the societal risk.

Gravity factor, g_{RF}

To assess the gravity factor g_{RF} , the empiric building vulnerability curve proposed by Agliardi et al. (2009) was used for buildings, streets, railways, and power lines.

For other types of exposed elements (vegetated, cultivated areas, and grass), it was considered that the effects of impact of a block of a given energy are higher than the ones affecting buildings. This would require new specific vulnerability curves. However, in lack of such curves, it was decided to use the same curve, and to artificially shift the kinetic energy (ke) in order to simulate higher damages (Tab.20).

Tab.20. Value of gravity factors for economic risk assessment.

Exposed elements	g_{RF} calculation
Vegetation	$F(2 ke)$
Wooden cultivations	$F(3 ke)$
Grass	1
Roads, railways, power lines, buildings	$F(Ke)$

Exposure factor, e_{RF}

The attribution of this value is based on the assumption that, differently from people, the elements at risk occupy in general the whole cell. For this reason, the exposure factor e_{RF} was considered always equal to 1.

Economic physical risk

For each of the 7 scenarios, the economic physical risk was calculated by eq. 5. The rockfall scenarios are assumed among them independent, and the total economic risk (R_{tot}) is:

$$R_{tot} = \sum R_i \quad (13)$$

where R_i is the physical risk of each scenario.

Results are shown in Tab. 21 and in Fig 39 and 40.

Clearly, mountain settlements and slopes are the most impacted areas, and present the highest economic losses. Rockfall risk is quite diffused, rarely reaching extremely high values in a single cell. However, total values of risk are considerable. It is important to remember that the presence of mitigation works (e.g. embankments) is not taken into account.

Tab. 21. Economic risk values for the two study areas

	Valtellina	Brescia
Range (€/year/cell)	<i>0 – 6,548</i>	<i>0 – 2,500</i>
Total (€/year)	<i>14,842,306</i>	<i>5,555,265</i>

The highest risk values are observed in Valtellina, where a larger surface is interested by the phenomena. The higher economic level corresponds to a lower societal risk: this is related to the type of impacted elements. In Valtellina, woods and cultivations are more impacted and more valuable, even if a small number of people is present.

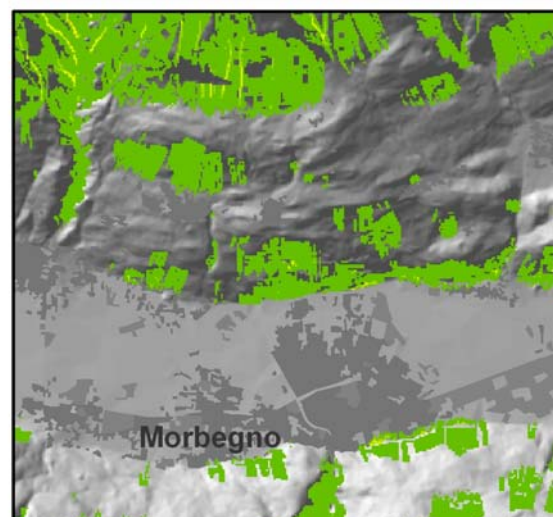
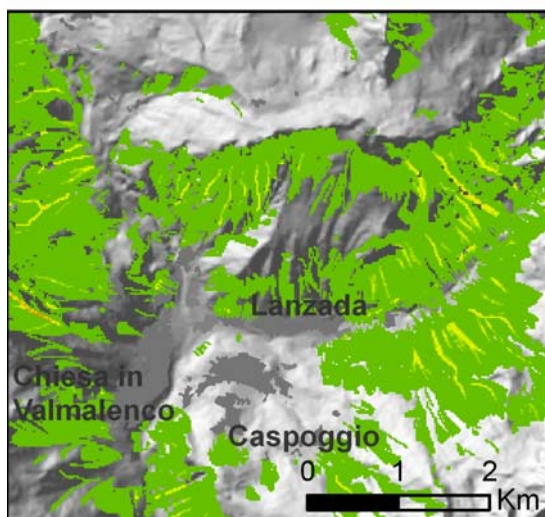
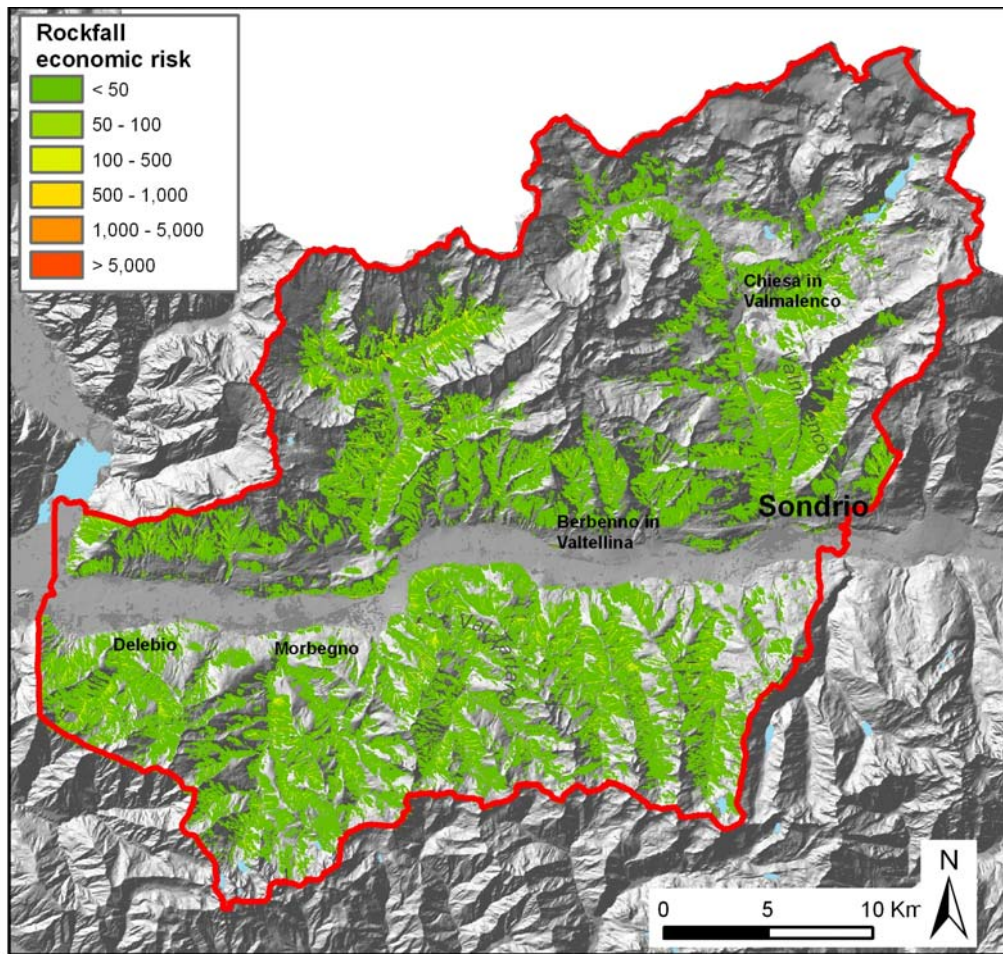


Fig.39. Map of economic physical risk for rockfalls, in euros/year, in Valtellina

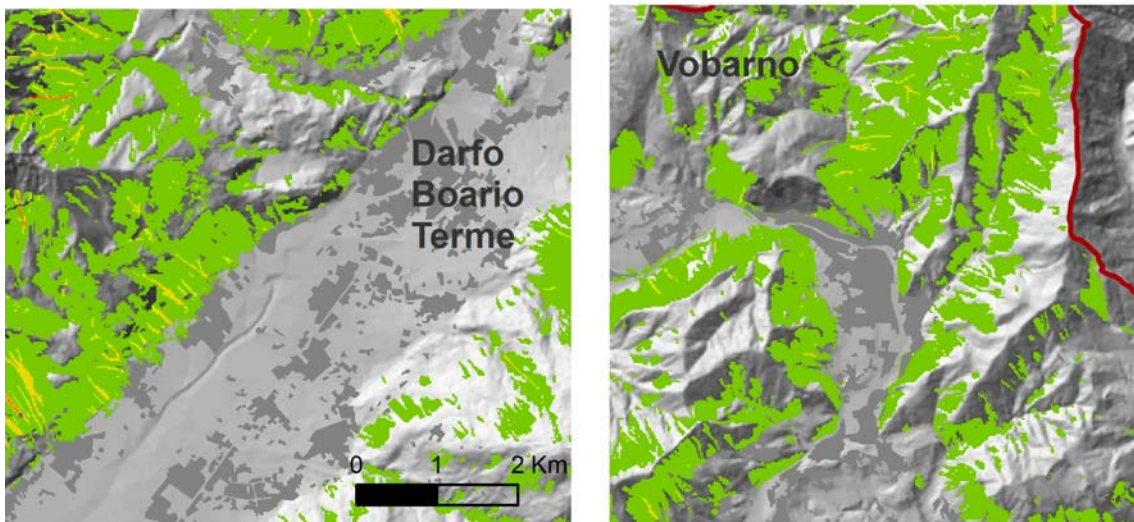
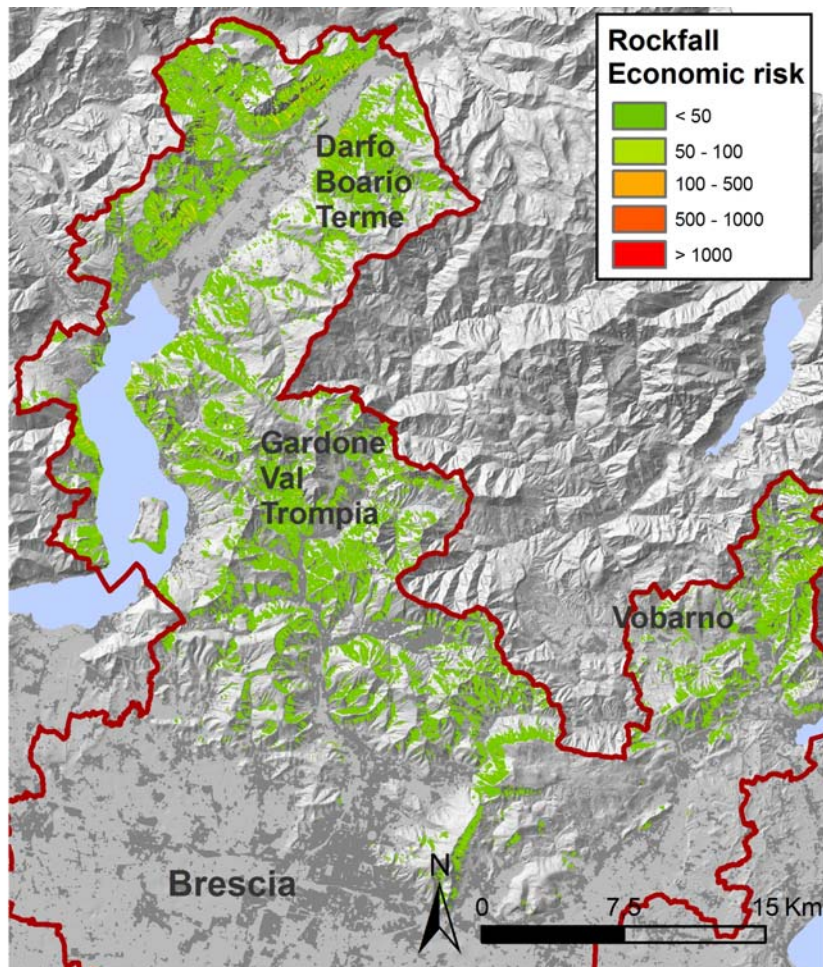


Fig.40. Map of economic physical risk for rockfalls, in euros/year, for the Brescia study area

6.2 SHALLOW LANDSLIDES

6.2.1 SHALLOW LANDSLIDES SIMULATION

Shallow landslides are phenomena limited in extension, involving superficial deposits, and can dominate sediment transport in steep, soil-mantled landscapes (Dietrich et al., 1986; Benda, 1990; Seidl and Dietrich, 1992). Three factors are considered responsible for triggering: sediment availability, presence of water and slope gradient. Shallow landsliding

Convergence of both soil and runoff, controlled by the topography, favours the triggering of shallow landslides in fine-scale topographic depressions (Williams and Guy, 1971; Dietrich et al., 1986). The downstream disturbance, scour and deposition from shallow landslides evolving into debris flows can affect channels, people, fish and property. Land use and lithology influence sediment availability, and can affect shallow landsliding. Many studies have demonstrated the acceleration of landsliding following road construction and trees harvesting (e.g. Fredriksen, 1970; Brown and Krygier, 1971; Mersereau and Dyrness, 1972; Swanson and Dyrness, 1975; Gresswell et al., 1979), but the role of deforestation on the initiation of shallow landslides is still not clear (e.g. Skaugest et al., 1993; Martin et al., 1996).

Shallow landslide hazard assessment is based on a variety of approaches and assumptions. Many approaches consider the multivariate correlations between mapped landslides and landscape attributes (e.g. Neuland, 1976; Carrara et al., 1977, 1991; Carrara, 1983; Mark, 1992; Busoni et al., 1995), or derive landslide susceptibility from classifications based on slope, lithology, morphology or geological structure (e.g. Brabb et al., 1972; Campbell, 1975; Hollingsworth and Kovacs, 1981; Lanyon and Hall, 1983; Seely and West, 1990; Montgomery et al., 1991; Niemann and Howes, 1991; Derbyshire et al., 1995). The approach used here (Montgomery et al., 1998) is based on the physically-based modelling proposed by Okimura et al. (Okimura and Ichikawa, 1985; Okimura and Nakagawa, 1988) and extended by others (e.g. Dietrich et al., 1993, 1995; van Asch et al., 1993; Montgomery and Dietrich, 1994) to develop a simple model of hazard from shallow landsliding. The approach is based on coupling a steady state hydrological model to a limit equilibrium infinite slope stability model.

Considering the most important controlling parameters, sediment availability was included in the analysis by means of the geo-environmental map (Regione Lombardia, 1983), containing slope deposits, but not considering fractures, alteration and tectonic origin. For hydrology, the presence and flow direction of water was calculated from the DTM, by means of a spatial function identifying the contributing area to each cell. Slope was also derived, together with curvature, by means of DTM. Land use map (DUSAF, 2007) was also included in the model to improve the characterisation of the study area. In particular, it helped to identify some potential source areas localised in settled areas, and to characterize the contribution of root cohesion to stability.

Hydrological model

The steady state hydrological model adopted in this study simulate the spatial pattern of soil moisture based on analysis of contributing areas, soil transmissivity and local slope (O'Loughlin, 1986) and has similarities to TOPOG (Beven and Kirkby, 1979).

The basic assumptions of the model are:

1. sub-superficial flow parallel to topographic gradients. The contributing area of the flux in each point is given by the related basin, as deriving from DTM.
2. the lateral flux in each point is in equilibrium with a steady state recharge r [LT^{-1}] given from the effective recharge on the contributing area (Fig.41); the effective recharge is expressed as precipitations diminished by the evapotranspiration, the surface runoff and the infiltration. This assumption is acceptable for prolonged and non intense precipitations.
3. the lateral flux capacity in each point is equal to $T \cdot \sin\theta$, where T is soil transmissivity [L^2T^{-1}], assumed to be equal to the mean permeability K [LT^{-1}] of the section multiplied for soil depth z (Fig.41); some authors use some functions expressing the decrease of permeability with depth (Beven, 2000).

Under these assumptions, the steady state is a one-dimensional model, easily implemented in hazard analyses with parameters distributed in raster format (Montgomery e Dietrich, 1994; Pack et al, 1998).

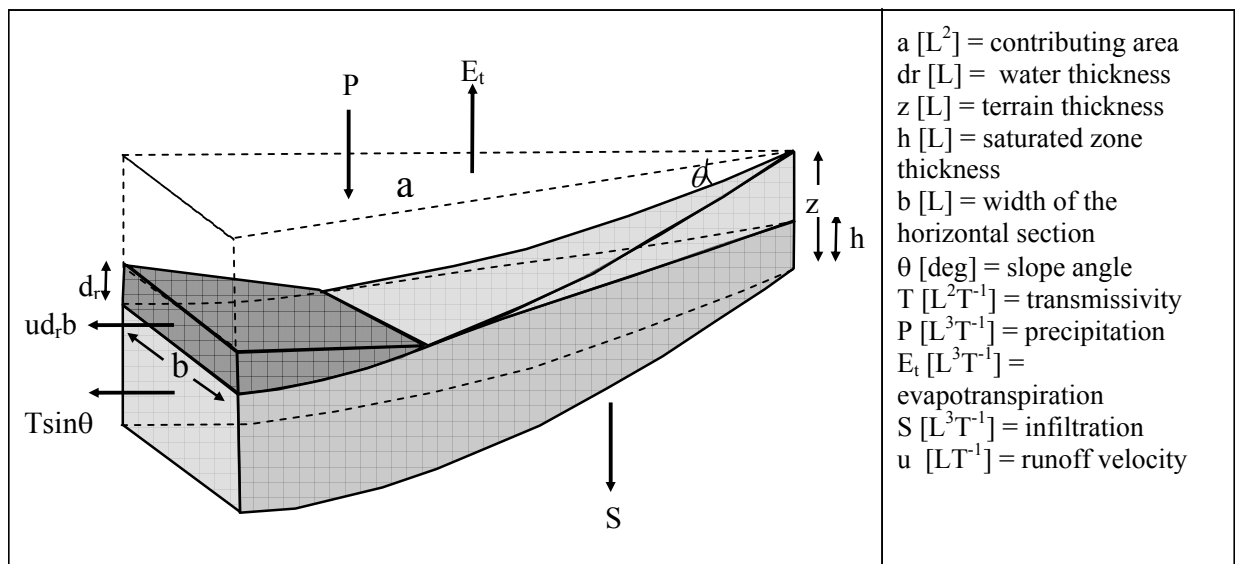


Fig. 41. Scheme of runoff as in Montgomery and Dietrich (1994)

Assuming steady state flow, it is possible to introduce a strong simplification of the law describing water flow along the slope. The assumption of steady state recharge is effective in the rare case of prolonged and constant rainfalls, where the time dependence becomes negligible. In steady state conditions, the variation in water table height in time is null.

Flow is assumed to infiltrate down to a low conductivity layer, and then to follow topographically determined flow paths. Local wetness (W) is calculated as the ratio of the local flux at a given steady-state rainfall (Q) to that upon complete saturation of the soil profile

$$W = \frac{Qa}{bT \sin \theta} \quad (14)$$

where a is the upslope contributing area (m^2), b is the length across which flow is accounted for (m), T is the depth-integrated soil transmissivity (m^2/day) and θ is the local slope (degrees). Adopting the simplifying assumption that the saturated conductivity does not vary with depth, Eq (14) can be reduced for the case where $W < 1$ to

$$W = \frac{h}{z} \quad (15)$$

where h is the thickness of the saturated soil above the impermeable layer and z is the total thickness of the soil. Combining Equations (14) and (15) allows expression of the relative saturation of the soil profile as

$$\frac{h}{z} = \frac{Qa}{bT \sin \theta} \quad (16)$$

which predicts relative soil moisture as a function of steady-state rainfall, specific catchment area (a/b), soil transmissivity and local slope. h/z increases in convergence areas (high a/b), in low permeability zones (low T) and in less steep zones (low gradient, $\sin \theta$).

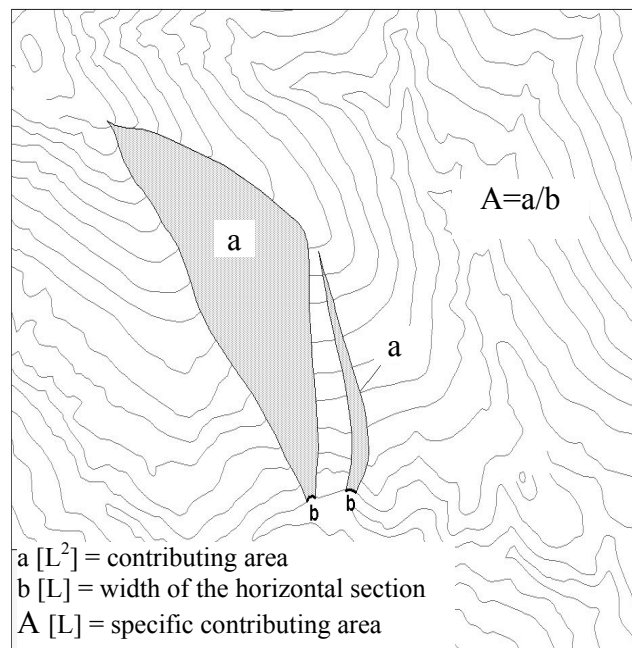


Fig.42. Example of topographic control on the specific contributing area

The steady state model simulates what the relative spatial pattern of wetness (h/z) would be during an intense natural storm which is not in steady state. This assumption would break down if precipitation events are sufficiently intense that thin soils on non-convergent sites can quickly reach destabilizing values of h/z before shallow subsurface flow can converge on unchanneled valleys (Iverson, 2000).

Infinite slope stability model

The infinite-slope stability model provides a one-dimensional model for failure of shallow soils neglecting arching and lateral root reinforcement.

An infinite slope is a geometric idealization describing a tabular mass of terrain, inclined, with lateral and longitudinal dimensions many times the soil thickness. Infinite slope method is mechanically mono dimensional (Iverson et al, 1997): all the quantities vary as a function of only a spatial coordinate, normal to slope surface (Fig.43). The infinite slope model is preferred, in case of shallow landslides, due to its direct solution, for the simplicity in introducing water flow and for the geometry characterised by a low ratio thickness/length.

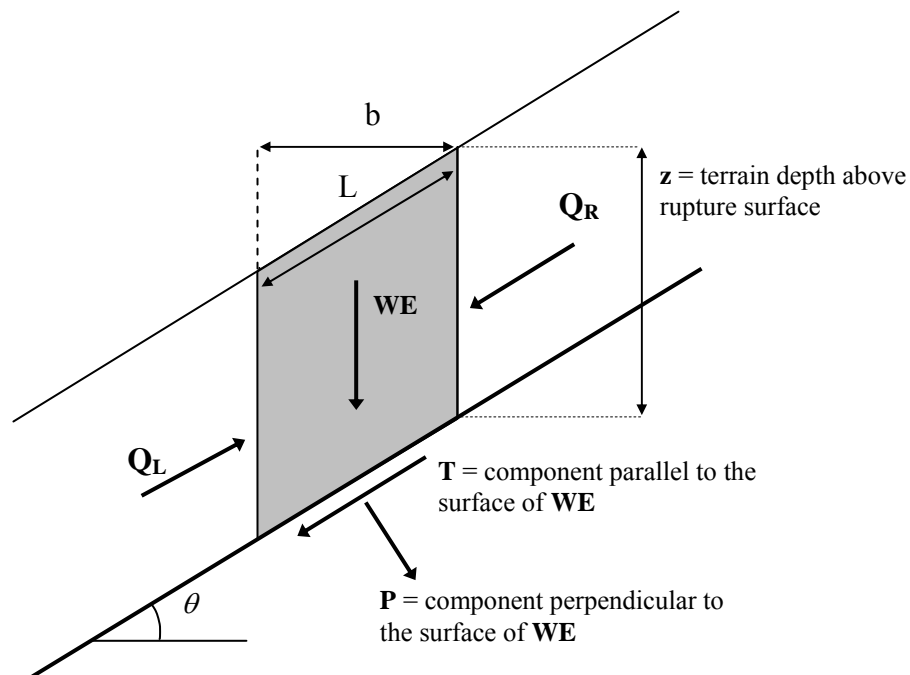


Fig.43. Scheme of forces of infinite slope method

This model assumes that the resistance to movement along the sides of the unstable mass is not significant.

Considering an element having volume $V = zb$, in case of infinite slope, lateral forces Q_L and Q_R are equal and opposite, so that their resultant is null. The weight of

the element is: $WE = \gamma_s V$, where γ_s is the unit weight of the soil, $\gamma_s = \rho_s g$, ρ_s being the bulk density of the soil, and g the gravitational acceleration.

The normal (P) and longitudinal (T) components of the weight are: $P = WE \cos \theta = \sigma L$ e $T = WE \sin \theta = \tau L$,

where τ is the shear stress, and σ is the total normal stress. Being $L = b/\cos \theta$,

$$\sigma = \frac{WE}{b} \cos^2(\theta) = \gamma_s z \cos^2(\theta) \quad (18)$$

$$\tau_{mobil} = \frac{WE}{b} \sin \theta \cos \theta = \gamma_s z \sin \theta \cos \theta \quad (19)$$

Being $FS = \frac{\tau}{\tau_{mobil}}$, where $\tau = c' + \sigma' \tan \phi'$

where c' is the cohesion soil cohesion and/or root strength, $\tan \phi'$ is the angle of internal friction of the soil mass at the failure plane. Hence,

$$\gamma_s z \sin \theta \cos \theta = \frac{c' + (\gamma_s z \cos^2 \theta - u) \tan \phi}{FS} \quad (20)$$

being u the pore pressure, from which:

$$FS = \frac{c' + (\gamma_s z \cos^2 \theta - u) \tan \phi}{\gamma_s z \sin \theta \cos \theta} \quad (21)$$

Evaluation of slope failure

Under these assumptions, the criterion for slope failure may be expressed as (Montgomery et al., 1999)

$$\rho_s g z \sin \theta \cos \theta = C' + [z \rho_s - h \rho_w] g \cos^2 \theta \tan \phi \quad (22)$$

where z is soil thickness, C' is the effective cohesion of the soil including the effect of reinforcement by roots that penetrate the basal failure surface, ρ_w is the bulk density of water and ϕ is the friction angle of the soil. Combining Equations (16) and (22) and rearranging in terms of the critical steady-state rainfall (Q_c) necessary to trigger slope instability, yields (Montgomery et al., 1999)

$$Q_c = \frac{T \sin \theta}{a/b} \left[\frac{C'}{\rho_w g z \cos^2 \theta \tan \phi} + \frac{\rho_s}{\rho_w} \left(1 - \frac{\tan \theta}{\tan \phi} \right) \right] \quad (23)$$

The physical interpretation of $W > 1$ is that the excess water runs off as overland flow; hence, there is no mechanism in this model for generating pore pressures in excess of hydrostatic pressures (Montgomery et al., 1999). Slopes that are stable even when $W=1$ are interpreted to be unconditionally stable and to require excess pore pressures to generate slope instability. The condition for unconditionally stable slopes can be expressed as

$$\tan \theta < \frac{C'}{\rho_s g z \cos^2 \theta} + \left(1 - \frac{\rho_w}{\rho_s}\right) \tan \phi \quad (24)$$

Similarly, slopes predicted to be unstable even when dry (i.e. $W = 0$) are considered to be unconditionally unstable areas where soil accumulation would be difficult and therefore one would expect to find rock outcropping. The condition for unconditionally unstable slopes can be expressed as (Montgomery et al., 1999)

$$\tan \theta \geq \tan \phi + \frac{C'}{\rho_s g z \cos^2 \theta} \quad (25)$$

Critical rainfall values can be calculated for locations with slopes between the criteria of Equations (24) and (25).

Reinforcement introduced laterally by roots across the side of potential failures (Burroughs, 1984; Reneau and Dietrich, 1987) and systematic variations in soil thickness influence the probability of slope failure (Dietrich et al., 1995). Spatial variations in soil properties also influence the probability of failure and the location of specific failures may be strongly influenced by site-specific properties such as interaction of flow in colluvial soil and near-surface fractured bedrock (e.g. Montgomery et al., 1997). Variation in the infiltration to deeper groundwater flow may also strongly influence the distribution of landsliding. Consequently, it is likely that within areas of equal topographic control on shallow landslide triggering, some locations will be more or less susceptible to failure. Moreover, soil thickness increases through time in topographic hollows (e.g. Dietrich and Dunne, 1978; Dietrich et al., 1995) and these changes will lead to an increasing probability of slope failure as a hollow infills with colluvium (Dunne, 1991; Montgomery, 1991).

The magnitude of soil cohesion by root strength varies both between species and as a consequence to timber harvesting (Takahasi, 1968; Burroughs and Thomas, 1977; Ziemer and Swanston, 1977; Wu et al., 1979; Reneau and Dietrich, 1987). Much of the total tensile strength of roots resides in the finest roots, which die rapidly after deforestation (Burroughs and Thomas, 1977; Ziemer and Swanston, 1977). Total root strength decreases to a minimum between 3 and 15 years after timber harvest and returns to values comparable to mature forest only after several decades (e.g. Sidle, 1992). Burroughs and Thomas (1977) estimated total tensile strength per unit area of soil imparted by '*Pseudotsuga menziesii*' to be about 17 kN/m², declining rapidly after cutting to about 2 kN/m² for stumps. Less cohesion is attributable to root systems of other species; hardwood species range from 2 to 13 kN/m² (Takahasi, 1968; Endo and Tsuruta, 1969; Riestenberg and Sovonick-Dunford, 1983; Reneau and Dietrich, 1987); woody shrubs and ground cover are typically 53 kN/m² (Burroughs, 1984; Terwilliger and Waldron, 1991). The effective cohesion due to tree roots varies spatially, with depth and distance among trees, and with their age. Comparison of the net root strength required for slope stability under the infinite-slope model and a lateral root strength model (Reneau and Dietrich, 1987) reveals that significantly greater root strength is required for the finite (i.e. lateral) than the infinite-slope model. Hence, calculations based on the infinite-slope model should yield a minimum constraint on the contribution of root strength to soils in which roots do not extend through the basal failure surface.

In this work, parameters in Tab.22 were used.

Tab.22. Parameters for the modelling, defined for deposit type and soil cover. Adapted from Frattini et al. (2009).

Deposit	Soil cover	Cr (kN/m ²)	C (kN/m ²)	C' (kN/m ²)	z (m)	γ_s (kN/m ³)	ϕ (°) mean	ϕ (°) rad	K _s (m/s)
Alluvium	Shrub	3	5	8	1	18	35	0.6109	0.000005
	Wood	5	5	10	1	18	35	0.6109	0.000005
	No vegetation	0	5	5	1	18	35	0.6109	0.000005
	Grass	1	5	6	1	18	35	0.6109	0.000005
Alluvial fans	Shrub	3	0	3	1	18	45	0.7854	0.00005
	Wood	5	0	5	1	18	45	0.7854	0.00005
	No vegetation	0	0	0	1	18	45	0.7854	0.00005
	Grass	1	0	1	1	18	45	0.7854	0.00005
Eluvial-colluvial deposit	Shrub	3	10	13	1	18	40	0.6981	0.000001
	Wood	5	10	15	1	18	40	0.6981	0.000001
	No vegetation	0	10	10	1	18	40	0.6981	0.000001
	Grass	1	10	11	1	18	40	0.6981	0.000001
Glacial deposit	Shrub	3	15	18	1	18	35	0.6109	0.0000005
	Wood	5	15	20	1	18	35	0.6109	0.0000005
	No vegetation	0	15	15	1	18	35	0.6109	0.0000005
	Grass	1	15	16	1	18	35	0.6109	0.0000005
Outcrops	Shrub	3	3	6	0.5	18	40	0.6981	0.000001
	Wood	5	3	8	0.5	18	40	0.6981	0.000001
	No vegetation	0	3	3	0.5	18	40	0.6981	0.000001
	Grass	1	3	4	0.5	18	40	0.6981	0.000001

6.2.2 EXPECTED FREQUENCY OF OCCURRENCE, W_{SL}

For the evaluation of w for shallow landslides, an intensity-frequency relationship was not considered, needing the calculation of a frequency for each intensity class. Shallow landslides are, for definition, of small dimension, and have a limited variability of intensity.

Frequency was calculated multiplying the mean frequency for each cell, \bar{w} , with a susceptibility factor s that expresses a spatial relative probability of landslide at the area

$$w = \bar{w} * s$$

The mean frequency of occurrence for each cell, \bar{w} , was calculated from inventory maps including also debris flow events, assuming that most of debris flows are triggered as shallow landslides.

The overall number of landslides in Valtellina, mapped for the period 1983-2008, equals to 2,819 events, meaning an annual frequency of 112 events/year, calculated only on mountainous areas.

For the Brescia area, the frequency w was calculated by means of datasets provided by European Project LESSLOSS for the Val Trompia and part of the Val

Sabbia (LESSLOSS, 2007). For these two sample areas, 1874 events for the period 1954-2000 were recorded, meaning an annual frequency of 130 events/year calculated for the whole study area, only on mountain zones. The mean annual frequency of shallow landslides in mountainous areas is therefore of $5 \cdot 10^{-5}$ events/year/cell for Valtellina and $5 \cdot 10^{-4}$ events/year/cell for Brescia. This difference can be explained considering the different lithological and morphological conditions of the two areas, in particular Valtellina is characterised in some parts by very steep rocky slopes where the triggering of shallow landslides is not probable. This is also supported by historical data.

Susceptibility factor, s , was calculated using the physically based model described above (Montgomery and Dietrich, 1994), and implemented in MATLAB. The model provides an estimate of the critical steady-state rainfall (Q_c) necessary to trigger slope instability. The value of critical recharge was rescaled to respect the condition $\bar{s} = 1$.

A *downscaling* of the frequency was effectively performed, based on the spatial susceptibility of the area.

Expected frequency of occurrence in Valtellina is on average one order of magnitude lower than in the Brescia area, as suggested by historical events (Fig.44).

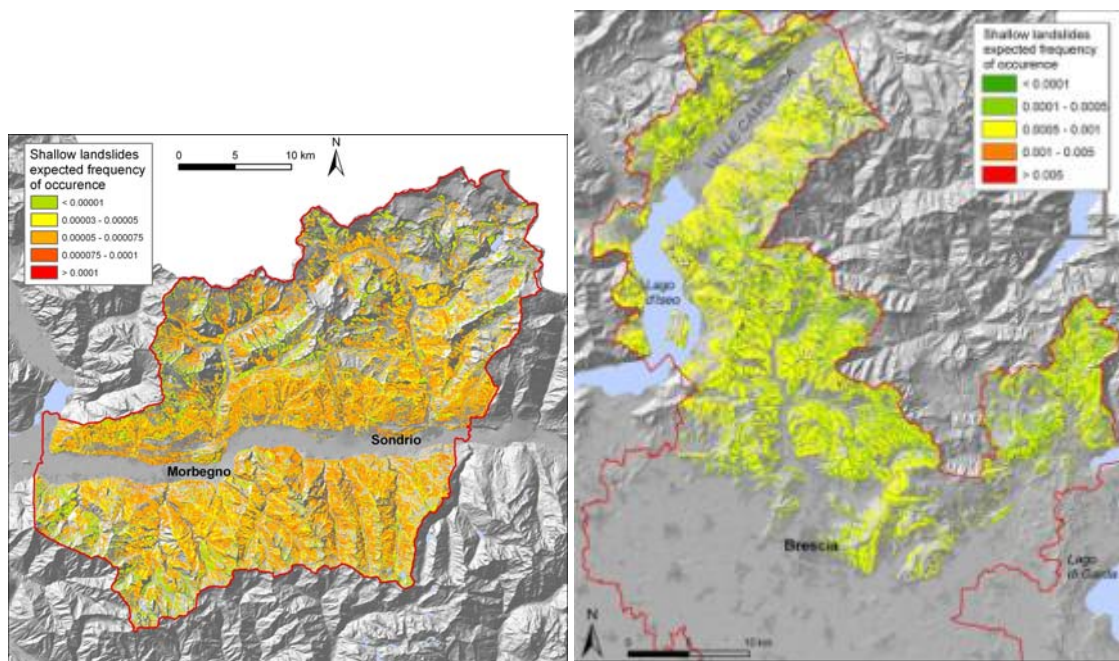


Fig.44. Expected frequencies of occurrence, w_{SL} , for shallow landslides

6.2.3 SOCIETAL RISK ASSESSMENT

Gravity factor, g_{SL}

The intensity of shallow landslides is quite low, unless they evolve in a debris flow. For this reason, even in case of impacted people or vehicles, the probability to

undergo heavy damages is very low. From expert evaluation, a gravity factor $g_{SL} = 0.1$ was assigned.

Exposure factor, e_{SL}

In case that shallow landslides do not evolve in debris flows, these phenomena do not have enough energy to damage structures. Hence, people potentially involved are the only ones localised on open air and along communication lines. With respect to equivalent inhabitants, only the ones being outside buildings are considered. Lacking of information requested to calculate the number of these people exactly, about 5% of exposed people was assumed to be located outside buildings. This assumption leads to an overestimation of risk in productive areas, and probably an underestimation for communication lines. The probability of people on open air to be effectively impacted is independent from civil protection systems, because shallow landslides are sudden and unpredictable events. The e value depends also on the area of expected landsliding with respect to the entire cell area, in the reasonable hypothesis that a cell can be affected only by one landslide at a time. Assuming that shallow landslides have a mean area of 50 m^2 (assumption supported by the analysis of the inventory landslide map for the study areas) and the cell area equals 400 m^2 , the population potentially impacted was corrected also for $50/400 = 0.125$.

As a consequence, the e_{SL} factor assumes the value of $0.05 \cdot 0.125 = 0.00625$.

To account for the vehicles impacting on occurred landslide, soon after the event, e_{SL} was corrected by a factor of 2, indicating that, for each landslide, there is the possibility that two people are successively impacted by the phenomena at the same place. With this correction, we finally obtain: $e_{SL} = 0.0125$.

Societal physical risk

Societal physical risk has very low values (Fig.45,46 and 47, Tab.23). Diffused shallow landsliding mostly develops in scarcely vegetated slopes in high mountains, scarcely settled, and along riverbed slopes. In Valtellina, risk values range from 0 to 10^{-7} for the day scenario and from 0 to $6 \cdot 10^{-6}$ for the night scenario. In Brescia area, in some zones along the valleys, the number of expected annual casualties reaches values of the order of magnitude of $3 \cdot 10^{-5}$. For the whole study areas, in Valtellina the daily societal risk equals $6 \cdot 10^{-6}$ casualties/year and the night one $9 \cdot 10^{-5}$ casualties/year. The expected number of victims for the study area of Brescia is 0.005 victims/year.

Tab.23. Societal risk values

	Valtellina day scen	Valtellina night scen	Brescia
Range (cas/year/cell)	$0-10^{-7}$	$0-6 \cdot 10^{-7}$	$0-3 \cdot 10^{-5}$
Total (cas/year)	$6 \cdot 10^{-6}$	$9 \cdot 10^{-5}$	$5 \cdot 10^{-3}$

. In the area of Brescia, societal risk is slightly higher, mainly due to the higher frequency of occurrence, w , and to the localisation of shallow landslides in proximity of densely urbanised areas (Fig. 55).

The model for risk assessment does not consider mitigation works, realised for instance to protect the city of Sondrio. The analysis of historical data show that no victims are recorded in the last century, hence the obtained results are in accordance with historical data.

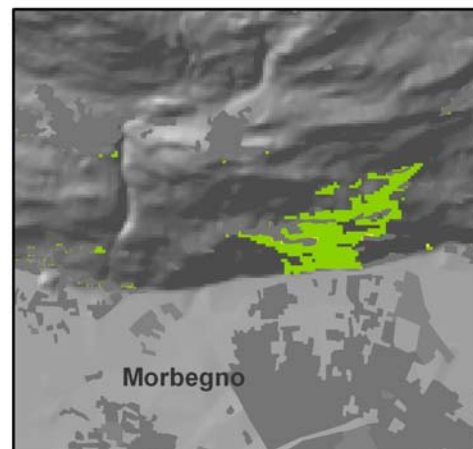
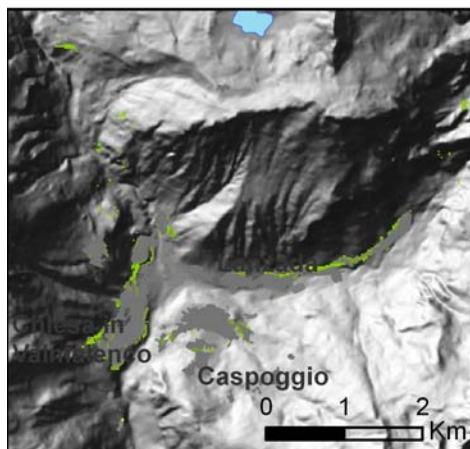
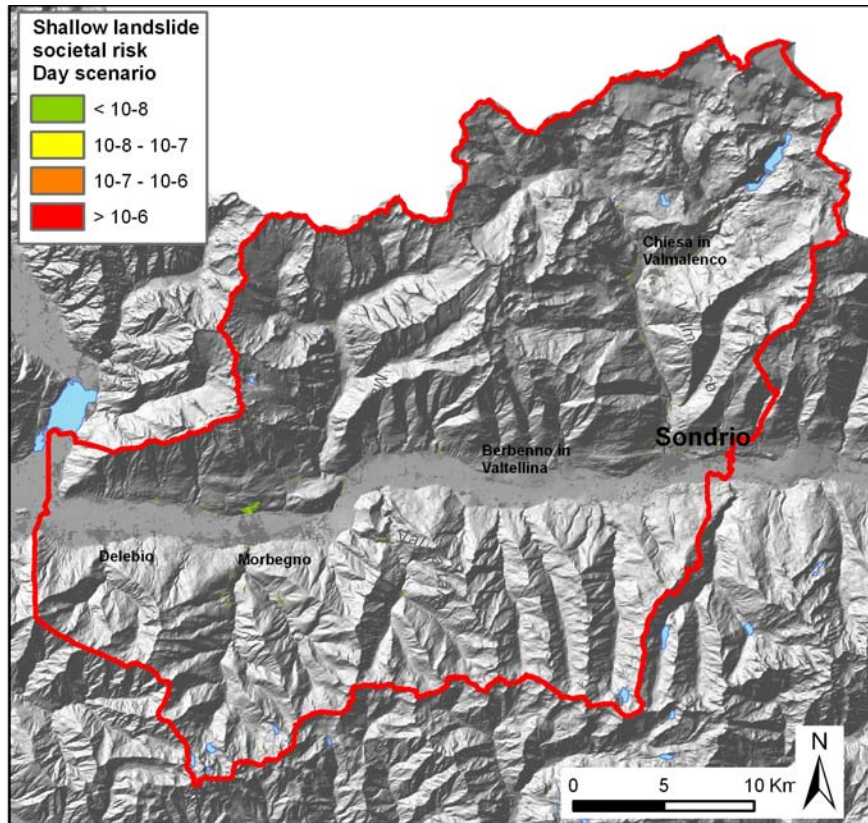


Fig.45. Map of societal physical risk for shallow landslides, for day scenario, Valtellina Risk values are expressed in terms of casualties per year.

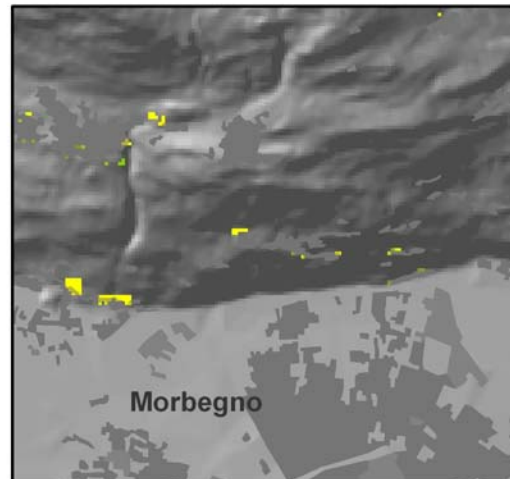
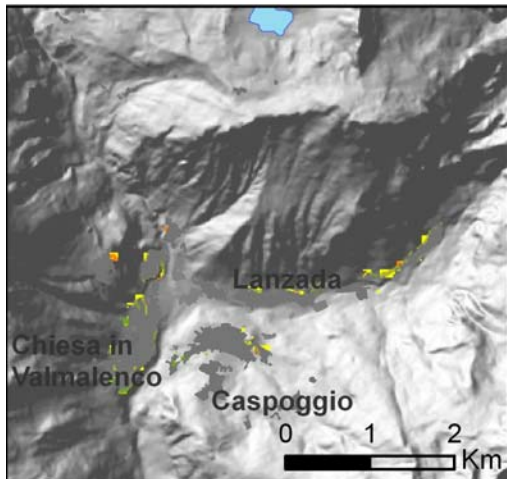
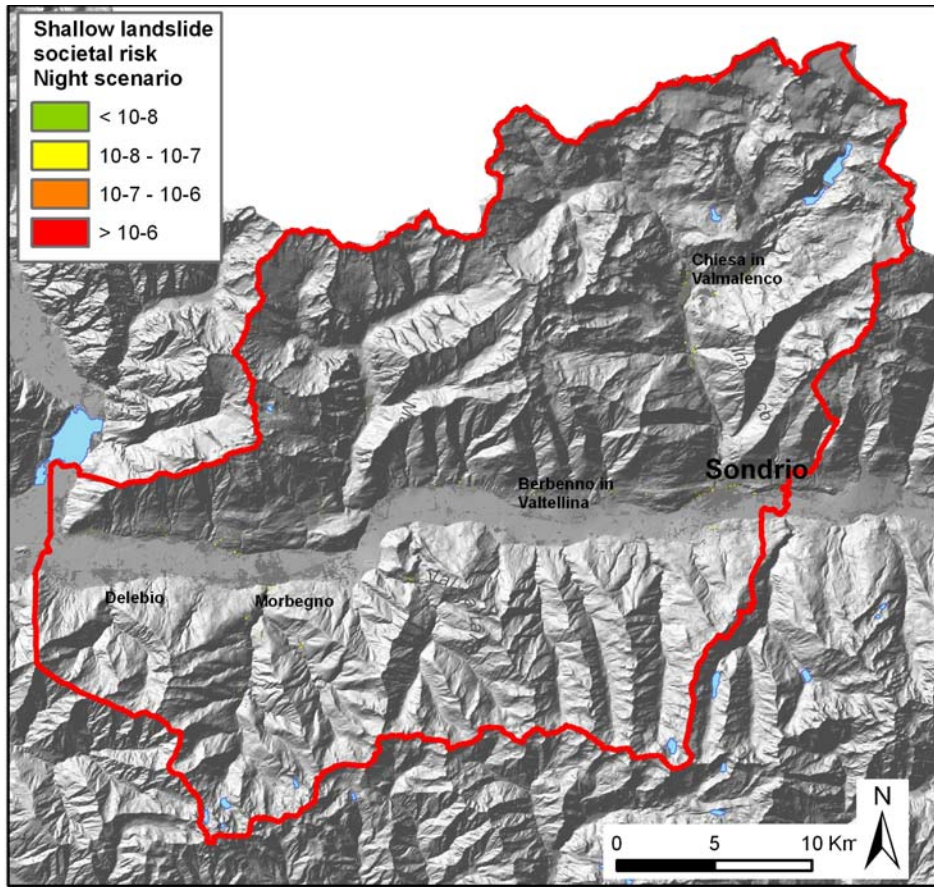


Fig.46. Map of societal physical risk for shallow landslides, night scenario, Valtellina. Risk values are expressed in terms of casualties per year.

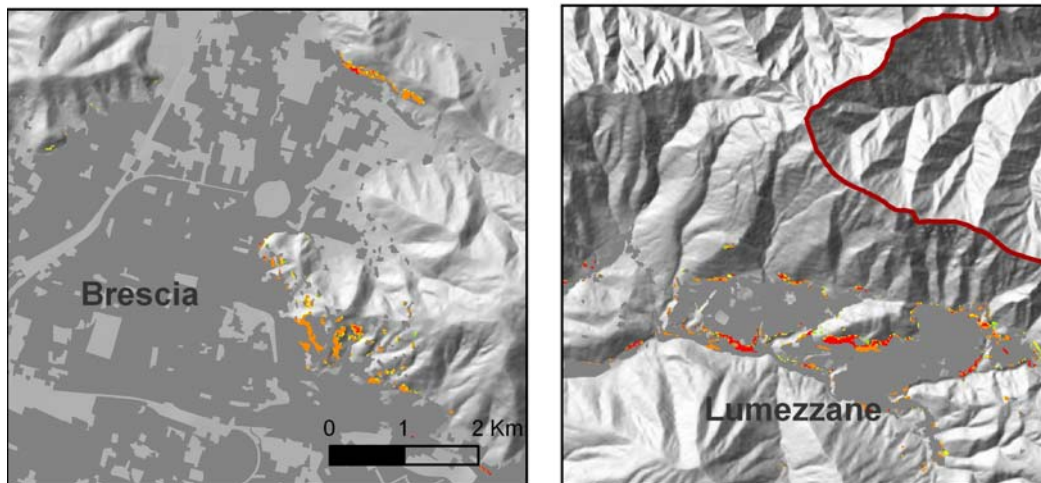
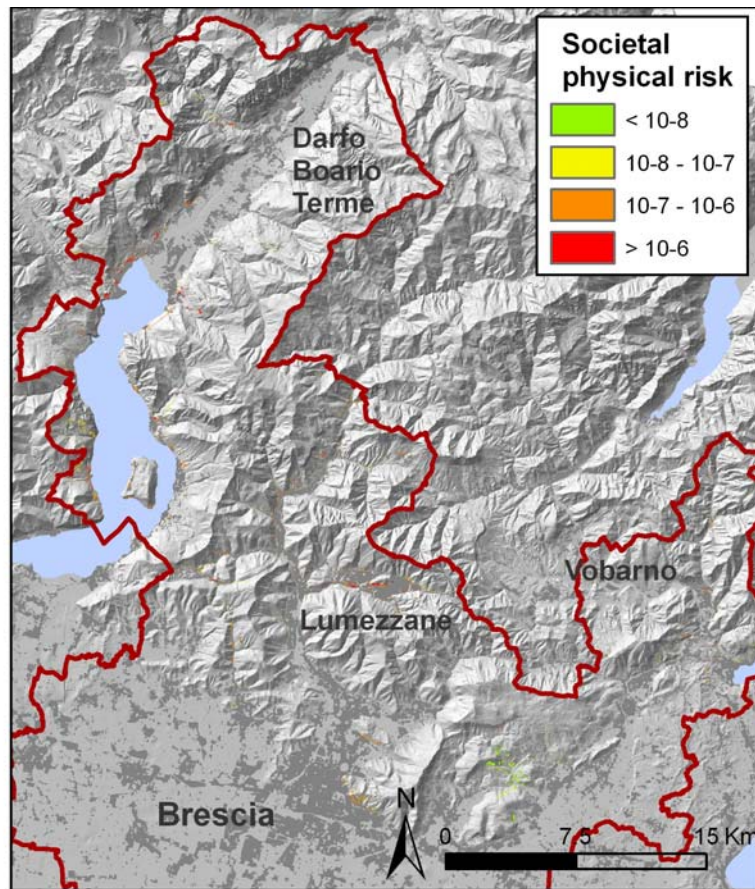


Fig.47. Map of societal physical risk for shallow landslides, Brescia study area. Risk values are expressed in terms of casualties per year.

6.2.4 ECONOMIC RISK ASSESSMENT

Gravity factor, g_{SL}

By means of an expert evaluation, different values were attributed to the factor of gravity to different categories of exposed elements. Due to the low intensity and to the type of phenomenon, the only economic direct damage is the one undergone by cultivations of different types, and woods (Tab.24.).

Tab. 24. Factor of gravity, g for economic risk by shallow landsliding

Exposed elements	g_{SL}
Roads, railways, power lines	0
Woods	0.3
Orchards, olive groves	0.5
Vineyards	0.7
Buildings	0

Exposure factor, e_{SL}

As said for societal risk, the value of e_{SL} depends on the area of expected landslides with respect to the entire cell area, in the reasonable hypothesis that a cell can be affected only by one landslide at a time. Assuming that shallow landslides have a mean area of 50 m^2 (assumption supported by the analysis of the inventory landslide map for the study areas) and the cell area equals 400 m^2 , we deduce that the value of the exposure factor e_{SL} was evaluated as $50/400 = 0.125$.

Economic physical risk

Shallow landslides do not induce a significant economic damage (Fig. 48 and 49). This is due to the low occurrence frequency of the events and to the low gravity factors assigned to buildings, which are not damaged by these events ($g = 0$). Moreover, as said for societal risk assessment, diffused shallow landsliding in most cases develop in scarcely vegetated slopes in high mountains.

In Valtellina, economic risk ranges from 0 to $0.098 \text{ €/year/cell}$, with a total value for the whole area of $7,110 \text{ €/year}$. In the Brescia area, it ranges from 0 to 0.24 €/year/cell , with a total value for the whole area of $58,109 \text{ €/year}$ (Tab.25).

Tab.25. Economic risk values for the two study areas

	Valtellina	Brescia
Range (€/year/cell)	0 - 0.098	0 - 0.24
Total (€/year)	7,110	58,109

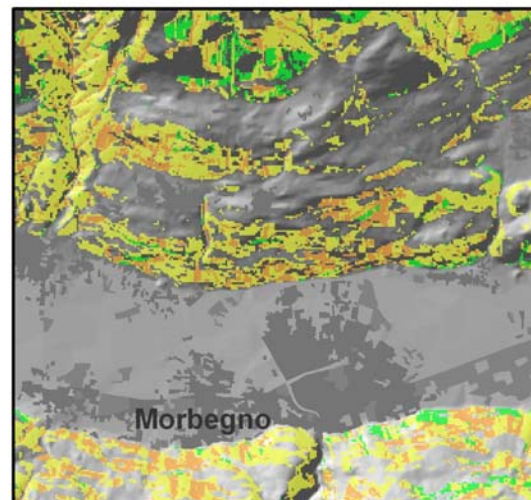
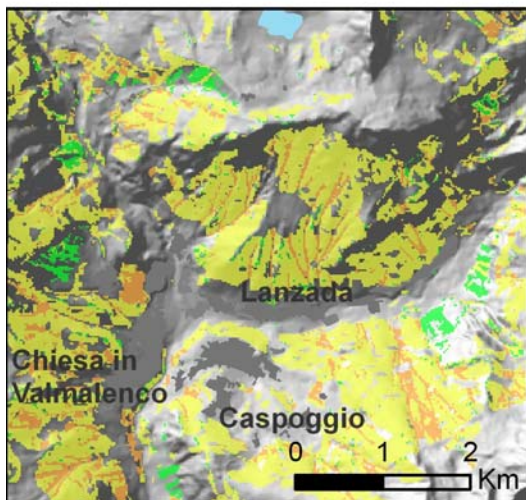
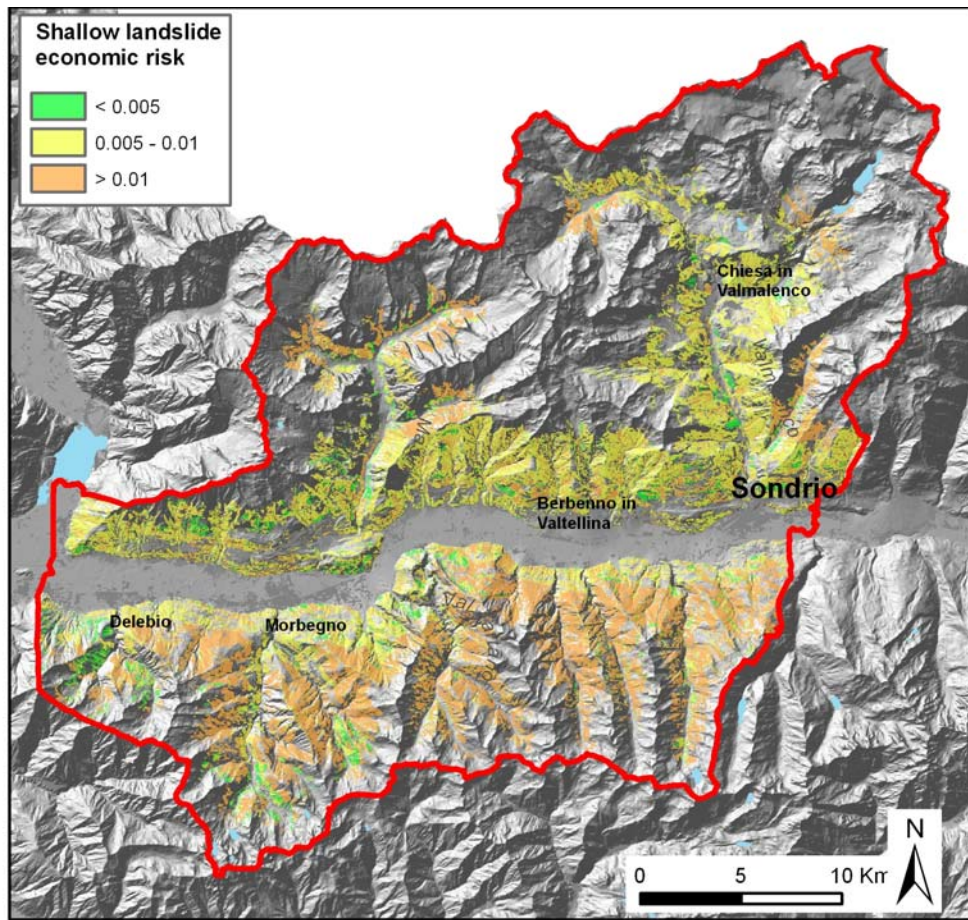


Fig.48. Map of economic physical risk for shallow landslides, in euros/year, for Valtellina

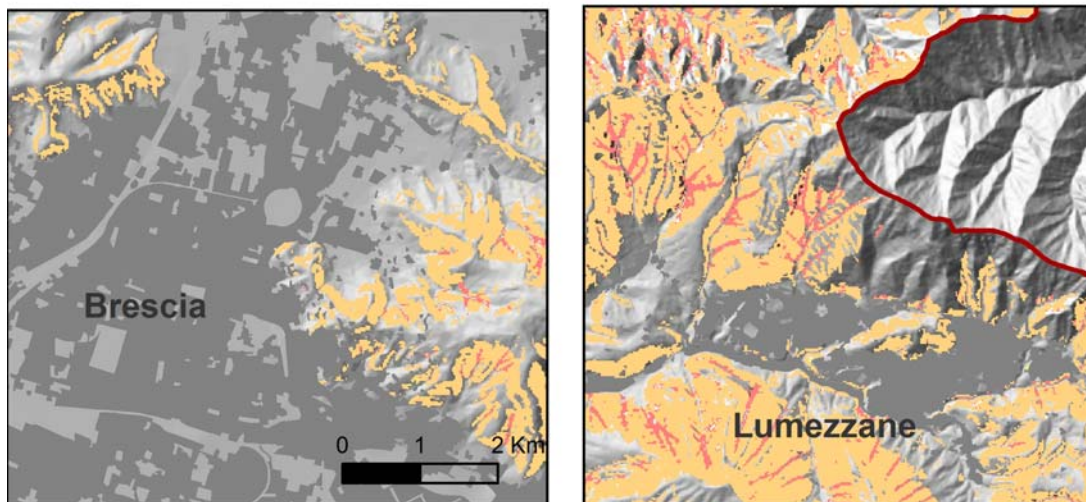
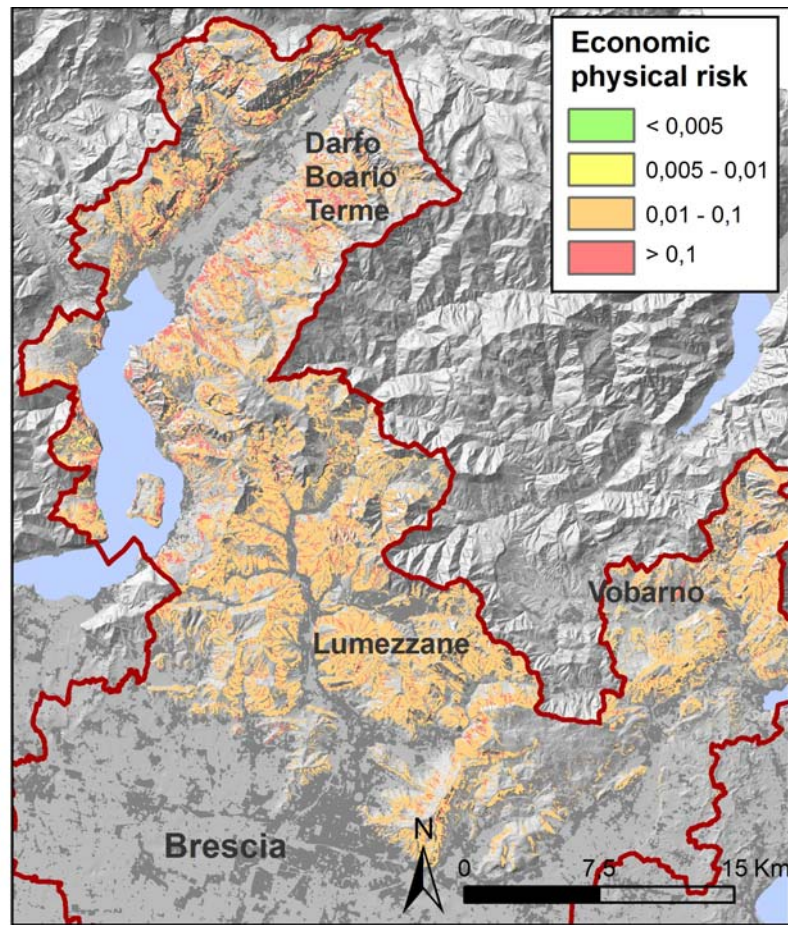


Fig.49. Map of economic physical risk for shallow landslides, in euros/year, for Brescia study area

6.3 DEBRIS FLOW RISK

For debris flow risk assessment, a semi-empirical model (Horton et al., 2008) was used. This model allows to define the maximum extent of flow propagation starting from previously identified source areas, and provides an associated qualitative probability qualifying the susceptibility potential. The kinetic energy is also provided by the computations (Horton et al., 2008). The model allows a free choice of the algorithms for calculation of flow direction and propagation distance.

6.3.1 DEBRIS FLOW SIMULATION

The code allows to compute the maximum extent of debris-flow propagation using the DTM, the geology, the geo-environmental map (Regione Lombardia, 1983) and the land use map (DUSAF, 2007). The complexity of the phenomenon and the variability of the controlling factors make debris flow modelling quite difficult. The methodology includes:

1. the identification of debris flow source areas by means of geomorphologic, hydrologic, geologic maps, combined with active debris flow inventory map.
2. the simulation of propagation by means of a probabilistic and energetic approach.

Source areas are identified by means of the shallow landslide simulation model as described above (par. 6.2) integrated with historical debris flow inventory maps, which are supposed to potentially reactivate in the future.

Flow direction algorithm

Flow direction algorithms distribute the flow from one cell to its eight neighbours. Some conditions are defined so that there is always at least one cell in which the flow can run, so that runoff algorithms only determine if flow continues or if it stops (Horton et al, 2008). The distribution of the flow, expressed as probabilities of flow for each cell, is a function of both the slope and the persistence, which is a weighting of the directions according to the previous direction, accounting for the concept of inertia.

The slope has a strong effect on the debris flow direction. Many different algorithms have been proposed in the literature. In the simple single-flow D8 approach, the flow is entirely transferred from each cell to the neighbouring cell along the steepest direction. The multiple flow direction method (Quinn et al. 1991) considers the spreading over every downward cell in a continuous, and not random way:

$$f_{si} = \frac{\tan \beta_i}{\sum_{j=1}^8 \tan \beta_j} \quad \text{for } \tan \beta > 0 \quad (26)$$

where:

i, j = flow direction;

f_{si} = flow proportion in direction i ;
 $\tan \beta_i$ = slope gradient between the central cell and cell in one downslope direction

Holmgren (1994) introduced an exponent, x , in the algorithm, to allow a control on the spreading of the flow

$$f_{si} = \frac{(\tan \beta_i)^x}{\sum_{j=1}^8 (\tan \beta_j)^x} \tag{27}$$

The higher is the exponent x , the more convergent the flow becomes (Fig.50). In particular,

- if $x = 1$, f_{si} = multiple flow direction method
- if $x \rightarrow \infty$, single flow direction (D8)

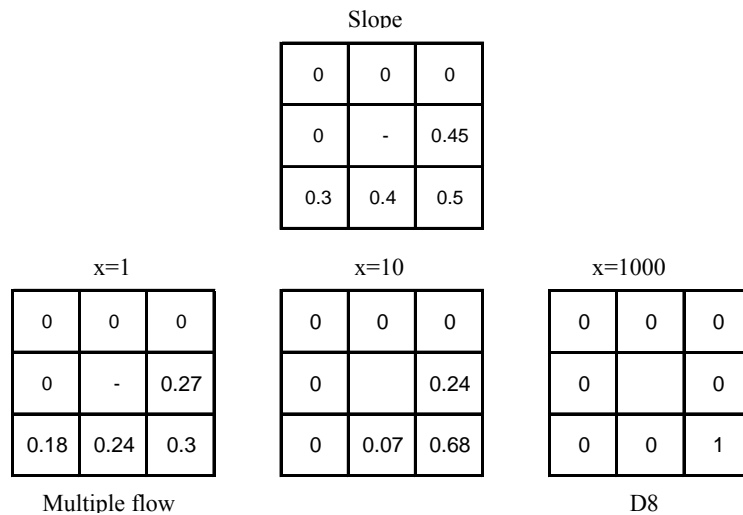


Fig.50. Example of flow distribution for three different values of exponent x (Holmgren, 1994).

A further weighting of the flow direction is included in the code to take into account the persistence of the debris flow, representing its inertia, which is the tendency of the flow to maintain its direction. Based on Gamma (2000), the persistence weight is a function of the change α in angle from the last flow direction.

$$\begin{aligned} f_{pi} &= w_0 \quad \text{if } \alpha=0^\circ \\ f_{pi} &= w_{45} \quad \text{if } \alpha=45^\circ \\ f_{pi} &= w_{90} \quad \text{if } \alpha=90^\circ \\ f_{pi} &= w_{135} \quad \text{if } \alpha=135^\circ \\ f_{pi} &= 0 \quad \text{if } \alpha=180^\circ \end{aligned}$$

where i = flow directions, f_{pi} = persistence term of flow proportion in direction i , α_i =angle between the previous flow direction and the new flow direction from the central cell i , w = weights for the corresponding change in direction.

Resulting probabilities are the combination of the slope-related algorithm and the persistence (Fig 51).

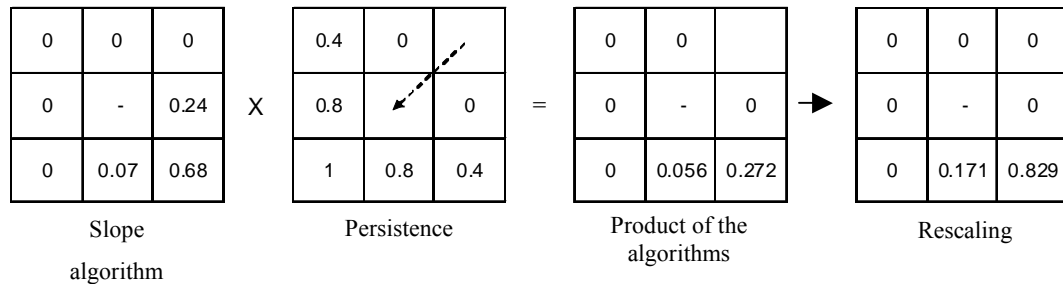


Fig.51. Example of flow apportionment with persistence effect. Provenience of flow is indicated by the flesh, and it is divided into the lower cells. The probability deriving from the product of slope algorithm and persistence is rescaled to 0-1

Runout distance calculation

Runout distance algorithms are energy-based calculations that define, for each cell, if the debris flow can potentially reach another cell. Thus, they control the distance reached by the debris flow. Moreover, they influence the flow direction: in fact, some of the cells that could receive a flow from the direction algorithm, are not reached by the flow because of energy, and their debris flow probability is set to zero. The source mass, is unknown, thus, runout distance calculation is based on unit energy balance, a constant loss function and a maximum velocity threshold. This approach does not aim to exactly represent the physical processes, but to provide a realistic figure of the phenomena.

Potential energy is in part transformed in kinetic energy, and in part lost as friction. Energy loss is modelled with a pre-determined friction angle. Kinetic energy is limited by a upper velocity threshold to avoid excessive or unrealistic energies.

At the beginning, a debris flow source has a certain unit potential energy (without considering the volume) (Fig.60) (a). During propagation, part of the energy is lost in friction (b). The kinetic energy increases and may reach the maximum threshold value, leading to an energy line having the same profile as the terrain. In fact, while the threshold is reached, energy loss is equal to the difference in potential energy (c). The debris flow stops when the energy becomes null (d) (Horton, et al., 2008).

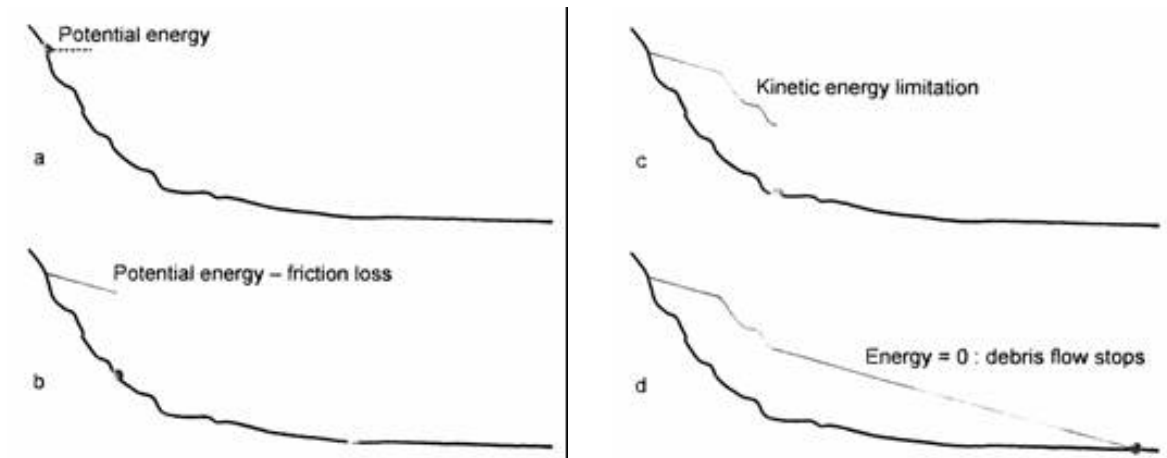


Fig.52. illustration of the runout distance calculation principles, from Horton et al., 2008

Calibration of the model

Outputs of each simulation are: the maximum kinetic energy of the debris flow in each cell, and the propagation probability for each cell. To calibrate the model, it was necessary to make a number of simulations modifying each time the control parameters. After several attempts, 6 parameterizations were identified which performed well, based on the comparison of simulation results and actual debris flows (Tab.26).

For Valtellina, the adopted model was n.1, better representing the real case. For Brescia, it was n.2.

Tab.26.Parameters for debris flow model calibration

	MODEL 1	MODEL 2	MODEL 3	MODEL 4	MODEL 5	MODEL 6
Flow accumulation (m ²)	10000	10000	10000	10000	10000	10000
Buffer (m)	2000	1000	1000	1000	1000	1000
Direction Algorithm	Holmg. exp10	Holmg. exp10	Holmg. exp10	Holmg. exp15	Holmg. exp5	Holmg. exp7
Inertial Algorithm	Weights	Weights	Weights	Weights	Weights	Weights
Friction loss function	c. loss 15°	c. loss 25°	c. loss 30°	c. loss 20°	c. loss 20°	c. loss 20°
Limiting Kinetic Energy	<10mps	<30mps	<30mps	<30mps	<30mps	<30mps

6.3.2 EXPECTED FREQUENCY OF OCCURRENCE, W_{DF}

For debris flow frequency assessment, it was decided not to consider the frequency/intensity relation, that would have required the calculation of an occurrence frequency for each class of intensity. Considering the high level of uncertainty in the calculation of debris flow intensity, also with respect to other types of landslide, this approach was discarded, and an overall frequency was assessed.

The expected frequency of occurrence w_{DF} is composed of a triggering frequency and a transit frequency. Triggering frequency was assumed to be the same as for shallow landslides. This assumption is supported by the fact that the majority of debris flow occurring in the area triggers as shallow landslides and that the number of debris flows triggered in different circumstances (debris erosion in riverbed, effects at the foot of the slope) is assumed to be balanced by the number of shallow landslides not evolving in debris flow. Triggering frequency was assumed as constant in each study area, given by the frequency of the events, divided by the number of source areas (i.e. Valtellina: 120,438 cells, in Brescia area: 290,987 cells). Triggering frequency results to be $9.4 \cdot 10^{-4}$ in Valtellina and $1.5 \cdot 10^{-4}$ in the Brescia area.

To calculate the probability associated to the propagation at each cell, the semi-empirical model proposed by Horton et al (2008), was used.

The expected frequency of occurrence w_{DF} for each cell of the areas was calculated as the product of triggering frequency of the single source area and the propagation frequency. For Valtellina, frequency for day and night scenarios were distinguished.

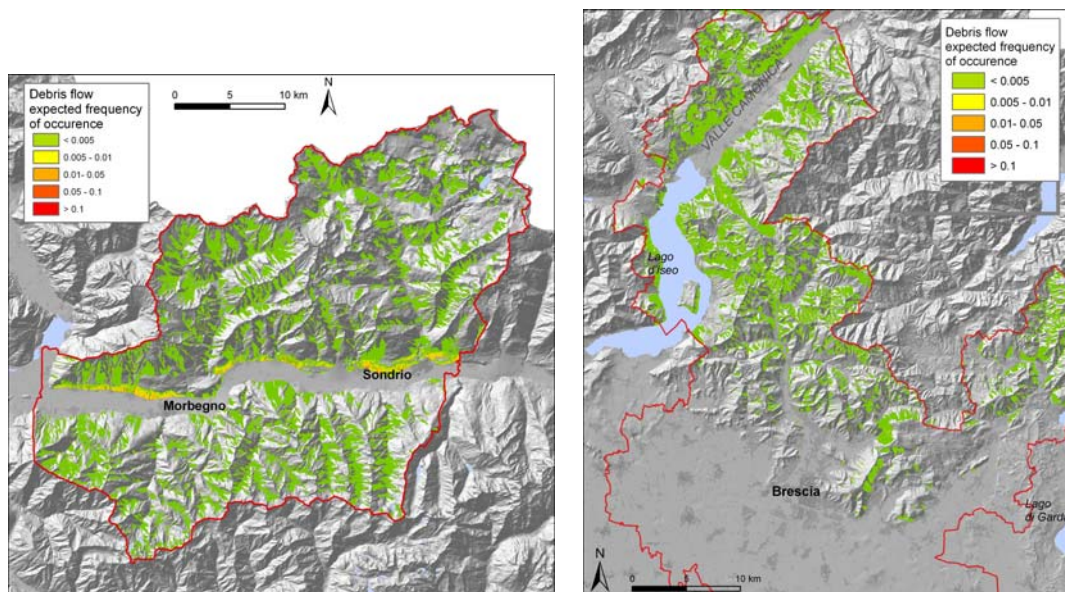


Fig.53. Expected frequency of occurrence w for debris flow

6.3.3 SOCIETAL RISK ASSESSMENT

Gravity factor, g_{DF}

Gravity related to debris flows is strictly dependant on the intensity, in terms of depth and velocity of the flow, and the vulnerability of people. Intensity for debris flows is in general quite high. The flow proceeds with high velocities and it carries debris having a great destructive power. For this reason, people impacted by debris flow are supposed to have a high probability of being damaged. By means of expert evaluations, a value of $g_{DF} = 0.75$ was fixed.

Exposure factor, e_{DF}

The probability that potentially exposed people can be effectively impacted by a debris flow (e_{DF}) is largely independent from civil protection systems, being debris flows sudden, fast and in general unpredictable phenomena. The e_{DF} value depends only on the possibility that people localised in a cell is impacted. This is a function of:

- mean debris flow extent with respect to cell dimension (400 m²)
- proportion of people living or working in the first floors of buildings.

It is assumed that debris flows in the areas have a mean width of 5 m, and they affect the whole length of the cell, that is 20 m, in the hypothesis that the cell is crossed normally. In case of oblique crossing, the length can range from 0 (at the corner) to almost 29 m in the central zone of the cell. The area impacted by debris flow equals to almost $5 \times 20 \text{ m} = 100 \text{ m}^2$, corresponding to 0,25 of the cell area.

Assuming that almost 50% of people in the buildings is located at the first floors, the exposure factor is then $0,25 \times 0,5 = 0,125$

Societal physical risk

In Valtellina, societal risk ranges from 0 to 0.014 casualties/year/cell for the day scenario and from 0 to 0.02 casualties/year/cell for the night scenario. On the whole area, the overall risk is 0.23 casualties/year for day scenario and 2.58 casualties/year for night scenario. The upper Val Masino and Valmalenco are the most impacted zones (Fig. 54 and 55).

In the area of Brescia, societal risk is concentrated on the western slope of Val Camonica, and Val Trompia with values reaching 0.017 casualties/year/cell, while in Valle Sabbia and in the municipality of Salò it shows very low values (10^{-4} - 10^{-5} casualties/year/cell) (Fig.56). The overall risk for the area is about 0.772 casualties/year.

The results show that Valtellina is more heavily impacted, especially during the evening and the night. This means that the most impacted are urban and residential zones. Considering that debris flows in Valtellina killed more than 20 people in the last 20 years, the modelling results seem compatible with historical data.

Tab.27. Societal risk values

	Valtellina day scen	Valtellina night scen	Brescia
Range (cas/year/cell)	$1.4 \cdot 10^{-2}$	$2 \cdot 10^{-2}$	$1.7 \cdot 10^{-2}$
Total (cas/year)	0.23	2.580	0.772

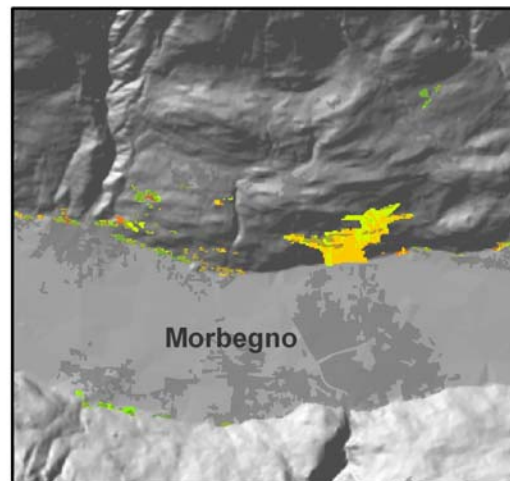
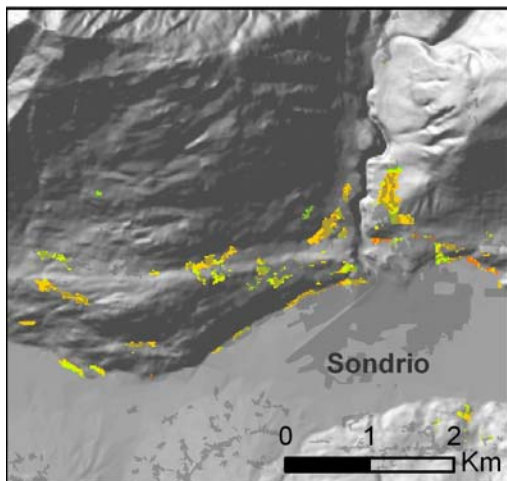
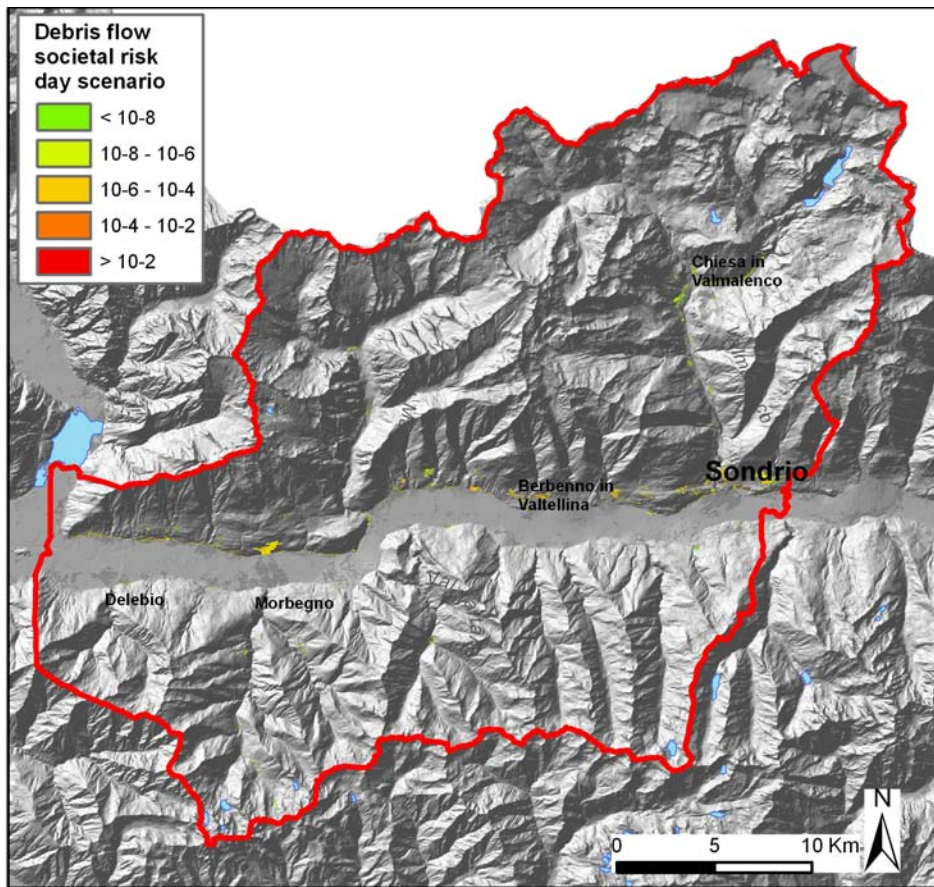


Fig.54. Map of societal physical risk for debris flows, day scenario, Valtellina. Risk values are expressed in terms of casualties per year.

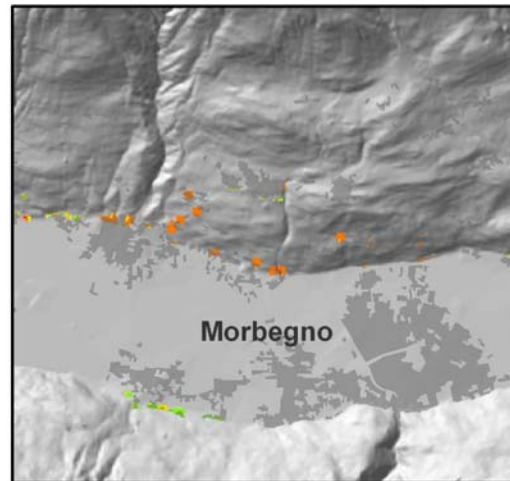
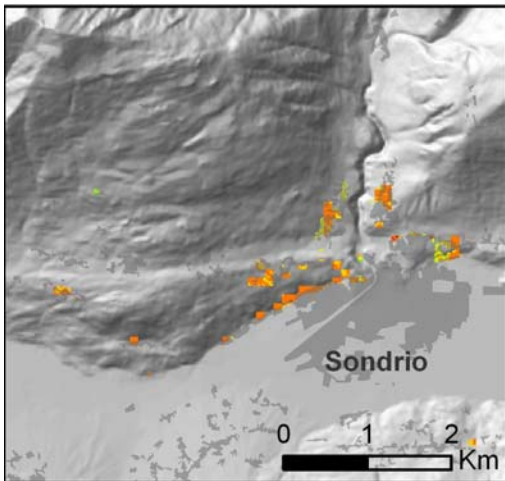
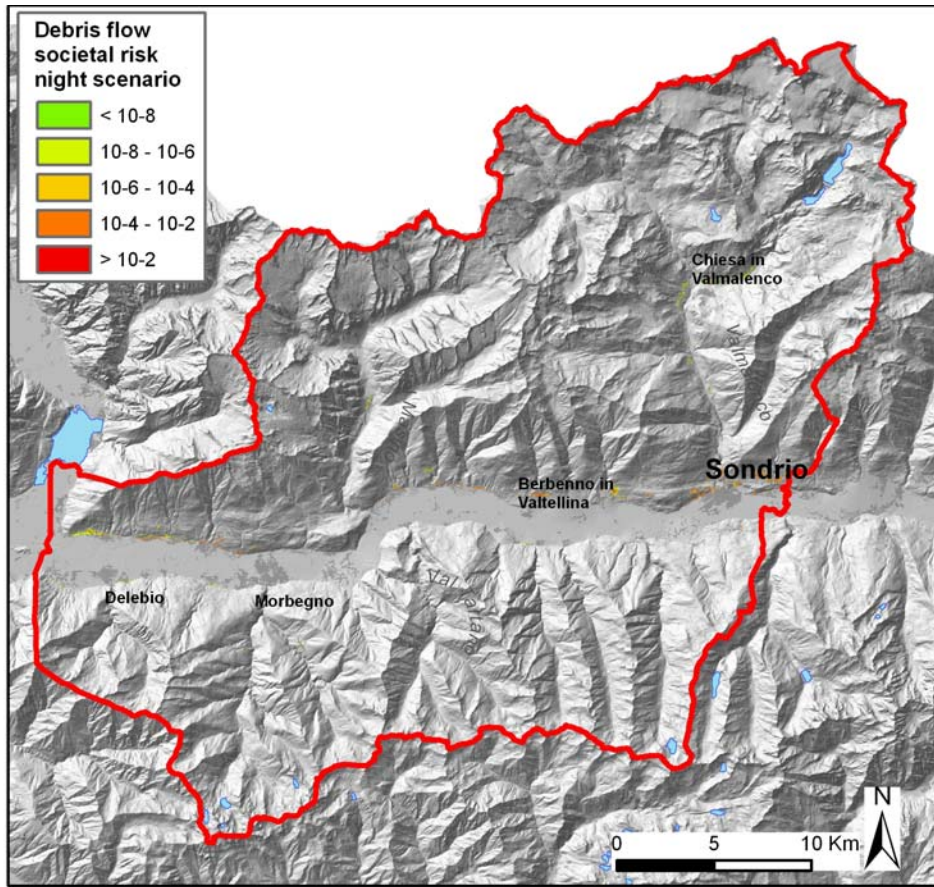


Fig.55. Map of societal physical risk for debris flows, night scenario, Valtellina. Risk values are expressed in terms of casualties per year.

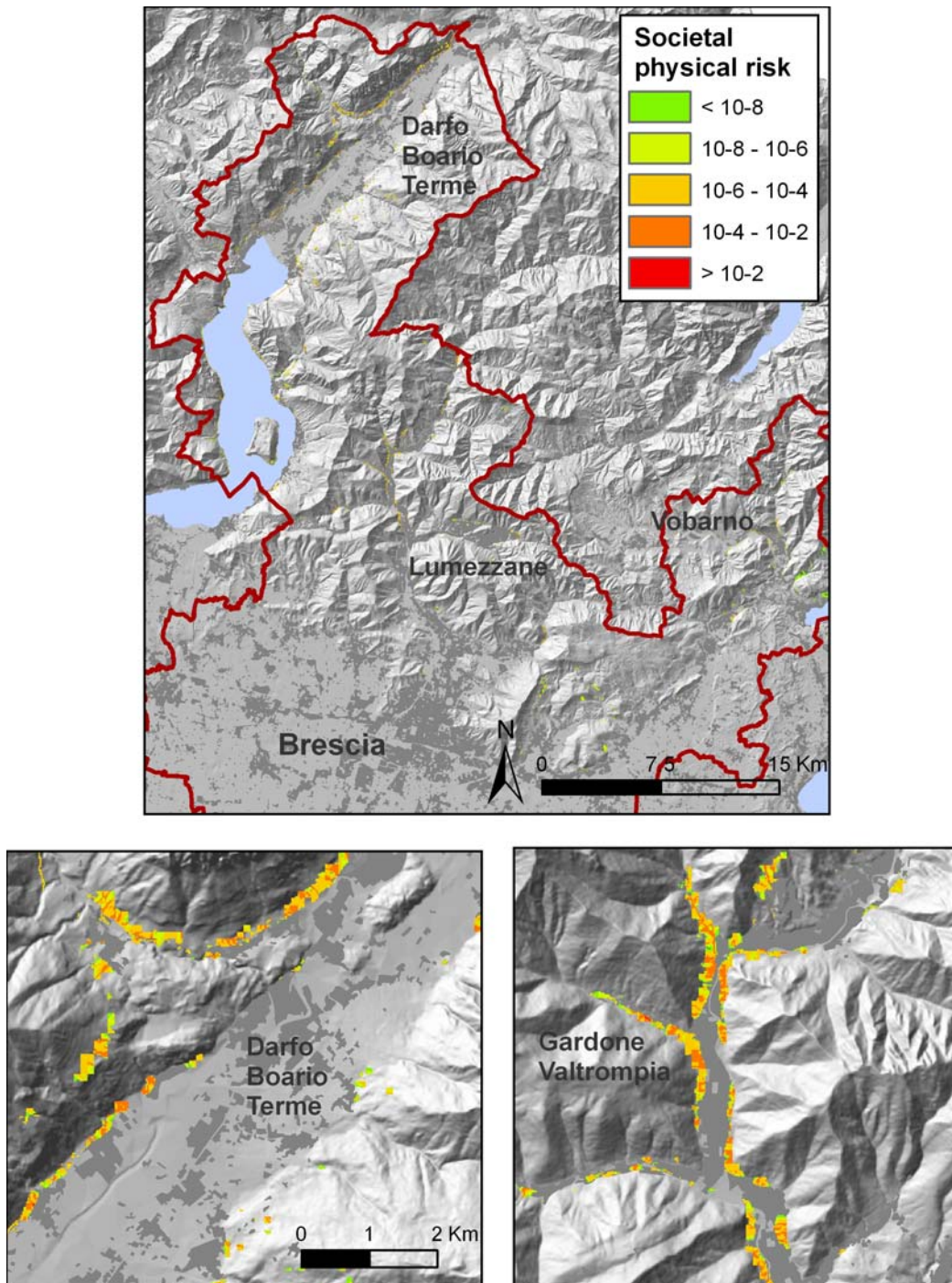


Fig.56. Map of societal physical risk for debris flows, Brescia study area. Risk values are expressed in terms of casualties per year.

6.3.4 ECONOMIC RISK ASSESSMENT

Gravity factor, g_{DF}

Gravity related to debris flows is strictly dependant on the intensity, in terms of depth and velocity of the flow, and on the vulnerability of exposed elements. To assess the value of g_{DF} , a debris flow with a depth of 2m was considered, and the relation proposed by Bovolin and Tagliatela (2002) was used:

$$g_{DF} = 0.125 * v$$

using as v the velocity obtained by the model. This function was used for buildings, without modifications. For other typologies of exposed elements, correction was introduced to account for higher vulnerability (Tab.28).

Tab.28. Factor of gravity, g for debris flow economic risk

Exposed elements	g_{DF}
Roads, power lines, railway	0
Woods	$0.125 * v * 2$
Orchards, olive groves, vineyards	$0.125 * v * 3$
Buildings	$0.125 * v$
Fields and grass	1

Exposure factor, e_{DF}

Similarly to what has been done for societal risk, an exposure factor e_{DF} considered equal to 0.25 was used.

Economic physical risk

Economic damages induced by debris flow range from 0 to 13,814 €/year/cell in Valtellina, from 0 to 18,112 €/year/cell in the area of Brescia. On the whole area, economic risk is equal to 2,583,644 €/year, and to 3,114,250 €/year in Valtellina and in the area of Brescia, respectively (Fig.57 and 58).

Tab.29. Economic risk values for the two study areas

	Valtellina	Brescia
Range (€/year/cell)	0 – 13,814	0 – 18,112
Total (€/year)	2,583,644	3,114,250

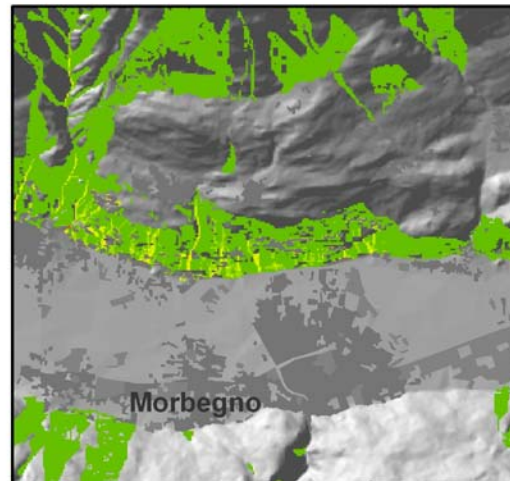
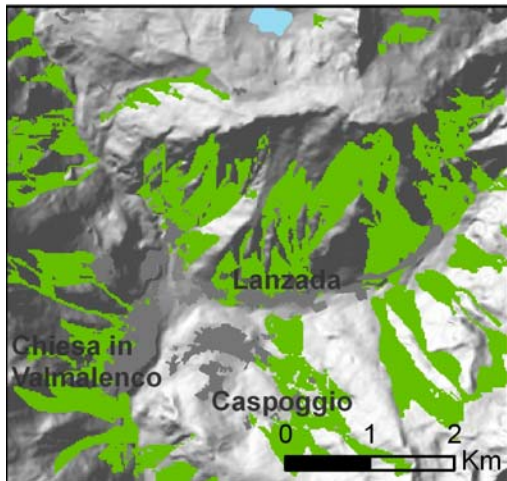
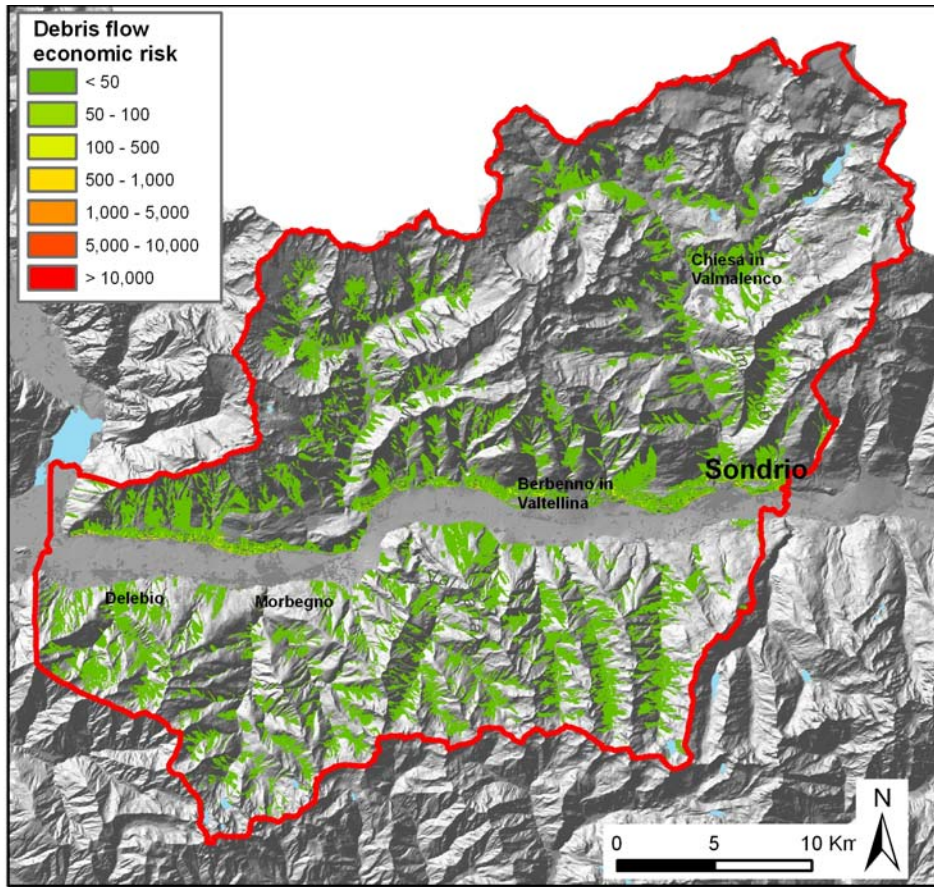


Fig.57. Map of economic physical risk for debris flows, in euros/year, for Valtellina

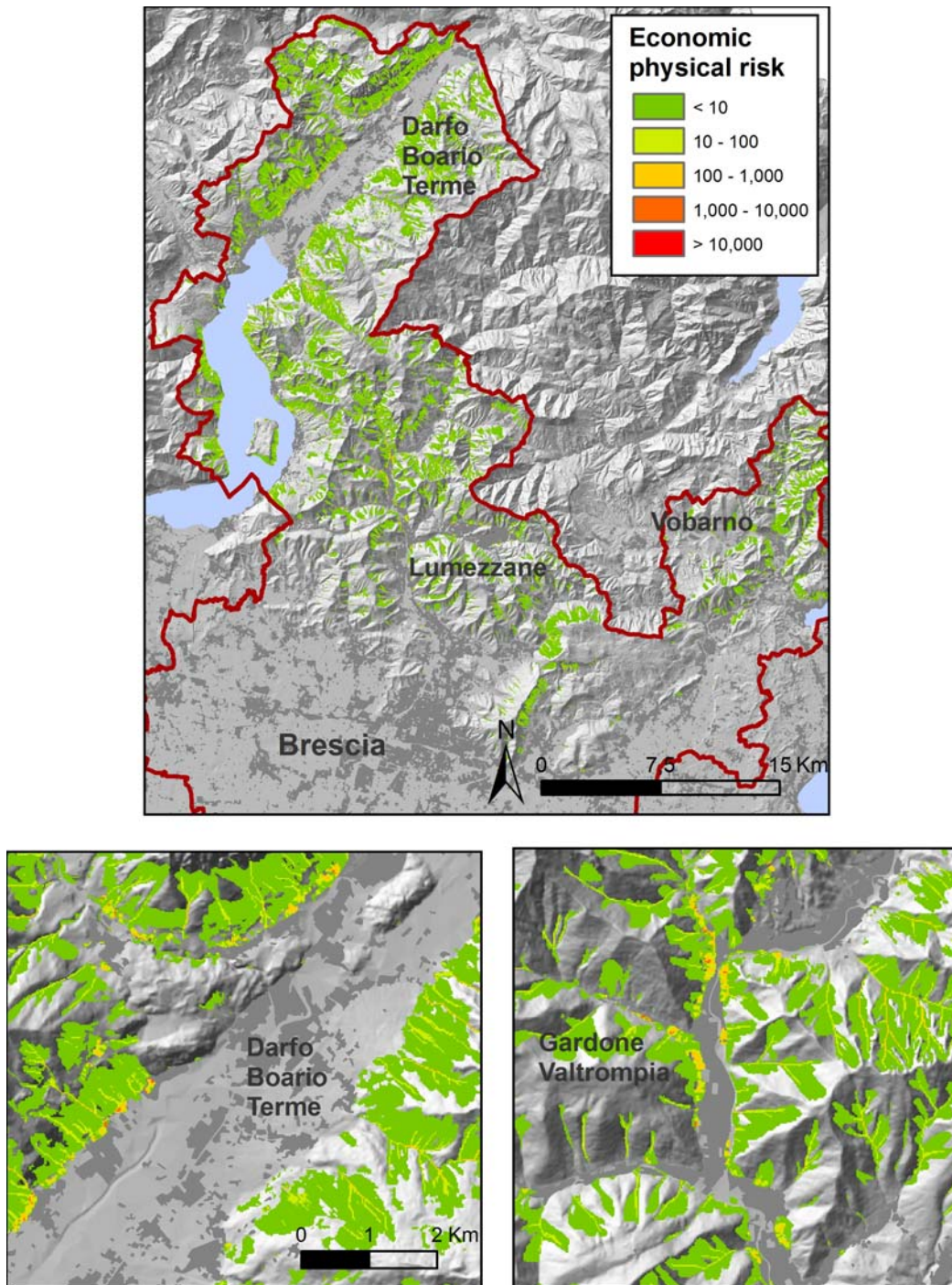


Fig.58. Map of economic physical risk for debris flows, in euros/year, Brescia study area

6.4 FLOODS ON ALLUVIAL FANS

For the analysis of floods on alluvial fans, the same model described for debris flows (Horton et al, 2008) was used (see section 6.3)

6.4.1 EXPECTED FREQUENCY OF OCCURRENCE, W_{FA}

To calculate the expected frequency of occurrence for floods on alluvial fans, the intensity-frequency curve was not used, because it requires the calculation of a frequency for each class of intensity of the floods, which was unknown. The expected frequency of occurrence for each cell of the model is composed of the frequency of the flooding events, and by the probability of transit in the flooding zone. The event frequency was calculated by means of AVI catalogue (AVI, 2007), landslide and flood database of Lombardy Region (Progetto IFFI, 2007), and the study by Govi and Turitto (1994). Historical events include indistinctly torrential floods, where liquid discharge is prevalent on solid discharge, and alluvial fan debris flows, where solid discharge is dominant. Catalogues include 477 fan floods for Valtellina, and 200 for Brescia area. Many of the events are concentrated on few active fans, and their activation frequency is significantly higher than the mean. For this reason, it was inappropriate to attribute to all the fans the same frequency. A specific frequency was calculated for each fan, based on historical data. In Valtellina, the maximum frequency is almost 0.090 events/year/cell, whereas in the Brescia area, 0.045 events/year/cell. For fans where no activation was recorded in historical data, a value of 10^{-3} events/year was assigned, corresponding to a return time of 1000 years (Fig.59).

To obtain the probability associated to the propagation of the flood, the semi-empirical model proposed by Horton et al. (2008) was used. The model allows to calculate the zones of the fan where the event can propagate, with an estimate of propagation frequency for each cell. Some models were trained and calibrated (Tab.30). For Valtellina, the best model representing the morphology of the mapped fans is n.3. For Brescia, n.4.

The expected frequency of occurrence for each cell was calculated as the product of reactivation frequency of the fan and propagation frequency (Fig.60). For Valtellina, the day and night frequency w_{FA} were distinguished.

Tab .30. Parameters of the debris flow simulation models for alluvial fan flooding

	MODEL 1	MODEL 2	MODEL 3	MODEL 4	MODEL 5	MODEL 6
Flow accumulation (m²)	400000	400000	400000	10000	10000	10000
Buffer (m)	60	60	60	1000	1000	1000
Direction Algorithm	Wichmann Betch	Wichmann Betch	Holmg. exp9	Holmg exp5	Holmg Exp10	Holmg Exp10
Inertial Algorithm	Weights	Weights	Weights	Weights	Weights	Weights
Friction loss function	c.loss10°	c.loss 5°	c.loss 5°	c.loss 20°	c.loss 20°	c.loss 20°
Limiting Kinetic Energy	<30 m/s	<30 m/s	<30 m/s	<30 m/s	<30 m/s	<30 m/s

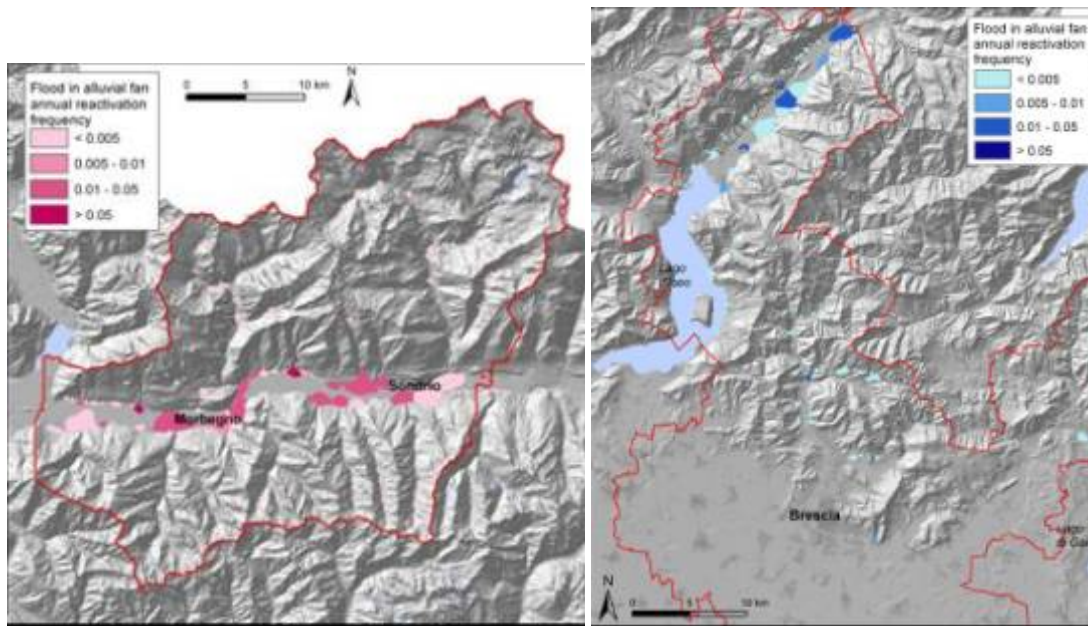


Fig. 59. Reactivation frequency, from historical events

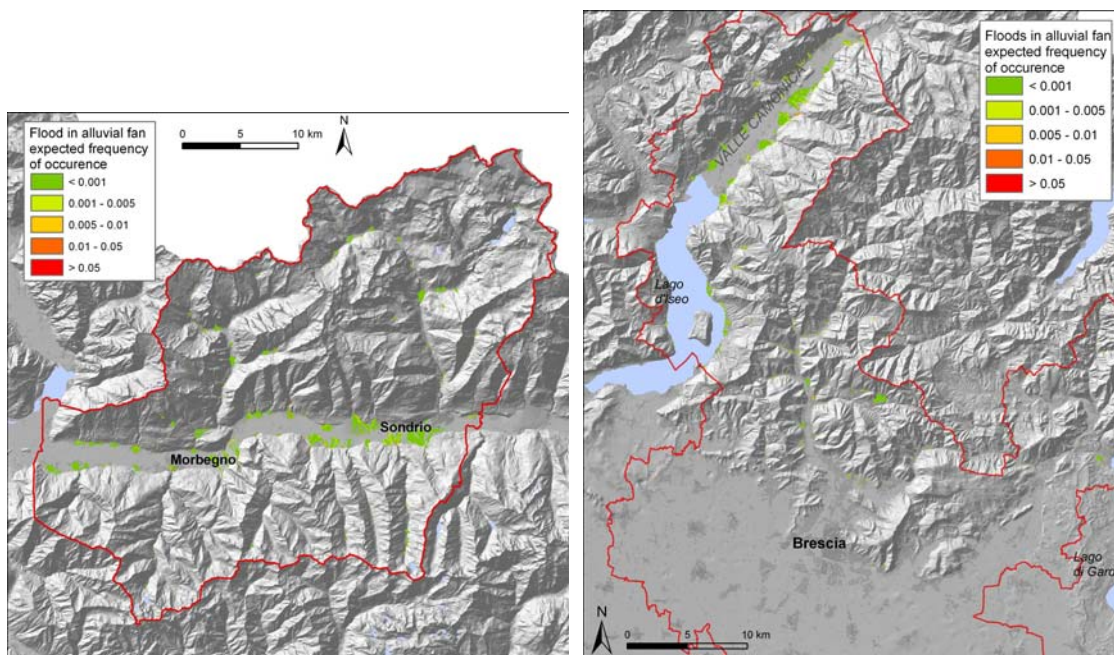


Fig.60. Flood in alluvial fan frequency of occurrence

6.4.2 SOCIETAL RISK ASSESSMENT

Gravity factor, g_{FA}

The gravity of fan floods depends on the intensity of the phenomenon, in terms of depth and velocity, and on the vulnerability of human life. The intensity of floods on alluvial fans is generally high. For this reason, probability of dying of people impacted by fan floods was assumed to be high. By expert evaluations, a g_{FA} value of 0.5 was used.

Exposure factor, e_{FA}

In the case of flooding on alluvial fans, the probability that exposed people is effectively impacted (e_{FA}) relatively depends on civil protection systems, even if these phenomena occur quite suddenly. Civil protection systems are supposed to be effective in 75% of the cases. The value of the factor e_{FA} significantly depends on the possibility that people is located at the lowest floors of the buildings. This is supposed here to be the 20% of people.

The value of e_{FA} derives from: $0.2 \times (1-0.75) = 0.05$

Societal physical risk

Alluvial fan risk is concentrated on active fans where the highest number of historical events were registered. In Valtellina, fan flood societal risk ranges from 0 to 0.001 casualties/year/cell in day scenario, and from 0 to 0.02 casualties/year/cell in the night scenario. The overall risk value for the whole area is of 0.04 casualties/year in the day scenario and 0.79 casualties/year in the night scenario (Tab.31).

For the entire Brescia area, the overall risk is of 0.53 casualties/year. Considering that fan floods produced a large number of victims in the last centuries (Berruti, 1998), these values are reasonable with respect to historical data (Fig. 61,62 and 63).

Tab.31. Societal risk values

	Valtellina day scen	Valtellina night scen	Brescia
Range (cas/year/cell)	0,001	0,020	0,0086
Total (cas/year)	0,040	0,79	0,5324

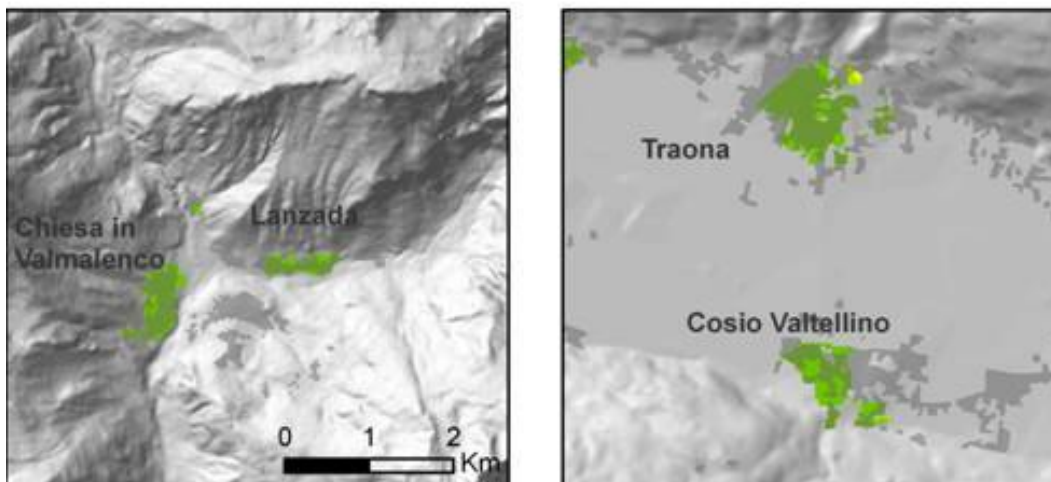
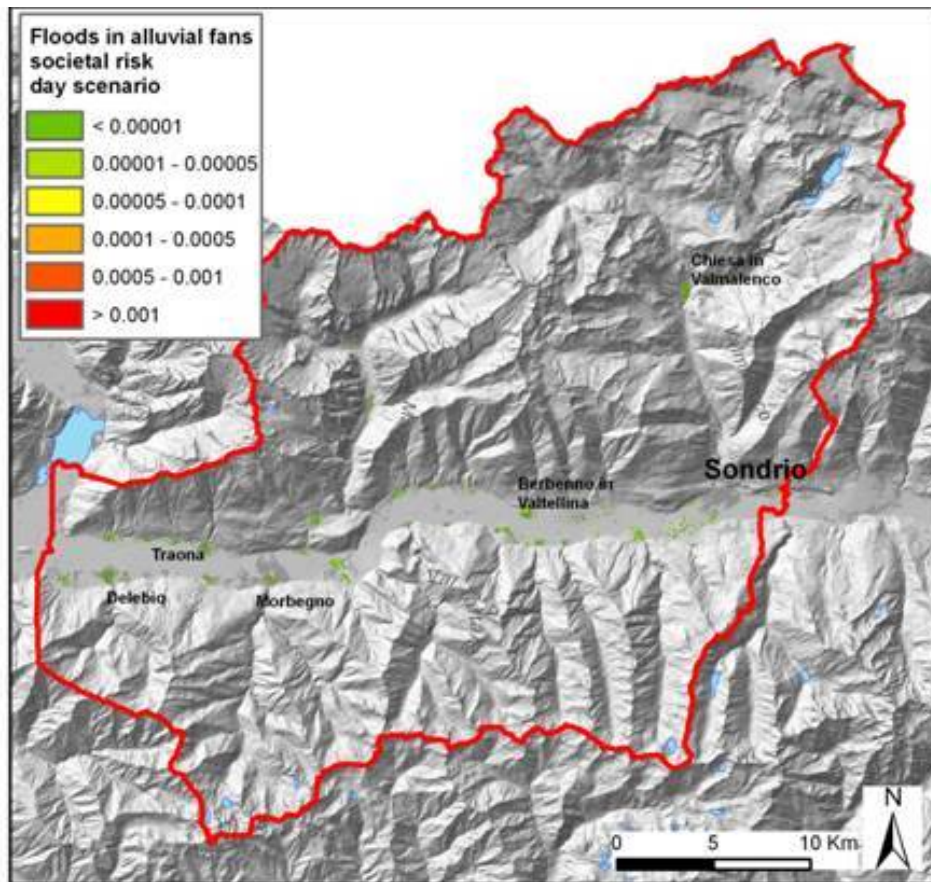


Fig.61. Map of societal physical risk for floods on alluvial fan, day scenario, Valtellina. Risk values are expressed in terms of casualties per year.

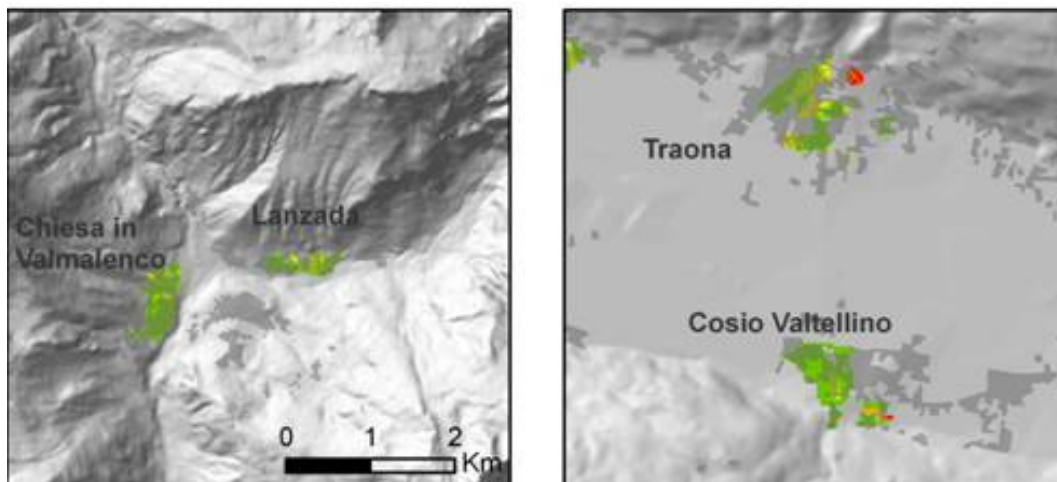
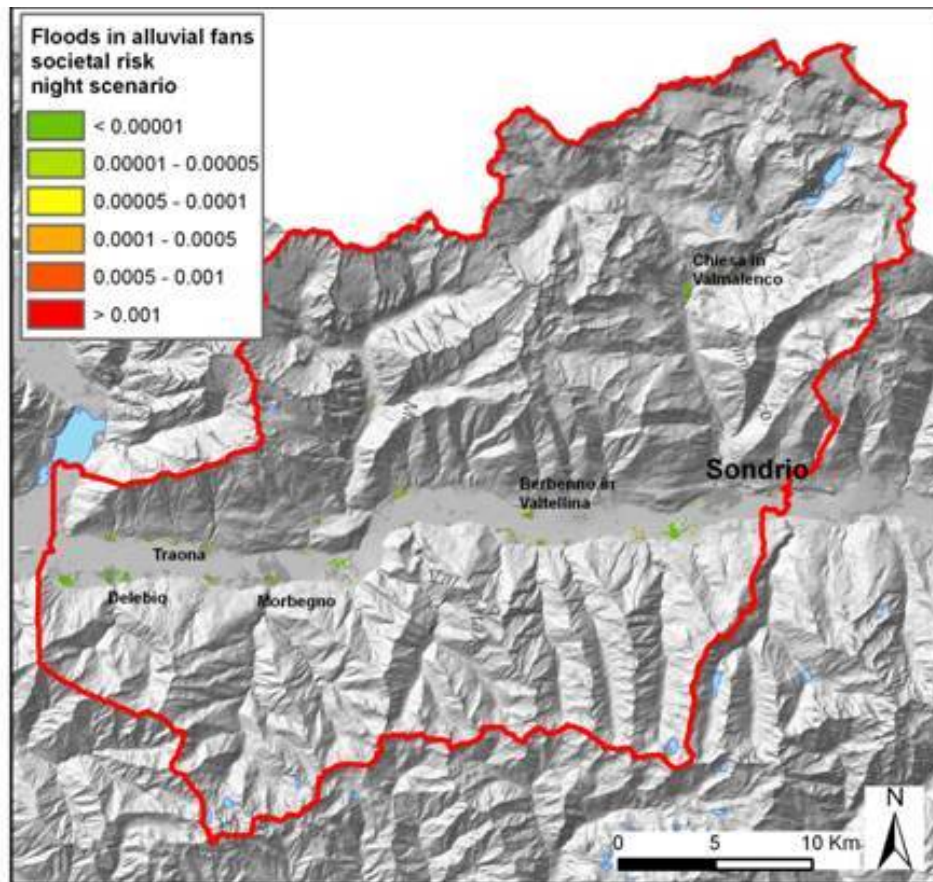


Fig.62. Map of societal physical risk for floods on alluvial fan, night scenario, Valtellina. Risk values are expressed in terms of casualties per year.

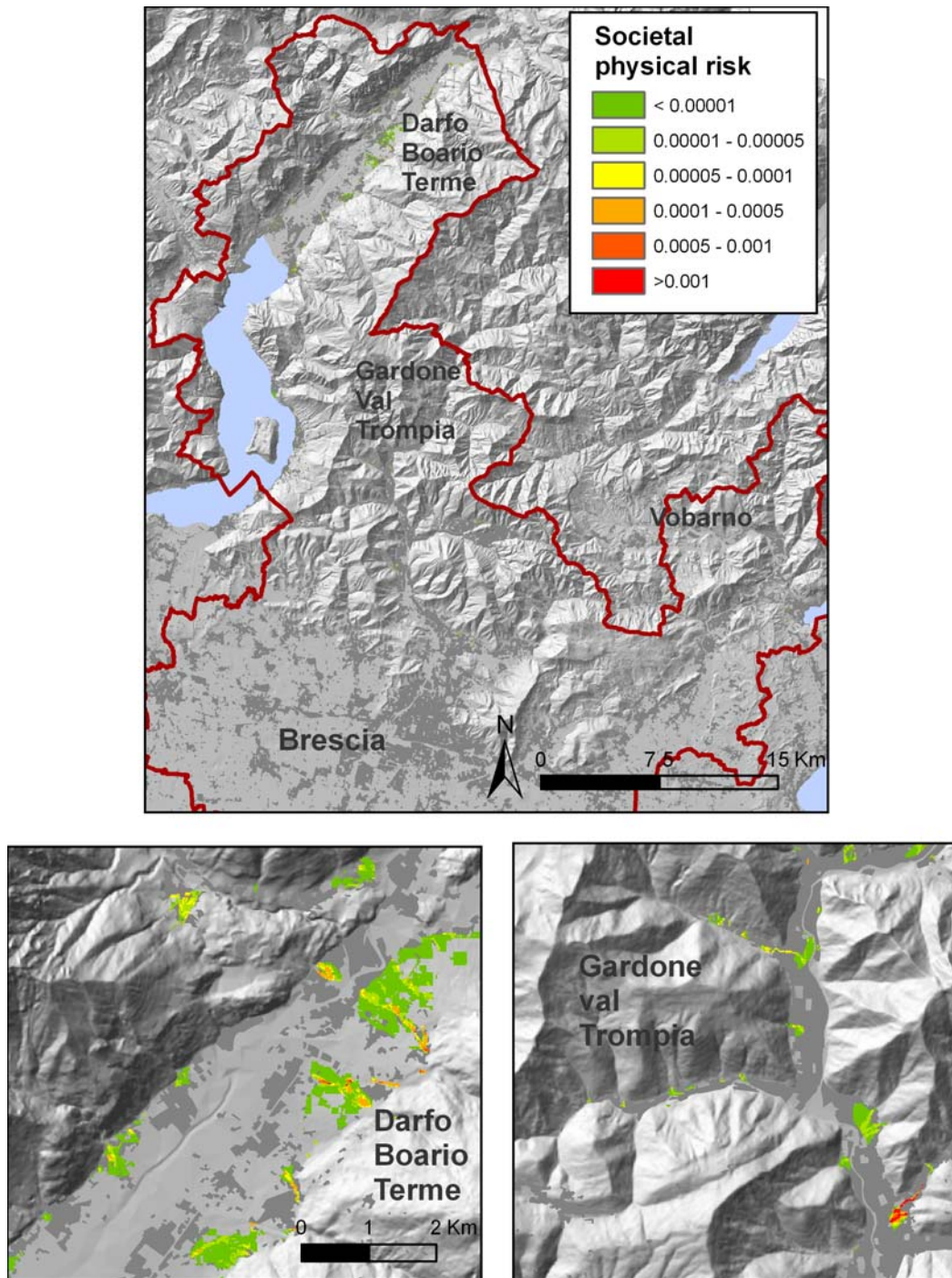


Fig.63. Map of societal physical risk for floods on alluvial fan, Brescia study area. Risk values are expressed in terms of casualties per year.

6.4.3 ECONOMIC RISK ASSESSMENT

Gravity factor, g_{AF}

The same gravity factor of debris flows was used (see Tab.28)

Exposure factor, e_{AF}

Floods in alluvial fans occur fast and often are unpredictable, but they generally involve only the first floor of buildings. By expert judgment, the value of the exposure factor is assumed to be 0.125.

Economic physical risk

In Valtellina, the economic damage caused by floods on alluvial fan shows risk values ranging from 0 to 7,178 €/year/cell. Summing the economic risk for the whole study area, it reaches 209,524 €/year (Fig.64). In the area of Brescia, the economic damage ranges from 0 to 7,556 €/year/cell. The total economic risk amounts to 794,289 €/year (Fig. 65).

Tab. 32. Economic risk values for the two study areas

	Valtellina	Brescia
Range (€/year/cell)	<i>7,178</i>	<i>7,556</i>
Total (€/year)	<i>209,524</i>	<i>794,289</i>

Impacted areas are quite localised, with limited extension, and considerable values of risk. Clearly, the villages located at the outlet of the secondary valleys, built on the fans, are the most impacted.

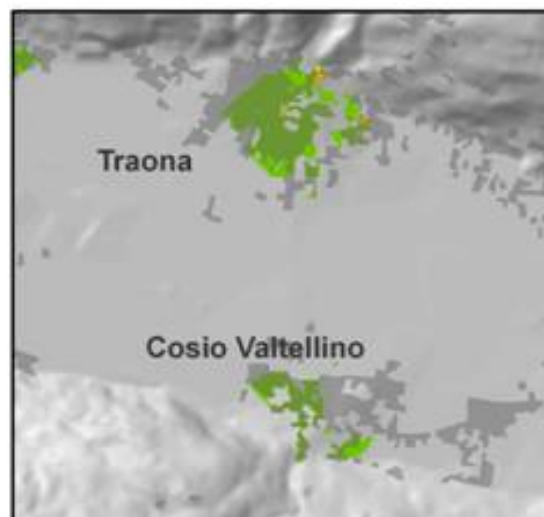
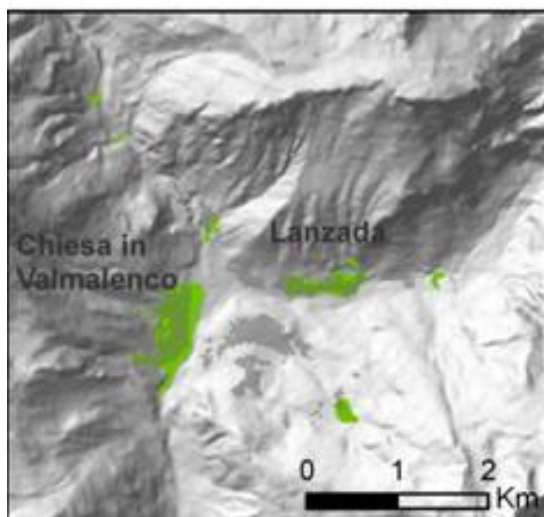
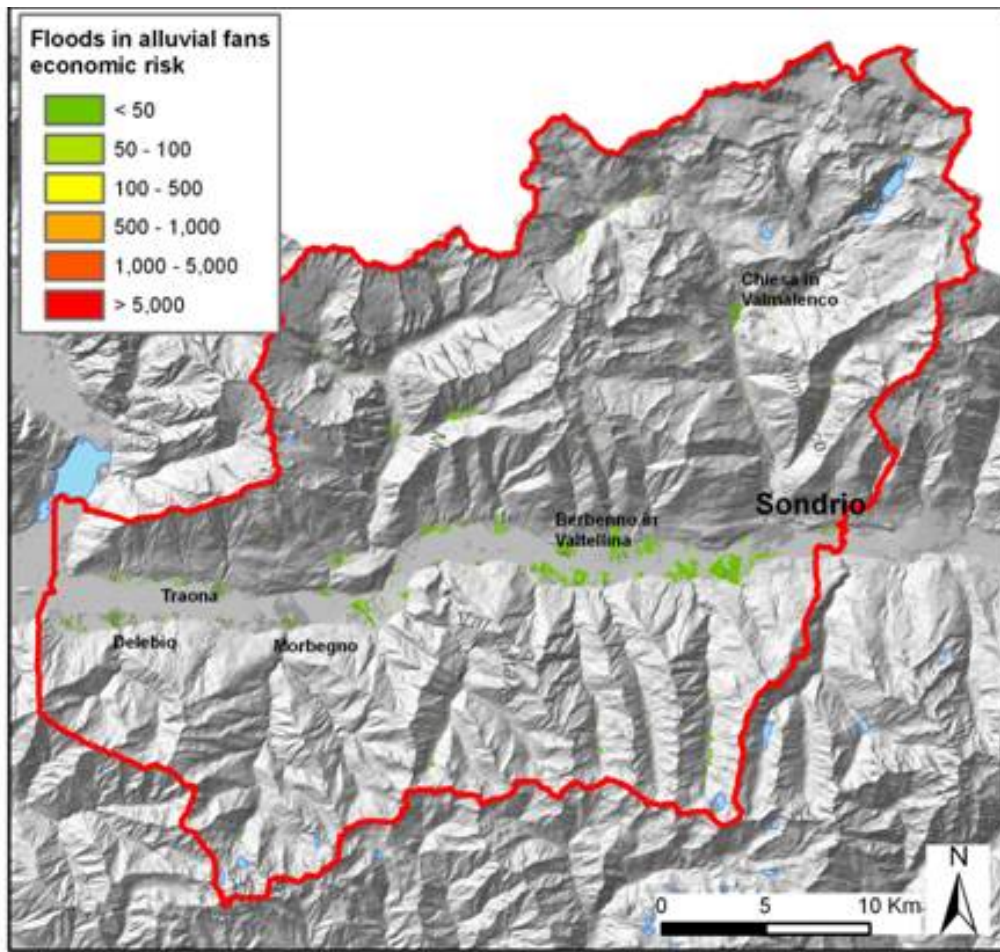


Fig.64. Map of economic physical risk for floods in alluvial fan, in euros/year, for Valtellina

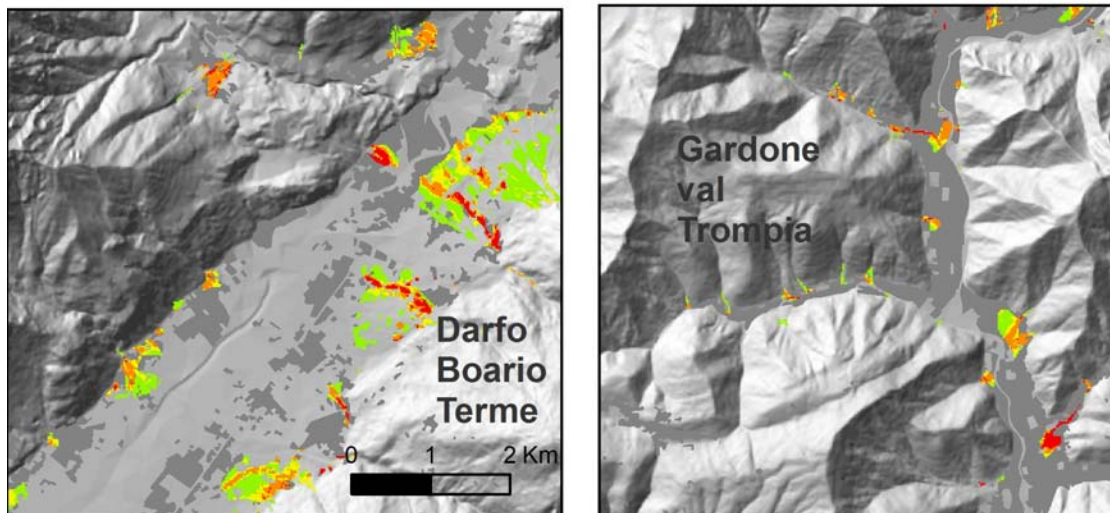
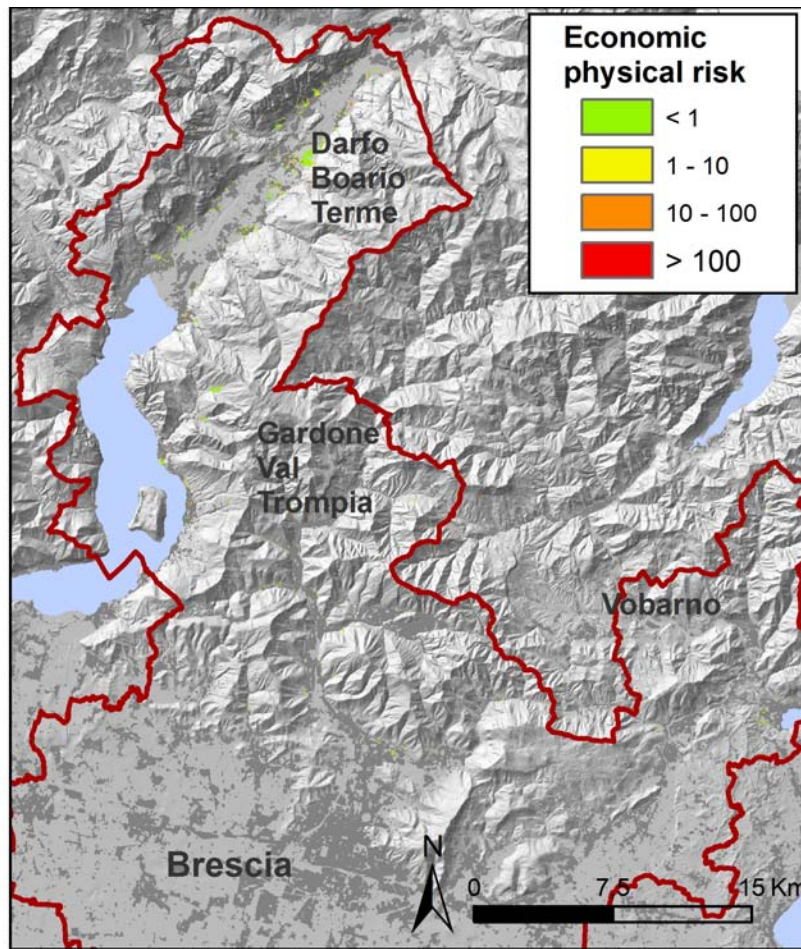


Fig.65. Map of economic physical risk for floods in alluvial fan, in euros/year, for Brescia study area

6.5 RIVER FLOODS

For river flood risk assessment, the zonation of PAI for river Adda, Oglio, Mella and Chiese were used, supported by the database of Regione Lombardia (REF) and the work of Berruti, (1998), (Fig.66).

P.A.I. (Piano Stralcio per l'Assetto Idrogeologico) delimitates the flooding zones according to their hydraulic hazard:

- Zone A: runoff of at least 80% of the discharge for the flood with 200 years return time. Outside, the velocity must be less than 0.4 m/s

- Zone B: interested by flood with a return time of 200 years. It extends as far as natural elevation exceeds the hydrometric elevation, or up to existing or planned hydraulic interventions (embankments).

- Zone C: inundation for catastrophic flood (return time 500 years or maximum recorded). It extends as far as natural elevation exceeds the hydrometric elevation, or, for embanked rivers, up to the overflowing height or flood height for embankment break (among these, most adverse condition is taken into account) .

Considering that gravity factor, g , is strictly dependent on the intensity of the flood, in terms of velocity and water depth, 6 different scenarios were considered (3 for zone A, 2 for zone B, 1 for zone C) each of them owning a different gravity factor.

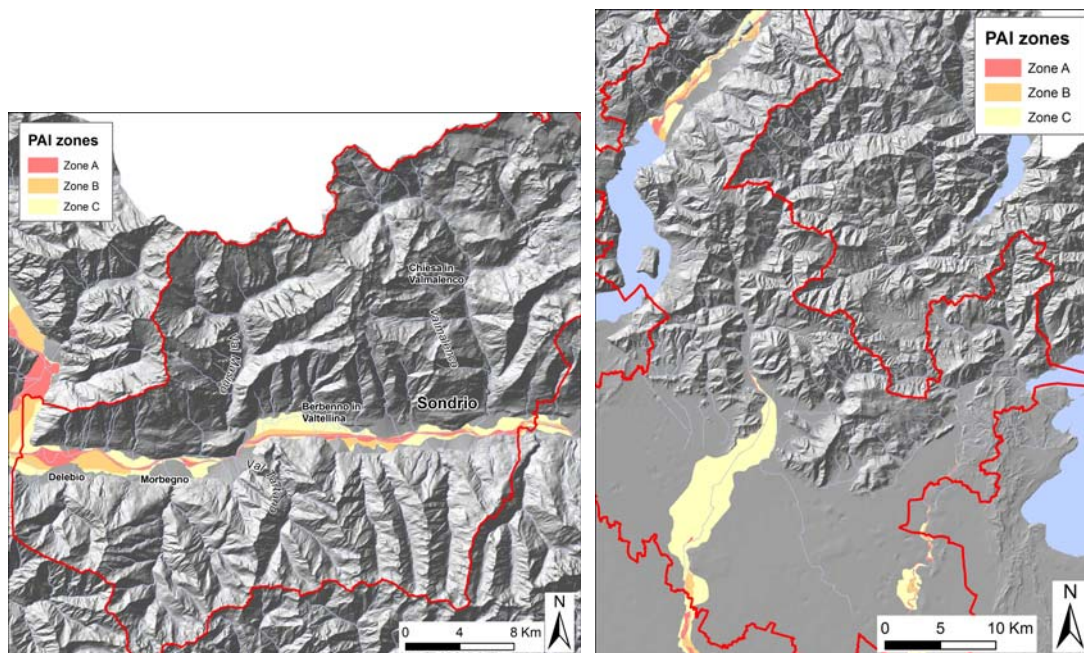


Fig.66. PAI zoning in the study areas

6.5.1 EXPECTED FREQUENCY OF OCCURRENCE, W_{FL}

Flood frequency for different flood scenarios is the following:

- zone A: it has for its definition an original frequency of occurrence $w = 1/200$ years = 0.005. It is referred to the 80% of the flood with higher velocity. For this

reason, in this analysis it is assumed to be $w_{FL} = 1/10 = 0.1$. It is assimilated to a time of return of 10 years, assuming that the zone of the ordinary flood is often activated. This assumption is supported by the analysis of the detailed studies for rivers Ticino, Adda and Olona (PAI, 2007). It was experimentally verified that in these studies, the area interested by floods with a recurrence interval of 10 years coincides quite well with zone A of PAI.

- zone B: $w_{FL} = 1/200$ years = 0.005

- zone C: $w_{FL} = 1/500$ years = 0.002

Expected occurrence frequency w_{FL} , for Valtellina, was recalculated for day and night scenarios.

6.5.2 SOCIETAL RISK ASSESSMENT

Gravity factor, g_{FL}

Gravity for river floods depends on the intensity of the event, expressed in terms of velocity and water depth, and on the vulnerability of people.

Intensity of floods changes in space as a function of the discharge (depending on time of return) and of the morphology. In a rigorous way, gravity should have been evaluated using the results of hydrological models used to delimitate PAI zones. Models should provide both velocity and water depth. In a simplified way, it is possible to use the DTM and/or the available hydraulic sections to obtain areas with different depth of the flood. To obtain velocity, simple hydraulic checks can be completed for each section, assuming a steady-state and uniform flow and using Chezy equation. To perform them it could be necessary to know the slope of the riverbed and the roughness of the surface where the flood runs. Interpolating between the sections, it could be possible to model depth and velocities along all the flooding area.

People vulnerability depends on velocity and depth of the flow. For low velocity and high depth also the swimming capacity becomes important. Using empiric relations available in the literature (Anon, 1980, French, 1987; FEMA, 2005), it is possible to get an approximate assessment of people vulnerability as a function of velocity and water depth.

From these considerations, it is clear that gravity evaluation is subjected to a strong uncertainty, that can be resumed as:

- methodological uncertainty in the use of simplified models (e.g. Chezy equation) with assumptions not always consistent with the reality (e.g. steady state and uniform flow)

- spatial uncertainty depending on the quality and resolution of DTM of the valley bottom and plain areas

- uncertainty in the interpolation of hydraulic sections, very distant along the riverbed and not always of good quality (many sections are obtained using contours of the 1:10,000 Regional Technical Maps, not very reliable in alluvial plain areas)

- uncertainty connected to vulnerability, both for the difficulty of accounting for the capacity of the individual of facing the flood, and for the objectively uncertainty in intensity, as said above.

Considering all the uncertainties, it was decided to develop a simplified approach.

For each of the PAI zones, a mean value of the water depth was calculated (h_a , h_b , h_c), assuming that zone A is necessarily involved in the events with return time of 10, 200 and 500 years, zone B in the events with 200 and 500 years return time, and zone C in the events with 500 years return time. Values of water depth, h , for the three scenarios are shown in Tab33 and 34.

Tab.33. Calculation of water depth for the three hazard zones

Frequency	Zone		
	A	B	C
0.1	h_a	0	0
0.005	h_b	h_b-h_a	0
0.002	h_c	h_c-h_a	h_c-h_b

Tab.34. Calculation of water depth for the three zones, in meters

Frequency	Zone		
	A	B	C
0.1	3	0	0
0.005	4	1	0
0.002	5	2	1

Considering the high level of uncertainty, and considering that the conversion factor for floods is very low and makes improbable that a flood effectively impacts people, a gravity level was assessed as in Tab 35.

Tab.35. Gravity factors for flood scenarios

Frequency	Zone		
	A	B	C
0.1	1	0	0
0.005	1	0.1	0
0.002	1	0.5	0.05

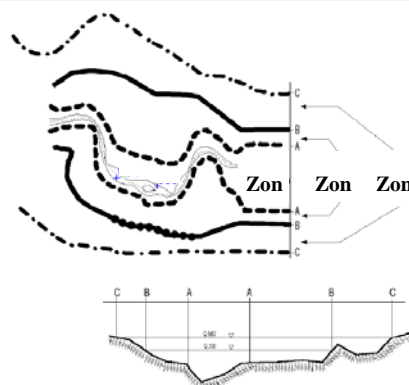


Fig.67. Exemplificative scheme of PAI zones, plan and section, for the evaluation of water depth

Exposure factor, e_{FL}

The probability of exposed people to be effectively impacted depends essentially on the possibility of people to evacuate the area before the arrival of the flood wave or on the possibility that people find a safe place at higher floors of buildings. Values of factor e were estimated by means of expert knowledge, considering that

- river flood is characterised by a quite slow and predictable propagation of the flood wave, and prevision and alert systems are in general effective in order to obtain almost a complete evacuation of the areas;

- road network during a flood event is interrupted, preventing people localised in streets from being impacted

The possibility that people are effectively impacted by a river flood is minor in the areas close to the river bed (e.g. Zone A), being here the perception of risk higher and inducing people to a more prudent behaviour.

After these considerations, a value of $e_{FL} = 0.005$ was assumed.

Societal physical risk

Flood risk analysis was performed by considering three different event scenarios (zone A, B and C) with three return times (10, 200 and 500 years). F/N curves were used to aggregate them in a societal risk value.

Societal river flood risk in Valtellina ranges from 0 to 0.001 casualties/year/cell for day scenario and from 0 to 0.002 casualties/year/cell for night scenario (Tab.36, Fig.68 and 69). The overall societal risk value for the study area is 0.0197 casualties/year for day scenario and 0.158 casualties/year for night scenario. Considering that the last casualties due to Adda flood date back to 1987, the obtained results seems in accordance with historical data.

In the Brescia area, the main contribution to societal risk is provided by river Mella. This is due to the fact that, as shown in Fig.25 of equivalent population, it passes through highly urbanised areas (the town of Brescia). Risk value reaches 10^{-4} casualties/year/cell (Fig.70). In the whole area, the total societal risk amounts to 0.069 casualties/year. Considering that the last casualties connected to Oglio and Mella floods date back to 1959-60, the results obtained are in accordance with historical data.

Tab.36. Societal risk values

	Valtellina day scen	Valtellina night scen	Brescia
Range (cas/year/cell)	0.00117	0.00200	0.00012
Total (cas/year)	0.01974	0.15834	0.069

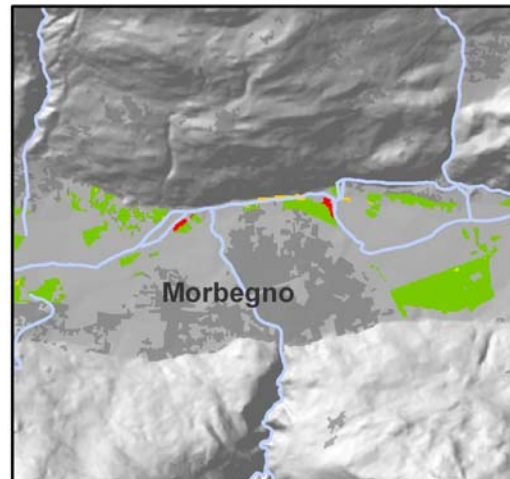
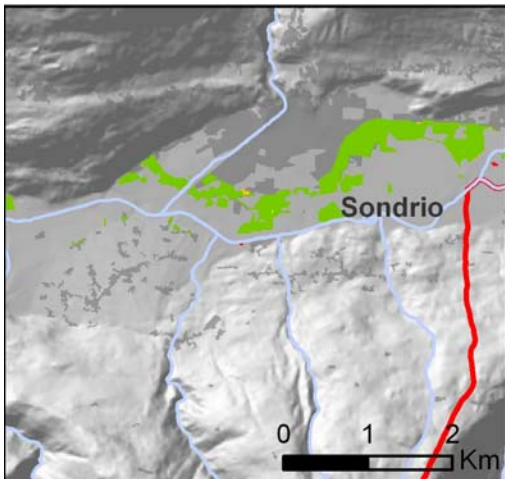
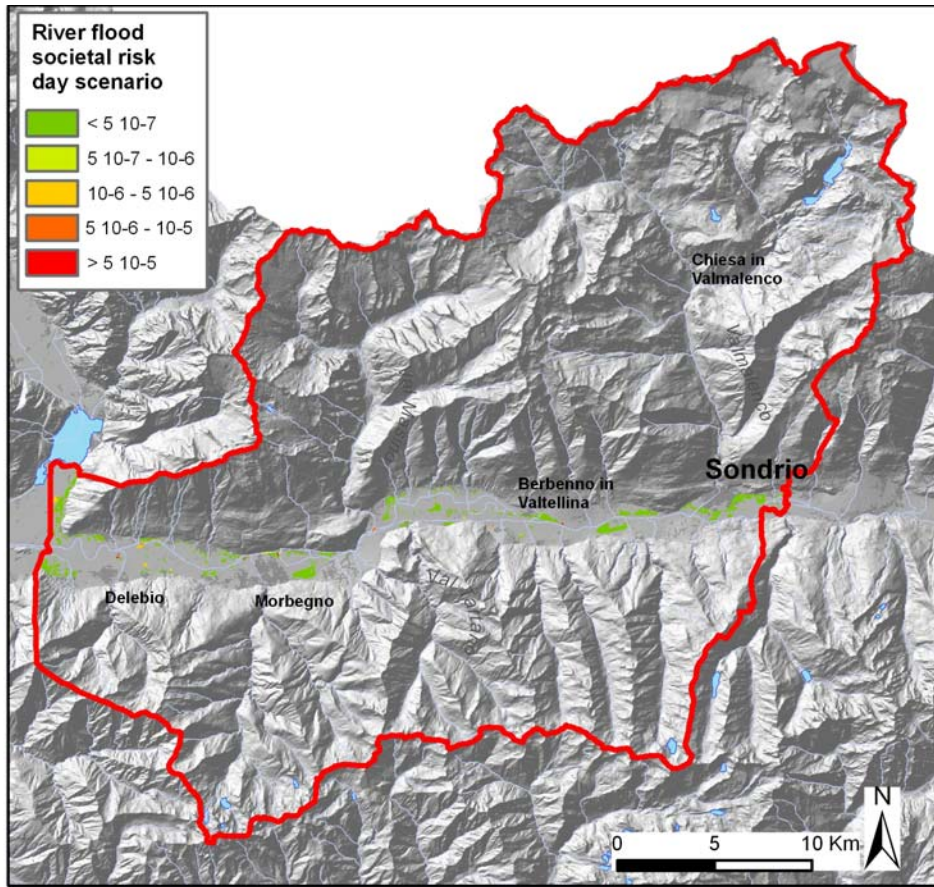


Fig.68. Map of societal physical risk for river flooding, day scenario, Valtellina. Risk values are expressed in terms of casualties per year.

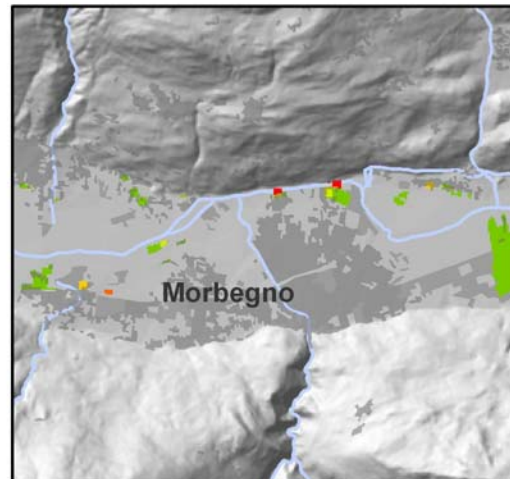
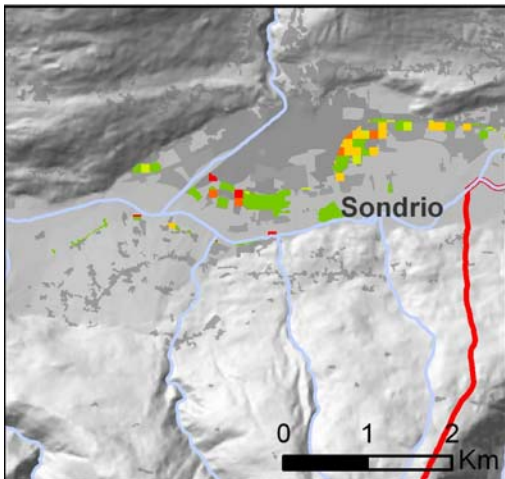
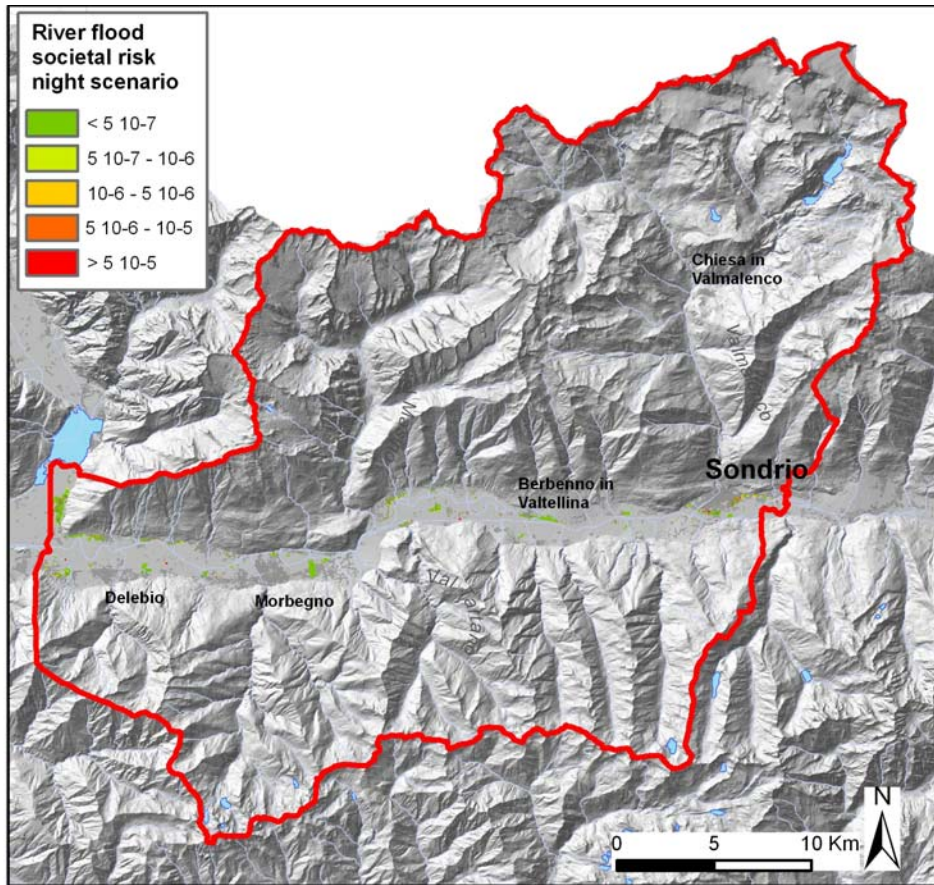


Fig. 69. Map of societal physical risk for river flooding, night scenario, Valtellina. Risk values are expressed in terms of casualties per year.

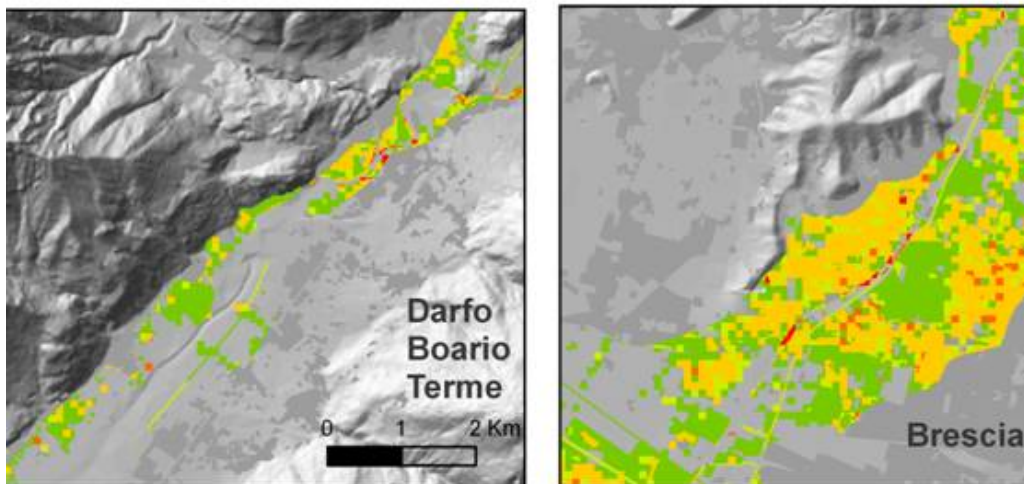
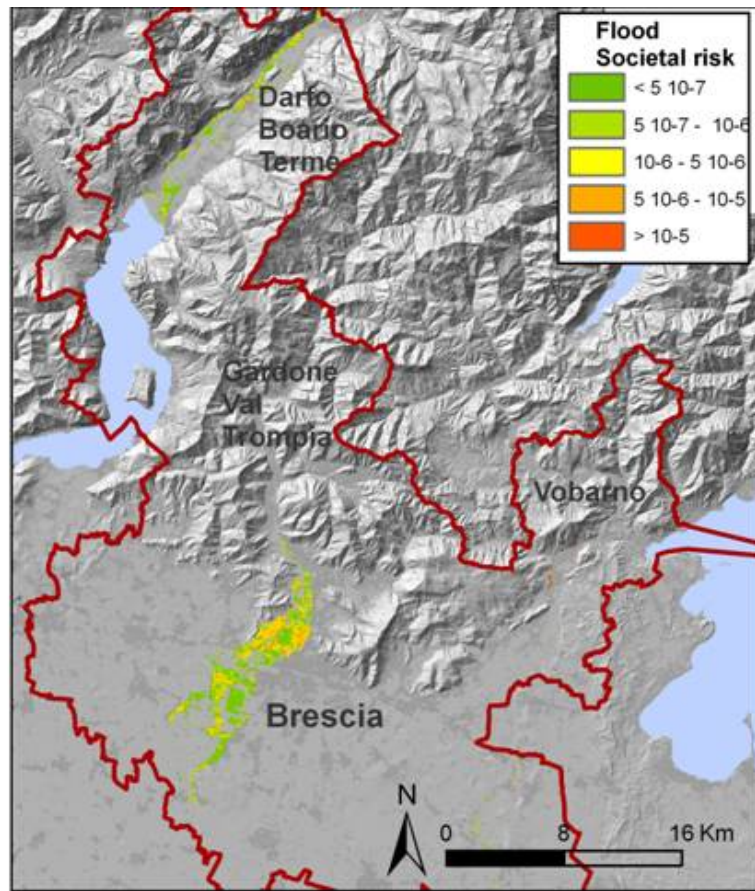


Fig.70. Map of societal physical risk for river flooding, Brescia study area. Risk values are expressed in terms of casualties per year.

6.5.3 ECONOMIC RISK ASSESSMENT

Gravity factor, g_{FL}

For the evaluation of gravity factor, g_{FL} , for buildings, *USACE* (United States Army Corps of Engineers) vulnerability curves were used (*USACE*, 2003) (Tab.37, Fig.71). They have been developed on the basis of flood data of Corps of Engineers for different zones of USA for the period 1996 and 1998 for buildings without basement, and for the period 1996 and 2001 for buildings with basement. In both cases, different types of buildings were distinguished (one floor, two or more floors, etc), and related contents damage was evaluated. Direct costs for cleaning and repairing, prevention of damages and other indirect costs connected to river flooding are not considered here.

Tab.37. Values of vulnerability for 1 floor buildings with basement (*USACE*, 2003)

Water depth (m)	Mean damage (%)	g
-2.856	0	0
-2.499	0.7	0.007
-2.142	0.8	0.008
-1.785	2.4	0.024
-1.428	5.2	0.052
-1.071	9	0.09
-0.714	13.8	0.138
-0.357	19.4	0.194
0	25.5	0.255
0.357	32	0.32
0.714	38.7	0.387
1.071	45.5	0.455
1.428	52.2	0.522
1.785	58.6	0.586
2.142	64.5	0.645
2.499	69.8	0.698
2.856	74.2	0.742
3.213	77.7	0.777
3.57	80.1	0.801
3.927	81.1	0.811
4.284	81.1	0.811
4.641	81.1	0.811
4.998	81.1	0.811
5.355	81.1	0.811
5.712	81.1	0.811

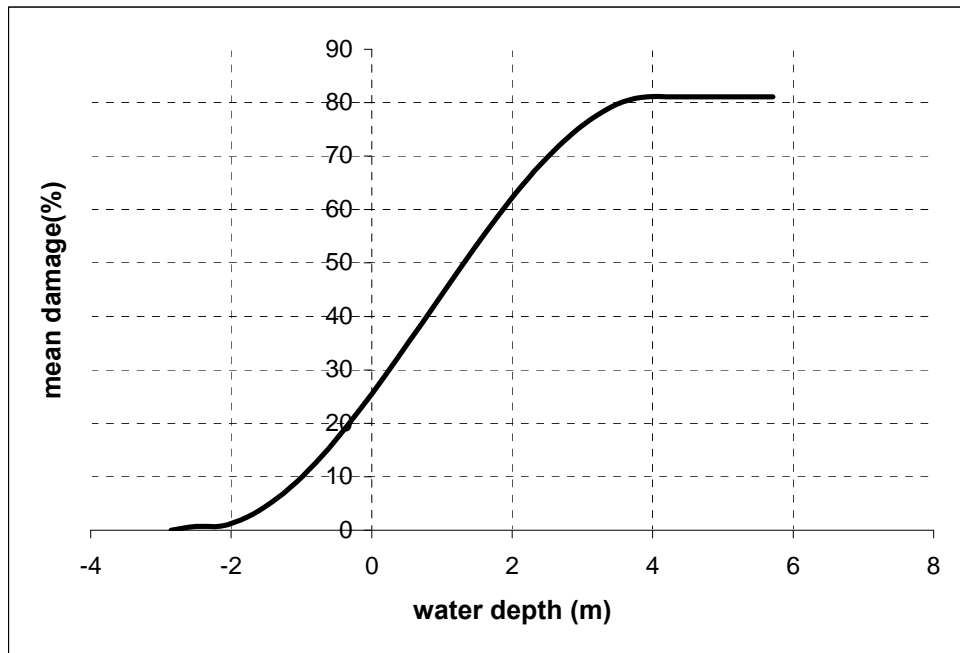


Fig.71. Vulnerability curve to floods for 1 floor buildings with basement, USACE,2003

For the other exposed elements, different values of g were defined by means of expert judgment, as a function of water depth for each of the 6 sub-scenarios (Tab.38).

Tab.38. Values of gravity factor g for exposed elements

	g value				
	1m	2m	3m	4m	5m
Buildings	<i>USACE curve</i>	<i>USACE curve</i>	<i>USACE curve</i>	<i>USACE curve</i>	<i>USACE curve</i>
Protected areas and wooden cultivations	0	0	0.2	0.3	0.4
Green areas and grasses	0.4	0.6	0.8	1	1
Markets and cemeteries	0	0.2	0.5	1	1
Road, railways, power lines	0	0	0	0	0

Exposure factor, e_{FL}

Considering that water flows out of the embankments and covers the whole areas of the involved cells, we considered an exposure factor $e_{FL} = 1$. All the exposed elements of the zones are considered completely exposed.

Economic physical risk

F/D curves were used to aggregate the three scenarios in an economic risk value.

In Valtellina, economic risk ranges from 0 to 39,577 €/year/cell. On the whole area, it amounts to 9,532,702 €/year. Similar values are obtained for the area of Brescia, as in Tab.39 The economic damage is very high, and clearly concentrated in the valley bottom. Most urbanised and productive areas result strongly damaged (Fig 72 and 73).

Tab.39. Economic risk values for the two study areas

	Valtellina	Brescia
Range (€/year/cell)	<i>39,577</i>	<i>50,587</i>
Total (€/year)	<i>9,532,702</i>	<i>20,665,701</i>

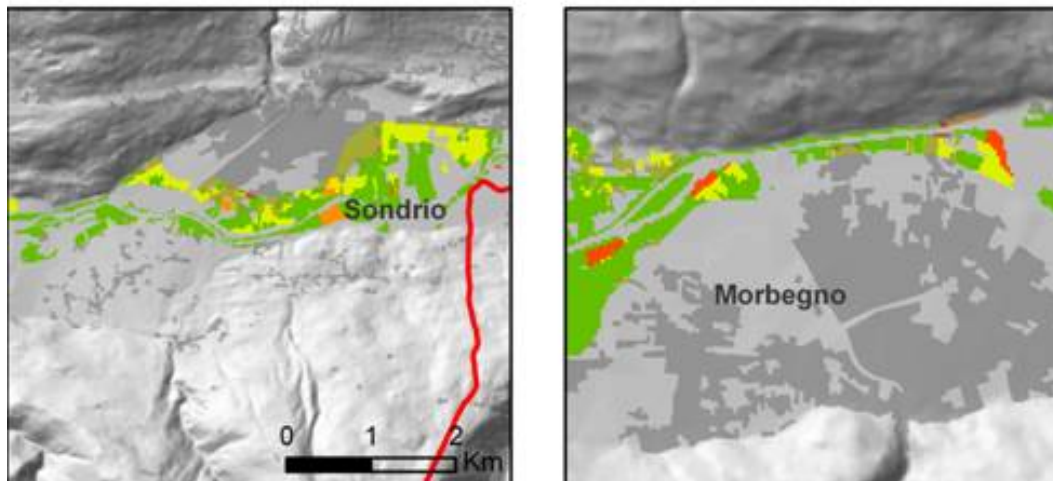
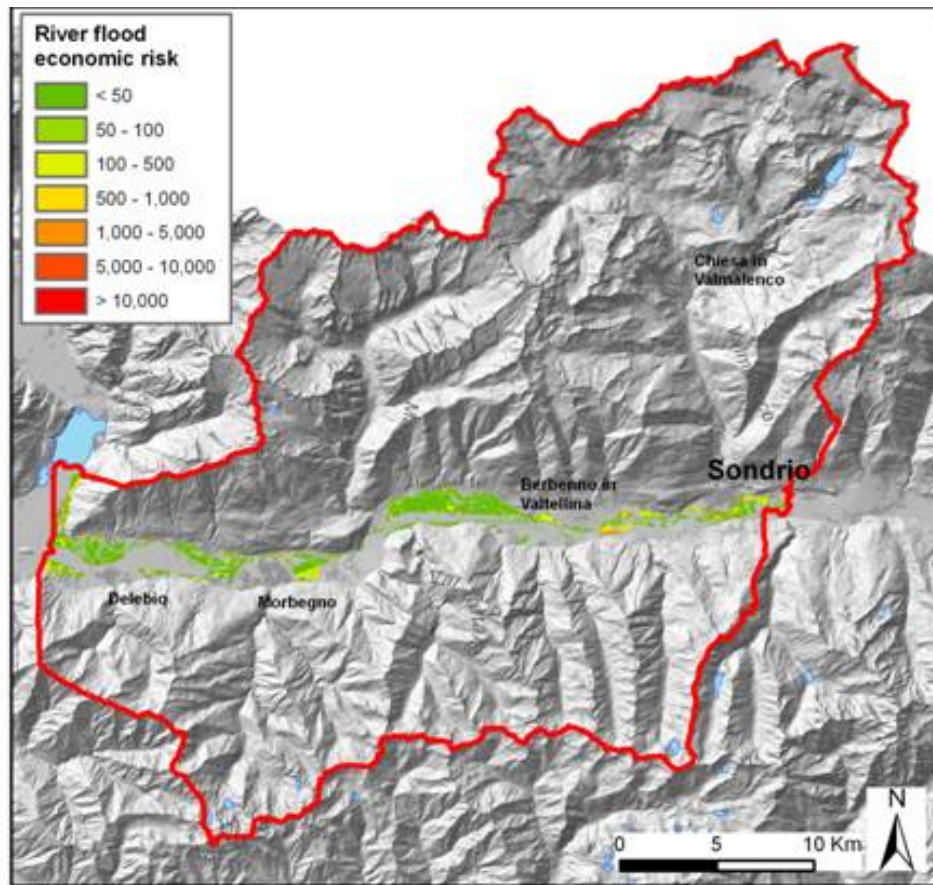


Fig. 72. Map of economic physical risk for river flooding, in euros/year, for Valtellina

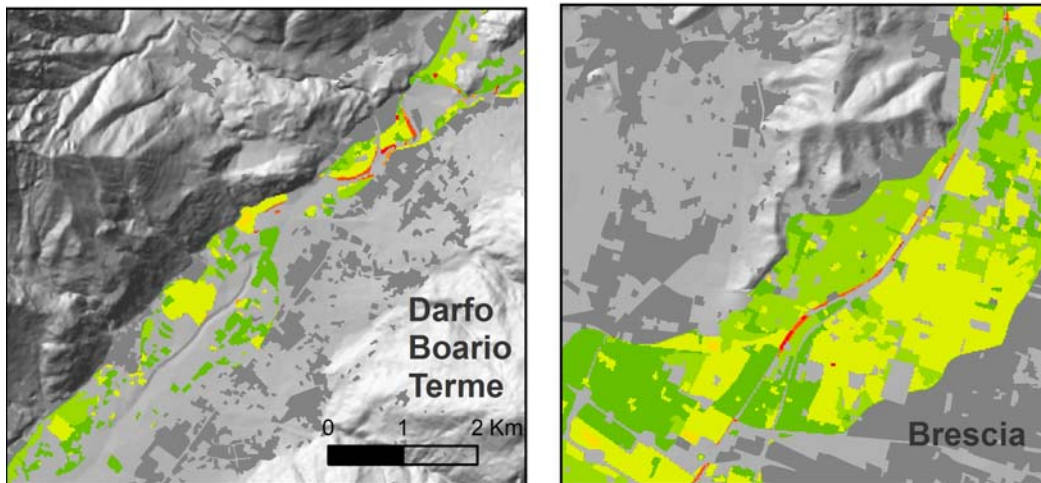
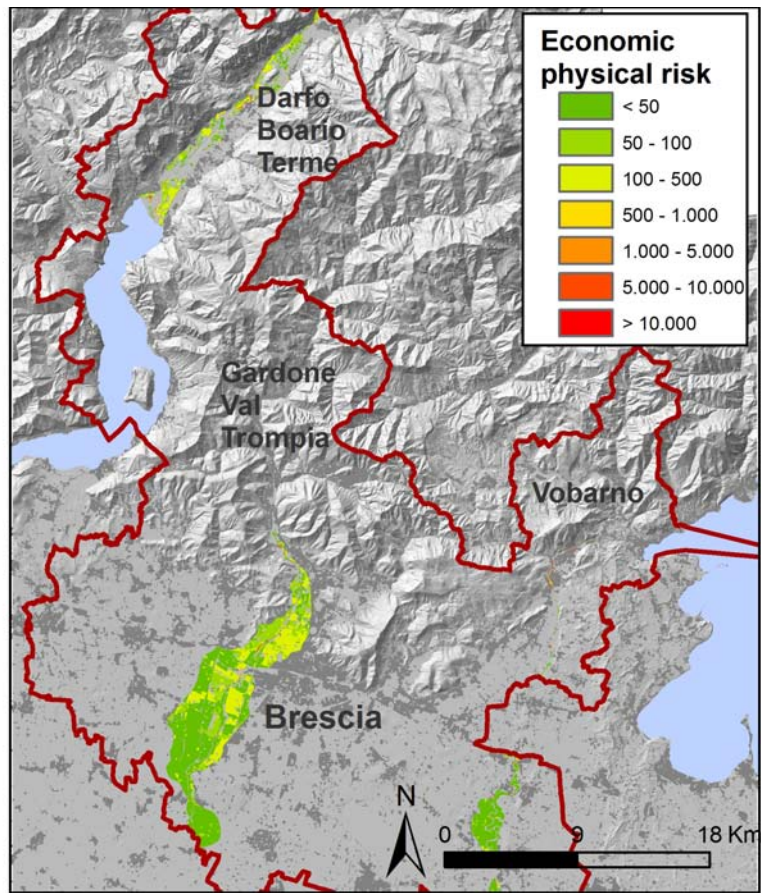


Fig.73. Map of economic physical risk for river flooding, in euros/year, for Brescia study area

6.6 SEISMIC RISK

6.6.1 METHODOLOGY

In Italy, the seismic classification of the municipalities is regulated by the ordinance n°3274/03. To face technical-administrative problems related to the management of the territory, each Region classifies its municipalities into one of the four seismic zones (for Lombardy, D.g.r. 28/05/2008 n.8/7374), defined in the following, on the basis of the maximum value of a parameter of seismic hazard. Seismic hazard is expressed by the maximum horizontal soil acceleration $a_{g,475}$, related to the 50th percentile with an exceedence probability of 10% in 50 years. As a function of the values of $a_{g,475}$, four seismic zones are defined:

- Zone 1: municipalities where $a_{g,475} \geq 0,25g$
- Zone 2: municipalities where $0,25g > a_{g,475} \geq 0,15g$
- Zone 3: municipalities where $0,15g > a_{g,475} \geq 0,05g$
- Zone 4: municipalities where $a_{g,475} < 0,05g$

Referring to the 4 zones, the study area of lower Valtellina belongs to zone 3 with acceleration values ranging from 0,050 g to 0,010 g. This is in general a safe area, not often interested by earthquakes.

The study area of Brescia belongs to zones 2 and 3, with acceleration values ranging from 0,08 and 0,162. In the regional context, the area of Brescia is the most prone to earthquake damages.

Five scenarios were evaluated for Brescia area, due to its high level of hazard, (72, 140, 475, 975 and 2500 years of return time), only three for Valtellina (72, 475, and 2500 years).

For risk assessment, different input data were used:

- Census parcels (ISTAT, 2001) and related data about the number of buildings, their different construction material, their structure and height, their use.
- values of horizontal soil acceleration, factor of amplification of the spectrum in horizontal acceleration and starting period of constant velocity of the spectrum in horizontal acceleration, for each municipality, for each return time (Presidenza del Consiglio dei Ministri, 2008).

The basic seismic hazard classification of a site is the first element necessary for the determination of seismic actions on buildings. Seismic hazard is defined in terms of maximum horizontal acceleration, a_g .

The methodology for seismic risk assessment is quite different with respect to the other threats included in the Integrated Area Plans. The nature of the process is quite complex, it is a largely treated problem in the literature, and a lot of methodological studies have been done. Due to the number of available data for the study areas, a great effort was made to implement here a higher level of detail than for the other risks.

Societal risk assessment was calculated as

$$RF = Fr * P_{ex} * p_i * N \quad (28)$$

where F_r is the overall fragility of the census parcels, and P_{ex} is the annual exceeding probability of the seismic risk scenario, which is the probability per year of having at least one event exceeding the intensity of a given scenario.

Similarly, economic risk was calculated as

$$RF = F_r * P_{ex} * V$$

where F_r is the overall fragility of the census parcels, and P_{ex} is the annual exceeding probability of the seismic risk scenario, and V is the overall economic value of the parcel.

In order to calculate the overall fragility for each census parcel, some important elements must be considered:

- number and types of buildings for each section
- period of each building
- horizontal spectral acceleration for each building
- terrain amplification and topographic effects

Elastic response spectrum in acceleration of the horizontal components

The spectrum of elastic response of the horizontal component is defined by the expressions in Tab.40:

Tab 40. Equations used for the calculation of coefficient S_e per building type (D.M 14/01/08)

Interval of period	Horizontal spectral acceleration- S_e
$0 \leq T \leq T_B$	$S_e(T) = a_g * S * \eta * F_0 * \left[\frac{T}{T_B} + \frac{1}{\eta * F_0} * \left(1 - \frac{T}{T_B} \right) \right]$
$T_B \leq T \leq T_C$	$S_e(T) = a_g * S * \eta * F_0$
$T_C \leq T \leq T_D$	$S_e(T) = a_g * S * \eta * F_0 * \left(\frac{T_C}{T_B} \right)$
$T_D \leq T$	$S_e(T) = a_g * S * \eta * F_0 * \left(\frac{T_C * T_D}{T_B} \right)$

where T and S_e are respectively, oscillation period of the building and horizontal spectral acceleration; S is the coefficient accounting for the ground category and for topographical conditions through the relation:

$$S = S_S \cdot S_T \quad (29)$$

S_S being the coefficient of stratigraphic amplification and S_T the coefficient of topographic amplification

η = factor correcting the elastic spectrum for viscous coefficient of attenuation che ξ different from 5% in the relation:

$$\eta = \sqrt{\frac{10}{5 + \xi}} \geq 0,55 \quad (30)$$

where ξ (in percentage) is evaluated on the basis of materials, typology of building and terrain;

F_0 is the factor quantifying the maximum spectral amplification, at a reference horizontal rigid site, and has a minimum value equal to 2,2;

T_C is the period corresponding to the beginning of the part at constant velocity, given from:

$$T_C = C_C \cdot T_C^* \quad (31)$$

where C_C is a coefficient function of the ground category (Tab.44);

T_C^* is the period corresponding to the beginning of the part of the spectrum at constant velocity

T_B is the period corresponding to the beginning of the part of the spectrum at constant acceleration

$$T_B = T_C/3 \quad (32)$$

T_D is the period corresponding to the beginning of the part at constant displacement of the spectrum, expressed in seconds through the relation:

$$T_D = 4,0 \cdot \frac{a_g}{g} + 1,6.$$

For particular terrain categories, for specific geotechnical systems or if there is the necessity of increasing the accuracy of the phenomena forecast, seismic actions to be considered in the design phase of a building can be determined by more rigorous analysis of seismic local response. These analyses presuppose a deep knowledge of geotechnical properties of terrains, and, in particular, of the strain-deformation functions in cyclic field, to be determined by means of specific tests. Lacking these conditions, for the horizontal components of the motion and for the defined terrain categories, the spectral response for category A is modified by means of the stratigraphic coefficient S_s , the topographic coefficient S_T and C_C coefficient modifying the value of period T_C .

The elastic response spectrum for the horizontal component of any type of terrain can be represented by a curve (Fig.74), on which it is possible to graphically detect the values of some parameters.

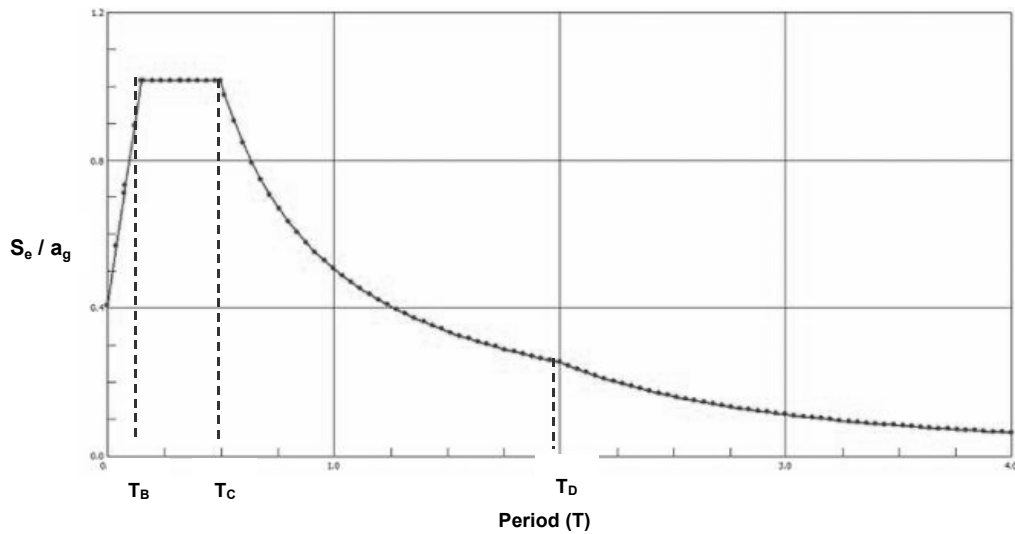


Fig.74. Elastic response spectrum representation

Ground categories

In order to assess seismic risk for buildings, it is necessary to evaluate the effect of the local seismic response through specific analysis as described in D.M 14/01/08, chap.7. In absence of those analysis, for the definition of the seismic action we can refer to a simplified approach, based on the individuation of reference ground categories (Tab.41). The geotechnical characterization of grounds in the significant volume is necessary, and in order to identify the category of the terrain, the classification is performed on the basis of equivalent velocity $V_{s,30}$ of propagation of S shear waves in the first 30 m of depth.

Tab.41. Description of the five ground categories (D.M 14/01/08)

Category	Description
A	<i>Outcrops or very rigid terrain characterised by $V_{s,30} > 800$ m/s eventually including superficial altered layer, with maximum depth of 3 m</i>
B	<i>Soft rocks and terrain deposit coarse grain very thick or fine grain very firm with depth > 30 m, characterised by a gradual increase of mechanic properties with depth and $360 < V_{s,30} < 800$ m/s</i>
C	<i>Terrain deposits coarse grain of intermediate thickness or fine grain medium firm with depth > 30 m, characterised by a gradual increase of mechanic properties with depth and $180 < V_{s,30} < 360$ m/s</i>
D	<i>Terrain deposits coarse grain of limited thickness or fine grain scarcely firm with depth > 30 m, characterised by a gradual increase of mechanic properties with depth and $V_{s,30} < 180$ m/s</i>
E	<i>Terrains of type C and D for depths < 20 cm, posed on the reference ground</i>

The equivalent velocity of S waves $V_{s,30}$ is defined as:

$$V_{s,30} = \frac{30}{\sum_{i=1}^N \frac{h_i}{V_{s,30}}} \quad (33)$$

where

h_i = depth (in m) of the layer i included in the first 30 m depth

$V_{s,30}$ = equivalent velocity of S waves for layer i

In Valtellina, due to the morphology of the area, only three terrain categories were considered (Fig.75), assigned on the basis of morphologic conformations (Tab.42) For Brescia area, a detailed characterisation was performed, based on (Fig.76):

- geological maps
- Quaternary deposit maps available for mountain areas (Geomabientale, RL, 1983)
- map of soils and landscape units for the plain areas
- geological studies realized for municipal planning zonation (PGT, Piani d Governo del Territorio)
- microzonation studies realized by private consulting companies

Tab. 42. Ground categories definition for risk assessment in Valtellina

Ground category	Description	Amplification
A	Slopes > 15°	Minimum
B	Alluvial fans	Medium
C	Valley bottom	Maximum

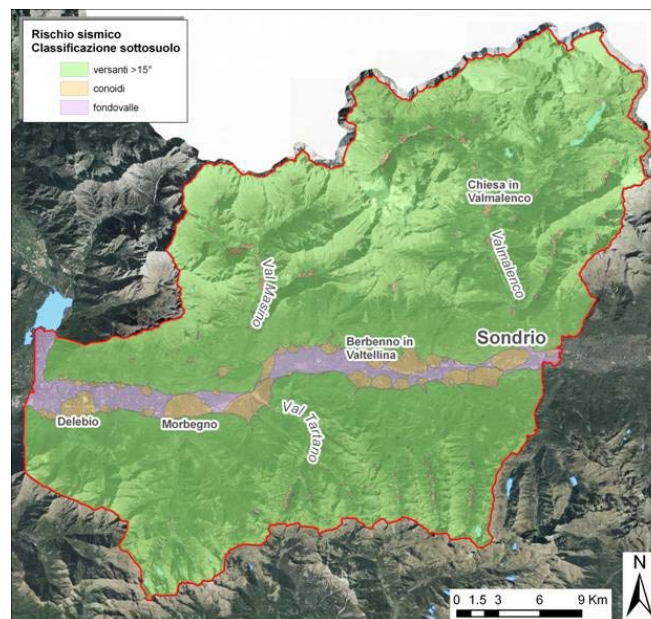


Fig.75. Ground categories, Valtellina.

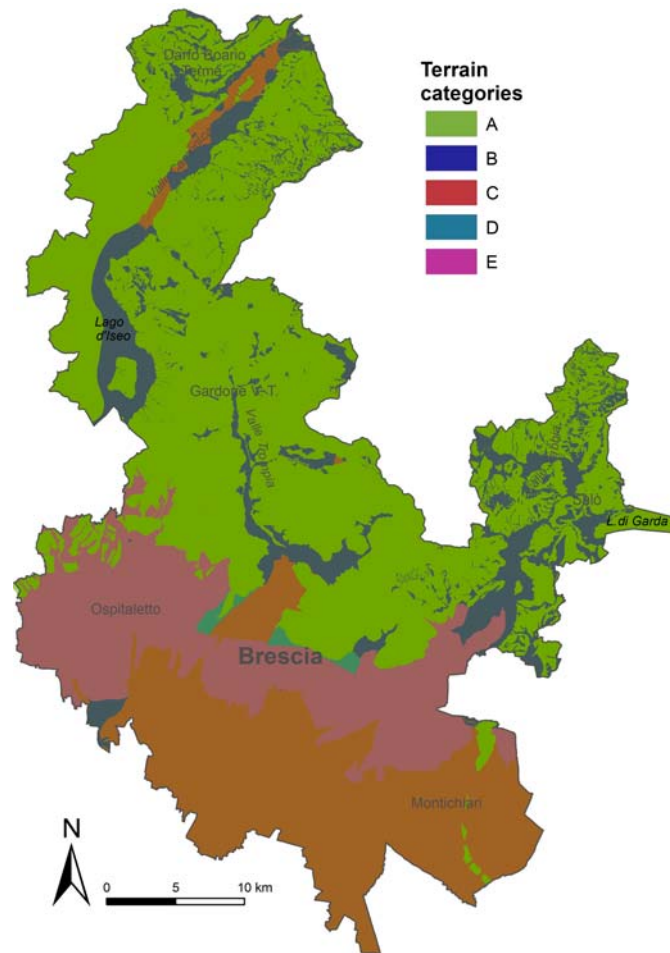


Fig.76. Ground categories, Brescia study area

Topographic conditions

Topographic conditions influence the local seismic response (D.M 14/01/08). For complex situations, specific analysis of seismic local response are required. In the present work, we consider simple superficial configurations and the corresponding values of the parameter S_T of topographic amplification (Tab.43) Categories refer to geometric bidimensional configurations, crests and long and narrow ridges, and must be considered if having an height superior to 30 m.

Tab.43. Categories of topographic conditions

Category	Characteristics of the topographic surface
T1	Plain surface, isolated slopes and relieves with mean inclination $i < 15^\circ$
T2	Slopes with inclination $i > 15^\circ$
T3	Relieves with sharp crest and mean inclination $15^\circ < i < 30^\circ$
T4	Relieves with sharp crest and mean inclination $i > 30^\circ$

Stratigraphic amplification

For terrain category A, the coefficients S_s and C_c are equal to 1.

For terrain categories B, C, D and E, the coefficients S_s e C_c can be calculated, as a function of values of F_0 and T_c^* related to ground of category, through expressions in Tab.44, where g is the gravity acceleration and the time is expressed in seconds.

Tab.44. Values of the coefficients S_s and C_c . (D.M 14/01/08)

Category	S_s	C_c
A	1	1
B	$1 < 1.4 - 0.4 * F_0 * a_g / g < 1.2$	$1.1 * (T_c^*)^{-0.2}$
C	$1 < 1.7 - 0.6 * F_0 * a_g / g < 1.5$	$1.05 * (T_c^*)^{-0.33}$
D	$0.9 < 2.4 - 1.5 * F_0 * a_g / g < 1.8$	$1.25 * (T_c^*)^{-0.5}$
E	$1 < 2 - 1.1 * F_0 * a_g / g < 1.6$	$1.15 * (T_c^*)^{-0.4}$

To each terrain category a distinct curve corresponds, representing the elastic response spectrum (Fig.77).

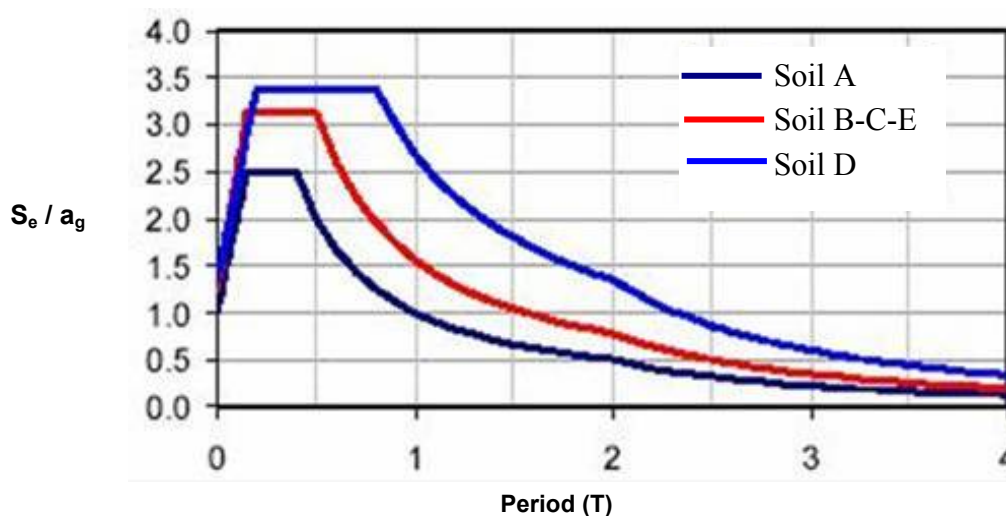


Fig.77. Representation of an elastic response spectrum for different round categories

Spectral Displacement

The methodology proposed by FEMA (2003) characterizes ground shaking using a standardized response shape, as shown in Fig.82. The standardized shape consists of four parts: peak ground acceleration (PGA), a region of constant spectral acceleration at periods from zero seconds to T_B (seconds), a region of constant spectral velocity at periods from T_B to T_c (seconds) and a region of constant spectral displacement for periods of T_d and beyond.

Spectral acceleration can be plotted as a function of spectral displacement (rather than as a function of period). This is the format of response spectra used for evaluation of damage to buildings and essential facilities. Eq.34 may be used to convert spectral displacement S_d , to period (seconds) for a given value of spectral acceleration S_e (units of g),

$$T = 0.32 \sqrt{S_d/S_e} \tag{34}$$

and Equation (35) may be used to convert spectral acceleration S_e (units of g) to spectral displacement S_d for a given value of period (FEMA, 2003).

$$S_d = 9.8 * S_e * T^2 \tag{35}$$

Building period

The period of buildings is necessary to evaluate their response to a seismic solicitations, as a function of their structure, the material they are composed of, the number of floors, the height.

An elaboration of statistical data (ISTAT, 2001) was performed in order to obtain, for each of the census parcels of the study areas, the number of buildings with different structural characteristics, that are:

- materials (masonry or reinforced concrete buildings)
- number of floors (1,2,3,4 or more)
- the use (residential or generic other use)

For non residential buildings, the number of floors and the materials were not available. They include plants, productive (e.g. sheds), and commercial buildings. They were considered in the analysis as 2 floors masonry buildings, to maintain a conservative approach.

Tab.45. Result of elaborations of ISTAT data related to buildings per census parcel

Structure	Residential buildings								Other uses
	1 floor		2 floors		3 floors		4 or more floors		2 floors
Materials	Masonry	Reinforced concrete	Masonry	Reinforced concrete	Masonry	Reinforced concrete	Masonry	Reinforced concrete	Masonry

The seismic action on buildings is characterised by three translation components, two horizontal (X and Y) and one vertical (Z), independent among them. In this work, the only horizontal component is considered, being the most damaging for buildings.

Buildings period was evaluated as in Castellani and Faccioli (2000) in (Tab.46 and 47) as:

Tab 46a. Rules for characteristic period of the buildings according to the material

Material	period
reinforced concrete	$T = 0.075 * h^{0.75}$
masonry	$T = 0.035 * h$

where h is building height, derived from the number of floors, assumed to be 3 m each.

Tab.47. Characteristic period of the buildings

Use	# floors	Height (m)	T masonry	T concrete
Residential	1	3	0,17	0,11
	2	6	0,29	0,21
	3	9	0,39	0,32
	4+	12+	0,6	
Other use	2	6	0,29	

Fragility curves

For each type of building, four limit states of damage are defined (FEMA, 2003)

- Slight Damage
- Moderate Damage
- Extensive Damage
- Complete Damage

On the basis of the available data, fragility curves were calculated, expressing, for any seismic acceleration, the probability that a limit state of damage is exceeded.

Building damage functions are in the form of lognormal fragility curves that relate the probability of being in, or exceeding, a building damage state for a given response spectrum displacement. Figure 78 provides an example of fragility curves for the four damage states used in this methodology.

Each fragility curve is defined by a median value of the spectral displacement that corresponds to the threshold of the damage state and by the variability associated with that damage state.

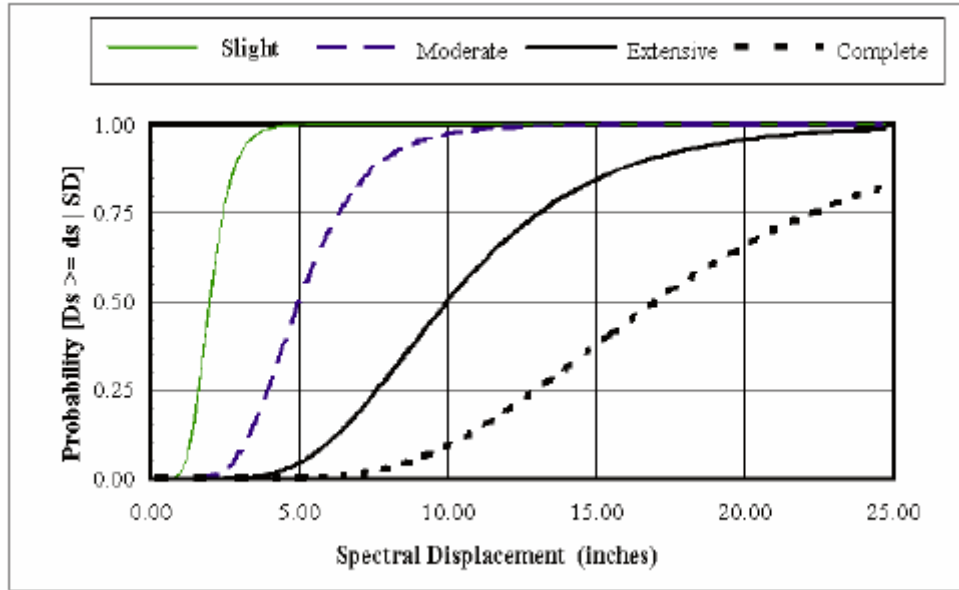


Fig.78. Example Fragility Curves for Slight, Moderate, Extensive and Complete Damage.
FEMA (2003)

In a more general formulation of fragility curves, the lognormal standard deviation, β , has been expressed in terms of the randomness and uncertainty components of variability, β_R and β_U , (Kennedy, et. al., 1980). Since it is not considered practical to separate uncertainty from randomness, the combined random variable term, β , is used to develop a composite “best-estimate” fragility curve. This approach is similar to that used to develop fragility curves for the FEMA-sponsored study of consequences of large earthquakes on six cities of the Mississippi Valley region (Allen & Hoshall, et al., 1985).

The conditional probability of being in, or exceeding, a particular damage state, ds , given the spectral displacement, S_d , is defined by the function:

$$P[ds | S_d] = \Phi \left[\frac{1}{\beta_{ds}} \ln \left(\frac{S_d}{S_{d,ds}} \right) \right] \quad (36)$$

where:

$S_{d,ds}$, is the median value of spectral displacement at which the building reaches the threshold of damage state, ds ,

β_{ds} is the standard deviation of the natural logarithm of spectral displacement for damage state, ds , and

Φ is the standard normal cumulative distribution function.

Median spectral displacement (or acceleration) values and the total variability are developed for each of the model building types and damage states of interest by the combination of performance data (from tests of building elements), earthquake experience data, expert opinion and judgment.

In general, the total variability of each damage state, β_{ds} , is modelled by the combination of following three contributors to damage variability:

- uncertainty in the damage state threshold,
- variability in the capacity (response) properties of the model building type of interest, and
- uncertainty in response due to the spatial variability of ground motion demand.

Each of these three contributors to damage state variability is assumed to be lognormally distributed random variables.

Values of the parameters β_{ds} and S_{dds} were provided by FEMA (2003). In particular, parameters identified for structures older than the formulation of NTC (Technical norms for construction) were selected, in order to be as conservative as possible. In the study areas, high magnitude earthquakes were never registered, and for this reason the norms were not used before their obligatoriness. Parameters are shown in Tab.48.

Tab. 48. Parameters of fragility curves– Pre-Code Seismic Design Level (FEMA, 2003).

Type of building	Spectral Displacement (inches)							
	Slight		Moderate		Extensive		Complete	
	$\bar{S}_{d,ds}$	β_{ds}	$\bar{S}_{d,ds}$	β_{ds}	$\bar{S}_{d,ds}$	β_{ds}	$\bar{S}_{d,ds}$	β_{ds}
C3L	0,43	1,19	0,86	1,15	2,16	1,15	5,04	0,92
C3M	0,72	0,90	1,44	0,86	3,60	0,90	8,40	0,96
C3H	1,04	0,73	2,07	0,75	5,18	0,90	12,10	0,95
URML	0,32	1,15	0,65	1,19	1,62	1,20	3,78	1,18
URMM	0,50	0,99	1,01	0,97	2,52	0,90	5,88	0,88

Two types of buildings were identified, in relation to FEMA definitions:

1. Concrete Frame Buildings with Unreinforced Masonry Infill Walls (C3): steel frame buildings with unreinforced masonry infill walls with the frame of reinforced concrete. In these buildings, the shear strength of the columns, after cracking of the infill, may limit the semi-ductile behaviour of the system. For these building typology, levels of damage are defined as:

- Slight Structural Damage: Diagonal (sometimes horizontal) hairline cracks on most infill walls; cracks at frame-infill interfaces.
- Moderate Structural Damage: Most infill wall surfaces exhibit larger diagonal or horizontal cracks; some walls exhibit crushing of brick around beam-column connections. Diagonal shear cracks may be observed in concrete beams or columns.
- Extensive Structural Damage: Most infill walls exhibit large cracks; some bricks may dislodge and fall; some infill walls may bulge out-of-plane; few walls may fall partially or fully; few concrete columns or beams may fail in shear resulting in partial collapse. Structure may exhibit permanent lateral deformation.
- Complete Structural Damage: Structure has collapsed or is in imminent danger of collapse due to a combination of total failure of the infill walls and nonductile failure of the concrete beams and columns. Approximately 15%(low-rise), 13%(mid-rise) or 5%(high-rise) of the total area of C3 buildings with Complete damage is expected to be collapsed.

2. Unreinforced Masonry Bearing Walls (URM): they include structural elements that vary depending on the building's age and, to a lesser extent, its geographic location. In buildings built before 1900, the majority of floor and roof construction consists of wood sheathing supported by wood framing. In large multistory buildings, the bottoms are cast-in-place concrete supported by the unreinforced masonry walls and/or steel or concrete interior framing. In unreinforced masonry constructed after 1950 (outside California) wood bottoms usually have plywood rather than board sheathing. In regions of lower seismicity, buildings of this type constructed more recently can include bottom and roof framing that consists of metal deck and concrete fill supported by steel framing elements. The perimeter walls, and possibly some interior walls, are unreinforced masonry. The walls may or may not be anchored to the diaphragms. Ties between the walls and diaphragms are more common for the bearing walls than for walls that are parallel to the bottom framing. Roof ties usually are less common and more erratically spaced than those at the bottom levels. Interior partitions that interconnect the bottoms and roof can reduce diaphragm displacements. For these building typology, levels of damage are defined as:

- Slight Structural Damage: Diagonal, stair-step hairline cracks on masonry wall surfaces; larger cracks around door and window openings in walls with large proportion of openings; movements of lintels; cracks at the base of parapets.
- Moderate Structural Damage: Most wall surfaces exhibit diagonal cracks; some of the walls exhibit larger diagonal cracks; masonry walls may have visible separation from diaphragms; significant cracking of parapets; some masonry may fall from walls or parapets.
- Extensive Structural Damage: In buildings with relatively large area of wall openings most walls have suffered extensive cracking. Some parapets and gable end walls have fallen. Beams or trusses may have moved relative to their supports.
- Complete Structural Damage: Structure has collapsed or is in imminent danger of collapse due to in-plane or out-of-plane failure of the walls. Approximately 15% of the total area of URM buildings with Complete damage is expected to be collapsed.

6.6.2 SOCIETAL RISK ASSESSMENT

We compute human casualties taking into account damages in each typology and the occupancy per typology, following FEMA & NIBS (1999) methodology. Casualty rates are presented in Tab.49 by injury level, typologies and damage states:

Tab.49. Values for equivalent casualties calculation per building typology and state of damage (FEMA, & NIBS, 1999).

Limit state of damage	Building type	Level of damage (%)				
		Light injuries	Injuries requiring hospitalisation	Severe injuries	Death	
Slight	<i>all</i>	0,05	0,005	0,0	0,0	
Moderate	<i>URM</i>	0,4	0,04	0,0	0,0	
	<i>C3</i>	0,2	0,02	0,0	0,0	
Extensive	<i>URM</i>	2,0	0,2	0,002	0,002	
	<i>C3</i>	1,0	0,1	0,001	0,001	
Complete	Partial collapse ^e	<i>URM</i>	10,0	2,0	0,02	0,02
		<i>C3</i>	5,0	1,0	0,01	0,01
	Total collapse	<i>1-2 floors URM / C3</i>	50,0	10,0	2,0	1,0
		<i>> 2 floors URM / C3</i>	50,0	10,0	2,0	2,0

For each limit state referred to each type of building, the percentages of damage level are calculated, obtaining, for each of them, the expected number of equivalent casualties.

Adding the expected casualties for each limit state, the total expected damage is calculated for each building type, for each census parcel. As a function of the percent presence of each building typology in each census parcel, the total fragility was evaluated for each parcel.

The exceedance probabilities of the seismic scenarios were calculated as a poissonian (eq.)

$$P_{ex} = 1 - e^{-1/T_R} \quad (37)$$

where:

P_{ex} = exceedance probability

-1 = time interval for P_{ex} evaluation, in this case one year

T_R = time of return of the event

Obtained values are shown in Tab.50

Tab.50. Exceedance probability values for return times

Return time (years)	Exceedance probability - P_{ex}
72	0,01367296
140	0,007117408
475	0,002102778
975	0,001025115
2500	0,00039992

For each census parcel, societal risk was then evaluated as

$$R_s = \text{fragility} * P_{ex} * \text{equivalent population}$$

The societal risk was then attributed only to the built part of the territory, being null the societal risk for people located in the open air. The aggregation of the scenarios was performed calculating the area of the F/N curve. In Valtellina, societal seismic risk for the three scenarios assumes values show in Tab.51.

Tab.51. Seismic societal risk range values for the day and night scenarios, for Valtellina

Return time	Day scenario (cas./year/cell)	Night scenario (cas./year/cell)	Tot day scenario (cas./year)	Tot night scenario (cas./year)
72	0 - 2.5 e-4	0 - 1.7 e-3	0.2165	0.2734
475	0 - 4.4 e-4	0 - 3.2 e-3	0.3462	0.4314
2500	0 - 3.4 e-4	0 - 2.5 e-3	0.2665	0.3330

Expected casualties per year are equivalent casualties, which means that injuries are included with the related coefficients (see Tab.49) The societal risk is higher where the highest density of population concentrates (Sondrio, Morbegno) (Fig.79 and 80).

For the area of Brescia, societal seismic risk for the three scenarios assumes values shown in Tab.52.

Societal seismic risk in the area of Brescia, as expected, is much more significant, due to the high level of hazard (Fig.81).

Tab.52. Overall seismic risk societal values for the day and night scenarios

Return time	Range (cas./year/cell)	Tot scenario (cas./year)
72	0-0.0013	3.88
140	0-0.0014	4.68
475	0-0.0014	5.45
975	0-0.0013	5.28
2500	0-0.0010	4.45

Tab.53. Societal risk values

	Valtellina day scen	Valtellina night scen	Brescia
Range (cas/year/cell)	0-0.0009	0-0.0007	0-0.004
Total (cas/year)	0.697	0.89	15,4

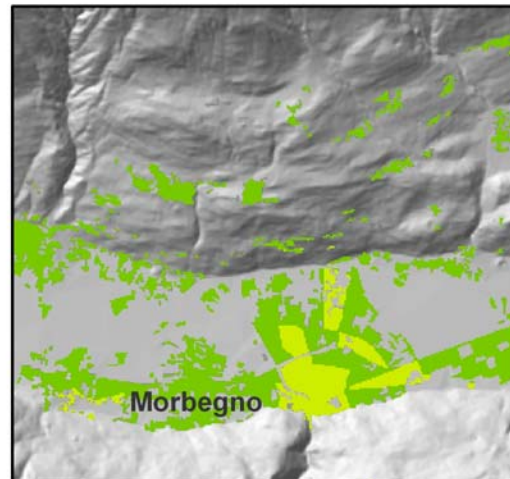
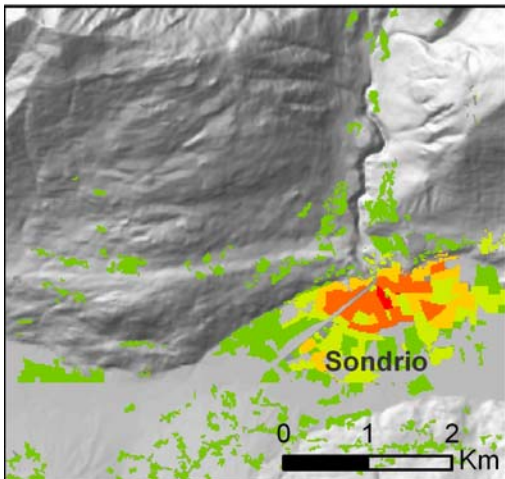
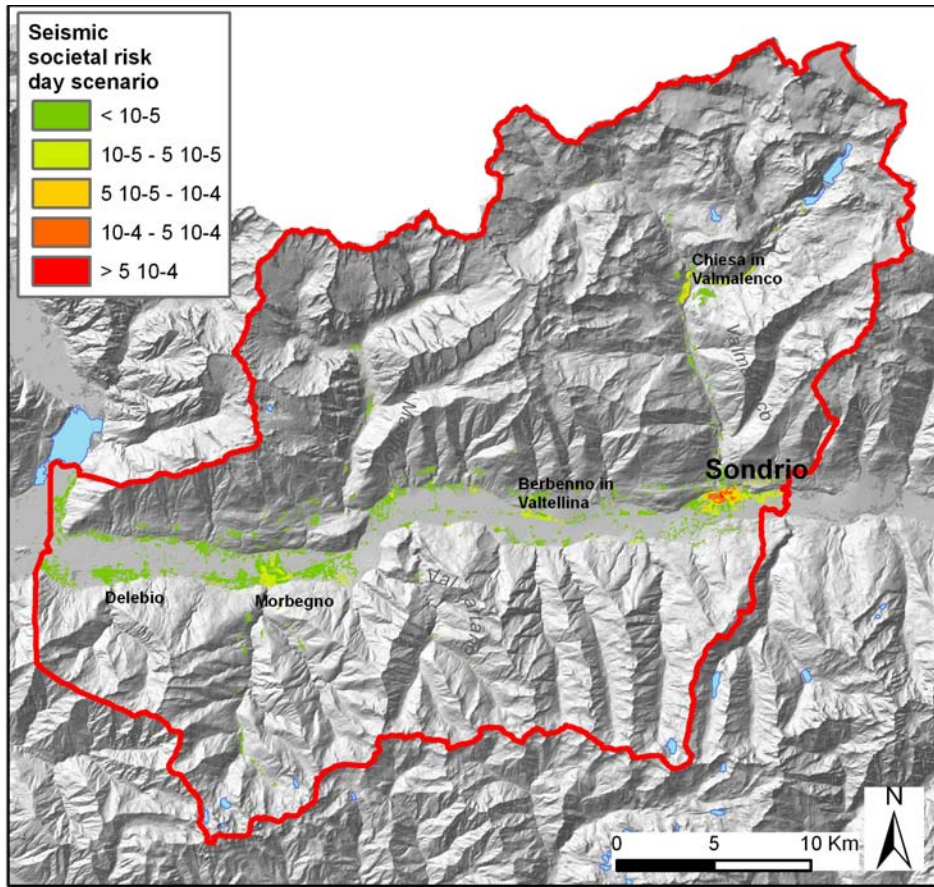


Fig.79. Map of societal seismic physical risk, day scenario, Valtellina. Risk values are expressed in terms of casualties per year.

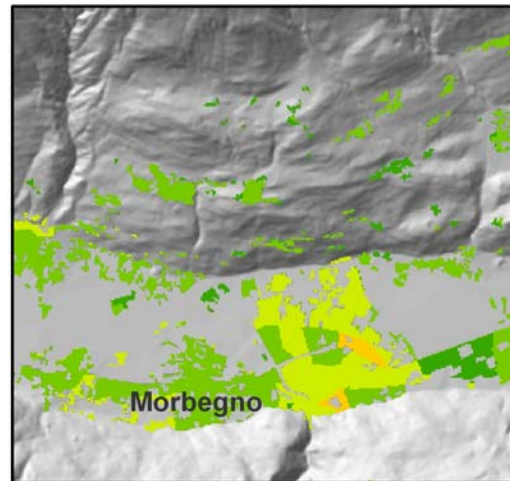
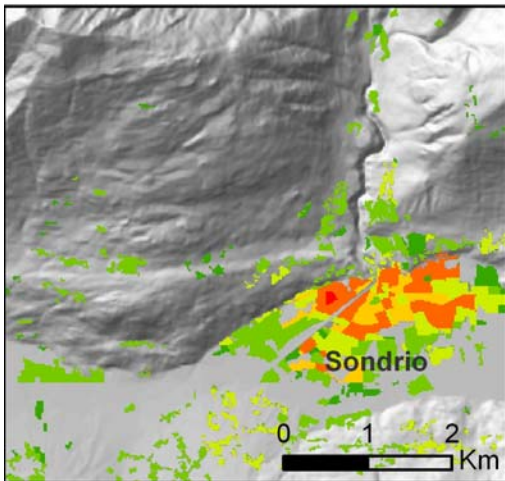
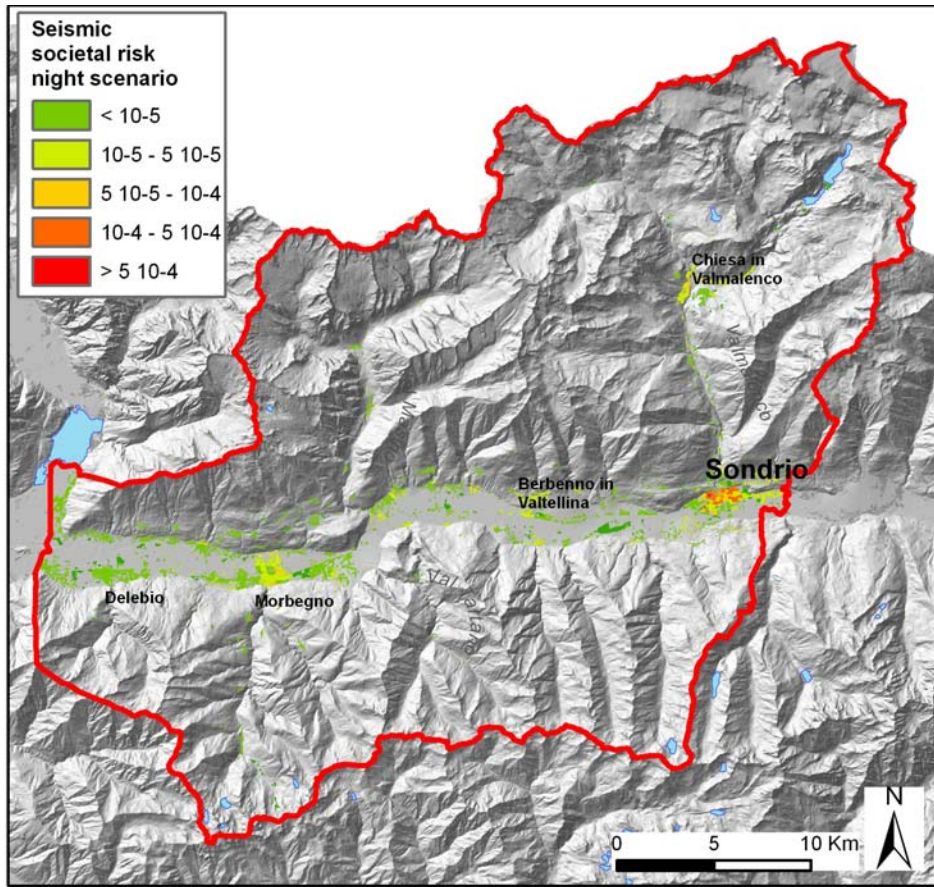


Fig.80. Map of societal seismic physical risk, night scenario, Valtellina. Risk values are expressed in terms of casualties per year.

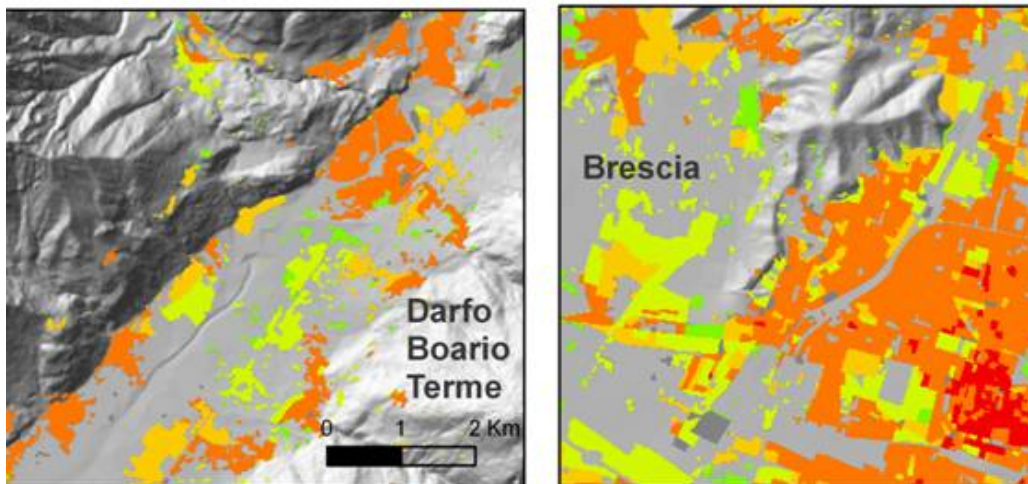
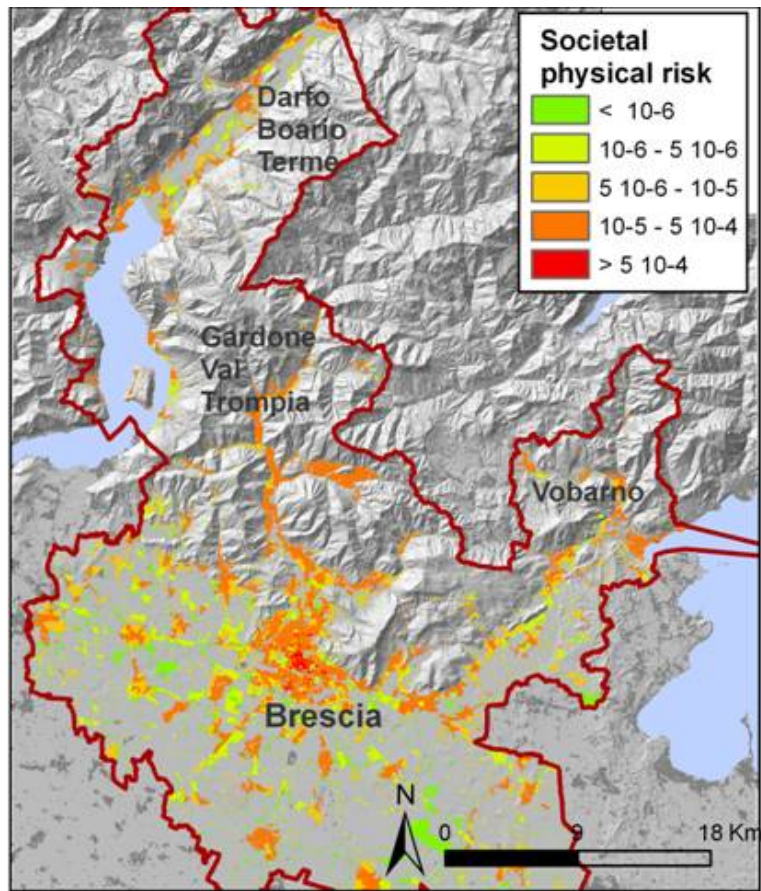


Fig.81. Map of societal seismic physical risk, Brescia study area. Risk values are expressed in terms of casualties per year.

6.6.3 ECONOMIC RISK ASSESSMENT

For economic risk assessment, for the building typologies an economic value was assessed, on the basis of a market research for the study areas (Tab.54). This was necessary in order to assess an overall value to each of the census parcels

Tab.54. Economic value for building typology

Building typology	surface m ²	Value €/ m ²	Building value €/ building
1 floor concrete	200	1500	300,000
1 floor masonry	200	1500	300,000
2 floors concrete	500	1500	750,000
2 floors masonry	500	1500	750,000
3 floors concrete	1200	1500	1,800,000
3 floors masonry	1200	1500	1,800,000
4+ floors concrete	2000	1500	3,000,000
4 + floors masonry	2000	1500	3,000,000
Other use			1,235,000

The calculation of the fragility F_r (from eq. 36) was the same as for societal risk. For each section, the potential economic loss was calculated. The economic risk was then attributed only to the built part of the territory, being referred only to building values and fragilities (Tab.55). The aggregation of the scenarios was performed calculating the area of the F/D curve. For both areas, economic risk is quite relevant (Tab.56).

Tab.55. Seismic economic risk values for the day and night scenarios

Return time	Valtellina (€/year/cell)	Brescia (€/year/cell)	Valtellina (€/year)	Brescia (€/year)
72	0-5,148	0-71,041	7,513,067	9,384,971
140	-	0-63,489	-	7,320,634
475	0-3'462	0-41,022	4,352,755	3,890,642
975	-	0-27,319	-	2,537,023
2500	0-1'302	0-15,622	1,655,619	1,292,115

Tab.56. Economic risk values for the two study areas

	Valtellina	Brescia
Range (€/year/cell)	0-8,398	0-131,423
Total (€/year)	12,419,634	65,078,752

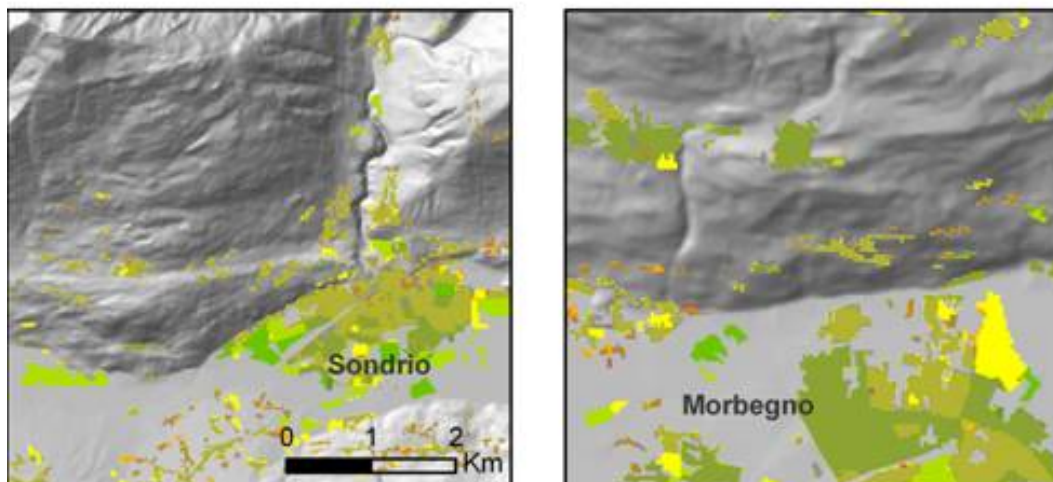
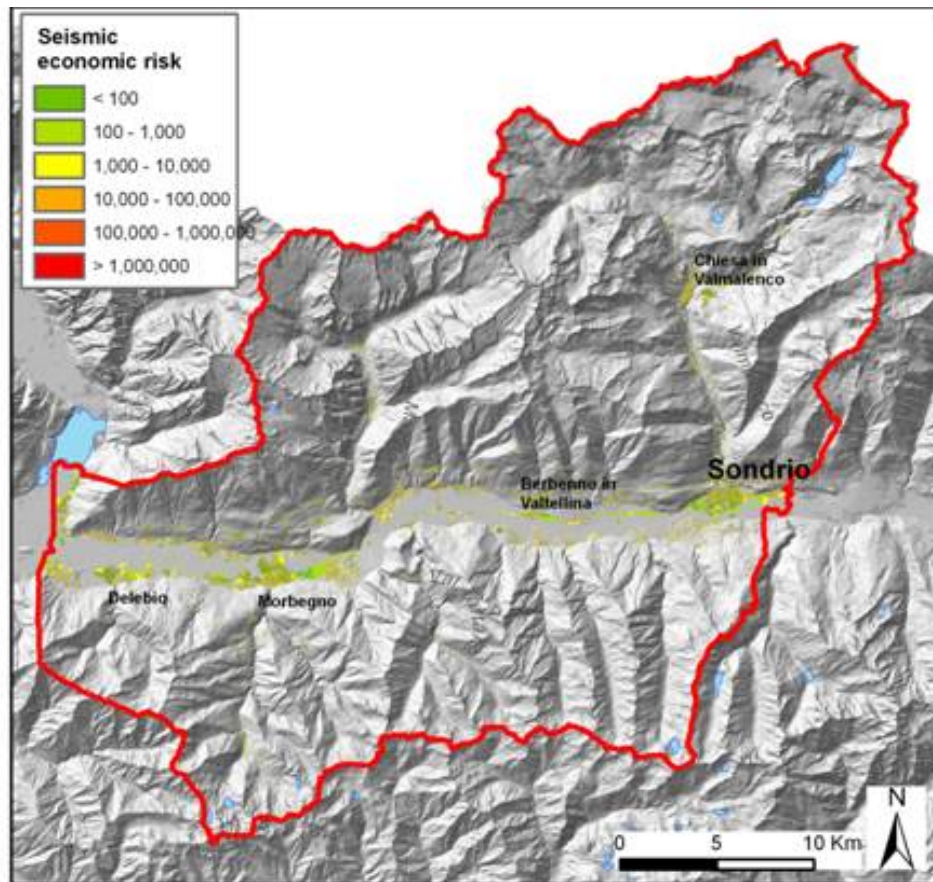


Fig.82. Map of economic seismic physical risk, in euros/year, for Valtellina

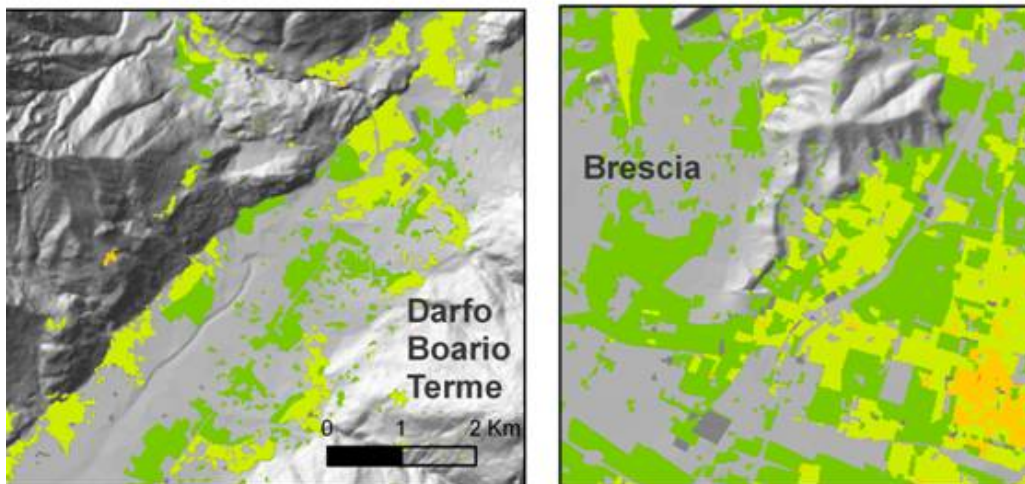
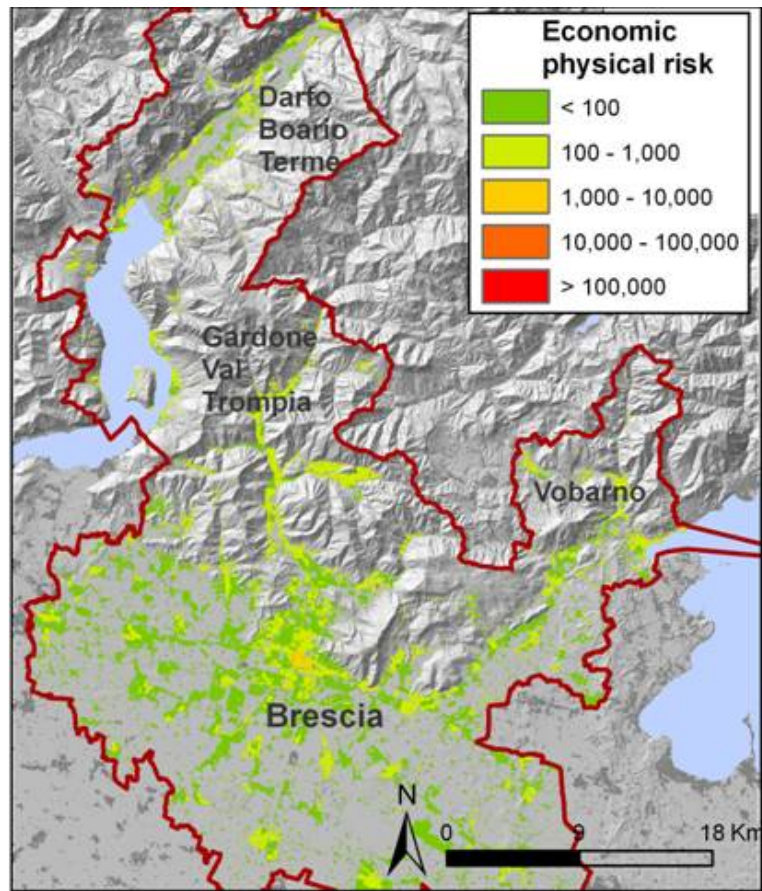


Fig.83. Map of economic seismic physical risk, in euros/year, for Brescia study area

6.7 WILDFIRE RISK

As said for the analysis at the regional scale, wildfires in Lombardy are only occasionally natural events. The anthropic nature of risk must be taken into account.

For the area of Brescia, wildfire risk was assessed. A number of data bases were available:

- SIAB – Information system anti wildfire (Database Regione Lombardia – D.G. Protezione Civile, Prevenzione e Polizia Locale, 2002)
- Map of destination of use for agricultural and forestal soils of Lombardy (Ersaf, 2000)
- Map of the forestal types of Lombardy (Ersaf, 2006)
- Paper Wildfire news of CFS
- Agro-climatic regional atlas
- Analysis and classification of risk areas of Regional plan of the prevision, prevention and active fight against wildfires of Lombardy, 2006

Wildfire risk often involves only volunteers employed in fire extinction. For this reason, societal risk was evaluated for both population and volunteers.

350 events were registered in the study area in the period 1997-2007.

6.7.1 EXPECTED FREQUENCY OF OCCURRENCE, W_w

Predictive models allow to define where a wildfire can occur and how likely, without explicitly defining return times and intensity. The expected frequency of occurrence is calculated as a function of territorial characteristics, influencing the susceptibility of an area. This value is normalised by means of the frequency of occurrence of the past events, expressed as spatial and temporal density of phenomena. In the methodology, a relevant importance was given to the statistics of past events, given the strongly anthropic component connected to the triggering of fire. For the historical series of 1997-2007, 350 triggering points were mapped and used for statistical elaborations (ERSAF).

The susceptibility of a territory to wildfire is defined as a function of determinant and predisposing factors.

Predisposing factors are connected to the intrinsic characteristics of the territory: morphology, vegetation, meteorological conditions. Dynamic and static factors can be distinguished. For the firsts, time has a limited incidence, because they change in a very slow way (e.g. morphology, wood extension), while the seconds are strictly dependent on temporal changes (e.g. temperature and wind trends). Dynamic variables as wind, temperature and precipitations can strongly influence both wildfire triggering and propagation. In this work, only static indicators were considered, because dynamic significant parameters for wildfires are not available for Lombardy. As a consequence, for meteorological variables, the agro-climatic atlas was used, describing the different climate conditions of the Region. This information is to be considered as static: for precipitations, the mean data referred to the second decade of march was used, and for temperatures the mean values for the same period. The choice was driven by the data provided by the regional anti-wildfire plan of 2006 (ERSAF, 2005-2006). The month of march resulted to be the most critical.

Tab.57. Predisposing factors for wildfires

	Indicator	Measure unit	Source
Static factors	Mean elevation	m s.l.m.	DTM
	Mean slope	degrees (°)	
	Surface exposed to north	m ²	
	Surface exposed to east		
	Surface exposed to south		
	Surface exposed to west		
	cultivations and pastures	Presence/absence	Map of destination of use of agricultural and forestall soils
	Pyrologic potential of cultivations and pastures	N (ranging 0-1)	
	Woods	Presence/absence	Map of the forestal types, Lombardy Region
	Pyrologic potential of wood types	N (ranging 0-1)	
Dynamic factors	Mean temperatures	°C	Agro-climatic atlas
	Mean precipitations	mm	

Tab.58. Determinant factors for wildfires

Indicator	Measure unit	Source
Distance from urbanised areas	m	DUSAF,2007
Distance from roads	m	DUSAF,2007

For the geomorphologic characterisation, elevation, aspect and slope were considered. Slope deeply influences fire diffusion, making fire closer to the combustible, and because ascensional hot air flow causes a heating and a dehydration of wood, favouring a faster lighting. Fire is more intense due to oxygen enrichment of the combustion zone due to the ascensional hot air flow. Burning woods easily roll down on steepest slopes, triggering new fires. Also aspect is a significant factor, influencing temperature and dampness of woods: slopes exposed to south result hotter, and dry. The preventing effect of rain is minor, such as the permanence of snow. Vegetation is more subjected to water stress, to a rapid withering and to a higher inflammability, due to high transpiration and reduction of water content. Similar considerations can be done with respect to elevation. Wildfire present a maximum in frequency in the elevation class ranging from 800 and 1100 m a.s.l., decreasing to zero above 1600 m a.s.l.

Another group of factors includes the use of agricultural and forestal areas, with particular reference to woods and pastures, which are the most interested by wildfires. The burnable surface was detected and characterised. To each category, a pyrologic potential was assigned (Del Favero, 2000), representing the degree of inflammability of vegetation. Chemically, the presence of oils and galipot increases the heat of combustion, due to the high energetic content, and burn intensively. Differently, the presence of mineral elements in wood and leaves can reduce the inflammability of some species of trees (Del Favero, 2000).

The determinant factors are referred to the anthropic presence on the territory. Often, potentially dangerous human behaviours take place along roads passing through woods (or in the immediate proximities): pic nic fires, cigarette ends thrown away,

stubble burning, cultivation cleaning, garbage deposits etc. Although road network is important to allow the access of workers and anti wildfire equipments, the statistical analysis of the events shows that the presence of roads is an element which increases wildfire occurrence. Most triggerings take place within 100 m from the roads, and the totality within 1 Km. Also the presence of urbanised areas determines a higher probability of frequentation of the area, for different activities and in different periods of the year.

The meteorological characterisation of the area helps in defining wildfire hazard: temperature and precipitation regime are predisposing factors.

The methodology of evaluation of the expected frequency of occurrence is based on a weighted sum of factors, where the weights assigned to each of them is representative of its potential incidence in the occurrence of a wildfire.

For each of the factors, a function of predisposition to wildfire was calculated, defined as:

$$\mu(x) = f(x_i) \quad (38)$$

assuming 0 to 1 values,

$\mu(x) = 1$ when the factor presents the higher predisposition to wildfire

$\mu(x) = 0$ when the factor presents the lowest predisposition to wildfire

$0 < \mu(x) < 1$ when the factor presents an intermediate predisposition to wildfire

The predisposition function can be of different types (linear, exponential, logistic). According to the literature (ERSAF, 2005-2006) and to the analysis of past events for the area, the frequency of the events shows a maximum between 800 and 110 m a.s.l., and becomes null above 1600 m a.s.l. Hence, a logistic function was applied to elevation (Fig.84a). The same is to be said for slope: the frequency of events shows minimum values until a 5-10% slope, and then increases to reach the maximum at 100% slope (Fig.84b). Slopes exposed to north show in general a minor predisposition to fire, eastern and western slopes an intermediate, and south slopes a maximum predisposition. This justifies the use of a logistic symmetric function, with its maximum at south and south-west and 0 in the north (Fig.84c).

For distances from roads and urbanised areas, a linear function was calculated (Fig.84d).

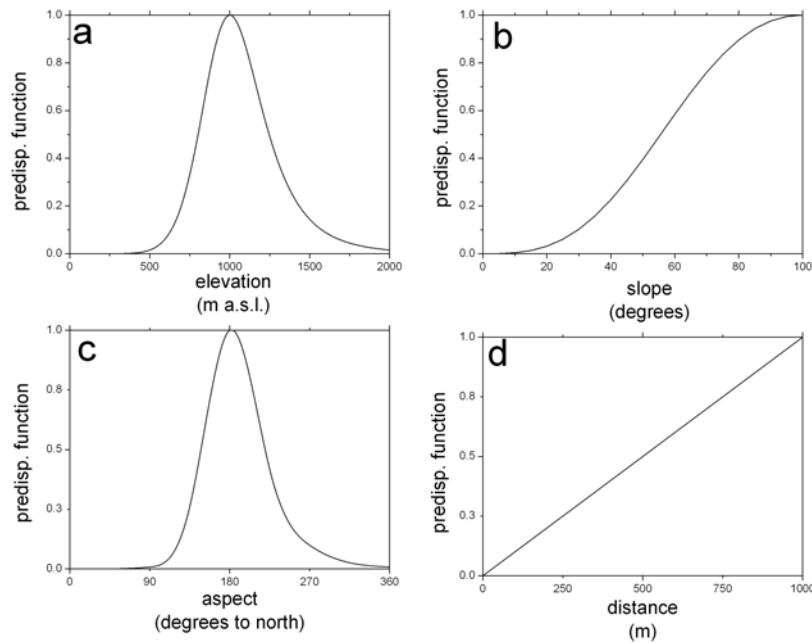


Fig.84. Function of conversion of some of the indicators

Each parameter was weighted according to an AHP, performed with the participation of 9 experts of ERSAF (Tab.59)

Tab.59. Indicators and related weights for susceptibility evaluation

	Indicator	Weight
Type indicators	Predisposing	0,003
	Determinant	0,003
Predisposing	mean elevation	0,061
	mean slope	0,079
	aspect	0,186
	pyrologic potential	0,165
	mean precipitations	0,308
	mean temperatures	0,200
Determinant	dist. From urbanised areas	0,163
	dist. From roads	0,837

By means of a weighted mean of the indicators, the susceptibility s of the area was evaluated, ranging from 0 (area non susceptible to wildfires) to 1 (area extremely prone to wildfires).

The statistical analysis of events has a determining role in the definition of the expected frequency of occurrence. The available data show the presence of 350 events in the study area of Brescia, which means a frequency value f of $1.9 \cdot 10^{-5}$ events/year/pixel.

The expected frequency of occurrence w was calculated as:

$w_w = s \cdot f$ on the whole vegetated area and on a buffer of 100 m calculated at its limits, to include in the analysis also the zone of interface between vegetated and urbanised areas. Expected frequency of occurrence on the study area presents values of order of magnitude 10^{-5} (Fig.85).

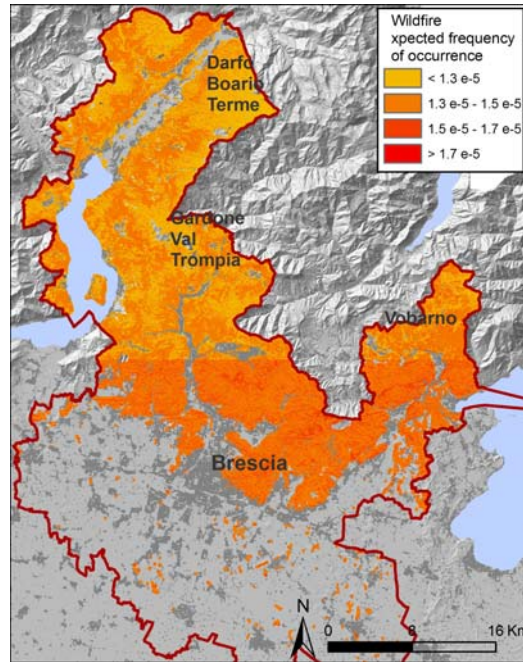


Fig.85. Expected frequency of occurrence for wildfires

6.7.2 SOCIETAL RISK ASSESSMENT

Societal risk assessment for wildfires is not only related to people living, working or being temporarily present in the study area.

Gravity factor, g_w

Supposing that in general fire has heavy effects on man health, a value of g of 0.8 was assigned by the experts of ERSAF.

Exposure factor, e_w

For risk assessment on population and on volunteers, two different values of exposure factor e were used. Volunteers are more exposed to wildfires. They are in close contact with fire, and in a large number they are involved in the exact moment of fire, while people in general is not easily directly involved. In most cases, casualties for wildfires among population are farmers, lighting fire to burn stubble or to clean the cultivations.

Mortality rates for the study area were used to calculate e_w , as number of equivalent casualties for event for year. Among volunteers, 5 people were injured in the period 1997-2007, which means $0.25*5 = 1.25$ equivalent casualties, which means $e_w = 1.25/350/10 = 0.00035714$.

Among population, 2 deaths were registered in the considered period, which means $e_w = 2/350/10 = 0.004$.

Elements at risk

For the assessment of wildfire risk on population, equivalent population was considered as element at risk, as for the other risks. For the assessment of risk on volunteers, 20 volunteers per pixel were considered to be active for each cell interested by wildfire, each of them staying in place for ten hours, meaning

$$p_i * N_{pe} = 20*10/24 = 8.33 \text{ volunteers/cell}$$

Societal risk assessment

Societal risk is quite homogeneous on the study area, in the order of magnitude of 10^{-7} . This is due to the narrow range of the values of the expected frequency of occurrence, and to the fact that most casualties take place among volunteers, working in the same number on the whole area.

On the whole area, 0.07 casualties/year/cell is the expected societal risk. It is important to say that in general wildfire triggering is not due to natural factors, but to anthropic activities or voluntary intentions. In this analysis, only partially they have been taken into account. The calculated value can be, for these reasons, underestimated with respect to the real value.

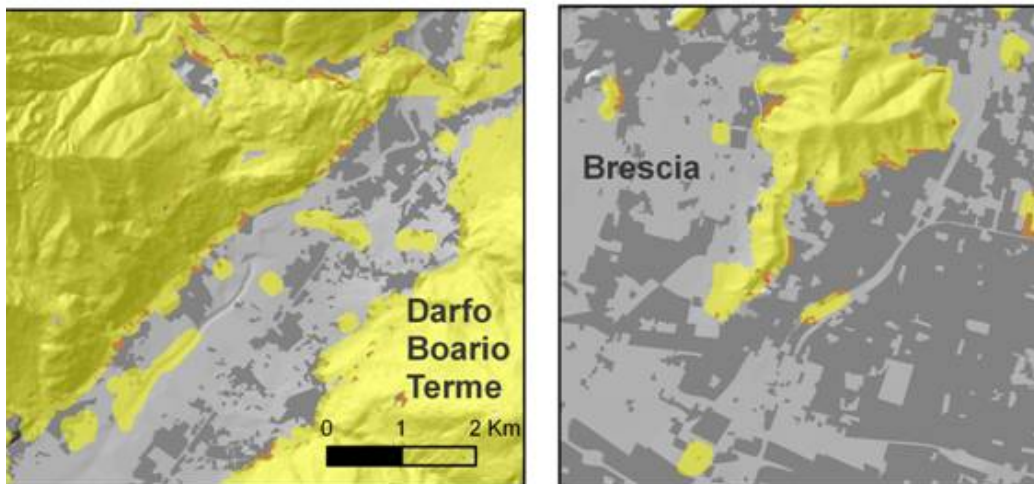
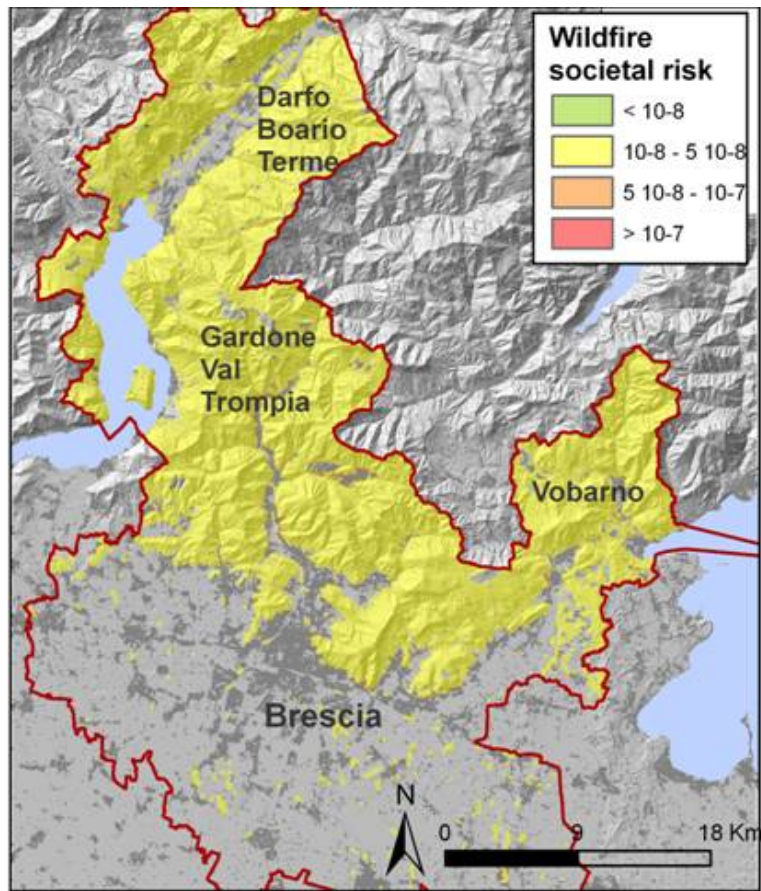


Fig.86. Map of societal physical risk for wildfires, Brescia study area. Risk values are expressed in terms of casualties per year.

6.7.3 ECONOMIC RISK ASSESSMENT

Gravity factor, g_w

The value of the factor of gravity for exposed elements was assessed with the expert knowledge of ERSAF operators, as in Tab.60.

Tab.60. gravity factors for elements exposed to wildfires

Exposed element	g_w
airports	0,4
forests	0,9
campings	0,5
commercial centres	0,4
cinemas	0,7
railways	0,3
fairs	0,4
orchards	1
technologic plants	0,3
olives	1
hospitals	0,7
agricultural productions	0,7
productive	0,5
residential	0,7
schools	0,7
crops	1
railway stations	0,7
streets	0,3
vines	1

Exposure factor, e_w

All the exposed elements are considered completely exposed. The exposure factor was considered always equal to 1.

Economic risk assessment

Economic risk for the area of Brescia is diffused on the whole burnable area, and very low, mainly related to the economic value of woods and cultivated areas. Highest losses reach 23 €/year/cell, while the total risk on the whole area equals 156,819 €/year (Fig.87).

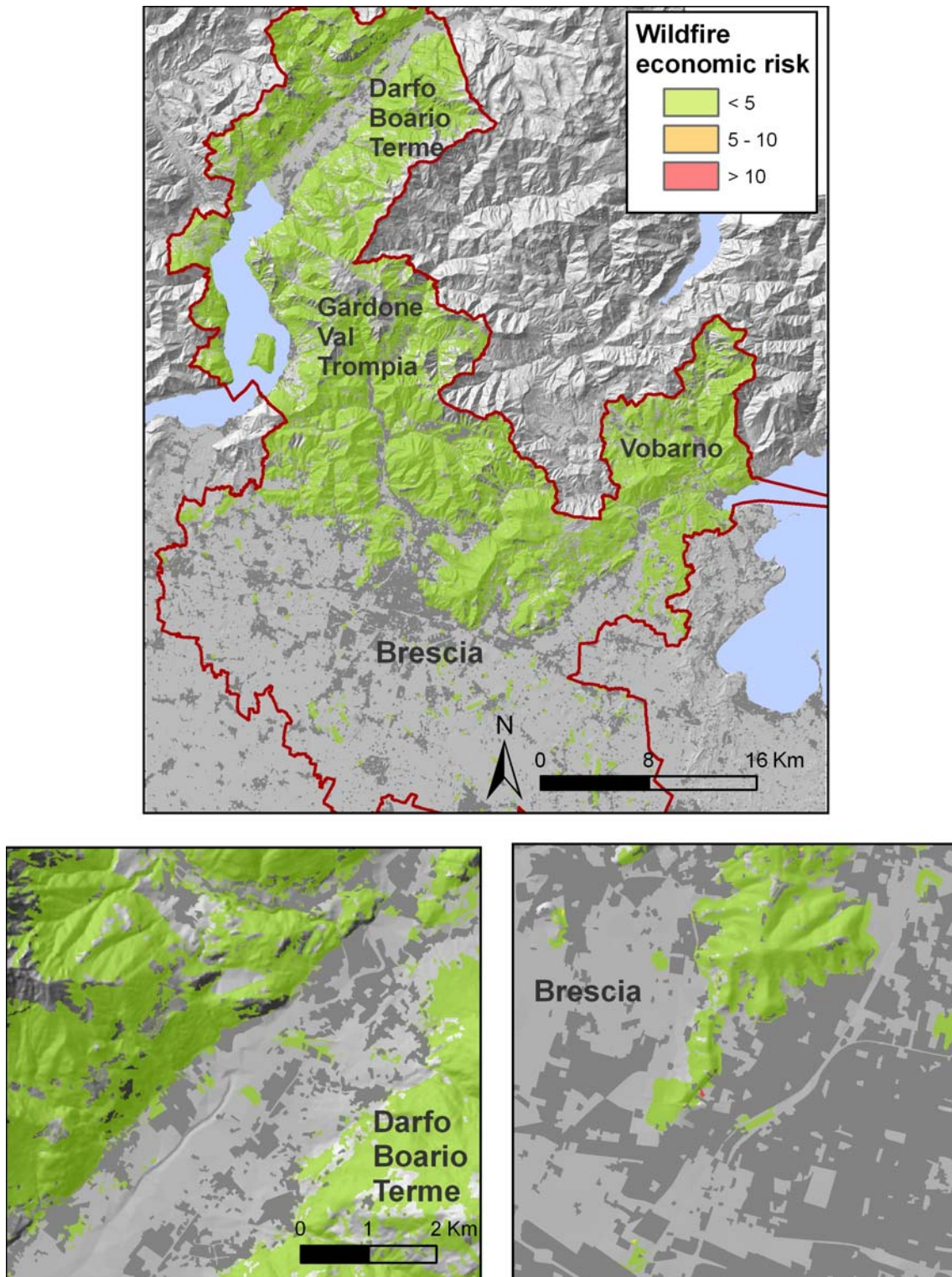


Fig.87. Map of economic physical risk for wildfires, in euros/year, for Brescia study area

6.8 TOTAL NATURAL RISK

6.8.1 INDIVIDUAL RISK

Individual risk is here expressed as the expected probability of being impacted by a phenomenon, in a year (Tab.61).

Tab.61. Maximum values of individual risk

	Valtellina day Scen	Valtellina night scen	Brescia
Rockfalls	<i>0,00176</i>	<i>0,00132</i>	<i>0,00600</i>
Shallow landslides	<i>0,00000</i>	<i>0,00000</i>	<i>0,00000</i>
Debris flows	<i>0,08462</i>	<i>0,01977</i>	<i>0,00554</i>
Floods in all. fans	<i>0,00049</i>	<i>0,01887</i>	<i>0,00125</i>
Floods	<i>0,00052</i>	<i>0,00050</i>	<i>0,00001</i>
Earthquakes	<i>0,00012</i>	<i>0,00012</i>	<i>0,00832</i>
wildfires	–	–	10^{-7}

6.8.2 SOCIETAL AND ECONOMIC TOTAL RISK

Outcomes of the risk assessment are resumed for the two study areas in Fig 88 and 89.

For the analysed natural risks, the area of Brescia shows significant values of societal risk, mainly due to seismic hazard. In lower Valtellina, people is prevalently threatened by debris flows. Floods have a relevant impact only on economic total risk, in both areas, such as rockfalls.

Results are strictly connected to the morphology and to the geography of the two study areas: while lower Valtellina is a completely mountainous territory, with many settlements localised on alluvial fans, the area of Brescia presents a plain zone, lower relieves, and is located in a seismic zone.

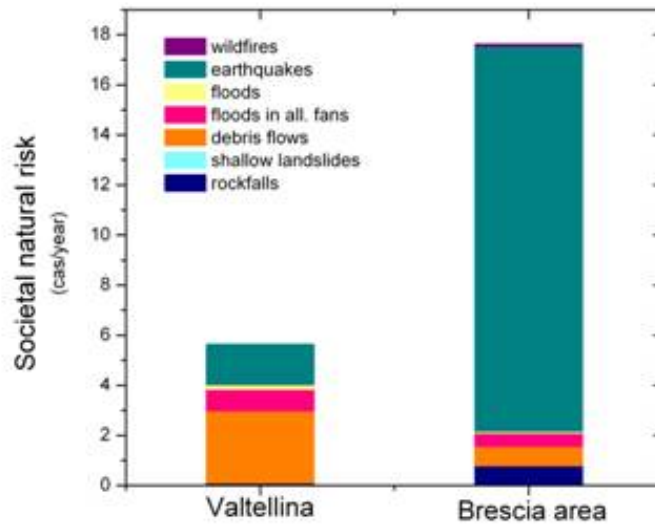


Fig.88. Societal natural risks for the two study areas

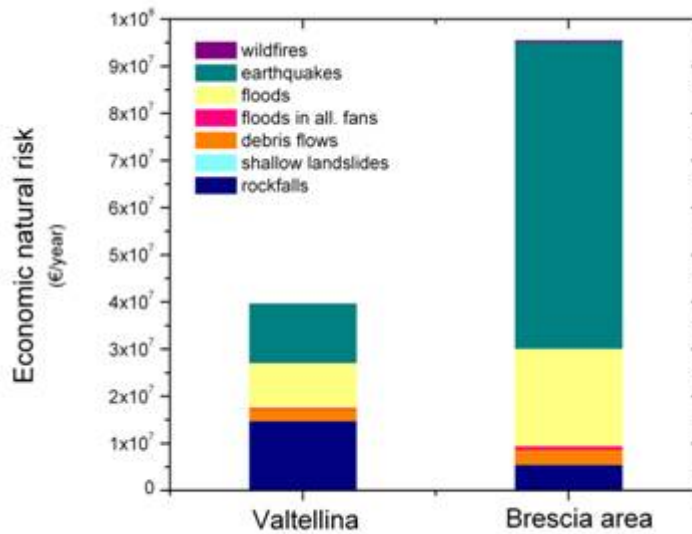


Fig.89. Economic natural risks for the two study areas

Lower Valtellina

Values of societal and economic risk related to natural threats (rockfalls, shallow landslides, debris flows, alluvial fan flooding, river floods, earthquakes) are resumed in Tab.62., and shown in Fig 90 and 91.

A scheme of risk values in relation to population and elevation is shown in Fig. 92.

Both societal and economic risk reach the highest values in correspondence of towns located in the valley bottom or on the alluvial fans, at lower elevations (e.g. Delebio, Morbegno, and Sondrio). Here, in fact, the highest number of residents, and as a consequence of buildings, facilities and activities, is observed.

The major component of economic risk at lower elevations is represented by flooding of the Adda river. As said before, river floods affect large part of the valley bottom, threatening productive activities, crops, buildings and towns. The correspondent societal risk is not so relevant: as explained before, river floods have a quite slow and predictable propagation of the flood wave, and prevision and alert systems are in general effective in order to obtain almost a complete evacuation of the areas. For this reason, a very low exposure factor, e_{FL} , was assumed (0.005).

Debris flows and alluvial fan flooding show a relevant importance in the societal risk, impacting the towns located on the alluvial fans of the main and of the secondary valleys. In general, the correspondent economic risk is not so high, because of the nature of these processes, threatening human life but usually generating economic damages only up to the first floors of the buildings.

Seismic risk is diffused on the whole territory, so that its distribution is controlled by the presence of buildings. The component of the total natural risk due to earthquakes is quite relevant for economic risk, less for societal, due to the modest intensity of earthquakes, which could slightly damage a large number of buildings without involving many people.

Above 700 m a.s.l., societal risk is negligible, due to the scarce human presence. On the contrary, economic risk is not negligible, mostly due to rockfalls impacting woods and roads.

FN and FD curves were calculated, for flood and seismic scenarios (Fig. 93 and 94).

Acceptability criteria proposed by Baecher (1982b) was used to observe economic risk acceptability, where damage economic values were discounted to the present (by means of Consumer Price Index, discounted to 2008).

Economic risk results to be marginally acceptable for the 200 years return time flood scenario, while it is not acceptable for the 10 years return time (showing high frequencies) and 500 years return time (showing very high damages), according to (Fig.94). Damages induced by seismic risk are in general not accepted.

Observing FN and FD curves, it is important to remind that existing measures to reduce risk are not taken into account in this risk assessment.

Societal risk related to floods and earthquakes never appears to be acceptable in lower Valtellina, if compared to Netherland Government Group risk criterion (Versteeg, 1987) (Fig.93)

Tab.62. Total values of societal and economic risk for Valtellina

	Valtellina societal risk	Valtellina economic risk
Range	0-0.028 <i>cas/year/cell</i>	0-39,577 <i>€/year/cell</i>
Total	5.6 <i>cas/year</i>	39,589,298 <i>€/year</i>

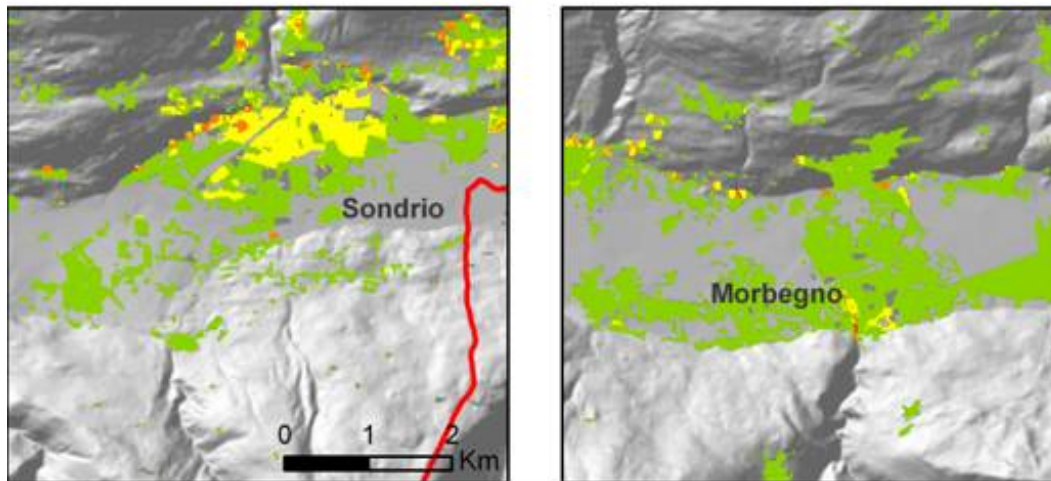
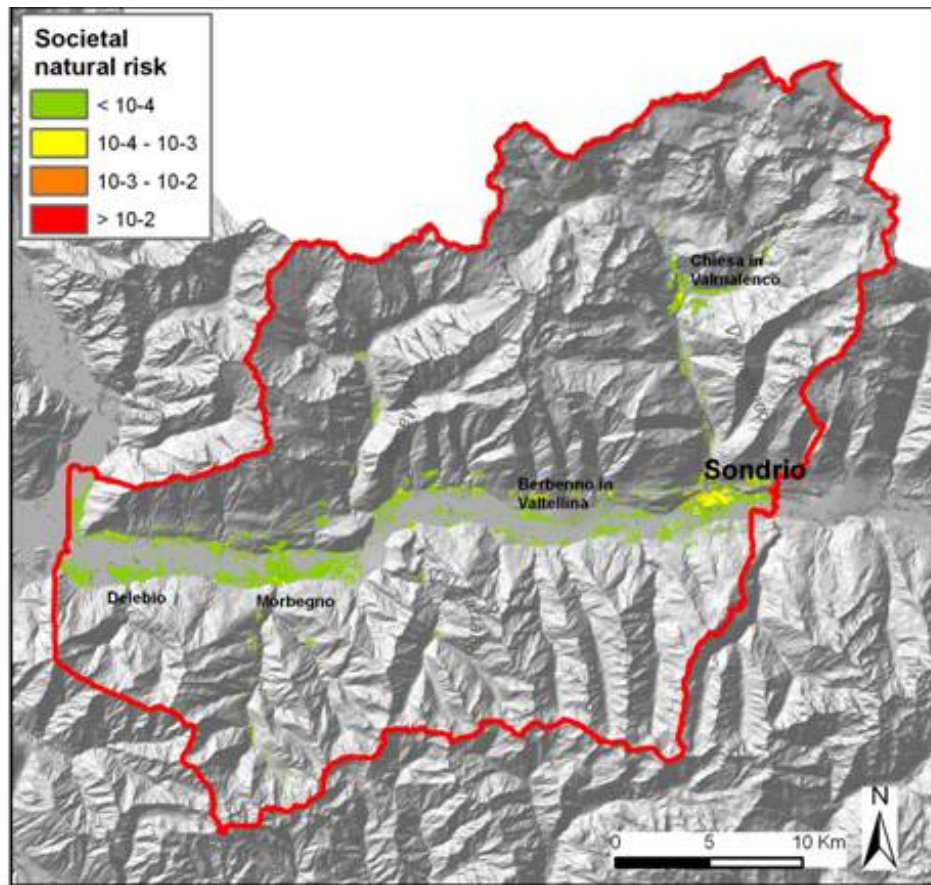


Fig.90. Map of total societal risk for natural hazards, Valtellina. Risk values are expressed in terms of casualties per year.

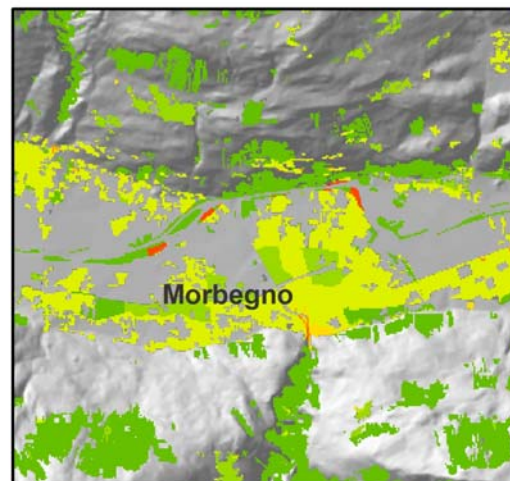
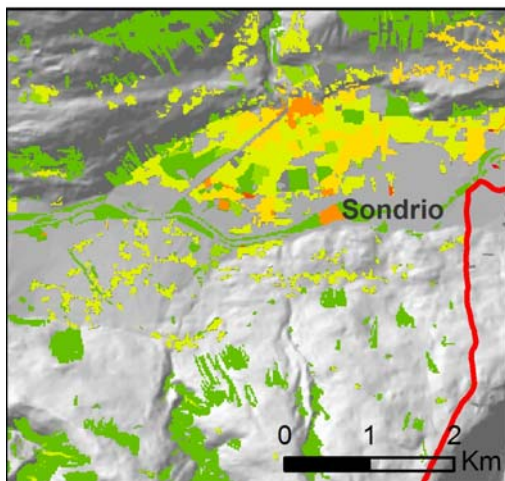
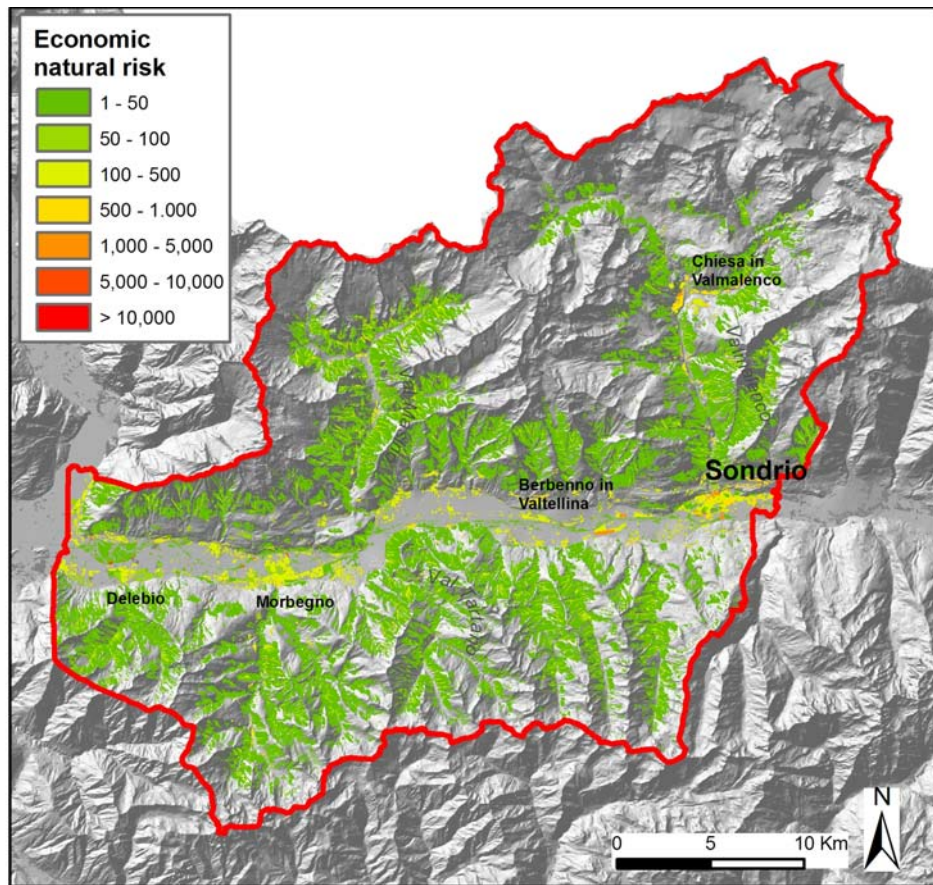


Fig.91. Map of total economic risk for natural hazards, in euros /year, for Valtellina

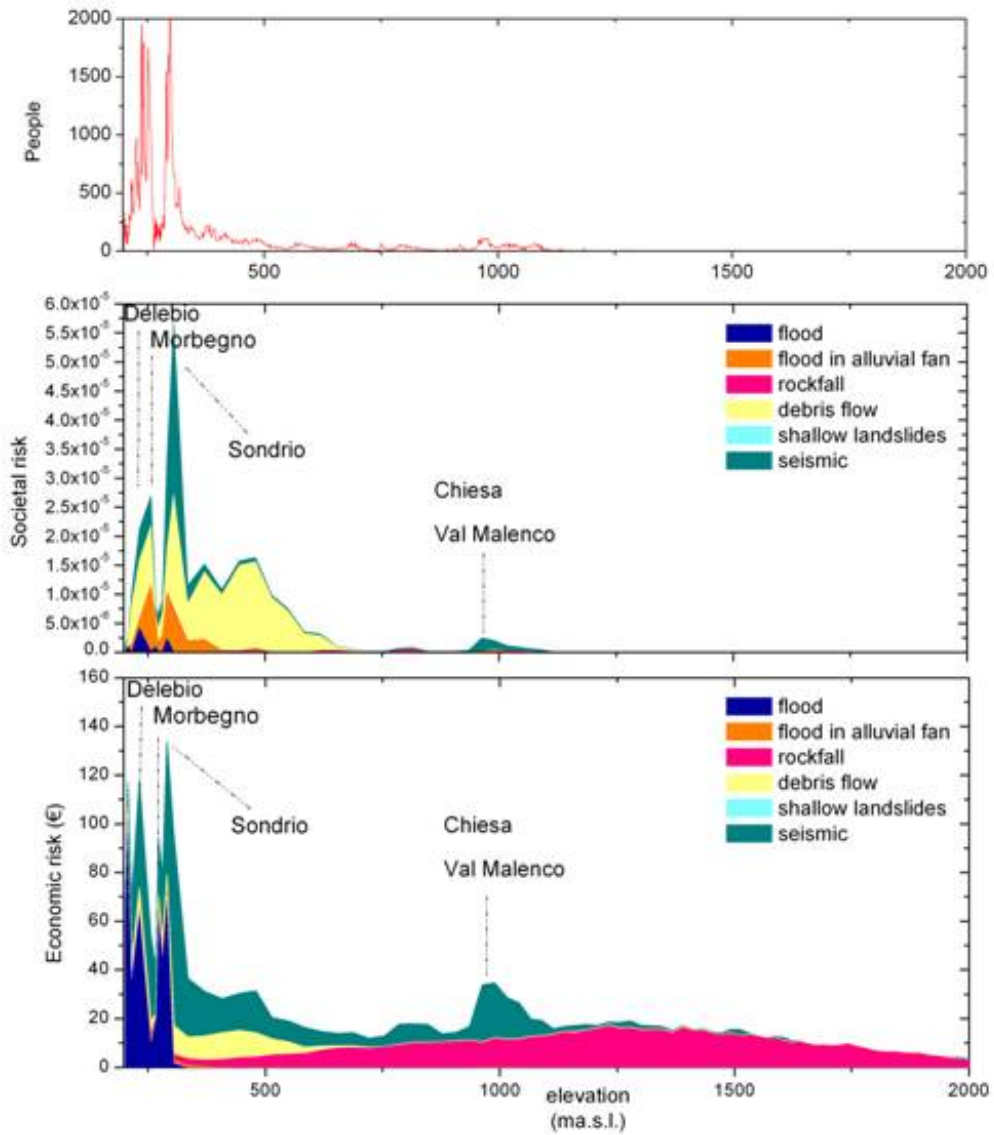


Fig.92. Cumulated values of societal and economic risk for lower Valtellina, compared with population distribution, in relation to elevation.

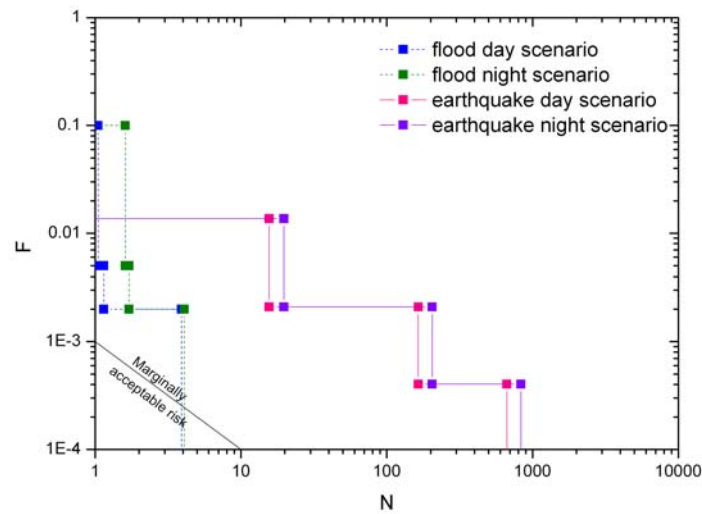


Fig.93. FN curves for flood and earthquake scenarios, compared to Netherland Government Group risk criterion (Versteeg, 1987)

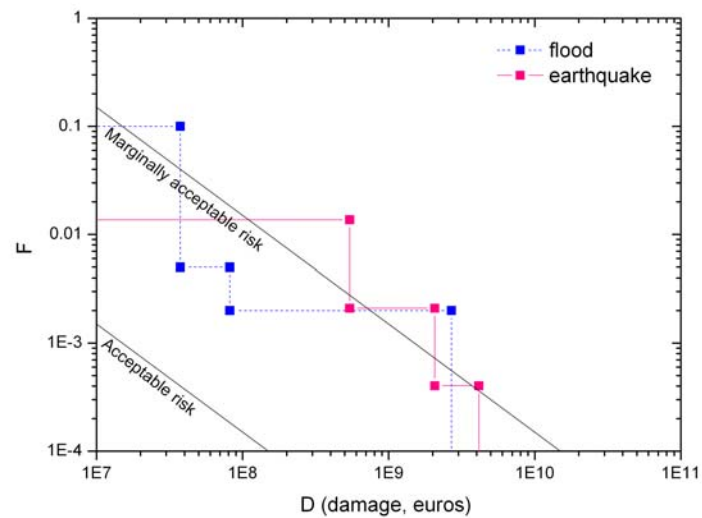


Fig.94. FD curves for flood and earthquake scenarios, compared to Baecher risk criterion (Baecher, 1982b)

Brescia area

Values of societal and economic risk related to natural threats (rockfall, shallow landslide, debris flow, alluvial fan flooding, river flood, earthquake, and wildfire) for the Brescia area are resumed in Tab.63., and shown in Fig 95 and 96.

A scheme of societal and economic risk values in relation to population and elevation is shown in Fig. 97. Most of population is concentrated in the plain zone, or in

the valley bottoms, corresponding to the zone lower than 300 m a.s.l. In this area, the most urbanised one, both societal and economic seismic risk are largely predominant. Floods on alluvial fans, rockfalls and debris flow affect the foots of the slopes, where minor settlements are located. Societal risk deriving from these threats is not negligible. River floods have not a role in societal risk. As said before, they threaten mainly buildings, crops and productive areas, but not significantly human life. Economic risk related to river floods, in fact, is very high.

As said for the area of lower Valtellina, above 700 m a.s.l., societal risk is negligible, due to the scarce human presence. On the contrary, economic risk is not negligible, mostly due to rockfalls impacting woods and roads.

FN and FD curves were calculated, for flood and seismic scenarios (Fig.98 and 99). Also in this case, acceptability criteria proposed by Baecher (1982b) was used to observe economic risk acceptability, where damage economic values were discounted to the present (by means of Consumer Price Index, discounted to 2008).

Economic risk results to be marginally acceptable for the 200 years return time flood scenario, whereas it is not acceptable for the 10 and 500 years return time, according to Baecher (1982b) (Fig.99). Damaged induced by seismic risk are in general not accepted.

Societal risk related to floods and earthquakes never appears to be acceptable in the area of Brescia (Fig.98) if compared to to Netherland Government Group risk criterion (Versteeg, 1987), except for the 200 years return time flood scenario

Tab.63. Total values of societal and economic risk, area of Brescia

	Brescia societal risk	Brescia economic risk
Range	<i>0-0.018</i> cas/year/cell	<i>0-131,423</i> €/year/cell
Total	<i>17.8</i> cas/year	<i>95,227,610</i> €/year

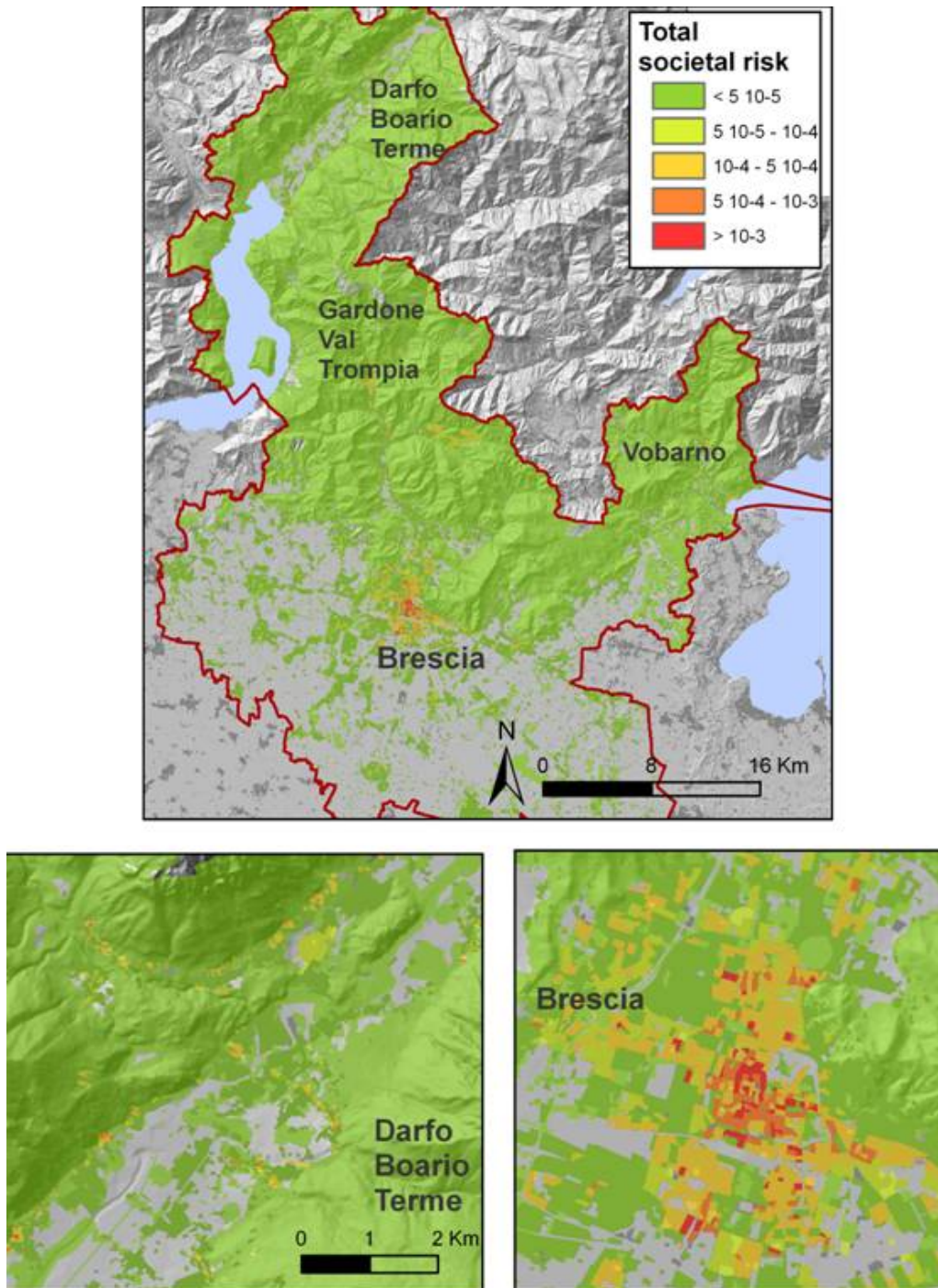


Fig.95. Map of total societal risk for natural hazards, area of Brescia

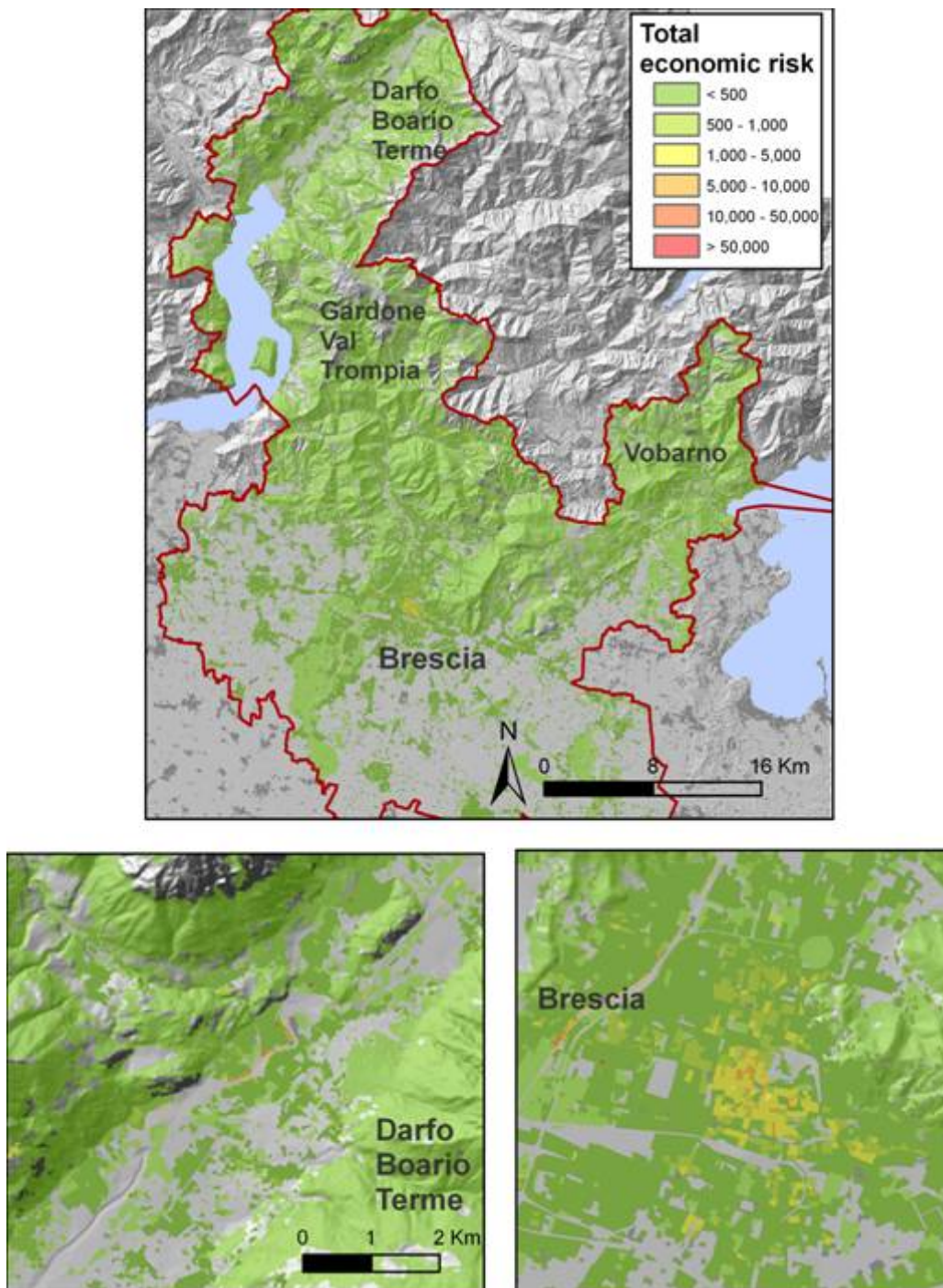


Fig.96. Map of total economic risk for natural hazards, area of Brescia

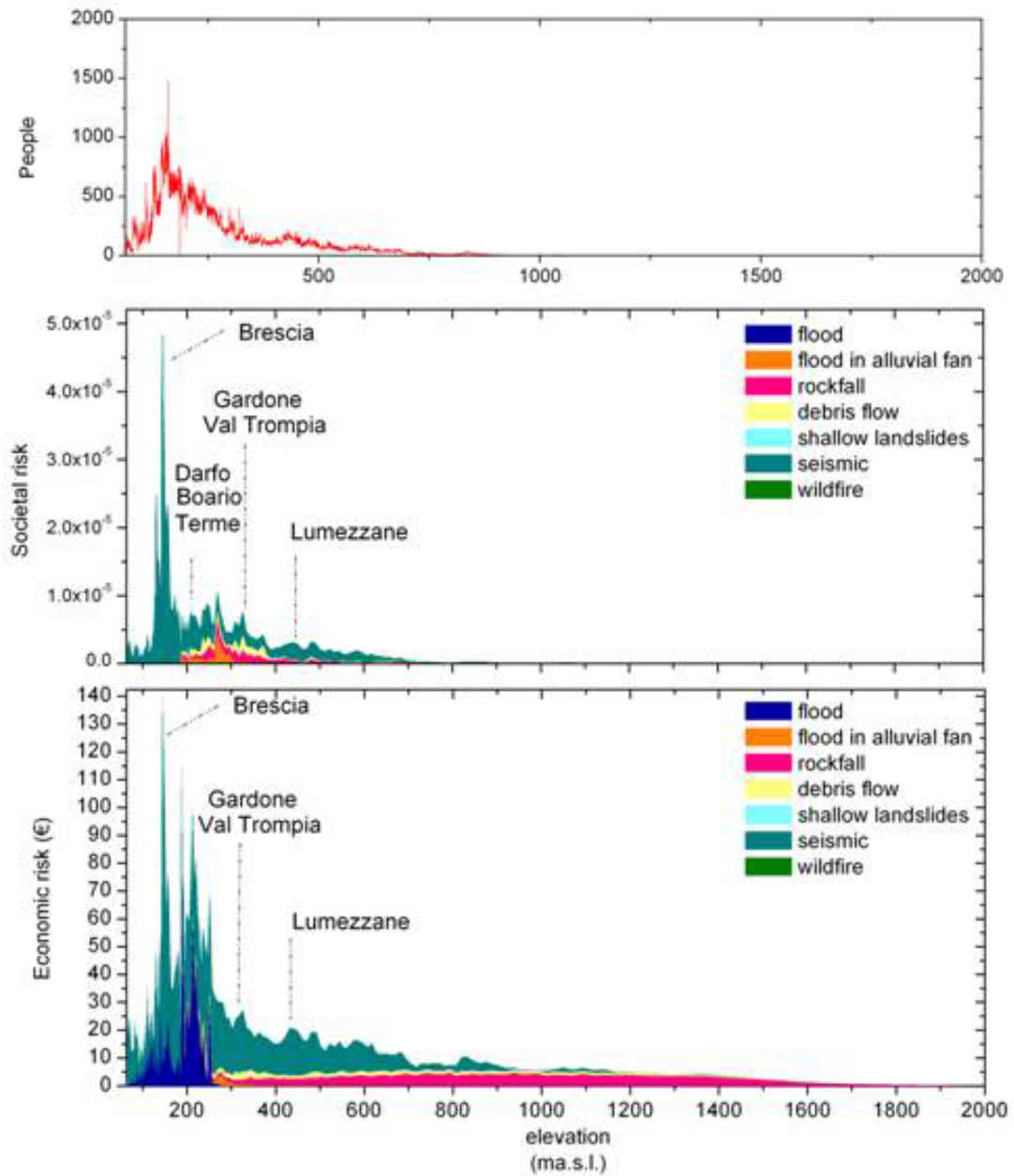


Fig.97. Cumulated values of societal and economic risk for lower Valtellina, compared with population distribution, in relation to elevation.

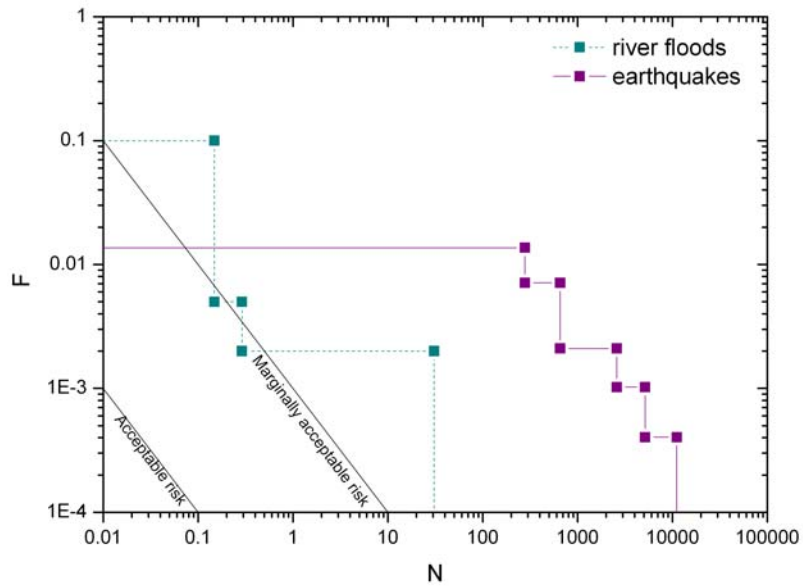


Fig.98. FN curves for flood and earthquake scenarios, compared to Netherland Government Group risk criterion (Versteeg, 1987)

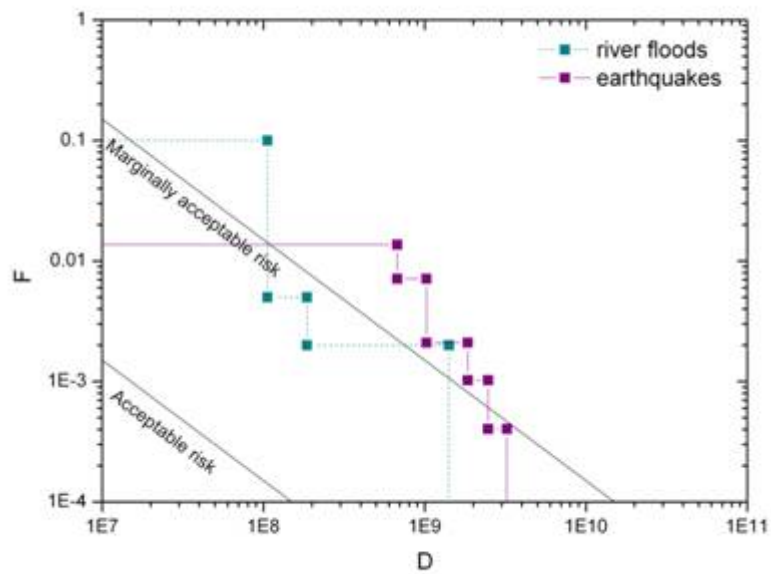


Fig.99. FD curves for flood and earthquake scenarios, compared to Baecher risk criterion (Baecher, 1982b)

7 TECHNOLOGICAL RISK ASSESSMENT

7.1 WORK INJURIES

A risk assessment for work injuries was performed on the area of Valtellina. Only mortal accidents were considered. Frequencies of accident for the whole province of Sondrio, referred to the period 2003-2005, were provided by INAIL (2007). Mortality coefficients were provided by INAIL (2009) and referred to the national context (Tab.64). For the analysis of risk, the number of people working in each of the following sectors, per cell, were considered:

- Workers of activities developed in urban centres
- Hospital workers
- Sport facilities workers
- School workers
- Natural reserves workers
- Workers of productive activities
- Quarry workers

A day and a night scenario were considered. Only hospital and sport facilities workers were considered to be working also during the evening and the night.

Work injuries risk map shows the results in Tab.65.

Tab. 64. Mortality coefficients (INAIL)

Type of work	Mortality coefficients
Quarry workers	0,00042
Productive sector workers	0,00010
Workers of activities developed in urban centres	0,00005
Hospital and sport facilities workers	0,00005

Tab.65. Risk values for typology of activity for day and night scenarios

	Societal risk for day scenario (casualties/year/cell)	Societal risk for night scenario (casualties/year/cell)
Quarry workers	0 - 1,84 10^{-4}	-
Productive sector workers	0 - 2,34 10^{-3}	-
Workers of activities developed in urban centres, hospitals, sport facilities	0 - 3,94 10^{-3}	0 - 5,02 e-004

Adding the expected risk for the day scenario, a value of 0.866 casualties/year is obtained, while for night scenario a value of 0.017 casualties/year. In particular, the values of risk for each type of activity are shown in Tab.66.

Tab.66. Overall risk values for typology of activity for day and night scenarios

	Societal risk for day Scenario (casualties/year)	Societal risk for night Scenario (casualties/year)
Quarry workers	<i>0.0874</i>	-
Productive sector workers	<i>0.506</i>	-
Workers of activities developed in urban centres, hospitals, sport facilities	<i>0.301</i>	<i>0.0175</i>

The zones where work injuries risk is higher are the northern part of Sondrio and the productive area located between Delebio and Morbegno, where the highest concentration of activities and workers are located (Fig.100 and 101).

Tab .67 Overall risk values for typology of activity for day and night scenarios

	Valtellina day scen	Valtellina night scen
Range (cas/year/cell)	<i>0-0.0039</i>	<i>0-0.0005</i>
Total (cas/year)	<i>0.8657</i>	<i>0.175</i>

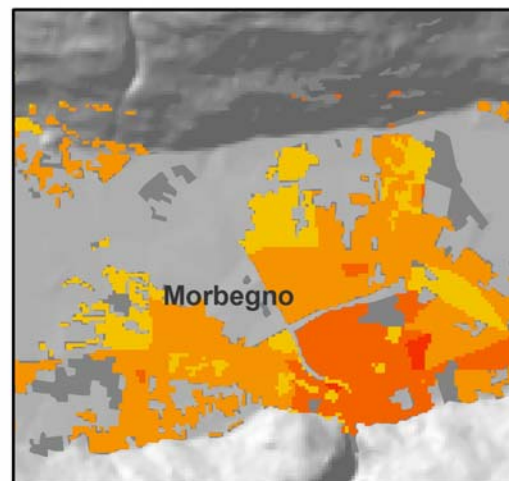
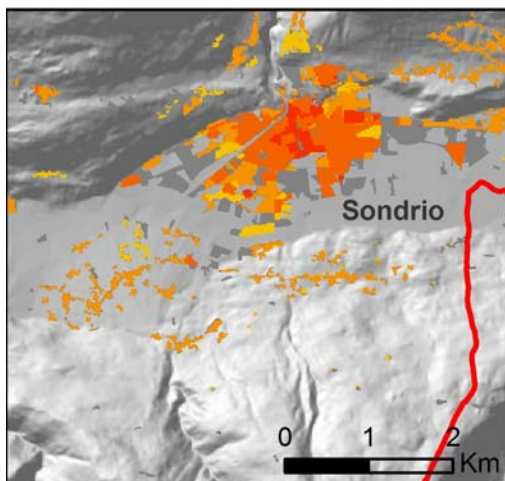
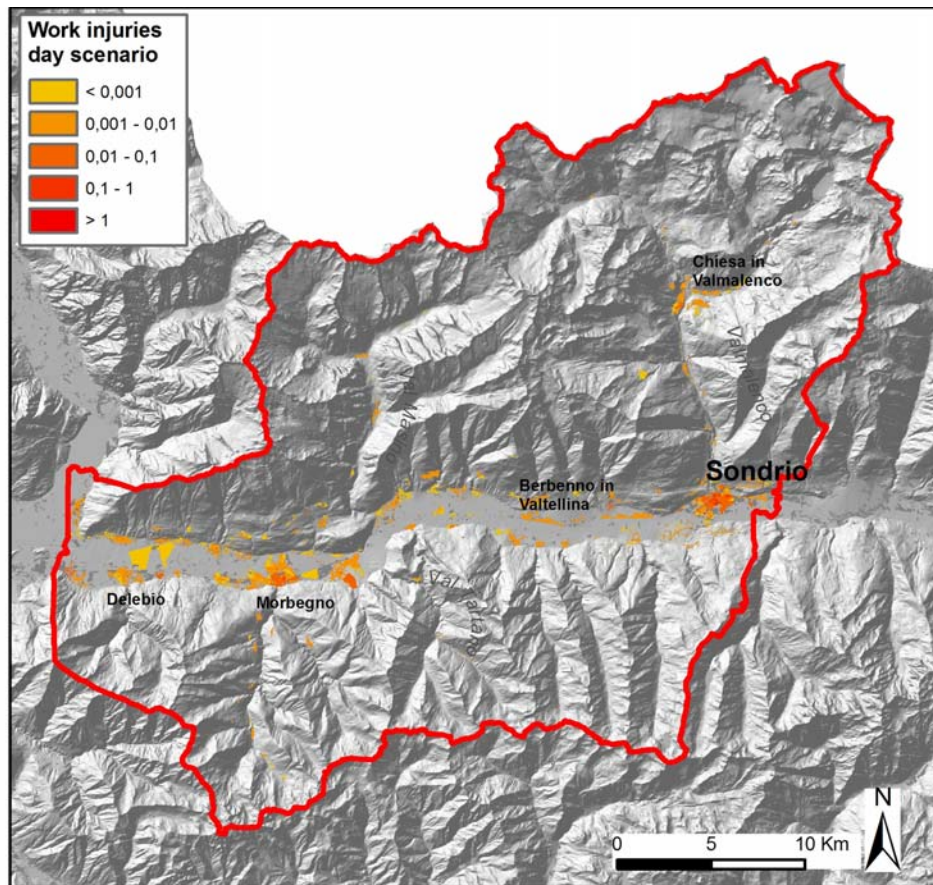


Fig.100. Map of societal physical risk for work injuries, day scenario. Risk values are expressed in terms of casualties per year.

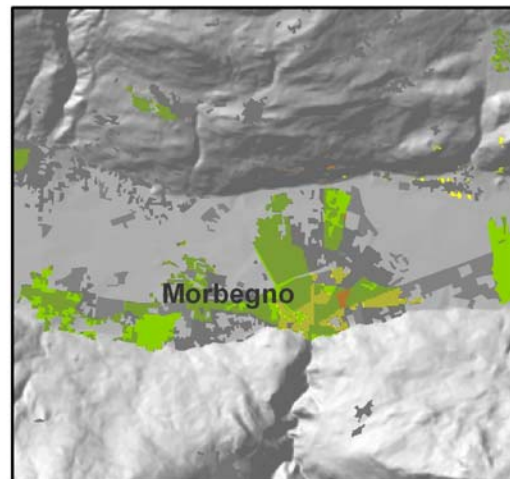
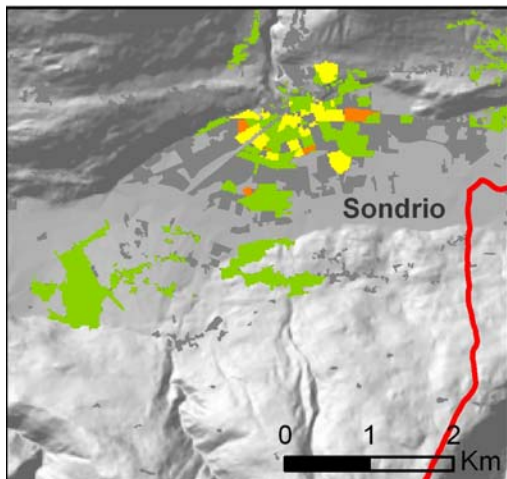
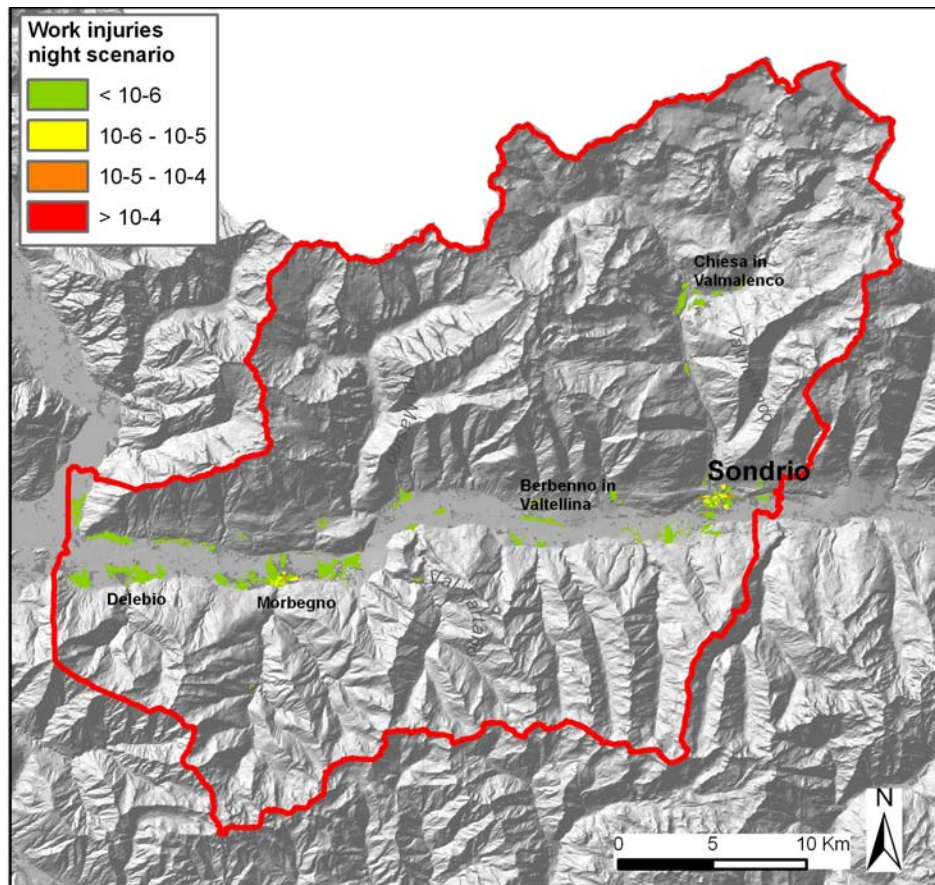


Fig.101. Map of societal physical risk for work injuries, night scenario. Risk values are expressed in terms of casualties per year.

7.2 ROAD ACCIDENT RISK

To assess road accidents risk, a classification of roads according to different typologies was performed (TELEATLAS, 2007):

- State streets
- Provincial streets
- Municipal street

Risk related to road accidents was calculated for each of the three typologies of streets (Fig.102), and then summed.

Data related to the mean annual number of casualties and injuries was provided for provincial and municipal streets by TELEATLAS (2007) and, for state streets, by ACI (2007), for the period 2000-2007.

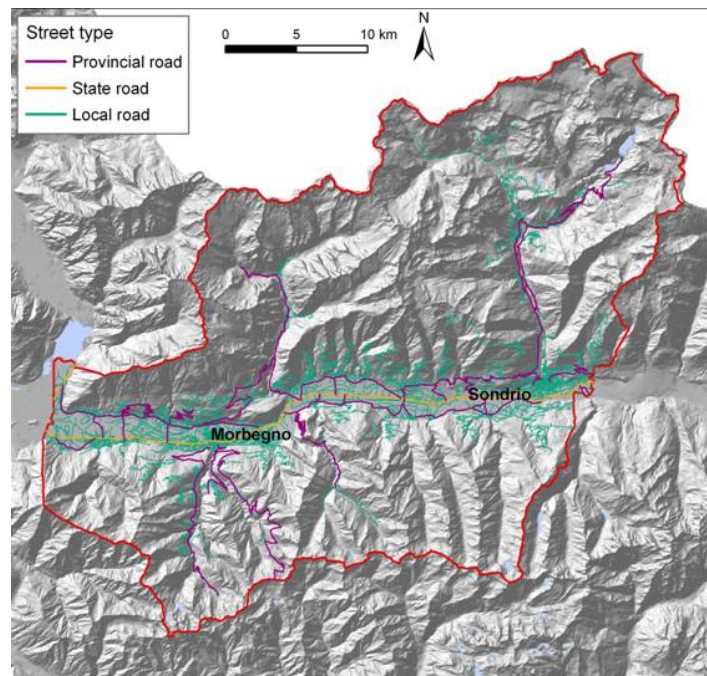


Fig.102. Road typologies for the study area

7.2.1 EXPECTED FREQUENCY OF OCCURRENCE, W_{RA}

For each km of the road network, the number of casualties and injured people due to road accidents were collected (ACI,2007). A value of w_{RA} for casualties and a value of w_{RA} for injuries were calculated as the frequency of accidents per year.

7.2.2 SOCIETAL RISK ASSESSMENT

Gravity factor, g_{RA}

As explained in Section 5.1.2, two values of g_{RA} were used in the analysis (Tab.68). All injuries were assimilated to heavy injuries, according to a conservative approach.

Tab.68. Values of gravity factor g for damage state (Buldrini, 2009).

Scenario	g_{RA}
Casualties	1
Injuries	0,25

Exposure factor, e_{RA}

For road accident risk, e_{RA} was supposed to be 1, being the casualties and injuries always the same people involved in the accidents.

Societal risk assessment

The map of road accident societal risk shows values ranging from 0 to 0,003 casualties/year/cell for municipal streets, values ranging from 0 to 0,24 casualties/year/cell for provincial streets and 0 to 0,0976 casualties/year/cell for state streets. Results are shown in Tab.69.

Tab.69. Risk values for typology of road

	Societal risk range (casualties/year/cell)	Societal risk (casualties/year)
State streets	0 – 0.0976	89.9
Provincial streets	0 – 0.24	214.5
Municipal streets	0 – 0.003	10,9

Tab.70. Risk values for day and night scenarios

	Valtellina day scen	Valtellina night scen
Range (cas/year/cell)	0-0.13	0-0.18
Total (cas/year)	183.25	256.55

Expected number of casualties include here also injured people, considered as $\frac{1}{4}$ of a casualty (1 injury = 0.25 casualties).

Streets affected by the highest number of casualties are the ones around the municipality of Sondrio and Morbegno, the most populated zones. Provincial street 15 in Valmalenco shows a high number of accidents, such as the state street 38 in the proximities of Sondrio and Morbegno (Fig.103).

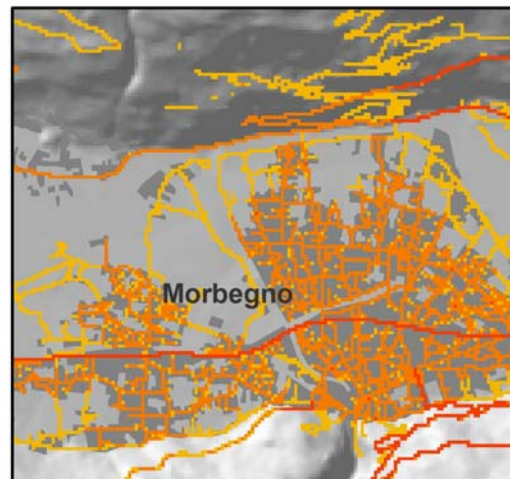
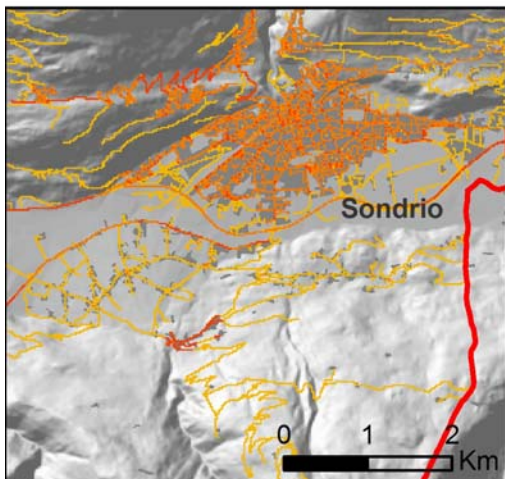
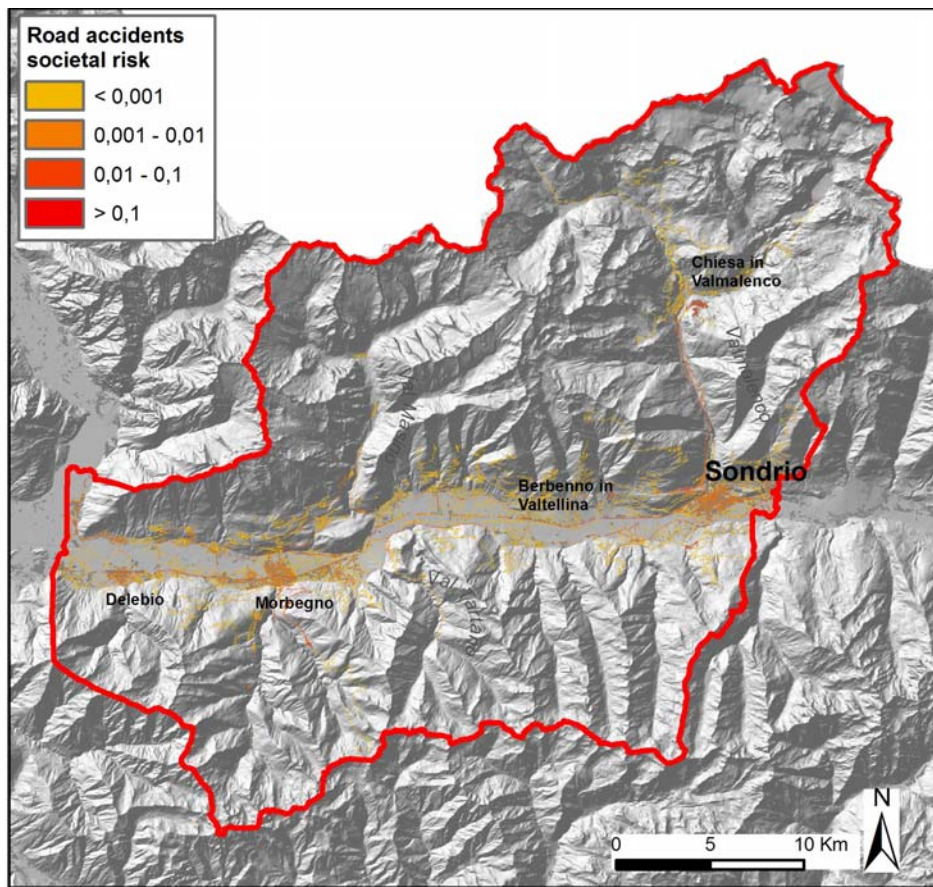


Fig.103. Map of societal physical risk for road accidents. Risk values are expressed in terms of casualties per year.

7.3 TRANSPORT OF HAZARDOUS MATERIALS

Risk related to transport of hazardous materials was assessed for roads and railways detected as potentially hazardous by CRASL (2008).

For each transport line, the scenarios concerned accidents deriving from transport of two classes of dangerous materials, defined according to ADR, (Accord européen relatif au transport international des marchandises Dangereuses par Route):

- class ADR 2 (compressed, liquefied or melted in pressure gas)
- class ADR 3 (liquid inflammable materials)

For each class, some materials of reference were assumed, as in Tab.71.

Tab.71. Materials assumed as reference for risk assessment

	ADR 2	ADR 3
Railway	Chlorine	Petrol
	Ammonia	
	GPL	
Street	Ammonia	Petrol
	GPL	

No hazardous materials were found to be transported in the area by means of railway.

7.3.1 IMPACT AREA, A_{IMP}

The potential areas of impact were calculated with respect to the materials taken as reference for the classes ADR 2 and 3 as:

$$A_{imp} = \pi \times r_i^2 \quad (39)$$

where r_i is the distance related to the high mortality threshold (PEE zone, DM 25/02/2005) for the scenario of each material (Buldrini, 2009) (Tab.72).

Tab.72. Characteristics of reference materials

Class	Material	Accident scenario	r_i (m)
ADR 2	Ammonia	Toxic release	677
	GPL	Flash fire	125
ADR 3	Petrol	Fire	44

7.3.2 EXPECTED FREQUENCY OF OCCURRENCE, W_{HM}

The expected frequency of occurrence was calculated for the three reference materials as follows (CRASL, 2008):

ADR 2 (NH3): $w = L^c \text{ [km]} \times N_{inc} \text{ [acc/year]} \times 1/TMA \text{ [vehic./year]} \times TMA_{NH3} \text{ [vehicle NH3/year]} \times 1/L \text{ [km]} \times 0,035$

ADR 2 (GPL): $w = L^c \text{ [km]} \times N_{inc} \text{ [acc/year]} \times 1/TMA \text{ [vehic./year]} \times TMA_{GPL} \text{ [vehicle GPL/year]} \times 1/L \text{ [km]} \times 0,035 \times 0,03$

ADR 3 (Petrol): $w = L^c \text{ [km]} \times N_{inc} \text{ [acc/year]} \times 1/TMA \text{ [vehic./year]} \times TMA_{benz} \text{ [vehicle petr/year]} \times 1/L \text{ [km]} \times 0,035 \times 2,5E-2$

where:

- $L^c \text{ [km]}$ = length of the i stretch of road belonging to the cell
- $N_{inc} \text{ [acc/year]}$ = number of accidents per year in the i stretch of road
- $TMA \text{ [vehic./year]}$ = mean annual traffic on the i stretch of road
- $TMA_{sost} \text{ [vehicle material/year]}$ = mean annual traffic of vehicles carrying an hazardous material on the i stretch of road
- $L \text{ [km]}$ = length of the i stretch of road

While numeric values correspond to:

- 0,035 is the probability of having a hole of 5 cm of diameter in the transport tank (Egidi, 1995, ARIPAR project)
- 0,03 is the probability of having a flash fire after transport tank breaking (Egidi, 1995, ARIPAR project)
- $2,5 \cdot 10^{-2}$ is the probability of having a fire after transport tank breaking (Egidi, 1995, ARIPAR project)

For each linear meter of street, w_{HM} was calculated.

Impact frequency for each cell was calculated, given its proximity to one or more stretches of road of various length. To do this, a density analysis was performed: each cell was considered as the centre of a circle having for radius the mortality threshold of the considered material (Tab.71). For each cell, the total length of the stretch of road within the circle was calculated (Fig.104).

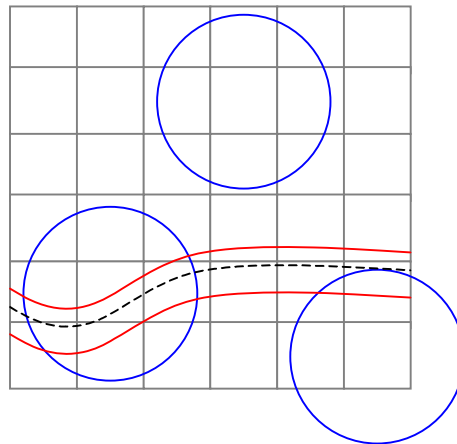


Fig.104. Scheme of the method for the calculation of the frequency of occurrence w .

7.3.3 SOCIETAL RISK ASSESSMENT

Gravity factor, g_{HM}

Gravity factor g was calculated referring to PEE zones (Piani di Emergenza Esterni), as defined by DM 25/02/2005:

- Zone 1 "of certain impact": (threshold high mortality) immediately adjacent to the road, characterised by effects causing a high mortality for people.
- Zone 2 "of damage": (threshold of irreversible lesions) external to the first, characterised by potential damages, also heavy and irreversible, for people not assuming the correct protection measures and by potential damages also lethal for vulnerable people as children and old people.
- Zone 3 "of attention": (threshold of reversible lesions) characterised by possible damages, in general not heavy also for vulnerable people

For the calculation of g , only zone 1 was taken into account, that is the zone where lethality ranges from 100% (source of release) to 50% detecting in this way a circular zone around the source. Factor g was evaluated for the three scenarios detecting, for each of them, the probability for a man to undergo a lethal damage.

A precautionary value of 0,90 for ammonia release was used (Buldrini, 2009). It is to be said that from the performed simulations, variations in the input data as quantity of released material and environmental conditions produce variations on the damage distances which are among them proportional. This means that these parameters do not influence strongly the gravity index g_{HM} .

For petrol release a precautionary value of $g_{HM} = 0,89$ was used (Buldrini, 2009).

For flash fire, due to the instantaneity of the phenomenon, lethal effects are assumed to be present only in the area of the flames, also accounting for its unhomogeneity. g_{HM} was assumed to be 1.

Exposure factor, e_{HM}

Due to the different geometry of the impacted areas, according to the scenario, some distinctions have to be done.

In case of toxic release generating a toxic cloud, it is reasonable to consider that the areas of damage are localised according to wind direction, approximated here with angular sectors of 45° : a factor $e_{HM} = 45/360 = 0.125$ was considered. Impacted people includes only people in the open air, or in a non protected place, assumed to the 25% of the residents. e results to be

$$e_{HM_{tox}} = 0,125 \times 0,25 = 0,03125.$$

In case of fire, the area impacted by thermic irradiation can be represented as a circle of influence around the source. Also in this case, impacted people includes only people in the open air, or in a non protected place, assumed to the 25% of the residents. e results to be

$$e_{HM_{fire}} = 0,25$$

In case of flash fire, the impacted area corresponds to the whole surface within the radius of total damage. Due to the instantaneity of the event, there is no reason to think that people have the time to get out of the zone. People inside buildings is also in this case protected.

$$e_{HM_{ff}} = 0,25$$

Societal risk assessment

Results of expected casualties per year due to transport accidents are shown in Tab 73 and 74.

Tab.73. Risk values for the different typologies of hazardous materials for the day and the night scenarios

	Risk for day scenario (casualties/year/cell)	Risk for night scenario (casualties/year/cell)
Ammonia	0 - 2,70 e-11	0 - 8,27 e-11
Petrol	0 - 1,20 e-09	0 - 3,68 e-09
GPL	0 - 9,35 e-11	0 - 2,86 e-10

Tab.74. Overall risk values for the different typologies of hazardous materials for the day and the night scenarios

	Risk for day scenario (casualties/year)	Risk for night scenario (casualties/year)
Ammonia	2,47 10^{-8}	3,71 10^{-8}
Petrol	3,57 10^{-8}	6,25 10^{-8}
GPL	9,96 10^{-9}	1,33 10^{-8}

The areas more exposed to this threat are the same affected by the highest number of road accidents: the area of Sondrio and the zone between Delebio and Morbegno.

Tab.75. Risk values

	Valtellina day scen	Valtellina night scen
Range (cas/year/cell)	$0 - 10^{-9}$	$0 - 4 \cdot 10^{-9}$
Total (cas/year)	$5.5 \cdot 10^{-8}$	$8.8 \cdot 10^{-8}$

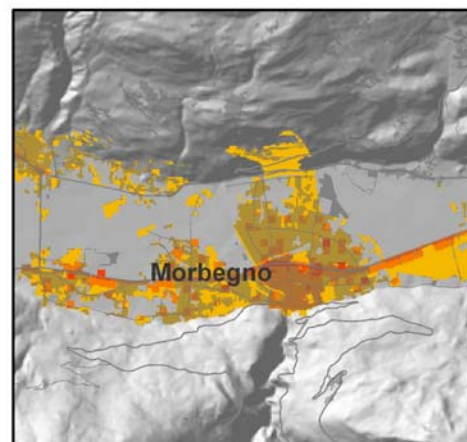
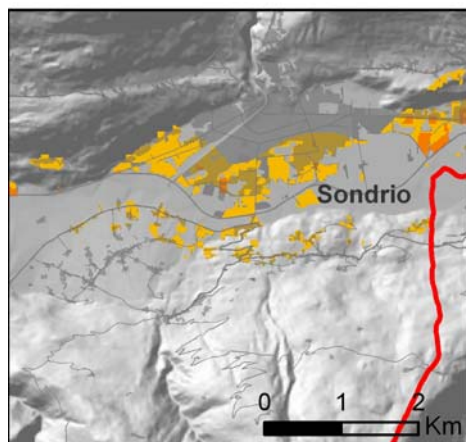
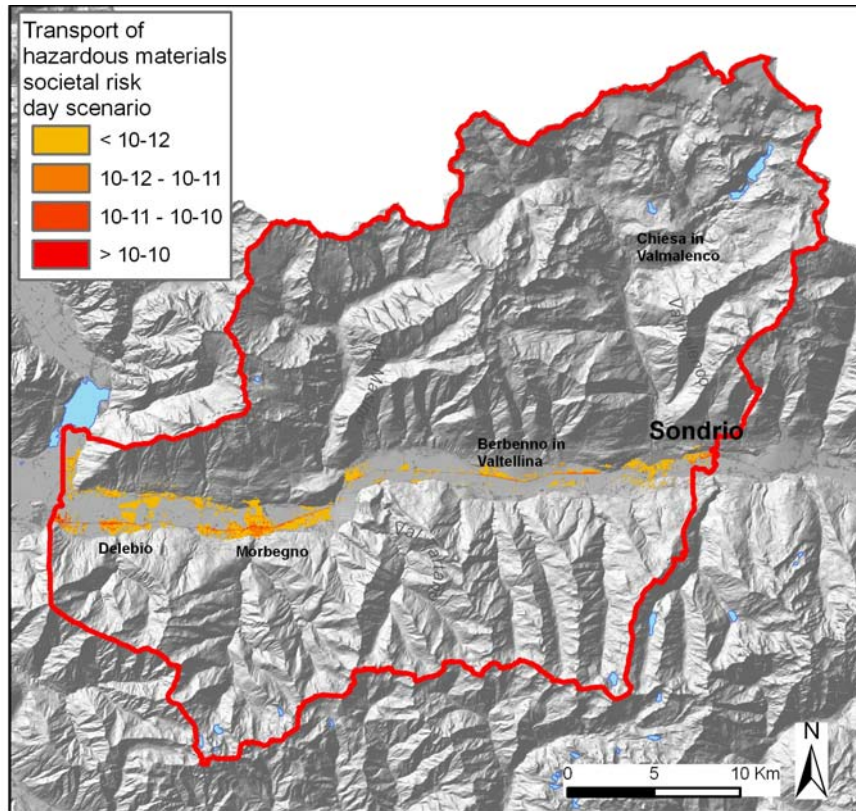


Fig. 105. Fig Map of societal physical risk for transport of hazardous materials, day scenario. Risk values are expressed in terms of casualties per year.

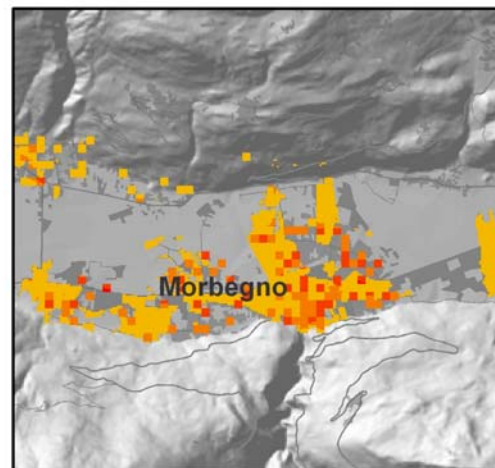
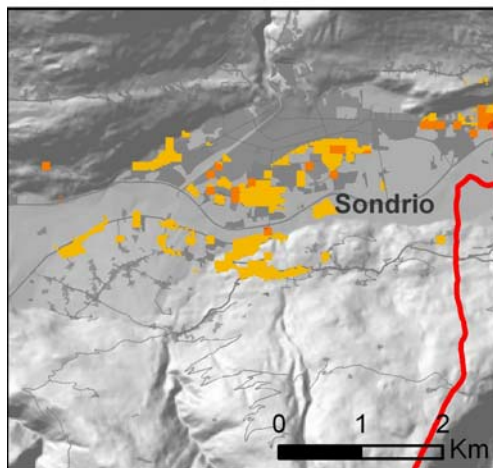
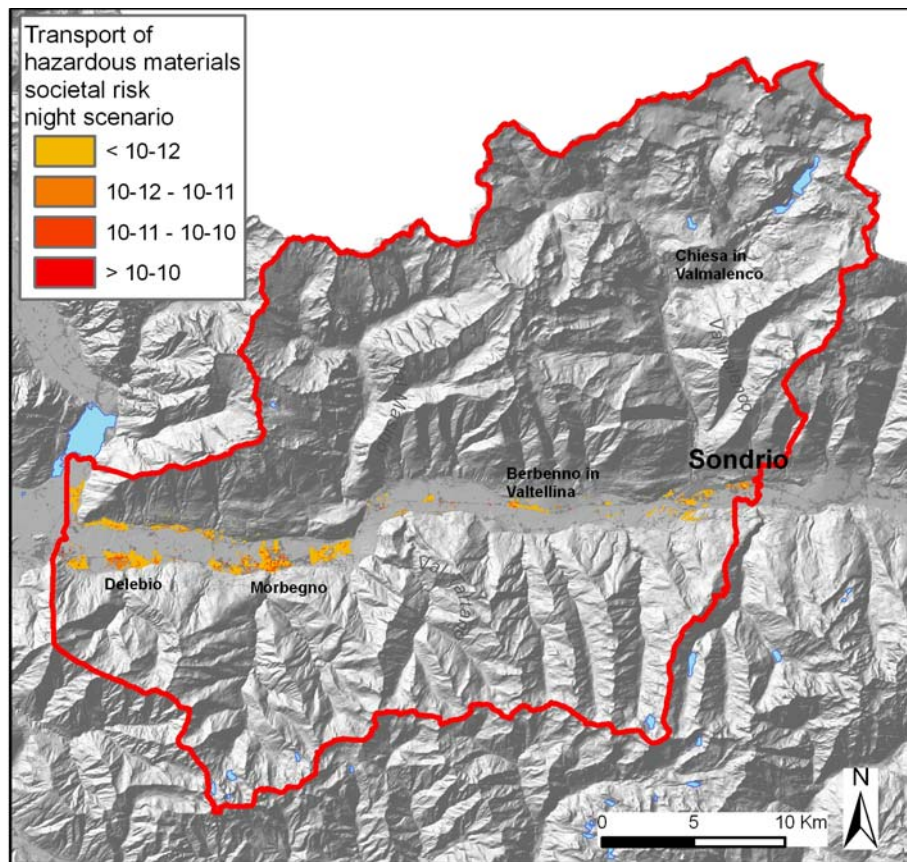


Fig.106. Map of societal physical risk for transport of hazardous materials, night scenario. Risk values are expressed in terms of casualties per year.

7.4 INDUSTRIAL RISK

Major risk plans, as defined by Direttiva Seveso (D.LGS 238/2005), are not present in the study area. Industrial risk analysis are referred to minor plants. Data related to industrial accidents were provided by statistical Italian yearbook of industry (ISTAT, 2001), by statistical yearbook of firemen (Ministero dell'Interno, 2008) containing the number of interventions per typology of plant, and the database of filling stations (Bordonaro, 2009).

Two categories of industries were distinguished, according to the different accident scenarios they can be interested by :

- plants involving inflammable liquids
- plants involving inflammable and combustible gas

In this analysis, scenarios involving only areas within the plant perimeter are not considered. These scenarios are included in work injuries, involving only plant workers.

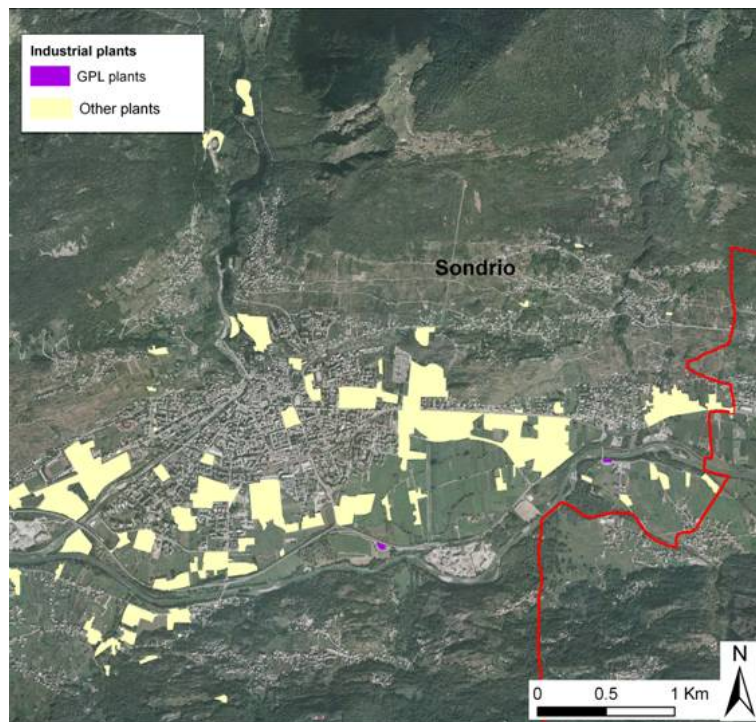


Fig.107. Industrial area in proximity of Sondrio

7.4.1 IMPACT AREA, A_{IMP}

For each industry typology, a reference material, a reference typology of accident scenario and three possible impact areas were defined (Buldrini, 2009) (Tab.76). As source point of the release, the centroid of the plant was considered, being unknown the exact localisation of the tanks or of the systems subject to failure (Fig.108).

Tab.76. Materials of reference, accident scenario of reference for the two typologies of plant

Typology	Material	Scenario	Zone 1 [m]	Zone 2 [m]	Zone 3 [m]
plants involving inflammable liquids	<i>Petrol</i>	<i>Fire</i>	20	30	35
plants involving inflammable, combustible gas	<i>GPL</i>	<i>Flash Fire</i>	70	115	-

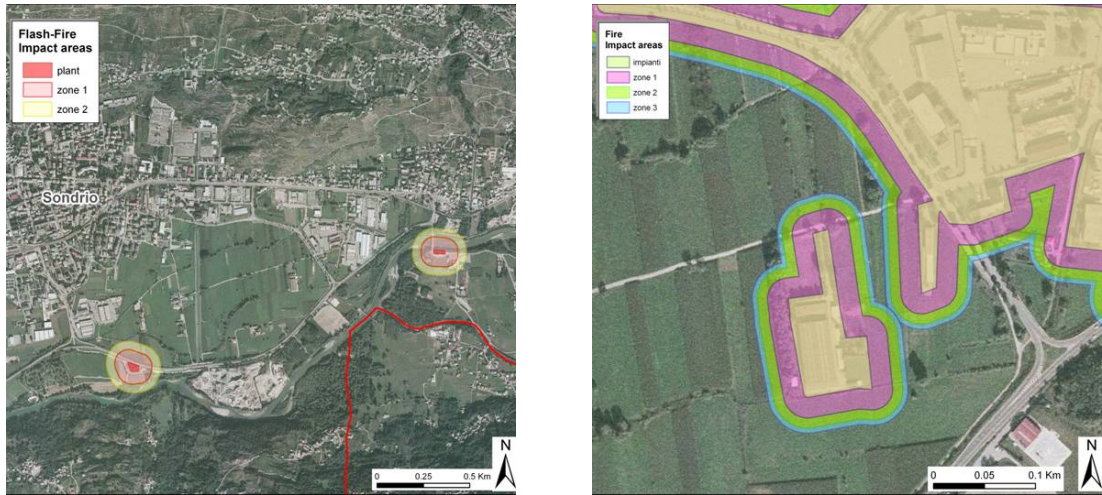


Fig108. Areas of impact for the two typologies of plants

7.4.2 EXPECTED FREQUENCY OF OCCURRENCE, w_I

The value of w_I was calculated for the two typologies of plants and for the different scenarios.

1. Plants involving inflammable liquids

Two different methodological approaches were compared, one based on the number of fires occurred at the provincial level, and the other based on the areal distribution of the productive areas detected in the land use map of DUSAF (DUSAF, 2007).

1°APPROACH:

The number of fires occurred each year between 2002 and 2007 were considered (Ministero dell'Interno, 2008) (Tab.77).

Tab.77. Firemen intervention for fires in the province of Sondrio, 2002 to 2007.

	N fires per year
2002	1127
2003	912
2004	767
2005	851
2006	568
2007	579

The annual mean number for the province of Sondrio was calculated in 800,66 fires/year, but considering that the study area covers almost half of the area of the whole province, the mean annual number for the study area lowers to 400,33 fires/year. Causes of fires were analysed at the national level (Tab.78).

Tab.78. National statistics of the number of fires triggered by different causes (Ministero dell'Interno, 2008)

Cause	n. fires
Auto combustion	1057
Chimney	8316
Electric causes	12531
Detonations	159
Sparks	4467
Lightning	326
Fireworks	373
Heating plants	359
Cigarette	7973
Chemical reactions	69
Backfire	279
Overheating of engines or similar	1431
Other	23044
Tot	60384

Among these, only the ones which could potentially trigger a fire in a plant were considered: detonations, chemical reactions, backfires, and overheating, for a total of 1938 fires. The percentage of fires due to these causes is 3,20946 %. This means, on the study area, $3,20946 (\%) * 400,33 = 12,848$ events/year.

2° APPROACH

The map of productive areas provided by DUSAF (DUSAF, 2007) was used to assess the value of w_l . The productive sector covers in the area 7,5482 km², which means a plant density of 80 plants/km². According to these calculations, in the productive sector almost 603 plants are located.

The interventions of firemen on the whole national territory for the years 2005 to 2007 were evaluated (Ministero dell'Interno, 2008) (Tab.79).

Tab.79. Firemen intervention for fires in Italy, 2002 to 2007.

PLACE	n° interventions		
	2005	2006	2007
Radioactive plants	20	17	21
Chemical plants	175	205	245
Electric energy plants	572	535	512
Rubber and plastic plants	369	453	531
Inflammable and explosive plants	59	162	140
Various productions	2284	2394	2666
Generic deposits	1271	1075	1114
Deposits of solid materials	2223	1818	1573
Deposits of inflammable materials	287	286	202
Deposits of plastic materials	455	315	242
Plants and deposits of combustibles	1347	1127	974
TOTAL events	9062	8387	8220
SUM events	25669		

The number of mean national events per year is

$25669 \text{ interventions} / 3 \text{ years} = 8556,33 \text{ interventions/year}$

The annual frequency for single plant was obtained referring to the number of plants of each category (Statistical Italian yearbook of industry ISTAT, 2001). The number of events per plant per year at the national level was calculated as

$(8556,33 \text{ events/year}) / \text{plants} = 0,0183 \text{ events/plant/year}$

Which means, for the study area

$603 \text{ plants} * 0,0183 \text{ events/plant/year} = 11,05 \text{ events/year}$

Comparing the results obtained by means of the two approaches, we notice that final values are quite similar. The value of w obtained by the second approach was chosen.

The number of events per cell was calculated as

$11,05 \text{ events/year} / 7,5482 \text{ km}^2 / 2500 \text{ (cell/km}^2) = 0,0005856 \text{ events/year/cell}$

The value of the expected frequency of occurrence, w , for plants using inflammable liquid is 0,0005856.

2. Plants involving inflammable, combustible gas

The national data of events/plant/year obtained by means of the second approach described above was used: $w = 0,0183$.

The expected frequencies of occurrence were normalised for time period for day and night scenarios, having a different length (10 and 14 hours, respectively).

7.4.3 SOCIETAL RISK ASSESSMENT

Gravity factor, g_I

As described for transportation of hazardous materials, the value of g was calculated referring to PEE zones, as defined by DM 25/02/2005.

The three zones of impact were considered for plants involving inflammable liquids, only the first two zones for plants involving inflammable, or combustible gas.

Factor g_I was evaluated for the reference scenarios for the two typologies of plants:

- fire, for plants involving inflammable liquids
- flash fire, for plants involving inflammable, or combustible gas.

Calculating, for both, the probability for people of undergo a lethal damage.

As a reference scenario for the first typology, a release of petrol was considered, and successive development of fire. Precautionary values of g were considered for the three zones (Tab.81)(Buldrini, 2009):

Tab.80. Gravity factor, g_I , for the three zones for plants involving inflammable liquids

	Zone 1	Zone 2	Zone 3
g	0,89	0,38	0,014

For flash fire, as said for transportation risk, the probability of dying in the first zone is considered equal to 1, to 0.63 for the second zone (Buldrini, 2009) (Tab.81).

Tab.81. Gravity factor, g_I , for the two zones for plants involving inflammable, or combustible gas.

	Zone 1	Zone 2
g	1	0,63

Exposure factor, e_I

In case of fire, if the effects do not include the formation of toxic clouds, the area affected by thermal irradiation is the whole circle having its centre in correspondence of the plant. The effective part of the population damaged by the accident is the one located in the open air or in non protected places, assumed to be, as for transportation risk, the 25% of the whole population. Hence, $e_{I_{fire}} = 0,25$.

IN case of flash fire, the impacted area includes a circle having the radius equal to the absolute distance of damage. Due to the instantaneity of the event, there is no reason to think that people have the time to get out of the zone. People inside buildings is, also in this case, protected: $e_{I_{ff}} = 0,25$.

Societal physical risk

Values of societal industrial risk for the different scenario are shown in Tab.82 and 83, and summarised in Tab. 84. Risk is very localised, but in some areas in the proximities of the plants, it can reach quite significant values. On the overall area, risk is however quite low.

Tab.82. Risk values for typology of plant and for zone, for day and night scenarios

Plant typology		Risk for day scenario (casualties/year/cell)	Risk for night scenario (casualties/year/cell)
plants involving inflammable liquids	Zone 1	$0 - 1,03 \cdot 10^{-2}$	$0 - 2,10 \cdot 10^{-3}$
	Zone 2	$0 - 3,02 \cdot 10^{-4}$	$0 - 8,77 \cdot 10^{-4}$
	Zone 3	$0 - 1,04 \cdot 10^{-5}$	$0 - 3,95 \cdot 10^{-5}$
plants involving inflammable, combustible gas	Zone 1	$0 - 4,49 \cdot 10^{-3}$	0
	Zone 2	$0 - 1,18 \cdot 10^{-3}$	0

Tab.83. Overall risk values for typology of plant and for zone, for day and night scenarios

Plant typology		Risk for day scenario (casualties/year)	Risk for night scenario (casualties/year)
plants involving inflammable liquids	Zone 1	$2,36 \cdot 10^{-1}$	$4,03 \cdot 10^{-1}$
	Zone 2	$2,22 \cdot 10^{-2}$	$4,45 \cdot 10^{-2}$
	Zone 3	$4,42 \cdot 10^{-4}$	$1,02 \cdot 10^{-3}$
plants involving inflammable, combustible gas	Zone 1	$1,83 \cdot 10^{-1}$	0
	Zone 2	$5,28 \cdot 10^{-1}$	0

Tab.84. Risk values for day and night scenarios

	Valtellina day scen	Valtellina night scen
Range (cas/year/cell)	0-0.01	0-0.0021
Total (cas/year)	0.48	0.445

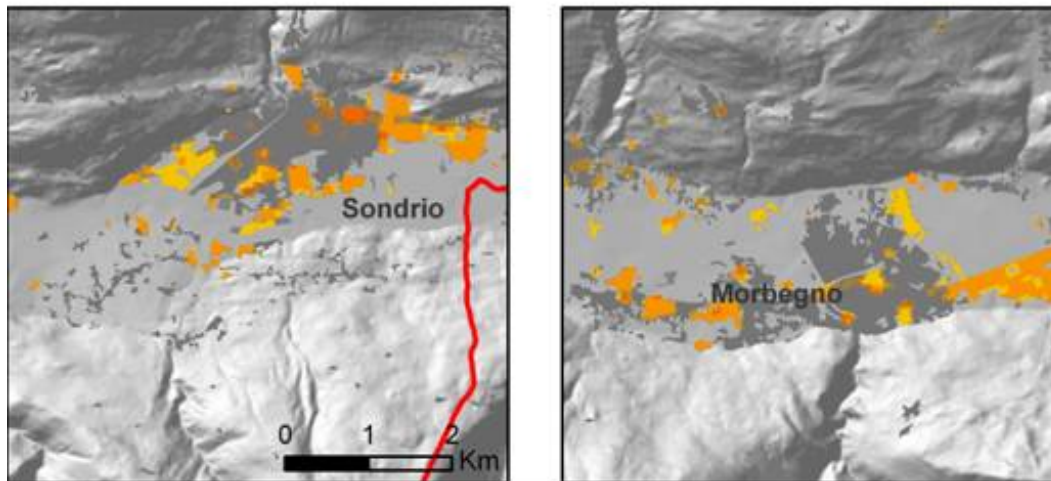
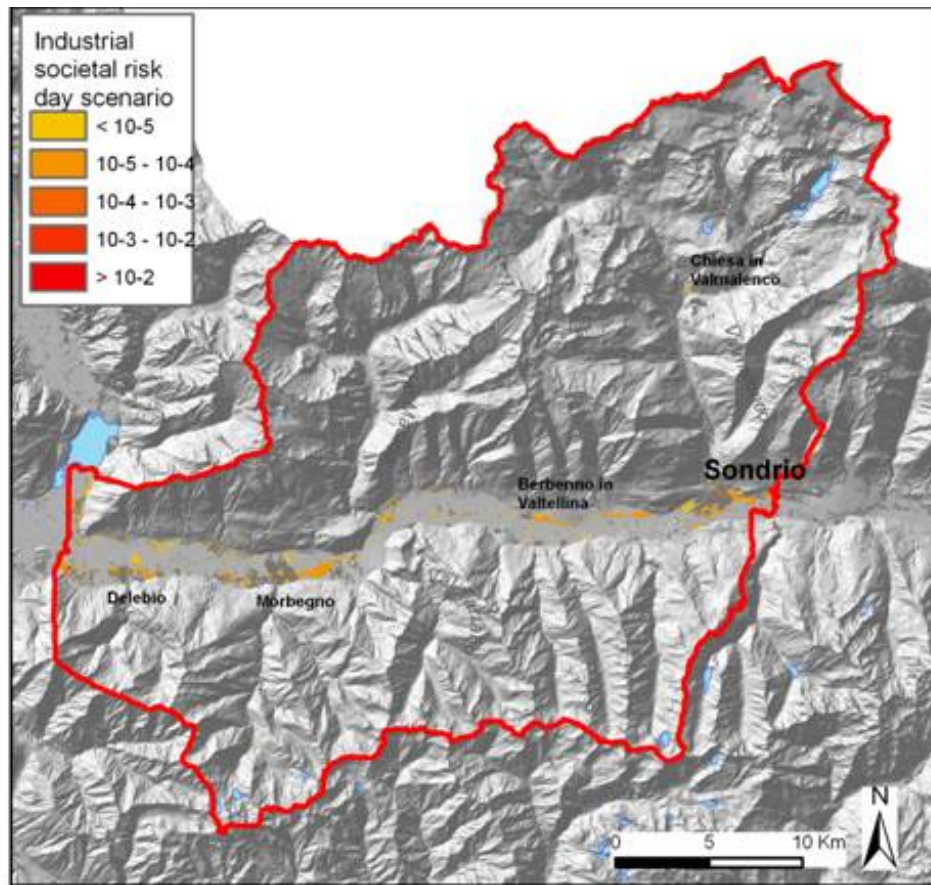


Fig.109. Fig Map of societal physical risk for industrial accident, day scenario. Risk values are expressed in terms of casualties per year.

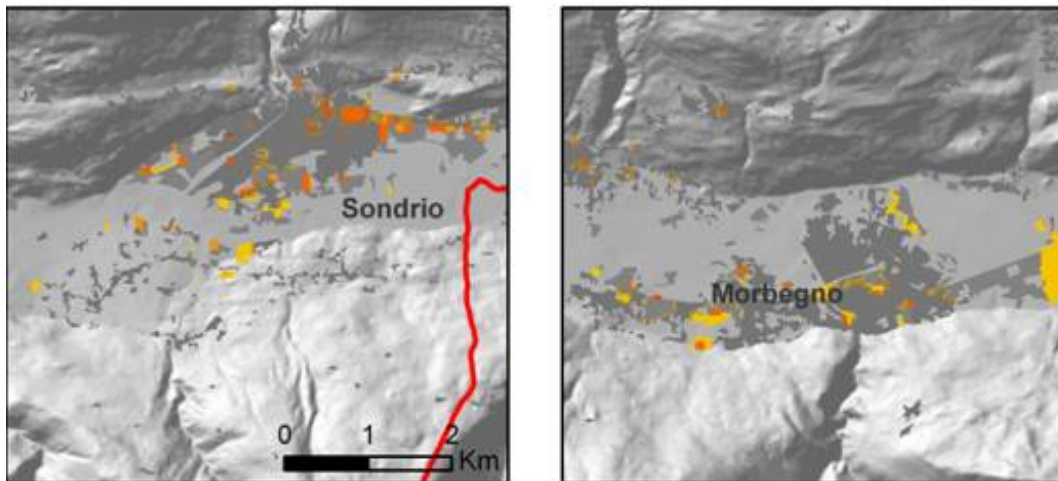
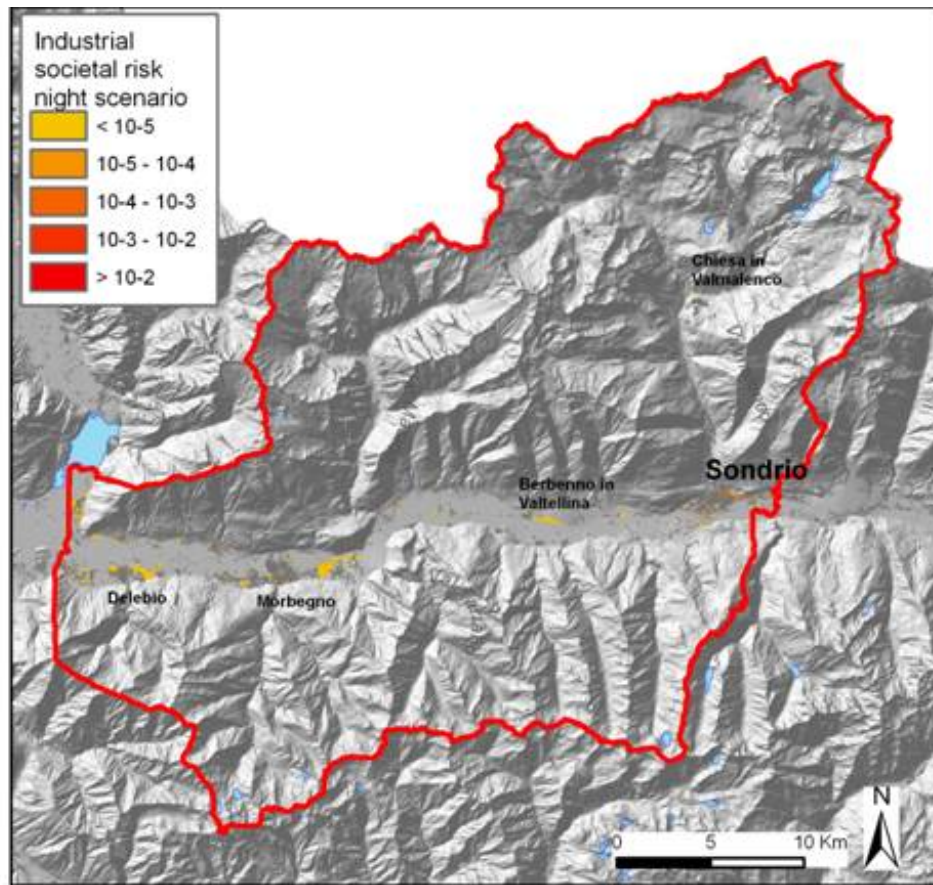


Fig.110. Map of societal physical risk for industrial accident, night scenario. Risk values are expressed in terms of casualties per year.

7.5 TOTAL TECHNOLOGICAL RISK

Total technological risk reaches very high values (Tab.85). It is clearly concentrated in the urbanised areas and mostly along communication lines.

Transport of hazardous materials have a very low impact on population, if compared to the other technological threats.

Work injuries and industrial accidents values show the same order of magnitude, but while work injuries take place with a strong predominance during the day, industrial accidents are likely to happen also during the night.

Road accidents show values three orders of magnitude higher than the previous ones. It is important to remember that expected casualties include in this analysis also injuries, adequately weighted. In any case, road accidents represent the main technologic threat in the area.

Tab.85. Total technological risk values for day and night scenarios

	Valtellina day scen	Valtellina night scen
Range (cas/year/cell)	0-0.13	0-0.18
Total (cas/year)	184	256.69

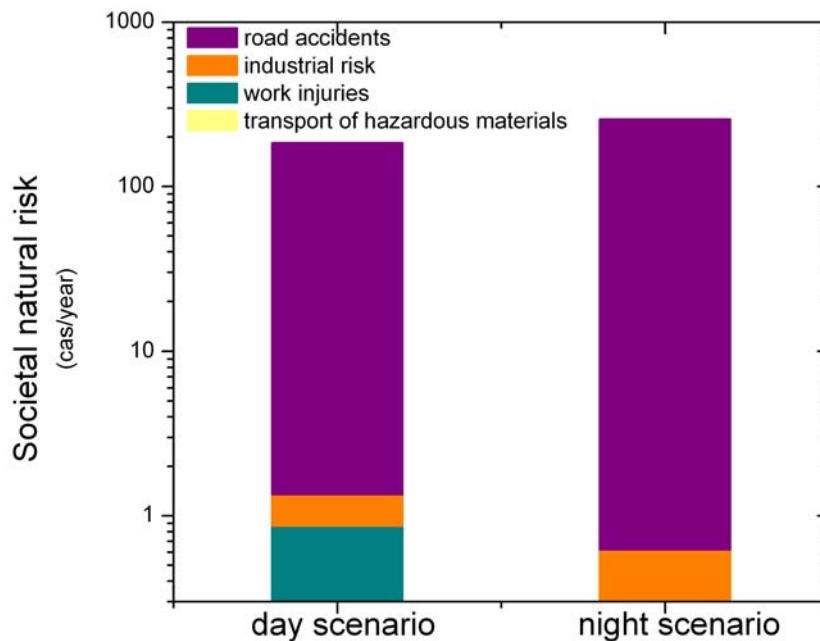


Fig.111. Values of societal risk values for day and night scenarios, in lower Valtellina

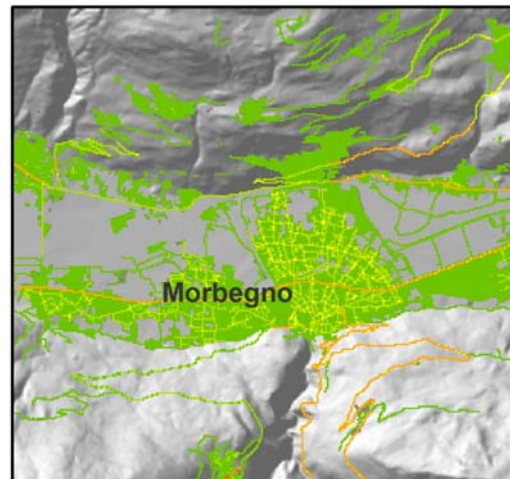
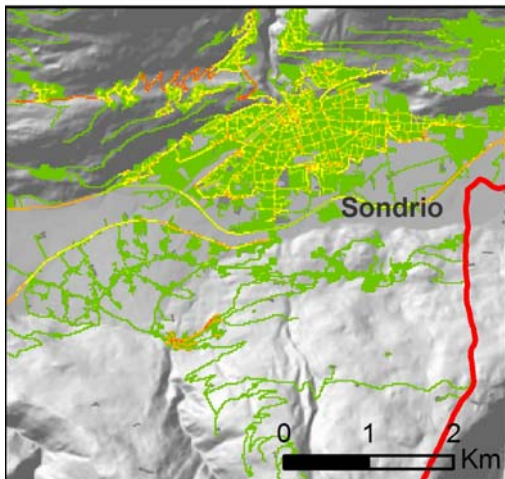
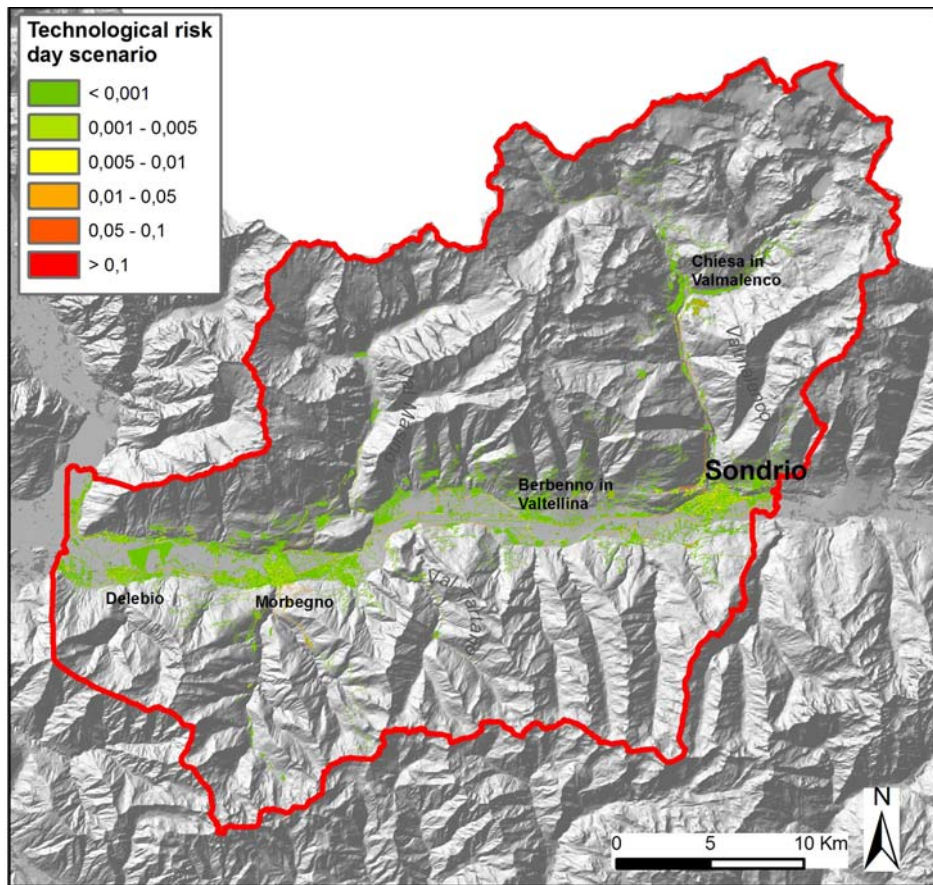


Fig.112. Map of societal technological risk, day scenario. Risk values are expressed in terms of casualties per year.

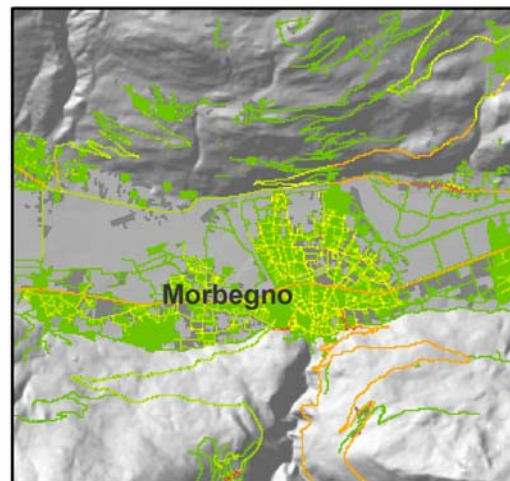
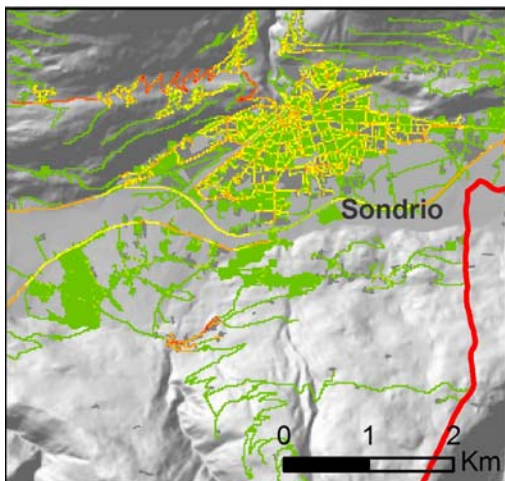
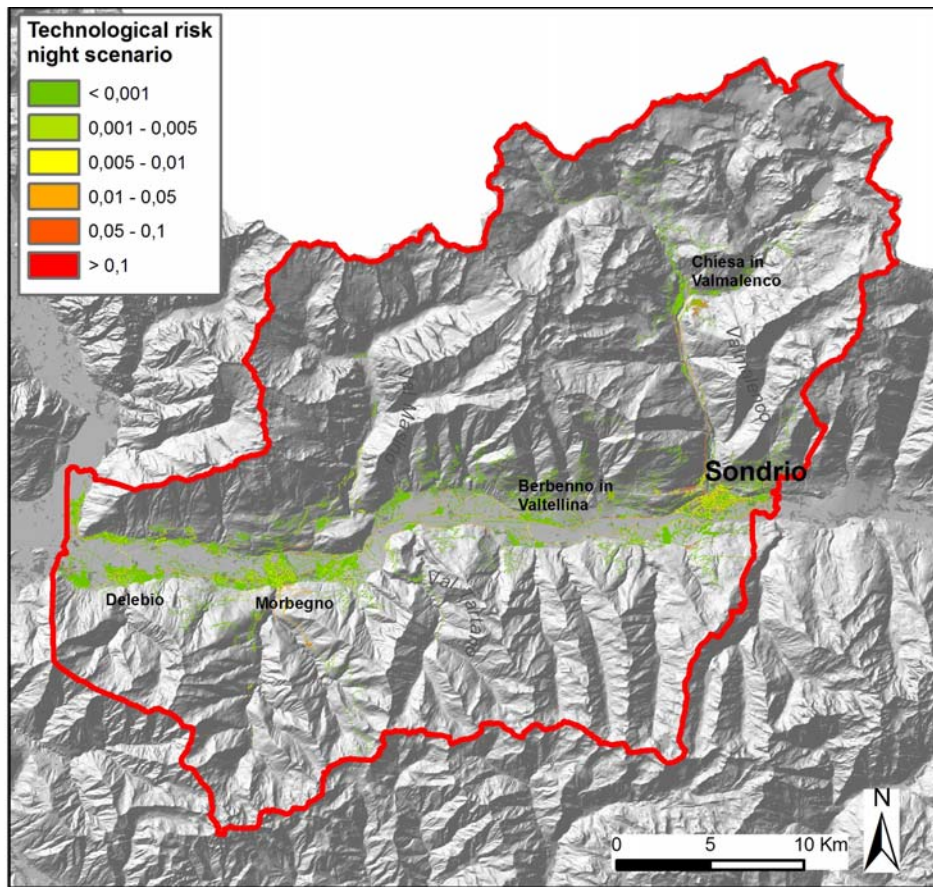


Fig.113. Map of societal technological risk, night scenario. Risk values are expressed in terms of casualties per year.

8 CONCLUSIONS

The multi risk quantitative analysis, aimed at the realization of Integrated Area Plans, led to the quantification of societal and economical risks, respectively in terms of casualties/year and €/year, for lower Valtellina and for the area of Brescia, including lower Val Trompia, Valcamonica and Val Sabbia. Both natural threats (rockfalls, shallow landslides, debris flows, alluvial fan flooding, river floods, earthquakes, and wildfires) and technological threats (transport of hazardous materials, road accidents, work injuries, industrial accident) were considered.

Different models were used to estimate the frequency of occurrence of the natural and technological phenomena. For each threat, vulnerability curves with respect to human life or to goods were used to assess damages, if available. In the other cases, some coefficients of gravity were estimated. Spatial and temporal exposition of people and goods was taken into account.

Results of the analysis allowed to study the effects of the considered natural threats, to contextualise them with respect to morphology and geography of the two study areas, and to compare the obtained values of risk with some acceptability curves proposed in the literature. Where possible, FN and FD curves were built. An analysis of the distribution of each risk with respect to elevation was performed.

This work could represent an important part of Integrated area Plans. The methodology, in fact, proved to be applicable at this scale of analysis, providing realistic results.

Domino effects were not included in the analysis yet, but this study provides data for their calculation, which will be implemented in the future, regarding:

- Earthquakes effects on landslides and industrial accidents
- Wildfire effects on industrial accidents
- Flooding effects on industrial accidents

In this study, risk assessment does not include all types of industrial accidents (e.g. dispersion of toxic substances, also in aquifers), or of landslides (e.g. deep-seated gravitational slope deformations), and it does not include other types of threat, as meteorological and climatic. The proposed methodology will be adapted and applied also to these threats.

The work could be further supported by a research of risk acceptability criteria and risk perceptions in population, stakeholders and administrations of the two study areas.

Quantitative risk assessment in Integrated Area Plans could become an important tool for the design of effective mitigation strategies, taking into account the complexity of the context, both from natural and social point of view. An integrated and holistic approach allows to optimise investments and risk reduction results.

PART III

UNCERTAINTY IN MULTI-RISK ASSESSMENT AT LOCAL SCALE

1 INTRODUCTION

In the framework of the Regional Program on Major Risk Mitigation (PRIM, 2007) we analysed and integrated with an indicator-based approach seven major territorial threats in the Lombardy Region, namely: hydrogeological, wildfire, seismic, meteorological, industrial (technological) risks; car accidents, and work injuries (Part I) result, a few risk hot-spot areas were identified in the region, on the basis of the number of risks simultaneously present, and their relative level.

One of the hot spots is the 420 km² area of Brescia and Val Trompia. The aim of this part of the thesis is to perform a Quantitative Risk Assessment on this risk hot-spot area, developing risk scenarios for flood, earthquake and industrial accident risk.

Due to the intrinsic uncertainty of the data and models used to assess the risk value, a strategy was developed to analyse this uncertainty and its propagation. Different methodologies (Monte Carlo simulation, Point Estimate and First Order Second Moment) for the evaluation of the uncertainties were applied to the case study, and compared.

Frequency-damage curves have been calculated, such as uncertainty propagation in the analysis. Monte Carlo Simulation, FOSM and Point Estimate uncertainty modelling were implemented and compared.

2 STUDY AREA

The 420 km² area of Brescia and Val Trompia (Fig.1) includes a plain zone (90 m a.s.l.) and a pre-alpine zone, with a maximum elevation of 1360 m a.s.l.. In low Val Trompia and in the area of Brescia, a high density of population settles, reaching a total of about 722,000 people, with a maximum density of 2,068 inhabitants / km², in the urban area of Brescia.

A variety of industrial activities is located in the area, supported by the presence of a well developed service offer: the area of Brescia and lower Val Trompia is economically strongly developed, and highly industrialised, since the beginning of the XX century: iron and steel, mechanics, chemicals and foundry industries are diffused, coupled with a strong urban development. In Val Trompia, the tourist activities are also relevant, coupled with the zootechnical and the agricultural sectors. 36 municipalities are involved in the study area.

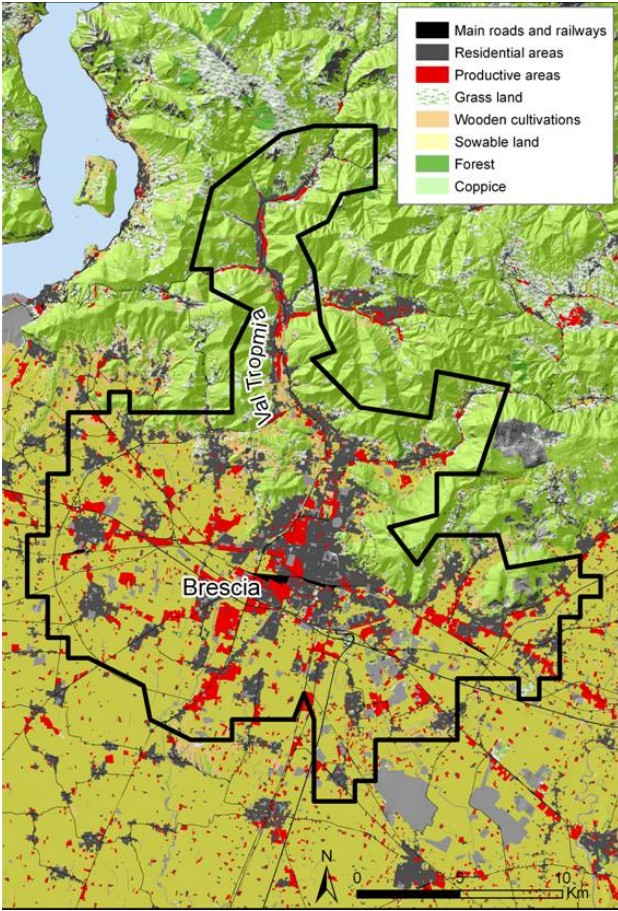


Fig.1. Hot spot area and elements at risk, from multi-risk analysis at the regional scale



Fig.2. Views of Gardone Val Trompia, in the lower valley

2.2 CONTEXT FOR RISK ANALYSIS AND DATA AVAILABILITY

The coexistence of technological and natural hazard sources in the hot spot area generates the necessity of a local scale analysis.

Due to the presence of river Mella, some floods can potentially occur in the area. The national regulatory map zonation (PAI - Piano stralcio di Assetto Idrogeologico, 2007) indicates areas with different hazard levels, with 200 and 500 years return time (see Part I and II for description).

In general, Lombardy has a low seismic risk, with respect to other Italian regions, with some exceptions in the eastern sector. The study area, close to the Lake Garda (max historical magnitude 6 Richter, 1222 A.D.), is one of the most exposed, with peak ground acceleration (pga) referred to a return time of 475 years (exceedance probability of 10% in 50 years) belonging to the range 0.125 - 0.15 g (Tab.1, Fig.3). Peak ground acceleration values have been computed for reference site conditions (stiff soils having shear wave velocities greater than 800 m/sec). Values have been grouped by 0.025 g, according to requirements of the Italian Government (Ord. 3274 Pres.cons.Min.,20/3/03) for the formulation of the seismic classification of the country. The study area belongs to class 3d (Tab.1, Fig.3).

Tab.1. Values of peak ground acceleration and correspondent hazard zones, (Ord. 3274 Pres.cons.Min., 20/3/03)

zone	Sub-zone	pga p(10%, 50 years) [g]
1	1d	0.325 – 0.350
	1c	0.300 – 0.325
	1b	0.275 – 0.300
	1a	0.250 – 0.275
2	2d	0.225 – 0.250
	2c	0.200 – 0.225
	2b	0.175 – 0.200
	2a	0.150 – 0.175
3	3d	0.125 – 0.150
	3c	0.100 – 0.125
	3b	0.075 – 0.100
	3a	0.050 – 0.075
4	4	≤ 0.050

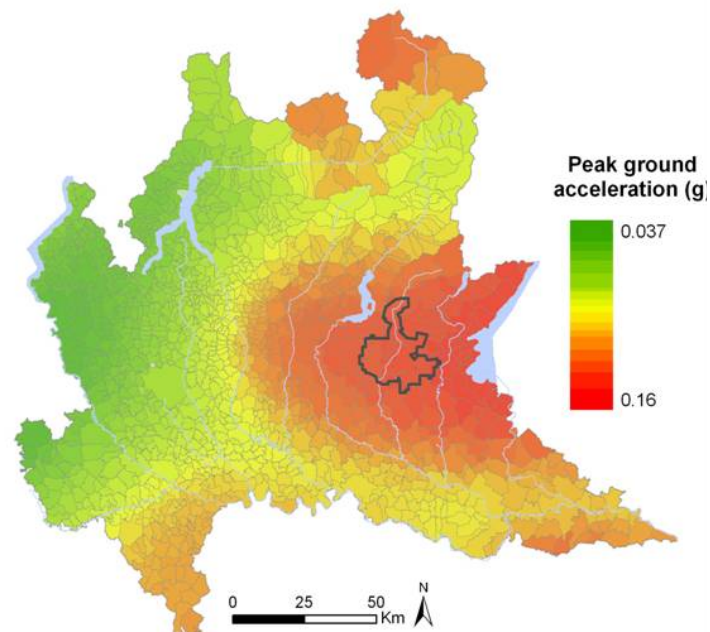


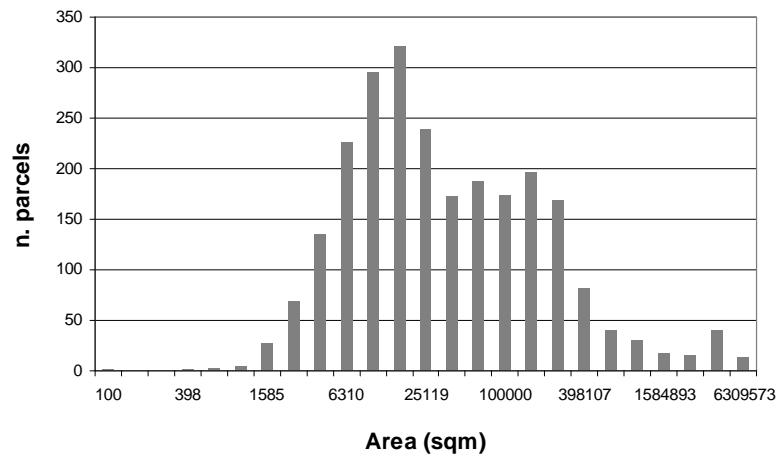
Fig.3. Values of peak ground acceleration referred to return time of 475 years (exceedance probability of 10% in 50 years) for Lombardy

Eight industrial plants classified as major risk plants, identified by a national law (D.Lgs. 238/05, according to Seveso Directive 96/82/CE), are located in the study area. For these plants, we analysed and mapped the areas of impact for different typologies of accident by means of security reports, compulsory provided by the companies. For each accident scenario, the security report includes the probability of occurrence, the area of impact, the intensity of the event and the effects on the structures and on the human life.

3 RISK ASSESSMENT AND UNCERTAINTY EVALUATION

3.1 METHODOLOGY

We performed a local-scale quantitative probabilistic risk analysis (QPRA), aimed at calculating the economic and human life expected annual loss for a set of risk scenarios with different probabilities and intensities of flood (2 scenarios), earthquake (3 scenarios) and industrial accident (8 scenarios). As terrain unit, we considered the census parcel (2460 parcels) of variable area, ranging from 0.0001 to 19 km² (Fig.4), for which we had detailed socio-economic data (e.g. residents, number and type of buildings) from the National Institute of Statistics (ISTAT, 2001).



$$E(D|event) = P(I|event) \cdot P(D|I) \cdot W \quad (3)$$

where $P(I|event)$ is the percentage of impacted area for each parcel, indicating the exposure to the specific threat. For each parcel, the portion of its surface potentially impacted by a threat was evaluated, for each scenario.

$P(D|I)$ is the vulnerability of a parcel, depending on the elements at risk located in it, calculated by means of process-specific vulnerability functions, described in the following.

W is the total value of a parcel, calculated on the basis of the number and typology of buildings and on the number of people living there. The value of the buildings, including the physical structure and the content, has been evaluated assuming an averaged value of 3,000 euros/m². For each of the census parcels, we disposed of the data related to the residential surfaces (ISTAT, 2001) and to the number of 1-floor, 2 floors etc. buildings. The total economic value of the buildings belonging to each parcel was computed (Fig5a). The number of people living in each parcel was also provided by ISTAT (2001) (Fig.5b).

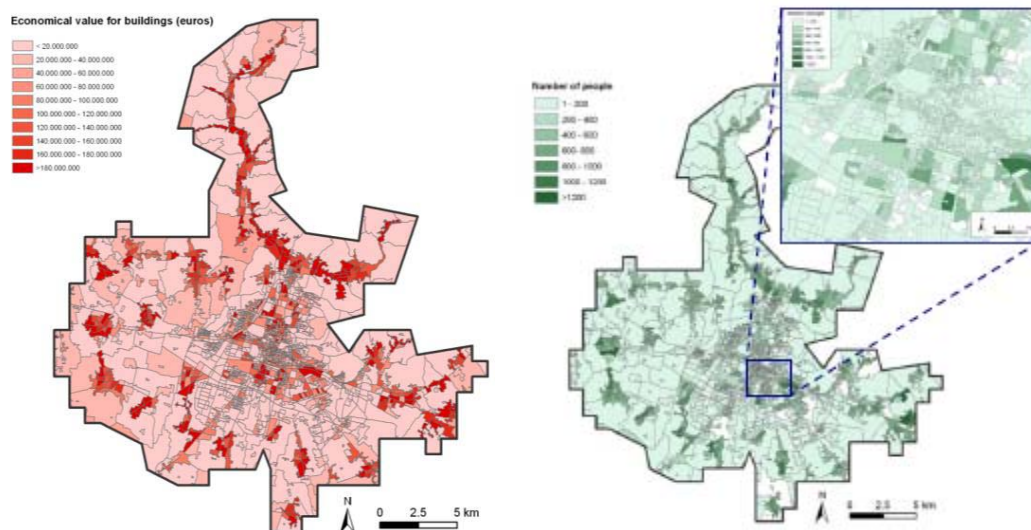


Fig. 5. Value of each census parcel, W , in terms of economical value of the buildings (a) and number of people (b)

A relevant level of uncertainty was perceived in some of the steps of risk assessment. In particular, some troubles were found in assessing with a high degree of reliability some of the input parameters of the model. We applied and compared different strategies for uncertainty modelling (Monte Carlo simulation, FOSM, and Point Estimate analysis) to assess and aggregate the uncertainty to the evaluation of hazards, values of the exposed elements and process-specific vulnerabilities. Epistemic and aleatory uncertainties were not distinguished, being at this scale of analysis strongly connected.

For what concerns the sources of hazard, some uncertainties were found in calculating the return time, and as a consequence the annual probability, and in

assessing the intensity of the event (e.g. depth of water for floods, peak ground acceleration for earthquakes).

Some uncertainties were introduced also in the treatment of the elements at risk, for instance in the evaluation of the position and value of the potentially impacted elements (e.g. value/m² for buildings, n. of buildings in a parcel), and in the vulnerability of each element. In addition, we found that the census parcel is not always the best territorial unit for risk analysis because the element at risk must be assumed homogeneously distributed within the parcel, while areas effectively impacted can be empty of elements (Fig. 6 and 7). To express this concept, an uncertainty was introduced also for the probability of impact given the event, $P(I|event)$. The uncertainty in this case is calculated as a function of the size of the parcel.

To some of the variables introduced in risk assessment, a constant uncertainty on the whole study area was assigned. This is the case for occurrence probability of the events, number of buildings for census parcel for the different typologies, number of people living in each census parcel, economic value of the buildings, and $P(D|I)$. In these cases, the lack of knowledge or the detail of the data were the same on the whole study area.

Since the values of intensity of the scenarios and of occurrence probability are averaged on the whole census parcel, the precision of the attributions is strongly dependent on the area they are averaged on, and the values of the coefficient of variation for these variables are expressed as a function of the census parcel area. The probability of impact also was considered as a function of the census parcel area, being the intensity value averaged on the whole parcel area and the elements assumed homogeneously distributed within the parcel.

COV values were assigned basing on expert knowledge of experts coming from the fields of geology and environmental sciences.

In the present work, variables for risk assessment were supposed to be random variables symmetrically distributed, non correlated.

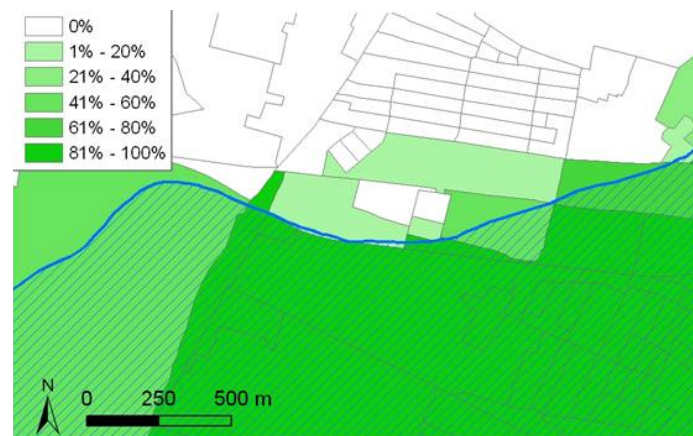


Fig.6. Example of calculation of impacted areas for floods, $P(I|event)$

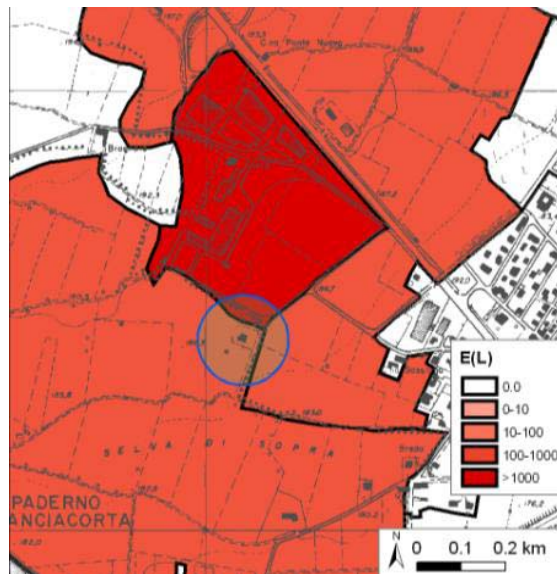


Fig.7. Expected loss, $E(L)$ in euros, for the whole census parcels. The blue circle indicates the exact location of the element at risk.

3.2 RISK ANALYSIS

1.1.1 FLOOD RISK

Flood risk was assessed for the Mella river (basin, 311 km² in size), passing through Brescia urban centre.

We calculated the intensity of two scenarios, having a return time of 200 and 500 years, according to national regulatory map zonation (PAI, 2007). Basing on a 20 x 20 m DTM, a modelization of the depth of the water was performed, and averaged on each parcel in a GIS environment (Fig. 8).

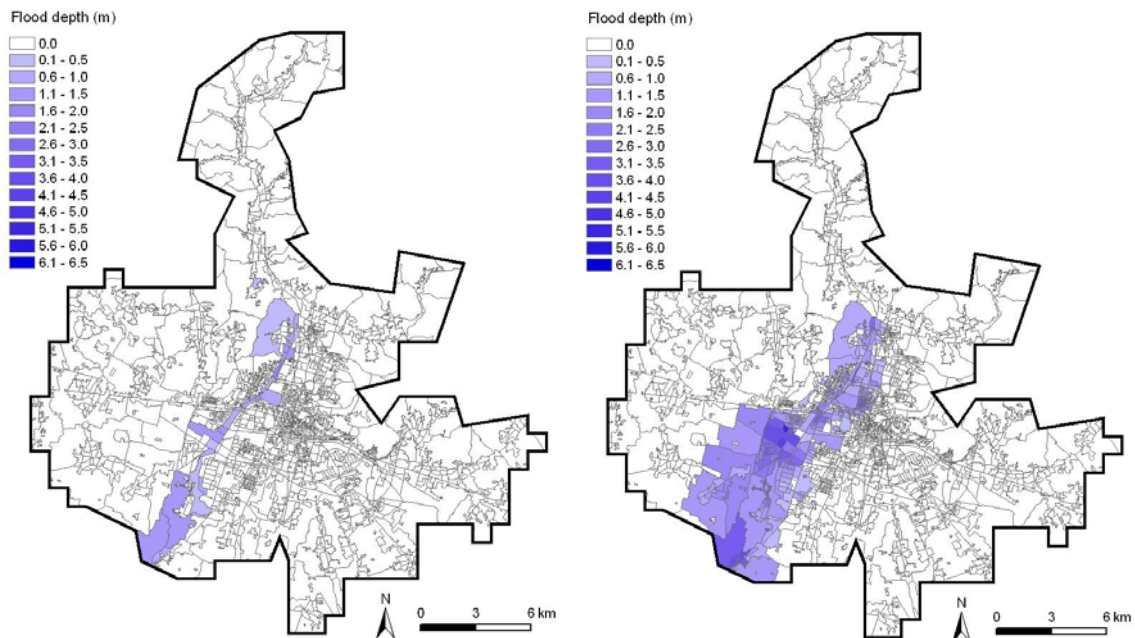


Fig. 8. Flow depth for the two scenarios: (a) return time 200 years (b): return time 500 years

As elements at risk, with respect to the hazard, two different typologies of buildings were considered, with one or more floors, and their content. For each census parcel, the number of buildings with one or more floors were provided by ISTAT (2001). Vulnerability curves were used to evaluate the damage (USACE, 2003) Tab.2, Fig.9)

Tab. 2. Percentages of damage related to water depth. Vulnerability curves (USACE, 2003)

Water Depth (m)	damage% 1 floor buil	damage% 2/more floor buil	damage% Content 1 floor buil	damage% Content 2/more floor buil
0.3	13.3	8.7	8.85	4.98
0.6	17.9	12.2	13.41	8.65
0.9	22	15.5	17.62	12.1
1.2	25.7	18.5	21.47	15.33
1.5	28.8	21.3	24.96	18.33
1.8	31.5	23.9	28.1	21.12
2.1	33.8	26.3	30.89	23.68
2.4	35.7	28.4	33.32	26.03
2.7	37.2	30.3	35.40	28.15
3	38.4	32	37.13	30.05
3.4	39.2	33.4	38.49	31.73
3.7	39.7	34.7	39.77	33.62
3.9	40	35.6	40.31	34.78
4.3	40	36.4	40.48	35.44
4.6	40	36.9	40.36	36.45
4.9	40	37.2	40.45	36.95

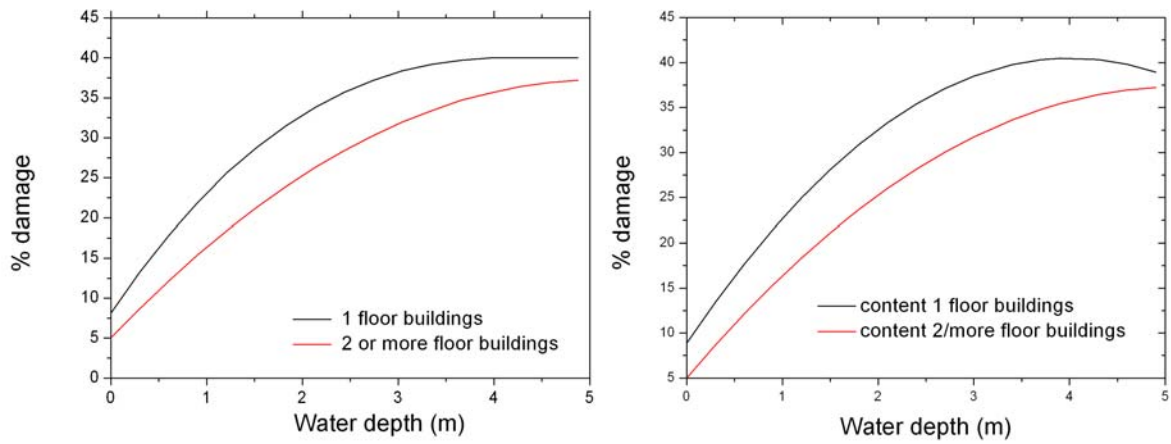


Fig. 9. Vulnerability curves to floods. USACE (2003)

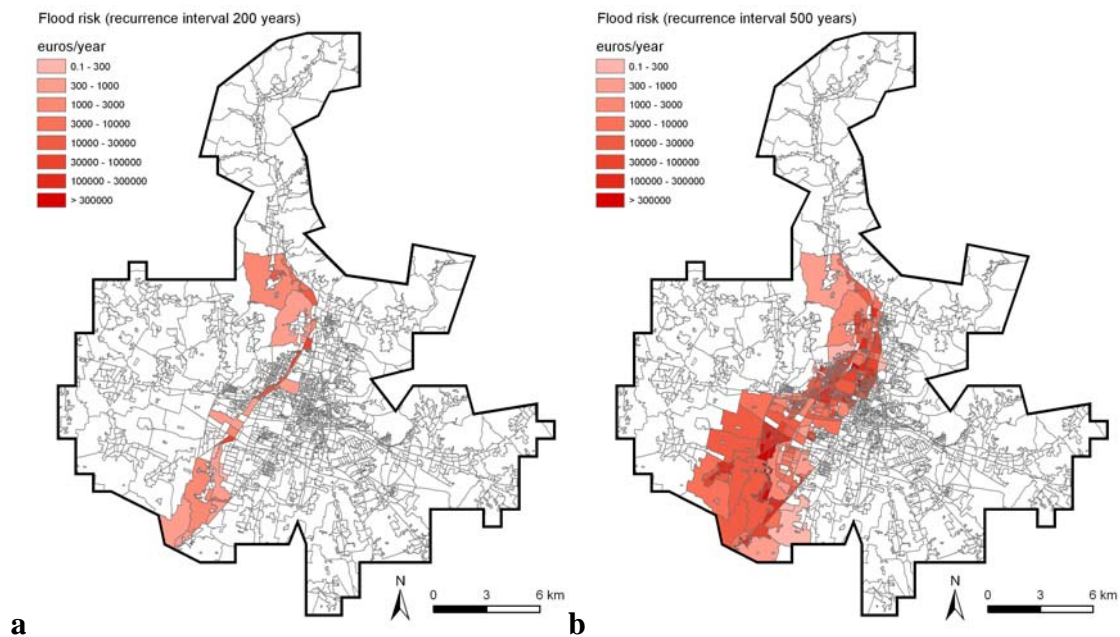


Fig. 10. a) flood risk values for return time 200 years, Monte Carlo Simulation; b) flood risk values for return time 500 years, Monte Carlo Simulation

The results obtained by means of the three methods for both flood scenarios were very similar (Tab.3).

Tab. 3. Expected losses for flood scenarios

		Monte Carlo Simulation	FOSM	Point Estimate
Tr 200 years	Range of E(L)	0-43,954 €	0-44,599 €	0-44,575 €
	Total loss	403,988 €	404,265 €	404,136 €
Tr 500 years	Range of E(L)	0-470,572 €	0-470,571 €	0-456,146 €
	Total loss	27,835,015 €	27,835,513€	26,955,987 €

The function linking the census parcel area and its uncertainty (COV) (Fig.11) has been chosen in order to account for a stronger uncertainty for larger parcels. Since the values of intensity, exposed elements, and impacted areas are averaged on the whole parcel, the bigger the parcel the greater the approximation is introduced on the values or the exact location of the variables. For this reason, the COV values assigned to $P(I|E)$ and mean water depth are dependent on the COV value of the corresponding census parcel area (Tab.4). In particular, the probability of impact was considered two times more uncertain for the scenario with return time 200 years, because of the presence of structures and embankments not considered in modelling of the water depth. Mean water depth was considered more uncertain for the scenario with return time of 500 years. In this case, in fact, the wide areas covered by the water and the limited detail of the DTM did not allow a precise calculation of water depth, and probably more errors were introduced than for the other scenario.

In assessing uncertainty to the quantity of buildings in each parcel, a higher COV was assigned to the percentage of buildings with two or more floors, including more different types of buildings, and being potentially more prone to errors in calculation of the exact number.

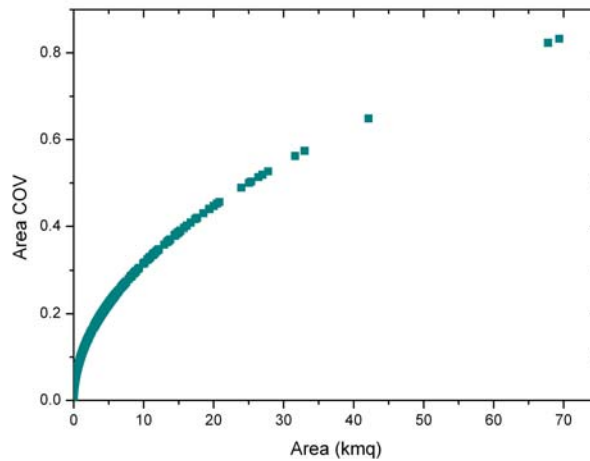


Fig. 11. COV values for area of the census parcels.

Tab. 4. Uncertain variables for the flood scenarios, and values for coefficients of variation

Floods	TR=200 years COV	TR=500 years COV
Parcel area	$(area^{0.5})/10000$	$(area^{0.5})/10000$
Mean water depth	$COV \text{ parcel area}$	$(COV \text{ parcel area}) * 1.2$
% 1 floor buildings	0.1	0.1
% 2 floor buildings	0.2	0.2
P(I E)	$(COV \text{ parcel area}) * 2$	$COV \text{ parcel area}$
Value euro m ²	0.333	0.333
P(E)	0.1	0.1

All the input variables are supposed to be independent, and non - skewed. For the evaluation of the uncertainty of the flood risk value expressed in terms of expected economical losses, for Monte Carlo simulation, we supposed a Gaussian distribution for all the variables, while for FOSM and Point Estimate a symmetric one. We performed the Monte Carlo Simulation with Latin Hypercube sampling, and 1000 iterations.

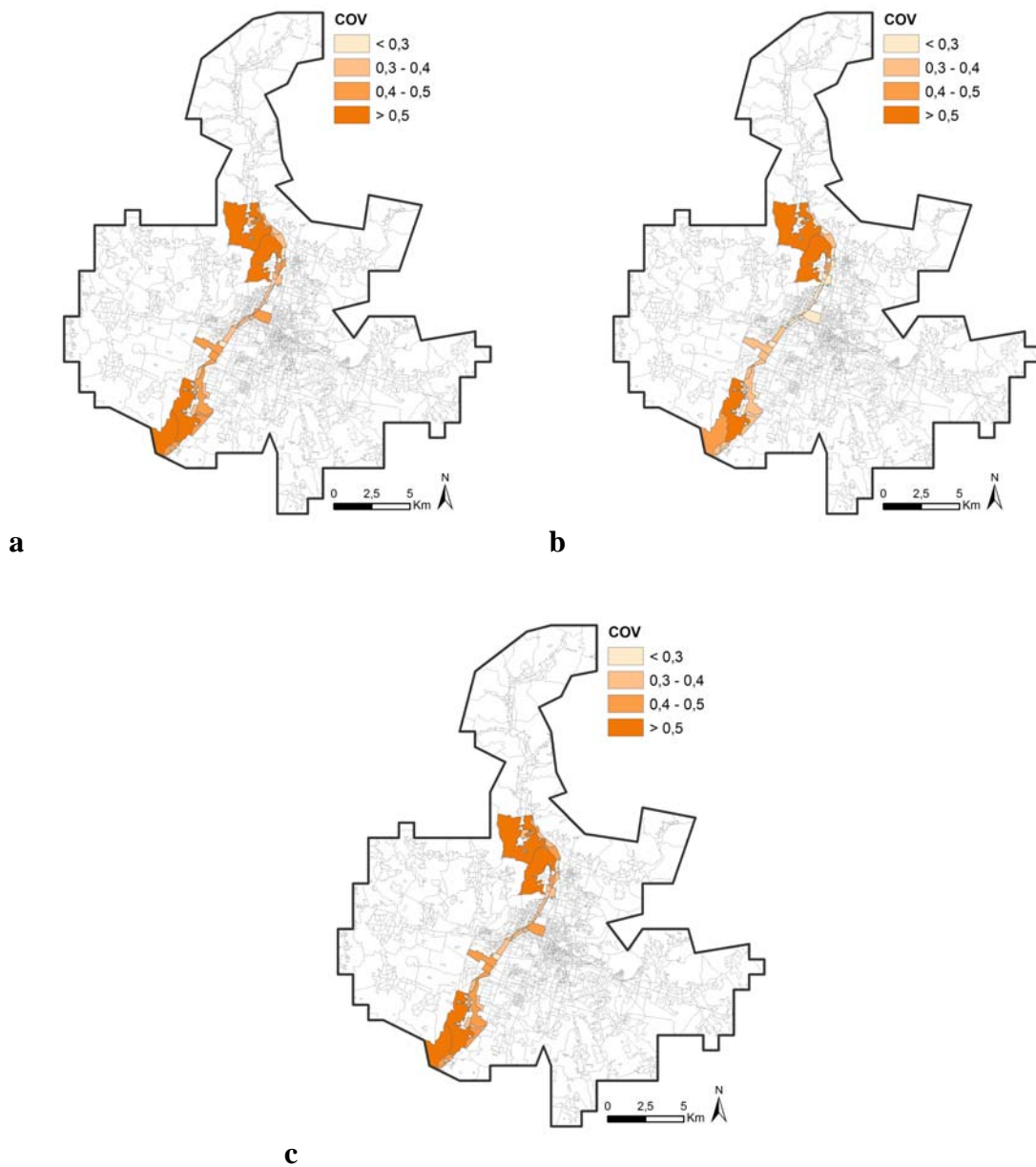


Fig. 12 (a): COV value for the T_r200 years scenario, calculated by means of a Monte Carlo simulation (b): COV value for the T_r200 years scenario, calculated with FOSM approach (c): COV value for the T_r200 years scenario, calculated with Point Estimate approach

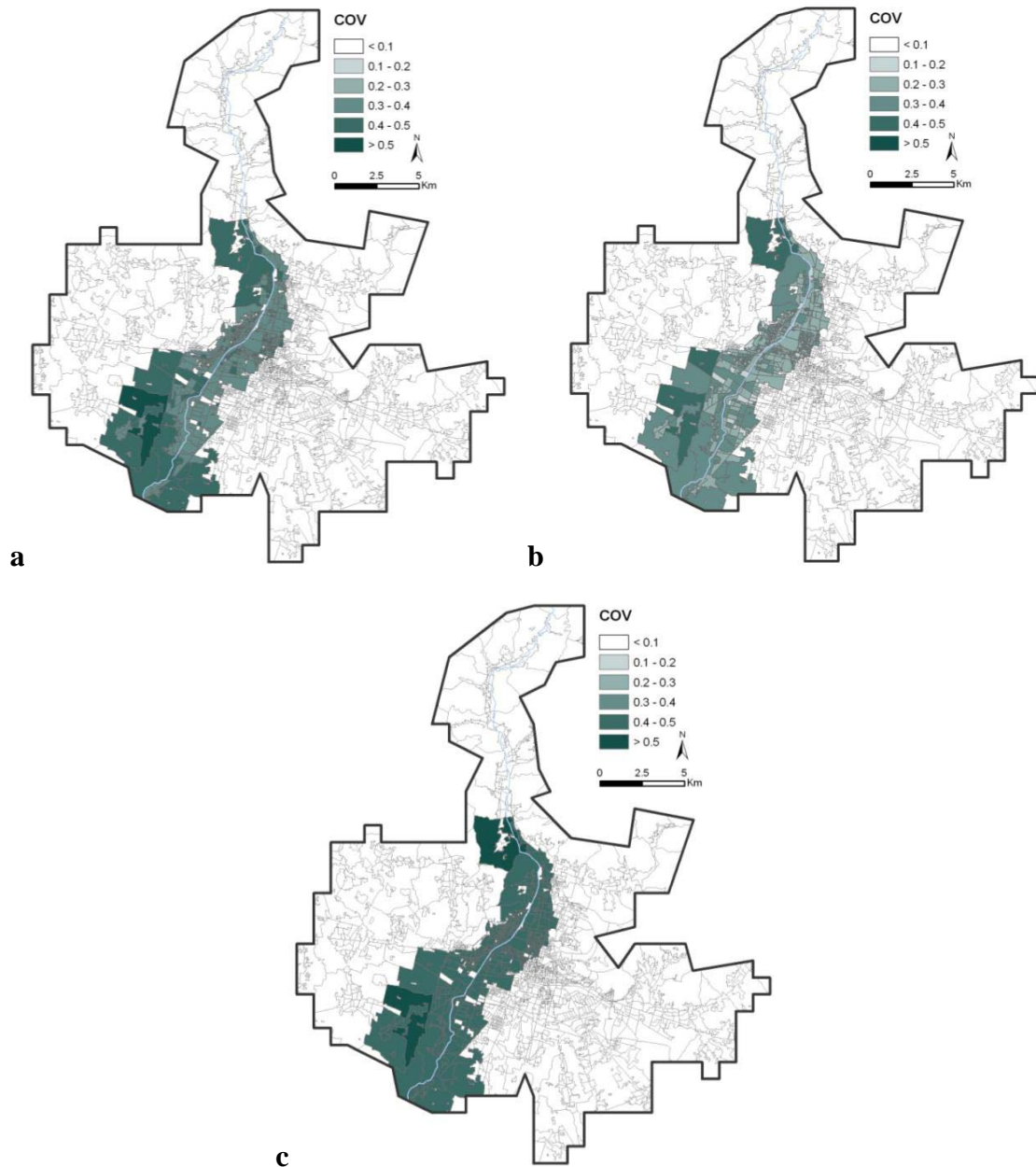


Fig. 13 (a): COV value for the Tr 500 years scenario, calculated by means of a Monte Carlo simulation (b): COV value for the Tr 500 years scenario, calculated with FOSM approach (c): COV value for the Tr 500 years scenario, calculated with Point Estimate approach

Tab.5. Values of Coefficients of variation on expected losses

	COV	Monte Carlo Simulation	FOSM	Point Estimate
Tr 200 years	Range	0-0.59	0.1-0.6	0-0.53
	Mean	0.36	0.29	0.36
Tr 500 years	Range	0-0.5	0.1-0.43	0-0.52
	Mean	0.36	0.28	0.4

Uncertainties propagated by means of FOSM show slightly lower values, and a smaller range of values.

1.1.2 SEISMIC RISK

For the probabilistic analysis at the local scale, we considered three scenarios with different return time: 75, 475 and 2500 years.

As elements at risk, we considered different typologies of buildings, concrete or masonry built, with different vulnerabilities to the events. Number of buildings for different materials, per census parcel, was provided by ISTAT (2001). For each type of buildings, a set of fragility curves was used, as in Kappos et al., (2006) (Fig.14 and 15).

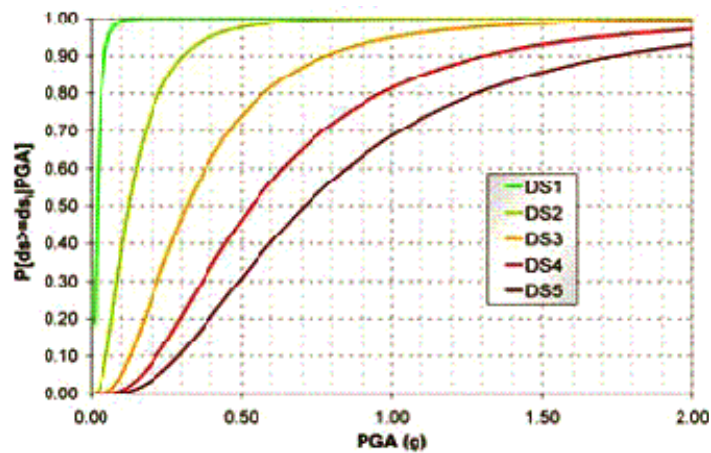


Fig. 14. Fragility curves for reinforced concrete buildings, 5 levels of damage (Kappos et al., 2006)

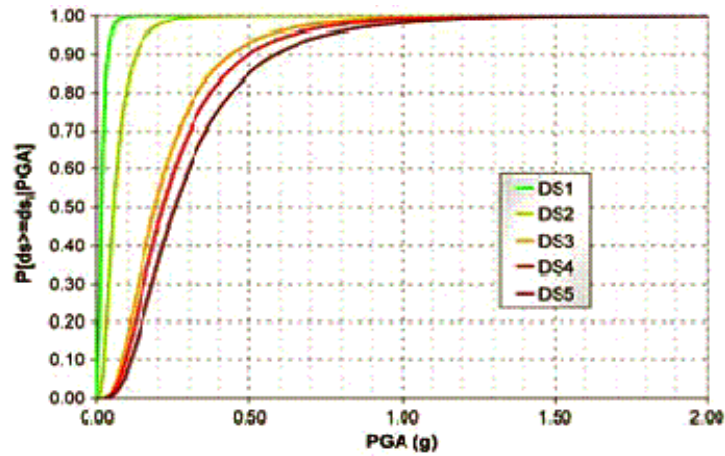
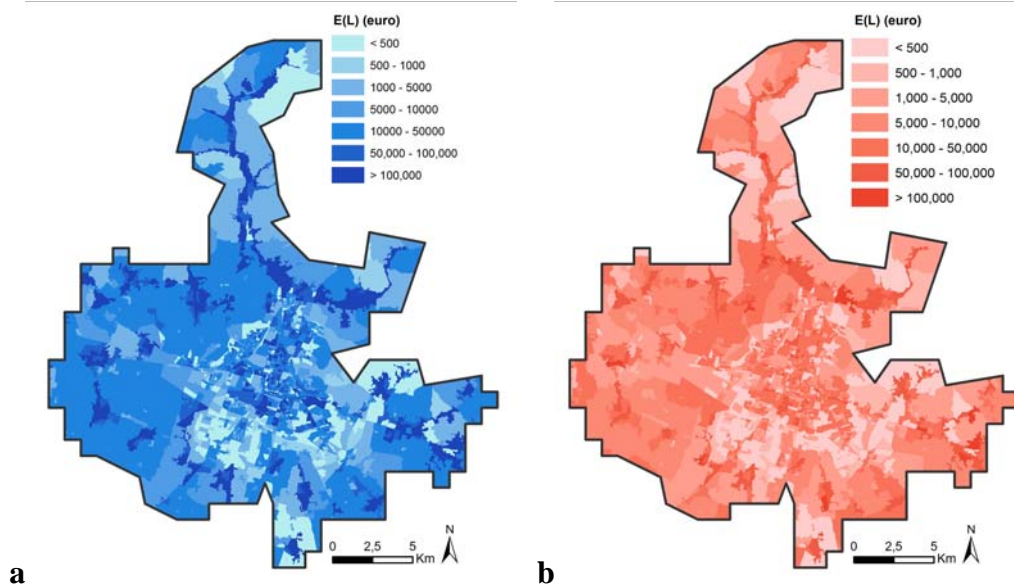


Fig. 15 Fragility curves for masonry buildings, 5 levels of damage (Kappos et al., 2006)

In risk assessment, the parcels are always supposed to be entirely impacted by the event, due to the diffused nature of the dangerous phenomenon, which means $P(I|event)=1$.

Also in this case, the input variables were supposed to be independent, and non-skewed. For Monte Carlo simulation, a Gaussian distribution was assumed for all the variables, while using FOSM and Point Estimate, a symmetric one. We performed the Monte Carlo Simulation with Latin Hypercube sampling, and 1000 iterations.



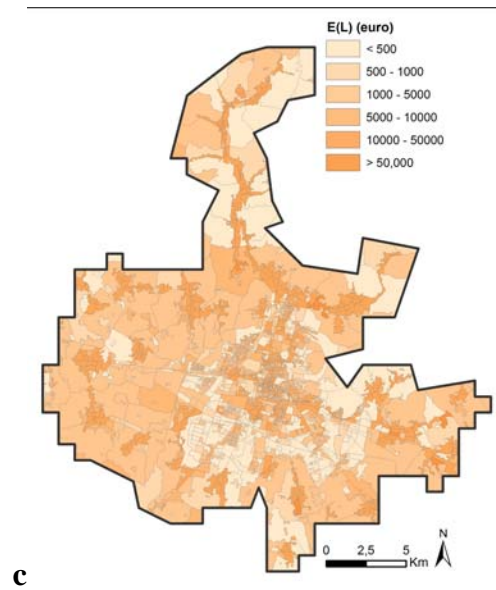


Fig. 16. a: Seismic risk values for Monte Carlo analysis, scenario a) Tr 75 years, b) 475 years and c) 2500 years

Tab. 6. Expected annual losses for seismic scenarios

		Monte Carlo Simulation	FOSM	Point Estimate
Tr 75	Range of E(L)	0-474,996 €	0-474,436 €	0-474,693 €
	Total loss	271,382,935 €	271,063,495 €	271,219,806 €
Tr 475	Range of E(L)	0-195,196 €	0-195,965 €	0-198,845 €
	Total loss	101,985,550 €	105,254,035 €	106,700,628 €
Tr 2500	Range of E(L)	0-107,188 €	0-83,618 €	0-85,722 €
	Total loss	51,861,135 €	41,508,402 €	42,712,091 €

Tab. 7. Uncertain variables for seismic risk years scenario, and values for their coefficient of variation

Seismic risk	COV
Parcel area	$(area^{0.5})/10000$
Peak ground acceleration	$(0.06+(2E-8*area)-(1E-16)*(area^2))$
% masonry buildings	0.1
% reinforced-concrete buildings	0.1
Value euro m2	0.333
P(E)	0.001

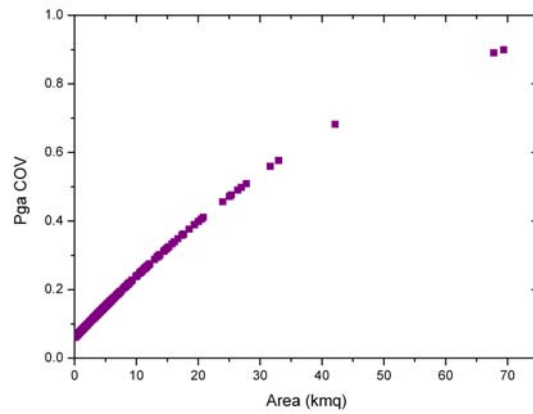
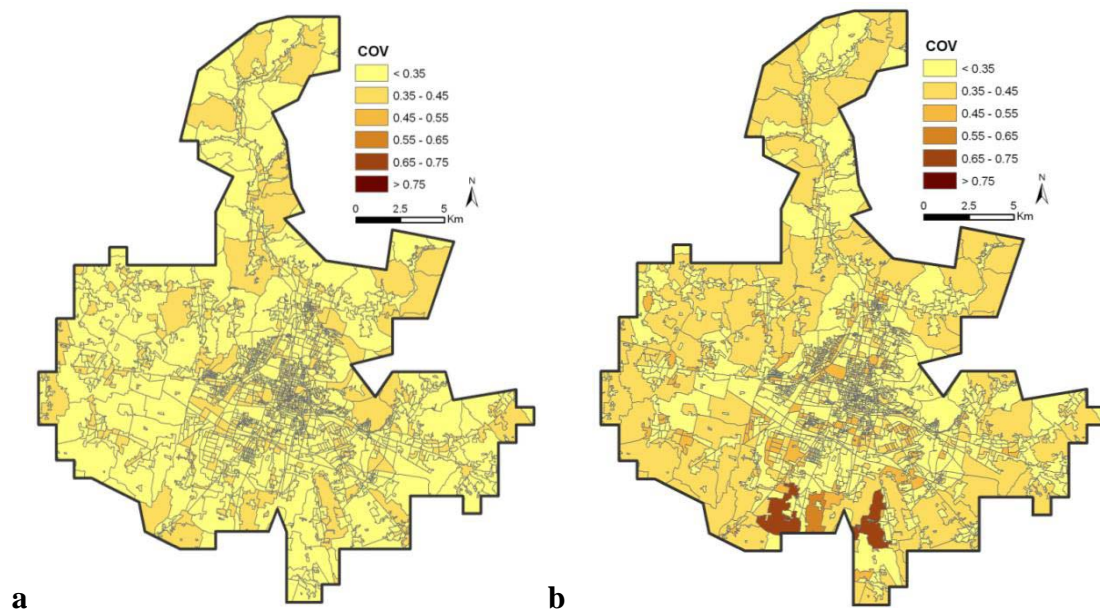


Fig. 17. COV values of peak ground acceleration values with respect to the area of the census parcels.



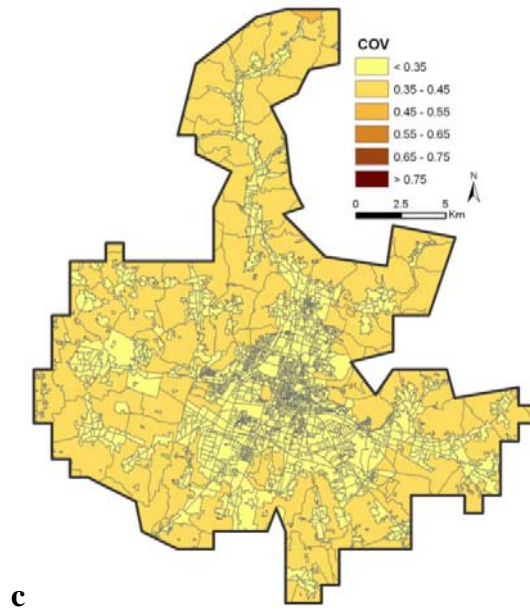


Fig. 18 (a): COV values for Monte Carlo analysis, scenario Rt 75 years (b): COV values for FOSM analysis, scenario Rt 75 years (c): COV values

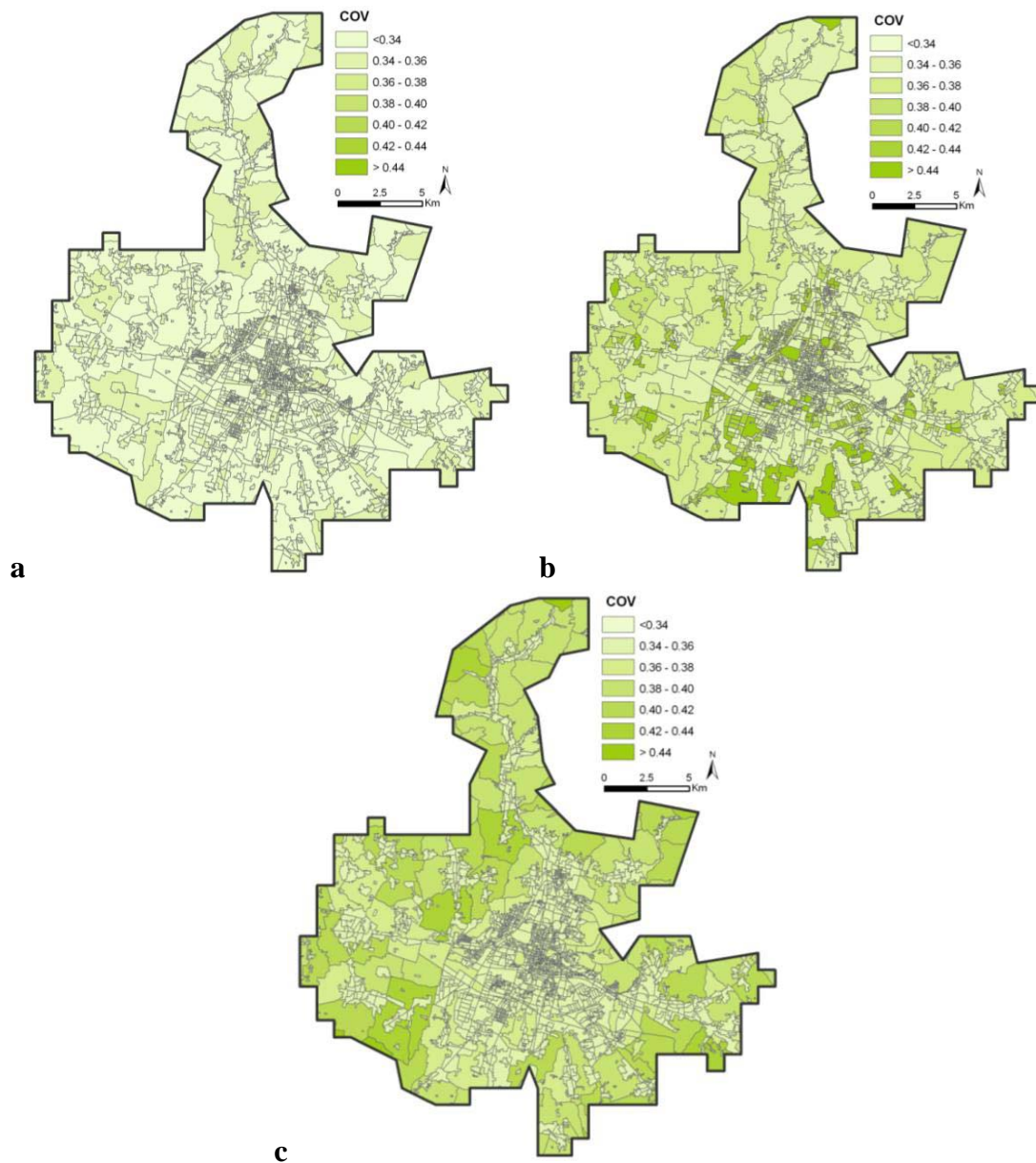


Fig. 19. (a): COV values for Monte Carlo analysis, scenario Rt 475 years (b): COV values for FOSM analysis, scenario Rt 475 years (c): COV values for Point Estimate analysis, scenario Rt 475 years

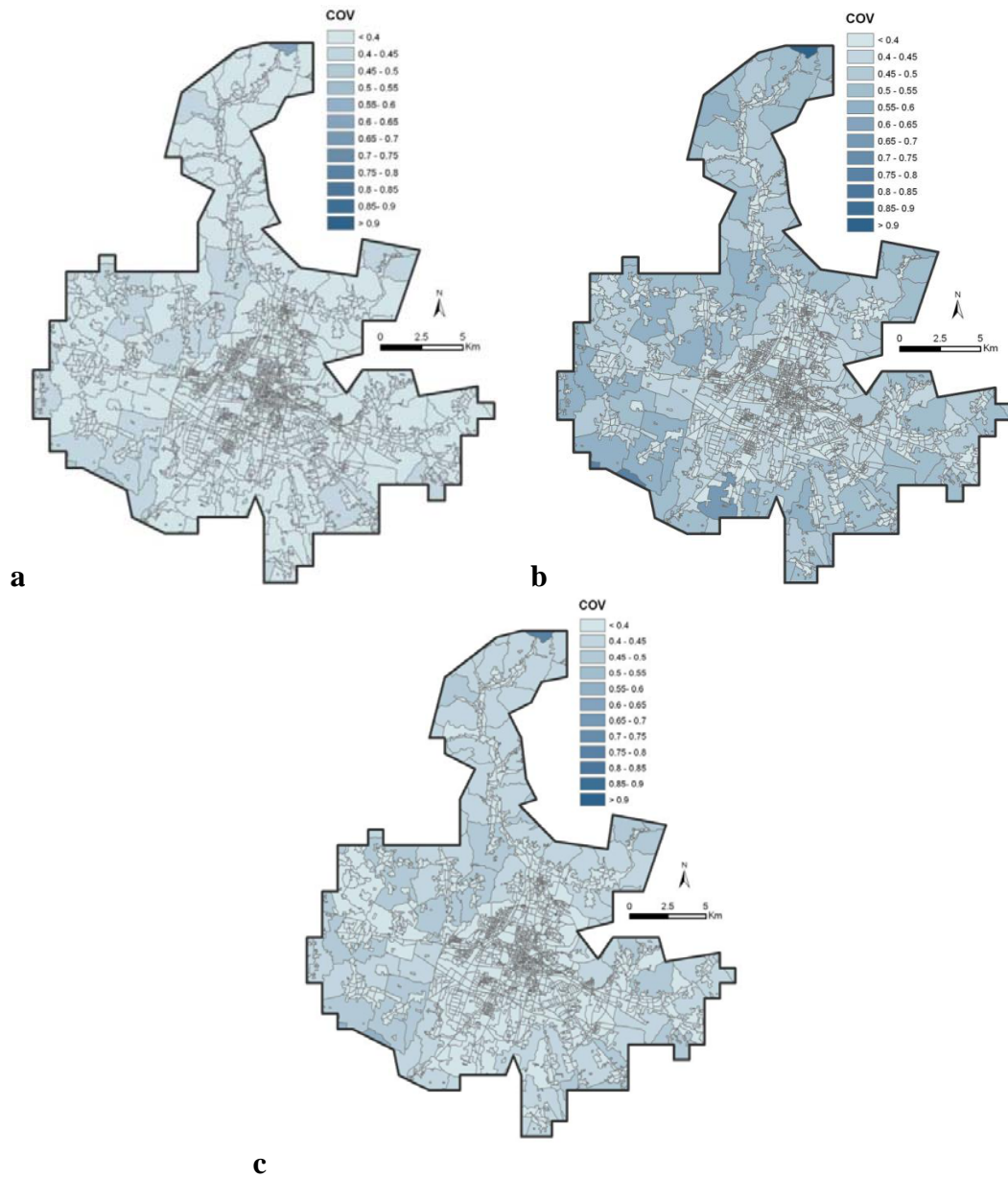


Fig. 20 COV values for seismic scenario Rt 2500 years a) Monte Carlo analysis, b) FOSM analysis c) PE analysis

Tab.8. Values of Coefficients of variation on expected losses

	COV	Monte Carlo Simulation	FOSM	Point Estimate
Tr 75 years	Range	0.3-0.39	0.33-1.2	0.34-1.8
	Mean	0.34	0.35	0.35
Tr 475 years	Range	0.32-0.35	0.34-0.83	0.33-1.06
	Mean	0.34	0.36	0.34
Tr 2475 years	Range	0.33-0.83	0.38-1.7	0.34-1.2
	Mean	0.35	0.43	0.37

1.1.3 INDUSTRIAL RISK

Only Major risk plants (RIR ex D.Lgs. 334/99) were considered: only for these plants, in fact, security reports are mandatory and available, carrying information about accident scenarios, probabilities and maps of impact. In the study, 8 scenarios were taken into account, related to 3 industrial plants (Fig.21). Due to incomplete documentation about the productive processes and the accident scenarios, only explosion-related accidents were considered, neglecting those related to the release of toxic gases and pollutants.

Vulnerability was calculated on the basis of the effects on people and on structures reported in the safety plans of the plants, compulsory provided by the companies (Tab.9).

All the input variables were supposed to be independent, and non - skewed. For Monte Carlo simulation, a Gaussian distribution was supposed for all the variables, while for FOSM and Point Estimate a symmetric one. Monte Carlo Simulation was performed with Latin Hypercube sampling, and 1000 iterations.

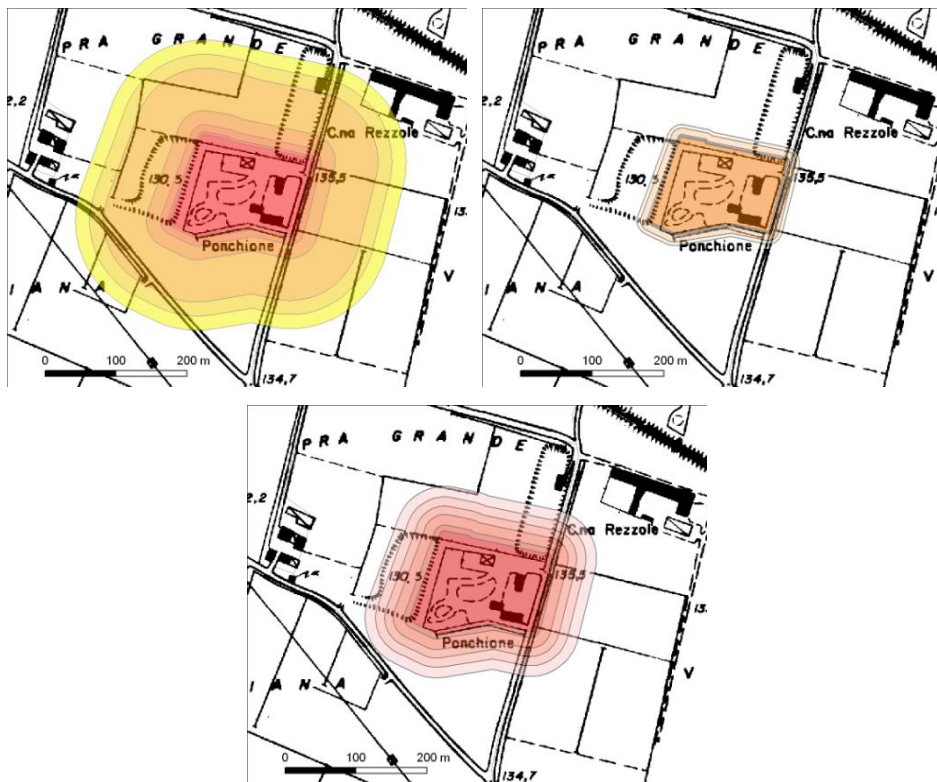


Fig. 21 a: Scenarios of industrial risk, plant n.1, TR = 2,949 Fig. b: Scenario TR =49,999 Fig. c: Scenario TR =99,999

Tab. 9. Vulnerability coefficients to industrial risk. From safety plans of the plants.

Accident	RADIUS (m)	SUBSTANCE	INTENSITY	expected damages	damage to buildings	damage to people
VCE	5	hydrogen	0.4 bar	high damages, demolition	0.90	0.90
VCE	10	hydrogen	0.15 bar	uninhabitable house, but repairable	0.50	0.50
VCE	20	hydrogen	0.04 bar	90% broken glasses	0.20	0.20
VCE	50	hydrogen	0.015 bar	50% broken glasses	0.10	0.10
UVCE	2	methanol	0.4 bar	high damages, demolition	1.00	0.90
UVCE	4	methanol	0.15 bar	uninhabitable house, but repairable	0.50	0.50
UVCE	13	methanol	0.04 bar	90% broken glasses	0.20	0.20
UVCE	60	methanol	0.015 bar	50% broken glasses	0.10	0.10
FF	7	GPL	37.5 kW/m2	damages to process machines	0.60	1.00
FF	30	GPL	12.5 kW/m2	high mortality - damages to structures, domino effects	0.30	1.00
FF	42	GPL	7 kW/m2	beginning of mortality	0.10	0.90
FF	55	GPL	5 kW/m2	irreversible lesions	0.10	0.70
FF	70	GPL	3 kW/m2	reversible lesions	0.10	0.40
VCE	6	GPL	0.8 bar	almost complete destruction,high mortality	0.95	1.00
VCE	10	GPL	0.4 bar	high damages, demolition, high mortality	0.90	1.00
VCE	20	GPL	0.3 bar	partial destruction,high mortality	0.60	1.00
VCE	40	GPL	0.14 bar	high mortality, mean damages to structures	0.40	1.00
VCE	100	GPL	0.07 bar	beginning of mortality	0.00	0.90
VCE	120	GPL	0.03 bar	irreversible lesions, 90% broken glasses	0.20	0.70
VCE	140	GPL	0.015 bar	reversible lesions, 50% broken glasses	0.10	0.40
FF	4	GPL	12.5 kW/m2	high mortality - damages to structures, domino effects	0.30	1.00
FF	6	GPL	7 kW/m2	beginning of mortality	0.10	0.90
FF	15	GPL	5 kW/m2	irreversible lesions	0.10	0.70
FF	20	GPL	3 kW/m2	reversible lesions	0.10	0.40
FF	86	propane	LFL	flammability limit, high mortality	1.00	1.00
FF	103	propane	1/2 LFL	1/2 flammability limit, lesions	0.50	0.60
FF	132	propane	LFL	flammability limit, high mortality	1.00	1.00
FF	158	propane	1/2 LFL	1/2 flammability limit, lesions	0.50	0.60
FF	140	propane	LFL	flammability limit, high mortality	1.00	1.00
FF	169	propane	1/2 LFL	1/2 flammability limit, lesions	0.50	0.60

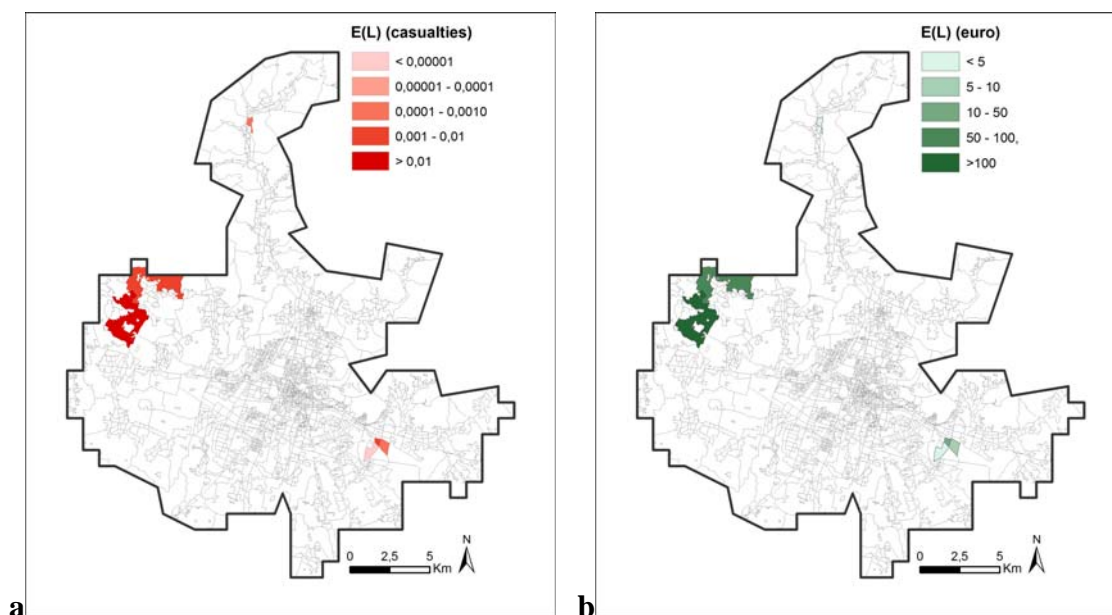


Fig. 22. industrial risk to a) people b) buildings

Tab. 10. Expected annual losses for industrial scenarios

		Monte Carlo Simulation	FOSM	Point Estimate
Economic	Range of E(L)	0-226 €	0-277 €	0-277 €
	Total loss	527 €	633 €	634 €
Societal	Range of E(L)	0-0.02 cas	0-0.02 cas	0-0.02 cas
	Total loss	0.035 cas	0.04 cas	0.04 cas

Tab. 11. Uncertain variables for industrial scenarios, and values for their coefficient of variation

Industrial to buildings	COV
Parcel area	$(area^{0.5})/10000$
N. buildings	0.4
Damage to buildings	0.4
Value euro m ²	0.333
P(E)	0.2

Tab. 12. Uncertain variables for industrial scenarios, and values for their coefficient of variation

Industrial to people	COV
Parcel area	$(area^{0.5})/10000$
N. affected people	0.4
Total n. people	0.4
Damage to people	0.2
Value euro m ²	0.333
P(E)	0.2

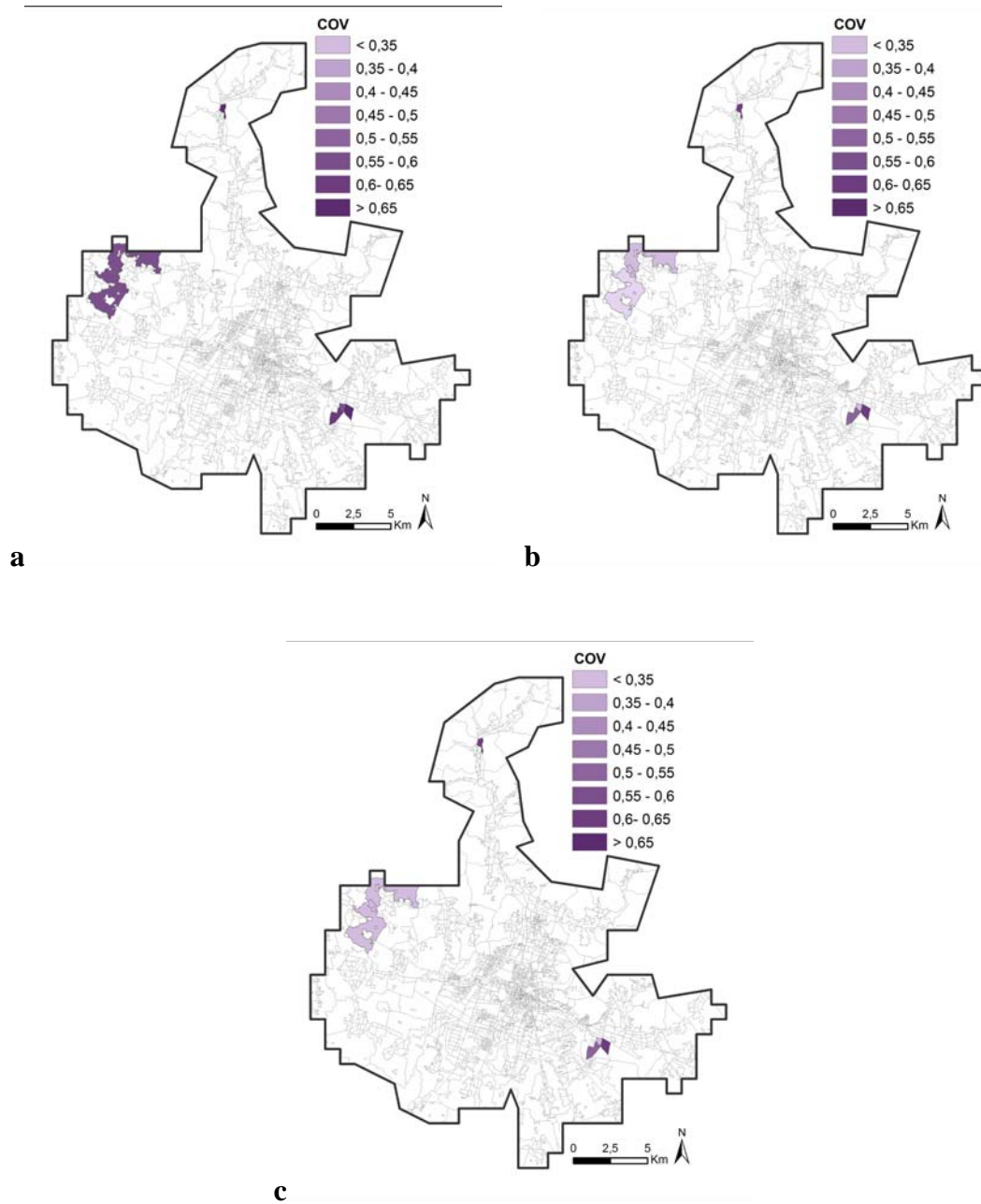


Fig. 23 COV values for industrial scenario economic risk a) Monte Carlo analysis, b) FOSM analysis c) PE analysis

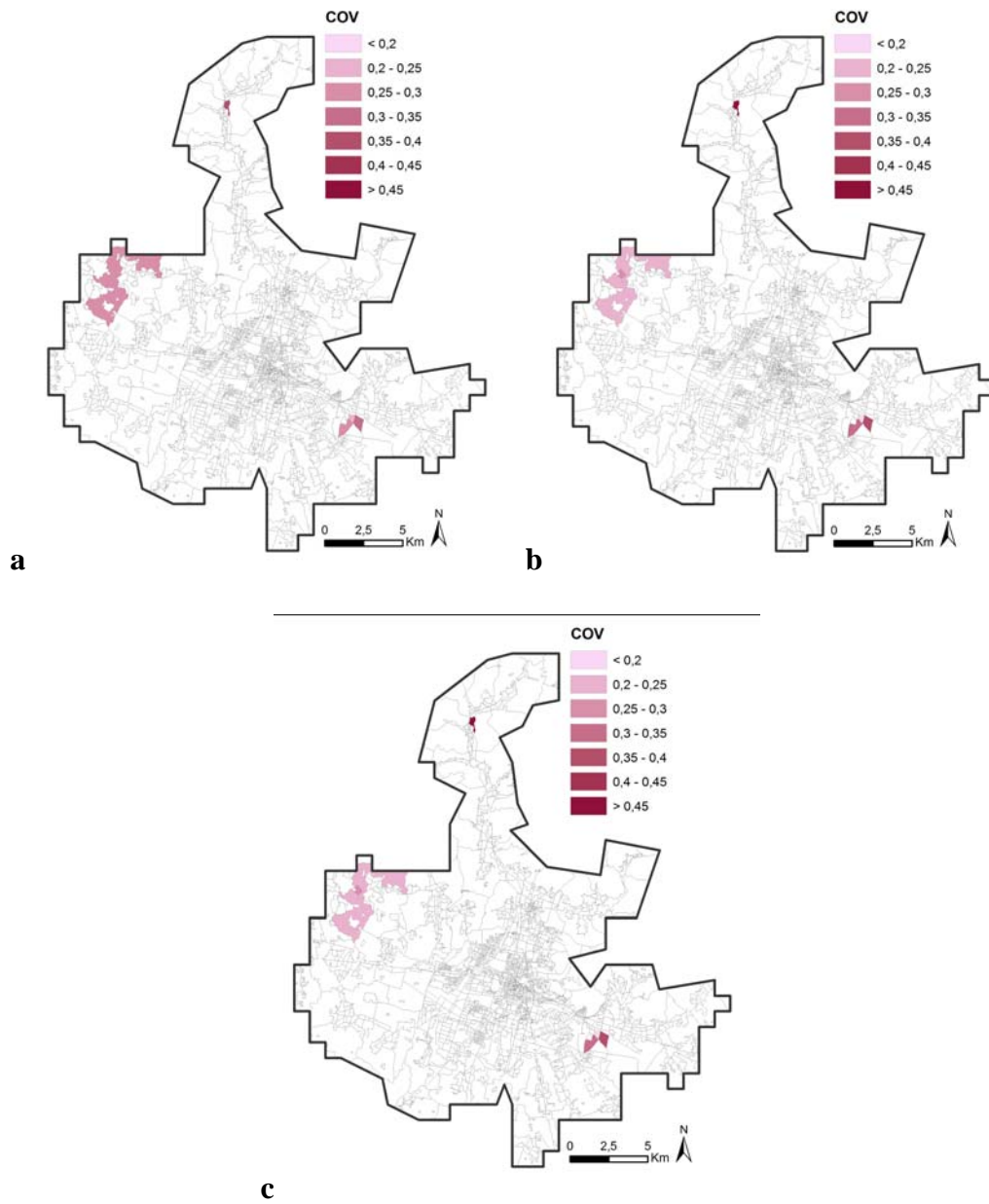


Fig. 24 COV values for industrial scenario societal risk a) Monte Carlo analysis, b) FOSM analysis c) PE analysis

Tab. 13. Values of Coefficients of variation on expected losses

	COV	Monte Carlo Simulation	FOSM	Point Estimate
Economic	Range	<i>0.57-0.7</i>	<i>0.31-0.62</i>	<i>0.31-0.61</i>
	Mean	<i>0.6</i>	<i>0.44</i>	<i>0.44</i>
Societal	Range	<i>0.24-0.4</i>	<i>0.18-0.46</i>	<i>0.16-0.46</i>
	Mean	<i>0.29</i>	<i>0.30</i>	<i>0.29</i>

As a result, FOSM, Monte Carlo simulations and Point Estimate show similar medium values of risk distributions. The slightly higher values for Monte Carlo simulation are probably due to the constraints imposed on the normal distributions of the variables, that cannot reach negative values and that consequently have been cut to positive ones. FOSM and Point Estimate do not account for the skewness of the distributions: in some cases the uncertainty is directional (e.g., toward lower values) and σ can be poorly significant with strongly asymmetrical distributions.

4 DISCUSSION AND CONCLUSIONS

4.2 RISK EVALUATION

In order to evaluate the risk level in the study area, F/D curves were built for the three risks, and then compared with the acceptability curves proposed by Baecher (1982b) (Fig.25), with damage economic values discounted to the present (by means of Consumer Price Index, discounted to 2008).

The expected loss due to earthquake is higher than what expected for the other events (Tab. 14). Industrial risk has a minor impact in the area, due to a low occurrence probability and a limited impact area. While industrial risk scenarios seem to be acceptable, flood risk is only marginally acceptable, and seismic risk scenarios are never considered as acceptable. For a more realistic evaluation of acceptability, an analysis of risk perception should also be made.

Regarding the assessment of economic risk, it should be stressed that the calculated risk is probably underestimated because it includes only buildings (i.e., lifelines and agricultural/natural resources are not included), without any discrimination according to use (e.g., an hospital has the same value per square meter of a private house). Moreover, the content of buildings have been considered only for residential buildings, neglecting other types of contents wich can have high value and a strong impact on the risk (e.g., industrial machineries, medical equipments).

The values assigned to the buildings was considered homogeneous for the whole study area. This is clearly an approximation, being the values of residential and productive structures strictly dependant on the exact location (e.g. big or small town, centre or suburbs, etc.). Hence, the spatial distribution of risk can be affected by this simplification.

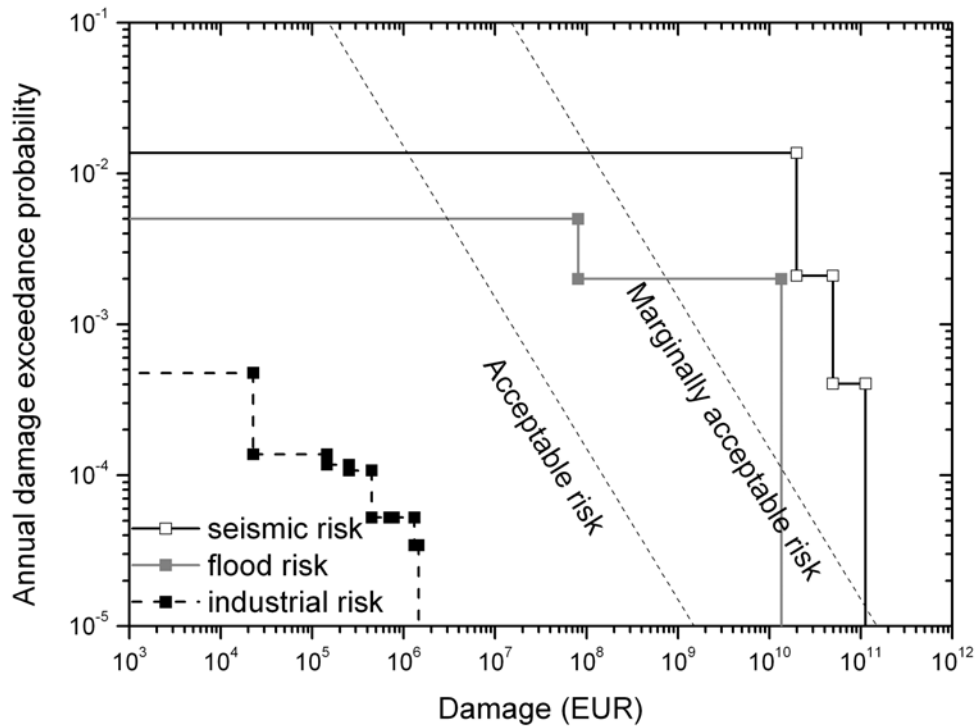


Fig. 25 F/N curves and acceptability curves for the analysed scenarios. The two dashed lines indicate the acceptable and marginally acceptable risk (Baecher, 1982b).

Tab. 14. Total expected annual losses for the scenarios, calculated on the whole study area by means of the three methods

	Flood TR 200y	Flood TR 500y	Seismic TR=75	Seismic TR=475	Seismic TR=2500	Industrial	Industrial societal
MC	403,988	27,835,015	271,382,935	101,985,550	51,861,136	527	0.035
FOSM	404,265	27,835,513	271,063,496	105,254,036	41,508,403	633	0.044
PE	404,136	26,955,987	271,219,806	106,700,628	42,712,092	634	0.044

4.3 UNCERTAINTY

The three methods for uncertainty assessment provide similar coefficient of variation of the output, ranging in mean from 0.28 to 0.6 (i.e., 28% and 60% of the expected value) (Tab. 15).

In the case of floods, a well defined relation exists between COV values and the distribution of the types of targets (e.g. buildings with 1 floor, buildings with two or

more floors, Fig. 26), due to the damage uncertainty, which is calculated based on the targets for each census parcel.

In general, the uncertainty evaluation performed by means of Monte Carlo Simulation is computationally more demanding, and time spending. Furthermore, the convergence of the simulation is quite difficult, and asks a very high number of samplings. The advantages of the method are related to the variety of distribution which can be chosen for the input variables, while in the deterministic approaches this is not possible. An advantage was found also in the possibility of truncating the distributions only to positive values (or to 0-1 values, in case of probabilities), where negative values have no physical meaning. The same operation can't be implemented easily in FOSM and PE methods. On the other side, these two methods are simpler, faster and provide however a good consistent result. FOSM requires the calculation of many derivatives, which in complex problems with many input variables can become a problem. In that case, a PE analysis should be preferred.

Tab. 15. Mean values of the coefficient of variation for the scenarios, calculated on the whole study area by means of the three methods

	Flood TR 200y	Flood TR 500y	Seismic TR=75	Seismic TR=475	Seismic TR=2500	Industrial buil	Industrial people
MC	0.36	0.36	0.34	0.34	0.35	0.6	0.29
FOSM	0.29	0.28	0.35	0.36	0.43	0.44	0.30
PE	0.36	0.40	0.35	0.34	0.37	0.44	0.29

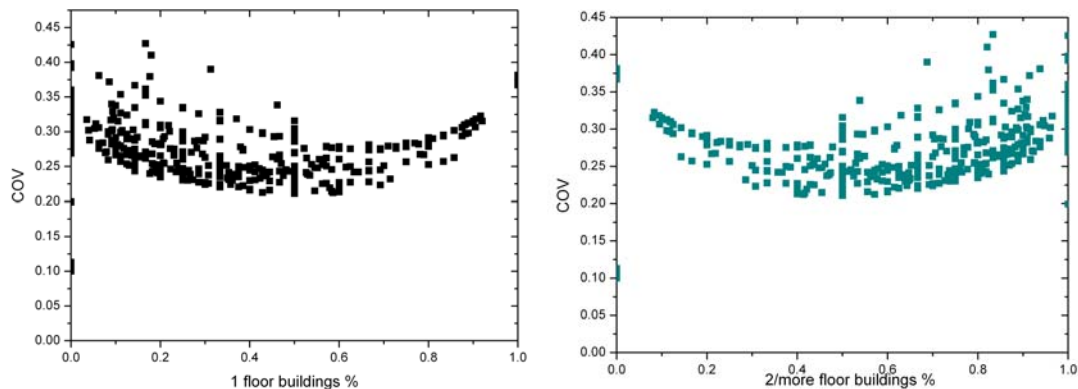


Fig. 26 Dependence COV – typologies of buildings for flood $T_R=500$ years scenario, evaluated by means of FOSM

PART IV

INDICATORS FOR PRIORITY AND EFFICACY EVALUATION OF MITIGATION WORKS

1 INTRODUCTION

This part of the study had the purpose of building a system of indicators for cost-efficiency evaluation of mitigation works, within the framework of risk prevention towards population, infrastructures and public structures safety.

The study for the definition of indicators of efficacy is focused on hydrogeological and wildfire mitigation strategies. The study leads to a methodology which is suitable for the evaluation of the efficacy and of the priority of mitigation projects presented by local administrations to the Regional Authorities.

This part of the thesis shows a state of the art of the available tools for work evaluation at the regional scale, the general objectives of the research, and the methodological scheme for the evaluation of the priority of actions aimed at risk mitigation.

2 PURPOSES OF THE STUDY

The purpose of this part of the research is to elaborate a system of indicators aimed at the evaluation of existing or planned mitigation works, as a function of their efficacy and economical convenience, with the purpose of a correct and functional use of the public economical resources. This tool could be useful in order to maximize risk mitigation, obtaining the maximum benefit for territory, goods and population. The tool can be used both in the evaluation of mitigation measures already realized (ex post), and in the preliminary evaluation of mitigation measures to be realized (ex ante). At the moment, the tool is implemented in Excel format. In the future, it will be developed for on-line usage.

The system is based on indicators, and the methodology is:

- easily applicable in all the different environmental conditions of Lombardy Region
- based on simple information already owned by the administrations
- adaptable to different work typologies

The methodology was applied to evaluate hydrogeological and wildfire mitigation works. For wildfires, a pre-existent regional model was available, which already offered a clear methodology to allocate resources and assess a priority (Piano Anti Incendio Boschivo).

Hydrogeological and wildfire risk are extremely different for distribution and impact on the territory, type of mitigation actions to be taken, and type of exposed elements. This has been taken into account in the choice of the indicators. As an example, hydrogeological risk can include both extremely localised events (sliding landslides), and spatially diffused events (rockfalls, shallow landslides). Moreover, wildfires include extremely variable phenomena, not easily predictable, whose mitigation is a function of many factors (e.g. distribution of monitoring networks, land use, vegetation, availability and distance of firemen).

Local and territorial administrations were involved in the definition and choice of indicators and in the assignment of their weights.

3 EXISTING PRACTICES IN LOMBARDY REGION

3.1 HYDROGEOLOGICAL RISK

Most of economic resources for the realization of mitigation works derive from the Italian Government, the Regions, or the local administrations and Basin authorities, through specific laws (L. 102/90 Valtellina, L. 267/98 Sarno, L. 183/90, Fondo di Protezione Civile L. 225/9 ...) and ordinances (various in 2000, 2002, 2003, 2004...). Lombardy Region allocates also its own funds (Pronto Intervento l.r. 34/73) to face very urgent events, when public or private safety is in danger, or when an interruption of strategic infrastructures (hospitals, streets, aqueduct, and drainage systems) is possible.

The regional law 5 January 2000, n. 1, art.3, assigns to the provinces, municipalities and mountain communities the functions related to project development, realization and management of mitigation works, included monitoring, prevention, emergency systems. Provinces and municipalities with more than 20.000 inhabitants provide in autonomy with their own funds to the realization of the works. Only in case of difficulties in the budget of the municipality, the Region can participate in financing the projects for a maximum of 50% of the whole cost.

When a disaster occurs the local administration have to perform a first recognition of the impacted area. The report is then validated by Lombardy Region that starts the financing procedures.

The activation of the financing procedures includes:

a) For works cheaper than 75.000 €, if the conditions requested by regional law 34/73 are present, the maximum urgency is approved. In this case, the local administration can contribute for a maximum import of € 75,000.

b) for works from 75,000 € to 150,000 €, for the part of the cost exceeding 75.000 €, the financing can be partial, and dependant on funds availability. When the Region cannot afford the whole cost, the exceeding import is covered by the local administration.

The assignment of a priority for the realization of the works, derives from a technical-political-territorial-economical evaluation of the work and of the territorial context, allowing to compare different requests. This occurs with non scientifically based qualitative criteria.

In terms of risk reduction, until now, an ex-post evaluation of the mitigation work is not codified. The only aspects that are now monitored are the administrative-financial aspects.

3.2 WILDFIRE RISK

At the regional level, the management of the wildfires mitigation works is treated in the *Piano regionale delle attività di previsione, prevenzione e lotta attiva contro gli incendi boschivi*, D.g.r. 27 december 2006 n. 8/3949. In the document, a methodology is

defined to help the allocation of the resources and the assessment of the priority of the works.

Base Areas are defined, i.e. territorial units chosen for the zonation and organization of anti-wildfire services. They are coincident with Mountain Communities in mountainous areas, with Provinces for the other parts of the regional territory. For each Base Area, two indicators are jointly evaluated:

1. **risk class**, that leads to the individuation of a priority scale with respect to risk management. Three groups of Base Area corresponding to three risk classes are detected.

Class 1: Wildfires of limited extension and relatively sporadic.

Class 2: Quite frequent wildfires, some of wide size

Class 3: Frequent wildfires, maximum territorial impact

2. In the Plan, the **work classes**, used to allocate the resources, are defined basing on the Work Coefficient (CDI). It summarises four other coefficients:

- Repartition coefficient (CR): proportion of the burnt surface in the Base Area with respect to the total burnt area in the Region.
- Incidence coefficient (CI): territorial incidence through the ratio between the surface actually burnt and the surface potentially burnt for each Base Area
- Relative Extension coefficient (CER): dimension of the potentially burnable for each Base Area with respect to the average potentially burnable surface of all the base areas.
- Park surface coefficient (CP): distribution of all types of protected natural areas. The coefficient can score three values:
 - o Base Areas with protected area less than 30%: CP = 1;
 - o Base Areas with protected area from 30% to 49%: CP = 1,2;
 - o Base Areas with protected area higher than 50%: CP = 1,5.

The repartition of the regional economical resources, is calculated in percentage terms for each Base Area through the ratio:

$$REPARTITION\% = \frac{CDI_{AdB}}{\sum CDI_{AdB}} \cdot 100 \quad (1)$$

where:

Repartition %: repartition in percentage of the resources

CDI_{AdB} : Work Coefficient of the Base Area

For a detailed description, see *Piano regionale delle attività di previsione, prevenzione e lotta attiva contro gli incendi boschivi*, D.g.r. 27 december 2006 n. 8/3949. It is worth noting that the criteria described above are independent from the typology and quality of the mitigation work that each Base Area plans for its own territory. In other words, the repartition is based only on territory characteristics, not on properties of the mitigation measures.

The contribution of the present work consists in the attempt of introducing also the project characteristics as a criteria for budget allocation and priority assessment.

4 METHODOLOGY

The methodology proposes three levels of evaluation of mitigation measures. The first consists in a general description of the territory where the work is situated, with the objective of detecting the major risk sources and define the risk level in the regional context.

The second level includes a multicriteria analysis based on indicators. Each indicator contributes with a score in defining the overall importance of a work, which is expressed explicitly in a synthetic index. This index expresses the existing relationship between the costs to afford and the capability of the work of pursuing the objective of safety.

The third level consists in a Cost-Benefit analysis, that evaluates both the ratio between expected costs and benefits (cost-benefit ratio, CBR), and the Net Present Value, (NPV).

At the moment, the methodology is supported by some Axcel worksheets. This guarantees a wide diffusion and a simple utilization of the tool, and allows an easy collection and utilization of the data. This is a temporary solution, adequate to this experimental phase of the work.

In the following, the worksheets will be described together with the information that the compiler need to provide.

4.1 LEVEL 1: RECOGNITION OF RISK LEVEL

The first part of the tool requires to input general information about the study area. In particular:

- the local administration proposing the work, the province, the mountain community
- the municipality, that is connected with the results of the risk analysis performed in Part I. The results of risk analysis at the municipal, provincial or mountain community level are then automatically shown on the worksheet, such as the number of inhabitants (tab...)
- the proposing administration
- the exact geographical location
- the exact coordinates of the place where the work will be located

In this phase, the level of risk of the area is shown, accounting for all the risk typologies analysed in Part I, referred both to the administrative unit, and to the 1 km² cell of PRIM. In particular, the level of each physical and total risk, and the value of the area (in terms of economical, human life, and environmental) are shown, normalised for the average regional value.

The resulting level of risk is very useful to contextualize the problem, to evaluate its relevance with respect to other similar areas of the region and at the same time to

verify that the work is not going to be realised in an area that should already be subjected to some mitigation measures or planning.

4.2 LEVEL 2: MULTI CRITERIA ANALYSIS

Multi criteria analysis allows to analyse and take into account very heterogeneous elements (people, works, costs, damages), to compare complex situations and evaluate importance and relevance. This level consists in two different sheets, one for each risk typology: hydrogeological (landslides, avalanches, floods) and wildfires. In each sheet there are qualitative information to be introduced, from a list, and quantitative values.

The methodology implies the evaluation of four indexes: scenario, I_s ; event, I_e ; work, I_o ; and project, I_p . Each index is calculated as the weighted sum of the respective indicators, scaled between 0 and 100:

$$I = \frac{\sum_{j=1}^n p_j i_j}{\sum_{j=1}^n p_j} \quad (2)$$

where I is the index, i the value of the j -*esim* indicator and p the j -*esim* weight. The four indexes are then aggregated by means of a weighted sum to calculate the complexive efficacy index of the work, I_{eff} .

All tables and values are shown in Appendix I.

- *Scenario index*

This index defines the scenario of risk represented by one or more events potentially occurring. The scenario indicators are referred to the occurring probability of the event, the spatial extension of the processes, and the exposed elements. The index expresses the criticality of the territory.

- *Event index*

Event indicators are related to the most recent and most significant event occurred in the analysed area. This is important because in most cases it is the direct reason why the work is proposed.

- *Work index*

It qualifies the mitigation work in terms of efficacy, efficiency and exhaustivity. Furthermore, the index quantifies the costs connected with the realization and the maintenance.

- *Project index*

It resumes the information related to the project phase and to the problems connected to its realization.

4.2.1 INDICATOR WEIGHTING

For indicators weighting, the AHP method has been used (Saaty, 1980).

The weight of each indicator is the result of a couple comparisons with respect to each of the other indicators referred to the same index (scenario, event, work, and project). The comparison is made by means of expert judgement. Thanks to the redundancy of the judgement expressed by the experts, AHP method generates weights that result to be not very sensitive to evaluation errors, and allows to verify the consistence of the coefficient matrix.

Weights have been obtained by the performance of AHP by all the experts involved in the research (for AHP method and application, see Part I) (Tab.1).

Tab 1. List of the indicators for the analysis of second level

Class	Indicators	weight
Scenario	Typology of the potential-occurring phenomenon	-
	Probability of occurrence	6.69
	Presence of strategic/relevant elements	7.12
	Presence of previous mitigation work	no
	Efficacy of previous mitigation work	6.61
	Actualised cost of previous mitigation work	2.83
	Scenario area	4.77
	Population exposed (per day)	-
	Population exposed in transit (per day)	-
	Population exposed temporarily (per day)	-
	Equivalent population in the scenario area	14.31
	Value of the exposed elements (reference table)	7.08
	Potential damage to exp. elements without interv. (% of value)	8.5
	Vulnerability of people in the scenario area	17.21
	N. historical events	5.63
	Damage induced by historical events	7.46
	N. deaths/injuries induced by historical events	11.79
Event	Event area	14.18
	Damages to exp. Elements induced by the event	29.68
	N. deaths/injuries induced by the event	56.14
Work	Typology of work (structural/non structural)	-
	Protected area	4.54
	Cost of the work	3.49
	Maintenance lifetime cost (% of the cost of the interv.)	3.28
	Spatial exhaustivity with respect to the scenario	6.82
	Efficacy % (function for which it is built)	11.11
	Efficiency % (work characteristics)	6.93
	Indirect costs avoided with the work	5.98
Relevance of the opera	5.31	

	Environmental impact	4.18
	Population exposed protected by the work(per day)	-
	Population exposed in transit protected by the int. (per day)	-
	Population exposed temporarily protected by the int. (per day)	-
	Equivalent population in the protected area	13.49
	Value of the exposed elements protected (reference table)	8.33
	Avoided damage to protected elements (% of value)	9.28
	Vulnerability of people in the protected area	17.26
Project	Authorizations required	12.05
	Project level	22.54
	Technical reports required	15.22
	Need for expropriation	18.97
	Financing and realization procedure	16.36
	Realization time	14.86

No weight is expressed for the indicators having the purpose of just describing the context (e.g. ‘typology of the potential-occurred phenomenon’, or ‘presence of previous mitigation work’), or for indicators becoming input data for numeric calculations (e.g. ‘population exposed per day’).

4.2.2 HYDROGEOLOGICAL INDICATORS

For ‘work’ both the project in its complexity (also when it is composed by more than one structure) or, in the case of an already-existing work, the existing structures, are intended. In both cases, only one sheet is to be filled.

No weight is expressed for the indicators having the purpose of just describing the context (e.g. ‘typology of the potential-occurred phenomenon’, or ‘presence of previous mitigation work’), or for indicators becoming input data for numeric calculations (e.g. ‘population exposed per day’).

- **Typology of work (structural/non structural)**

Indicates the structural or non structural nature of the work. Mitigation measures can be active, when they act directly on the hazard source, or passive, including all the other kind of works realised on the territory in order to mitigate the risk. Non structural works mitigate the risk in an indirect way, without physical actions on the area (e.g. information, education, etc.)

- **Typology of the potential-occurring phenomenon.** It refers to the most significant kind of event that endangers the area.
- **Probability of occurrence**

Evaluation of the probability, in qualitative terms (very high to very low) of the phenomenon. It is an important indicator since the benefits introduced with the work (including avoided losses) are proportional to this probability. For hydrogeological risk, the probability is indicated based on the expected return time of the event, and calculated with poissonian probability in 100 years.

- **Scenario area**

The area of the scenario is a key indicator for the evaluation of a work. It corresponds to the area that, based on the available knowledge of the phenomenon and on the direct experience, and given a certain occurrence probability, would be directly impacted, with possible direct damages to people and structures. The value of the vulnerable elements belonging to this area, in fact, influences the importance and the priority of the work.

It is however possible to project for the same scenario different works, to whom in general different final scores will correspond. It is also possible to hypothesize different scenarios, with different return times and occurrence probabilities. For landslide events, the area of the scenario can be detected quite easily. In the case of floods, the evaluation is more complex, and the area must be detected through spatial continuity, geomorphology, and triggering causes.



Fig.1. Example of Scenario area, Municipality of Varenna (300.000 mq)

- **Presence of strategic/relevant elements**

Shows if in the area of the scenario are located strategic elements, as defined in the d.d.u.o. 19904, 21/11/2003. All public buildings are strategic or relevant, such as the infrastructures if their interruption causes big problems and high indirect costs: es. an important street or the only access to a settlement.

- **Presence of previous mitigation work**

Indicates if mitigation works have already been realised in the scenario area. This indicator is not used in the calculation.

- **Efficacy of existing mitigation works**

Expresses the effective capability of the previous works in mitigation. The evaluation is based on expert knowledge and expressed in qualitative terms.

- **Actualised cost of previous mitigation work**

Expresses the actualised value of the mitigation works already existing in the area. A higher score is attributed to works realised in contexts where the previous investments were smaller.

- **N. historical events**

It's the number (estimated or known) of the past events occurred in the scenario area. A higher score is given to works realised where the event frequency is high.

- **Damage induced by historical events**

It's the expected and actualised cost related to the damages of known historical events. It is in general a difficult data to obtain: the local administration usually doesn't collect it. It must be estimated by the proposer, based on available historical sources (catalogues, professional studies). If an area had in time high losses, a higher score is assigned to the proposed work.

- **N. deaths/injuries induced by historical events**

Expresses the number of casualties, injuries or missing people as a consequence of the historical events occurred in the scenario area.

- **Population exposed (per day)**

Expresses the number of all the people living in the scenario area. It includes:

- inhabitants
- people in transit (on streets, railways...)
- people temporarily present (for work, ceremonies...)

The calculation is performed through a formula. Inhabitants are considered present for 16 hours per day in the area, people in transit for 0,2 hours, temporary people for 8 hours.

- **Vulnerability of people in the scenario area**

Qualitative index expressing the expected damage to people involved in an event. For instance, rockfalls and debris flows have high vulnerability indexes (are very dangerous for people), while a lacustrine flood the index is almost null (people have all the time to move to safer areas).

- **Value of the exposed elements**

Estimate of the value of all the goods located in the scenario area.

- **Potential damage to exp. elements without works (% of value)**

Percentage of the value of goods located in the scenario area that would be lost in case of an event.

- **Event area**

Area (expressed in m²) interested by an event (landslide, avalanche or flood), if existing. It corresponds to the area of the last event that induced the need of a mitigation measure. When the proposed work is a preventive one, the event area does not exist.



Fig.2. Exemple of event area (in yellow, almost 30.000 mq) and scenario area (in red) in the Municipality of Varenna (LC)

- **Damages to exposed elements induced by the event**

Estimate of all damages of the vulnerable goods in the event area, included evacuation costs.



Fig.5. Buildings damaged by the landslide of July 2008 in Colorina, Sondrio

- **N. deaths/injuries induced by the event**

Number of casualties and injuries as a consequence of the event.

- **Protected area.** The area (in m²) of influence of the work.



Fig.3. Example of protected area (in yellow, almost 48.000 mq) and of scenario area (in red), Municipality of Varenna

- **Cost of the work**

Cost of the work or of the group of proposed works. Classes of cost are indicative, and they are inspired by regulations of the Regional Administration (< 75.000 €; 5.000.000 €).

- **Maintenance lifetime cost (% of the cost of the work)**

Percentage value of the cost of the work due to its maintenance during its life.

- **Spatial exhaustivity with respect to the scenario**

Completeness of the work in terms of length – width, inside the scenario area. As an example, a rockfall protection net with a length of 100m protecting a scenario area of 100 m is 100% exhaustive. An embankment of 70 m of length protecting 140 m of cliff, has a 50% of exhaustivity (Fig.4). If it is not possible to exactly define the protected surface with respect to the exposed one, an approximated value can be assigned.

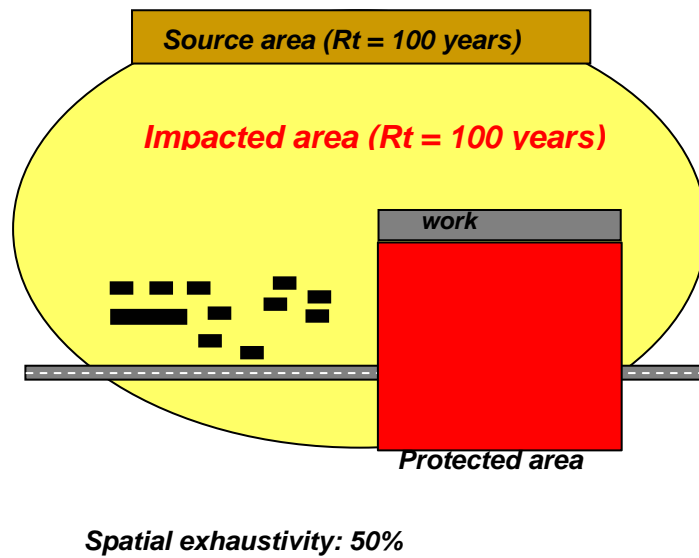


Fig.4. The concept of spatial exhaustivity.

- **Efficacy % (function for which it is built)**
Utility of the work and adequacy for the purpose it was built. It's a parameter including different factors(choice of work typology, design, dimensioning).
- **Efficiency % (work characteristics)**
State of the work, independent from the context in which it is located, considering the degree of response to its functions, and its physical-structural state (conservation, maintenance).



Fig.5. Example of non efficient dike (broken in the central part), Lanzada (Sondrio).

- **Indirect costs avoided with the work**

Indirect costs that the work will avoid in the future. Indirect costs represent the damage that the community and the territory could have, deriving not only from the loss of the goods, but also from the indirect induced damages (interruption of streets, limitations to accessibility, etc.)

- **Relevance of the work**

Strategic or ordinary (defined by d.d.u.o. 19904, 21/11/2003). Public buildings are strategic or relevant, such as the infrastructures that if interrupted generate strong losses of functionality and services. Works with strategic relevance are preferred.

- **Environmental impact**

Qualitative estimate of the environmental impact of the work. If it is negligible, the score of the indicator is high.

- **Population exposed protected by the work (per day)**

People present in the protected area, each day. It includes:

- inhabitants
- people in transit (on streets, railways...)
- people temporarily present (for work, ceremony...)

The calculation is performed through a formula. Inhabitants are considered present for 16 hours per day in the area, people in transit for 0,2 hours, temporary people for 8 hours.

- **Value of the exposed elements protected (reference table)**

Estimated value of all the goods located in the scenario area.

- **Avoided damage to protected elements (% of value)**

Percentage of damages potentially avoided in the area protected by the work.

- **Vulnerability of people in the scenario area**

- **Authorizations required**

Complexity of authorization procedure for the approval of the project. Works with a simplified and easy procedure are preferred. The procedure is ordinary if only ordinary administration authorizations are required, complex if the area is submitted to paesistic or hydrogeological constraints, environmental impact evaluation, etc.

- **Project phase**

Phase of the project realization. It can be indicative of the time necessary to develop and realise the project, and of its uncertainty. Where a project is already at the executive phase, a higher score is assigned.

- **Technical reports required**

Technical supports to the project which does not require supplementary technical report are preferred.

- **Need for expropriations**

Indirect indicator of the time needed for the realization of the work. When there is no necessity of expropriation, realization time is shorter, th procedure simpler.

- **Financing and realization procedure**

Financing procedures with respect to regional and national laws. The procedure indirectly influences the realization time and the administrative effort. Projects with extraordinary financing procedures or UE funds are preferred, with respect to works financed with only ordinary regional funds.

- **Realization time**

Expected time for work realization. Projects that can be realised in a short time are preferred.

4.2.3 WILDFIRES

In the case of wildfires, the indicators are in general referred to the Base Area, the territorial units on which the anti-wildfire activity is organised on the territory.

Indicators accounting for the description of the phenomenon in this case are not needed, because only one process is taken into account.

Tab.2. List of indicators of multi criteria analysis for wildfire risk

Class	Indicator	Weight (%)	
Scenario	Probability of occurrence	1.5	
	Risk class of the base area (Piano AIB)	1.73	
	Work class of the base area (Piano AIB)	2.43	
	Presence of strategic/relevant elements	3.16	
	Presence of previous mitigation work	-	
	Efficacy of previous mitigation work	1.51	
	Actualised cost of previous mitigation work	0.97	
	Scenario area	2.85	
	Population exposed (per day)	-	
	Population exposed in transit (per day)	-	
	Population exposed temporarily (per day)	-	
	Equivalent population in the scenario area	11.22	
	Vulnerability of people in the scenario area	8.4	
	Volunteers exposed and involved in activities in scenario area	15.36	
	Vulnerability of volunteers in the scenario area	12.04	
	Value of the exposed elements (reference table)	3.43	
	Potential damage to exp. elements without interv. (% of value)	2.34	
	Value of the forest exposed	4.05	
	Presence of natural protection regime	4.4	
	N. historical events	1.5	
	Damage induced by historical events	1.31	
	N. deaths/injuries induced by historical events	9.2	
	N. deaths/injuries among volunteers induced by historical events	12.6	
		Event area	4.06
	Event	Damages to exp. Elements induced by the event	7.2
		N. deaths/injuries induced by the event	44.37
N. deaths/injuries among volunteers induced by the event		44.37	
Typology of work (structural/non structural)		no	
		-	
Opera	Protected area	2.96	
	Cost of the work	2.05	

Maintenance lifetime cost (% of the cost of the interv.)	1
Spatial exhaustivity with respect to the scenario	2.48
Efficacy % (function for which it is built)	4
Efficiency % (work characteristics)	2.23
Indirect costs avoided with the work	2.43
Relevance of the opera	3.7
Environmental impact	3
Population exposed protected by the work(per day)	
Population exposed in transit protected by the int. (per day)	
Population exposed temporarily protected by the int. (per day)	
Equivalent population in the protected area	13.52
Vulnerability of people in the protected area	16.2
Safety of the volunteers in the protected area	18.28
Vulnerability of the volunteers in the protected area	16.8
Value of the exposed elements protected (reference table)	3.89
Avoided damage to protected elements (% of value)	5.06
Value of the forest protected by the work	2.4

- **Probability of occurrence**

For wildfires, the occurrence probability is expressed in terms of frequency of the event, i.e. the number of wildfires per year each 10 km². The data derives from the anti-wildfire regional plan for each Base Area referring to the historical series 1996-2005.

- **Risk class of the base area**

For a methodological continuity with the Regional Plan, the class of risk is taken into account. It is a determining indicator for the allocation of the available budget and the priority of the works. A higher score is assigned to high risk areas.

- **Work class of the base area**

Similar considerations can be done for the work class of Base Area defined by the Regional Plan. The work class is defined based on the incidence of the phenomena for each Base Area: higher scores are assigned to high work class areas.

- **Scenario area**

Surface potentially covered by fire. For its definition it is necessary to refer both to topographic or structural elements, able to control the propagation of fire (e.g. topographic divides, roads, rivers, etc.), and to operative strategies already active on the area (availability of volunteers, helicopters, airplanes, etc.). The scenario must include also a reasonable buffer (100 m) of interface between vegetation and settlements that could be damaged in case of wildfire.

- **Presence of natural protection regime**

The realization of a work in the framework of a protected area has a supplementary value, because it contributes to follow the objective of conservation and safety of an area that is considered valuable and important for its environment. The related score depends on the typology level of natural protection.

4.3 LEVEL 3: COST-BENEFIT ANALYSIS

The third level of the analysis consists in cost-benefit analysis. The method is inspired by the one implemented by FEMA (2006), which includes three different levels of analysis, to be chosen based on the available level of detail of data: *Very limited data*, *Limited data* and *Full data Module*.

With respect to the level of data available in Lombardy, the BCA that can be performed can be defined between *Very limited data* and *Limited data*.

However, there are many differences in the Italian and American socio-economic context: many data related to intensity-frequency relationship are not available in Italy, while they are public in USA. In the same time, public services in USA are often located in private structures, while in Italy it is the opposite: the evaluation of indirect costs must account for these differences.

4.3.1 B/C RATIO

The ratio between the benefits induced by the work (in terms of goods, people saved and indirect cost avoided), and the costs for realization and maintenance of the work, as:

$$\frac{\text{Benefit}}{\text{Cost}} = \frac{(\text{Direct losses avoided} + \text{Indirect losses avoided} + \text{people saved}) * P}{\text{Work cost} + \text{maintenance cost}} \quad (3)$$

P = occurring probability of the phenomenon

Direct losses = $E * V * L_T$

E = m² exposed for each type of element

V = value for m² in euro for each type of element

L_T = % of the exposed value lost in case of event

4.3.2 NET PRESENT VALUE, NPV

The difference between benefits and costs express the net benefit of the work, i.e. Net Present Value:

$$\text{NPV} = \left((\text{Direct losses avoided} + \text{indirect losses avoided} + \text{people saved}) * P \right) - (\text{Work cost} + \text{maintenance cost}) \quad (4)$$

4.3.3 NET BENEFIT/TOTAL COSTS OF THE SCENARIO

It compares the potential costs in case of event in presence and in absence of the work.

$$\frac{\text{Net Benefit}}{\text{Total Scenario Costs}} = \frac{(\text{Work benefits} - \text{Work Total Costs})}{\text{Costs without work}} \quad (5)$$

Where the benefit of the work is calculated as:

$$\text{Work benefit} = (\text{direct losses avoided} + \text{indirect losses avoided} + \text{people saved}) * P$$

The total cost of the opera is:

$$\text{Work total cost} = \text{work cost} + \text{maintenance cost} \quad (7)$$

The total costs of the scenario in absence of the work have been calculated as:

$$\text{Cost without work} = (\text{direct losses} + M) * P \quad (8)$$

where:

M = Economic value associated to potential casualties and injuries in the area exposed to the phenomenon, calculated based on the equivalent people present each day in the exposed area (see later on).

The direct losses avoided by the work, that is the benefits, must be multiplied by the probability of occurrence of the phenomenon, while costs are certain.

For works related to slope instability and for punctual works related to wildfire prevention, the benefits are represented by the safety of a portion of territory. In detail, all soil use typologies, services and infrastructures are considered, as protected surfaces, whose total value is calculated on the basis of the unit m² value used in PRIM.

In the case of works for the prevention of wildfire extended on the territory, the focus is on the wooden surface, testing the application of a methodology that explicit the multifunctional value of the forest: productive, protective, environmental, landscape, didactic, experimental and historical- cultural.

The economical quantification of the functions of the woods is particularly complex, mostly if applied to wide areas showing different situations and influences of different intensity.

4.3.4 DATA NEEDED FOR COST-BENEFIT ANALYSIS

- **Occurrence probability**

For hydrogeological risk, the probability is indicated based on the expected return time of the event, and calculated with poissonian probability in 100 years.

For wildfires, the occurrence probability is expressed as the frequency of occurrence of the event, referring to the number of wildfires per ear each 10 km² deriving from the Regional anti-Wildfire Plan for each Base Area in the period 1996-2005.

- **Work cost**

The exact cost in euro is provided by the operator, if known. In case it is not known, it can be expressed as a range of values, and considered in the calculation as the mean value of the range.

- **Project lifetime**

The expected lifetime of the work is directly provided by the operator. The consequent benefits will be calculated referring to this period of time, such as the maintenance costs.

- **Maintenance costs**

Maintenance costs per year are actualised through a discount rate defined by Lombardy Region with respect to the economic context, on the basis of the lifetime of the work.

- **Exhaustivity**

The indicator of exhaustivity expresses the percentage of the total problem solved by the introduction of the opera. It is used for the calculation of the protected value in the case it is not possible to exactly quantify the surfaces of the exposed elements.

- **Indirect losses avoided by the work**

The indirect losses avoided by the work are expressed as classes of values directly by the operator: the mean value is considered for the calculation. As for benefits and maintenance costs, indirect losses are actualised through a discount rate defined by Lombardy Region with respect to the economic context, on the basis of the lifetime of the work.

- **Type/quantity of the exposed elements**

The description of the exposed elements is used to calculate the direct losses avoided by the work. It is performed through some simple tables where the main categories of the exposed elements are listed, and the operator inserts the number, the surfaces and eventually the degree of loss. The economical mean value of each unit of surface of each element is pre-defined, based on economic data of the study area, and it is however modifiable.

Eventually, the data accounting for the localisation of the work (municipality, province) could be used to perform a more detailed regionalised analysis of the costs of the goods, differentiated for local contexts, in order to redefine corrected values for each different zone.

- **Economical losses avoided by the work**

Direct economical losses avoided by the presence of the work are calculated through the input of the surfaces belonging to the protected area, the calculation of their value and of the percentage of value lost in case of event (this parameter indicates in indirect way the efficiency of the work).

$$\text{Direct losses avoided} = A \cdot V \cdot L_p \quad (10)$$

A = m² protected for each element

V = value per m² in euro for each type of element

LP = % lost value in case of event

- **People saved through the work**

A quantification of the benefit deriving from rescued people is performed. The number of residents, of workers of different productive sectors and the number of people in transit is multiplied for a time index representative of the duration of the permanence in the safe area (8/24 for temporary people, 0.2/24 for those in transit, 16/24 for residents); in this way it is possible to calculate an equivalent number of people present in the area per day. The resulting value can be evaluated economically as a function of the estimated value of a human life.

The number of equivalent people damaged by the event is obtained multiplied the equivalent people for the percentage of deaths or injuries expected, defined by the operator:

$$\text{Damaged people} = \left(n.\text{resident} * \frac{16}{24} + n.\text{temporary} * \frac{8}{24} + n.\text{in transit} * \frac{0.2}{24} \right) * \% \text{deaths / injured}$$

The number of damaged people has been monetized considering an economical value of 1,000,000 euros per person (GEO, 1998; Fichs and McAlpin, 2006; Jonkman, 2006; Porter, et al. 2006), corrected for P (occurrence probability of the event).

5 APPLICATION

The application of the methodology and of the tool here presented was performed for some mitigation works by the operators of the General Direction of Civil Protection of Lombardy.

At the moment, the methodology of level 2 (multicriteria analysis) was applied on 21 works. For two case studies, more than one alternative is evaluated. The methodology of level three (cost-benefit) was applied only on two works: Fiumelatte (LC) and Cortenova (LC). This is mainly due to the difficulty in collecting the necessary data.

Tab.3. List of works to be evaluated in the training step by means of the proposed methodology.

Number	MUNICIPALITY	RISK	DESCRIPTION	SCENARIO INDEX	EVENT INDEX	WORK INDEX	PROJECT INDEX	EFFICIENCY INDEX
1	Colzate (BG)	1	Diffused rockfalls on residential area and road. Maintenance for works and road.	55.14	48.13	51.63	82.3	56.38
2	Santa Brigida (BG)	1	Reinforcement of flooded chalk quarries	64.53	11.48	32.92	82.3	44.67
3	Saviore dell'Ada-mello (BS)	1	Preliminar geotechnical analysis for slope stabilization	55.07	30.57	49.63	70.72	49.46
4	Braone, Ceto, Niardo (BS)	2	Forest improvement in degraded soils	28.05	4.78	16.45	80.98	26.65
5	Cremia (CO)	2	Realization of a water basin for helicopter anti wildfire service	24.96	3.76	69.45	80.98	39.61
6	Como	1	Realization of a floodgate	57.15	18.7	94.44	94.06	62.48
7	Bordolano (CR)	1	Stabilization of river Oglio Scarp to protect residential areas	51.09	9.35	80.68	98.87	55.09
8	Cremona	1	Delocalization of a camping	39.46	14.44	79.22	92.53	51.40
9	Crotta d'Adda (CR)	1	Lateral erosion and landslide on the scarp, involving an urbanised area. Completino of existant works and stabilization of the foot of the slope	59.56	20.38	79.5	94.06	59.68
10	Colico-Dorio (LC)	1	Geotechnical analysis and landslide monitoring	55.2	73.29	52.57	69.85	61.45
11	Cortenova (LC)	1	Landslide monitoring. Stabilization of slope	70.68	42.44	89.91	83.44	70.27
12	Varenna A (LC)	1	Extremely urgent realization of a rockfall embankment	62.58	68.06	61.05	98.48	68.95
13	Varenna B (LC)	1	Realization of rockfall embankment and completion of	62.58	68.06	83.05	78.55	71.89

			rockfall embankment					
14	Boffalora d'Adda (LO)	1	realization of an embankment for River Adda					
15	Vari comuni (LO)	1	Twinning between evacuated and hosting municipalities in case of river Po flooding	62.27	20.12	78.11	97.35	60.59
16	Nerviano-Rho (MI)	1	Realization of a basin					
17	Bussero-Gorgonzola (MI)	1	Realization of a basin					
18	Casaloldo (MN)	1	Realization of a filling channel for the protection of a residential area					
19	Belgioioso (PV)	1	Diffused floods. Road and residential area defence	64.3	13.6	68.45	58.26	51.12
20	Varzi (PV)	1	Slope stabilization	58.1	67.62	71.55	82.3	67.82
22	San Giacomo Filippo A (SO)	1	Slope stabilization	71.25	34.38	35.36	74.09	52.3
22	San Giacomo Filippo B (SO)	1	Slope stabilization	72.82	73.29	60.58	78.55	70.51
23	Sondrio (SO)	1	Adaptation of an existing dike as a protection of the city of Sondrio	77.35	31.99	97.44	70.72	69.77
24	CM Valtellina Morbegno	2	Video monitoring for wildfires	43.07	3.765	21.87	81.658	32.73
25	Cadegliano-Viconago (SO)	1	Works on landslide on state road. Stabilization and monitoring. Rebuilding of road surface.					
26	Paspardo (BS)	2	Environmental recover of burnt area	34.29	4.78	26.52	99.32	34.06
27	CM Val Brembana	2	Realization of inter municipal emergency plan for wildfires	61.86	7.97	23.86	99.32	42.99

1 = Hydrogeological risk, 2 = Wildfire risk,

5.1 LEVEL 2: MULTI CRITERIA ANALIYSIS

Multi criteria analysis was applied by the experts of Lombardy Regional Administration, University Milano Bicocca and ERSAF. In most of the cases, the experts had a deep knowledge of the analysed works and contexts.

In general they observed that works aimed at wildfire mitigation are in mean less efficient than those aimed at hydrogeological risk mitigation. This is due to the fact that indicators for the two types of works are slightly different, so that the results are not directly comparable. In particular, wildfire are penalized by the fact that works are diffused on the territory, with more uncertain results in terms of mitigation. This is an intrinsic characteristic of works applied to wildfire mitigation. The indicator related to past consequences of the events (deaths or injuries) is very low for wildfire: this contributes to keep low the priority obtained by these type of works.

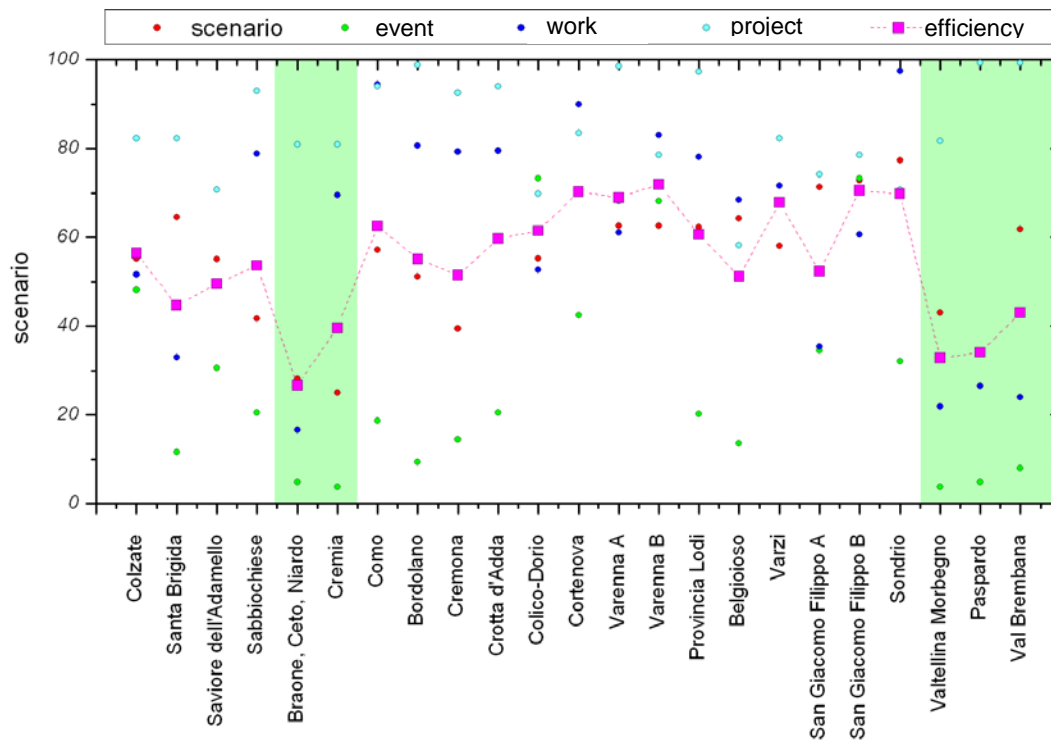


Fig.6. Graphical representation of efficiency indexes. The green area shows works of mitigation for wildfires.

The observation of the results (Fig.9) suggests that the works economically more conspicuous (large works) have a better efficiency than limited works, under the condition of being well built. Works, however, are evaluated individually, not taking into account their potential interaction and synergy, which could improve the performance of some small works.

To observe the range of variation of the indexes, a box chart was realised (Fig.10). The index of event shows the greater variations, ranging from 9,35 and 73,93. The work index ranges between 32,92 and 97,44 (Sondrio). On the other side, the scenario index is the less changing.

The different indexes impact on the final efficiency result as shown in Fig.11 The sum of the indexes represents the efficiency of the work. Weighted values of the indicators have a strong influence mainly on project and event indexes. Scenario and work event give a higher influence on the final result.

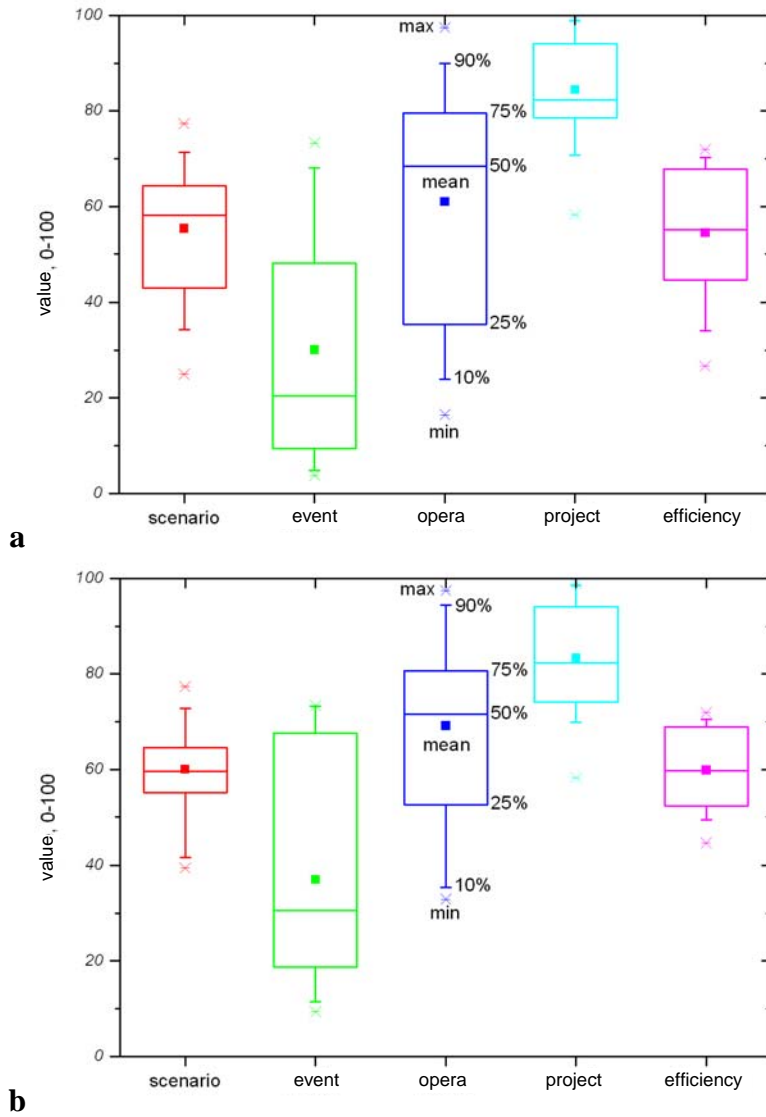


Fig.7. Box chart of efficiency index: a) overall, b) hydrogeological. Boxes allow to observe the value distribution by means of the representation of the percentiles. For hydrogeological risk, in general a minor variation is shown.

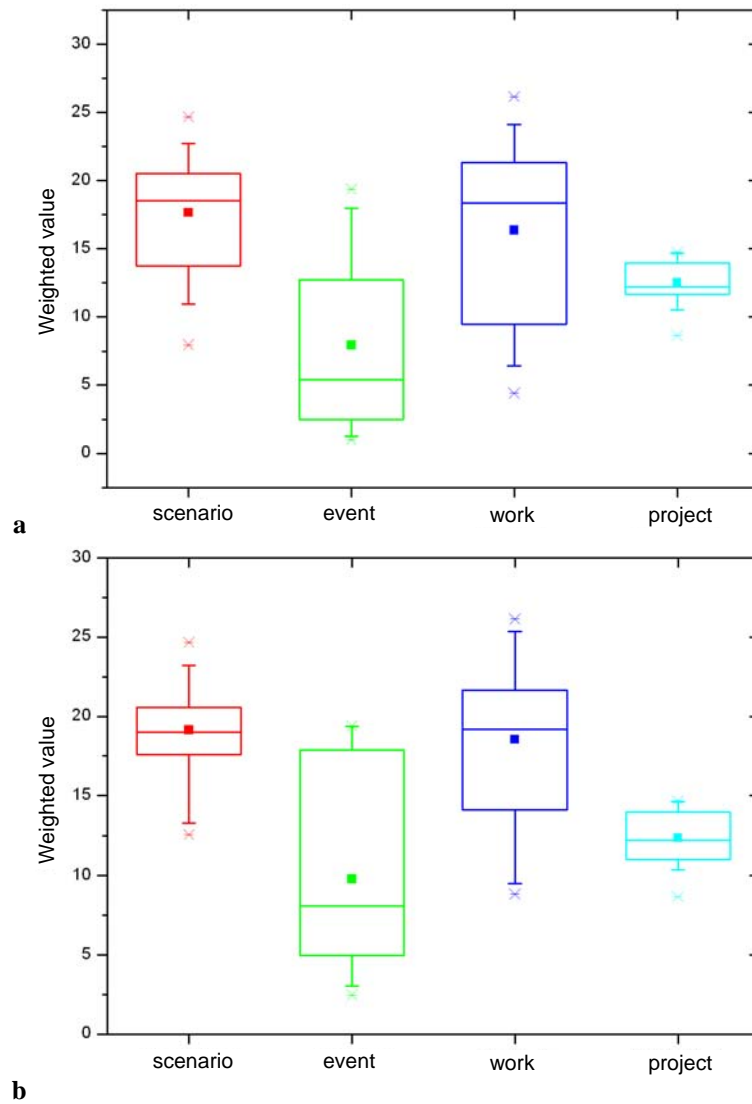


Fig.8. Box chart of weighted efficiency indexes: a) overall, b) only hydrogeological. Weighted values are summed to calculate, for each work, the value of efficiency. Scenario and work indexes are the most relevant.

5.2 LEVEL 3: COST-BENEFIT ANALYSIS

Cost benefit analysis was applied to two works: Fiumelatte (LC) and Cortenova (LC). For these events, a large amount of data, and studies of risk are available.



Fig.9. Landslide of Fiumelatte, Varenna (LC). Rockfall occurred on 13 November 2004 and caused 2 casualties and heavy damages to buildings and to railway. A rockfall embankment was realised in extreme urgency conditions. A bigger embankment was designed to protect all the slope of Fiumelatte (in the image on the left)

In the case of Fiumelatte (Fig.12), the Department of Geologic Sciences and Geotechnologies of the University of Milano Bicocca performed a detailed study of rockfall hazard by means of HY-STONE model (Agliardi et al., 2009). The model was applied on detailed topographies (Lidar, 2x2 m) where the projects of the mitigation works and buildings were included (Fig 13 and 14).

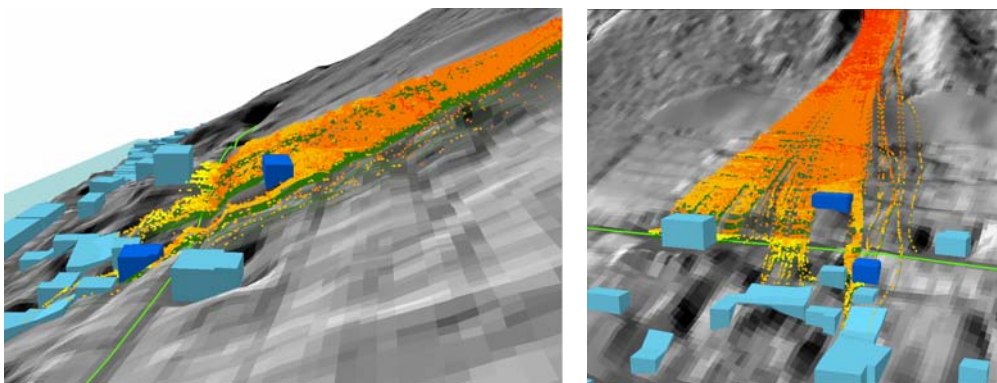


Fig.10. Examples of 3D simulation of block propagation, Hy-STONE, (Agliardi et al., 2009)

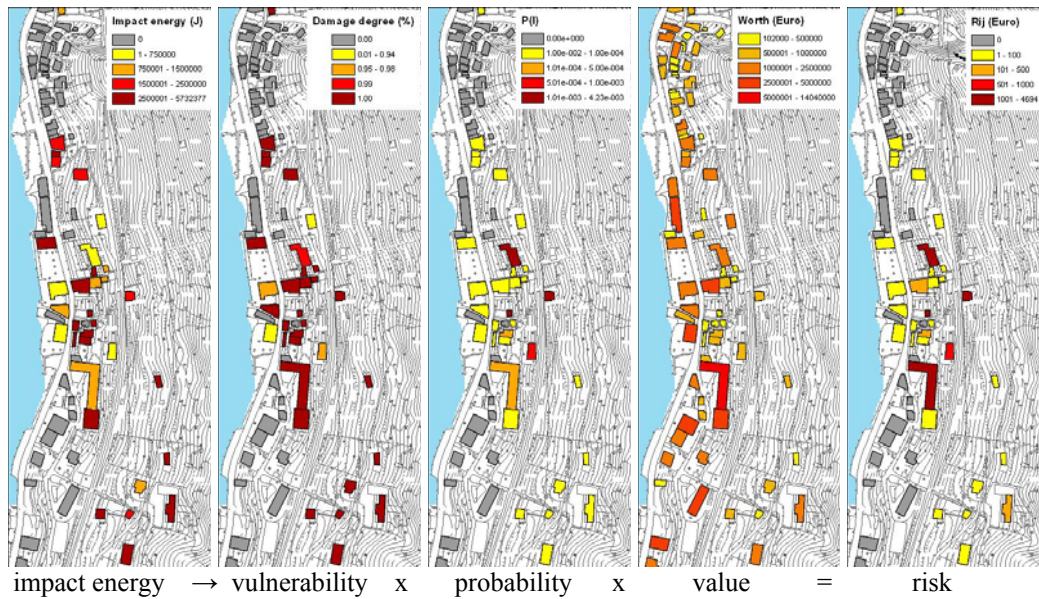


Fig.11. Steps for the evaluation of damages to the buildings (scenario without mitigation work)

The temporary embankment is quite effective, but protects only a part of the slope potentially exposed. The complete embankment, instead, shows a noticeable efficacy and efficiency, intercepting almost all the possible trajectories. The cost-benefit analysis was performed considering exposed buildings, people potentially hit and the possible damage to the railway, for the two works (Tab.4 and5).

Tab.4. Costs and benefits actualised to the present deriving from the building of the temporary embankment. Discount rate = 4.3%.

Costs	euro	benefits	euro
Work initial cost	482.000	Value saved every year	139.100
Maintenance costs	3.000	Deaths/casualties avoided by the work (per year)	685
		Indirect damages avoided by the work (per year)	9.060
Total on 40 years	563.900	Total on 40 years	4.346.200

Tab.5. Costs and benefits actualised to the present deriving from the building of the definitive embankment. Discount rate = 4.3%.

Costs	euro	benefits	euro
Work initial cost	2.480.000	Value saved every year	525.200
Maintenance costs	3.000	Deaths/casualties avoided by the work (per year)	3.200
		Indirect damages avoided by the work (per year)	9.060
Total on 40 years	2.559.000	Total on 40 years	15.691.600

For the landslide of Bindo in Cortenova (LC) (Fig.15), the Department of Geologic Sciences and Geotechnologies of the University of Milano Bicocca realised a study aimed at the quantification of different risk scenarios connected with different work alternatives (monitoring, removal of people, construction of an open or closed embankment dam) (Crosta et al, 2005). From the study, the best alternative resulted to be the construction of an open embankment associated with a continuous monitoring of the landslide (Crosta et al, 2005). Two different projects were considered: the first including the realization of an embankment requiring the demolition of 5 buildings, and the monitoring of the landslide. The second including also the reconstruction of the road, in a gallery. The second project is clearly much more costly, balanced by a limited gain in terms of benefits (evaluated in 25.000 euro/year of avoided costs for the positive impact on the practicability). However, the reconstruction of the road induces a benefit also in the quality of life and in wellness of resident people which is hardly quantified in economic terms.

Costs and benefits were calculated considering as exposed elements houses and residents. People in transit on the roads were considered as non exposed, for both scenarios (in one case there is no road, in the second there is a tunnel)(Tab.6).



Fig.12. Landslide of Bindo, Cortenova (LC). The event occurred on 1 December 2002. To mitigate the risk connected to the potential reactivation of the instable sectors, a big embankment is designed.

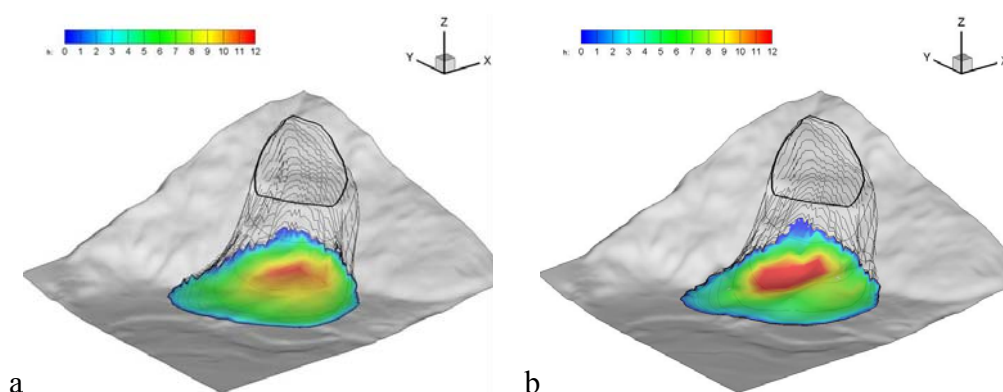


Fig.13. Simulation of the collapse of 1,2 millions m^3 of the unstable zone: a) without mitigation works; b) in presence of an opened embanked dam.

Tab.6. Costs and benefits actualised to the present deriving from the building of embanked dam and the maintenance of the monitoring system. Discount rate = 4.3%.

Costs	euro	benefits	euro
Work initial cost	<i>600.000</i>	Value saved every year	<i>58.500</i>
Maintenance costs	<i>35.000</i>	Deaths/casualties avoided by the work (per year)	<i>326.300</i>
Houses demolition	<i>1.880.000</i>	Indirect damages avoided by the work (per year)	<i>54.400</i>
Total on 40 years	<i>3.479.000</i>	Total on 40 years	<i>12.823.000</i>

Tab.7. Costs and benefits actualised to the present deriving from the building of embanked dam, the maintenance of the monitoring system and the reconstruction of the road. Discount rate = 4.3%.

Costs	euro	benefits	euro
Work initial cost	<i>600.000</i>	Value saved every year	<i>58.500</i>
Maintenance costs	<i>35.000</i>	Deaths/casualties avoided by the work (per year)	<i>326.300</i>
Bypass	<i>2.500.000</i>	Indirect damages avoided by the work (per year)	<i>80.000</i>
Houses demolition	<i>1.880.000</i>		
Total on 40 years	<i>5.979.000</i>	Total on 40 years	<i>13.570.000</i>

Both Fiumelatte and Bindo works present positive values for the benefit/cost ratio and of Net Present Value (NPV) (Tab.8). The best work appears to be the closed rockfall dam embankment of Fiumelatte, in accordance with the results of the multi criteria analysis. This work, having an initial cost of almost 2,500,000 euro, ensures protection and safety to a wide area, inducing noticeable benefits to the community (more than 13,000,000 euro in 40 years). Similarly valuable is the work realised in Fiumelatte with extreme urgency. It shows the highest cost/benefit ratio (7.75), showing a high efficacy obtained with container costs. The works of Cortenova are less performing, but surely positives.

Tab.8. Results of cost-benefit analysis

Number	MUNICIPALITY	RISK	DESCRIPTION	BENEFIT/COST BCR	NET BENEFIT NPV, euro	NPV/POTENTIAL COSTS WITHOUT WORK
12 a	Cortenova (LC)	1	Landslide monitoring – stabilization of residential area and slope	3.77	9.344.000	4.24
12 b	Cortenova (LC)	1	Landslide monitoring – stabilization of residential area and slope	2.30	7.591.000	3.45
13 a	Varenna A (LC)	1	realization embankment dam – extreme urgency	7.75	3.785.280	1.78
13 b	Varenna B (LC)	1	realization embankment dam – completion of embankment dam	6.13	13.132.680	6.19

6 CONCLUSIONS

The study faced the problem of finding a strategy to optimise the resources allocation for mitigation works. The research proposes a three-level methodology for the evaluation of the economic efficacy of the works, and a software for local administrations involved in work planning. The methodology was then applied by the operators of the General Direction of Civil Protection of Lombardy to real cases, to test its performance.

The proposed methodology introduces some new utilities with respect to what was currently in use. In particular, it is deeply connected to the regional context, both for competences and data availability requirements. According to the available level of data, different levels of the methodology can be implemented, in order to use all the detail of the available information.

The tool works in Excel environment. This allow a simple and effective distribution, and an easy applicability.

The application of the methodology to the real cases underlined some points:

- The comparison between mitigation works for hydrogeological and wildfire risks is a complex problem, both because selected indicators are slightly different for the two cases and because the typology of works and the mitigation philosophies are quite different.
- For a risk type, the methodology allows to evaluate and compare the different works quite easily. On the basis of the expert knowledge, results appear to be realistic.
- In the multi criteria analysis, a certain degree of subjectivity is not eliminable, as demonstrated by the results obtained by different compilers on the same study cases. Moreover, the attribution of value to the different indicators was realised in a quite subjective way, based on expert knowledge of the working group.
- Cost benefit analysis was applied only to two case studies, underlining a potential weakness of the method: not always the required data are easily available. On the other side, cost-benefit analysis offers advanced evaluation and comparison tools, more useful for a correct management of mitigation works.

In the future, the study will lead to the development of an intranet software, associated with the realisation of a digital database of works.

REFERENCES

- AAVV, 2007. Il rischio integrato in Lombardia: misurazioni di livello regionale e individuazione delle zone a maggiore criticità. In PRIM 20007-2010, Programma Regionale Integrato di Mitigazione dei Rischi. Regione Lombardia.
- Agliardi, F., Crosta, G., 2003. High resolution three-dimensional numerical modelling of rockfalls, *International Journal of Rock Mechanics and Mining Sciences* 40, 455-471.
- Agliardi, F., Crosta, G.B., Frattini, P., 2008. Integrating rockfall risk assessment and countermeasure design by 3D modelling techniques.
- Agliardi, F., Crosta, G. B., Frattini, P., 2009. Integrating rockfall risk assessment and countermeasure design by 3D modelling techniques *Natural Hazards and Earth System Science*, Volume 9, Issue 4, 2009, pp.1059-1073.
- AGS, Australian Geomechanics Society, 2000. Landslide management concepts and guidelines. *Australian Geomechanics* 37(1).
- Ale, B.J.M, Laheij, G.M.H., Uijt de Haag, P.A.M., 1996. Zoning instruments for major accident prevention, in: C. Cacciabue, I.A. Papazoglou (Eds.), *Probabilistic Safety Assessment and Management, ESREL 96, PSAM-III*, Crete, p. 1911.
- Allen and Hoshall, Benjamin J.R. and Associates, and Systan Inc., 1985. *An Assessment of Damage and Casualties for Six Cities in the Central United States Resulting from Earthquakes in the New Madrid Seismic Zone*. Prepared for FEMA.
- Annan, K.A., and United Nations, 1999. *Facing the humanitarian challenge: Towards a culture of prevention*, United Nations Department of Public Information, New York.
- ANON, 1980. *Potential flood hazards at Willow Beach, Lake Mead, Naional Redreation Area, US National Park*
- Apostolakis, G.E., (2004). How useful is quantitative risk assessment? *Risk Analysis* Vol. 24 No. 3, pp. 515-520.
- Archetti, R., Lamberti, A., 2003. Assessment of risk due to debris flow events, *Nat. Hazards Rev.* 4: 115-125
- ASFPM, 2006. *Use of Benefit/Cost Analysis for FEMA Programs: A Draft Discussion*, 14 pp, Association of State Floodplain Managers, Madison.

- Azioni, A., La Barbera, G., Zaninetti, A., 1995. Analysis and prediction of rock falls using a mathematical model, *International Journal of Rock Mechanics and Mining Sciences & Geomechanical Abstracts* 32 (7), 709-724.
- Baecher, G.B., 1982b. Statistical methods in site characterization. Updating subsurface samplings of soils and rocks and their in-situ testing, Santa Barbara, Engineering foundation: 463-492
- Baecher, G.B., Christian, J.T., 2003. Reliability and statistics in Geotechnical engineering, Wiley & sons.
- Ball, D. J., and Floyd, P. J., 1998. Societal Risks. London: HSE.
- Barbat, A. H. and Cardona O. D., 2003. Vulnerability and disaster risk indices from engineering perspective and holistic approach to consider hard and soft variables at urban level, IDB/IDEA Program on Indicators for Disaster Risk Management, <http://idea.unalmz.edu.co>, Universidad Nacional de Colombia, Manizales.
- Bariselli, C., 2009. Analisi del rischio sociale dovuto a frane e alluvioni in Val Trompia, Val Sabbia, bassa Valcamonica e pianura bresciana. Tesi di laurea.
- Bedford, T., Cooke, R.M., 2001. Probabilistic Risk Analysis: Foundations and Methods, Cambridge University Press, New York.
- Bell, R., Glade, T, 2004. Multi-hazard analysis in natural risk assessments, *Risk Analysis* IV. pp. 197-206.
- Benda, L., 1990. The influence of debris flows on channels and valley floors in the Oregon Coast Range, USA - *Earth Surface Processes and Landforms.*, Vol. 15, 457-446.
- Benson, C., 1998. The cost of disasters, in *Development at Risk? Natural Disasters and the Third World*, edited by J. Twigg, Oxford Centre for Disaster Studies, UK National Coordinated Committee for the International Decade for Natural Disaster Reduction (IDNDR), pp. 8-13, Oxford.
- Benson, C., and Clay, E.J., 2002. Disasters, Vulnerability and the Global Economy, World Bank, Washington, D.C.
- Benson, C., and Twigg, J., 2004. Measuring mitigation: Methodologies for Assessing Natural Hazard Risks and the Net Benefits of Mitigation - A Scoping Study, International Federation of the Red Cross and Red Crescent Societies, ProVention Consortium.
- Benson, C., Twigg, J., Rossetto, T., 2007. Tools for Mainstreaming Disaster Risk Reduction: Guidance Notes for Development Organisations, International Federation of Red Cross and Red Crescent Societies and ProVention Consortium Secretariat, Geneva, Switzerland, 178pp.
- Berruti, G., 1998. Levandosi i Fiumi Sopra le Rive. Per una Mappa Storica del Rischio Idrogeologico nel Bresciano. Grafo edizioni: Brescia (in Italian).
- Beven, K.J., 2000. Rainfall-runoff modelling, The primer. John Wiley & Sons, Chichester, UK.
- Beven, K.J. , Kirkby , M.J., 1979). A physically based, variable contributing area model of basin hydrology, *Hydrological Science Bulletin* 24, 43-69.

- Birkmann, J. (Ed.), 2006. *Measuring Vulnerability to Natural Hazards. Towards Disaster Resilient Societies*. United Nations, University Press, Tokyo.
- Blong, R., 2003. A new damage index *Nat. Hazards* 30, 1-23.
- Boardman, C.E., Thompson, M., Walter, C.E., Ehrman, C.S., 1996. *The Separations Technology and Transmutation System (STATS) Report—Implications for Nuclear Power Growth and Energy Sufficiency*, Pacific Basin Conference, Kobe, Japan, October, p. 411.
- Bohnenblust, H., 1998. Risk-based decision making in the transportation sector, In: R.E. Jorissen, P.J.M. Stallen (Eds.), *Quantified Societal Risk and Policy Making*, Kluwer Academic Publishers, Dordrecht.
- Bordonaro, D., 2009. *Analisi del rischio naturale e tecnologico nella media-bassa Valtellina*. Tesi di laurea.
- Bottelberghs, P.H., 2000. Risk analysis and safety policy developments in The Netherlands, *J. Hazard. Mater.*, 71 59–84.
- Bovolin, V and Taglialatela, L., 2002. V. Bovolin and L. Taglialatela, *Proceedings Scritti in onore di Lucio Taglialatela*, CNR-GNDCI Publication no. 2811, Naples, Italy (2002), pp. 429–437.
- Brabb, E.E., Pampeyan, E.H., and Bonilla, M.G., 1972. *Landslide susceptibility in San Mateo County, California, scale 1:62 500*, Miscellaneous Field Studies Map, MF-360. US Geological Survey, Washington, D.C.
- Breuer, L., Huisman, J.A., Frede, H.G., 2006. Monte Carlo assessment of uncertainty in the simulated hydrological response to land use change. *Environ Model Assess* 11:209–218.
- Brouwer, R., De Blois, C., 2007. Integrated modelling of risk and uncertainty underlying the cost and effectiveness of water quality measures. *Environmental Modelling & Software* xx 1e16.
- Brown, G. W. and Krygier, J. T., 1971. Clear-cut logging and sediment production in the Oregon Coast Range, *Wat. Resour. Res.*, 7, 1189±1198.
- Buldrini, M., 2009. PIA- Piano Integrato d'Area della provincia di Brescia, *Relazione metodologica*, Marzo 2009.
- Burroughs, E.R. Jr., 1984. Landslide hazard rating for portions of the Oregon Coast Range. In: O'Loughlin, C. L., and Pearce, A. J. (eds.), *Proceedings of the Symposium on Effects of Forest Land Use on Erosion and Slope Stability*, Honolulu, Hawaii, Environment and Policy Institute, University of Hawaii, Honolulu. pp. 265±274.
- Burroughs, E.R.Jr and Thomas, B. R., 1977. Declining root strength in Douglas-Fir after felling as a factor in slope stability, *Forest Service Research Paper INT-190*. US Department of Agriculture, Ogden. 27 pp.
- Busoni, E., Sanchis, P. S., Calzolari, C., and Romognoli, A., 1995. Mass movement and erosion hazard patterns by multivariate analysis of landscape integrated data: the Upper Orcia River Valley (Siena, Italy) case, *Catena*, 25, 169±185.

- Campbell, R.H., 1975. Soil slips, debris flows and rainstorms in the Santa Monica Mountains and vicinity, southern California, US Geological Survey Professional Paper 851. US Geological Survey, Washington, D.C. 51 pp.
- Cao, Y., Hussaini, M.Y., Zang, T.A., 2003. An Efficient Monte Carlo Method for Optimal Control Problems with Uncertainty USA Computational Optimization and Applications, 26, 219–230, 2003 Kluwer Academic Publishers.
- Cardona, O. D., Hurtado, J. E., 2000. Holistic seismic risk estimation of a metropolitan center, in Proceedings of 12th World Conference of Earthquake Engineering, Auckland, New Zealand.
- Cardona, O.D., 2001. Holistic evaluation of the seismic risk using complex dynamic systems (in Spanish), PhD Thesis, Technical University of Catalonia, Barcelona, Spain.
- Cardona, O.D., Hurtado, J.E., Duque, G., Moreno, A., Chardon, A.C., Velasquez, L.S., Prieto, S.D, 2004. Disaster Risk and Risk Management Benchmarking: a methodology based on indicators at National Level, IDB-IDEA Program on Indicators for Disaster Risk Management, Universidad Nacional De Colombian, Manizales, 101 pp.
- Carrara, A., 1983. Multivariate models for landslide hazard evaluation, *Math. Geol.*, 15, 403–426.
- Carrara, A., Cardinali, M., Detti, R., Guzzetti, F., Pasqui, V., and Reichenback, P. 1991. GIS techniques and statistical models in evaluating landslide hazard, *Earth Surf. Process. Landf.*, 16, 427–445.
- Carrara, A., Pugliese Carratelli, E., and Merenda, L., 1977. Computer-based bank and statistical analysis of slope instability phenomena, *Z. Geomorph.*, 21, 187–222.
- Carreño M., Cardona O., Barbat, A, 2007. A disaster risk management performance index, *Natural Hazards* 41(1):1–20.
- Carter D.A., 1995. The Scaled Risk Integral—A Simple Numerical Representation of Case Societal Risk for Land Use Planning in the Vicinity of Major Accident Hazards, *Loss Prevention in the Process Industries*, vol. II, Elsevier, Amsterdam, pp. 219–224.
- Carter D.A., Hirst I.L, 2000. Worst case methodology for the initial assessment of societal risk from proposed major accident installations, *J. Hazard. Mater.* 71 117–128.
- Castellani, A., Faccioli, E., 2000. *Costruzioni in zona sismica*. Hoepli, Milano, 312 pp.
- CEPAL/BID, 2000. A matter of development: how to reduce vulnerability in the face of natural disasters: confronting Natural Disasters: a Matter of Development, Seminar, New Orleans, 25 and 26 March.
- Christian, J.T., and Baecher G.B., 1999. Point-estimate method as numerical quadrature. *Journal of geotechnical and geoenvironmental engineering*, Vol. 125, No. 9 pp. 779–786.
- Chun-Lien, S., 2005. Probabilistic Load-Flow Computation Using Point Estimate Method, *IEEE transactions on power systems*, vol. 20, no. 4.

- Coburn, A.W., Spence, R.J.S., Pomonis, A., 1994. *Vulnerability and Risk Assessment*, UNDP and Department of Humanitarian Affairs, United Nations. 2nd Editino.
- Consiglio Nazionale delle Ricerche (CNR), 1998. *Eventi alluvionali e frane nell'Italia Settentrionale, Periodo 1972-1974*, Torino.
- Consiglio Nazionale delle Ricerche (CNR), 1999. *Eventi alluvionali e frane nell'Italia Settentrionale, Periodo 1975-1981*, Torino.
- Crosta, G.B. and Agliardi, F., 2003. A methodology for physically based rockfall hazard assessment, *Natural Hazards and Earth System Sciences* 3, 407-422.
- Crosta, G.B., D. Negro, P., Frattini, P., 2003. Soil slips and debris flows on terraced slopes, *Nat. Hazards Earth Syst. Sci.* 3, 31-42.
- Crosta, G.B., Agliardi, F., Frattini, P., Imposimato, S., 2004. A three-dimensional hybrid numerical model for rockfall simulation. *Geophysical Research Abstracts* 6, n. 04502.
- Crosta, G.B., Chen, H., and Frattini, P., 2005. Forecasting hazard scenarios and implications for the evaluation of countermeasure efficiency for large debris avalanches, *Engineering Geology*, Vol 83, Issues 1-3, 28 February 2006, Pages 236-253
- Crosta, G.B., Carrara, A., Agliardi, F., Campedel, P., Frattini P., 2006. Valutazione della pericolosità da caduta massi tramite un approccio integrato statistico e deterministico. *Giornale di Geologia Applicata*, 4 41-48.
- Crosta, G.B., Chen, H., Frattini, P., 2006. Forecasting Hazard Scenarios and implications for the evaluation of Countermeasure Efficiency for Large Debris Avalanches. *Engineering Geology*, 83:236-253.
- Crosta, G.B., Frattini, P., 2003. Distributed modelling of shallow landslide triggered by intense rainfall. *Natural Hazards and Earth System Sciences*, 3:81-93,
- Crosta, G.B., Frattini, P., 2008. Rainfall induced landslides and debris flows, *Hydrological Processes*, 22: 473-477.
- Crosta, G.B., Frattini, P., Fugazza, F., Caluzzi, L., Chen, H., 2005. Cost-Benefit analysis for debris avalanche risk management. In: Hungr O., Fell R., Couture R., Eberhart E. (eds.) *Landslide risk management*. Balkema, Rotterdam, 517-524.
- Crovelli, R.A., 2000. *Probability Models for Estimation of Number and Costs of Landslides'* Open-File Report 00-249, <http://pubs.usgs.gov/of/2000/ofr-00-0249/ProbModels.html>
- Cruden, D.M. and Varnes, D.J., 1996. Landslide types and processes. In: Turner, A.K. and Schuster, R.L., Editors, 1996. *Landslides Investigation and Mitigation*, National Research Council, Transportation Research Board, Washington, DC, pp. 36-75.
- D.LGS 238/2005 - Decreto Legislativo 21 settembre 2005, n. 238 "Attuazione della direttiva 2003/105/CE, che modifica la direttiva 96/82/CE, sul controllo dei pericoli di incidenti rilevanti connessi con determinate sostanze pericolose"
- D.M 14/01/08, Decreto ministeriale 14 gennaio 2008, Norme Tecniche per la Costruzione (NTC).

- Dasgupta, A.K., and Pearce, D.W., 1978. *Cost-Benefit Analysis: Theory and Practice*, Macmillan, London.
- Dedeuwaerdere, A., 1998. *Cost-benefit analysis for natural disaster management: A case study in the Philippines*, 87 pp., Center for Research on the Epidemiology of Disasters (CRED), Brussels.
- Del Favero, R., 2000. *Biodiversità e indicatori nei tipi forestali del Veneto*. Regione Veneto, Dip. Foreste, Mestre (Venezia), 335 pp.
- Derbyshire, E., van Asch, T., Billard, A., and Meng, X., 1995. Modelling the erosional susceptibility of landslide catchments in thick loess: Chinese variations on a theme by Jan de Ploey, *Catena*, 25, 315±331.
- Diamantidis, D., Duzgun, S., Nadim, F., Wöhrle, M., 2006. On the Acceptable Risk for Structures Subjected to Geohazards, ECI Conference on Geohazards, Lillehammer, Norway.
- Dietrich, W.E., Montgomery, D.R., 1998. A digital terrain model for mapping shallow landslide potential. technical report. <http://socrates.berkeley.edu/~geomorph/shalstab/>
- Dietrich, W.E., Dunne, T., Humphrey, N., and Reid, L., 1982. Construction of sediment budgets for drainage basins. In: Swanson, F. J., Janda, R. J., Dunne, T., and Swanson, D. N. (eds), *Sediment Budgets and Routing in Forested Drainage Basins*, US Department of Agriculture, Forest Service General Technical Report PNW-141. Pacific Northwest Forest and Range Experiment Station, Portland, Oregon. pp. 2±23.
- Dietrich, W.E., Wilson, C.J., Reneau S.L., 1986. Hollows, colluvium, and landslides in soil-mantled landscapes Hillslope Processes, edited by A.D. Abrahams, pp.361-388, Allen and Unwin, Winchester, Mass.
- Dietrich, W. E., Reiss, R., Hsu, M.-L., and Montgomery, D. R., 1995. A process-based model for colluvial soil depth and shallow landsliding using digital elevation data, *Hydrol. Process.*, 9, 383±400.
- Dietrich, W. E., Wilson, C. J., Montgomery, D. R., and McKean, J., 1993. Analysis of erosion thresholds, channel networks and landscape morphology using a digital terrain model, *J. Geol.*, 101, 259±278.
- Dilley, M., Chen, R.S., Deichmann, U., Lerner-Lam, A.L., Arnold, M., 2005. *Natural disaster hotspots: a global risk analysis*. Disaster Risk Management Series No.5 Washington, DC: The World Bank.
- Dreze, J., and Sen, A., 1989. *Hunger and Public Action*, 373 pp., Clarendon Press, Oxford.
- Dunne, T., 1991. Stochastic aspects of the relations between climate, hydrology and landform evolution, *Trans. Jpn. Geomorph. Union*, 12, 1±24.
- Durham, K., 2003. Treating the risks in Cairns, *Natural Hazards*, 30: 251-261.
- Dussauge, C, Grasso, J.R., Helmstetter, A., 2003. *Journal of Geophysical Research-Part B-Solid Earth*, 2003 - Richmond, Va.: William Byrd Press for John Hopkins Press.
- E.R.S.A.L., 1992, Progetto “Carta Pedologica” – I suoli del fondovalle valtellinese.

- Egidi, D., Foraboschi, F.P., Spadoni, G., 1995. The ARIPAR project: analysis of the major accident risks connected with industrial and transportation activities in the Ravenna area. *Reliability Engineering and System Safety*, 49 75-89.
- El-Ramly, H., Morgenstern, N.R., and Cruden, D..M., 2003. Reply to the discussion by J.M. Duncan, M. Navin, and T.F. Wolff on —Probabilistic slope stability analysis for practice *Can. Geotech. J.* 40: 851–855.
- Endo, T. and Tsuruta, T., 1969. The effect of tree roots on the shearing strength of soil, *Annual Report. Forest Experiment Station, Hokkaido.* pp. 167±182.
- Epstein, S., 1994. Integration of the cognitive and psychodynamic unconscious, *American Psychologist* 49 pp. 709–724.
- ERSAF, 2005-2006. Piani di previsione, prevenzione e lotta attiva dei parchi regionali, Campo dei Fiori, Groane, Pineta di Appiano Gentile e Tradate, Valle del Ticino, Sud Milano, Orobie valtelinesi, Alto Garda Bresciano.
- ESPO, 2005. The Spatial Effects and Management of Natural and Technological Hazards in Europe. Final report of the ESPON Project 1.3.1, pp. 197.
- Evans A.W., Verlander N.Q., 1997. What is wrong with criterion FN-lines for judging the tolerability of risk, *Risk Anal.* 17 (2) 157–168.
- Fairfield, J., and Leymarie, P., 1991. Drainage networks from grid elevation models. *Water Resources Research*, 27, 709–717.
- Fell, R., 1994. Landslide risk assessment and acceptable risk. *Canadian Geotechnical Journal/Revue Canadienne de Geotechnique* Vol. 31, no. 2, pp. 261-272.
- Fell, R., Ho, K.K.S., Lacasse, S., Leroi, E., 2005. A framework for landslide risk assessment and management - in *Landslide risk management- Hungr, Fell, Couture & Eberhardt*, Taylor and Francis Group, London.
- FEMA, 1997. Report on Costs and Benefits of Natural Hazard Mitigation, 57 pp., Federal Emergency Management Agency, Washington DC.
- FEMA, 1998. Protecting Business Operations: Second Report on Costs and Benefits of Natural Hazard Mitigation, 50 pp., Federal Emergency Management Agency, Washington DC.
- FEMA, 1999. Earthquake Loss Estimation Methodology, HAZUS, Federal Emergency Management Agency, Washington, D.C.
- FEMA, 1999. Hazard Mitigation Grant Program Desktop Reference, 252 pp., Federal Emergency Management Agency, Washington DC.
- FEMA - Department of Homeland Security Emergency Preparedness and Response Directorate, Mitigation Division, 2003. Multi-hazard Loss Estimation Methodology Earthquake Model HAZUS-MH MR3 Technical Manual, Washington DC.
- FEMA - Department of Homeland Security, 2005. Multi-hazard Loss Estimation Methodology - Flood Model HAZUS MH MR3. Technical Manual. Washington, D.C. 471 pp.

- FEMA - Mitigation Directorate, 2006. Guidelines for Benefit-Cost Analysis, How to Determine Cost-Effectiveness of Hazard Mitigation Projects. A New Process for Expediting Application Reviews. Washington, D.C.
- FEMA & NIBS, 1999. Earthquake loss estimation methodology – HAZUS 99. Federal Emergency Management Agency and National Institute of Buildings Sciences, Washington, D.C.
- Ferrier, N. and Haque, C.E., 2003. Hazards risk assessment methodology for emergency managers: A standardized framework for application, *Nat. Hazards* 28(2/3), 271–290.
- Fishman, G.S., 1996. Monte Carlo. Concepts, Algorithms, and Applications: Concepts, Algorithms, and Applications, Springer.
- Frattini, P., Crosta, G.B., Soso, R., 2009. Approaches for defining thresholds and return periods for rainfall-triggered shallow landslides. *Hydrol. Process.* 23, 1444–1460.
- French, R. H., 1987. *Hydraulics processes on alluvial fans*, Elsevier, Amsterdam, The Netherlands. 241 pp.
- Fuchs, S. and McAlpin, M. C., 2005. The net benefit of public expenditures on avalanche defence structures in the municipality of Davos, Switzerland, *Nat. Hazards Earth Syst. Sci.*, 5, 319–330.
- Fuchs, S., Heiss K., Hubl, J., 2007. Towards an empirical vulnerability function for use in debris flow risk assessment. *Natural Hazards. Natural Hazards and Earth System Science*, Volume 7, Issue 5, 2007, pp.495- 506.
- Fuchs, S., Thöni, M.; Mcalpin, M.C.; Gruber, U., Briindl M., 2006. Avalanche hazard mitigation strategies assessed by cost effectiveness analysis and cost benefit analyses – evidence from Davos, Switzerland, *Natural Hazards DOI 10.1007/s11069-006-9031-z*.
- Galli, M. and Guzzetti, F., 2007. Landslide Vulnerability Criteria: A Case Study from Umbria, Central Italy. *Environmental Management* 40, 649–664.
- Gamma, P., 2000. Dfwalf- Ein Murgang Simulationsprogramm zur Gefahrenzonierung. Geographisches Institut der Universität Bern.
- Geotechnical engineering office, 1997. strategic plan on slope safety, 1997-2002, Geotechnical engineering office, Hong Kong, 7p.
- GEO, Geotechnical engineering office, 1998. Landslides and boulder falls from natural terrain: interim risk guidelines. GEO report n.75. Geotechnical engineering office, the government of the Hong Kong special Administrative region.
- Glade, T., 2003. Vulnerability assessment in landslide risk analysis.- *Die Erde*, 134: 121-138.
- Glade, T., Anderson, M., and Crozier, M. J., 2004. *Landslide hazard and risk*, Wiley.
- Govi, M. and Turitto, O., 1994. Ricerche bibliografiche per un catalogo sulle inondazioni; piene torrentizie e frane in Valtellina e Valchiavenna.
- Granger, K. and Hayne, M., 2001. *Natural hazards and the risks they pose to South-East Queensland*, Australian Geological Survey Organisation, Canberra.

- Granger, K., Jones, T., Leiba, M., and Scott, G., 1999. Community Risk in Cairns: A Multi-Hazard Risk Assessment, Australian Geological Survey Organisation, Canberra.
- Gresswell, S., Heller, D., and Swanston, D.N., 1979. Mass movement response to forest management in the central Oregon Coast Ranges, Forest Service Resources Bulletin PNW-84, US Department of Agriculture, Portland. 26 pp.
- Gunderson, L.H., and Holling, C.S. (Eds.), 2002. Panarchy: Understanding Transformations in Human and Natural Systems, 507 pp., Island Press, Washington, D.C.
- Guzzetti, F., 2000. Landslide fatalities and evaluation of landslide risk in Italy. *Engineering Geology*, Vol. 58: 89-107.
- Hall, B.D., 2006. Monte Carlo uncertainty calculations with small-sample estimates of complex quantities. *Metrologia* 43 220–226.
- Harr, M.E., 1989. Probabilistic estimates for multivariate analyses. *Appl. Math. Modelling*, Vol. 13.
- He, J. and Siillfors, G., 1994. An optimal point estimate method for uncertainty studies. *Appl. Math. Modelling*, 18.
- HSE, Health and Safety Executive, 1989. Risk criteria for land use planning in the vicinity of major industrial hazards, HSE Books ISBN 0-11-885491-7.
- HSE, Health and Safety Executive, 1992. The Tolerability of risks from nuclear power stations, HSE Books ISBN 0-11-886368-1.
- HSE, Health and Safety Executive, 2001. Reducing risks, protecting people—HSE's decision making process, ISBN 0-7176-2151-0, <http://www.he.gov.uk/dst/r2p2.pdf>.
- Hill, G. and Greathead, D., 1999. Economic Evaluation in Classical Biological Control. In: Perrings, C., Williamson, M. and Dalmazzone, S., eds. (1999) *The Economics of Biological Invasions*.
- Hoffman, F.O., and Hammonds, J.S., 1994. Propagation of uncertainty in risk assessment: the need to distinguish between uncertainty due to lack of knowledge and uncertainty due to variability. *Risk analysis*, 14, 707-712.
- Hollingsworth, R. and Kovacs, G.S., 1981. Soil slumps and debris flows: prediction and protection, *Bull. Assoc. Engng. Geol.*, 18, 17±28.
- Holmgren, P. 1994. Multiple flow direction algorithms for runoff modelling in grid based elevation models: an empirical evaluation, *Hydrological Processes* 8 (4), pp. 327–334.
- Hong, H.P., 1998. An efficient point estimate method for probabilistic analysis. *Reliability Engineering and System Safety* 59 261-267.
- Horton, P., Jaboyedoff, M., Bardou, E., 2008. Debris Flow susceptibility mapping at a regional scale, 4th Canadian Conference on Geohazards, Université de Laval, Quebec, Canada.
- Hoyois, P., and Guha-Sapir, D., 2004. Disasters caused by flood : Preliminary data for a 30 year assessment of their occurrence and human impact, paper presented at Health and Flood Risk Workshop; A Strategic Assessment of Adaptation Processes and Policies,

- International workshop organised by the Tyndall Centre for Climate Change Research, University of East Anglia, Norwich, 18th to 20th July 2004.
- Hubert, Ph., Bamy M. H., and Moatti J. P., 1991. Elicitation of decision makers' preferences of management of major hazards, *Risk Analysis*, 11:199-206.
- Hungr, O., Evans, S.G., 1988. Engineering evaluation of fragmental rockfall hazards. Proc. 5th International Symposium on Landslides, vol. 1. University of Lausanne, Lausanne, pp. 685– 690.
- Hungr, O., Evans, S.G., and Hazzard, J., 1999. Magnitude and frequency of rock falls and rock slides along the main transportation corridors of southwestern British Columbia, *Canadian Geotechnical Journal*, 36, 224-238.
- Hydropower & Dams, 1998. Risk Based Dam Safety Evaluations, Conference Report: Part 2, Hydropower & Dams.
- IFRC, 2002. World Disasters Report 2002, International Federation of the Red Cross and Red Crescent Societies, Geneva, 240 pp.
- Ichem, Institute of Chemical Engineering, 1985. Nomenclature for hazard and risk assessment in the process industries.
- IPCC, 2007. Climate Change 2007: The Physical Science Basis, Summary for Policymakers, 18 pp, Intergovernmental Panel on Climate Change, Geneva.
- ISDR, 2007. Guidance note on the Costs and Benefits of Disaster Risk Reduction,
- IUGS, 1997. Quantitative risk assessment for slopes and landslides – the state of the art. IUGS working group on landslides, committee on risk assessment in Landslide Risk Assessmentm Cruden and Fell (eds.), Balkema, Rotterdam, 3-14.
- IUSSE Press, 2007. Earthquake Disaster Scenario Prediction and Loss Modelling for Urban Areas, LESSLOSS Report n° 2007/07.
- Iverson, R.M., 1997. The physics of debris flow, *Reviews of geophysics*, Vol. 35 No. 3 pp. 245-296, Agosto
- Iverson, R.M., 2000. Landslide triggering by rain infiltration *WATER RESOURCES RESEARCH*, VOL. 36, NO. 7, PAGES 1897–1910.
- Jaboyedoff, M. and Labiouse, V. 2003. Preliminary assessment of rockfall hazard based on GIS data. *ISRM 2003–Technology roadmap for rock mechanics*, South African Institute of Mining and Metallurgy, Vol. 1, 575-578.
- Jansen, H.M.A. ,1988..Financieel economische risicolimiet (financial economic risk limit, in Dutch), *Min. van Volkshuisvesting, Ruimtelijke Ordening en Milieu, directie stralenbescherming*.
- Jongejan, R.B.. How safe is safe enough? The government's response to industrial and flood risks. PhD thesis, 2008
- Jonkman, S.N., van Gelder P.H.A.J.M., Vrijling J.K., 2002. Loss of life models for sea- and river floods, in: Wu et al. (eds) *proc. Of Flood Defence*, Volume 1, pp. 196 - 206, Science Press, New York Ltd.

- Jonkman, S.N., van Gelder P.H.A.J.M., Vrijling J.K., 2003. An overview of quantitative risk measures for loss of life and economic damage, *Journal of Hazardous Materials*, A99, pp.1-30.
- Jonkman, S. N., 2007. Loss of life estimation in flood risk assessment. Theory and applications, PhD Thesis, Technical University of Delft, Delft, Netherlands, 354 pp.
- Kabat, P., van Vierssen, W. Veraart, J. Vellinga, P., Aerts, J. 2005. Climate proofing the Netherlands, *Nature*, 438, 283-284.
- Kaplan, S. and Garrick, B.J, 1981. On the quantitative definition of risk, *Risk analysis*, 1(1):11-27.
- Kappos, AJ, Panagopoulos, G, Panagiotopoulos, Ch, Penelis, G., 2005. A hybrid method for the vulnerability assessment of R/C and URM buildings. In: Spence R, Le Brun B (eds) *Bulletin of earthquake engineering*, special issue: the risk-ue Project—Methodology.
- Kennedy, R.P., Cornell C.A, Campbell R.L., Kaplan S., and Perla H.F., 1980. Probabilistic Seismic Safety of an Existing Nuclear Power Plant. *Nuclear Engineering and Design* 59 (2): 315-38.
- Klecka, W.R., 1980. *Discriminant Analysis*, Sage Publications, Newbury Park, California.
- Kopp, R.J., et al., 1997. *Cost-Benefit Analysis and Regulatory Reform: An Assessment of the Science and the Art*, 67 pp, Resources for the Future, Washington DC.
- Kramer, R. A., 1995. Advantages and Limitations of Benefit-Cost Analysis for Evaluating Investments in Natural Disaster Mitigation, in *Disaster Prevention for Sustainable Development: Economic and Policy Issues*, edited by M. Munasinge and C. Clarke, pp. 61-76, World Bank, Washington DC.
- Laheij, G.M.H., Post, J.G., Ale B.J.M, 2000. Standard methods for land-use planning to determine the effects on societal risk, *J. Hazard. Mater.* 71 269–282.
- Lanyon, L. E. and Hall, G. F., 1983. Land-surface morphology: 2. Predicting potential landscape instability in eastern Ohio, *Soil Sci.*, 136, 382±386.
- Lari, S., Frattini P., Crosta G.B., 2009. Local scale multi-risk assessment and uncertainty evaluation: the case of Brescia (Italy), in review.
- Lee, E.M., Jones, D.K.C., 2004. *Landslide risk assessment*. Thomas Telford, London, pp 454.
- Leroi, E., Bonnard, C., Fell, R., McInnes, R., 2005. Risk assessment and management. In: Hungr, O., Fell, R., Couture, R., Eberhardt, E. (Eds.), *Landslide Risk Management*. Taylor and Francis, London, pp. 159–198.
- LESSLOSS Project N. GOCE-CT-2003-50544, 2007. *Risk Mitigation for Earthquakes and Landslides*, LESSLOSS ANNUAL REPORT, Publishable Final Activity Report
- Luhmann, N., 1995. *Social systems*, Stanford, CA, Stanford University Press.
- Mark, R.K., 1992. Map of debris - flow probability, San Mateo County, California, scale 1:62 500, *Miscellaneous Investigations Map*, I-1257-M. US Geological Survey, Washington, D.C.

- Marthaler, M. 2001. *Le Cervin est-il africain ? Une histoire géologique entre les Alpes et notre planète*. Editons LEP (Loisirs et Pédagogie), Le Mont-sur-Lausanne.
- Martin, K., Skaugset, A., and Pyles, M.R., 1996. Forest management of landslide prone sites: the effectiveness of headwall leave areas, part II, COPE Report, 9, 8±12.
- Masure, P., 2003. Variables and indicators of vulnerability and disaster risk for land-use and urban on territorial planning, IDB/IDEA Programa de indicadores para la gestion de riesgos, Universidad Nacional de Colombia, Manizales.
- Mechler, R., 2002. Natural Disaster Risk and Cost-Benefit Analysis. In Kreimer, A, M. Arnold and A.Carlin (eds.). *The Future of Disaster Risk: Building Safer Cities*. Conference papers. Washington, DC: The World Bank.
- Mechler, R., 2004a. Natural Disaster Risk Management and Financing Disaster Loss in Developing Countries, 284 pp, Universität Fridericiana zu Karlsruhe, Karlsruhe.
- Mechler, R., 2004b. Piura Case Study, Deutsche Gesellschaft fuer Technische Zusammenarbeit (GTZ), Eschborn.
- Mechler, R., 2004c. Semarang Case Study, Deutsche Gesellschaft fuer Technische Zusammenarbeit (GTZ), Eschborn.
- Mechler, R., 2005. Cost-benefit analysis of natural disaster risk management in developing countries. Working paper. Deutsche Gesellschaft fuer Technische Zusammenarbeit (GTZ), Eschborn.
- Mersereau, R.C. and Dyrness, C.T.. 1972. Accelerated mass wasting after logging and slash burning in western Oregon', *J. Soil Wat. Conserv.*, 27, 112±114.
- Middelmann, M. and Granger, K. (eds), 2000. *Community risk in Mackay: A multi-hazard risk assessment*, Australian Geological Survey Organisation, Canberra.
- Ministry of Agriculture, 2001. *Flood and Coastal Defence Project, Appriaisal Guidance*. Overview. London.
- Mizina, S.V., Smith J.B. , Gossen E., Spiecker K.F., Witkowski S.L.,1999. An Evaluation of Adaptation Options for Climate Change Impacts on Agriculture in Kazakhstan, *Mitigation and Adaptation Strategies for Global Change*, 4, 25-41.
- Moench, M., and Dixit, A. (Eds.), 2004. *Adaptive Capacity and Livelihood Resilience: Adaptive Strategies for Responding to Floods and Droughts in South Asia*, 214 pp., Institute for Social and Environmental Transition, Boulder, Kathmandu.
- Moench, M., and Stapleton, S., 2007. *Water, Climate, Risk and Adaptation*, edited, 88 pp., Cooperative Programme on Water and Climate, The Netherlands, In Press.
- Moench, M., Mechler, R., Stapleton, S., 2007. *Guidance note on the Costs and Benefits of Disaster Risk Reduction*, ISDR.
- Montgomery, D.R., 1991. *Channel initiation and landscape evolution*, PhD Thesis, University of California, Berkeley. 421 pp.
- Montgomery, D.R., Sullivan, K. and Greenberg1, H.M.,1998. Regional test of a model for shallow Landsliding Hydrological Processes, *Vol. 12*, 943±955.

- Montgomery, D. R. and Dietrich, W. E., 1994. A physically based model for topographic control on shallow landsliding. *Water Resources Research*, vol . 30 n.4 pp.1153-1171.
- Montgomery, D. R., Dietrich, W. E., Torres, R., Anderson, S. P., Heffner, J. T., and Loague, K., 1997. 'Hydrologic response of a steep unchanneled valley to natural and applied rainfall', *Wat. Resour. Res.*, 33, 91±109.
- Morales, J.M., and Pérez-Ruiz, J., 2007. Point Estimate Schemes to Solve the Probabilistic Power Flow. *IEEE transactions on power systems*, vol. 22, no. 4.
- Moser, D. A., 1996. The Use of Risk Analysis by the U.S. Army Corps of Engineers, *Water Resources Update*, 103, 27-34.
- MMC, Multihazard Mitigation Council, 2005. *Natural Hazard Mitigation Saves: An Independent Study to Assess the Future Savings from Mitigation Activities: Volume 2-Study Documentation*, 144 pp, Multihazard Mitigation Council, Washington DC.
- NACE rev2, 2006. *Regolamento (CE) n. 1893/2006 del parlamento europeo e del consiglio del 20 dicembre*
- NASA, 2002. *Probabilistic Risk Assessment procedures guide for NASA managers and practitioners*, prepared for Office of Safety and Mission Assurance NASA Headquarters. Washington D.C. 20546.
- Navarro, H., 2005. *Manual para la evaluacion de impacto de proyectos y programas de lucha contra la pobreza*, 85 pp, Instituto Latinoamericano y del Caribe de Planificacion Economica y Social (ILPES): Area de Proyectos y programacion de inversiones, Santiago de Chile.
- Neuland, H., 1976. A prediction model of landslips, *Catena*, 3, 215±230.
- Niemann, K.O. and Howes, D.E., 1991. Applicability of digital terrain models for slope stability assessment, *ITC J.*, 1991-3, 127±137.
- NORSOK, 2001. *Standard Z-013, Risk and emergency preparedness analysis* NTC (Norwegian Technology Centre), Oslo: Norway,
- Okimura, T. and Nakagawa, M., 1988. A method for predicting surface mountain slope failure with a digital landform model, *Shin Sabo*, 41, 48±56.
- Okimura, T., and Ichikawa, R.A., 1985. Prediction method for surface failures by movements of infiltrated water in a surface soil layer, *Natural Disaster Sci.*, 7, 41±51.
- O'loughlin E.M., 1981. Saturation regions in catchment and their relation to soil and topographic properties. *Journal of Hydrology* 53 (1981), 229–246.
- O'Loughlin, E. M., 1986. Prediction of surface saturation zones in natural catchments by topographic analysis, *Wat. Resour. Res.*, 22, 794±804.
- OMB, Office of Management and Budget, 1992, *Circular No. A-94 Revised: Guidelines and Discount Rates for Benefit-Cost Analysis of Federal Programs*, 17 pp, Office of Management and Budget, Washington DC.
- Osei, E.K., Amoh, G.E.A., and Schandorf, C., 1997. Risk ranking by perception. *Health Physics*, 72, 195–203.

- Pack, R., Tarboton, D., and Goodwin, C., 1998. The SINMAP Approach to Terrain Stability Mapping, Paper Submitted to 8th Congress of the International Association of Engineering Geology, Vancouver, British Columbia, Canada.
- Parker, D.J., Green, C.H., Thompson, P.M., 1987. Urban Flood Protection Benefits, Gower Technical Press.
- Parry, G.W., 1996. The characterization of uncertainty in Probabilistic Risk Assessments of complex systems. *Reliability engineering and system safety*, 54, 119-126.
- Paté-Cornell, M.E., 1995. Risk analysis and the probabilistic treatment of uncertainties. Report to the electric Power Research Institute, Projects RP 2955 and RP 3550, EPRI, Palo Alto, CA.
- Paté-Cornell, M.E., 1996. Uncertainties in risk analysis: Six levels of treatment. *Reliability Engineering and System Safety* 54 95-1.
- Pawlicki, T., Jiang S.B., Li, J., Deng, J., and Ma C. M., 2000. Including Setup Uncertainty in Monte Carlo Dose Calculation for IMRT . Proceedings of the 22nd Annual EMBS International Conference, July 23-28, 2000 Chicago IL.
- Pedersoli, G. S., 1960. La lunga alluvione, Edizioni Toroselle 1992.
- Penning-Roswell, E., C. Green, P. Thompson, A. Coker, S. Tunstall, C. Richards, D. Parker, 1992. The Economics of Coastal Management - A Manual of Benefit Assessment Techniques (The Yellow Manual). London.
- Pettenella, D., Baiguera, M., 1997. La contabilita` ambientale delle risorse forestali: un'applicazione alla regione Lombardia. *L'Italia Forestale e Montana* 5, 347-365.
- Piers, M., 1998.. Methods and models for the assessment of third party risk due tot aircraft accidents in the vicinity of airports and their implications for societal risk, In: R.E. Jorissen, P.J.M. Stallen (Eds.), *Quantified Societal Risk and Policy Making*, Kluwer Academic Publishers, Dordrecht.
- Plattner, T., 2005. .Modelling public risk evaluation of natural hazards: a conceptual approach, *Nat. Hazards Earth Syst. Sci.*, 5, 357-366.
- Porter, K.A., Kiremidjian, A.S., LeGrue, J.S., 2001. Assembly-based vulnerability of buildings and its use in performance evaluation, *Earthquake spectra*, 17 (2), 291-312.
- Porter, K. A., Shoaf, K., and Seligson, H., 2006. Value of injuries in the Northridge Earthquake, *Earthq. Spectra*, 22, 555-563.
- Powers, K., 2003. Benefit-Cost Analysis and the Discount Rate for the Corps of Engineers' Water Resource Projects: Theory and Practice, 29 pp, Congressional Research Service, Washington DC.
- PRIM 2007-2010, 2007. Programma Regionale Integrato di Mitigazione dei Rischi, Studi Preparatori – Il rischio integrato in Lombardia: misurazioni di livello regionale e individuazione delle zone a maggiore criticità, Regione Lombardia - Protezione civile, Prevenzione e Polizia Locale.
- PRIM 2007-2010, 2007. Programma Regionale Integrato di Mitigazione dei Rischi, Studi Preparatori – Incidenti ad elevata rilevanza sociale in Lombardia, Regione Lombardia - Protezione civile, Prevenzione e Polizia Locale.

- PRIM 2007-2010, 2007. Programma Regionale Integrato di Mitigazione dei Rischi, Studi Preparatori – Rischi maggiori in Lombardia, Regione Lombardia - Protezione civile, Prevenzione e Polizia Locale.
- ProVention Consortium, 2005. Successful disaster prevention in Latin America: The Argentina Flood Rehabilitation and the Rio Flood Reconstruction and Prevention Project, ProVention Consortium.
- Public Law 106-390, Disaster Mitigation Act of 2000, 26 pp., 106th Congress of the United States, Washington DC.
- Quinn, P F, Beven, K J, Chevallier, P, and Planchon, O., 1991. The prediction of hillslope flow paths for distributed hydrological modeling using digital terrain models. *Hydrological Processes* 5: 59-79.
- Rackwitz, R., 2002. Optimization and risk acceptability based on the Life Quality Index, *Structural Safety* 24, 297–331.
- Reneau, S. L. and Dietrich, W. E., 1987. Size and location of colluvial landslides in a steep forested landscape, in Beschta, R. L., Blinn, T., Grant, G. E., Ice, G. G., and Swanson, F. J. (eds), *Proceedings of the International Symposium on Erosion and Sedimentation in the Pacific Rim*, IAHS Pub., 165, 39±48.
- Riestenberg, M. M. and Sovonick-Dunford, S., 1983. The role of woody vegetation in stabilizing slopes in the Cincinnati area, Ohio, *Geol. Soc. Am. Bull.*, 94, 506±518.
- Roberds, W., 2005. Estimating temporal and spatial variability and vulnerability. In: *Landslide Risk Management*-Hungr, Fell, Couture & Eberhardt (eds), 2005 Taylor & Francis Group, London.
- Rosenblueth, E., 1981. Two-point estimates In probabilities-. *Appl. Math. Modelling*, 1981, Vol. 5.
- Saaty, T.L., 1980. *The Analytic Hierarchy Process: Planning, Priority Setting, Resource Allocation*, McGraw-Hill.
- Saaty, T.L., 1990. *Multicriteria Decision Making: The Analytic Hierarchy Process*, Vol. 1, AHP Series, RWS Publications, 502 pp,
- Seeley, M. W. and West, D. O., 1990. Approach to geologic hazard zoning for regional planning, Inyo National Forest, California and Nevada, *Bull. Assoc. Eng. Geol.*, 27, 23±35.
- Seidl, M., Dietrich, WE, 1992. The problem of channel erosion in bedrock. In: K.H. Schmidt and J. de Ploey, Editors, *Functional Geomorphology: Landform Analysis and Models*, *Catena Supplement* vol. 23 (1992), pp. 101–124.
- Sen, A. 1999b. *Poverty and Famines*, 257 pp., Oxford University Press, Delhi.
- Sen, A., 1999a. *Development as Freedom*, 366 pp., Alfred Knopf, New York.
- Shmid, S.M., Fügenschuh1, B., Kissling, E, Schuster, R, 2004. Tectonic map and overall architecture of the Alpine orogen, *Eclogae geol. Helv.* 97 (2004) 93–117
- Skaugset, A., Froehlich, H., and Lutz, K., 1993. The effectiveness of headwall leave areas, *COPE Report*, 6, 3±6.

- Slijkhuis, K.A.H., van Gelder, P.H.A.J.M., Vrijling, J.K., 1997. Optimal dike height under statistical-, damage- and construction-uncertainty. In: N. Shiraishi, M. Shinozuka, Y.K. Wen (Eds.), *Structural Safety and Reliability*, vol. 7, Kyoto, Japan, pp. 1137–1140.
- Slovic, P., 1987. Perception of risk, *Science* 236 (4798): 280–85.
- Slovic, P., Fischhoff, B., & Lichtenstein, S., 1984. Behavioral decision theory perspectives on risk and safety. *Acta Psychologica*, 56, 183-203.
- Smith, V.K., 1992. Environmental risk perception and valuation: conventional versus prospective reference theory. In: Bromley, D.W. and Segerson, K., Editors, 1992. *The social response to environmental risk: policy formulations in an age of uncertainty*, Kluwer Academic Publishers, Boston, pp. 23–56.
- Smyth, A.W., Altay, G., Deodatis, G., Erdik, M., Franco, G., Gülkan, P., Kunreuther, H., Luş, H., Mete, E., Seeber, N., Yüzügüllü, Ö., 2003. Benefit-Cost Analysis for Mitigating Seismic Losses: Probabilistic Evaluation of Retrofit Measures for Residential Buildings in Turkey, in *International Conference on Applications of Statistics and Probability in Civil Engineering, ICASP*, San Francisco.
- Società Geologica Italiana, 1990. *Guide Geologiche Regionali, Alpi e Prealpi Lombarde* (a cura di M. B. Cita, R. Gelati, A. Gregnanin), Roma.
- Stallen, P. J. M., Geerts, R., and Vrijling, J. K., 1996. Three conception of quantified societal risk. *Risk Analysis*, 16(5), 635– 644.
- Starr, C. , 1969. Social benefit vs. technological risk, *Science* 165, 1232:1238
- Swanson, F. J., and Dyrness, C. T. 1975. Impact of clear-cutting and road construction of soil erosion by landslides in the western.Cascade Range, Oregon, *Geology*, 3, 393±396.
- Takahasi, T., 1968. Studies of the forest facilities to prevent landslides, *Bull Fac. Agric., Shizuoka Univ.*, 18, 85±101.
- TAW, Technical Advisory Committee on Water Defences, 1985. Some considerations of an acceptable level of risk in The Netherlands, TAW.
- Terwilliger, V.J. and Waldron, L.J., 1991. Effects of root reinforcement on soil-slip patterns in the Transverse Ranges of southern California, *Geol. Soc. Am. Bull.*, 103, 775±785.
- Tropeano, D., Govi, M., Mortasa, G., Turitto,O., Soriana, P., Negrini, G., Arattano, M., 1999. -Eventi alluvionali e frane nell'Italia settentrionale – Periodo 1975-1981.
- Tweeddale, H.M.,1992. Balancing quantitative and non-quantitative risk assessment, *Process Safety & Environmental Protection*, 72 (B), 70-74 .
- Tyagunov, S., Heneka, P., Zschau J., Ruck, B. and Kottmeier, C. CEDIM, 2005. From Multi-Hazards to Multi-Risks, paper presented at Amonia Conference, December 2005 <http://www.cedim.de/english/904.php>.
- UNDP (United Nations Development Programme Bureau for Crisis Prevention and Reco), 2004. *Reducing disaster risk: a challenge for development*. New York, NY: United Nation Development Programme, Printed by John S. Swift Co., USA.

- Upadhyay, R.R., Ezekoye, O.A., 2008. Treatment of design fire uncertainty using Quadrature Method of Moments. *Fire Safety Journal* 43 127–139.
- USACE (US Army Corps of Engineers), 2000. Economic Guidance Memo (EGM) 01-03, Generic Depth-Damage Relationships Washington, DC.
- USACE (US Army Corps of Engineers), 2003. Generic depth–damage relationships for residential structures with basements. Report EGM 04-01, Economic Guidance Memorandum, p. 17.
- USACE (US Army Corps of Engineers), 2003. Hydrologic Engineering Center HEC-ResSi - Reservoir System Simulation User's Manual Version 2.0, CPD-82. US Army Corps of Engineers, Davis, CA.
- Uzielli, M, Düzgün, Ş, and Vangelsten, BV, 2006. A first-order second-moment framework for probabilistic estimation of vulnerability to landslides - Proceedings of Geohazards - Technical, Economic and Social Risk Evaluation, Lillehammer, June 18-21.
- van Asch, T., Kuipers, B., and van der Zanden, D.J., 1993. An information system for large scale quantitative hazard analyses of landslides, *Z. Geomorph.*, 87 (Suppl.), 133±140.
- van Danzig, D., 1956. Economic decision problems for flood prevention, *Econometrica* 24 276–287.
- van Griensven, A. , Meixner, T., Grunwald, S., Bishop, T., Diluzio, M., Srinivasan, R., 2006. A global sensitivity analysis tool for the parameters of multi-variable catchment models. *Journal of Hydrology* 324 10–23.
- van Westen, C. J., Montoya, L., and Boerboom, L., 2002. Multi-Hazard Risk Assessment using GIS in urban areas: A case study for the city of Turrialba, Costa-Rica, In: Proc. Regional workshop on Best Practise in Disaster Mitigation, Bali, pp. 120–136.
- Venton, C.C., and Venton P., 2004. Disaster preparedness programmes in India: A cost benefit analysis, 26 pp, Humanitarian Practice Network: Overseas Development Institute, London.
- Vermeiren, J. C., and Stichter S., 1998. Costs and Benefits of Hazard Mitigation for Building and Infrastructure Development: A case study in small island developing states, in Conference of the International Emergency Management Society, edited.
- Versteeg, M., 1987. External safety policy in the Netherlands: an approach to risk management. *Journal of hazardous materials*, 17: 215-221.
- Vinai, P., 2007. Development and Application of Objective Uncertainty Measures for Nuclear Power Plant Transient Analysis. Thèse no 3897 école polytechnique fédérale de Lausanne.
- Voortman, H.G., 2004. Risk-based design of large-scale flood defence systems, PhD thesis, Delft University.
- Vrijling, J.K., van Gelder, P.H.A.J.M, 1997. Societal risk and the concept of risk aversion, In: C. Guedes Soares (Ed.), *Advances in Safety and Reliability*, vol. 1, Lissabon, pp. 45–52.
- Vrijling, J. K., van Hengel, W., and Houben, R.J., 1995. A framework for risk evaluation. *Journal of Hazardous Materials*, 43(3), 245–261.

- Vrijling, J. K., van Hengel, W., and Houben, R.J., 1998. Acceptable risk as a basis for design. *Reliability Engineering and System Safety*, 59, 141–150.
- Vrouwenvelder, A.C.W.M., Lovegrove, R., Holicky, M., Tanner, P., Canisius, G., 2001. Risk assessment and risk communication in civil engineering, Safety, risk and reliability: trends in engineering, Malta, ISBN 3-85748-102-4, (<http://www.web.cvut.cz/ki/710/pdf/1812.pdf>).
- Warren, R., 2002. Ohio Natural Hazard Mitigation Planning Guidebook: A step-by-step guide to help communities prepare natural hazard mitigation plans and minimize future losses, 113 pp, Ohio Department of Natural Resources and Ohio Emergency Management Agency.
- Williams, G.P. and Guy, H.P., 1971. Debris avalanches: a geomorphic hazard. In: Coates, D. R. (ed.), *Environmental Geomorphology*. SUNY Publications in Geomorphology, Binghamton. pp. 25±46.
- Wisner, B., Blaikie, P.M., Cannon, T., 2004. *At Risk: Natural hazards, people's vulnerability and disasters*, Second Edition ed., 471 pp., Routledge, London.
- World Bank, 1996. *Appraisal of Argentinean Flood Protection Project*.
- Wu, T.H., McKinnell, W.P., and Swanston, D.N., 1979. Strength of tree roots and landslides on Prince of Wales Island, Alaska, *Can. Geotech. J.*, 16, 19±33.
- Yelokhin, A.N., 1997. Complex risk analysis for Novgorodsky's region's population, in: B.-M. Drottz Sjöberg (Ed.), *Proceedings of the Annual Meeting of the Society for Risk Analysis-Europe: New Risk Frontiers*, Stockholm,
- Yen, B.C., Cheng, S.T., Melching, C.S., 1986. First order reliability analysis. In: Yen BC (ed) *Stochastic and risk analysis in hydraulic engineering*. Water Resources Publications, Littleton, pp 1–36
- Zadeh, L.A., 1965. Fuzzy sets, *Information and control*, 8:338-353.
- Zhou, H.M., 1995. *Towards an Operational Risk Assessment in Flood Alleviation*, Delft University Press, ISBN 90-407-1146-1.
- Ziemer, R.R. and Swanston, D.N., 1977. 'Root strength changes after logging in southeast Alaska', Research Note PNW-306. US Forest Service, Pacific Northwest Forest and Range Experiment Station, Portland.

DATA SOURCES

- ACI, Automobile Club Italia, www.aci.it, I dati sugli incidenti stradali rilevati nel 2007, 2007
- ARPA Lombardia, 2007, database della popolazione.
- AVI - Aree Vulnerate Italiane da frane ed inondazioni, <http://avi.gndci.cnr.it>, visited on April 2007
- Regione Lombardia, 2009. Catalogo degli eventi di frana e di inondazione della Regione Lombardia.
- Centostazioni s.p.a, www.centostazioni.it, visited in 2009
- CRASL, 2008. Studio dei trasporti pericolosi in Regione Lombardia, Università Cattolica del Sacro Cuore.
- CRASL, 2009. Piano Integrato d'Area per la provincia di Brescia, rischi tecnologici, , Università Cattolica del Sacro Cuore.
- CTR – Carta Tecnica Regionale
<http://www.cartografia.regione.lombardia.it/geoportale/ptk?command=openchannel&channel=143>, visited on April 2007
- D.Lgs. 334/99
- DUSAF - Uso del Suolo Agricolo Forestale.
<http://www.cartografia.regione.lombardia.it/geoportale/ptk?command=openchannel&channel=157>, visited on April 2007
- ERSAF, 2000. Map of destination of use for agricultural and forestal soils of Lombardy
- ERSAF, 2006, Map of the forestal types of Lombardy
- Gruppo di lavoro CPTI: Catalogo Parametrico dei Terremoti Italiani, versione 2004 (CPTI04), INGV, Bologna, 2004.
- INAIL, Istituto Nazionale per l'assicurazione contro gli infortuni sul lavoro, www.inail.it, visited on April 2007
- ISTAT- Istituto nazionale di statistica 2001, censimento dell'industria <http://www.istat.it/>, visited on April 2007

- ISTAT Istituto nazionale di statistica, <http://www.istat.it/>, visited on April 2007
- ISTAT Istituto nazionale di statistica, <http://www.istat.it/>, visited on April 2007
- ISTAT-Istituto nazionale di statistica, 2001, censimento della popolazione
<http://www.istat.it/>, visited on April 2007
- MINISTERO DELL'INTERNO Dipartimento dei Vigili del Fuoco del Soccorso Pubblico e della Difesa Civile, 2008. Annuario statistico del corpo nazionale vigili del fuoco.
- MISURC - Mosaico Informatizzato degli Strumenti Urbanistici Comunali.
<http://www.cartografia.regione.lombardia.it/geoportale/ptk?command=openchannel&channel=154>, April 2007
- MPS Working Group, 2004 Redazione della mappa di pericolosità sismica prevista dall'Ordinanza PCM 3274 del 20 marzo 2003. Rapporto Conclusivo per il Dipartimento della Protezione Civile, INGV, Milano-Roma, 2004 aprile (2004) 65 pp. + 5 appendixes. <http://zonesismiche.mi.ingv.it>, visited on April 2007
- MPS Working Group, 2004 Redazione della mappa di pericolosità sismica prevista dall'Ordinanza PCM 3274 del 20 marzo 2003. Rapporto Conclusivo per il Dipartimento della Protezione Civile, INGV, Milano-Roma, 2004 aprile (2004) 65 pp. + 5 appendixes. <http://zonesismiche.mi.ingv.it>, visited on April 2007
- PAI - Piano stralcio di Assetto Idrogeologico
<http://www.adbpo.it/online/ADBPO/Home/Pianificazione/Pianistralcioapprovati/PianostralcioperlAssettoIdrogeologicoPAI/Pianovigente.html>, visited on April 2007
- PAI - Piano stralcio di Assetto Idrogeologico
<http://www.adbpo.it/online/ADBPO/Home/Pianificazione/Pianistralcioapprovati/PianostralcioperlAssettoIdrogeologicoPAI/Pianovigente.html>, visited on April 2007
- Piano Antincendi Boschivi (AIB), Regione Lombardia, 2006
<http://www.incendiboschivi.regione.lombardia.it/>, visited on April 2007
- Presidenza del Consiglio dei Ministri, Dipartimento di Protezione Civile, 2008. Indirizzi e criteri per la microzonazione sismica, DVD.
- PROGETTO IFFI - Inventario dei Fenomeni Fransi in Lombardia.
<http://www.cartografia.regione.lombardia.it/geoportale/ptk?command=openchannel&channel=152>, visited on April 2007
- PS267 - Piano straordinario per le aree a rischio idrogeologico molto elevato.
<http://www.adbpo.it/online/ADBPO/Home/Pianificazione/Pianistraordinariapprovati/PianostradaordinarioperleareearischioidrogeologicomoltoelevatoPS267/Pianovigente.html>, visited on April 2007
- Regione Lombardia - Direzione Generale Territorio e Urbanistica - Infrastruttura per l'Informazione Territoriale, Province, Comunità Montane, 1983, Carta Geoambientale.
- Regione Lombardia (D.G. Territorio ed urbanistica): Il bacino Lariano - nuove tecnologie per la generazione di un modello tridimensionale del terreno, CD, edizione 2007.
- SIAB - Sistema Informativo Antincendio Boschivo- D.G. Protezione Civile Prevenzione Polizia Locale Regione Lombardia, data base Regione Lombardia, 2002

SIBCA, Sistema Informativo Bacini e Corsi d'acqua,
<http://www.cartografia.regione.lombardia.it>, 2008

SIRF-CESI, mappe di densità di fulminazione 1996-2005 <http://www.fulmini.it/>, visited on April 2007

SIRVAL - Sistema Informativo Regionale Valanghe.
<http://www.cartografia.regione.lombardia.it/geoportale/ptk?command=openchannel&channel=152>, visited on April 2007

TELEATLAS www.teleatlas.com/index.htm, visited in 2007

UNI- Ente Nazionale Italiano di Unificazione, www.uni.com, visited in May 2009.

APPENDIX I

Indicators for hydrogeological risk. Possible choices and correspondent values.

Probability of occurrence	value
Very low (TR > 1000 years)	0.02
low (100 < TR < 1000 years)	0.20
medium (10 < TR < 100 years)	0.70
high (1 < TR < 10 years)	0.90
Very high (TR < 1 years)	1.00

Scenario area (km²)	value
>1.000.000	1
1.001-10.000	0.6
10.000-100.000	0.75
100.000-1.000.000	0.9
101-1.000	0.45
1-100	0.3
unknown	0.3

Efficacy of existing mitigation works	value
unknown	0
negative	-1
null	0
sufficient	0.3
good	0.7
excellent	1

Actualised cost of previous mitigation work (€)	value
--	--------------

0	1
<75.000	-0.1
> 5.000.000	-1
1.000.000 - 2.500.000	-0.7
150.000 - 400.000	-0.5
2.500.000 - 5.000.000	-0.9
400.000 - 1.000.000	-0.6
75.000 - 150.000	-0.3

N° historical events	value
0	0.0
>3	1.0
1-2	0.7
unknown	0.1

Damage induced by historical events (direct and indirect costs)	value
-	0.01
<100.000	0.1
>50.000.000	1
100.000-500.000	0.2
2.000.000-5.000.000	0.6
20.000.000-50.000.000	0.9
5.000.000-20.000.000	0.8
500.000-2.000.000	0.4

N. deaths/injuries induced by historical events	value
0	0
>10	1
1 - 3	0.7
3 - 5	0.8
5 - 10	0.9

Population exposed	value
0	0
> 1000	1
0-10	0.25
100 - 1000	0.9
10- 100	0.6

Vulnerability of people in the scenario area	value
null	0.1
Very low	0.3
low	0.5
high	0.9
Very high	1

Value of the exposed elements	value
-	0.01
<100.000	0.1
>50.000.000	1
100.000-500.000	0.2
2.000.000-5.000.000	0.6
20.000.000-50.000.000	0.9
5.000.000-20.000.000	0.8
500.000-2.000.000	0.4

Potential damage to exp. Elements without work (% of value)	value
0	0
>50	1
0,1 - 3	0.2
11 - 25	0.6
26 - 50	0.8
4 - 10	0.4

Event area (mq)	value
>1.000.000	1
1.001-10.000	0.6
10.000-100.000	0.75
100.000-1.000.000	0.9
101-1.000	0.45
1-100	0.3
unknown	0.3

Damages to exposed elements	value
-	0.01
<100.000	0.1
>50.000.000	1
100.000-500.000	0.2
2.000.000-5.000.000	0.6

20.000.000-50.000.000	0.9
5.000.000-20.000.000	0.8
500.000-2.000.000	0.4

N. deaths/injuries induced by the event	value
0	0
>10	1
1 - 3	0.7
3 - 5	0.8
5 - 10	0.9

Protected area	value
>1.000.000	1
1.001-10.000	0.6
10.000-100.000	0.75
100.000-1.000.000	0.9
101-1.000	0.45
1-100	0.3
unknown	0.3

Cost of the work	value
-	
<75.000	1
> 5.000.000	0.1
1.000.000 - 2.500.000	0.5
150.000 - 400.000	0.7
2.500.000 - 5.000.000	0.3
400.000 - 1.000.000	0.6
75.000 - 150.000	0.9

Maintenance cost (% of the building cost)	value
0	1
1 -3	0.9
3-5	0
5-10	0.5
>10	0.2

Spatial exhaustivity (% of the scenario area)	value
<30%	0
30-50%	0.3

50-80%	0.7
80-100%	1
Efficacy % (function for which it is built)	value
0-30%	0
31-50%	0.3
51-80%	0.7
81-100%	1
Efficiency % (work characteristics)	value
0-30%	0
31-50%	0.3
51-80%	0.7
81-100%	1
Indirect costs avoided with the work	value
-	
<75.000	0.1
> 5.000.000	1
1.000.000 - 2.500.000	0.7
150.000 - 400.000	0.5
2.500.000 - 5.000.000	0.9
400.000 - 1.000.000	0.6
75.000 - 150.000	0.3
Relevance	value
ordinary	0.1
Strategic and/or relevant	1
Environmental impact	value
high	0
low	0.8
medium	0.5
null	1
Population protected	value
0	0
> 1000	1
0-10	0.25
100 - 1000	0.9
10- 100	0.6

Value of protected elements	value
-	0.01
<100.000	0.1
>50.000.000	1
100.000-500.000	0.2
2.000.000-5.000.000	0.6
20.000.000-50.000.000	0.9
5.000.000-20.000.000	0.8
500.000-2.000.000	0.4
Avoided damage to protected elements (% of value)	value
0	1
>50	-1
0,1 - 3	-0.2
11 - 25	-0.6
26 - 50	-0.8
4 - 10	-0.4
Vulnerability of people in the scenario area	value
null	1
very low	-0.1
low	-0.3
high	-0.9
very high	-1
Authorizations required	value
ordinary	0.1
complex	1
Project level	value
feasibility	0.1
definitive	0.95
executive	1
Technical reports	value
Missing	0
Non necessary	0.9
Geologic Report	1
Hydraulic/hydrologic report	1
Expropriations	value
no	1
yes	0.5

Financing and realization procedure	value
ordinary	0.1
extraordinary	1
Realization time	value
<6 months	1
6 months -1 year	0.8
1-3 years	0.6
>3 years	0.3

Indicators for wildfire risk. Possible choices and correspondent values.

N. wildfires per year	Value
0,01-0,252	0.20
0,253-0,495	0.40
0,496-0,738	0.60
0,739-0,981	0.80
>0,981	1.00

Risk class	Value
0	0
1	0.6
2	0.3
3	1

Work class	Value
0	0
1	0.15
2	0.3
3	0.45
4	0.6
5	0.75
6	1
7	1

Scenario area	Value
>1.000.000	1
1.001-10.000	0.6

10.000-100.000	0.75
100.000-1.000.000	0.9
101-1.000	0.45
1-100	0.3
unknown	0.3

Presence of natural protection	Value
None	0
Regional park	0.5
Natural reserve	0.8
Natural park	1
SIC (Communitarian Interest Site)	1
ZPS (Special Protection Zones)	1

Indicators for cost-benefit analysis. Values and parameters to fill.

Occurrence probability	poisson Rt = 100
Very low (Rt > 1000 years)	0.02
low (100 < Rt < 1000 years)	0.18
medium (10 < Rt < 100 years)	0.86
high (1 < Rt < 10 years)	0.99
Very high (Rt < 1 year)	1.00

Exposed element	Extension of the exposed element (m ²)	Not protected by the work (m ²)	%losses with work in the protected area	% losses without work
Agricultural				
Building Areas				
Major risk industries				
Forest				
Quarry				
Houses				
Cemetery				
Cableways				
Industrial plants				
Sport structures				
Zootechnic plant				
Untilled soil				
Protection works				
Ponds				
Grasses or grazing land				
Productive craftsman like				
Industrial				
Crops				
Railway station				
Olive grove / vineyard				
Railway 1 binary				
Railway 2+ binary				

Aqueduct				
Airport				
High speed railway				
Motorway				
Strategic buildings				
Power plant				
Church				
Penstock				
Purification plant				
Dam				
Dump				
Power lines				
Tunnel				
Incinerator				
Oil/Gas pipeline				
Hospitals				
Bridge				
Port				
Schools				
Main road				
Secondary road				
Discontinuous urban area				
Continuous urban area				

Exposed people (per day)	n. people in the impacted area	protected by the work	% deaths or injured for the specific phenomenon
resident			
in transit (transport)			
temporary			

ACKNOWLEDGEMENTS

Particular thanks to Prof. Giovanni Battista Crosta and to Dr. Paolo Frattini for the precious guide and help over these pleasant years.

Thanks to Dr. Federico Agliardi, for the help on rockfall simulations, to Massimo Ceriani and Francesco Pozza (Regione Lombardia) for data providing; Bruna Comini, Elena Gagliazzi and Giacomo Borromeo (ERSAF) for methodological support on wildfire risk; Stefano Oliveri (CRASL), Giuseppe Triacchini (JRC) and Marco Buldrini for methodological support on technological risk, Prof. Michel Jaboyedoff and Pascal Horton, for the use of the debris-flow simulation model, Elena Valbuzzi (Università degli Studi di Milano Bicocca) for the application of indicators for priority and efficacy evaluation of mitigation works.

Thanks to Antonio Pola, Stefano Basiricò, and Rosanna Sosio for friendship, and for having shared long afternoons, breaks, and the office with me.